frontiers | Research Topics

# Women in avian physiology 2023

**Edited by**
Sandra G. Velleman, Francesca Soglia and Servet Yalcin

**Published in**
Frontiers in Physiology

ISSN 1664-8714
ISBN 978-2-8325-4625-3
DOI 10.3389/978-2-8325-4625-3

## About Frontiers

Frontiers is more than just an open access publisher of scholarly articles: it is a pioneering approach to the world of academia, radically improving the way scholarly research is managed. The grand vision of Frontiers is a world where all people have an equal opportunity to seek, share and generate knowledge. Frontiers provides immediate and permanent online open access to all its publications, but this alone is not enough to realize our grand goals.

## Frontiers journal series

The Frontiers journal series is a multi-tier and interdisciplinary set of open-access, online journals, promising a paradigm shift from the current review, selection and dissemination processes in academic publishing. All Frontiers journals are driven by researchers for researchers; therefore, they constitute a service to the scholarly community. At the same time, the *Frontiers journal series* operates on a revolutionary invention, the tiered publishing system, initially addressing specific communities of scholars, and gradually climbing up to broader public understanding, thus serving the interests of the lay society, too.

## Dedication to quality

Each Frontiers article is a landmark of the highest quality, thanks to genuinely collaborative interactions between authors and review editors, who include some of the world's best academicians. Research must be certified by peers before entering a stream of knowledge that may eventually reach the public - and shape society; therefore, Frontiers only applies the most rigorous and unbiased reviews. Frontiers revolutionizes research publishing by freely delivering the most outstanding research, evaluated with no bias from both the academic and social point of view. By applying the most advanced information technologies, Frontiers is catapulting scholarly publishing into a new generation.

## What are Frontiers Research Topics?

Frontiers Research Topics are very popular trademarks of the *Frontiers journals series*: they are collections of at least ten articles, all centered on a particular subject. With their unique mix of varied contributions from Original Research to Review Articles, Frontiers Research Topics unify the most influential researchers, the latest key findings and historical advances in a hot research area.

Find out more on how to host your own Frontiers Research Topic or contribute to one as an author by contacting the Frontiers editorial office: frontiersin.org/about/contact

# Women in avian physiology: 2023

**Topic editors**

Sandra G. Velleman — The Ohio State University, United States

Francesca Soglia — University of Bologna, Italy

Servet Yalcin — Ege University, Türkiye

**Citation**

Velleman, S. G., Soglia, F., Yalcin, S., eds. (2024). *Women in avian physiology: 2023*. Lausanne: Frontiers Media SA. doi: 10.3389/978-2-8325-4625-3

# Table of contents

frontiers | Frontiers in Physiology

TYPE Editorial
PUBLISHED 07 March 2024
DOI 10.3389/fphys.2024.1392506



OPEN ACCESS

EDITED AND REVIEWED BY
Colin Guy Scanes,
University of Wisconsin–Milwaukee,
United States

*CORRESPONDENCE
Sandra G. Velleman,
velleman.1@osu.edu

RECEIVED 27 February 2024
ACCEPTED 04 March 2024
PUBLISHED 07 March 2024

CITATION
Velleman SG, Soglia F and Yalcin S (2024), Editorial: Women in avian physiology: 2023. *Front. Physiol.* 15:1392506. doi: 10.3389/fphys.2024.1392506



# Editorial: Women in avian physiology: 2023

Sandra G. Velleman[1]*, Francesca Soglia[2] and Servet Yalcin[3]

[1]Department of Animal Sciences, The Ohio State University, Wooster, OH, United States, [2]Department of Agricultural and Food Sciences, University of Bologna, Bologna, Italy, [3]Department of Animal Science, Ege University, Bornova, Türkiye

KEYWORDS

**avian physiology, nutrition, reproduction, muscle, temperature**

Editorial on the Research Topic
Women in avian physiology: 2023

## Introduction

The "Women in Avian Physiology: 2023" is the second in a series of Research Topics focused on Women by Frontiers in Avian Physiology. The series on Women in Avian Physiology is aimed at showcasing research especially from early career women to help promote their careers in the area of avian physiology. Submissions from all areas of Avian Physiology were accepted. A total of 12 submissions were accepted for publication spanning the areas of Nutrition, Reproduction, Breast Muscle Physiology and Myopathies, and the Effects of Temperature.

## Nutrition

Three contributions addressed nutrition by Ashayerizadeh et al., Dayan et al., and Johnson et al. Ashayerizadeh et al. found that adding turmeric powder to diets increased growth in Japanese quail and the effect was enhanced with black pepper powder and may be an alternative to the addition of antibiotics in feed. Dayan et al. focused on improving immediate post hatch energy and breast muscle development by in-ovo feeding with creatine monohydrate. They found increased expression of genes related to muscle growth potential and an increased number of myofibers in the breast muscle. Johnson et al. reported findings with the addition of a microencapsulate feed additive containing botanicals and organic acids on jejunum and ileum health in 15-day old broiler chicks. The research showed that the microencapsulated feed additive resulted in a more anti-inflammatory phenotype in the jejunum and the ileum had a greater immunometabolic response.

## Reproduction

The area of reproduction was covered by four contributions. Brady et al. investigated how artificial insemination affects sperm storage tubules in turkey hens. The storage of sperm in the sperm tubules directly impacts hen fertility. Transcriptome analysis revealed

that the inseminated group had the greatest change in the sperm storage tubule transcriptome which may have a direct effect on fertility. Kosonsiriluk et al. also studied the effects of turkey hen artificial insemination. They investigated the effect of insemination on the transcriptome of the uterovaginal junction where the semen storage tubules are located. In brief, they found that repeated inseminations caused a local immune response and increased aging of the turkey hen uterovaginal junction. Long non-coding RNA (lnc RNA) are a class of non-coding RNAs over 200 nucleotides in length and may regulate ovarian development. In Taihe Black-Bone Chickens, Huang et al. identified 136 differentially expressed lncRNAs. Network analysis of lncRNA-mRNA interactions identified 16 pairs of lncRNA-target gene associations with 7 differentially expressed lncRNAs with 14 target genes associated with reproductive traits. Interestingly, the target genes identified were primarily associated with follicle and ovary development. Keel bone damage in Japanese Quail hens was addressed by Hilebrand et al. using a radiography approach to detail the development of the keel bone. Damage to the keel bone is an animal welfare issue in laying hens and can have an occurrence up to 100% within a single flock. They found between 8 and 19 weeks of age that there was decreased radiographic density, lateral surface area and length of the keel bone. Furthermore by 23 weeks of age, 82% of the quail hens had deviations of the keel bone.

## Breast muscle physiology and myopathies

The broiler breast muscle is the most economically valuable cut due to increasing consumer demand. To meet this increase in consumer demand, the poultry industry has developed broiler lines with improved growth rates, increased meat yield, and higher feed efficiencies. Despite the improvements, breast muscle myopathies like Wooden Breast have emerged in recent years. Alnahhas et al. provided a comprehensive review of hypoxia-inducible factor 1 and how it plays a key role in the development of these conditions. Hypoxia is one of the primary causes of broiler breast muscle myopathies. The review included a discussion of the causes and consequences of hypoxia with focus given to the hypoxia-inducible factor pathway. In an opinion paper by Xu and Velleman on the role of mTOR pathway in breast muscle growth and development, the importance of mTOR signal transduction in regulating muscle fiber hypertrophy and satellite cell mediated growth was discussed. They viewed the mTOR pathway as being critical in breast muscle growth through its stimulation of myofiber protein synthesis and regulating satellite cell-mediated myogenesis. Satellite cells are located at the periphery of each muscle fiber and are responsible for all post hatch muscle fiber growth and the regeneration of muscle.

## Effects of temperature

Uyanga et al. did a bibliometric analysis of papers published in the area of poultry research from 2000 to 2021. They found that the top 10 globally cited manuscripts focused on the effects heat stress, alleviating heat stress, and the relationship between oxidative stress and heat stress poultry in poultry. The findings of this literature search underscore the concern associated with climate change and its association with heat stress. The sensitivity of primary broiler pectoralis major muscle satellite cells to temperature was investigated by Gregg et al. Since broiler body temperature is 41°C and *in vitro* assays of satellite cells are typically run at 38°C, experiments were run to determine the effect of temperature on broiler satellite cell myogenesis. It was found that culturing at 41°C compared to 38°C altered satellite cells myogenic kinetics with promoting a more rapid progression through the myogenic process and increase the number of apoptotic cells. Thus, birds that are thermally stressed post hatch may have altered myogenesis and post hatch muscle growth.

## Author contributions

SV: Writing–original draft, Writing–review and editing. FS: Writing–review and editing. SY: Writing–review and editing.

## Funding

The author(s) declare that no financial support was received for the research, authorship, and/or publication of this article.

## Conflict of interest

The authors declare that the research was conducted in the absence of any commercial or financial relationships that could be construed as a potential conflict of interest.

The author(s) declared that they were an editorial board member of Frontiers, at the time of submission. This had no impact on the peer review process and the final decision.

## Publisher's note

frontiers | Frontiers in Physiology

TYPE Original Research
PUBLISHED 24 January 2023
DOI 10.3389/fphys.2023.1079638



OPEN ACCESS

EDITED BY
Xiaofei Wang,
Tennessee State University, United States

REVIEWED BY
Monika Proszkowiec-Weglarz,
Agricultural Research Service (USDA), United States
Sonia Metayer Coustard,
Other, France

*CORRESPONDENCE
Zehava Uni,
zehava.uni@mail.huji.ac.il

SPECIALTY SECTION
This article was submitted to Avian Physiology, a section of the journal Frontiers in Physiology

RECEIVED 25 October 2022
ACCEPTED 11 January 2023
PUBLISHED 24 January 2023

CITATION
Dayan J, Melkman-Zehavi T, Reicher N, Braun U, Inhuber V, Mabjeesh SJ, Halevy O and Uni Z (2023), Supply and demand of creatine and glycogen in broiler chicken embryos.
*Front. Physiol.* 14:1079638.
doi: 10.3389/fphys.2023.1079638



# Supply and demand of creatine and glycogen in broiler chicken embryos

Jonathan Dayan[1], Tal Melkman-Zehavi[1], Naama Reicher[1], Ulrike Braun[2], Vivienne Inhuber[2], Sameer J. Mabjeesh[1], Orna Halevy[1] and Zehava Uni[1]*

[1]Department of Animal Science, Robert H. Smith Faculty of Agriculture, Food and Environment, The Hebrew University of Jerusalem, Rehovot, Israel, [2]AlzChem Trostberg GmbH, Trostberg, Germany

Optimal embryonic development and growth of meat-type chickens (broilers) rely on incubation conditions (oxygen, heat, and humidity), on nutrients and on energy resources within the egg. Throughout incubation and according to the embryo's energy balance, the main energy storage molecules (creatine and glycogen) are continuously utilized and synthesized, mainly in the embryonic liver, breast muscle, and the extraembryonic yolk sac (YS) tissue. During the last phase of incubation, as the embryo nears hatching, dynamic changes in energy metabolism occur. These changes may affect embryonic survival, hatchlings' uniformity, quality and post hatch performance of broilers, hence, being of great importance to poultry production. Here, we followed the dynamics of creatine and glycogen from embryonic day (E) 11 until hatch and up to chick placement at the farm. We showed that creatine is stored mainly in the breast muscle while glycogen is stored mainly in the YS tissue. Analysis of creatine synthesis genes revealed their expression in the liver, kidney, YS tissue and in the breast muscle, suggesting a full synthesis capacity in these tissues. Expression analysis of genes involved in gluconeogenesis, glycogenesis, and glycogenolysis, revealed that glycogen metabolism is most active in the liver. Nevertheless, due to the relatively large size of the breast muscle and YS tissue, their contribution to glycogen metabolism in embryos is valuable. Towards hatch, post E19, creatine levels in all tissues increased while glycogen levels dramatically decreased and reached low levels at hatch and at chick placement. This proves the utmost importance of creatine in energy supply to late-term embryos and hatchlings.

KEYWORDS

**incubation, chicken, embryo, creatine, glycogen**

## Introduction

The phase of embryonic development has great importance to the production chain of meat-type chickens (broilers) as the 21-day of incubation constitutes more than a third of the broiler lifespan, starting with incubation and ending with marketing at 35–42 days (Havenstein et al., 2003a; Havenstein et al., 2003b; Zuidhof et al., 2014; Givisiez et al., 2020). During the period of incubation, in order to ensure optimal development and growth, avian embryos depend on levels of oxygen, heat and humidity together with the supply of nutrients and energy (Decuypere et al., 2001; Moran, 2007; De Oliveira et al., 2008). Embryos utilize the nutrients within the egg to form high energy-value compounds such as glycogen and creatine with the final aim of ATP production (Christensen et al., 1999; 2000; 2001; Moran, 2007).

Glycogen is the main storage form of glucose in tissues, its high-energetic value is derived from the potential to release glucose and the production of ATP by aerobic respiration or by anaerobic glycogen breakdown (glycolysis). Two key enzymes are involved in glycogen metabolism; glycogen synthase (GYS), a rate limiting enzyme in glycogen synthesis, and glycogen phosphorylase L (PYGL), which catalyzes the release of glucose-1-phosphate from glycogen (Blaxter, 1989; Scanes, 2022). During most of incubation period, up to embryonic day (E) 19, gas exchange is achieved through chorioallantoic respiration and oxygen is sufficient to support aerobic processes of energy metabolism and lipid oxidation (Tazawa et al., 1983; Decuypere et al., 2001; Moran, 2007). Along this period, sufficient glucose is produced, and the unutilized glucose is funneled to storage, i.e., glycogen synthesis in the embryonic liver, muscles, and the extraembryonic yolk sac (YS) tissue (Romanoff, 1960; Romanoff, 1967; Noble and Cocchi, 1990; Speake et al., 1998; Yadgary and Uni, 2012; Wong and Uni, 2021). Post E19, prior to the initiation of the hatching process, oxygen levels become limiting. At this phase, energy production in the embryo switches from lipid oxidation to anaerobic catabolism, by the breakdown of glycogen to glucose and by gluconeogenesis with the breakdown of amino acids for glucose and ATP production. The latter is apparent with the activation of two key gluconeogenic enzymes; fructose-1,6-bisphosphatase 1 (FBP1), which catalyzes the hydrolysis of fructose 1,6-bisphosphate to fructose 6-phosphate, and glucose-6-phosphatase 2 (G6PC2), which catalyzes the hydrolysis of glucose-6-phosphate to glucose and inorganic phosphate, leading to the release of glucose into the bloodstream. By the time the embryo hatches, almost all glycogen is exploited, and its stores are depleted (Uni and Ferket, 2004; De Oliveira et al., 2008; Yadgary and Uni, 2012).

Creatine, another high-energy value molecule, is deposited by the hen in the egg compartments (yolk and albumen) where it is available to the embryo (Reicher et al., 2020). However, as only small amounts are deposited, the embryo relies also on *de novo* synthesis of creatine during incubation (Walker, 1979). Creatine synthesis involves two main steps driven by two enzymes. The first enzyme, L-arginine: glycine amidinotransferase (AGAT), catalyzes the reaction between glycine and arginine to create ornithine and guanidinoacetic acid (GAA). The second enzyme is guanidinoacetate N-methyltransferase (GAMT), which is responsible for GAA methylation *via* S-adenosylmethionine (SAM) to form creatine. Once inside the cells, as shown in rats and mice, creatine is phosphorylated into phosphocreatine, initiating the conversion of ADP into ATP during its dephosphorylation. Thus, creatine functions as an energy storage molecule, which can generate ATP on demand (Bessman and Carpenter, 1985; Wyss, 2000; Da Silva et al., 2009). Additionally, unlike glycogen or fat, no metabolic breakdown is needed for ATP production from the creatine/phosphocreatine system, making it the fastest way of ATP provision. In chicken embryos and hatchlings, creatine was shown to play a major role in energy metabolism, with the potential to promote their energetic status and the post-hatch performance (Murakami et al., 2014; Zhang et al., 2016). However, little is known about the dynamics of creatine during chicken embryogenesis and its relation to glycogen stores, as well as to the energetic status of late-term embryos and hatchlings. Moreover, previous studies have not shown an inclusive comparison of glycogen and creatine dynamics simultaneously in the liver, YS tissue, and breast muscle.

This study examined creatine and glycogen dynamics from E11 until hatch and up to chick placement at the farm. Embryos and hatchlings were sampled and examined for; (1) creatine and glycogen levels in the liver, YS tissue, and breast muscle, (2) levels of blood glucose and ketones, and (3) the expression levels of genes encoding for enzymes involved in creatine synthesis in the liver, kidney, YS tissue and breast muscle (AGAT and GAMT), along with genes that are encoding for gluconeogenic enzymes (FBP1 and G6PC2), and enzymes responsible for glycogen synthase (GYS), and glycogenolysis (PYGL).

# Materials and methods

## Eggs, incubation and sampling procedure

Fertile eggs ($n$ = 100; mean weight = 70.04 g, SD = 2.19 g) from 40-week-old broiler hens (Cobb 500) were purchased from a commercial breeder farm (Y. Brown and Sons Ltd., Hod Hasharon, Israel). Eggs were incubated in a Petersime hatchery at the Faculty of Agriculture of the Hebrew University under standard conditions (37.8°C and 56% relative humidity). On embryonic day (E) 10, eggs were candled, unfertilized eggs and dead embryo eggs were removed. Tissue sampling was performed at E11, E13, E15, E17, E19, at hatch (actual time of hatch at the hatchery, 480–483 h in incubation) and at chick placement (31–34 h post hatch, prior to the exposure to feed at the farm). At each sampling day, six embryos/hatchlings were randomly selected, euthanized by cervical dislocation and the following parameters were recorded: embryo yolk free body mass (YFBM), yolk content weight, YS tissue weight (according to Yadgary et al., 2010), liver weight and breast muscle weight. The relative weights of liver, breast muscle and YS tissue were calculated as percent of YFBM. Blood glucose and ketone levels were also recorded. In addition, liver, YS tissue and breast muscle samples were collected for creatine and glycogen content determination and for the evaluation of expression levels of genes involved in creatine synthesis, gluconeogenesis, glycogenesis, and glycogenolysis. Kidney samples were collected for the evaluation of expression of creatine synthesis. Immediately after collection, tissue samples were placed in liquid nitrogen and kept under −80°c until further processing.

## Creatine and glycogen content determination

Liver, YS tissue and breast muscle samples were lyophilized and later examined for their creatine and glycogen content by Swiss-BioQuant-AG (Reinach, Switzerland). The concentrations of creatine and glycogen (mg/g dry weight tissue) were determined, and the total amounts (mg) in each tissue were calculated. Due to insufficient material load, breast muscle samples were analyzed only at E15, E17, E19, hatch and chick placement.

## Glucose and ketones measurements

Blood glucose and ketones levels were obtained directly from the jugular vein of embryos and determined using FreeStyle Optimum Gluco/Keto meter and test strips (Abbott Diabetes Care Ltd., Witney Oxon, United Kingdom) according to the manufacturer's instructions.

**TABLE 1** Primers used for real-time PCR gene expression analysis.

| Target[a] | Accession number | Primer F (5′-3′) | Primer R (5′-3′) | Amplicon | References |
|---|---|---|---|---|---|
| AGAT | NM204745.1 | ACATCTTGCACCTGACTACCG | ACAGTGGGTGATCATCAGGAA | 206 | Reicher et al. (2020) |
| GAMT | XM015299974.2 | ACACAAGGTGGTGCCACTGA | CGAGGTGAGGTTGCAGTAGG | 199 | Reicher et al. (2020) |
| GYS1 | AB090806 | GATGAAACGCGCCATCTTCG | CGCACGAACTCCTCGTAGTC | 213 | Primer Blast |
| GYS2 | XM_015291547.2 | CATCTGTACACTGTGCCCATGTG | TTTGGAGTGACAACATCAGGATTT | 92 | Yadgary and Uni. (2012) |
| PYGL | NM_204392.2 | CCGTCCTCCATGTTTGATGTG | TCTTGATGCGGTTGTACATGGT | 100 | Yadgary and Uni. (2012) |
| FBP1 | NM_001278048.1 | TTCCATTGGGACCATATTTGG | ACCCGCTGCCACAAGATTAC | 100 | Yadgary and Uni. (2012) |
| G6PC2 | NC_052538.1 | CCTTCACAGACTGACATGGTCATTA | ATGAGGGAAATGTGTTGCTATGAAT | 100 | Yadgary and Uni. (2012) |
| HPRT | NM_204848 | AAGTGGCCAGTTTGTTGGTC | GTAGTCGAGGGCGTATCCAA | 110 | Boo et al. (2020) |
| β-actin | NM_205518.1 | AATGGCTCCGGTATGTGCAA | GGCCCATACCAACCATCACA | 112 | Primer Blast |

[a]Arginine-glycine amidinotransferase (**AGAT**), catalyzes the reaction between glycine and arginine to create GAA; guanidinoacetate N-methyltransferase (**GAMT**), catalyzes the methylation of GAA, to create creatine; glycogen synthase (**GYS**), catalyzes the rate-limiting step in the synthesis of glycogen (GYS1 is the muscle variant and GYS2 is expressed in other tissues); glycogen phosphorylase L (**PYGL**), catalyzes the release of glucose-1-phosphate from glycogen; fructose-1,6-bisphosphatase 1 (**FBP1**), catalyzes the hydrolysis of fructose 1,6-bisphosphate to fructose 6-phosphate; glucose-6-phosphatase 2 (**G6PC2**), catalyzes the hydrolysis of glucose-6-phosphate, allowing the release of glucose into the bloodstream; β-actin is a housekeeping cytoskeletal protein (β-**actin**), and hypoxanthine phosphoribosyl transferase 1 (**HPRT**) is an enzyme in the purine synthesis in salvage pathway, also a housekeeping gene.

## RNA isolation, cDNA synthesis and determination of mRNA abundance by real-time PCR

Total RNA was isolated from 100 mg of tissue (from YS tissue, liver, kidney and breast muscle) using TRI-Reagent (Sigma-Aldrich, St. Louis, MO) according to the manufacturer's protocol. RNA concentration was determined using a Nano Drop ND-1000 instrument (Thermo Fisher Scientific, Wilmington, DE). Total RNA was treated with DNase using a Turbo DNA-free Kit according to the manufacturer's protocol (Ambion; Thermo Fisher Scientific, Wilmington, DE). cDNA was created from 1 μg of DNA-free RNA using the qPCRBIO cDNA synthesis kit according to the manufacturer's protocol (PCRBIOSYSTEMS, London, United Kingdom). Relative mRNA expression was evaluated using gene-specific primers (Table 1) of genes involved in creatine synthesis [arginine-glycine amidinotransferase (AGAT), guanidinoacetate N-methyltransferase (GAMT)], gluconeogenesis [fructose-1,6-bisphosphatase 1 (FBP1), glucose-6-phosphatase 2 (G6PC2)], glycogenesis [glycogen synthase (GYS)], and glycogenolysis [glycogen phosphorylase L (PYGL)] and the housekeeping genes; cytoskeletal protein (β-actin) and hypoxanthine phosphoribosyl transferase 1 (HPRT). Primer sequences were designed using Primer-BLAST software (Ye et al., 2012) based on published cDNA sequences where available and purchased from Sigma-Aldrich (Rehovot, Israel). PCR products were validated by gel electrophoresis in 1.5% agarose gel. Real-time qPCR reactions were conducted in triplicate in a Roche Light cycler 96 (Roche Molecular Systems, Inc., Pleasanton, CA). Each reaction (20 μL) included 3 μL of cDNA sample diluted 1:20 in ultrapure water (UPW, Biological Industries, Beit HaEmek, Israel), 4 μM of each primer, and Platinum SYBR Green qPCR super mix-UDG (Thermo Fisher Scientific, Wilmington, DE). Reaction conditions: preincubation at 95°C for 60°s, followed by 40 cycles of a 2-step amplification cycle of 95°C for 10°s and 60°C for 30°s, ended with a melting curve generated by the following conditions: 95°C for 60°s, 65°C for 60°s, and 97°C for 1 s. Relative mRNA expression was calculated by subtracting the geometric mean of cycle threshold (Ct) values of β-Actin and HPRT reference genes from sample Ct (Pfaffl, 2007).

## Statistical analysis

Data of creatine and glycogen concentrations in tissues and data of blood glucose and ketone levels were subjected to one-way ANOVA analysis with the embryonic day (age) as main effect. Data of creatine and glycogen amount and of gene expression in tissues were subjected to two-way ANOVA analysis with the embryonic day (age), tissue and their interaction as the main effects. Differences between means were tested by using Tukey's HSD test and considered significantly different with $p$-value lower than or equal to 0.05 ($p \leq 0.05$). Values are presented as mean ± standard error mean (SEM). All statistical analyses were carried out using JMP-pro 16 software (SAS Institute Inc., Cary, NC).

# Results

## Creatine and glycogen levels in the breast muscle, liver and YS tissue of chicken embryos

Measurements of creatine concentration (mg/g of dry tissue) in the breast muscle showed a significant increase by 47% ($p$-value, $p = 0.0009$) from embryonic day (E) 15 to E17 (Figure 1A, and Supplementary Table S1). Then, throughout E19, hatch and chick placement, creatine levels did not differ significantly between consecutive days. The liver and yolk sac (YS) tissue exhibited similar patterns (Figures 1B, C, and Supplementary Table S1), as creatine concentration increased by 3.8-fold and 3.4-fold respectively from E13 up to the highest value at hatch ($p < 0.0001$). Different from the breast muscle, creatine concentration decreased in the liver and YS tissue at chick placement by 2-fold and 1.5-fold, respectively. The total amount of creatine in each organ (Figure 1D and Supplementary Table S2) was calculated by multiplying the total dry tissue weight (Suppl. Table 6) by the concentration of creatine (Figures 1A–C and Supplementary Table S1). A two-way ANOVA test revealed a significant interaction between the effects of age and tissue ($p < 0.0001$). This was mainly due to the breast muscle tissue, as its

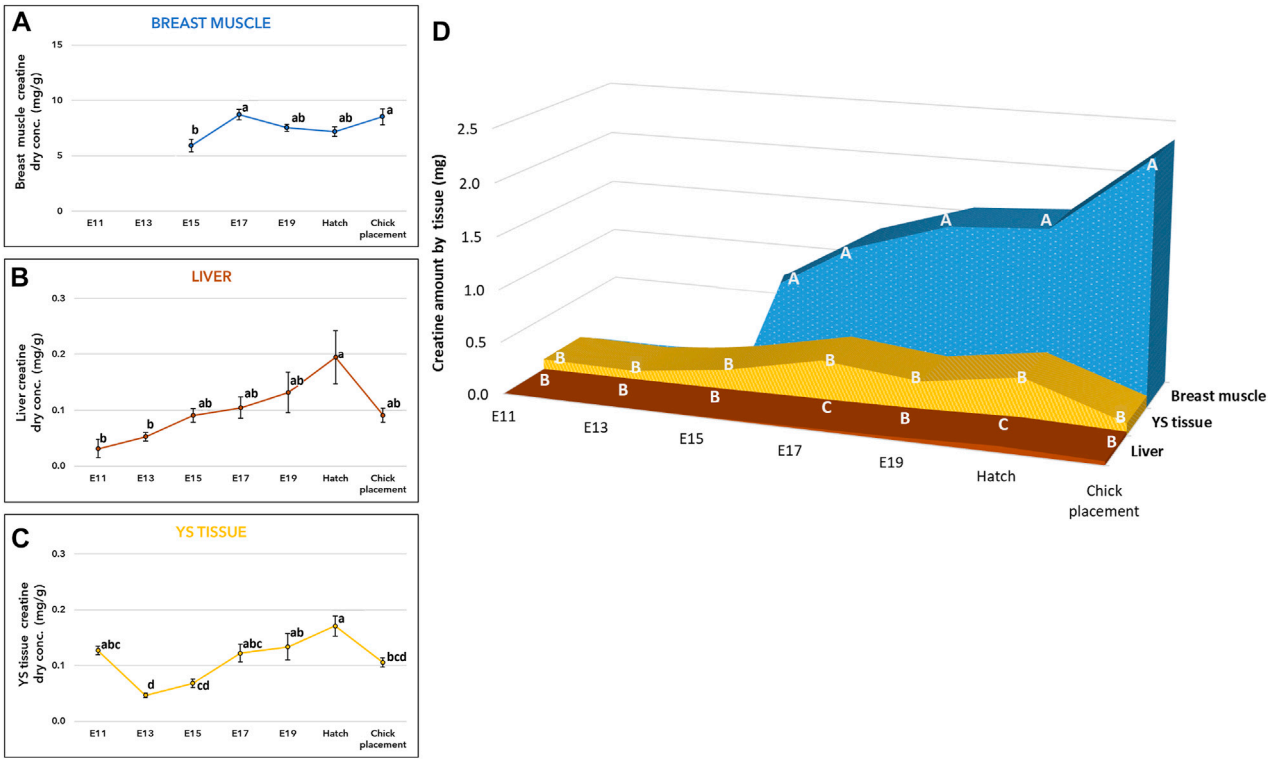


FIGURE 1
Creatine levels from E11 until hatch and at chick placement **(A–C)** Dry weight concentration (mg/g) and **(D)** total tissue amount (mg) of Yolk sac (YS) tissue, liver, and breast muscle **(A–C)** The lower-case letters denote for means significantly different between days within each organ, as derived from a one-way ANOVA Tukey's HSD test **(D)** The capital letters denote for means significantly different between organs within each day as derived from a two-way ANOVA followed by Tukey's HSD test. $p \leq 0.05$ $n = 6$ per day.

creatine amount showed a constant elevation pattern unlike the liver and YS tissue. Results also show that creatine is stored mainly in the breast muscle, as its amount was 3-fold higher at hatch and 15-fold higher at chick placement compared with combined amounts of the liver and YS tissue. It should be noted that compared to the liver, the YS tissue had higher amounts of creatine throughout incubation, significantly higher on E17 and at hatch (Figure 1D and Supplementary Table S2).

As for glycogen, its concentration (mg/g of dry tissue) exhibited similar patterns in the breast muscle, liver, and YS tissue (Figures 2A–C, and Supplementary Table S1). Towards E17 an increase in glycogen levels was observed in all tissues, then towards hatch, glycogen levels were significantly decreased reaching the lowest levels at chick placement ($p < 0.0001$). The total amount of glycogen in each organ (Figure 2D and Supplementary Table S1) was also calculated by multiplying the total dry tissue weight (Supplementary Table S6) by the concentration in tissues (Figures 2A–C and Supplementary Table S1). A two-way ANOVA test revealed a significant interaction between the effects of age and tissue ($p < 0.0001$). The interaction was mainly due to the YS tissue, as its glycogen amount showed the most dynamic pattern, with a rapid increase up to E17 followed by a sharp decrease. In addition, throughout incubation the YS tissue had the highest amount of glycogen, as it was 27-fold higher on E11 compared to the liver and 3.3-fold higher at hatch and at chick placement, compared to the combined amount in the liver and breast muscle (Figure 2D and Supplementary Table S2).

## Blood glucose and ketones levels of chicken embryos

Glucose (mg/dL) and ketones (β-HBA; mmol/L) levels were measured from E11 to chick placement and exhibited altered patterns. From E11 to E17, glucose levels were relatively constant ranging between values of 123.5–143.6 mg/dL (Figure 3A). From E19 and until hatch and chick placement, blood glucose levels increased significantly by 38% ($p < 0.0001$), reaching values of 191.9–208.3 mg/dL. Ketone levels (Figure 3B) showed a dynamic pattern, starting on E11 with the lowest level (2.09 mmol), increasing gradually up to the highest value on E17 (4.33 mmol/L; $p < 0.0001$). On E19, ketones level decreased to 3.24 mmol/L while at hatch levels increased again to 4.06 mmol/L.

## Creatine synthesis genes in the breast muscle, kidney, liver, and YS tissue of chicken embryos

The potential of creatine *de novo* synthesis in the tissues was evaluated by the examination of arginine-glycine amidinotransferase

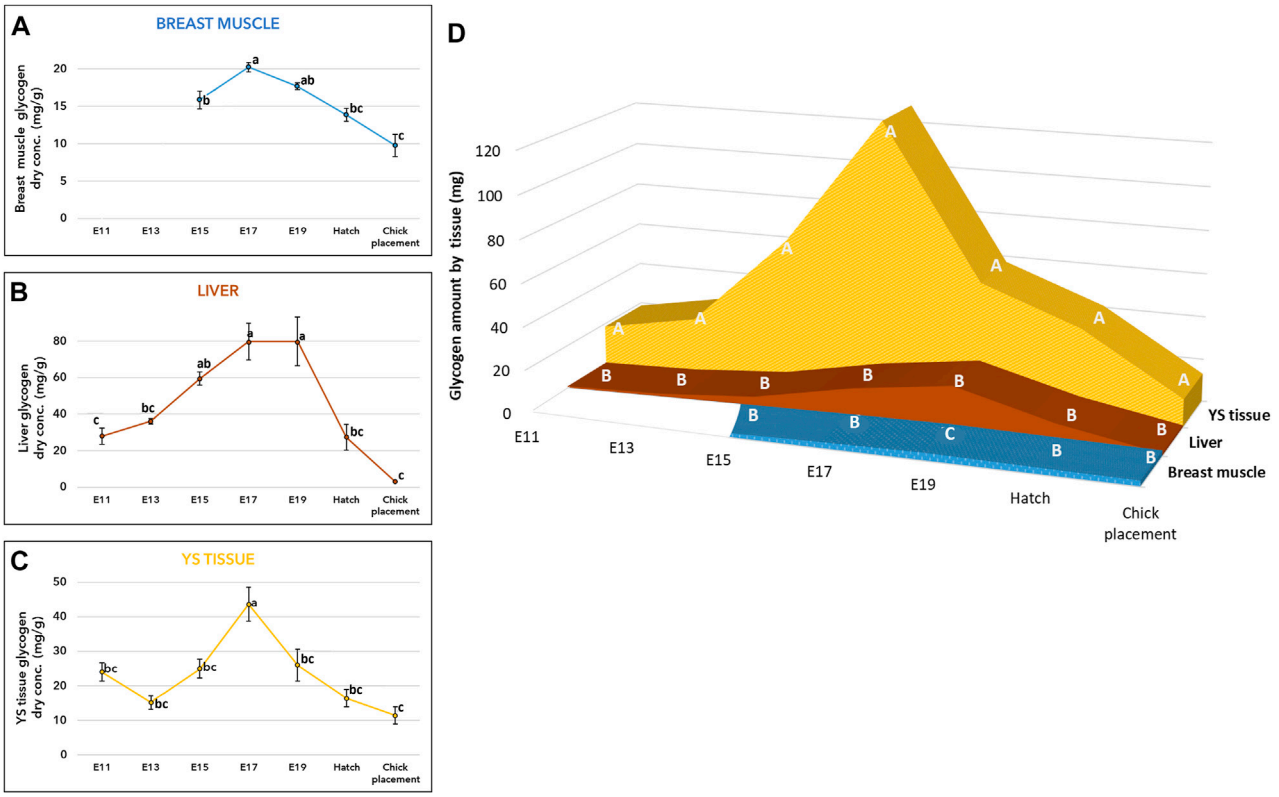


FIGURE 2
Glycogen levels from E11 until hatch and at chick placement **(A–C)** Dry weight concentration (mg/g) and **(D)** total tissue amount (mg) of YS tissue, liver, and breast muscle **(A–C)** The lower-case letters denote for means significantly different between days within each organ, as derived from a one-way ANOVA Tukey's HSD test **(D)** The capital letters denote for means significantly different between organs within each day as derived from a two-way ANOVA followed by Tukey's HSD test. ($p \leq 0.05$), $n = 6$ per day.

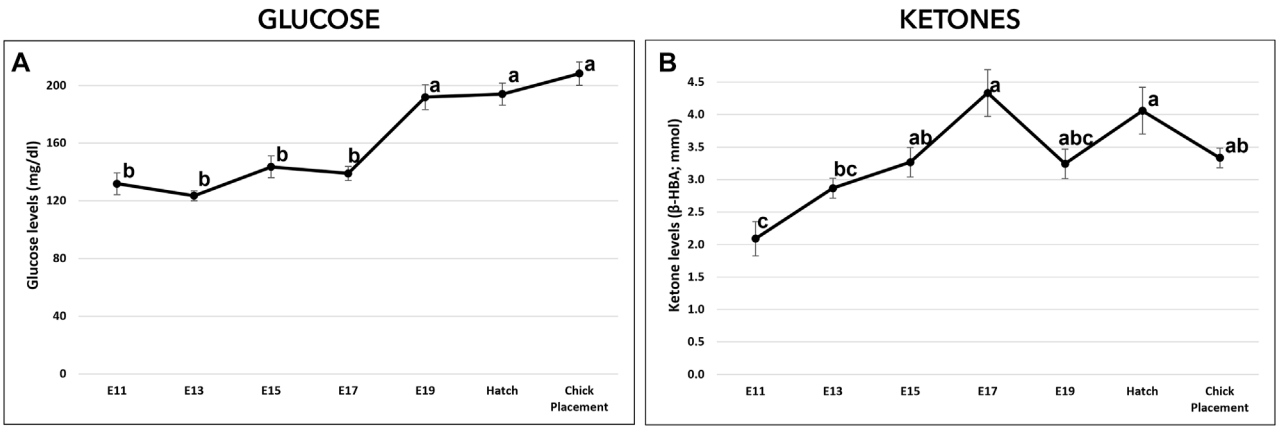


FIGURE 3
Glucose and ketones levels from E11 until hatch and at chick placement. **(A)**-Glucose (mg/di) and **(B)**-ketones ((3-HBA; mmol) were measured by FreeStyle Optimum Gluco/Keto meter. The lower-case letters denote for means significantly different between days, as derived from a one-way ANOVA Tukey's HSD test ($p < 0.05$), $n = 6$ per day.

(AGAT), and guanidinoacetate N-methyltransferase (GAMT) (Figure 4 and Supplementary Table S3). Expression analysis of AGAT and GAMT by a two-way ANOVA test revealed significant interactions between the effects of age and tissue ($p < 0.0001$). The interaction was mainly associated with the varying expression patterns in tissues. In the breast muscle, AGAT expression showed a dynamic pattern, as it was increased from E11 to E19, followed by a decrease at hatch, then, sharply increased again reaching the highest level at chick

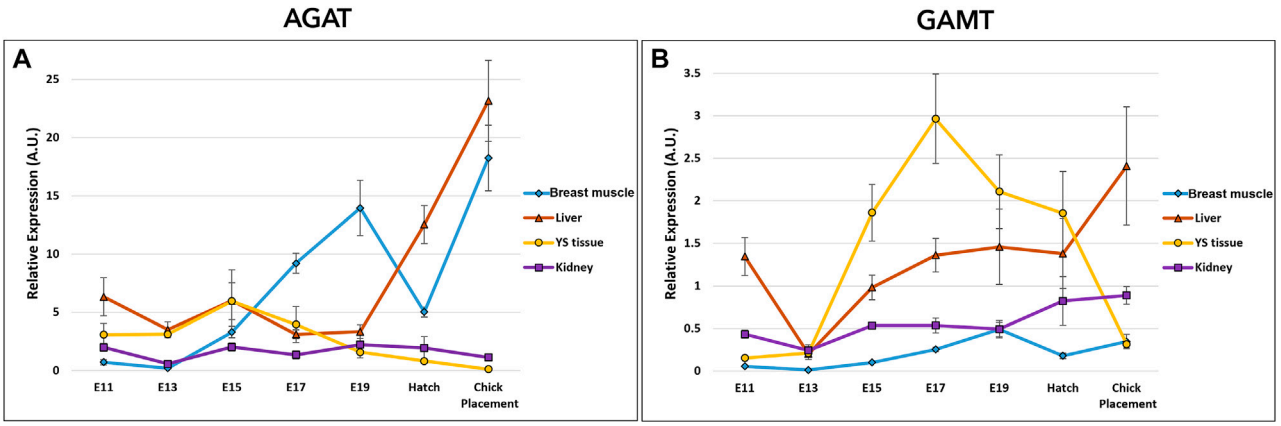


FIGURE 4
Dynamic expression of genes involved in creatine synthesis **(A)** Arginine-glycine amidinotransferase (AGAT), catalyzes the reaction between glycine and arginine to create GAA **(B)** Guanidinoacetate N-methyltransferase (GAMT), responsible for the methylation of GAA to create creatine. Expression analysis of AGAT and GAMT by a two-way ANOVA followed by Tukey's HSD test revealed significant interactions between the effects of age and tissue. ($p < 0.05$), $n$ = 6 per day.

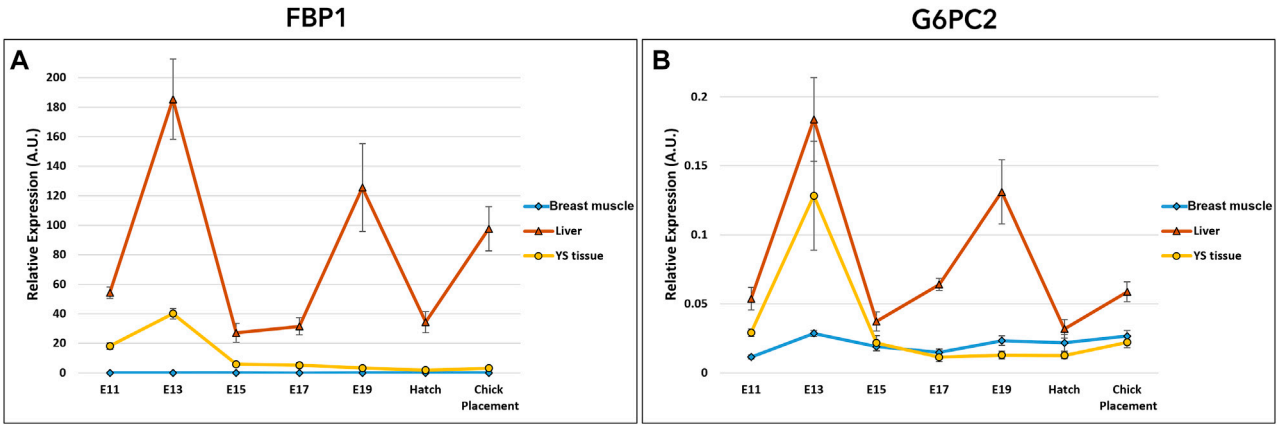


FIGURE 5
Dynamic expression of genes involved in gluconeogenesis **(A)** Fructose-1,6-bisphosphatase 1 (FBP1), regulatory enzyme, catalyzes the hydrolysis of fructose 1,6-bisphosphate to fructose 6-phosphate **(B)** Glucose-6- phosphatase 2 (G6PC2), catalyzes the hydrolysis of glucose-6-phosphate, allowing the release of glucose into the bloodstream. Expression analysis of FBP1 and G6PC2 by a two-way ANOVA followed by Tukey's HSD test revealed significant interactions between the effects of age and tissue. ($p < 0.05$), $n$ = 6 per day.

placement. GAMT expression in the breast muscle also showed a dynamic pattern, increasing from E11 to E19 followed by a decrease at hatch. In the kidney, expression of AGAT remained stable and was not significantly different between consecutive embryonic days, however, GAMT expression increased gradually from E13 along the second half of incubation, reaching highest values at hatch and at placement. The liver and YS tissue showed alternating expression patterns as liver AGAT expression increased towards hatch and chick placement, and YS tissue AGAT expression decreased. As for GAMT expression, in the liver significantly different values were found on E13 as levels were decreased, while at chick placement levels were significantly increased. In the YS tissue GAMT expression increased up to E17, followed by a decrease up to chick placement. Altogether, results demonstrate a shift in expression levels of AGAT and GAMT, decreasing in the extraembryonic YS tissue towards hatch and placement, and increasing in the embryonic liver, breast muscle and kidney.

## Gluconeogenic genes in the liver, YS tissue, and breast muscle of chicken embryos

Gluconeogenesis potential was evaluated by the examination of two genes: fructose-1,6-bisphosphatase 1 (FBP1) and glucose-6-phosphatase 2 (G6PC2) (Figure 5 and Supplementary Table S4). Expression analysis of FBP1 and G6PC2 by a two-way ANOVA test revealed significant interactions between the effects of age and tissue ($p < 0.0001$). Also here, the interaction is associated with the altering expression patterns in tissues. Results showed daily fluctuation in liver FBP1 expression. In the

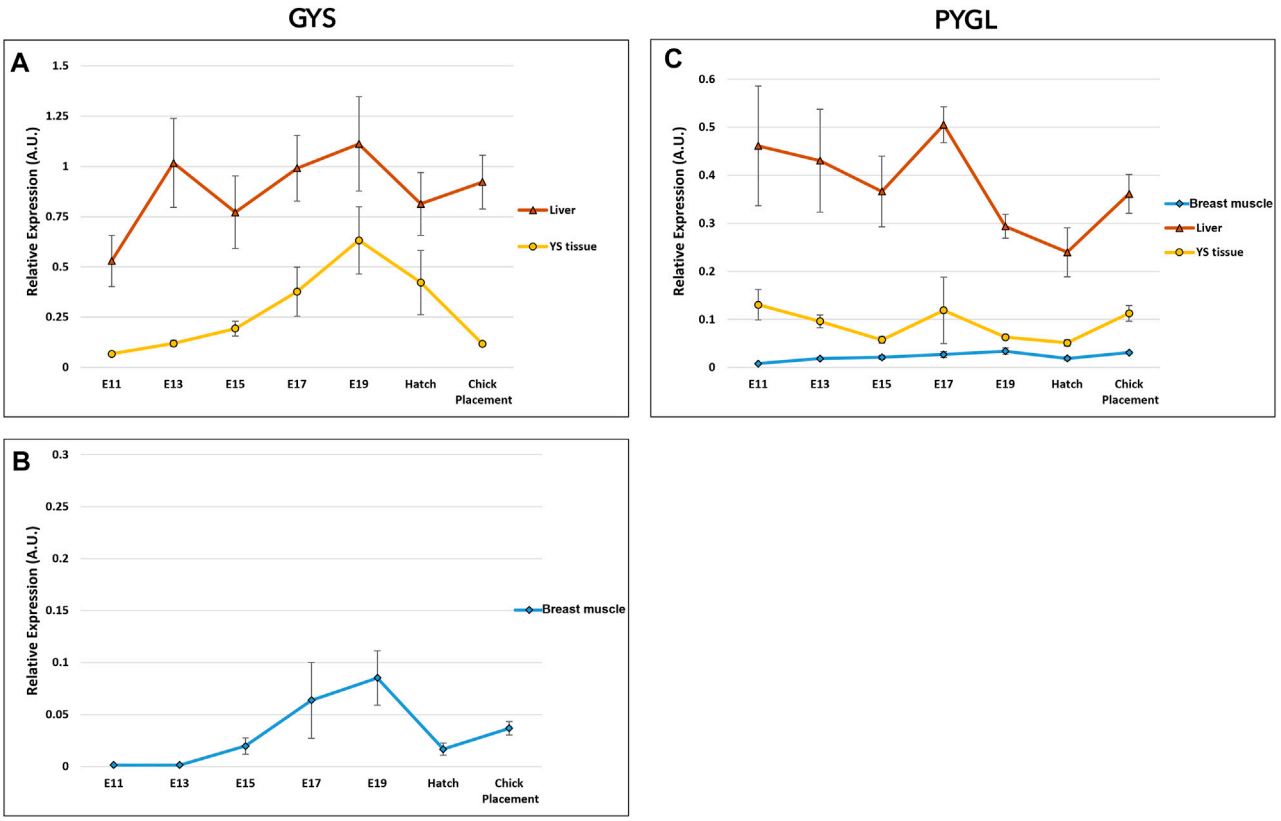


FIGURE 6
Dynamic expression of genes involved in glycogen synthesis and breakdown. **(A, B)** Glycogen synthase (GYS*) catalyzes the rate-limiting step in the synthesis of glycogen; **(C)** Glycogen phosphorylase L (PYGL), catalyzes the release of glucose- 1 -phosphate from glycogen. As derived from a two-way ANOVA followed by Tukey's HSD test, the factor of tissue was found to be significantly different in GYS and PYGL (highest in the liver, mean in the YS tissue and lowest in the breast muscle). The factor age was also significant, as E 1 9 was highest in GYS and E17 was highest in PYGL ($p < 0.05$), $n = 6$ per day. *Two variants were used for glycogen synthase gene; **(A)** GYS2 in the liver and YS tissue and **(B)** GYS one in the breast muscle.

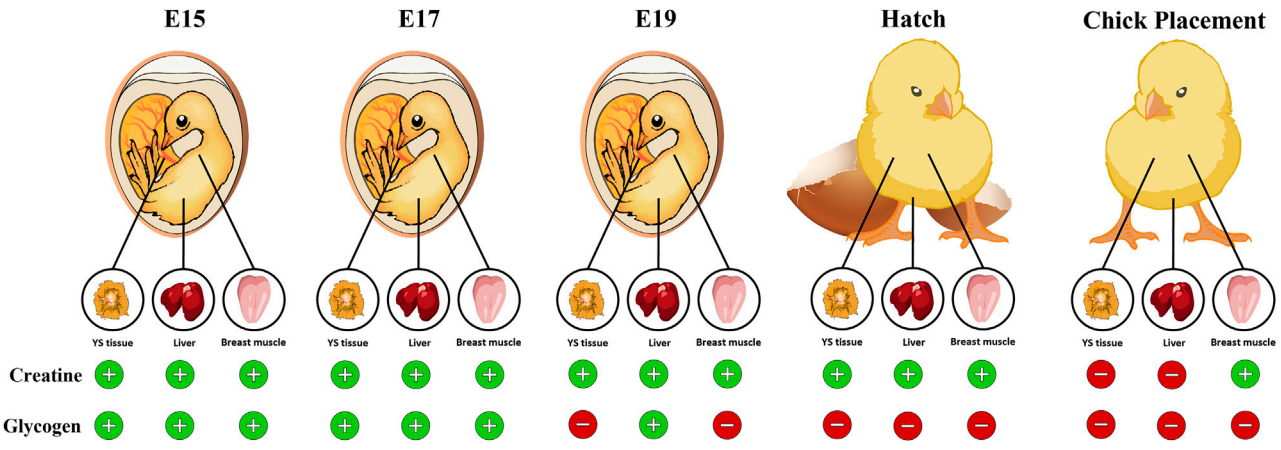


FIGURE 7
Graphical illustration demonstrating the available energy resources (creatine and glycogen) in the chicken embryo during the pre-post hatch period. Towards hatch, creatine levels in the YS tissue, liver and breast muscle increase while glycogen levels dramatically decrease, reaching low levels at hatch and at chick placement. In the breast muscle, as glycogen levels are depleted, creatine levels are elevated. Thus, highlighting the importance of creatine as an available energy source for the late-term embryo and hatchling.

YS tissue, FBP1 expression was elevated on E13 and significantly decreased on E15, then remained constant throughout incubation up to chick placement. In the breast muscle, FBP1 expression level was relatively low, decreasing between E15 and E17, and increasing again at placement. The variation in expression pattern of G6PC2 was similar to that of FBP1 expression in the liver, breast muscle and YS tissue. In

general, when comparing the expression of gluconeogenic genes between the liver, YS tissue and breast muscle within days, the liver showed the highest values throughout incubation.

### Glycogen synthesis and breakdown in the liver, YS tissue, and breast muscle of chicken embryos

The potential of glycogen synthesis and breakdown was evaluated by two genes: glycogen synthase (GYS) and glycogen phosphorylase L (PYGL) (Figure 6 and Supplementary Table S5). Glycogen synthase (GYS) has two isoforms/variants: glycogen synthase 1 (GYS1) and GYS2 (Roach et al., 1998). GYS1 is expressed at lower levels in muscle, whereas GYS2 is primarily responsible for glycogen synthesis in the liver (Browner et al., 1989; Nuttall et al., 1994). Accordingly, in the breast muscle, the muscle variant GYS1 was used for expression analysis of glycogen synthase, while in the YS tissue and liver, GYS2 was used. As for, glycogen phosphorylase, the variant PYGL was used for the breast muscle, YS tissue and liver. PYGL was shown to be expressed at the protein level also in the breast muscle (Zambonelli et al., 2016). A two-way ANOVA test revealed that there was no significant interaction between the effects of age and tissue in GYS and PYGL expression. The tissue factor had statistically significant effect on GYS expression ($p < 0.0001$) with the highest expression levels in the liver, medium values in the YS tissue and lowest in the breast muscle. Similarly, the age factor was also found to be significant ($p = 0.00035$), with a peak in overall GYS expression at E19, significantly different from all sampling points apart from E17. As for PYGL, the tissue factor had a significant effect ($p < 0.0001$) with the highest expression levels in the liver, medium values in the YS tissue and lowest in the breast muscle. The age factor was also found to be significant ($p = 0.049$), with the highest PYGL expression at E17. As in the gluconeogenic genes, expression analysis of glycogen synthesis and breakdown genes between tissues within each day, showed the highest expression levels in the liver, with medium values in the YS tissue and lowest in the breast muscle.

## Discussion

The fertile egg contains trace amounts of available energy molecules in the form of carbohydrates (Yadgary and Uni, 2012; Réhault-Godbert et al., 2019) and creatine (Reicher et al., 2020). Accordingly, chicken embryos depend on the supply of high energy-value molecules that are synthesized, stored, and utilized by the embryonic and extraembryonic tissues. The current study investigated the dynamics of the two major energy-value molecules, creatine and glycogen, in key tissues for energy metabolism, from mid incubation (E11) until hatch and placement at the farm. Based on our findings, creatine is stored mainly in the breast muscle, while glycogen is stored mainly in the YS tissue. We demonstrate, for the first time, that creatine synthesis genes (AGAT, GAMT) are expressed in the chicken breast muscle as early as mid-incubation. The expression analysis of genes related to gluconeogenesis (FBP1, G6PC2), glycogenesis (GYS), and glycogenolysis (PYGL), reveals that the liver constitutes the main site of glycogen metabolism activity. However, due to the relatively large size and high storage capacity of the breast muscle and YS tissue, their contribution to glycogen metabolism is substantial. Towards hatch, creatine levels in all tissues increased, while glycogen levels decreased post E19 reaching low levels at hatch and at chick placement. Together, the findings suggest that when glycogen stores are depleted, creatine serves as an available energy source for late-term embryos and hatchlings.

In accordance with the traditional description of spatial separation between the supply and demand organs of endogenous creatine (Wyss, 2000), our results show that in chicken embryos creatine synthesis genes (AGAT, GAMT) are expressed in the liver and kidney. Here we show, that AGAT and GAMT are also expressed in the extraembryonic YS tissue. This fits the concept of the YS tissue as a multifunctional metabolic organ, which supports embryonic development (Yadgary et al., 2010; Yadgary et al., 2011; Yadgary and Uni, 2012; Yadgary et al., 2013; Yadgary et al., 2014; Dayan et al., 2020; Wong and Uni, 2021). To the best of our knowledge, we are the first to show AGAT and GAMT expression in the breast muscle of chicken embryos; the expression of these genes was previously found in the skeletal muscle of fish, mice, cattle, and pigs (Borchel et al., 2019). Ostojic (2021) points towards a metabolic advantage of *de novo* creatine synthesis in myocytes to maintain muscle creatine levels and cellular energy. The levels of creatine in the liver, YS tissue and breast muscle show similar pattern of increase up to hatch, where creatine is stored mainly in the breast muscle. Nevertheless, considering the relative size of organs, the significance of the YS tissue, the largest organ during incubation is highlighted as a superior creatine source vs the liver, with higher total creatine amount (19-fold higher on E17 and 7-fold higher at hatch). Together, we conclude that during incubation the supply of creatine depends on its *de novo* synthesis by the embryonic and extraembryonic tissues. As creatine levels increase towards hatch, it serves as an essential energy source, especially to late-term embryos and hatchlings.

Comparable patterns of glycogen levels were exhibited in the breast muscle, liver and YS tissue where all tissues reached peak values on E17-E19, followed by a sharp decrease towards chick placement. Previous studies showed a similar pattern corresponding with the changes in energy metabolism towards hatch and decreased glycogen levels in tissues (Christensen et al., 1999; Christensen et al., 2000; Christensen et al., 2001; Uni and Ferket, 2004; Uni et al., 2005; Foye et al., 2006; Moran 2007; De Oliveira et al., 2008; Yadgary and Uni, 2012). This study shows that throughout incubation, the majority of glycogen is stored in the YS tissue. This agrees with a previously published study by Yadgary and Uni (2012), which showed the importance of the YS tissue as the major glycogen storage organ. Our results suggest a pivotal role of the YS tissue, not only in creatine supply, but also in the supply of glycogen during mid-term incubation up to the initiation of the energy-demanding hatching process. Expression analysis of genes involved in glycogen synthesis and breakdown (GYS and PYGL, respectively), showed the highest expression levels in the liver compared with mid values in the YS tissue and the lowest values in the breast muscle. According to these findings, E19 marks a critical time point, showing a shift in balance between glycogen synthesis and breakdown. The decrease in GYS expression but not in PYGL expression fits the observed decrease in glycogen levels. On this day (E19), as oxygen becomes limited (Tazawa et al., 1983), other metabolic pathways are involved in glucose and ATP production, shifting towards anaerobic catabolism of glucose, with the breakdown of glycogen and gluconeogenesis (Uni and Ferket, 2004; Moran, 2007; De Oliveira et al., 2008; Yadgary and Uni 2012). Indeed,

the increase in ketones levels up to E17 correspond with β-oxidation of yolk-derived fatty acids, and the rise in blood glucose levels (starting on E19) correspond with the metabolic shift and the decrease in tissue glycogen levels from E17 onwards. At hatch, when oxygen supply was restored, ketones levels increase again. The expression of the two key genes FBP1 and G6PC2 was the highest in the liver along the incubation period with mid values in the YS tissue and lowest in the breast muscle. Together, our results lead to the conclusion that during the second half of incubation the gluconeogenic pathway as well as glycogen synthesis and breakdown is most active in the liver. However, due to the relatively large size and high storage capacity of the breast muscle and YS tissue, their contribution to energy supply for the chicken embryo should not be neglected.

In conclusion, this study evaluated the dynamics of creatine, glycogen, and their synthesis during the second half of the broiler embryonic development period. We demonstrate that during incubation, creatine is stored mainly in the breast muscle while glycogen is stored mainly in the YS tissue. The exhibited decrease in glycogen levels towards hatch in all tissues, starting on E19, opposes the increase in creatine levels, suggesting the significance of creatine in energy supply for late-term embryos and hatchlings (summarized in Figure 7). Moreover, in breast muscle, as glycogen levels are depleted, high creatine levels are maintained until chick placement, emphasizing the utmost importance of creatine involvement in supplying available energy for the hatching chick before placement at the farm. The fact that creatine is involved in maintaining available energy supply for the hatching broiler chick could have a great impact when considering hatchling quality, uniformity, chick survival and post-hatch performance.

## Data availability statement

The original contributions presented in the study are included in the article/Supplementary Materials, further inquiries can be directed to the corresponding author.

## Ethics statement

The animal study was reviewed and approved by IACUC: AG-20-16298.

## Author contributions

JD: experimental design and execution, data analysis, manuscript writing. TM-Z: experimental methodologies, data analysis, manuscript review. NR: experimental methodologies. OH and ZU: supervision, manuscript review. SM: experimental methodologies, manuscript review. UB and VI: funding. All authors contributed to the article and approved the submitted version.

## Funding

This study received partial funding from AlzChem Trostberg GmbH. The funder was not involved in the study design, analysis, interpretation of data, the writing of this article or the decision to submit it for publication.

## Conflict of interest

UB and VI were employed by AlzChem Trostberg GmbH.

The remaining authors declare that the research was conducted in the absence of any commercial or financial relationships that could be construed as a potential conflict of interest.

## Publisher's note



## Supplementary material

The Supplementary Material for this article can be found online at: https://www.frontiersin.org/articles/10.3389/fphys.2023.1079638/full#supplementary-material.

## References

Bessman, S. P., and Carpenter, C. L. (1985). The creatine-creatine phosphate energy shuttle. *Annu. Rev. Biochem.* 54 (1), 831–862. doi:10.1146/annurev.bi.54.070185.004151

Blaxter, K. (1989). *Energy metabolism in animals and man*. Cambridge, United Kingdom: Cambridge University Press.

Boo, S. Y., Tan, S. W., Alitheen, N. B., Ho, C. L., Omar, A. R., and Yeap, S. K. (2020). Identification of reference genes in chicken intraepithelial lymphocyte natural killer cells infected with very-virulent infectious bursal disease virus. *Sci. Rep.* 10 (1), 8561–8569. doi:10.1038/s41598-020-65474-3

Borchel, A., Verleih, M., Kühn, C., Rebl, A., and Goldammer, T. (2019). Evolutionary expression differences of creatine synthesis-related genes: Implications for skeletal muscle metabolism in fish. *Sci. Rep.* 9 (1), 5429–5438. doi:10.1038/s41598-019-41907-6

Browner, M. F., Nakano, K., Bang, A. G., and Fletterick, R. J. (1989). Human muscle glycogen synthase cDNA sequence: A negatively charged protein with an asymmetric charge distribution. *Proc. Natl. Acad. Sci.* 86 (5), 1443–1447. doi:10.1073/pnas.86.5.1443

Christensen, V. L., Donaldson, W. E., Nestor, K. E., and McMurtry, J. P. (1999). Effects of genetics and maternal dietary iodide supplementation on glycogen content of organs within embryonic turkeys. *Poult. Sci.* 78 (6), 890–898. doi:10.1093/ps/78.6.890

Christensen, V. L., Grimes, J. L., Donaldson, W. E., and Lerner, S. (2000). Correlation of body weight with hatchling blood glucose concentration and its relationship to embryonic survival. *Poult. Sci.* 79 (12), 1817–1822. doi:10.1093/ps/79.12.1817

Christensen, V. L., Wineland, M. J., Fasenko, G. M., and Donaldson, W. E. (2001). Egg storage effects on plasma glucose and supply and demand tissue glycogen concentrations of broiler embryos. *Poult. Sci.* 80 (12), 1729–1735. doi:10.1093/ps/80.12.1729

Cogburn, L. A., Trakooljul, N., Chen, C., Huang, H., Wu, C. H., Carré, W., et al. (2018). Transcriptional profiling of liver during the critical embryo-to-hatchling transition period in the chicken (Gallus gallus). *BMC genomics* 19 (1), 695. doi:10.1186/s12864-018-5080-4

Collin, A., Berri, C., Tesseraud, S., Rodon, F. R., Skiba-Cassy, S., Crochet, S., et al. (2007). Effects of thermal manipulation during early and late embryogenesis on thermotolerance and breast muscle characteristics in broiler chickens. *Poult. Sci.* 86 (5), 795–800. doi:10.1093/ps/86.5.795

Da Silva, R. P., Nissim, I., Brosnan, M. E., and Brosnan, J. T. (2009). Creatine synthesis: Hepatic metabolism of guanidinoacetate and creatine in the rat *in vitro* and *in vivo*. *Am. J. Physiology-Endocrinology Metabolism* 296 (2), E256–E261. doi:10.1152/ajpendo.90547.2008

Dayan, J., Reicher, N., Melkman-Zehavi, T., and Uni, Z. (2020). Incubation temperature affects yolk utilization through changes in expression of yolk sac tissue functional genes. *Poult. Sci.* 99 (11), 6128–6138. doi:10.1016/j.psj.2020.07.037

De Oliveira, J. E., Uni, Z., and Ferket, P. R. (2008). Important metabolic pathways in poultry embryos prior to hatch. *World's Poult. Sci. J.* 64 (4), 488–499. doi:10.1017/s0043933908000160

Decuypere, E., Tona, K., Bruggeman, V., and Bamelis, F. (2001). The day-old chick: A crucial hinge between breeders and broilers. *World's Poult. Sci. J.* 57 (2), 127–138. doi:10.1079/wps20010010

Foye, O. T., Uni, Z., and Ferket, P. R. (2006). Effect of in ovo feeding egg white protein, β-hydroxy-β methylbutyrate, and carbohydrates on glycogen status and neonatal growth of turkeys. *Poult. Sci.* 85 (7), 1185–1192. doi:10.1093/ps/85.7.1185

Givisiez, P. E., Moreira Filho, A. L., Santos, M. R., Oliveira, H. B., Ferket, P. R., Oliveira, C. J., et al. (2020). Chicken embryo development: Metabolic and morphological basis for in ovo feeding technology. *Poult. Sci.* 99 (12), 6774–6782. doi:10.1016/j.psj.2020.09.074

Havenstein, G. B., Ferket, P. R., and Qureshi, M. A. (2003a). Carcass composition and yield of 1957 versus 2001 broilers when fed representative 1957 and 2001 broiler diets. *Poult. Sci.* 82 (10), 1509–1518. doi:10.1093/ps/82.10.1509

Havenstein, G. B., Ferket, P. R., and Qureshi, M. A. (2003b). Growth, livability, and feed conversion of 1957 versus 2001 broilers when fed representative 1957 and 2001 broiler diets. *Poult. Sci.* 82 (10), 1500–1508. doi:10.1093/ps/82.10.1500

Leksrisompong, N., Romero-Sanchez, H., Plumstead, P. W., Brannan, K. E., and Brake, J. (2007). Broiler incubation. 1. Effect of elevated temperature during late incubation on body weight and organs of chicks. *Poult. Sci.* 86 (12), 2685–2691. doi:10.3382/ps.2007-00170

Moran, E. T., Jr (2007). Nutrition of the developing embryo and hatchling. *Poult. Sci.* 86 (5), 1043–1049. doi:10.1093/ps/86.5.1043

Murakami, A. E., Rodrigueiro, R. J. B., Santos, T. C., Ospina-Rojas, I. C., and Rademacher, M. (2014). Effects of dietary supplementation of meat-type quail breeders with guanidinoacetic acid on their reproductive parameters and progeny performance. *Poult. Sci.* 93 (9), 2237–2244. doi:10.3382/ps.2014-03894

Noble, R. C., and Cocchi, M. (1990). Lipid metabolism and the neonatal chicken. *Prog. lipid Res.* 29 (2), 107–140. doi:10.1016/0163-7827(90)90014-c

Nuttall, F. Q., Gannon, M. C., Bai, G., and Lee, E. Y. (1994). Primary structure of human liver glycogen synthase deduced by cDNA cloning. *Archives Biochem. biophysics* 311 (2), 443–449. doi:10.1006/abbi.1994.1260

Ostojic, S. M. (2021). Creatine synthesis in the skeletal muscle: The times they are a-changin'. *Am. J. Physiology-Endocrinology Metabolism* 320 (2), E390–E391. doi:10.1152/ajpendo.00645.2020

Pfaffl, M. W. (2007). "Relative quantification," in *Real-time PCR* (Abingdon, UK: Taylor & Francis), 89–108.

Réhault-Godbert, S., Guyot, N., and Nys, Y. (2019). The golden egg: Nutritional value, bioactivities, and emerging benefits for human health. *Nutrients*, 11(3), 684, doi:10.3390/nu11030684

Reicher, N., Epstein, T., Gravitz, D., Cahaner, A., Rademacher, M., Braun, U., et al. (2020). From broiler breeder hen feed to the egg and embryo: The molecular effects of guanidinoacetate supplementation on creatine transport and synthesis. *Poult. Sci.* 99 (7), 3574–3582. doi:10.1016/j.psj.2020.03.052

Roach, P. J., Cheng, C., Huang, D., Lin, A., Mu, J., Skurat, A. V., et al. (1998). Novel aspects of the regulation of glycogen storage. *J. basic Clin. physiology Pharmacol.* 9 (2-4), 139–151. doi:10.1515/jbcpp.1998.9.2-4.139

Romanoff, A. L. (1967). *Biochemistry of the avian embryo*. New York, NY: Wiley.

Romanoff, A. L. (1960). "The extraembryonic membranes," in *The avian embryo: Structural and functional development* (New York, NY: The Macmillan Company), 1041–1140.

Scanes, C. G. (2022). "Carbohydrate metabolism," in *Sturkie's avian physiology* (Massachusetts, United States: Academic Press), 593–625.

Speake, B. K., Murray, A. M., and Noble, R. C. (1998). Transport and transformations of yolk lipids during development of the avian embryo. *Prog. Lipid Res.* 37, 1–32. doi:10.1016/s0163-7827(97)00012-x

Tazawa, H., Visschedijk, A. H. J., Wittmann, J., and Piiper, J. (1983). Gas exchange, blood gases and acid-base status in the chick before, during and after hatching. *Respir. Physiol.* 53 (2), 173–185. doi:10.1016/0034-5687(83)90065-8

Uni, Z., Ferket, P. R., Tako, E., and Kedar, O. (2005). In ovo feeding improves energy status of late-term chicken embryos. *Poult. Sci.* 84 (5), 764–770. doi:10.1093/ps/84.5.764

Uni, Z., and Ferket, R. P. (2004). Methods for early nutrition and their potential. *World's Poult. Sci. J.* 60 (1), 101–111. doi:10.1079/WPS20038

Walker, J. B. (1979). Creatine: Biosynthesis, regulation, and function. *Adv. Enzym. Relat. Areas Mol. Biol.*, 50(177), 177–242. doi:10.1002/9780470122952.ch4

Wong, E. A., and Uni, Z. (2021). Centennial Review: The chicken yolk sac is a multifunctional organ. *Poult. Sci.*, 100(3), 100821. doi:10.1016/j.psj.2020.11.004

Wyss, M. (2000). Creatine and creatinine metabolism. *Physiol. Rev.* 80, 1107–1213. þdoi:10.1152/physrev.2000.80.3.1107

Yadgary, L., Cahaner, A., Kedar, O., and Uni, Z. (2010). Yolk sac nutrient composition and fat uptake in late-term embryos in eggs from young and old broiler breeder hens. *Poult. Sci.* 89 (11), 2441–2452. doi:10.3382/ps.2010-00681

Yadgary, L., Kedar, O., Adepeju, O., and Uni, Z. (2013). Changes in yolk sac membrane absorptive area and fat digestion during chick embryonic development. *Poult. Sci.* 92 (6), 1634–1640. doi:10.3382/ps.2012-02886

Yadgary, L., and Uni, Z. (2012). Yolk sac carbohydrate levels and gene expression of key gluconeogenic and glycogenic enzymes during chick embryonic development. *Poult. Sci.* 91 (2), 444–453. þdoi:10.3382/ps.2011-01669

Yadgary, L., Wong, E. A., and Uni, Z. (2014). Temporal transcriptome analysis of the chicken embryo yolk sac. *BMC genomics* 15 (1), 690–715. doi:10.1186/1471-2164-15-690

Yadgary, L., Yair, R., and Uni, Z. (2011). The chick embryo yolk sac membrane expresses nutrient transporter and digestive enzyme genes. *Poult. Sci.* 90 (2), 410–416. doi:10.3382/ps.2010-01075

Ye, J., Coulouris, G., Zaretskaya, I., Cutcutache, I., Rozen, S., and Madden, T. L. (2012). Primer BLAST: A tool to design target-specific primers for polymerase chain reaction. *BMC Bioinforma.* 13 (1), 134–211. doi:10.1186/1471-2105-13-134

Zambonelli, P., Zappaterra, M., Soglia, F., Petracci, M., Sirri, F., Cavani, C., et al. (2016). Detection of differentially expressed genes in broiler pectoralis major muscle affected by White Striping–Wooden Breast myopathies. *Poult. Sci.* 95 (12), 2771–2785. doi:10.3382/ps/pew268

Zhang, L., Zhu, X. D., Wang, X. F., Li, J. L., Gao, F., and Zhou, G. H. (2016). Individual and combined effects of in-ovo injection of creatine monohydrate and glucose on somatic characteristics, energy status, and post hatch performance of broiler embryos and hatchlings. *Poult. Sci.* 95 (10), 2352–2359. doi:10.3382/ps/pew130

Zuidhof, M. J., Schneider, B. L., Carney, V. L., Korver, D. R., and Robinson, F. E. (2014). Growth, efficiency, and yield of commercial broilers from 1957, 1978, and 2005. *Poult. Sci.* 93 (12), 2970–2982. doi:10.3382/ps.2014-04291

frontiers | Frontiers in Physiology

TYPE Systematic Review
PUBLISHED 07 February 2023
DOI 10.3389/fphys.2023.1123582



OPEN ACCESS

EDITED BY
Colin Guy Scanes,
University of Arkansas, United States

REVIEWED BY
Mahmoud Madkour,
National Research Centre, Egypt
Servet Yalcin,
Ege University, Türkiye
Monika Proszkowiec-Weglarz,
Agricultural Research Service (USDA),
United States
Wen-Chao Liu,
Guangdong Ocean University, China

*CORRESPONDENCE
Victoria Anthony Uyanga,
victoriauyanga@yahoo.com
Hai Lin,
hailin@sdau.edu.cn

SPECIALTY SECTION
This article was submitted to Avian Physiology,
a section of the journal
Frontiers in Physiology

RECEIVED 14 December 2022
ACCEPTED 23 January 2023
PUBLISHED 07 February 2023

CITATION
Uyanga VA, Musa TH, Oke OE, Zhao J, Wang X, Jiao H, Onagbesan OM and Lin H (2023), Global trends and research frontiers on heat stress in poultry from 2000 to 2021: A bibliometric analysis. *Front. Physiol.* 14:1123582.
doi: 10.3389/fphys.2023.1123582



# Global trends and research frontiers on heat stress in poultry from 2000 to 2021: A bibliometric analysis

Victoria Anthony Uyanga[1]*, Taha H. Musa[2], Oyegunle Emmanuel Oke[3], Jingpeng Zhao[1], Xiaojuan Wang[1], Hongchao Jiao[1], Okanlawon M. Onagbesan[3] and Hai Lin[1]*

[1]Shandong Provincial Key Laboratory of Animal Biotechnology and Disease Control and Prevention, Key Laboratory of Efficient Utilization of Non-Grain Feed Resources (Co-Construction by Ministry and Province), Ministry of Agriculture and Rural Affairs, College of Animal Science and Technology, Shandong Agricultural University, Tai'an, China, [2]Biomedical Research Institute, Darfur University College, Nyala, Sudan, [3]Department of Animal Physiology, Federal University of Agriculture, Abeokuta, Nigeria

**Background:** Heat stress remains a major environmental factor affecting poultry production. With growing concerns surrounding climate change and its antecedent of global warming, research on heat stress in poultry has gradually gained increased attention. Therefore, this study aimed to examine the current status, identify the research frontiers, and highlight the research trends on heat stress in poultry research using bibliometric analysis.

**Methods:** The literature search was performed on the Web of Science Core Collection database for documents published from 2000 to 2021. The documents retrieved were analyzed for their publication counts, countries, institutions, keywords, sources, funding, and citation records using the bibliometric app on R software. Network analysis for co-authorship, co-occurrence, citation, co-citation, and bibliographic coupling was visualized using the VOSviewer software.

**Results:** A total of 468 publications were retrieved, and over the past two decades, there was a gradual increase in the annual number of publications (average growth rate: 4.56%). China had the highest contribution with respect to the number of publications, top contributing authors, collaborations, funding agencies, and institutions. Nanjing Agricultural University, China was the most prolific institution. Kazim Sahin from Firat University, Turkey contributed the highest number of publications and citations to heat stress in poultry research, and Poultry Science was the most productive and the most cited journal. The top 10 globally cited documents mainly focused on the effects of heat stress, alleviation of heat stress, and the association between heat stress and oxidative stress in poultry. All keywords were grouped into six clusters which included studies on "growth performance", "intestinal morphology", "heat stress", "immune response", "meat quality", and "oxidative stress" as current research hotspots. In addition, topics such as; "antioxidants", "microflora", "intestinal barrier", "rna-seq", "animal welfare", "gene expression", "probiotics", "feed restriction", and "inflammatory pathways" were identified for future research attention.

**Conclusion:** This bibliometric study provides a detailed and comprehensive analysis of the global research trends on heat stress in poultry over the last two decades, and it is expected to serve as a useful reference for potential research that will help address the impacts of heat stress on poultry production globally.

KEYWORDS
bibliometric, chickens, growth performance, heat stress, oxidative stress, VOSviewer

# 1 Introduction

With the imminent challenge of climate change and its antecedent of global warming, the growing increase in ambient temperature affects all life forms including humans, plants, and animals. This raises a major concern about the extent to which the ongoing variability in climatic conditions would directly and/or indirectly affect the future of animal production (Oke et al., 2021). Heat stress is a significant environmental stressor, especially in the tropics and sub-tropical regions of the world. It occurs under prevailing high temperatures where the animal cannot dissipate its body temperature to the surrounding environment, causing a negative balance between the amount of heat generated and the body's heat loss (Lara and Rostagno, 2013). Heat stress largely affects poultry production since modern-day birds are highly vulnerable to high temperatures and they have limited heat dissipation capacity (Uyanga et al., 2022a). The feather coverage of birds and their lack of sweat glands makes them prone to high ambient temperatures relative to other monogastric animals (Zaboli et al., 2019). Thus, the incidence of heat stress is associated with severe detrimental effects on the health, welfare, and productivity of poultry species, accruing to significant economic losses (Oke et al., 2021; Madkour et al., 2023). Importantly the effects of heat stress on poultry production are directly associated with food safety issues, thus warranting special attention in order to bridge the protein demand to supply gap.

Studies have shown that heat stress negatively affects growth performance, production indices, behavior, immunity, metabolism, welfare, and physiological responses of poultry (Azad et al., 2010; Soleimani et al., 2011; Farag and Alagawany, 2018). It is characterized by an increase in body temperature, higher respiratory rate, decreased feed intake, lowered body weight, poor feed efficiency, low egg production, decreased reproduction, impaired immunity, impaired metabolism, alterations in intestinal microflora, poor intestinal morphology, increased inflammatory response, increased production of reactive oxygen species, deteriorated meat quality, and in extreme cases, results to death of the animals (Wang et al., 2018; Liu et al., 2020; Alagawany et al., 2021; Nawaz et al., 2021; Uyanga et al., 2021; Madkour et al., 2022). The effects of heat stress have been studied on different poultry species, and the findings reported are multifaceted, and interwoven. To better understand the impacts of heat stress in poultry and the strategies for its alleviation, various studies have been conducted under varied experimental conditions. Several works have extensively reviewed the impacts of heat stress and the approaches for its mitigation in poultry. It can be surmised that these mitigating approaches center on environmental modification, management techniques, nutritional manipulation, genetic manipulation, and perinatal conditioning of the birds (Lin et al., 2006; Saeed et al., 2019; Wasti et al., 2020; Abdel-Moneim et al., 2021; Kumar et al., 2021; Uyanga et al., 2022b; Madkour et al., 2023). Therefore, it is evident that a reasonable number of scientific information has been generated on heat stress in poultry, however, to the best of our knowledge, there currently exists no bibliometric study that has comprehensively examined the available literature to stimulate further research in this area.

Bibliometric analysis has been described as a scientific methodology that utilizes computer-assisted review to examine all the publications on a specific topic or field in order to identify the core research, authors of the subject, and their relationships over a given period (Nicolaisen, 2010; Liu et al., 2022). The conduct of bibliometric analysis provides information on the topic of interest and further gives an overall understanding of the intellectual landscape. Attributes such as the author or citation information, titles, keywords, and abstract data have been developed for network analysis and sociometric analysis (Han et al., 2020; Musa et al., 2020). Bibliometric is increasingly important in managing the increasing number of academic publications which often involve empirical contributions producing voluminous, fragmented, and controversial research outcomes (Aria and Cuccurullo, 2017). Compared to other scientific review techniques, bibliometric provides highly objective and reliable analyses since it employs a "systematic, transparent, and reproducible review process that is based on the statistical measurement of science, scientists, or scientific activity" (Wallin, 2005). Therefore, with the increasing number of research reporting on heat stress in poultry production, it was deemed necessary to provide evidence-based insights *via* a bibliometric analysis of the research productivity by authors, countries, keywords, funding agencies, and collaboration networks. The findings of this study would help unveil the research progress on heat stress in poultry and its development in recent decades. This would also provide organized information for researchers, poultry industry experts and further advance research in this area.

Therefore, this bibliometric study was conducted to investigate, identify and visualize the network of publications that have shaped the intellectual discourse and research structure on heat stress in poultry from 2000 to 2021. The mapping of the thematically related publications and an examination of the contributions, co-operations, and recent trends as it relates to the heat stress in poultry was also carried out.

# 2 Materials and methods

## 2.1 Data sources

Relevant documents for the bibliometric study were retrieved from the Web of Science Core Collection (WoSCC). This database is considered appropriate to retrieve eligible literature on the subject matter in an appropriate reference format. WoSCC is the world's foremost citation database covering articles from over 21,000 peer-reviewed journals, with about 1.9 billion cited references. It is a reliable database and is widely utilized for bibliometric studies in various disciplines (Chen et al., 2021; Cheng et al., 2022; Shan et al., 2022)

## 2.2 Search strategy

For this study, published peer-reviewed articles on heat stress and poultry were retrieved from the WoSCC database through a comprehensive search of online documents published from 2000 to 2021. The search was carried out by two investigators (VAU and THM) on a single day, 10 October 2022 to eliminate variations arising from database updates. To build a valid search query that will retrieve as many relevant documents as possible, specific keywords were used. Several "systematic reviews" and "bibliometric analyses" articles were reviewed to build a search query for heat stress and poultry production (Liu et al., 2020; Leishman et al., 2021; Siddiqui et al., 2022).

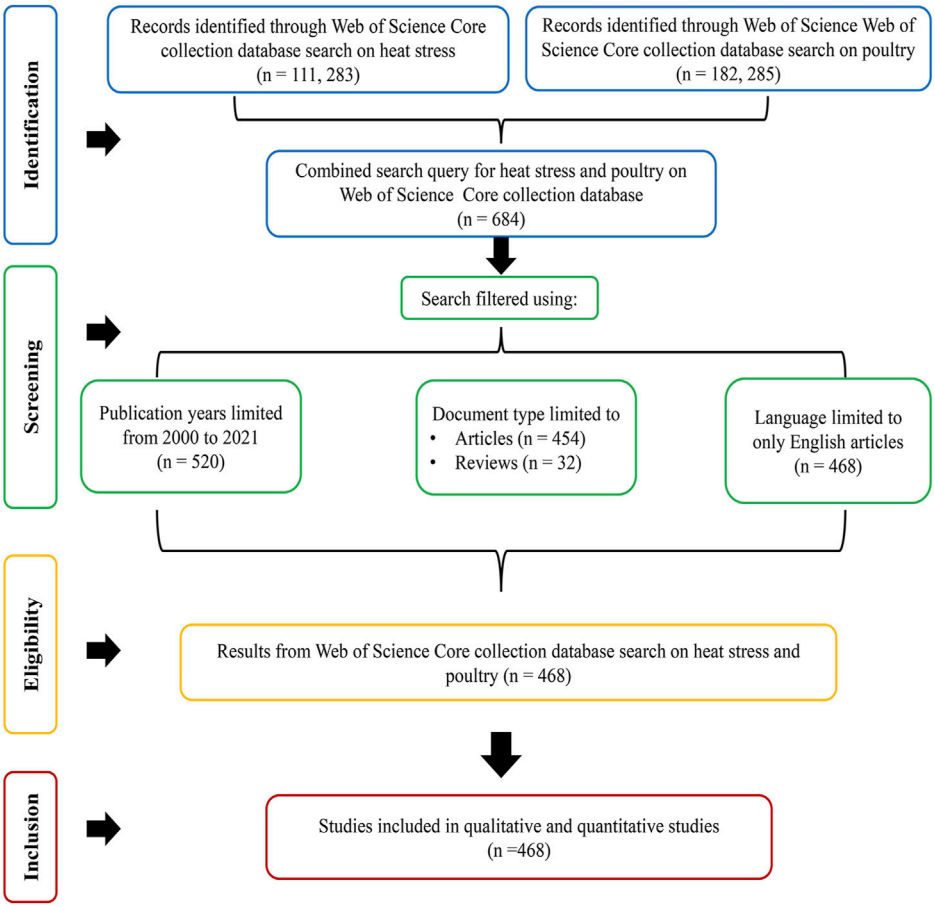


FIGURE 1
Schematic illustration of the search strategy conducted to retrieve published articles on heat stress in poultry from 2000 to 2021.

The search strategy was as follows:

#1: "poultry" (Title) OR "chicken" (Title) OR "guinea fowl" (Title) OR "turkey" (Title) OR "geese" (Title) OR "duck" (Title) OR "quail" (Title) OR "pigeon" (Title) OR "broilers" (Title) OR "laying hen" (Title) OR "fowl" (Title) OR "ostriches" (Title) OR "pheasants" (Title)
#2: "heat stress" (Title) OR "thermal stress" (Title) OR "high temperature" (Title) OR "hot temperature" (Title) OR "thermal condition" (Title) OR "high ambient temperature" (Title) OR "heat exposure" (Title) OR "heat conditioning" (Title) OR "high environmental temperature" (Title) OR "high environmental temperature" (Title). The two queries were combined to generate the final dataset: #1 and #2. Details of the search methodology are provided as Supplementary Material.

The quotation mark (" ") was used as the Boolean search modifier to retrieve exact phrases for search terms and to avoid the split up of search terms that contained more than one word/phrase into single-word components. The search query was built mainly on the "Title" field tag to ensure that the retrieved documents were directly related to heat stress and poultry. The time span was limited to the period of research interest, from 2000 to 2021. Publication type was limited to "articles" and "review, and document type was restricted to only English language. A schematic illustration of the search strategy is presented in Figure 1.

## 2.3 Data extraction

The retrieved documents were extracted using the "Export Records to File" button and the "Full Records and Cited References" option on WoSCC. The plain text, RIS, BibTeX, excel, and tab-delimited files were downloaded for further processing. The exported data included information on authors, publication years, document types, web of science categories, affiliations, journals, funding agencies, countries, research areas, citations, and keywords. The journal impact factor (IF) and category quartile were obtained from the 2021 Journal Citation Reports. The quality of publications was evaluated using the number of citations and the Hirsh-index (h-index).

## 2.4 Bibliometric analysis

Qualitative and quantitative analysis was performed using the Biblioshiny app on R studio (version 2022.07.1 + 554) (Aria and Cuccurullo, 2017). This platform was used to generate results for main publication information, annual production and citations, author's impact, relevant affiliations, relevant sources, most cited countries, WordCloud analysis, thematic evolution, and factorial analysis. The bibliometric online analysis platform (https://

**TABLE 1** Main characteristics of the published articles on heat stress and poultry.

| Description | Results |
|---|---|
| Timespan | 2000:2021 |
| Document sources (Journals, Books, etc.) | 144 |
| Number of documents | 468 |
| Annual growth rate (%) | 4.56 |
| Document average age | 6.12 |
| Average citations per document | 24.11 |
| References | 13,844 |
| Document contents | |
| Keywords plus | 1,381 |
| Author's keywords | 1,068 |
| Authors | |
| Authors | 1,679 |
| Authors of single-authored documents | 13 |
| Author Productivity through Lotka's Law (no. of authors) | |
| Document written by one author | 1,333 |
| Document written by two author | 207 |
| Document written by three author | 60 |
| Authors collaboration | |
| Single-authored documents | 13 |
| Co-authors per documents | 5.2 |
| International co-authorships (%) | 24.36 |
| Document types | |
| Article | 436 |
| Review | 32 |

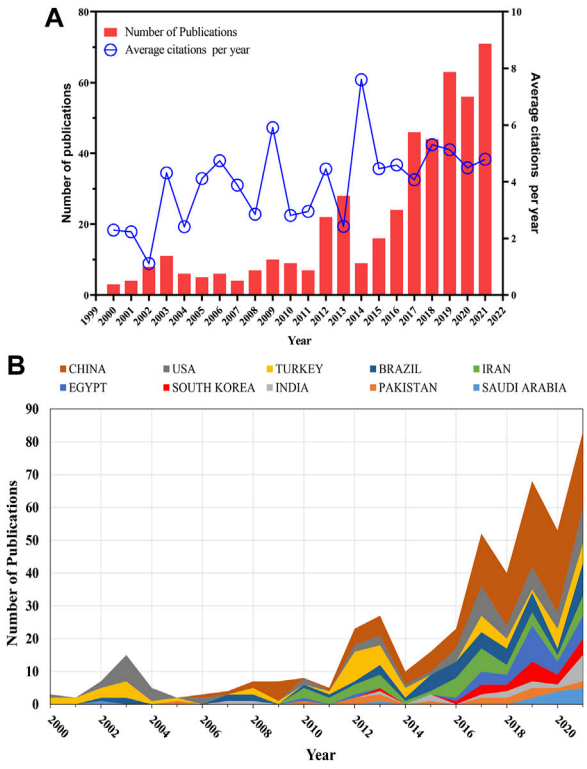


FIGURE 2
Trends in annual publications on heat stress in poultry. **(A)** Annual number of publications and average citation of articles. **(B)** Annual publication trends from top productive countries.

bibliometric.com), was used to analyze and visualize the partnership analysis between countries.

The VOSviewer software (version 1.6.11) developed by Nees Jan van Eck and Ludo Waltman (van Eck and Waltman, 2010), was used for creating, visualizing, and exploring bibliometric maps based on network data. VOSviewer was used to analyze the co-authorship of authors, countries, and institutions; co-occurrence of all keywords; citation analysis of documents, sources, authors, institutions, and countries; bibliographic coupling of documents, sources, authors, and countries; and the co-citation analysis of cited references, cited sources and cited authors. The network data were generated as network visualization and overlay visualization and interpreted accordingly. The nodes on the maps were representative of the analyzed element (that is, author, country, institution, source, or document). The line between nodes represents the link between two elements, and the thickness of the lines represents the link strength of their connections. The size of an element was determined based on its total link strength (TLS), and different colors were used to differentiate elements into different clusters (van Eck and Waltman, 2010; Cheng et al., 2022).

## 2.5 Data analysis

R software (version 4.2.1), GraphPad Prism (version 8.0.2), and Microsoft Excel 2016 were used to perform descriptive statistics and plot charts. The Spearman correlation coefficients were conducted using GraphPad Prism. Data were considered statistically significant at $p < 0.05$.

# 3 Results

## 3.1 Annual growth of publication and citations

A total of 468 documents on heat stress and poultry research. These included 93.16% of articles and 6.84% of reviews from 144 sources. The average citation per document was 24.11, and the documents had an average age of 6.12 years. The studies involved a total of 1, 679 authors, with 13 single-authored documents and 5.2 co-authors per document. The results revealed an international collaboration rate of 24.36% among the authors as shown in Table 1.

The annual publications and average citations from 2000 to 2021 are shown in Figure 2A. The annual production of publications on heat stress in poultry rose steadily from three documents as at 2000 to 79 documents in 2021, with an annual growth rate of 4.56%. Correspondingly, the average citations increased from 2.29 in 2000 to the highest point of 7.60 in 2014, and it was at 4.79 in 2021. A significant correlation coefficient was established between the number of publications and the average number of citations for the past 22 years ($r = 0.5438$, $p > 0.0089$). Figure 2B shows the United States dominated the number of publications until 2005. However, China made significant developments from 2006 and has increasingly dominated the number of publications in this field.

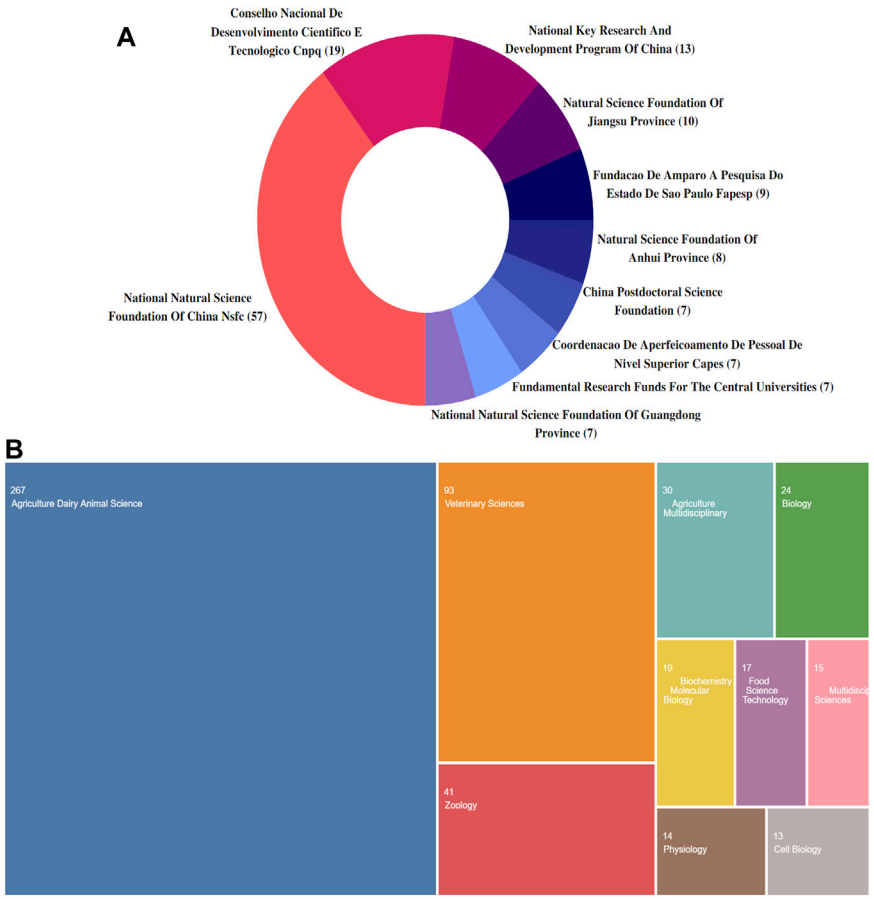


FIGURE 3
Overview of global research on heat stress in poultry. **(A)** Contribution of various funding bodies. **(B)** Research areas according to subject categories.

## 3.2 Contribution of funding agencies and institutions

A summary of the top 10 most active funding agencies is shown in Figure 3A. Five of these were from China and the top three funding agencies that supported research on heat stress in poultry were the National Natural Science Foundation of China (n = 57, 12.18%), Conselho Nacional De Desenvolvimento Cientifico E Tecnologico (n = 19, 4.06%), and National Key Research and Development Program of China (n = 13, 2.78%). Figure 3B shows that among the WoSCC subject categories, the top three areas with the highest contribution to heat stress in poultry were Agriculture, Dairy, Animal Science (n = 267), Veterinary Science (n = 93), and Zoology (n = 41).

As shown in Figure 4A, the most relevant institutions that published on heat stress in poultry were majorly from China (25%) and the United States (15%). The top institutions with the highest number of publications were Nanjing Agricultural University (China, n = 96), Firat University (Turkey; n = 69), and Universiti Putra Malaysia (Malaysia, n = 40). Co-authorship analysis of the author's institutions (minimum of three documents) showed that 58 institutions formed the largest set of connections (Figure 4B). A total of 11 institutional clusters were formed with five links and 151 TLS. In the network visualization map, Nanjing Agricultural University had the largest node with the greatest total link strength (TLS = 26). Other top collaborating institutions were Iowa State University (TLS = 19), University Estadual Maringa (TLS = 14), Firat University (TLS = 13), and Zagazig University (TLS = 12).

For the citation analysis, a total of 139 institutions (minimum number of documents of two) met the threshold and formed the largest connection (Figure 4C). The density between the institutions showed that they were closely related in terms of their citation links. Key institutions were Nanjing Agricultural University (TLS = 503), Zagazig University (TLS = 242), Firat University (TLS = 200), Iowa State University (TLS = 150), and Nanjing Normal University (TLS = 130). Importantly, it was observed that Nanjing Agricultural University had the greatest citation linkages with the Chinese Academy of Agricultural Sciences, Anhui University of Science and Technology, and University of Veterinary Medicine Hanover.

## 3.3 Contribution of countries

From Table 2, analysis for the most relevant country based on the corresponding authors revealed that China had the highest number of publications, followed by Turkey, Brazil, United States, and Iran. These accrued from both single- and multi-country publications. Interestingly, the multiple-country publication (MCP) analysis showed that France (MCP_Ratio:0.750) and the Netherlands

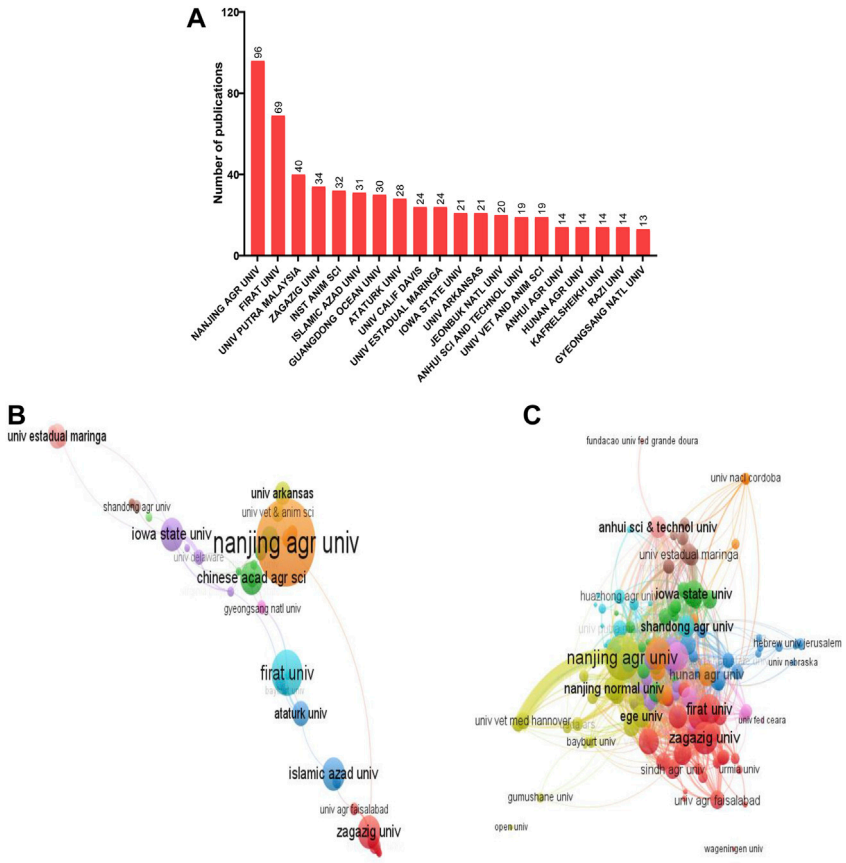


FIGURE 4
Analysis on the institutional contributions to research on heat stress in poultry. **(A)** Most relevant affiliations. **(B)** Network visualization for co-authorship analysis of contributing institutions. **(C)** Network visualization for the citation analysis of contributing institutions. *The larger the node, the greater the institutional contribution, and the thicker the line, the greater the link strength between the connected institutions.*

**TABLE 2 Top 10 productive countries contributing to research on heat stress in Poultry.**

| | Corresponding author's country | | | | | | Most cited countries | | |
|---|---|---|---|---|---|---|---|---|---|
| Rank | Country | Articles | SCP | MCP | Freq | MCP ratio | Country | TC | AAC |
| 1 | China | 137 | 113 | 24 | 0.293 | 0.175 | China | 3,912 | 28.55 |
| 2 | Turkey | 56 | 42 | 14 | 0.120 | 0.250 | Turkey | 1,671 | 29.84 |
| 3 | Brazil | 49 | 45 | 4 | 0.105 | 0.082 | United States | 1,288 | 29.95 |
| 4 | United States | 43 | 30 | 13 | 0.092 | 0.302 | Iran | 706 | 20.17 |
| 5 | Iran | 35 | 32 | 3 | 0.075 | 0.086 | Japan | 445 | 49.44 |
| 6 | Egypt | 23 | 14 | 9 | 0.049 | 0.391 | Brazil | 435 | 8.88 |
| 7 | Korea | 16 | 12 | 4 | 0.034 | 0.250 | Egypt | 387 | 16.83 |
| 8 | India | 15 | 14 | 1 | 0.032 | 0.067 | Pakistan | 384 | 48.00 |
| 9 | Japan | 9 | 4 | 5 | 0.019 | 0.556 | Belgium | 321 | 80.25 |
| 10 | Pakistan | 8 | 5 | 3 | 0.017 | 0.375 | Israel | 180 | 36.00 |

AAC, average article citations; MCP, multiple country publication; SCP, single country publication; TC, total citations.

(MCP_Ratio: 0.750) had the highest collaboration ratio (data not shown). Among the top 20 most cited countries, China had the highest total citations, followed by Turkey, United States, Iran, and Japan. Correspondingly, the collaboration network among contributing countries showed that China had close collaboration with Unites States, Germany, Australia, Egypt, Japan, and Turkey (Figure 5A).

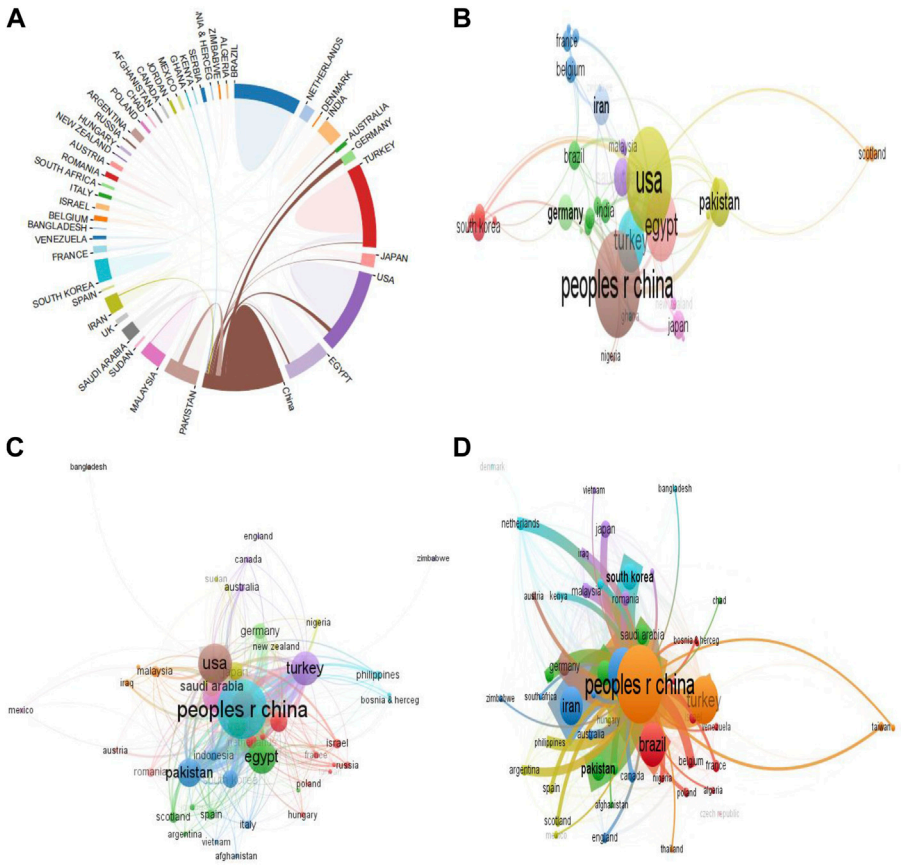


FIGURE 5
Countries contributions to research on heat stress in poultry. **(A)** Interrelationship between contributing countries. **(B)** Co-authorship mapping of countries. **(C)** Citation analysis of countries. **(D)** Bibliographic coupling of countries. *The larger the node, the greater the country's contribution, and the thicker the line, the greater the link strength between two connected countries.*

Co-authorship analysis of contributing countries showed that 46 countries constituted the largest connection (Figure 5B). They were grouped into 12 clusters, having 10 links and 178 TLS. Prominent countries with the largest connections were the People's Republic of China (TLS = 45), United States (TLS = 44), Egypt (TLS = 29), Pakistan (TLS = 18), and Saudi Arabia (TLS = 14). The network analysis revealed that China had great co-authorship linkages with the United States, Pakistan, Germany, and Egypt. Correspondingly, the citation analysis showed that 49 countries were connected, with a total TLS of 265, 42 links, and were grouped into 11 clusters. The five most prominent countries were the People's Republic of China (TLS = 1,055), United States (TLS = 538), Turkey (TLS = 413), Egypt (TLS = 416), and Pakistan (TLS = 314) (Figure 5C). Evidently, China had greater citation linkages with United States, Pakistan, Iran, Egypt, and Turkey.

In addition, the bibliographic coupling analysis of contributing countries (Figure 5D) showed that all 54 countries were connected and were categorized into 8 clusters having 109 links and 108, 141 TLS. Among the countries, People's Republic of China (TLS = 40 822), United States (TLS = 20,421), Egypt (TLS = 20,213), Iran (TLS = 14,097), and Turkey (TLS = 13,270) had the highest TLS. Importantly, the People's Republic of China was able to establish strong connections with countries such as United States, Brazil, Pakistan, Turkey, Iran, and South Korea.

## 3.4 Document sources

A total of 144 sources of documents were identified in this study. The top 20 journals with publications on heat stress in poultry are shown in Table 3. Based on the number of articles produced the most prolific journal was Poultry Science. This was followed by British Poultry Science, Journal of Thermal Biology, Animals, and Brazilian Journal of Poultry Science. Correspondingly, the total citations increased with these journals (Poultry Science and British Poultry Science), except that Worlds Poultry Science Journal had higher citations than Journal of Thermal Biology, which was followed by Biological Trace Element Research. Among these top 20 journals, the Journal of the Science of Food and Agriculture had the highest impact factor, and 60% of these journals were partitioned into JCR Q1.

A total of 111 sources formed the largest set of connections for citation analysis (Figure 6A). These sources had 681 links and 1,572 TLS. They were grouped into 17 clusters and the document sources with the strongest TLS were Poultry Science (TLS = 574), Journal of Thermal Biology (TLS = 243), World's Poultry Science Journal (TLS = 207), Animals (TLS = 150) and British Poultry Science (TLS = 146). Interestingly, Poultry Science journal formed the greatest citation network with co-journals including Journal of Thermal Biology, British Poultry Science, World's Poultry Science Journal, and Animals. The bibliographic coupling of sources showed

**TABLE 3** Top 20 most productive journals contributing to research on heat stress in poultry.

| Rank | Journal | Number of articles | Total citation | h_index | IF | Rank | Journal |
|---|---|---|---|---|---|---|---|
| 1 | Poultry Science | 66 | 3,067 | 28 | 4.014 | 4.192 | Q1 |
| 2 | British Poultry Science | 23 | 768 | 13 | 1.892 | 2.429 | Q2 |
| 3 | Journal of Thermal Biology | 17 | 524 | 12 | 3.189 | 3.342 | Q1 |
| 4 | Animals | 16 | 302 | 9 | 3.231 | 3.312 | Q1 |
| 5 | Brazilian Journal of Poultry Science | 15 | 170 | 9 | 1.019 | 1.492 | Q3 |
| 6 | Worlds Poultry Science Journal | 12 | 593 | 10 | 3.452 | 3.762 | Q1 |
| 7 | Biological Trace Element Research | 11 | 445 | 9 | 4.081 | 3.755 | Q2 |
| 8 | Plos One | 10 | 333 | 8 | 3.752 | 4.069 | Q1 |
| 9 | Cell Stress and Chaperones | 9 | 160 | 7 | 3.827 | 3.940 | Q3 |
| 10 | Asian-Australasian Journal of Animal Sciences | 9 | 89 | 6 | 2.694 | 2.816 | Q1 |
| 11 | Animal Science Journal | 8 | 180 | 5 | 1.974 | 2.027 | Q2 |
| 12 | Journal of Applied Poultry Research | 8 | 104 | 5 | 2.162 | 2.000 | Q2 |
| 13 | Italian Journal of Animal Science | 8 | 37 | 4 | 2.552 | 2.785 | Q1 |
| 14 | Tropical Animal Health and Production | 8 | 109 | 4 | 1.893 | 1.930 | Q2 |
| 15 | Animal Feed Science and Technology | 6 | 267 | 6 | 3.313 | 3.914 | Q1 |
| 16 | Journal of Animal Physiology and Animal Nutrition | 5 | 209 | 5 | 2.718 | 2.747 | Q1 |
| 17 | Journal of the Science of Food and Agriculture | 5 | 158 | 5 | 4.125 | 4.096 | Q1 |
| 18 | International Journal of Biometeorology | 5 | 235 | 4 | 3.738 | 3.951 | Q2 |
| 19 | Animal | 4 | 40 | 4 | 3.730 | 3.908 | Q1 |
| 20 | Journal of Animal Science | 4 | 118 | 4 | 3.338 | 3.243 | Q1 |

that 128 sources formed the largest bibliographic connection with 4,262 links, TLS of 55,653 and they were grouped into 9 clusters (Figure 6B). Poultry Science had the largest network (TLS = 13,909), followed by Journal of Thermal Biology (TLS = 9,995), World's Poultry Science Journal (TLS = 7,046), Animals (TLS = 6,092), and British Poultry Science (TLS = 3,719). Similar to the citation analysis, it was revealed that Poultry Science established strong bibliographic coupling with co-journals including Journal of Thermal Biology, World's Poultry Science Journal, Animals, and British Poultry Science.

In total, 142 sources of documents (minimum number of citations per source = 20) were analyzed for the co-citation network of their cited sources (Figure 6C). Similar to the citation and bibliographic coupling networks, Poultry Science journal had the largest network of co-cited sources (TLS: 115,035). Other top co-cited sources were British Poultry Science (TLS = 31,960), World's Poultry Science Journal (TLS = 20,901), Journal of Thermal Biology (TLS = 13,199), and Journal of Animal Science (TLS = 12,769). Importantly, Poultry Science had a great co-citation network with other journals especially, British Poultry Science, World's Poultry Science Journal, International Journal of Poultry Science, and Journal of Animal Science and Biotechnology.

## 3.5 Authorship analysis

A total of 1,679 authors contributed to the 468 documents on heat stress in poultry from 2000 to 2021. Table 4 shows that the top five authors with the highest global contributions were Kazim Sahin (Firat University, Turkey), followed by Nurhan Sahin (Firat University, Turkey), Feng Gao (Nanjing Agricultural University, China), Li Zhang (Guangdong Ocean University, China) and Endong Bao (Nanjing Agricultural University, China). Interestingly, researchers from Nanjing Agricultural University, China constituted about 45% of the top 20 contributing authors, while China alone had 75% of the top 20 authors, followed by Turkey at 20%.

The co-authorship analysis showed that several of the authors were not connected, whereas the largest network had 69 authors, 304 links, and 309 TLS. Figure 7A shows that the five authors with significant co-authorship connections were Alagawany, Mahmoud (TLS = 26), Naiel Mohammed A.E (TLS = 21), Abd El-Hack, Mohamed E. (TLS = 21), Abdel-Moneim, Abdel-Moneim Eid (TLS = 17), and Shehata, Abdelrazeq M (TLS = 15). The co-authorship network revealed that of the few connected researchers, there was a close association between the different clusters. This suggests that the active authors on heat stress in poultry had established a centralized and concentrated network, but still lacked extensive collaboration with other scholars. Citation analysis of authors with a minimum of two documents showed that 308 authors formed the largest connection, with a total TLS of 10,244; 5,504 links, and they were categorized into 10 clusters (Figure 7B). Five authors with the strongest TLS were Gao, Feng (TLS = 366), Bao, Endong (TLS = 331), Tang, Shu (TLS = 282), Lamont, Susan J (TLS = 193), and Alagawany Mahmoud (TLS = 160).

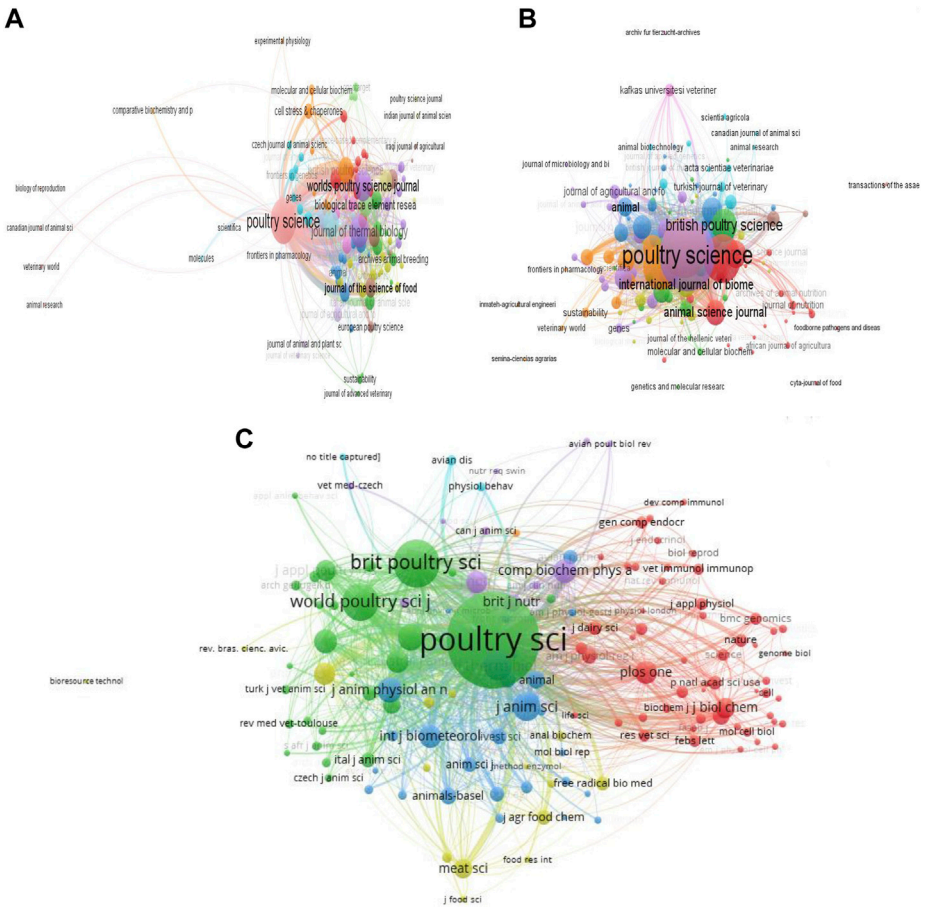


FIGURE 6
Journals contributing to research on heat stress in poultry. **(A)** Citation analysis of sources. **(B)** Bibliographic coupling of sources. **(C)** Co-citation analysis of cited sources. *The larger the node, the greater the journal's contribution, and the thicker the line, the greater the link strength between two journals.*

The co-citation network of cited authors revealed that a total of 115 authors were connected (minimum number of citations per author: 20) with 5,440 links; 42; 054 TLS, and they formed 5 clusters (Figure 7C). Top co-cited authors in the network were Sahin, K (TLS = 5,081), Yahav, S. (TLS = 2,849), Attia, Y.A (TLS = 2,551), Quinteiro, W.M (TLS = 2,183), and Lin, H (TLS = 5,081). Results from both the citation and bibliographic coupling analysis showed that Bao, Endong, and Tang, Shu who are major contributors affiliated with Nanjing Agricultural University, China were isolated in a distinct cluster.

Network visualization map showing the bibliographic coupling of authors also revealed that a total of 125 authors were connected (minimum number of documents: 3), with 6,721 links, total TLS of 152,247, and that they were grouped into 6 clusters (Figure 7D). Gao, Feng (TLS = 7,084), Lamont, Susan (TLS = 6,529), Bao, Endong (TLS = 5,435), Gasparino, Eliane (TLS = 5,097), and Sahin K (TLS = 5,054) were among the authors with the greatest TLS.

## 3.6 Documents and co-cited documents

The top 10 most globally cited documents on heat stress in poultry are presented in Table 5. "Effect of heat stress on oxidative stress, lipid peroxidation and some stress parameters in broiler" by Altan O. et al. (2003) was the most cited document. Two review articles were included in the top 10 globally cited documents. "Strategies for preventing heat stress in poultry" by Lin H et al. (2006) and "Association between heat stress and oxidative stress in poultry; mitochondrial dysfunction and dietary interventions with phytochemicals" by Akbarian A. et al. (2016).

Following citation analysis (Figure 8A), the network visualization map showed that a total of 304 documents (minimum number of citations per document = 5) formed the largest set of connected items, which were grouped into 19 clusters. From the citation analysis, the following documents: Altan et al. (2003) (citations = 294, links = 39), Lin et al. (2006) (citations = 250, links = 35), Bartlett (2003) (citations = 246, links = 35), Akbarian et al. (2016) (citations = 219, links = 43), and Sohail et al. (2010) (citations = 215, links = 37) had the highest citation and linkages. Bibliographic coupling of documents revealed that 156 documents were connected (minimum number of citations per documents: 20) with a total TLS of 10,770, 406 links and they were distributed into 7 clusters (Figure 8B). The following; Wang et al. (2021) (TLS = 554), Abdel-Moneim et al. (2021) (TLS = 504), Farag and Alagawany (2018) (TLS = 430), Lin et al. (2006) (TLS = 338), and Kumar et al. (2021) (TLS = 325) were among the top documents with high TLS.

**TABLE 4 Most productive authors contributing to global researches on heat stress in poultry.**

| Rank | Author | Institution | h_index | TC | NP |
|---|---|---|---|---|---|
| 1 | Kazim Sahin | Firat University, Turkey | 14 | 736 | 17 |
| 2 | Nurhan Sahin | Firat University, Turkey | 11 | 482 | 13 |
| 3 | Feng Gao | Nanjing Agricultural University, China | 10 | 383 | 10 |
| 4 | Li Zhang | Guangdong Ocean University, China | 10 | 343 | 12 |
| 5 | Endong Bao | Nanjing Agricultural University, China | 9 | 262 | 14 |
| 6 | Jiaolong Li | Nanjing Agricultural University, China | 9 | 301 | 10 |
| 7 | Shu Tang | Nanjing Agricultural University, China | 8 | 150 | 13 |
| 8 | Jiao Xu | Nanjing Agricultural University, China | 8 | 147 | 11 |
| 9 | Yun Jiang | Nanjing Normal University, China | 7 | 268 | 7 |
| 10 | Zhuang Lu | Nanjing Agricultural University, China | 7 | 260 | 7 |
| 11 | Bingbing Ma | Nanjing Agricultural University, China | 7 | 268 | 7 |
| 12 | Bin Yin | Shandong Academy of Agricultural Science, China | 7 | 86 | 7 |
| 13 | M. Zhang | Jinling Institute of Technology, China | 7 | 161 | 13 |
| 14 | Guanghong Zhou | Nanjing Agricultural University, China | 7 | 254 | 7 |
| 15 | Mohamed E. Abd El-Hack | Zagazig University, Egypt | 6 | 208 | 6 |
| 16 | Recep Gümüş | Cumhuriyet University, Turkey | 6 | 102 | 6 |
| 17 | Jianhua He | Hunan Agricultural University, China | 6 | 210 | 8 |
| 18 | Shaojun He | Anhui Science and Technology University, China | 6 | 185 | 10 |
| 19 | Xiaofang He | Nanjing Agricultural University, China | 6 | 245 | 6 |
| 20 | Halit İmik | Ataturk University, Turkey | 6 | 102 | 6 |

NP, number of publications, TC: total citation.

Analysis of the co-citation network of cited references (minimum number of citations per cited reference = 20) showed that 59 cited references formed a network of 1,548 links, 6,334 TLS and were grouped into 4 clusters (Figure 8C). Top five cited references included Lara and Rostagno (2013) (TLS = 1,377) which was published in Animals (Basel), followed by Quinteiro-Filho et al. (2010) (TLS = 994), Mashaly MM (2004) (TLS = 737), Sohail MU (2012) (TLS = 700), and Zhang ZY (2012) (TLS = 629). The last four cited references were all published in Poultry Science. Moreover, the strongest co-citation connection was found between the cited references, Lara and Rostagno (2013); and Quinteiro-Filho et al. (2010) (link strength = 37)

## 3.7 Keyword analysis

WordCloud analysis showed that "chickens" (127), "growth performance" (125), "supplementation" (75) "performance" (74), and "oxidative stress" (60) were the top five Keyword Plus with the highest frequency (Figure 9A). Co-occurrence analysis (minimum occurrence of each keyword = 5) categorized all the keywords into six clusters (Figure 9B). The top six keywords in terms of co-occurrence were "heat stress" (TLS = 1,884), "growth performance" (TLS = 1,027), "chickens" (TLS = 988), "broiler" (TLS = 961), "performance" (TLS = 781), and "oxidative stress" (TLS = 684) (Figures 9B, C). The overlay visualization showed that the keyword "heat stress" co-occurred with several current topics including "meat quality", "antioxidants", "microflora", "intestinal barrier", "expression", and "rna-seq" (Figure 9C).

To understand the research trend on heat stress in poultry over time, a thematic evolution analysis was conducted by grouping the Keyword Plus into four periods (2000–2005, 2006–2010, 2011–2015, and 2016–2021). Supplementary Table S1 gives detailed information on Keyword plus classification and the properties of the clusters/time series. As shown in Figure 10A, from 2000 to 2005 had key terms such as environmental temperature, oxidative stress, and chickens; 2006 to 2010 had terms such as lipid-peroxidation, oxidative stress; environmental temperature; 2011 to 2015 had high frequency for performance, supplementation, and chickens, and the period between 2016 and 2021 included terms such as oxidative stress, growth performance, and temperature.

Thematic map analysis was carried out for the Keyword plus and Author keywords (Figures 10B, C). For the Keywords plus, the motor theme covered terms such as growth performance, ascorbic acid, and meat quality. The niche themes were terms related to oxidative stress, gene expression, and muscle metabolism. The emerging or declining themes covered terms such as stress, dietary supplementation, microflora, intestinal morphology, and probiotic mixture, while the basic themes included terms related to broiler chickens, lipid peroxidation, and ambient temperature (Figure 10B). Thematic

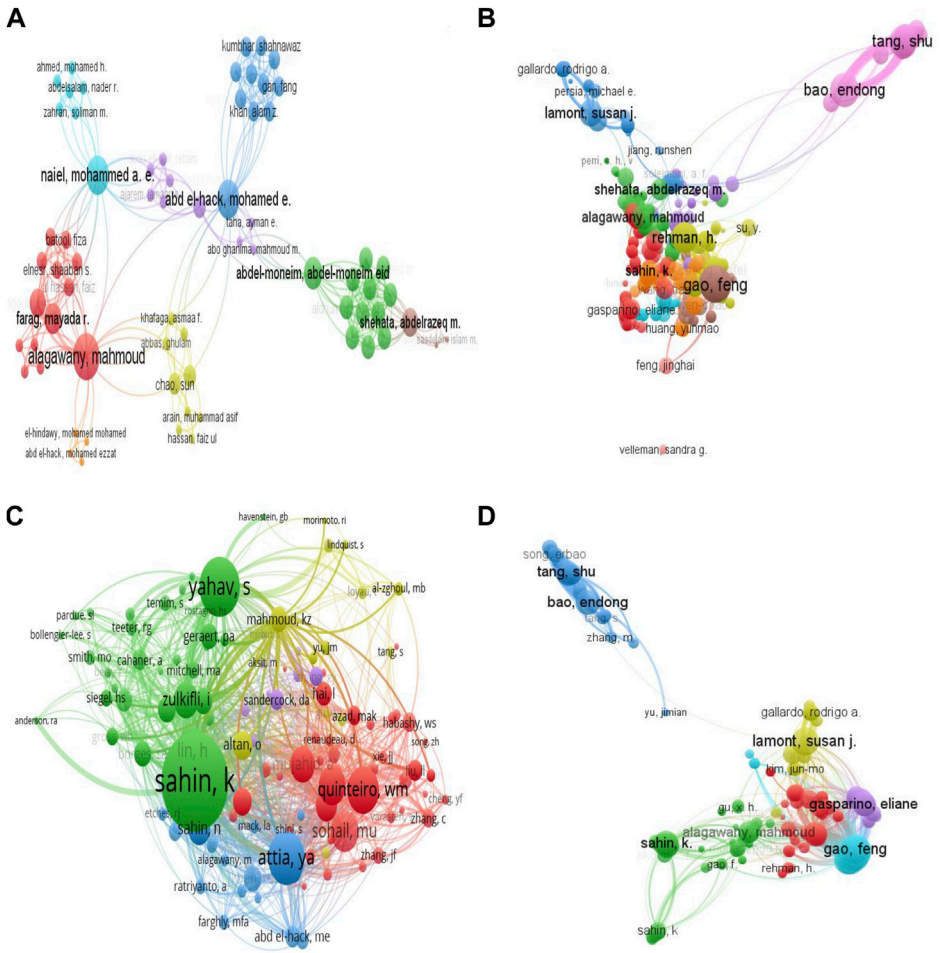


FIGURE 7
Analysis of the authorship network for global research on heat stress in poultry. **(A)** Co-authorship mapping of authors. **(B)** Citation analysis of authors. **(C)** Co-citation analysis of authors. **(D)** Bibliographic coupling analysis of authors. *The larger the node, the greater the author's contribution, and the thicker the line, the greater the link strength between two authors.*

mapping of the Authors keywords showed that the motor theme included immunity, nutrition, and thermal stress. The niche theme had terms associated with oxidative stress, heat shock proteins, and chronic heat exposure. The emerging or declining themes featured terms such as chicken, hsp 70, rna-seq, co-enzyme 10, and transcriptome, while the basic theme had growth performance, terms related to heat stress, and gene expression (Figure 10C). Figure 10D shows the conceptual framework of Author keywords (n = 50) using the multiple correspondence analysis. The results showed that the keywords were categorized into four clusters of 4, 5, 8, and 33 elements, respectively. Key terms including "acute heat stress, "cyclic heat stress" and "oxidative status" were covered in the first cluster, whereas, the last cluster which had the largest number of elements (n = 33) covered terms closely related to heat stress, growth performance, gene expression, production, and metabolism.

## 4 Discussion

Over the last decades, with the increasing awareness and global actions towards climate change and global warming, research on heat stress in farm animals especially poultry has gained attention, as evidenced by the annual increment in the number of publications. The number of publications and citation counts achieved each year is an indicator of the research interest and progress made by researchers in that specific area (Musa et al., 2020; Xu et al., 2022). Several researchers, countries, institutions, and industry partners have collaborated on studies to address "heat stress in poultry", thus necessitating this bibliometric analysis to understand the milestones achieved, research gaps uncovered, and the trends for future research. Over the past two decades, the annual publications on heat stress in poultry showed a significant increase, and so far, the highest number of articles was achieved in 2021. The annual number of publications increased relatively slowly from 2000 until 2011, with fewer than 15 articles per year. The increase observed from 2012 could possibly occur due to increasing awareness of the impacts of heat stress on poultry (Lin et al., 2006; Yahav, 2009) and its association with oxidative stress (Altan et al., 2003; Mujahid et al., 2005), as seen from the records of top globally cited documents. More so, the dietary manipulation of heat stress in poultry using prebiotics and probiotics (Lan et al., 2004; Sohail et al., 2010), polyphenols (Pena et al., 2008; Aengwanich and Suttajit, 2010), amino acids (Zarate et al., 2003; Dai

TABLE 5 Top 10 most globally cited documents on heat stress in poultry.

| Rank | Title | First author | Type | Source | PY | TC | TCY |
|---|---|---|---|---|---|---|---|
| 1 | Effect of heat stress on oxidative stress, lipid peroxidation and some stress parameters in broiler | Altan O. | Article | British Poultry Science | 2003 | 294 | 14.7 |
| 2 | Strategies for preventing heat stress in poultry | Lin H. | Review | World's Poultry Science Journal | 2006 | 250 | 14.71 |
| 3 | Effects of different levels of zinc on the performance and immunocompetence of broilers under heat stress | Bartlett JR. | Article | Poultry Science | 2003 | 246 | 12.3 |
| 4 | Association between heat stress and oxidative stress in poultry; mitochondrial dysfunction and dietary interventions with phytochemicals | Akbarian, A. | Review | Journal of Animal Science and Biotechnology | 2016 | 219 | 31.29 |
| 5 | Effect of a probiotic mixture on intestinal microflora, morphology, and barrier integrity of broilers subjected to heat stress | Song J. | Article | Poultry Science | 2014 | 215 | 23.89 |
| 6 | Effect of supplementation of prebiotic mannan-oligosaccharides and probiotic mixture on growth performance of broilers subjected to chronic heat stress | Sohail MU | Article | Poultry Science | 2012 | 215 | 19.55 |
| 7 | Superoxide Radical Production in Chicken Skeletal Muscle Induced by Acute Heat Stress | Mujahid A. | Article | Poultry Science | 2005 | 206 | 11.44 |
| 8 | Effect of Chronic Heat Exposure on Fat Deposition and Meat Quality in Two Genetic Types of Chicken | Lu Q. | Article | Poultry Science | 2007 | 193 | 12.06 |
| 9 | Effects of different levels of vitamin E on growth performance and immune responses of broilers under heat stress | Niu ZY. | Article | Poultry Science | 2009 | 180 | 12.86 |
| 10 | Alleviation of cyclic heat stress in broilers by dietary supplementation of mannan-oligosaccharide and Lactobacillus-based probiotic: Dynamics of cortisol, thyroid hormones, cholesterol, C-reactive protein, and humoral immunity | Sohail MU. | Article | Poultry Science | 2010 | 159 | 12.23 |

PY, published year; TC, total citation; TCY, total citation per year.

et al., 2011), as well as, minerals and vitamins (Sahin et al., 2002; Niu et al., 2009; Mohiti-Asli et al., 2010; Vakili et al., 2010; Moeini et al., 2011) etc., were gradually gaining research attention. The last 5 years have witnessed production exceeding 40 documents annually, accounting for 61.9% of the total documents. The increase in the number of publications was positively associated with the rise in the average annual citation in a monotonic relationship. Also, it is expected that with an increase in the number of citable years, the average citation will continue to increase. Therefore, consistent efforts to foster research and collaboration are necessary to drive annual publications, growth rate, and article citations on heat stress and poultry.

Importantly, China ranked foremost in its contribution to research on heat stress in poultry in terms of publications, top contributing authors, funding agencies, institutional affiliations, and corresponding authorship. The network analysis also revealed that China significantly cooperated with other countries including United States, Egypt, Turkey, Germany, and Australia. In terms of co-authorship, citations, and bibliographic coupling, China had the greatest connections, networks, and TLS with other countries. This may be closely attributed to the significant financial investments by the Chinese government to support research on heat stress in poultry. The study revealed that out of the top 10 funding agencies, five were sponsors from China including the National Natural Science Foundation of China, National Key Research and Development Program of China, and Natural Science Foundation of Jiangsu Province. Evidently, the most productive institutions were also from China, with the most significant being the Nanjing Agricultural University. The institutional networks for co-authorship and citation analysis further revealed that Nanjing Agricultural University played a significant role in establishing strong research cooperation and collaboration with other institutions both within and outside China.

With respect to the authors, Kazim Sahin from Firat University, Turkey, Nurhan Sahin from Firat University, Turkey, and Feng Gao from Nanjing Agricultural University, China contributed the highest to global research on heat stress in poultry. Studies by Kazim Sahin and Nurhan Sahin were majorly centered on vitamin and mineral metabolism, quail production, phytochemicals, oxidative stress, and heat stress alleviation (Sahin et al., 2012; Sahin et al., 2013; Sahin et al., 2017; Orhan et al., 2021). Both authors were closely affiliated and collaborated on most of their research. On the other hand, Feng Gao focused on studies related to muscle metabolism, taurine supplementation, heat stress-induced oxidative damage, and the effects of chronic heat stress on broilers (Lu et al., 2017; Ma et al., 2018; Lu et al., 2019; Ma et al., 2021). Furthermore, the co-authorship analysis revealed that several of the authors, even those with a higher number of publications were excluded from the network. In line with this, the international co-authorship of authors was found to be 24.36%, thus suggesting that the inter-collaborative efforts of authors in this research field were relatively low. In addition, research works from Gao, Feng; Bao, Endong; Tang, Shu; Lamont, Susan J; and Alagawany Mahmoud were highly cited by other authors, while the works from Sahin, K., Yahav, S., Attia, Y.A., Quinteiro, W.M., and Lin, H. were among the top co-cited papers, suggesting that they contributed to the high impact papers sought after in the field. Consequently, documents from these authors were also found among the top globally cited research in this field (Sahin and Kucuk, 2003; Lin et al., 2006; Yahav, 2009; Attia et al., 2021). The

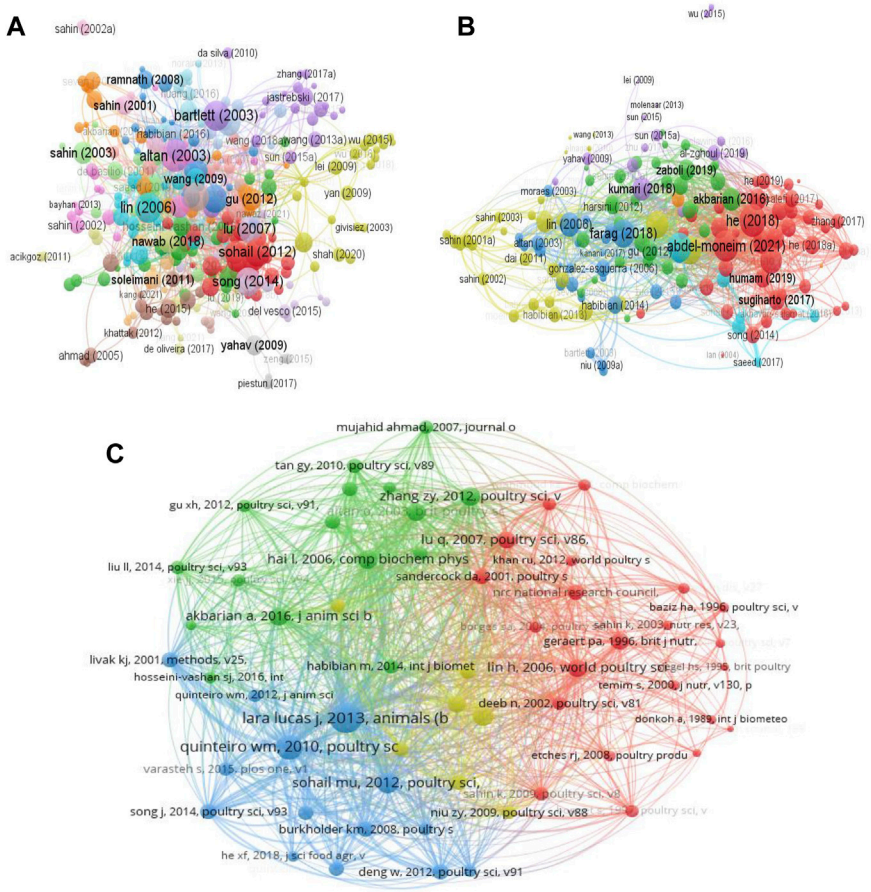


FIGURE 8
Network visualization of documents on heat stress in poultry. **(A)** Citation analysis of documents. **(B)** Bibliographic coupling analysis of documents. **(C)** Co-citation network of documents.

bibliographic coupling of authors characterizes the phenomenon where two authors cite similar document (s) in the articles that they have published (Ma, 2012; Zhang and Yuan, 2022). Findings from both the citation and bibliographic coupling analysis showed that Bao, Endong and Tang, Shu who were affiliated with Nanjing Agricultural University, China had a strong connection in their bibliographic network, suggesting that these authors have close similarities in their research outputs. Altogether, key scholars who have contributed quantitatively or qualitatively to promoting research on heat stress in poultry were identified, indicating their substantial contributions to the field.

Bibliometric analysis of document sources (including journals, books, etc.) is important in providing updated insights and trends for a particular research area, as well as in guiding scholars to select suitable journals for their research communication (Cheng et al., 2022; Liu et al., 2022). Journals including Poultry Science, British Poultry Science, Journal of Thermal Biology, Animal, and Brazilian Journal of Poultry Science were the most prolific sources of articles on heat stress in poultry and they also accrued higher citation index. Journal co-citation analysis and bibliographic coupling further emphasized that Poultry Science had the largest network and was strongly connected with other journals such as Journal of Thermal Biology, World's Poultry Science Journal, Animals, and British Poultry Science. These may be related to the publication of high-impact findings in these journals, thus suggesting that the hot topics and future trends emanating from research on heat stress in poultry are likely to be reported in these journals. Evidently, Poultry Science journal produced most of the top globally cited articles, revealing that this journal is a relevant, consistent, and authoritative source for high-caliber research and information related to poultry production.

The article, titled "Effect of heat stress on oxidative stress, lipid peroxidation and some stress parameters in broiler" by Altan O. et al. (2003) was identified as the most globally cited document on heat stress in poultry. Key findings of this study were that heat stress increased fearfulness, induced oxidative stress, and initiated significant physiological responses in broilers (Altan et al., 2003). Two review articles also contributed significantly to the global research progress on heat stress in poultry. They were "Strategies for preventing heat stress in poultry" by Lin H et al. (2006) and "Association between heat stress and oxidative stress in poultry; mitochondrial dysfunction and dietary interventions with phytochemicals" by Akbarian A. et al. (2016). Given the widespread concerns on how to mitigate the adverse impacts of heat stress in poultry production, Lin et al. (2006) was among the early reports to surmise various methods, which included, genetic, nutritional, feeding, and environmental strategies that can be

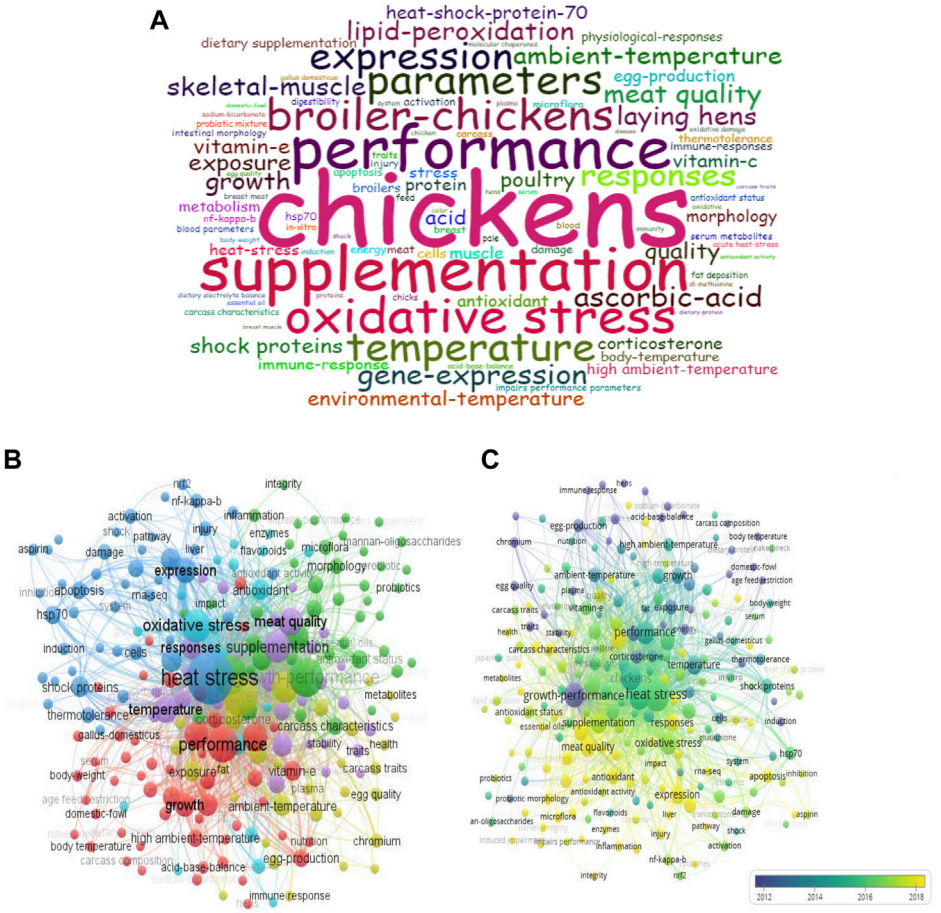


FIGURE 9
Analysis for Keywords associated with global research on heat stress in poultry. **(A)** Word cloud analysis of Keyword Plus. **(B)** Network visualization for all keywords co-occurrence. **(C)** Overlay visualization for the co-occurrence analysis of all keywords.

adopted to cope with heat stress in poultry. In addition, following the discovery that oxidative stress was closely associated with heat stress in poultry, Akbarian et al. (2016) provided a detailed discussion that explained the mechanisms through which heat stress induces oxidative stress, and also presented the use of antioxidant phytochemicals as a nutritional strategy for the alleviation of mitochondrial dysfunction in heat-stressed birds. From the citation networks, documents including Altan et al. (2003), Bartlett (2003), Lin et al. (2006), Akbarian et al. (2016), and Sohail et al. (2010) had the greatest linkages and also contributed substantially to the advancement of research on heat stress in poultry. Several documents were commonly cited by scholars in this research area, especially the works of Lara and Rostagno (2013) which reported on the "Impact of heat stress on poultry production" and Quinteiro-Filho et al. (2010) which reported that "Heat stress impairs performance parameters, induces intestinal injury, and decreases macrophage activity in broiler chickens".

Keywords are considered important terms and phrases from a research paper that rightly expresses the content covered, help generate new information and frontiers of knowledge, and assist in the retrieval of relevant content. Commonly, author-generated keywords (that is, Author keywords) are provided during article submission to describe the main contents/concepts addressed in their research. Also, the Keyword Plus is generated by Web of Science from the words and phrases that occur in the titles of cited references (Tripathi et al., 2018). Therefore the use of both author keywords and Keyword Plus explicitly expresses the knowledge structure, the article's content, and the interactions of various research in a given subject area (Zhang et al., 2016). In this study, the top five keywords with the highest WordCloud frequency were "chickens", "growth performance", "supplementation", "performance", and "oxidative stress". Word Cloud provides a visual representation of texts that are frequently occurring, such that the bigger and bolder a word appears, the higher its frequency of occurrence. Interestingly, the keyword "oxidative stress" had a higher occurrence than "heat stress" revealing a shift in research interest, which suggest that more researchers were gradually getting involved with studies that addressed oxidative stress in poultry. In addition, the thematic evolution of Keyword plus identified that research on oxidative stress had gained momentum over the years. Importantly, the thematic growth on oxidative stress had evolved to integrate other terms related to performance, supplementation, gene expression, and growth performance. This was also consistent with the overlay visualization which showed that heat stress co-

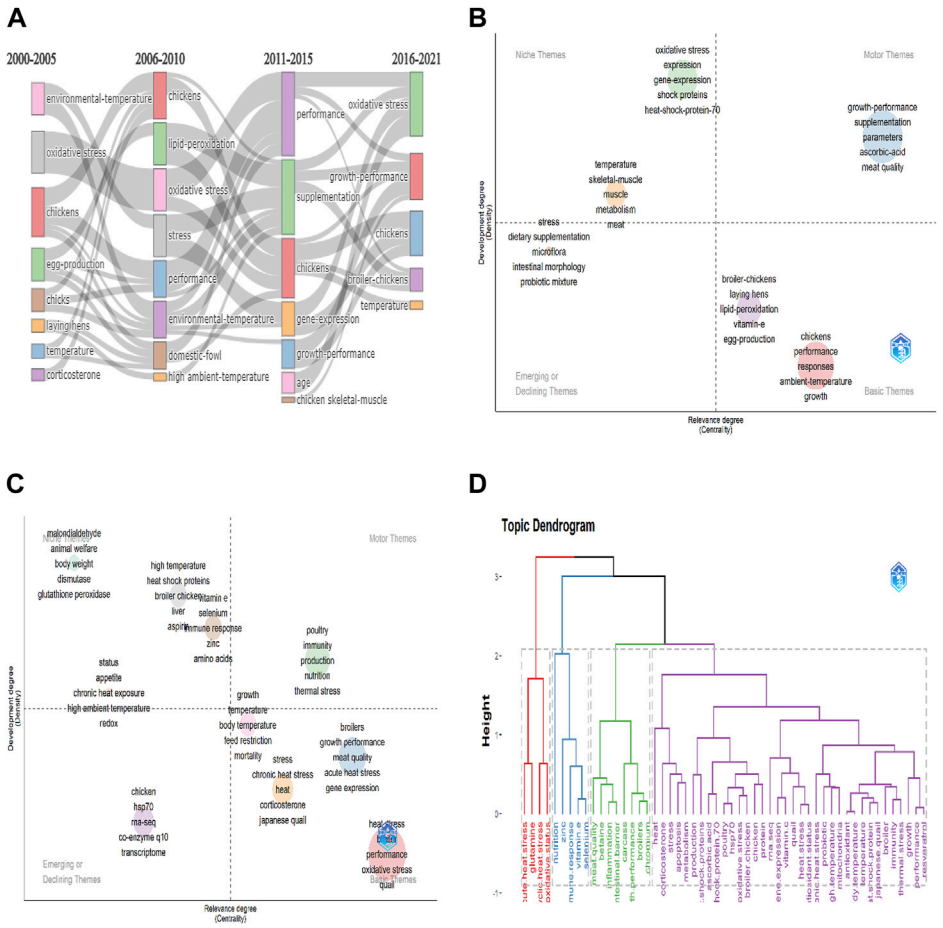


FIGURE 10
Keywords analysis for global research terms on heat stress in poultry. **(A)** Thematic evolution of Keyword Plus from 2000 to 2021. **(B)** Thematic map analysis of Keyword Plus **(C)** Thematic map analysis of authors keywords. **(D)** Topic dendrogram using multiple correspondence analysis of authors keywords to show the hierarchical relationship between terms.

occurred with various new topics such as "meat quality", "antioxidants", "microflora", "intestinal barrier", "expression", and "rna-seq".

The co-occurrence network of all keywords unveiled that current research on heat stress in poultry mainly focused on studies of growth performance, environment and production (red nodes), studies on intestinal morphology, and microbiota (green nodes), studies on the molecular mechanisms of heat stress (blue nodes), studies on immune response and metabolites, studies on meat quality and carcass characteristics (purple nodes), and studies on oxidative stress (aqua nodes). With the recent development in research, it is interesting to note that several terms have emerged in relation to heat stress such as "essential oils", "resveratrol", "betaine", "curcumin", "probiotic mix", "flavonoids", and "plant extracts". These are important agents provided as supplements to poultry in a bid to alleviate the detrimental effects of heat stress. Several studies have demonstrated their protective and beneficial effects on the growth performance, behavior and welfare, immune system, antioxidant capacity, egg production, nutritional metabolism, intestinal health, thermotolerance, and other physiological variables of heat-stressed birds (Nawab et al., 2020; Sariozkan et al., 2020; Jiang et al., 2021; Liu et al., 2021; Mohammadi, 2021; Wen et al., 2021; Yang et al., 2021).

The thematic map analysis of keywords allows for the organization of keyword groupings according to their density and centrality into a single circle for mapping as a two-dimensional image (Ejaz et al., 2022). From the Keyword plus, it was identified that motor topics including "growth performance", "supplementation", "ascorbic acid research", and "meat quality", have been well-researched with respect to heat stress in poultry (Mahmoud et al., 2004; Abidin and Khatoon, 2013; Kumar et al., 2021; Piray and Foroutanifar, 2021). However, some topics that were weakly developed from both the emerging and declining themes (microflora, intestinal morphology, and probiotic mixture) and the basic themes (lipid-peroxidation, egg production, and ambient temperature) could be of research interest for further studies on heat stress in poultry. In examining the Author keywords, some underdeveloped and marginally important topics grouped into the emerging and declining themes were "hsp70", "rna-seq", "co-enzyme q10", and "transcriptome". To address this, studies have reported that co-enzyme q10 protects the chicken primary myocardial cells against

damage and apoptosis during *in vivo* heat stress by upregulating hsp70 expression and HSF1 binding activity (Xu et al., 2017a; Xu et al., 2017b; Xu et al., 2019b), and that co-enzyme q10 induced autophagy and suppressed the PI3K/AKT/mTOR signaling as a protective mechanism against heat stress (Xu et al., 2019a). Alongside this, several studies have employed the whole transcriptomics approach, as well as other RNA sequencing technology to investigate the effects of heat stress in poultry (Saelao et al., 2018; Te Pas et al., 2019; Kim et al., 2021; Liang et al., 2021). With the advent of this tool, the molecular mechanisms that occur in distinct cells or tissues of various poultry species during heat stress exposure can be profiled, quantified, and comprehensively understood, thus presenting useful information to advance research in this field. The transcriptomics approach has been utilized to investigate the effects of heat stress on various tissues including the liver (Jastrebski et al., 2017; Wang et al., 2020), bursa (Monson et al., 2018; Chanthavixay et al., 2020), thymus (Monson et al., 2019), cardiac and skeletal muscle (Srikanth et al., 2019), hypothalamus (Sun et al., 2015), and heart (Zhang et al., 2017; Zhang et al., 2019). In addition, some topics which are relevant but weakly developed were identified in the basic theme, such as "corticosterone", "acute heat stress"' "chronic heat stress", "oxidative stress", "feed restriction, "meat quality", and "gene expression". Importantly, these topics may be considered highly relevant and of great potential in stimulating future research and scientific development on heat stress in poultry.

To the best of our knowledge, the present study is the first to examine the global research status and emerging trends on heat stress in poultry species using the bibliometric approach. Noteworthy, research progress in this field is gradually developing with greater growth potential. Presently, the need for extensive global cooperation between authors, institutions, and countries cannot be overemphasized. Current research on heat stress in poultry could be identified as focusing on production performance, physiological responses, oxidative stress, and dietary supplements. However, it is deduced that future research trends will focus more on topics such as; "antioxidants", "meat quality", "microflora", "intestinal barrier", "rna-seq", "animal welfare", "gene expression", "probiotics", "feed restriction", and "inflammatory pathways". Therefore, this comprehensive analysis of the current status and emerging topics on heat stress in poultry would serve as a useful reference for researchers, policymakers, and other stakeholders in the poultry industry.

## 5 Limitations of the study

It is important to point out that despite the novelty of this work and the important findings established from this study, there are a few limitations associated with it.

1. The documents retrieved for this study were solely based on the WoSCC database, as such not inclusive of other database collections such as Scopus, Pubmed, Dimension *etcetera*, which may have more information to deliver. However, it is agreed that Web of Science is the most suitable database and the most recommended for bibliometric studies in a specific field (Cheng et al., 2022; Shan et al., 2022).
2. The documents mined from the search may not necessarily obtain all the related literature due to the diversity of keywords. However, the detailed search strategy employed, the advanced search technique, and the logical use of Boolean operators have helped to improve the relevance and accuracy of retrieved results.
3. The key term in this study "heat stress in poultry" was expressed as "heat stress" AND "Poultry", with the use of "AND" as a Boolean operator to ensure that all related keywords were retrieved and the search result was narrowed down to only the relevant terms.

## Data availability statement

The original contributions presented in the study are included in the article/Supplementary Material, further inquiries can be directed to the corresponding authors.

## Author contributions

VU conceptualized the research, and drafted the manuscript. VU and TM conducted the bibliometric analysis, collected the data, and interpreted the results. OEO, JZ, XW, HJ, OO, and HL revised the manuscript and supervised the study. All authors contributed to the final version of the article.

## Funding

This work was supported by the Key Technologies Research and Development Program of China (2021YFD1300405), Key Technology Research and Development Program of Shandong province (2019JZZY020602), the Earmarked Fund for China Agriculture Research System (CARS-40-K09), and National Natural Science Foundation of China (31772619).

## Conflict of interest

The authors declare that the research was conducted in the absence of any commercial or financial relationships that could be construed as a potential conflict of interest.

## Publisher's note



## Supplementary material

The Supplementary Material for this article can be found online at: https://www.frontiersin.org/articles/10.3389/fphys.2023.1123582/full#supplementary-material

# References

Abdel-Moneim, A. M. E., Shehata, A. M., Khidr, R. E., Paswan, V. K., Ibrahim, N. S., El-Ghoul, A. A., et al. (2021). Nutritional manipulation to combat heat stress in poultry – a comprehensive review. *J. Therm. Biol.* 98, 102915. doi:10.1016/j.jtherbio.2021.102915

Abidin, Z., and Khatoon, A. (2013). Heat stress in poultry and the beneficial effects of ascorbic acid (Vitamin C) supplementation during periods of heat stress. *Worlds Poult. Sci. J.* 69, 135–151. doi:10.1017/S0043933913000123

Aengwanich, W., and Suttajit, M. (2010). Effect of polyphenols extracted from Tamarind (*Tamarindus indica L.*) seed coat on physiological changes, heterophil/lymphocyte ratio, oxidative stress and body weight of broilers (*Gallus domesticus*) under chronic heat stress. *Animal Sci. J.* 81, 264–270. doi:10.1111/j.1740-0929.2009.00736.x

Akbarian, A., Michiels, J., Degroote, J., Majdeddin, M., Golian, A., and De Smet, S. (2016). Association between heat stress and oxidative stress in poultry; mitochondrial dysfunction and dietary interventions with phytochemicals. *J. Animal Sci. Biotechnol.* 7, 37. doi:10.1186/s40104-016-0097-5

Alagawany, M., Elnesr, S. S., Farag, M. R., Abd El-Hack, M. E., Barkat, R. A., Gabr, A. A., et al. (2021). Potential role of important nutraceuticals in poultry performance and health - a comprehensive review. *Res. Veterinary Sci.* 137, 9–29. doi:10.1016/j.rvsc.2021.04.009

Altan, O., Pabuccuoglu, A., Altan, A., Konyalioglu, S., and Bayraktar, H. (2003). Effect of heat stress on oxidative stress, lipid peroxidation and some stress parameters in broilers. *Br. Poult. Sci.* 44, 545–550. doi:10.1080/00071660310001618334

Aria, M., and Cuccurullo, C. (2017). bibliometrix: An R-tool for comprehensive science mapping analysis. *J. Inf.* 11, 959–975. doi:10.1016/j.joi.2017.08.007

Attia, Y. A. E. W., De Oliveira, M. C., Abd El-Hamid, A. E. H. E., Al-Harthi, M. A., Alaqil, A., and Mohammed, N. A. E. M. (2021). Cyclical heat stress and enzyme supplementation affect performance and physiological traits of Japanese quail during the early stage of laying. *Animal Sci. Pap. Rep.* 39, 89–100.

Azad, M. A. K., Kikusato, M., Maekawa, T., Shirakawa, H., and Toyomizu, M. (2010). Metabolic characteristics and oxidative damage to skeletal muscle in broiler chickens exposed to chronic heat stress. *Comp. Biochem. Physiology - A Mol. Integr. Physiology* 155, 401–406. doi:10.1016/j.cbpa.2009.12.011

Chanthavixay, G., Kern, C., Wang, Y., Saelao, P., Lamont, S. J., Gallardo, R. A., et al. (2020). Integrated transcriptome and histone modification analysis reveals NDV infection under heat stress affects bursa development and proliferation in susceptible chicken line. *Front. Genet.* 11, 567812. doi:10.3389/fgene.2020.567812

Chen, Y., Long, T., Xu, Q., and Zhang, C. (2021). Bibliometric analysis of ferroptosis in stroke from 2013 to 2021. *Front. Pharmacol.* 12, 817364. doi:10.3389/fphar.2021.817364

Cheng, K., Guo, Q., Shen, Z., Yang, W., Wang, Y., Sun, Z., et al. (2022). Bibliometric analysis of global research on cancer photodynamic therapy: Focus on nano-related research. *Front. Pharmacol.* 13, 927219. doi:10.3389/fphar.2022.927219

Dai, S. F., Gao, F., Zhang, W. H., Song, S. X., Xu, X. L., and Zhou, G. H. (2011). Effects of dietary glutamine and gamma-aminobutyric acid on performance, carcass characteristics and serum parameters in broilers under circular heat stress. *Animal Feed Sci. Technol.* 168, 51–60. doi:10.1016/j.anifeedsci.2011.03.005

Ejaz, H., Zeeshan, H. M., Ahmad, F., Bukhari, S. N. A., Anwar, N., Alanazi, A., et al. (2022). Bibliometric analysis of publications on the omicron variant from 2020 to 2022 in the Scopus database using R and VOSviewer. *Int. J. Environ. Res. Public Health* 19, 12407. doi:10.3390/ijerph191912407

Farag, M. R., and Alagawany, M. (2018). Physiological alterations of poultry to the high environmental temperature. *J. Therm. Biol.* 76, 101–106. doi:10.1016/j.jtherbio.2018.07.012

Han, J., Kang, H.-J., Kim, M., and Kwon, G. H. (2020). Mapping the intellectual structure of research on surgery with mixed reality: Bibliometric network analysis (2000–2019). *J. Biomed. Inf.* 109, 103516. doi:10.1016/j.jbi.2020.103516

Jastrebski, S. F., Lamont, S. J., and Schmidt, C. J. (2017). Chicken hepatic response to chronic heat stress using integrated transcriptome and metabolome analysis. *PLoS ONE* 12, e0181900. doi:10.1371/journal.pone.0181900

Jiang, S., Yan, F. F., Hu, J. Y., Mohammed, A., and Cheng, H. W. (2021). Bacillus subtilis-based probiotic improves skeletal health and immunity in broiler chickens exposed to heat stress. *Animals* 11, 1494. doi:10.3390/ani11061494

Kim, H., Kim, H., Seong, P., Arora, D., Shin, D., Park, W., et al. (2021). Transcriptomic response under heat stress in chickens revealed the regulation of genes and alteration of metabolism to maintain homeostasis. *Animals* 11, 2241. doi:10.3390/ani11082241

Kumar, M., Ratwan, P., Dahiya, S. P., and Nehra, A. K. (2021). Climate change and heat stress: Impact on production, reproduction and growth performance of poultry and its mitigation using genetic strategies. *J. Therm. Biol.* 97, 102867. doi:10.1016/j.jtherbio.2021.102867

Lan, P. T. N., Sakamoto, M., and Benno, Y. (2004). Effects of two probiotic Lactobacillus strains on jejunal and cecal microbiota of broiler chicken under acute heat stress condition as revealed by molecular analysis of 16S rRNA genes. *Microbiol. Immunol.* 48, 917–929. doi:10.1111/j.1348-0421.2004.tb03620.x

Lara, L., and Rostagno, M. (2013). Impact of heat stress on poultry production. *Animals* 3, 356–369. doi:10.3390/ani3020356

Leishman, E. M., Ellis, J., van Staaveren, N., Barbut, S., Vanderhout, R. J., Osborne, V. R., et al. (2021). Meta-analysis to predict the effects of temperature stress on meat quality of poultry. *Poult. Sci.* 100, 101471. doi:10.1016/j.psj.2021.101471

Liang, Z. L., Jin, Y. Y., Guo, Y., Qiu, S. J., Zhao, Y., Zhao, Z. H., et al. (2021). Heat stress affects duodenal microbial community of indigenous yellow-feather broilers as determined by 16S rRNA sequencing. *Italian J. Animal Sci.* 20, 1222–1231. doi:10.1080/1828051X.2021.1970034

Lin, H., Jiao, H. C., Buyse, J., and Decuypere, E. (2006). Strategies for preventing heat stress in poultry. *Worlds Poult. Sci. J.* 62, 71–86. doi:10.1079/WPS200585

Liu, F. H., Yu, C. H., and Chang, Y. C. (2022). Bibliometric analysis of articles published in journal of dental sciences from 2009 to 2020. *J. Dent. Sci.* 17, 642–646. doi:10.1016/j.jds.2021.08.002

Liu, L., Ren, M., Ren, K., Jin, Y., and Yan, M. (2020). Heat stress impacts on broiler performance: A systematic review and meta-analysis. *Poult. Sci.* 99, 6205–6211. doi:10.1016/j.psj.2020.08.019

Liu, W. C., Guo, Y., An, L. L., and Zhao, Z. H. (2021). Protective effects of dietary betaine on intestinal barrier function and cecal microbial community in indigenous broiler chickens exposed to high temperature environment. *Environ. Sci. Pollut. Res.* 28, 10860–10871. doi:10.1007/s11356-020-11326-6

Lu, Z., He, X. F., Ma, B. B., Zhang, L., Li, J. L., Jiang, Y., et al. (2017). Chronic heat stress impairs the quality of breast-muscle meat in broilers by affecting redox status and energy-substance metabolism. *J. Agric. Food Chem.* 65, 11251–11258. doi:10.1021/acs.jafc.7b04428

Lu, Z., He, X. F., Ma, B. B., Zhang, L., Li, J. L., Jiang, Y., et al. (2019). The alleviative effects and related mechanisms of taurine supplementation on growth performance and carcass characteristics in broilers exposed to chronic heat stress. *Poult. Sci.* 98, 878–886. doi:10.3382/ps/pey433

Ma, B. B., He, X. F., Lu, Z., Zhang, L., Li, J. L., Jiang, Y., et al. (2018). Chronic heat stress affects muscle hypertrophy, muscle protein synthesis and uptake of amino acid in broilers via insulin like growth factor-mammalian target of rapamycin signal pathway. *Poult. Sci.* 97, 4150–4158. doi:10.3382/ps/pey291

Ma, B. B., Zhang, L., Li, J. L., Xing, T., Jiang, Y., and Gao, F. (2021). Heat stress alters muscle protein and amino acid metabolism and accelerates liver gluconeogenesis for energy supply in broilers. *Poult. Sci.* 100, 215–223. doi:10.1016/j.psj.2020.09.090

Ma, R. (2012). Author bibliographic coupling analysis: A test based on a Chinese academic database. *J. Inf.* 6, 532–542. doi:10.1016/j.joi.2012.04.006

Madkour, M., Aboelazab, O., Abd El-Azeem, N., Younis, E., and Shourrap, M. (2023). Growth performance and hepatic antioxidants responses to early thermal conditioning in broiler chickens. *J. Anim. Physiol. Anim. Nutr. Berl.* 107, 182–191. doi:10.1111/jpn.13679

Madkour, M., Salman, F. M., El-Wardany, I., Abdel-Fattah, S. A., Alagawany, M., Hashem, N. M., et al. (2022). Mitigating the detrimental effects of heat stress in poultry through thermal conditioning and nutritional manipulation. *J. Therm. Biol.* 103, 103169. doi:10.1016/j.jtherbio.2021.103169

Mahmoud, K. Z., Edens, F. W., Eisen, E. J., and Havenstein, G. B. (2004). Ascorbic acid decreases heat shock protein 70 and plasma corticosterone response in broilers (*Gallus gallus domesticus*) subjected to cyclic heat stress. *Comp. Biochem. Physiology B-Biochemistry Mol. Biol.* 137, 35–42. doi:10.1016/j.cbpc.2003.09.013

Moeini, M. M., Bahrami, A., Ghazi, S., and Targhibi, M. R. (2011). The effect of different levels of organic and inorganic chromium supplementation on production performance, carcass traits and some blood parameters of broiler chicken under heat stress condition. *Biol. Trace Elem. Res.* 144, 715–724. doi:10.1007/s12011-011-9116-8

Mohammadi, F. (2021). Effect of different levels of clove (*Syzygium aromaticum L.*) essential oil on growth performance and oxidative/nitrosative stress biomarkers in broilers under heat stress. *Trop. Animal Health Prod.* 53, 84. doi:10.1007/s11250-020-02517-x

Mohiti-Asli, M., Shariatmadari, F., and Lotfollahian, H. (2010). The influence of dietary vitamin E and selenium on egg production parameters, serum and yolk cholesterol and antibody response of laying hen exposed to high environmental temperature. *Arch. fur Geflugelkd.* 74, 43–50.

Monson, M. S., Van Goor, A. G., Ashwell, C. M., Persia, M. E., Rothschild, M. F., Schmidt, C. J., et al. (2018). Immunomodulatory effects of heat stress and lipopolysaccharide on the bursal transcriptome in two distinct chicken lines. *BMC Genomics* 19, 643. doi:10.1186/s12864-018-5033-y

Monson, M. S., Van Goor, A. G., Persia, M. E., Rothschild, M. F., Schmidt, C. J., and Lamont, S. J. (2019). Genetic lines respond uniquely within the chicken thymic transcriptome to acute heat stress and low dose lipopolysaccharide. *Sci. Rep.* 9, 13649. doi:10.1038/s41598-019-50051-0

Mujahid, A., Yoshiki, Y., Akiba, Y., and Toyomizu, M. (2005). Superoxide radical production in chicken skeletal muscle induced by acute heat stress. *Poult. Sci.* 84, 307–314. doi:10.1093/ps/84.2.307

Musa, T. H., Ahmad, T., Li, W., Kawuki, J., Wana, M. N., Musa, H. H., et al. (2020). A bibliometric analysis of global scientific research on scrub typhus. *Biomed. Res. Int.* 2020, 5737893. doi:10.1155/2020/5737893

Nawab, A., Tang, S., Li, G., An, L., Wu, J., Liu, W., et al. (2020). Dietary curcumin supplementation effects on blood immunological profile and liver enzymatic activity of laying hens after exposure to high temperature conditions. *J. Therm. Biol.* 90, 102573. doi:10.1016/j.jtherbio.2020.102573

Nawaz, A. H., Amoah, K., Leng, Q. Y., Zheng, J. H., Zhang, W. L., and Zhang, L. (2021). Poultry response to heat stress: Its physiological, metabolic, and genetic implications on meat production and quality including strategies to improve broiler production in a warming world. *Front. veterinary Sci.* 8, 699081. doi:10.3389/fvets.2021.699081

Nicolaisen, J. (2010). Bibliometrics and citation analysis: From the science citation index to cybermetrics. *JASIST* 61, 205–207. doi:10.1002/asi.21181

Niu, Z. Y., Liu, F. Z., Yan, Q. L., and Li, W. C. (2009). Effects of different levels of vitamin E on growth performance and immune responses of broilers under heat stress. *Poult. Sci.* 88, 2101–2107. doi:10.3382/ps.2009-00220

Oke, O. E., Uyanga, V. A., Iyasere, O. S., Oke, F. O., Majokdunmi, B. C., Logunleko, M. O., et al. (2021). Environmental stress and livestock productivity in hot-humid tropics: Alleviation and future perspectives. *J. Therm. Biol.* 100, 103077. doi:10.1016/j.jtherbio.2021.103077

Orhan, C., Sahin, N., Sahin, K., and Kucuk, O. (2021). Influence of dietary genistein and polyunsaturated fatty acids on lipid peroxidation and fatty acid composition of meat in quail exposed to heat stress. *Trop. Animal Health Prod.* 53, 494. doi:10.1007/s11250-021-02933-7

Pena, J. E. M., Vieira, S. L., Lopez, J., Reis, R. N., Barros, R., Furtado, F. V. F., et al. (2008). Ascorbic acid and citric flavonoids for broilers under heat stress: Effects on performance and meat quality. *Braz. J. Poult. Sci.* 10, 125–130. doi:10.1590/s1516-635x2008000200008

Piray, A., and Foroutanifar, S. (2021). Chromium supplementation on the growth performance, carcass traits, blood constituents, and immune competence of broiler chickens under heat stress: A systematic review and dose–response meta-analysis. *Biol. Trace Elem. Res.* 200, 2876–2888. doi:10.1007/s12011-021-02885-x

Quinteiro-Filho, W. M., Ribeiro, A., Ferraz-de-Paula, V., Pinheiro, M. L., Sakai, M., Sá, L. R. M., et al. (2010). Heat stress impairs performance parameters, induces intestinal injury, and decreases macrophage activity in broiler chickens. *Poult. Sci.* 89, 1905–1914. doi:10.3382/ps.2010-00812

Saeed, M., Abbas, G., Alagawany, M., Kamboh, A. A., Abd El-Hack, M. E., Khafaga, A. F., et al. (2019). Heat stress management in poultry farms: A comprehensive overview. *J. Therm. Biol.* 84, 414–425. doi:10.1016/j.jtherbio.2019.07.025

Saelao, P., Wang, Y., Chanthavixay, G., Yu, V., Gallardo, R. A., Dekkers, J. C. M., et al. (2018). Integrated proteomic and transcriptomic analysis of differential expression of chicken lung tissue in response to NDV infection during heat stress. *Genes* 9, 579. doi:10.3390/genes9120579

Sahin, K., and Kucuk, O. (2003). Zinc supplementation alleviates heat stress in laying Japanese quail. *J. Nutr.* 133, 2808–2811. doi:10.1093/jn/133.9.2808

Sahin, K., Orhan, C., Akdemir, F., Tuzcu, M., Iben, C., and Sahin, N. (2012). Resveratrol protects quail hepatocytes against heat stress: Modulation of the Nrf2 transcription factor and heat shock proteins. *J. Animal Physiology Animal Nutr.* 96, 66–74. doi:10.1111/j.1439-0396.2010.01123.x

Sahin, K., Orhan, C., Smith, M. O., and Sahin, N. (2013). Molecular targets of dietary phytochemicals for the alleviation of heat stress in poultry. *Worlds Poult. Sci. J.* 69, 113–124. doi:10.1017/S004393391300010X

Sahin, K., Sahin, N., Sari, M., and Gursu, M. F. (2002). Effects of vitamins E and A supplementation on lipid peroxidation and concentration of some mineral in broilers reared under heat stress (32°C). *Nutr. Res.* 22, 723–731. doi:10.1016/S0271-5317(02)00376-7

Sahin, N., Hayirli, A., Orhan, C., Tuzcu, M., Akdemir, F., Komorowski, J. R., et al. (2017). Effects of the supplemental chromium form on performance and oxidative stress in broilers exposed to heat stress. *Poult. Sci.* 96, 4317–4324. doi:10.3382/ps/pex249

Sariozkan, S., Guclu, B. K., Konca, Y., Aktug, E., Kaliber, M., Beyzi, S. B., et al. (2020). The effects of thyme oil and vitamin combinations on performance, carcass quality and oxidation parameters in broilers exposed to heat stress. *Ank. Univ. Veteriner Fak. Derg.* 67, 357–364. doi:10.33988/auvfd.626707

Shan, M., Dong, Y., Chen, J., Su, Q., and Wang, Y. (2022). Global tendency and frontiers of research on myopia from 1900 to 2020: A bibliometrics analysis. *Front. Public Health* 10, 846601. doi:10.3389/fpubh.2022.846601

Siddiqui, S. H., Khan, M., Kang, D., Choi, H. W., and Shim, K. (2022). Meta-analysis and systematic review of the thermal stress response: Gallus gallus domesticus show low immune responses during heat stress. *Front. Physiol.* 13, 809648. doi:10.3389/fphys.2022.809648

Sohail, M. U., Ijaz, A., Yousaf, M. S., Ashraf, K., Zaneb, H., Aleem, M., et al. (2010). Alleviation of cyclic heat stress in broilers by dietary supplementation of mannan-oligosaccharide and lactobacillus-based probiotic: Dynamics of cortisol, thyroid hormones, cholesterol, C-reactive protein, and humoral immunity. *Poult. Sci.* 89, 1934–1938. doi:10.3382/ps.2010-00751

Soleimani, A. F., Zulkifli, I., Omar, A. R., and Raha, A. R. (2011). Physiological responses of 3 chicken breeds to acute heat stress. *Poult. Sci.* 90, 1435–1440. doi:10.3382/ps.2011-01381

Srikanth, K., Kumar, H., Park, W., Byun, M., Lim, D., Kemp, S., et al. (2019). Cardiac and skeletal muscle transcriptome response to heat stress in Kenyan chicken ecotypes adapted to low and high altitudes reveal differences in thermal tolerance and stress response. *Front. Genet.* 10, 993. doi:10.3389/fgene.2019.00993

Sun, H. Y., Jiang, R. S., Xu, S. Y., Zhang, Z. B., Xu, G. Y., Zheng, J. X., et al. (2015). Transcriptome responses to heat stress in hypothalamus of a meat-type chicken. *J. Animal Sci. Biotechnol.* 6, 6. doi:10.1186/s40104-015-0003-6

Te Pas, M. F. W., Park, W., Srikanth, K., Kemp, S., Kim, J. M., Lim, D., et al. (2019). Transcriptomic profiles of muscle, heart, and spleen in reaction to circadian heat stress in Ethiopian highland and lowland male chicken. *Cell Stress Chaperones* 24, 175–194. doi:10.1007/s12192-018-0954-6

Tripathi, M., Kumar, S., Sonker, S. K., and Babbar, P. (2018). Occurrence of author keywords and keywords plus in social sciences and humanities research: A preliminary study. *COLLNET J. Sci. Inf. Manag.* 12, 215–232. doi:10.1080/09737766.2018.1436951

Uyanga, V. A., Oke, E. O., Amevor, F. K., Zhao, J., Wang, X., Jiao, H., et al. (2022a). Functional roles of taurine, L-theanine, L-citrulline, and betaine during heat stress in poultry. *J. Animal Sci. Biotechnol.* 13, 23. doi:10.1186/s40104-022-00675-6

Uyanga, V. A., Wang, M., Tong, T., Zhao, J., Wang, X., Jiao, H., et al. (2021). L-citrulline influences the body temperature, heat shock response and nitric oxide regeneration of broilers under thermoneutral and heat stress condition. *Front. Physiology* 12, 671691. doi:10.3389/fphys.2021.671691

Uyanga, V. A., Zhao, J., Wang, X., Jiao, H., Onagbesan, O. M., and Lin, H. (2022b). Dietary L-citrulline modulates the growth performance, amino acid profile, and the growth hormone/insulin-like growth factor axis in broilers exposed to high temperature. *Front. Physiology* 13, 937443. doi:10.3389/fphys.2022.937443

Vakili, R., Rashidi, A. A., and Sobhanirad, S. (2010). Effects of dietary fat, vitamin E and zinc supplementation on tibia breaking strength in female broilers under heat stress. *Afr. J. Agric. Res.* 5, 3151–3156.

van Eck, N. J., and Waltman, L. (2010). Software survey: VOSviewer, a computer program for bibliometric mapping. *Scientometrics* 84, 523–538. doi:10.1007/s11192-009-0146-3

Wallin, J. A. (2005). Bibliometric methods: Pitfalls and possibilities. *Basic & Clin. Pharmacol. Toxicol.* 97, 261–275. doi:10.1111/j.1742-7843.2005.pto_139.x

Wang, G. J., Li, X. M., Zhou, Y., Feng, J. H., and Zhang, M. H. (2021). Effects of heat stress on gut-microbial metabolites, gastrointestinal peptides, glycolipid metabolism, and performance of broilers. *Animals* 11, 1286. doi:10.3390/ani11051286

Wang, Y., Saelao, P., Chanthavixay, K., Gallardo, R., Bunn, D., Lamont, S. J., et al. (2018). Physiological responses to heat stress in two genetically distinct chicken inbred lines. *Poult. Sci.* 97, 770–780. doi:10.3382/ps/pex363

Wang, Y., Saelao, P., Kern, C., Jin, S. H., Gallardo, R. A., Kelly, T., et al. (2020). Liver transcriptome responses to heat stress and newcastle disease virus infection in genetically distinct chicken inbred lines. *Genes* 11, 1067. doi:10.3390/genes11091067

Wasti, S., Sah, N., and Mishra, B. (2020). Impact of heat stress on poultry health and performances, and potential mitigation strategies. *Animals open access J. MDPI* 10, 1266. doi:10.3390/ani10081266

Wen, C., Leng, Z. X., Chen, Y. P., Ding, L. R., Wang, T., and Zhou, Y. M. (2021). Betaine alleviates heat stress-induced hepatic and mitochondrial oxidative damage in broilers. *J. Poult. Sci.* 58, 103–109. doi:10.2141/jpsa.0200003

Xu, J., Huang, B., Tang, S., Sun, J. R., and Bao, E. D. (2019a). Co-enzyme Q10 protects primary chicken myocardial cells from heat stress by upregulating autophagy and suppressing the PI3K/AKT/mTOR pathway. *Cell Stress Chaperones* 24, 1067–1078. doi:10.1007/s12192-019-01029-4

Xu, J., Tang, S., Song, E., Yin, B., Wu, D., and Bao, E. (2017a). Hsp70 expression induced by Co-Enzyme Q10 protected chicken myocardial cells from damage and apoptosis under *in vitro* heat stress. *Poult. Sci.* 96, 1426–1437. doi:10.3382/ps/pew402

Xu, J., Tang, S., Yin, B., Sun, J. R., Song, E. B., and Bao, E. D. (2017b). Co-enzyme Q10 and acetyl salicylic acid enhance Hsp70 expression in primary chicken myocardial cells to protect the cells during heat stress. *Mol. Cell. Biochem.* 435, 73–86. doi:10.1007/s11010-017-3058-1

Xu, J., Yin, B., Huang, B., Tang, S., Zhang, X. H., Sun, J. R., et al. (2019b). Co-enzyme Q10 protects chicken hearts from *in vivo* heat stress via inducing HSF1 binding activity and Hsp70 expression. *Poult. Sci.* 98, 1002–1011. doi:10.3382/ps/pey498

Xu, L., Ding, K., and Lin, Y. (2022). Do negative citations reduce the impact of cited papers? *Scientometrics* 127, 1161–1186. doi:10.1007/s11192-021-04214-4

Yahav, S. (2009). Alleviating heat stress in domestic fowl: Different strategies. *Worlds Poult. Sci. J.* 65, 719–732. doi:10.1017/S004393390900049X

Yang, C., Luo, P., Chen, S. J., Deng, Z. C., Fu, X. L., Xu, D. N., et al. (2021). Resveratrol sustains intestinal barrier integrity, improves antioxidant capacity, and alleviates inflammation in the jejunum of ducks exposed to acute heat stress. *Poult. Sci.* 100, 101459. doi:10.1016/j.psj.2021.101459

Zaboli, G., Huang, X., Feng, X., and Ahn, D. U. (2019). How can heat stress affect chicken meat quality? - a review. *Poult. Sci.* 98, 1551–1556. doi:10.3382/ps/pey399

Zarate, A. J., Moran, E. T., and Burnham, D. J. (2003). Exceeding essential amino acid requirements and improving their balance as a means to minimize heat stress in broilers. *J. Appl. Poult. Res.* 12, 37–44. doi:10.1093/japr/12.1.37

Zhang, J. B., Schmidt, C. J., and Lamont, S. J. (2017). Transcriptome analysis reveals potential mechanisms underlying differential heart development in fast- and slow-growing broilers under heat stress. *BMC Genomics* 18, 295. doi:10.1186/s12864-017-3675-9

Zhang, J., Yu, Q., Zheng, F., Long, C., Lu, Z., and Duan, Z. (2016). Comparing keywords plus of WOS and author keywords: A case study of patient adherence research. *J. Assoc. Inf. Sci. Technol.* 67, 967–972. doi:10.1002/asi.23437

Zhang, Q., Zhang, B., and Luo, Y. (2019). Cardiac transcriptome study of the effect of heat stress in yellow-feather broilers. *Italian J. Animal Sci.* 18, 971–975. doi:10.1080/1828051X.2019.1610338

Zhang, R., and Yuan, J. (2022). Enhanced author bibliographic coupling analysis using semantic and syntactic citation information. *Scientometrics* 127, 7681–7706. doi:10.1007/s11192-022-04333-6

frontiers | Frontiers in Physiology

TYPE Original Research
PUBLISHED 22 March 2023
DOI 10.3389/fphys.2023.1147483



OPEN ACCESS

EDITED BY
Gale Strasburg,
Michigan State University, United States

REVIEWED BY
Giri Athrey,
Texas A&M University, United States
Jiahui Xu,
University of California, Irvine, United States
Eric Wong,
Virginia Tech, United States

*CORRESPONDENCE
Christina L. Swaggerty,
christi.swaggerty@usda.gov

SPECIALTY SECTION
This article was submitted to Avian Physiology, a section of the journal Frontiers in Physiology

RECEIVED 18 January 2023
ACCEPTED 10 March 2023
PUBLISHED 22 March 2023

CITATION
Johnson CN, Arsenault RJ, Piva A, Grilli E and Swaggerty CL (2023), A microencapsulated feed additive containing organic acids and botanicals has a distinct effect on proliferative and metabolic related signaling in the jejunum and ileum of broiler chickens. *Front. Physiol.* 14:1147483. doi: 10.3389/fphys.2023.1147483



# A microencapsulated feed additive containing organic acids and botanicals has a distinct effect on proliferative and metabolic related signaling in the jejunum and ileum of broiler chickens

Casey N. Johnson[1], Ryan J. Arsenault[2], Andrea Piva[3,4], Ester Grilli[3,5] and Christina L. Swaggerty[1]*

[1]Southern Plains Agricultural Research Center, Agricultural Research Service, United States Department of Agriculture, College Station, TX, United States, [2]Department of Animal and Food Sciences, University of Delaware, Newark, DE, United States, [3]DIMEVET, University of Bologna, Bologna, Italy, [4]Vetagro S.p.A, Reggio Emilia, Italy, [5]Vetagro Inc., Chicago, IL, United States

Well designed and formulated natural feed additives have the potential to provide many of the growth promoting and disease mitigating characteristics of in-feed antibiotics, particularly feed additives that elicit their effects on targeted areas of the gut. Here, we describe the mechanism of action of a microencapsulated feed additive containing organic acids and botanicals (AviPlus® P) on the jejunum and ileum of 15-day-old broiler-type chickens. Day-of-hatch chicks were provided *ad libitum* access to feed containing either 0 or 500 g/MT of the feed additive for the duration of the study. Fifteen days post-hatch, birds were humanely euthanized and necropsied. Jejunum and ileum tissue samples were collected and either flash frozen or stored in RNA-later as appropriate for downstream applications. Chicken-specific kinome peptide array analysis was conducted on the jejunum and ileum tissues, comparing the tissues from the treated birds to those from their respective controls. Detailed analysis of peptides representing individual kinase target sites revealed that in the ileum there was a broad increase in the signal transduction pathways centering on activation of HIF-1α, AMPK, mTOR, PI3K-Akt and NFκB. These signaling responses were largely decreased in the jejunum relative to control birds. Gene expression analysis agrees with the kinome data showing strong immune gene expression in the ileum and reduced expression in the jejunum. The microencapsulated blend of organic acids and botanicals elicit a more anti-inflammatory phenotype and reduced signaling in the jejunum while resulting in enhanced immunometabolic responses in the ileum.

KEYWORDS

**broiler chicken, antibiotic alternatives, botanicals (thymol and vanillin), essential oils, organic acids (citric and sorbic), immunometabolism, kinome, gut health**

# 1 Introduction

Natural products are being explored as potential antibiotic alternatives for use in animal agriculture. Promising alternatives include, but are not limited to, organic acids, botanicals, short chain fatty acids, and bacterial fermentates (Postbiotics) (Johnson et al., 2019; Swaggerty et al., 2020a; 2020b; Liu et al., 2021; Salminen et al., 2021). These natural products have been used and evaluated in the animal agriculture industry for a number of years and numerous primary and review articles in the literature support the use of such products for use as antibiotic alternatives, to enhance production parameters, and improve animal health and welfare (Zeng, et al., 2015; Abd El-Hack et al., 2016; Jazi et al., 2018; Yadav and Jha, 2019). Extensive studies are being conducted to measure and evaluate the performance enhancing and disease mitigating effects of these products (EFSA Panel et al., 2020 on Additives and Products or Substances used in Animal Feed (FEEDAP); Swaggerty et al., 2020a; 2020b; 2022). Microencapsulated feed additives have been shown to allow such products to survive the upper gastrointestinal tract (GI tract) and be delivered along the small intestine (Grilli et al., 2007; Piva et al., 2007). The small intestine is the main site of digestion and nutrient absorption in chickens (Svihus, 2014). The different gut segments have been reported to serve different functions in relation to nutrient absorption, with the jejunum being the major site of absorption of fat, starch, and protein, and the ileum, anatomically following the jejunum, being the major site of water and mineral absorption (Svihus, 2014). Although microencapsulation allows for the product to be delivered to the small intestine, the concentration of included compounds have been shown to decrease down the length of the gut (Grilli et al., 2007; Piva et al., 2007).

The chicken-specific kinome peptide array and accompanying software are designed to measure and evaluate the immunometabolic signaling changes that occur between treatment and control groups (Jalal et al., 2009; Li et al., 2012). The technology utilizes 15 amino acid (AA) long peptides from the chicken proteome corresponding to known kinase target sites in the human proteome (orthologues sequences). Kinases are enzymes which catalyze phosphorylation events, the transfer of a phosphate group from ATP to a target protein, and act as key regulators of cell signaling. This post-translational modification can act to increase or inhibit the target protein's activity and modulate its capacity to interact with other molecules. Proteins also can contain multiple kinase target sites sometimes with complementary or enhancing functions and sometimes with antagonistic or competing functions. In the peptide array assay, active kinases in the samples phosphorylate their target sites represented on the array. Many sites on the array have known physiological functions in the human phospho-proteome and therefore can provide valuable insight into chicken intracellular signaling cascades and thus physiological changes between treatment groups (Jalal et al., 2009). Using a kinomic approach to explore the changes to intracellular signaling cascades associated with immune and metabolic processes in response to the blend, we are able to better understand the changes conferred resulting in improved production measures and disease outcomes (Swaggerty et al., 2020a; Swaggerty et al., 2022).

There is a well-documented complex interplay between cellular metabolism and immunity and *vice versa*, the study of which is deemed immunometabolism (Pearce and Pearce, 2013). The emphasis on immunometabolic signaling allows researchers to look closely at the immune and metabolic changes imparted by products, therapeutics, and diseases in tissues (*in vivo*), cell populations (*ex vivo*), or monocultures (*in vitro*). Using the immunometabolic chicken-specific kinome peptide array we are able to elucidate differences in key cell signaling cascades which can provide insight into the immune and metabolic alterations imparted under different treatment conditions. Thus, providing insight into potential mode-of-action.

In a previous study, our group determined the kinome profile of jejunum and ileum tissue samples from birds fed the microencapsulated blend of organic acids and botanicals compared to corresponding tissue samples from control fed birds. That analysis provided the framework for the present study, providing valuable insight into the changes in cell signaling pathways conferred by the product and highlighting the presence of a distinction between the tissue responses (Swaggerty et al., 2020a). The objectives of the current study were to further characterize the mechanism of action of this microencapsulated blend of organic acids and botanicals by defining the site-specific changes in phosphorylation status of proteins and inferring the physiological consequences of those changes. Further elucidating the mode of action of these products will allow us to create more efficacious health promoting products that will help mitigate foodborne and poultry diseases while increasing production efficiency.

# 2 Materials and methods

## 2.1 Experimental design and chickens

Trial was conducted as previously reported (Swaggerty et al., 2020a) and briefly summarized here. Day-of-hatch by-product broiler breeder chicks (from here on referred to simply as broilers) were obtained from a commercial hatchery (Timpson, TX). Chicks were placed in 3 m × 3 m floor pens containing pine shavings and provided *ad libitum* access to feed and water throughout the study. Chicks were fed a corn and soybean meal starter diet that met or exceeded the established nutrient requirements of poultry (National Research Council, 1994). Control birds were fed a non-supplemented diet while treatment birds were fed the same diet base supplemented with 500 g/metric ton (MT) of a commercially available lipid-microencapsulated blend of citric (25%) and sorbic (16.7%) acids, thymol (1.7%), and vanillin (1.0%) (AviPlus®*p*, Vetagro S. p.A, Reggio Emilia, Italy). Two replicate trials were conducted. From each replicate trial control (n = 10) and treatment (n = 10) birds were euthanized by cervical dislocation and necropsied at 15 days post hatch. Sampling time was established based on previous work (Grilli et al., 2015; Swaggerty et al., 2020a) and in consideration of the productive cycle of broilers. In a commercial setting, the first diet change typically occurs between 10 and 15 days-of-age. Additionally, the first 2 weeks of grow out are critical to the development of the gastrointestinal and immunological function and by 2–3 weeks of age broilers are considered mature. All bird studies were overseen by the on-site

attending veterinarian under the approved experimental procedures outlined in protocol #2017008 and were approved by the USDA/ARS Institutional Animal Care and Use Committee. The IACUC operates under the Animal and Plant Health Inspection Service (APHIS) establishment number 334299. The experiments were conducted in accordance with the recommended code of practice for the care and handling of poultry and followed the ethical principles according to the Guide for the Care and Use of Agricultural Animals in Research and Teaching, fourth edition (Ag Guide, 2020).

During necropsy, jejunum and ileum samples were taken and stored for later use. Samples for the kinome peptide array protocol were flash frozen in liquid nitrogen and stored at -80°C. Samples for quantitative real-time RT-PCR (qRT-PCR) were placed in RNA-Later (Qiagen, Valencia, CA) and stored at -20°C for later use.

## 2.2 Chicken-specific immunometabolic kinome peptide array

Kinome peptide array protocol was carried out as previously described (Arsenault et al., 2017) and briefly summarized here. Samples from 5 birds per replicate trial (n = 10) were used to represent each treatment group, the same birds were used for both tissues (jejunum and ileum). Tissue samples (40 mg) were submerged in PBS and vortexed to clear the sample of any gut contents and homogenized by a Bead Ruptor 24 homogenizer (Omni International, Kennesaw, GA) in 100 µL of lysis buffer containing protease inhibitors. An activation mix containing ATP was then added to the lysate and applied to peptide arrays. Peptide arrays have 771 15-mer peptides each printed 9 times per array. These peptides represent known kinase target sites. Kinases present in our samples are able to phosphorylate target peptides using the ATP supplied in the activation mix. Arrays were then incubated at 37°C with 5% CO2 in a humidity chamber, allowing kinases in the samples to phosphorylate their target sites. Samples were then washed and a phospho-specific florescent stain was applied. Stain not bound to phosphorylated sites was removed *via* a de-staining process. Arrays were then imaged using a Tecan PowerScanner microarray scanner (Tecan Systems, San Jose, CA) at 532–560 nm with a 580-nm filter to detect dye fluorescence.

GenePix Pro software (Molecular Devices, San Jose, CA) was then used to grid the array images, ensuring peptide spots were correctly associated with their phosphorylation site and the spot intensity signal was collected. Greater intensity florescence correlates to greater phosphorylation at the target site. Florescent intensities for treatments were then compared with those for controls using the data normalization and analysis program, Platform for Intelligent, Integrated Kinome Analysis 2 (PIIKA 2) (Li et al., 2012; Trost et al., 2013). PIIKA two performs data normalization and variance stabilization prior to making specified comparisons to generate fold-change values (treatment/control) and significance values (*p*-value). *p*-values are calculated *via* one-sided paired *t*-test between treatment and control for a given peptide. The resulting data output was then used in downstream applications such as Search Tool for the Retrieval of Interacting Genes/Proteins (STRING) (Szklarczyk et al., 2021) and Kyoto Encyclopedia of Genes and Genomes (KEGG) (Kanehisa et al., 2021) databases used to pinpoint changes in protein-protein interactions and signal transduction pathways.

## 2.3 RNA extraction for quantitative real-time reverse transcription polymerase chain reaction

Jejunum and ileum tissue samples (30–40 mg) were placed in BeadBugTM tubes (#Z763799-50 EA, Sigma-Aldrich®, St. Lois, MO). Lysis buffer (600 µL; RNeasy Mini Kit; Qiagen) was added and the samples were homogenized in the Omni International Bead Ruptor Elite (Kennesaw, GA) on speed setting six for 2 min. Total RNA was then isolated from the homogenized samples according to the manufacturer's instructions, eluted with 50 µL of RNase-free water, and stored at -80°C until quantitative real-time reverse transcription polymerase chain reaction (qRT-PCR) analyses were performed.

## 2.4 Quantitative real-time RT-PCR for mRNA expression

mRNA expression was analyzed for Interferon gamma (IFNγ), Interleukin 4 (IL-4), and Hypoxia Inducible Factor 1 alpha (HIF-1α) in jejunum and ileum. All primer and probe sequences are provided in Table 1. Genes of interest were selected due to up and downstream relation to pathways of interest identified during the kinome peptide

**TABLE 1** Primer and probe sequences for qRT PCR.

| RNA target | Forward (5′ to 3′) | Reverse (5′ to 3′) | Probe (5′ to 3′) | References | Accession # |
|---|---|---|---|---|---|
| 28s | GGC GAA GCC AGA GGA AAC T | GAC CGA TTT GCA CGT C | 6FAM-AGG ACC GCT ACG GAC CTC CAC CA-TAMRA | Kaiser et al. (2000) | X59,733 |
| IFNy | GTG AAG GTG AAA GAT ATC ATG GA | GCT TTG CGC TGG ATT CTC A | 6FAM-TGG CCA AGC TCC CGA TGA ACG A-TAMRA | Kaiser et al. (2000) | Y07922 |
| IL-4 | AAC ATG CGT CAG CTC CTG AAT | TCT GCT AGG AAC TTC TCC ATT GAA | 6FAM-AGC AGC ACC TCC CTC AAG GCA CC-TAMRA | Avery et al. (2004) | AJ621735 |
| HIF-1α | GCA GAC TCA GAC ACC ATC AA | GGA CAG GAG ATG GAA CAA | 6FAM-TGG CAG AAC GTG TGG ATG TGA -TAMRA | Present Study | NM_204,297 |

array data analysis. The qRT-PCR was performed using the TaqMan one-step RT-PCR master mix reagents (Applied Biosystems, Branchburg, NJ). Amplification and detection of specific products were performed using the Applied Biosystems 7,500 Fast Real-Time PCR System with the following cycle profile: one cycle of 48°C for 30°min and 95°C for 20°s and 40 cycles of 95°C for 3°s and 60°C for 30 s. Quantification was based on the increased fluorescence detected by the 7,500 Fast Sequence Detection System due to hydrolysis of the target-specific probes by the 5′ nuclease activity of the rTth DNA polymerase during PCR amplification. Sample standardization was done using 28 S RNA. Results were calculated as 40-cycle threshold (CT) for each tissue sample from control- and supplement-fed chickens and the data are presented as the fold-change from controls. Fold change was calculated as 2(supplement-fed corrected mean–control-fed corrected mean) for each tissue.

# 3 Results

## 3.1 Kinome analysis

### 3.1.1 Protein and peptide assessment

Statistically significant differentially phosphorylated peptides were identified by kinome peptide array analysis in ileum and jejunum tissue samples collected. The Venn diagrams shown in Figure 1 highlight the differential treatment effect between the two tissues. The overlapping and distinct alterations in phosphorylation events on proteins represented on the array are shown in Figure 1A while the distinct and overlapping peptides represented on the array with significantly altered phosphorylation status are shown in Figure 1B. Using both Venn diagrams, the distinction between significant changes to individual protein phosphorylation status and changes to different peptides on those proteins can begin to be observed.

Figure 1A shows that the largest proportion of proteins with statistically significant differential phosphorylation events between treatment and control tissues (219 proteins) are shared between the two tissues (46.9%). While a large proportion (35.4%) of the peptides significantly differentially phosphorylated are indeed overlapping between the two tissues (234 peptides) (Figure 1B), the largest proportion (46.9%) are significantly differentially phosphorylated in the ileal tissue (310 peptides). The remaining 17.7% of significantly differentially phosphorylated peptides are in the jejunum (117 peptides).

A visualization comparison of the kinome results from the ileum and jejunum was generated by PIIKA two showing the phosphorylation level of each spot compared to control (Figure 2) (Trost et al., 2013). Ileum phosphorylation level is represented on the left side of each circle while jejunum phosphorylation level is on the right side. Figure 2 shows that ~52% of the peptides on the array share a common phosphorylation status in both ileum and jejunum (or is not statistically significant). The other ~48% of the peptides show a differential phosphorylation state between jejunum and ileum; i.e. increased in one and decreased in the other (or is not statistically significant). This relatively large proportion of peptides that display opposite phosphorylation status between the two tissues indicates distinct responses to the product and/or an effect of delivery of the product down the GI tract.

Collectively, the Venn diagrams show that even though the same proteins are affected in the two tissues they are likely to have different peptides being differentially phosphorylated between the tissues. Additionally, the peptides shared between the tissues in Figure 1B may be differentially phosphorylated in opposite directions, as indicated in Figure 2. Taken together, these figures show that the treatment has a distinct effect between the two tissues, including differential effects on the same proteins.

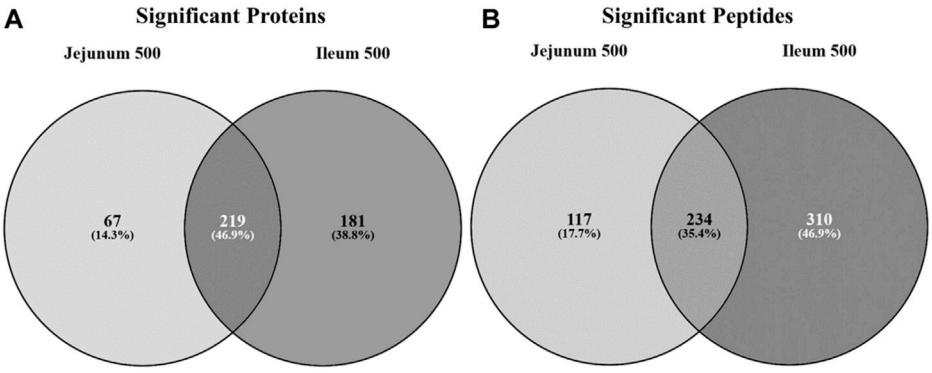


FIGURE 1
Venn diagram of significantly differentially phosphorylated proteins and peptides in ileum and jejunum from birds provided feed supplemented with 500 g/MT of a microencapsulated blend of organic acids and botanicals compared to their respective controls fed a non-supplemented diet at 15 days post-hatch. Kinase target peptides are printed on the array and are phosphorylated by active kinases; there are multiple peptides present on the array for a given protein. Proteins **(A)** and peptides **(B)** statistically significantly differentially phosphorylated in jejunum and ileum from birds fed product containing feed ($p < 0.05$) from their respective control tissue were input into the Venn diagram-generating program Venny (http://bioinfogp.cnb.csic.es/tools/venny/).

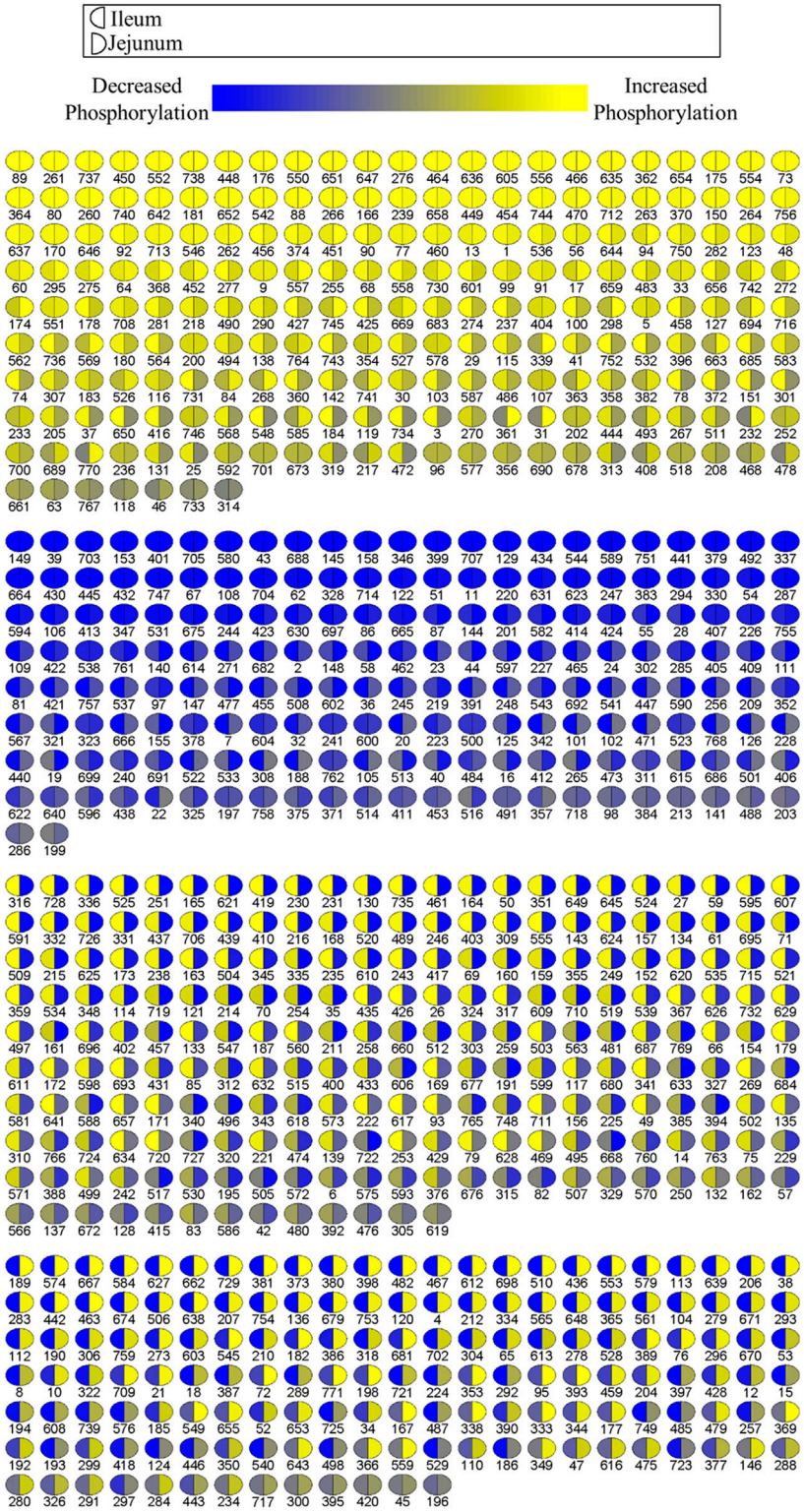


FIGURE 2
Comparison of relative phosphorylation of array peptides between ileum and jejunum due to product. Each spot represents a peptide on the array which corresponds to a kinase recognition site. The left half of each spot shows the differential phosphorylation status relative to control birds for ileum. The right side of each spot shows the phosphorylation status relative to control birds for jejunum.

### 3.1.2 KEGG and reactome pathways

The proteins significantly altered for each tissue (relative to control) were input into the STRING protein-protein interaction database to generate a list of KEGG pathways overrepresented in the data (Szklarczyk et al., 2021) highlighting the physiology and response to stimuli within a

10.3389/fphys.2023.1147483

**TABLE 2 Top 30 KEGG Pathways Enriched in Jejunum and Ileum. The top 30 KEGG pathways, as determined by STRING, for each tissue are represented here. Proteins showing statistically significant differential phosphorylation status between treatment and control fed birds for each tissue were provided to STRING for protein-protein interaction analysis. False Discovery Rate (fdr) is a significance metric (*p*-value) provided by STRING. *p*-values are generated using the Benjamini–Hochberg procedure. Key pathways in immune and metabolic regulation have been bolded.**

| Top 30 KEGG pathways in jejunum | | Top 30 KEGG pathways in ileum | |
|---|---|---|---|
| KEGG pathway | fdr | KEGG pathway | fdr |
| **MAPK signaling pathway** | **4.93E-39** | Pathways in cancer | 6.03E-41 |
| **PI3K-Akt signaling pathway** | **2.32E-32** | **MAPK signaling pathway** | **2.66E-36** |
| Pathways in cancer | 2.32E-32 | MicroRNAs in cancer | 1.64E-32 |
| **Insulin signaling pathway** | **1.90E-29** | **PI3K-Akt signaling pathway** | **1.81E-32** |
| Ras signaling pathway | 3.25E-29 | **Insulin signaling pathway** | **4.70E-31** |
| ErbB signaling pathway | 1.12E-28 | Hepatitis B | 1.84E-27 |
| MicroRNAs in cancer | 1.68E-28 | Proteoglycans in cancer | 1.53E-26 |
| Neurotrophin signaling pathway | 1.28E-26 | **HIF-1 signaling pathway** | **2.83E-26** |
| Hepatitis B | 3.58E-25 | **Central carbon metabolism in cancer** | **2.83E-26** |
| **Central carbon metabolism in cancer** | **5.20E-24** | ErbB signaling pathway | 1.21E-25 |
| Growth hormone synthesis, secretion and action | 6.37E-24 | Shigellosis | 3.87E-25 |
| PD-L1 expression and PD-1 checkpoint pathway in cancer | 3.58E-23 | **AMPK signaling pathway** | **5.89E-25** |
| EGFR tyrosine kinase inhibitor resistance | 4.94E-23 | Neurotrophin signaling pathway | 1.70E-24 |
| Focal adhesion | 1.09E-22 | Kaposi sarcoma-associated herpesvirus infection | 1.70E-24 |
| T cell receptor signaling pathway | 5.70E-22 | Human cytomegalovirus infection | 2.64E-24 |
| Chemokine signaling pathway | 2.43E-21 | EGFR tyrosine kinase inhibitor resistance | 4.04E-24 |
| Proteoglycans in cancer | 1.01E-19 | Ras signaling pathway | 7.86E-24 |
| Acute myeloid leukemia | 2.19E-19 | *Yersinia* infection | 1.47E-23 |
| **HIF-1 signaling pathway** | **3.06E-19** | T cell receptor signaling pathway | 1.13E-22 |
| Kaposi sarcoma-associated herpesvirus infection | 3.06E-19 | FoxO signaling pathway | 2.37E-22 |
| Insulin resistance | 3.39E-19 | Prostate cancer | 3.94E-22 |
| Prostate cancer | 5.73E-19 | Insulin resistance | 3.98E-22 |
| FoxO signaling pathway | 7.68E-19 | Hepatitis C | 4.62E-22 |
| Human cytomegalovirus infection | 1.08E-18 | PD-L1 expression and PD-1 checkpoint pathway in cancer | 6.19E-22 |
| Autophagy - animal | 1.16E-18 | Focal adhesion | 4.49E-21 |
| **mTOR signaling pathway** | **2.28E-18** | Chemokine signaling pathway | 6.24E-21 |
| Prolactin signaling pathway | 5.79E-18 | Osteoclast differentiation | 8.12E-21 |
| Glioma | 1.13E-17 | Glucagon signaling pathway | 1.22E-20 |
| Rap1 signaling pathway | 1.36E-17 | Growth hormone synthesis, secretion and action | 3.78E-20 |
| B cell receptor signaling pathway | 4.03E-17 | Rap1 signaling pathway | 5.80E-20 |

specific tissue. The top 30 overrepresented KEGG pathways for each tissue are shown in Table 2. Many of the top pathways in both tissues are broadly related to growth and proliferation (Mitogen-activated protein kinase (MAPK), cancer, phosphatidylinositol 3-kinase- RAC (Rho family)-alpha serine/threonine-protein kinase (PI3k-Akt)) and specifically glucose metabolism (insulin, central carbon metabolism in cancer, Hypoxia-Inducible Factor-1 (HIF-1) signaling). As these pathways represent a physiological response centered around growth/proliferation and glucose metabolism and, as we have reported previously (Perry et al., 2020), glycolysis is closely related to inflammation and innate immunity, these pathways were considered in more detail.

**TABLE 3 Top 30 Reactome Pathways Enriched in Jejunum and Ileum. The top 30 Reactome pathways, as determined by STRING, for each tissue are represented here. Proteins showing statistically significant differential phosphorylation status between treatment and control fed birds for each tissue were provided to STRING for protein-protein interaction analysis. False Discovery Rate (fdr) is a significance metric (*p*-value) provided by STRING. *p*-values are generated using the Benjamini–Hochberg procedure. Key pathways in immune and metabolic regulation have been bolded.**

| Top 30 reactome pathways in jejunum | | Top 30 reactome pathways in ileum | |
|---|---|---|---|
| Reactome pathway | fdr | Reactome pathway | fdr |
| Signaling by Receptor Tyrosine Kinases | 6.23E-38 | **Immune System** | 5.27E-42 |
| Signal Transduction | 6.25E-36 | Signal Transduction | 9.23E-40 |
| **Immune System** | **3.25E-35** | Signaling by Receptor Tyrosine Kinases | 1.16E-38 |
| Disease | 1.13E-30 | **Innate Immune System** | **3.81E-33** |
| Diseases of signal transduction by growth factor receptors and second messengers | 1.16E-29 | **Cytokine Signaling in Immune system** | **4.35E-33** |
| **Innate Immune System** | **7.67E-29** | Disease | 1.51E-31 |
| **MAPK family signaling cascades** | **2.49E-26** | Signaling by Interleukins | 1.88E-31 |
| Signaling by Interleukins | 7.62E-25 | Diseases of signal transduction by growth factor receptors and second messengers | 1.13E-28 |
| **Cytokine Signaling in Immune system** | **1.46E-24** | Intracellular signaling by second messengers | 2.31E-26 |
| Signaling by NTRK1 (TRKA) | 3.94E-22 | Toll-like Receptor Cascades | 2.59E-24 |
| Signaling by NTRKs | 9.28E-22 | **MAPK family signaling cascades** | **8.44E-24** |
| Toll-like Receptor Cascades | 1.41E-21 | **PI3K/AKT Signaling in Cancer** | **3.70E-20** |
| Intracellular signaling by second messengers | 2.39E-21 | Signaling by VEGF | 4.27E-20 |
| RAF/MAP kinase cascade | 7.47E-20 | VEGFA-VEGFR2 Pathway | 6.27E-20 |
| VEGFA-VEGFR2 Pathway | 3.95E-19 | **PIP3 activates AKT signaling** | **8.27E-20** |
| Toll Like Receptor 7/8 (TLR7/8) Cascade | 1.70E-18 | Toll Like Receptor 4 (TLR4) Cascade | 2.11E-18 |
| **PI3K/AKT Signaling in Cancer** | **1.74E-18** | Signaling by NTRK1 (TRKA) | 2.54E-18 |
| MyD88:MAL (TIRAP) cascade initiated on plasma membrane | 2.71E-18 | **MAPK1/MAPK3 signaling** | **3.35E-18** |
| Toll Like Receptor 4 (TLR4) Cascade | 4.39E-18 | MyD88:MAL (TIRAP) cascade initiated on plasma membrane | 3.58E-18 |
| MyD88 cascade initiated on plasma membrane | 4.39E-18 | Signaling by NTRKs | 6.35E-18 |
| **TRAF6 mediated induction of NFκB and MAP kinases upon TLR7/8 or 9 activation** | **1.09E-17** | Toll Like Receptor 7/8 (TLR7/8) Cascade | 1.75E-17 |
| Fc epsilon receptor (FCERI) signaling | 6.63E-17 | Axon guidance | 2.82E-17 |
| **PIP3 activates AKT signaling** | **7.82E-17** | Toll Like Receptor 9 (TLR9) Cascade | 3.14E-17 |
| **MAP kinase activation** | **1.28E-16** | Nervous system development | 3.14E-17 |
| Toll Like Receptor 3 (TLR3) Cascade | 2.53E-16 | MyD88 cascade initiated on plasma membrane | 3.74E-17 |
| Axon guidance | 4.99E-16 | RAF/MAP kinase cascade | 4.81E-17 |
| TRIF(TICAM1)-mediated TLR4 signaling | 5.08E-16 | **Negative regulation of the PI3K/AKT network** | **8.82E-17** |
| **Negative regulation of the PI3K/AKT network** | **7.08E-15** | **TRAF6 mediated induction of NFκB and MAP kinases upon TLR7/8 or 9 activation** | **9.82E-17** |
| **PI5P, *p*P2A and IER3 Regulate PI3K/AKT Signaling** | **2.87E-14** | Toll Like Receptor 3 (TLR3) Cascade | 2.02E-15 |
| **FCERI mediated MAPK activation** | **1.16E-12** | Fcgamma receptor (FCGR) dependent phagocytosis | 7.91E-15 |

In addition to KEGG pathway analysis, Reactome pathways were also determined. The top 30 Reactome pathways overrepresented in the data for jejunum and ileum are shown in Table 3. Similarly, many of the Reactome pathways also indicate alterations in growth and metabolic related signaling, but also highlights the immune related signaling

**TABLE 4 HIF-1α and related proteins' phosphorylation events. Here, the kinome peptide array results are shown. Jejunum 500 and ileum 500 were compared to their respective control tissues. Phosphorylation events represented in this table show significant (*p*-value <0.05) for each site in ileum while these sites are not significantly altered in jejunum. Significant values are highlighted in bold.**

| UniProt ID | Protein | Query site | Chicken site | Peptide AA sequence | Jejunum 500 v Control | | Ileum 500 v Control | |
|---|---|---|---|---|---|---|---|---|
| | | | | | Fold-change | *p*-value | Fold-change | *p*-value |
| Q16665 | HIF-1α | T796 | T781 | ESGLPQL**T**SYDCEVN | 1.078 | 0.165 | **1.220** | **0.000** |
| Q16665 | HIF-1α | S247 | S247 | KTFLSRH**S**LDMKFSY | -1.124 | 0.208 | **-2.187** | **0.000** |
| P68400 | CK2α | T360 | T360 | SGISSVP**T**PSPLGPL | 1.082 | 0.105 | **1.496** | **0.000** |
| Q15118 | PDK1 | Y243 | Y215 | AKSLCDL**Y**YMSSPEL | **-1.533** | **0.000** | **-1.493** | **0.003** |
| O15530 | PDK1 | S241 | S245 | SRQARAN**S**FVGTAQY | **1.194** | **0.013** | **1.172** | **0.010** |

**TABLE 5 AKT3 and related proteins' phosphorylation events. Here, the kinome peptide array results are shown. Jejunum 500 and ileum 500 were compared to their respective control tissues. Phosphorylation events represented in this table show significant (*p*-value <0.05) for sites as described above. Significant values are highlighted in bold.**

| UniProt ID | Protein | Query site | Chicken site | Peptide AA sequence | Jejunum 500 v Control | | Ileum 500 v Control | |
|---|---|---|---|---|---|---|---|---|
| | | | | | Fold-change | *p*-value | Fold-change | *p*-value |
| Q9Y243 | AKT3 | S476 | S476/S472 | RPHFPQF**S**Y**S**ASGRE | -1.038 | 0.255 | **-1.118** | **0.018** |
| Q9Y243 | AKT3 | T305 | T305 | TDAATMK**T**FCGTPEY | -1.075 | 0.126 | **1.207** | **0.002** |

changes. Of note are the pathways related to Toll-like receptor (TLR) signaling and those that indicate changes in Nuclear factor kappa B (NFκB) signaling, which will be further evaluated herein.

### 3.1.3 Site-specific functional analysis

HIF-1α, a subunit of a transcription factor that promotes the expression of genes related to energy metabolism in response to hypoxic and normal oxygen conditions (Lu et al., 2002) is downstream of multiple pathways represented in Table 2 including, but not limited to Insulin signaling, PI3K-Akt, Mechanistic target of rapamycin (mTOR) signaling, MAPK signaling, as well as metabolic signaling, glycolysis and the citric acid cycle. Phosphorylation of T796 (query sites referred to in text, see tables for chicken site) is an activating phosphorylation (Gradin et al., 2002), and in the current study is phosphorylated in the ileum but not significantly altered in the jejunum. Casein kinase 2α (CK2α) is an enzyme which phosphorylates HIF-1α at T796, activating HIF-1α, and is significantly phosphorylated at T360 (resulting in increased CK2α activity) in ileum but is not significantly altered in jejunum. Additionally, S247, an inhibitory site on HIF-1α (Kalousi et al., 2010) shows a significant decrease in phosphorylation in the ileum but is not significantly altered in the jejunum. The phosphorylation of HIF-1α and its related proteins are summarized in Table 4.

As HIF-1α activates glycolysis, it is also related to the uptake of glucose to feed this metabolic pathway (LaMonte et al., 2013). HIF-1α induces the expression of genes shown to be involved in the transport and metabolism of glucose (Harris, 2002; Semenza, 2009) while limiting the entry of metabolites into the mitochondria by activating pyruvate dehydrogenase 1 (PDK1) (Kim et al., 2006; Papandreou et al., 2006). PDK1's activating site Y243 shows statistically significantly decreased phosphorylation in both ileum and jejunum.

The insulin signaling pathway incorporates the response to insulin (i.e., uptake of glucose) as well as glycolysis, MAPK, and PI3K-Atk (Kanehisa et al., 2021). A significant part of the insulin signaling pathway is PI3K-Akt signaling (along with MAPK and glycolysis). AKT Serine/Threonine Kinase 3 (AKT3), a central part of the PI3K-AKT signaling, shows altered phosphorylation only in the ileum. AKT3 shows decreased phosphorylation at S472/S476 (Sarbassov et al., 2005). AKT3 at site T305 is significantly increased in ileum and is not significant in jejunum. AKT3 and related peptide's kinome data is summarized in Table 5.

mTOR is a serine/threonine kinase that affects a swath of cellular processes including cell growth, differentiation, and metabolism. mTOR induces transcription of HIF-1α and also regulates insulin signaling by altering Insulin Receptor Substrate 1 (IRS1), an early molecule in the insulin signaling pathway. IRS1 phosphorylation is increased in both tissues. mTOR phosphorylation was significantly altered in both ileum and jejunum as a result of feeding the product (Table 6). mTOR phosphorylates Eukaryotic translation initiation factor 4 E (eIF4E)-binding protein 1 (4EBP1) inducing transcription (Cheng et al., 2004). In the current study, 4EBP1 had significantly increased phosphorylation at S65 and T46 in both tissues, whereas, T37 had significantly increased phosphorylation in ileum but not in the jejunum. Regulatory-Associated Protein of mTOR Complex 1 (RPTOR) has two key sites for activation (S863 and T706). Both activation sites were statistically increased in ileum and unchanged in the jejunum.

Numerous sites were significantly different between the tissues (Figure 1). mTOR's phosphorylation site S2448 increased

**TABLE 6 mTOR and related proteins' phosphorylation events. Here, the kinome peptide array results are shown. Jejunum 500 and ileum 500 were compared to their respective control tissues. Phosphorylation events represented in this table show significant (*p*-value <0.05) for sites as described above. Significant values are highlighted in bold.**

| UniProt ID | Protein | Query site | Chicken site | Peptide AA sequence | Jejunum 500 v Control | | Ileum 500 v Control | |
|---|---|---|---|---|---|---|---|---|
| | | | | | Fold-change | *p*-value | Fold-change | *p*-value |
| P42345 | MTOR | S2448 | S2352 | RSRTRTD**S**YSASQSV | 1.049 | 0.247 | **1.231** | **0.002** |
| P42345 | MTOR | S2481 | S2387 | TVPESIH**S**FIGDGLV | **1.269** | **0.000** | **-1.318** | **0.000** |
| Q8N122 | RPTOR | S863 | S864 | LTQSAPA**S**PTNKGMH | 1.111 | 0.062 | **1.401** | **0.000** |
| P42345 | MTOR | T2446 | T2350 | NKRSRTR**T**DSYSASQ | 1.063 | 0.212 | **1.179** | **0.008** |
| Q8N122 | RPTOR | T706 | T707 | PAEGGSL**T**PVRDGPC | 1.091 | 0.075 | **1.323** | **0.000** |
| Q13541 | EIF4EBP1 | S65 | S66 | FLMECRN**S**PVAKTPP | **1.213** | **0.004** | **1.265** | **0.000** |
| Q13541 | EIF4EBP1 | T46 | T47 | GGTVFGT**T**PGGTRII | **1.228** | **0.001** | **1.248** | **0.000** |
| Q13541 | EIF4EBP1 | T37 | T38 | PPGDYST**T**PGGTVFG | -1.035 | 0.267 | **1.165** | **0.007** |

**TABLE 7 AMPK and related proteins' phosphorylation events. Here, the kinome peptide array results are shown. Jejunum 500 and ileum 500 were compared to their respective control tissues. Phosphorylation events represented in this table show significant (*p*-value <0.05) for sites as described above. Significant values are highlighted in bold.**

| UniProt ID | Protein | Query site | Chicken site | Peptide AA sequence | Jejunum 500 v Control | | Ileum 500 v Control | |
|---|---|---|---|---|---|---|---|---|
| | | | | | Fold-change | *p*-value | Fold-change | *p*-value |
| Q13131 | AMPK (PRKAA1) | S172 | S174 | KIADFGL**S**NMMSDGE | -1.066 | 0.142 | **1.193** | **0.004** |
| O43741 | AMPK (PRKAB2) | S108 | S110 | TKIPLIK**S**HNDFVAI | **-1.299** | **0.001** | **-1.442** | **0.000** |
| Q96RR4 | CAMKK2 | S511 | S483 | RREERSL**S**APGNLLP | 1.084 | 0.098 | **1.145** | **0.008** |

**TABLE 8 NFκB and Related proteins' phosphorylation events. Here, the kinome peptide array results are shown. Jejunum 500 and ileum 500 were compared to their respective control tissues. Phosphorylation events represented in this table show significant (*p*-value <0.05) for sites as described above. Significant values are highlighted in bold.**

| UniProt ID | Protein | Query site | Chicken site | Peptide AA sequence | Jejunum 500 v Control | | Ileum 500 v Control | |
|---|---|---|---|---|---|---|---|---|
| | | | | | Fold-change | *p*-value | Fold-change | *p*-value |
| P19838 | NFKB1 | S337 | S345 | FVQLRRK**S**DLETSEP | -1.038 | 0.2426 | **1.080** | **0.038** |
| P19838 | NFKB1 | S932 | S946 | CDSGVET**S**FRKLSFT | **1.115** | **0.028** | 1.106 | 0.064 |
| O15111 | CHUK | T23 | T37 | EMRDRLG**T**GGFGNVC | -1.058 | 0.124 | **1.239** | **0.000** |
| O15111 | CHUK | S180/S176 | S194 | DQG**S**LCT**S**FVGTLQY | **1.310** | **0.000** | 1.097 | 0.130 |
| Q14164 | IKBKE | S172 | S172 | EDDEKFV**S**VYGTEEY | 1.055 | 0.120 | **1.141** | **0.012** |
| Q05769 | COX2 | Y446 | Y446 | DQSRQMR**Y**QSLNEYR | 1.014 | 0.412 | **1.226** | **0.001** |

phosphorylation in ileum while no significant change is seen in jejunum. Increased phosphorylation also occurred in the ileum at site T2446, while no significant change was observed in jejunum. Further, site S2481 had significantly decreased phosphorylation in ileum.

The multiprotein complex formed by interaction of RPTOR and mTOR is called mTORC1. This complex has been shown to be essential for the phosphorylation of 4EBP1 (Hara et al., 2002).

Table 7 lists three 5' AMP-activated protein kinase (AMPK) related phosphorylation sites within the kinome data. AMPK is an energy sensor that plays a role in cellular energy homeostasis (Hardie et al., 2012). Calcium/Calmodulin Dependent Protein Kinase 2 (CAMKK2) phosphorylates AMPK at S172 (activating

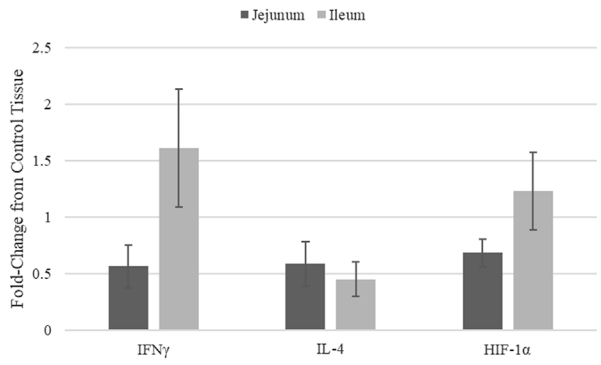


FIGURE 3
mRNA Expression in jejunum and ileum samples from blend-fed chickens compared to those on control diet.

site). CAMKK2 phosphorylation (S511) was significantly increased in ileum, but not jejunum. AMPK beta-2 at site S108 is shown to be an activating phosphorylation (Warden et al., 2001), and in the current study showed statistically significantly decreased phosphorylation in both the ileum and jejunum.

As described above, PI3K-Atk signaling is part of insulin signaling. Akt activates NFκB by phosphorylating Inhibitor of nuclear factor kappa-B kinase subunit alpha (IKKa) (Nidai Ozes et al., 1999; Romashkova and Makarov, 1999). NF-kB transcription factor activity is crucial in immune and inflammatory processes, cell cycle and proliferative processes, and cell death. Phosphorylation of NFκB is summarized in Table 8. NF-kB p50 (S337) shows increased phosphorylation in the ileum. This site is important for DNA binding (Hou et al., 2003; Guan et al., 2005). NF-kB p105 (S932) shows increased phosphorylation in the jejunum. This site has been shown to allow for the processing for p105 to p50 (active form of subunit) (Heissmeyer et al., 1999; Lang et al., 2003). IKKa (T23) phosphorylation activates the kinase, which then phosphorylates nuclear factor of kappa light polypeptide gene enhancer in B-cells inhibitor, alpha (IkBa) (inhibitor of NFκB) which then dissociates from NFκB allowing NFκB to translocate to the nucleus (Cahill and Rogers, 2008). IKKa (T23) is phosphorylated in ileum, not significant in jejunum. IKKa (S176/S180, S180 is on the array, S176 is included in the peptide) both activating phosphorylations (Ling et al., 1998; Senftleben et al., 2001). This site shows increased phosphorylation in jejunum while not significantly altered in ileum. Inducible IκB kinase (IKK-i) autophosphorylates at S172, this is an activating phosphorylation which results in activation of activates NFκB. (Shimada et al., 1999). IKK-i shows increased phosphorylation in Ileum while not being significant in jejunum. COX-2 is activated by phosphorylation at Y446 (Alexanian et al., 2014). This site is significantly increased in the ileum and not significantly altered in the jejunum. NFκB is reported to induce HIF-1α *via* a multitude of cellular stimuli including Interleukin-1beta (IL-1β) and Tumour Necrosis Factor alpha (TNFα) mediated signaling.

## 3.2 Quantitative RT-PCR to measure mRNA expression

Quantitative real-time RT-PCR was used to validate kinome peptide array data analysis (Figure 3). ThemRNA expression levels of interferon gamma (INFγ). Interleukin 4 (IL-4), and HIF-1α in jejunum and ileum were measured. The mRNA expression was compared in tissues from broilers fed the microencapsulated bend relative to their respective control tissues. Fold-change (FC) was calculated using the $40^{-\Delta\Delta CT}$ method and error bars show Standard Error. FC for IFNγ, IL-4, and HIF-1α in jejunum were 0.57, 0.59, and 0.69 respectively. FC for IFNγ, IL-4, and HIF-1α in Ileum were 1.61, 0.45, and 1.23 respectively. Student's *t*-test was performed and *p*-values for IFNγ, IL-4, and HIF-1α for jejunum were 0.12, 0.57, 0.15 respectively, while in ileum *p*-values were 0.78, 0.09, and 0.92 respectively.

Though mRNA expression is not necessarily correlated with protein translation or protein activity, coupling gene expression data with the kinome data provides a method of validating the signal transduction observed in the kinome data. Key indicators of immune stimulation (IFNy (Figure 3), other immune genes from (Swaggerty et al., 2020a)) and glycolysis related genes (HIF-1α) show increases in the ileum vs. the jejunum, in agreement with the kinome data. HIF-1α transcription does not necessarily mean HIF-1α function is active, however this in conjunction with Kinome data indicate increased activity in ileal tissue, suggest that HIF-1α is indeed functioning.

## 3.3 Summary of results

Figure 4 summarizes how the proteins listed in Tables 4–8 are related to one another and how a selection of relevant pathways (Tables 2, 3) come together to form this network. The consequences of the signaling changes result in changes to biological and metabolic processes. In jejunum, the signaling changes observed using both the kinome data and qPCR results indicate an increase in tricarboxylic acid cycle (TCA cycle) signaling and a reduction in pro-inflammatory processes, cell survival, protein synthesis, and glycolysis. In ileum, the same increase in TCA cycle as seen in the jejunum is observed, however the other processes were also increased in the ileum, whereas they were decreased in the jejunum.

# 4 Discussion

The botanical blend product studied here has been shown previously to have both a performance and disease mitigation effects (EFSA Panel on Additives and Products or Substances used in Animal Feed (FEEDAP) et al., 2020; Swaggerty et al., 2020a; Swaggerty et al., 2022). Here we attempt to describe a mechanism of action behind those observations. A possible mechanism for the improved chicken growth and performance shown previously is the enhanced glycolysis related signaling observed in this study in the ileum. This enhanced glycolysis occurs in the presence of adequate oxygen and can be considered aerobic glycolysis, otherwise known as the Warburg effect (Vaupel and Multhoff, 2021). In both tissues you see altered glycolysis, in the ileum which results in signaling that may lead to the enhanced production of anabolic building blocks, in the jejunum the lack of glycolytic signaling resulted in decreased expression of cytokines and chemokines typically associated with inflammation (Tables 4–8; Figure 3). Rapidly growing or highly active cells require a high level

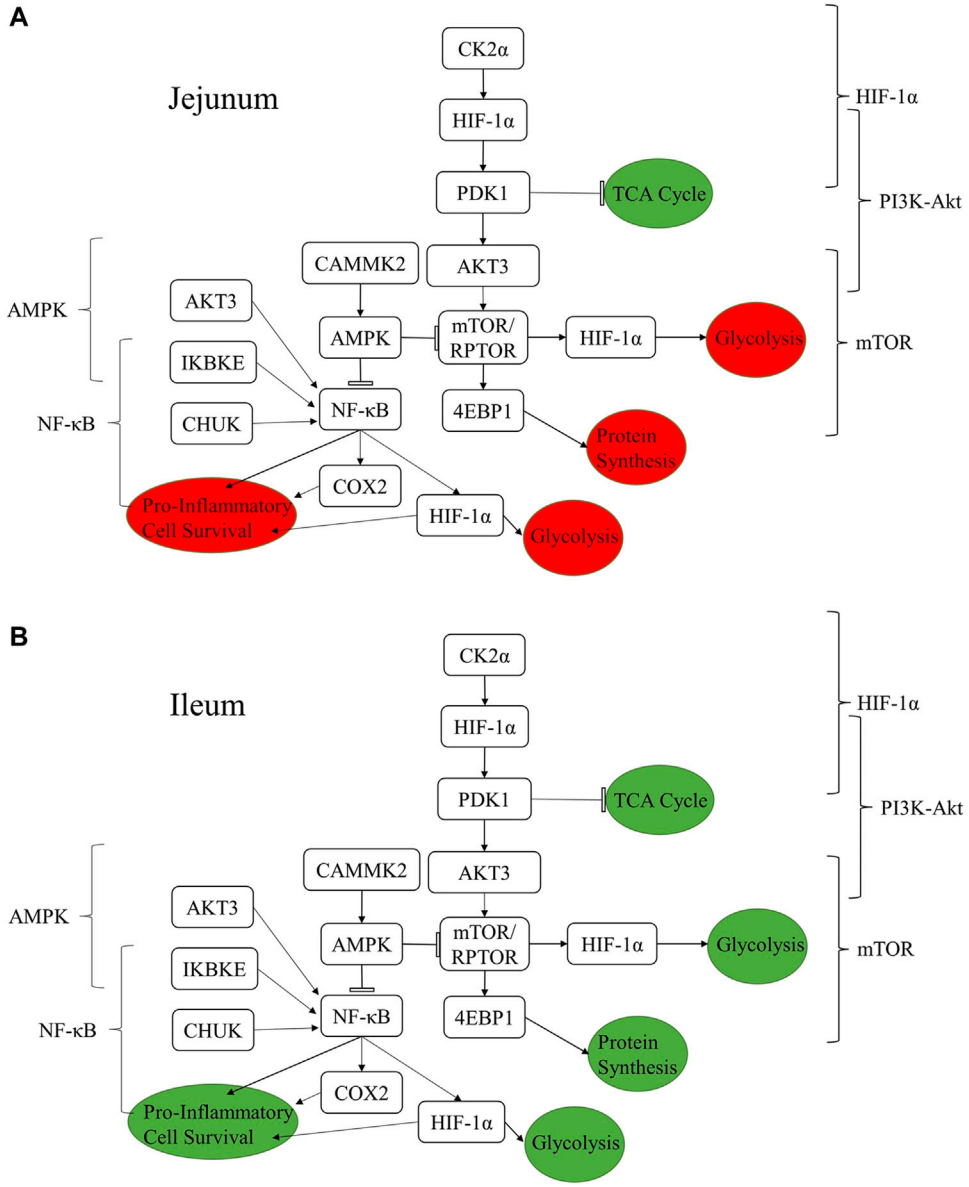


FIGURE 4
Summary figure showing the relationships between proteins discussed in the results and the resulting functional changes imparted by the product in jejunum **(A)** and ileum **(B)**. The brackets on either side of the figure denote the relevant signaling pathway. The colored circles represent the downstream functional effects of the signaling represented. The colors of the circles show whether the downstream functional effect is increased (green) or decreased (red).

of metabolites. Many of these metabolites come in the form of glycolytic or TCA cycle intermediates. By increasing aerobic glycolysis, a ready pool of metabolites and NADPH reducing agents are available for growth and activity (Vander Heiden et al., 2009). The Warburg effect was first discovered in cancer, a situation of high proliferation. More recently this phenotype has been found in immune cells and rapidly developing tissue as well. A phenotype similar to a growing broiler chicken (Johnson, 2021).

Insulin signaling activates AKT which activates mTOR which induces the transcription factors HIF-1 and NFκB (DeBerardinis et al., 2008). HIF-1 induces pro-glycolysis genes such as hexokinase, among others, which activates and perpetuates the cycle of increased glycolysis leading to greater HIF-1 activity (Semenza, 2013; Cheng et al., 2014). Pyruvate dehydrogenase kinase 1's (PDK1) activating site Y243 shows statistically significantly decreased phosphorylation in both ileum and jejunum. This site being phosphorylated is shown to increase PDK1's activity and increase conversion of pyruvate into lactate (Hitosugi et al., 2011), supporting a pro-glycolysis/Warburg phenotype in the ileum and a reduction in said signaling in jejunum. NFκB is activated *via* insulin signaling/Akt which induces the expression of HIF-1α and several pro-inflammatory cytokines (several of which show increased expression in the ileum and not in the jejunum) as seen published previously with this product (Swaggerty et al., 2020a; Swaggerty et al., 2022). These results

describe the mechanistic pathway leading to the increased glycolysis in the ileum as well as the mRNA expression results observed previously. This was accomplished by tracing the activation status and upstream signaling events leading to the activation of NFκB, which is a transcription factor transcribing proinflammatory cytokines and chemokines (Swaggerty et al., 2020a).

Previous research has shown that this product enhances growth and improves outcomes related to necrotic enteritis (NE) (Swaggerty et al., 2022). qPCR in that previous study (Swaggerty et al., 2022), looking at the same blend in the context of a NE model, mRNA expression in the jejunum for interleukin 6 (IL-6), interleukin 10 (IL-10), and IFNy were all increased (10.9, 5.03, and 5.66-fold respectively). In the context of this study, without a disease challenge, the blend resulted in reduced mRNA expression of IL-6 and IFNy (0.57 and 0.6 respectively) and less of an increase in IL-10 (1.39). These data support the hypothesis that the blend results in a more quiescent (potentiated) state in the jejunum and increases the capacity to respond to challenge. The inflammatory response to a pathogen is critical to the clearance of the pathogen. Jejunum is a more important site of nutrient absorption and also a more basally inflammatory tissue than ileum (Johnson et al., 2020). This may be explained by the fact that immune cells are more represented in the jejunum than the ileum, thus we observe changes that may represent a more growth effect in the ileum and anti-inflammatory effect in the jejunum.

Anti-inflammatory effects seen in the jejunum may be allowing for better barrier integrity and function, while allowing more proliferative signaling systemically (as reflected in ileum) thus better chicken growth with less permeable (leaky gut) GI tract. Thus, feed additive's primary function appears to be to decease inherent innate immune signaling, at least in the gut. This interpretation of our results is supported by the findings in a recent publication by Bialkowski et al. (2023) which showed an increase in gut barrier function in broilers in response to the same product reported on here. This increases the capacity to respond in the event of a disease or stress challenge (Perry et al., 2022; Swaggerty et al., 2022). You see more of an increase in cytokine expression and pro-inflammatory signaling in the jejunum with the treatment fed groups in the context of a challenge, but as reported here, in the absence of a challenge the gut is relegated to a more quiescent (potentiated) state. This means that the products are enabling greater capacity, or potential, to respond to these challenges. Given the results presented here, as well as the results referenced from studies testing similar products, it would be prudent to conduct a study that looks not only at the effect of this or similar products on the gut tissues, but more systematically as well. Previous work has shown that a subclinical *Salmonella* challenge can have a measurable effect on muscle metabolism (Kogut et al., 2016). As such, a specific site of further study should be the muscle tissue, as a major site of nutrient utilization in a broiler chicken it would be very likely to show effects related to any systemic change in proliferative and/or inflammatory signaling.

The jejunum and ileum are both segments of the small intestine and are being exposed to the same product. These segments have distinct physiological functions related to nutrient absorption and immunity (Svihus, 2014). The kinome data shows a clear distinction in the activation status of key immunometabolic signaling pathways (Tables 2, 3) between jejunum and ileum following the feeding of the blend product. These pathways are active in the ileum and absent or turned off in the jejunum. While some have argued that there is no anatomical or physiological distinction to be made between the jejunum and ileum in a chicken (Duke, 1986) our results here and elsewhere (Swaggerty et al., 2020a) have shown significant differences along the GI tract, not only between duodenum, cecum and ileum/jejunum but stark differences between the ileum and jejunum as well (Bialkowski et al., 2023). This post-translational and gene expression differences highlight the need for researchers to study multiple segments of the intestine in order to generate a clear picture of challenge or intervention effects.

Though many of the same pathways were altered by the product, as measured by phosphorylation changes in the proteins of those pathways, in both the jejunum and ileum, the members of the pathways show differential responses between the tissues as reflected in the changes in phosphorylation status of individual phosphorylation sites (Figures 1, 2). These differences show how in one tissue (Jejunum) proliferative signaling (transcription factors, gene expression) can be curtailed while in an adjacent tissue (Ileum) proliferative signaling (transcription factors, gene expression) can be heightened in response to the same treatment. Though, it is possible part of this difference is due to different concentrations of the product as it passes along the GI tract (Grilli et al., 2007; Piva et al., 2007). Future studies could evaluate the differential effects between these gut segments by utilizing organoids designed to represent the ileum and jejunum. Research is currently being done to develop and utilize organoids for such studies, however the technology may not yet be advanced enough to represent different segments of the gut perfectly (Li et al., 2018; Ghiselli et al., 2021; Nash et al., 2021; Zhao et al., 2022). Looking at the site-specific functions of phosphorylation status allows for determining the mechanism of action of the product in a context specific way (Tables 4–8). These site-specific changes highlight the importance of determining the functional effect of differential phosphorylation rather than rely on the phosphorylation status itself (increased phosphorylation doesn't always mean on nor the inverse).

## Data availability statement

The raw data supporting the conclusion of this article will be made available by the authors, without undue reservation.

## Ethics statement

The animal study was reviewed and approved by USDA/ARS Institutional Animal Care and Use Committee (IACUC). The IACUC operates under the Animal and Plant Health Inspection Service (APHIS) establishment number 334299.

## Author contributions

CS, AP, and EG conceived the study. CJ conducted the experiments, analyzed the data, and prepared the manuscript for submittal. CJ, CS, and RA contributed to writing, reviewing, and

editing the manuscript. AP and EG reviewed the manuscript. All authors read and approved the final manuscript.

## Funding

This research was supported, in part, by Vetagro ((CS) Agreement number 58-3091-8-005; https://www.vetagro.com) and the USDA/ARS (3091-32000-035-00D; https://www.ars.usda.gov/research/project/?accnNo=430283). There was no additional external funding received for this study. Vetagro provided support in the form of salaries for AP and EG, and supplied the AviPlus feed amendment, but did not have any additional role in data collection and analysis, decision to publish, or preparation of the manuscript. USDA/ARS provided support in the form of salary for CLS and CNJ but did not have any additional role in the study design, data collection and analysis, decision to publish, or preparation of the manuscript. The specific roles of these authors are articulated in the 'author contributions' section.

## Acknowledgments

The authors thank M. Reiley Street, Jr (United States. Department of Agriculture, Agricultural Research Service (USDA/ARS), College Station, TX) for outstanding technical support and assistance with daily animal care. Additionally, the authors thank Dr. Cristiano Bortoluzzi for the design and use of the HIF-1α primer/probe pair for qRT-PCR. The USDA is an equal opportunity provider and employer. Mention of trade names or commercial products in this publication is solely for the purpose of providing specific information and does not imply recommendation or endorsement by the USDA.

## Conflict of interest

Author AP was employed by Vetagro S.p.A. and EG was employed by Vetagro Inc.

The remaining authors declare that the research was conducted in the absence of any commercial or financial relationships that could be construed as a potential conflict of interest.

## Publisher's note



## References

Abd El-Hack, M. E., Alagawany, M., Ragab Farag, M., Tiwari, R., Karthik, K., Dhama, K., et al. (2016). Beneficial impacts of thymol essential oil on health and production of animals, fish and poultry: A review. *J. Essent. Oil Res.* 28, 365–382. doi:10.1080/10412905.2016.1153002

Ag Guide (2020). *Guide for the care and use of agricultural animals in research and teaching*. 4th edition. Available at: https://www.asas.org/services/ag-guide (Accessed January 17, 2023).

Alexanian, A., Miller, B., Chesnik, M., Mirza, S., and Sorokin, A. (2014). Post-translational regulation of COX2 activity by FYN in prostate cancer cells. *Oncotarget* 5, 4232–4243. doi:10.18632/oncotarget.1983

Arsenault, R. J., Lee, J. T., Latham, R., Carter, B., and Kogut, M. H. (2017). Changes in immune and metabolic gut response in broilers fed β-mannanase in β-mannan-containing diets. *Poult. Sci.* 96, 4307–4316. doi:10.3382/ps/pex246

Avery, S., Rothwell, L., Degen, W. D. J., Schijns, V. E. J. C., Young, J., Kaufman, J., et al. (2004). Characterization of the first nonmammalian T2 cytokine gene cluster: The cluster contains functional single-copy genes for IL-3, IL-4, IL-13, and GM-CSF, a gene for IL-5 that appears to Be a pseudogene, and a gene encoding another cytokinelike transcript, KK34. *J. Interferon Cytokine Res.* 24, 600–610. doi:10.1089/jir.2004.24.600

Bialkowski, S., Toschi, A., Yu, L., Schlitzkus, L., Mann, P., Grilli, E., et al. (2023). Effects of microencapsulated blend of organic acids and botanicals on growth performance, intestinal barrier function, inflammatory cytokines, and endocannabinoid system gene expression in broiler chickens. *Poult. Sci.* 102, 102460. doi:10.1016/j.psj.2022.102460

Cahill, C. M., and Rogers, J. T. (2008). Interleukin (IL) 1beta induction of IL-6 is mediated by a novel phosphatidylinositol 3-kinase-dependent AKT/IkappaB kinase alpha pathway targeting activator protein-1. *J. Biol. Chem.* 283, 25900–25912. doi:10.1074/jbc.M707692200

Cheng, S.-C., Quintin, J., Cramer, R. A., Shepardson, K. M., Saeed, S., Kumar, V., et al. (2014). mTOR- and HIF-1α–mediated aerobic glycolysis as metabolic basis for trained immunity. *Science* 345, 1250684. doi:10.1126/science.1250684

Cheng, S. W. Y., Fryer, L. G. D., Carling, D., and Shepherd, P. R. (2004). Thr2446 is a novel mammalian target of rapamycin (mTOR) phosphorylation site regulated by nutrient status. *J. Biol. Chem.* 279, 15719–15722. doi:10.1074/jbc.C300534200

DeBerardinis, R. J., Lum, J. J., Hatzivassiliou, G., and Thompson, C. B. (2008). The biology of cancer: Metabolic reprogramming fuels cell growth and proliferation. *Cell Metab.* 7, 11–20. doi:10.1016/j.cmet.2007.10.002

Duke, G. E. (1986). "*Alimentary canal: Anatomy, regulation of feeding, and motility*," in *avian physiology*, ed. P. D. Sturkie (New York, NY: Springer), 269–288. doi:10.1007/978-1-4612-4862-0_11

EFSA PanelBampidis, V., Azimonti, G., Bastos, M. de L., Christensen, H., Dusemund, B., et al. (2020). *on Additives and Products or Substances used in Animal Feed (FEEDAP)*, 18, e06063. doi:10.2903/j.efsa.2020.6063Assessment of the application for renewal of authorisation of AviPlus® as a feed additive for all porcine species (weaned), chickens for fattening, chickens reared for laying, minor poultry species for fattening, minor poultry species reared for laying*EFSA J.*

Gessner, D. K., Ringseis, R., and Eder, K. (2017). Potential of plant polyphenols to combat oxidative stress and inflammatory processes in farm animals. *J. Anim. Physiol. Anim. Nutr.* 101, 605–628. doi:10.1111/jpn.12579

Ghiselli, F., Rossi, B., Felici, M., Parigi, M., Tosi, G., Fiorentini, L., et al. (2021). Isolation, culture, and characterization of chicken intestinal epithelial cells. *BMC Mol. Cell Biol.* 22, 12. doi:10.1186/s12860-021-00349-7

Gradin, K., Takasaki, C., Fujii-Kuriyama, Y., and Sogawa, K. (2002). The transcriptional activation function of the HIF-like factor requires phosphorylation at a conserved threonine. *J. Biol. Chem.* 277, 23508–23514. doi:10.1074/jbc.M201307200

Grilli, E., Bodin, J. C., Gatta, P. P., Tedaschi, M., and Piva, A. (2007). Microencapsulation allows slow release of organic acids in the GI tract of broilers. *Proc. 16th Eur. Symp. Poult. Nutr. Strasbg. Fr. CABI Publ.* Available at: https://www.vetagro.com/2021/07/12/microincapsulation-slow-release-poultry-organic-acids/ (Accessed February 23, 2023).

Grilli, E., Tugnoli, B., Passey, J. L., Stahl, C. H., Piva, A., and Moeser, A. J. (2015). Impact of dietary organic acids and botanicals on intestinal integrity and inflammation in weaned pigs. *BMC Vet. Res.* 11, 96. doi:10.1186/s12917-015-0410-0

Guan, H., Hou, S., and Ricciardi, R. P. (2005). DNA binding of repressor nuclear factor-kappaB p50/p50 depends on phosphorylation of Ser337 by the protein kinase A catalytic subunit. *J. Biol. Chem.* 280, 9957–9962. doi:10.1074/jbc.M412180200

Hara, K., Maruki, Y., Long, X., Yoshino, K., Oshiro, N., Hidayat, S., et al. (2002). Raptor, a binding partner of target of rapamycin (TOR), mediates TOR action. *Cell* 110, 177–189. doi:10.1016/S0092-8674(02)00833-4

Hardie, D. G., Ross, F. A., and Hawley, S. A. (2012). Ampk: A nutrient and energy sensor that maintains energy homeostasis. *Nat. Rev. Mol. Cell Biol.* 13, 251–262. doi:10.1038/nrm3311

Harris, A. L. (2002). Hypoxia — A key regulatory factor in tumour growth. *Nat. Rev. Cancer* 2, 38–47. doi:10.1038/nrc704

Heissmeyer, V., Krappmann, D., Wulczyn, F. G., and Scheidereit, C. (1999). NF-kappaB p105 is a target of IkappaB kinases and controls signal induction of Bcl-3-p50 complexes. *EMBO J.* 18, 4766–4778. doi:10.1093/emboj/18.17.4766

Hitosugi, T., Fan, J., Chung, T.-W., Lythgoe, K., Wang, X., Xie, J., et al. (2011). Tyrosine phosphorylation of mitochondrial pyruvate dehydrogenase kinase 1 is important for cancer metabolism. *Mol. Cell* 44, 864–877. doi:10.1016/j.molcel.2011.10.015

Hou, S., Guan, H., and Ricciardi, R. P. (2003). Phosphorylation of serine 337 of NF-kappaB p50 is critical for DNA binding. *J. Biol. Chem.* 278, 45994–45998. doi:10.1074/jbc.M307971200

Jalal, S., Arsenault, R., Potter, A. A., Babiuk, L. A., Griebel, P. J., and Napper, S. (2009). Genome to kinome: Species-specific peptide arrays for kinome analysis. *Sci. Signal.* 2, pl1. doi:10.1126/scisignal.254pl1

Jazi, V., Foroozandeh, A. D., Toghyani, M., Dastar, B., Rezaie Koochaksaraie, R., and Toghyani, M (2018). Effects of Pediococcus acidilactici, mannan-oligosaccharide, butyric acid and their combination on growth performance and intestinal health in young broiler chickens challenged with Salmonella Typhimurium. *Poult. Sci.* 97, 2034–2043. doi:10.3382/ps/pey035

Johnson, C. N. (2021). A kinomic analysis of the immunometabolic effects of antibiotic alternatives in necrotic enteritis disease models. Available at: https://www.proquest.com/docview/2588008294/abstract/E865D8008E5E4DA5PQ/1 (Accessed August 25, 2022).

Johnson, C. N., Hashim, M. M., Bailey, C. A., Byrd, J. A., Kogut, M. H., and Arsenault, R. J. (2020). Feeding of yeast cell wall extracts during a necrotic enteritis challenge enhances cell growth, survival and immune signaling in the jejunum of broiler chickens. *Poult. Sci.* 99, 2955–2966. doi:10.1016/j.psj.2020.03.012

Johnson, C. N., Kogut, M. H., Genovese, K., He, H., Kazemi, S., and Arsenault, R. J. (2019). Administration of a postbiotic causes immunomodulatory responses in broiler gut and reduces disease pathogenesis following challenge. *Microorganisms* 7, 268. doi:10.3390/microorganisms7080268

Kaiser, P., Rothwell, L., Galyov, E. E., Barrow, P. A., Burnside, J., and Wigley, P. (2000). Differential cytokine expression in avian cells in response to invasion by *Salmonella typhimurium*, Salmonella enteritidis and Salmonella gallinarum. *Microbiology* 146, 3217–3226. doi:10.1099/00221287-146-12-3217

Kalousi, A., Mylonis, I., Politou, A. S., Chachami, G., Paraskeva, E., and Simos, G. (2010). Casein kinase 1 regulates human hypoxia-inducible factor HIF-1. *J. Cell Sci.* 123, 2976–2986. doi:10.1242/jcs.068122

Kanehisa, M., Furumichi, M., Sato, Y., Ishiguro-Watanabe, M., and Tanabe, M. (2021). Kegg: Integrating viruses and cellular organisms. *Nucleic Acids Res.* 49, D545–D551. doi:10.1093/nar/gkaa970

Kim, J., Tchernyshyov, I., Semenza, G. L., and Dang, C. V. (2006). HIF-1-mediated expression of pyruvate dehydrogenase kinase: A metabolic switch required for cellular adaptation to hypoxia. *Cell Metab.* 3, 177–185. doi:10.1016/j.cmet.2006.02.002

Kogut, M. H., Genovese, K. J., He, H., and Arsenault, R. J. (2016). AMPK and mTOR: Sensors and regulators of immunometabolic changes during Salmonella infection in the chicken. *Poult. Sci.* 95, 345–353. doi:10.3382/ps/pev349

LaMonte, G., Tang, X., Chen, J. L.-Y., Wu, J., Ding, C.-K. C., Keenan, M. M., et al. (2013). Acidosis induces reprogramming of cellular metabolism to mitigate oxidative stress. *Cancer Metab.* 1, 23. doi:10.1186/2049-3002-1-23

Lang, V., Janzen, J., Fischer, G. Z., Soneji, Y., Beinke, S., Salmeron, A., et al. (2003). betaTrCP-mediated proteolysis of NF-kappaB1 p105 requires phosphorylation of p105 serines 927 and 932. *Mol. Cell. Biol.* 23, 402–413. doi:10.1128/MCB.23.1.402-413.2003

Li, J., Li, J., Zhang, S. Y., Li, R. X., Lin, X., Mi, Y. L., et al. (2018). Culture and characterization of chicken small intestinal crypts. *Poult. Sci.* 97, 1536–1543. doi:10.3382/ps/pey010

Li, Y., Arsenault, R. J., Trost, B., Slind, J., Griebel, P. J., Napper, S., et al. (2012). A systematic approach for analysis of peptide array kinome data. *Sci. Signal.* 5, pl2. doi:10.1126/scisignal.2002429

Ling, L., Cao, Z., and Goeddel, D. V. (1998). NF-kappaB-inducing kinase activates IKK-alpha by phosphorylation of Ser-176. *Proc. Natl. Acad. Sci.* 95, 3792–3797. doi:10.1073/pnas.95.7.3792

Liu, L., Li, Q., Yang, Y., and Guo, A. (2021). Biological function of short-chain fatty acids and its regulation on intestinal health of poultry. *Front. Vet. Sci.* 8, 736739. doi:10.3389/fvets.2021.736739

Lu, H., Forbes, R. A., and Verma, A. (2002). Hypoxia-inducible factor 1 activation by aerobic glycolysis implicates the Warburg effect in carcinogenesis. *J. Biol. Chem.* 277, 23111–23115. doi:10.1074/jbc.M202487200

Micciche, A. C., Foley, S. L., Pavlidis, H. O., McIntyre, D. R., and Ricke, S. C. (2018). A review of prebiotics against Salmonella in poultry: Current and future potential for microbiome research applications. *Front. Vet. Sci.* 5, 191. doi:10.3389/fvets.2018.00191

Nash, T. J., Morris, K. M., Mabbott, N. A., and Vervelde, L. (2021). Inside-out chicken enteroids with leukocyte component as a model to study host–pathogen interactions. *Commun. Biol.* 4, 377. doi:10.1038/s42003-021-01901-z

Nidai Ozes, O., Mayo, L. D., Gustin, J. A., Pfeffer, S. R., Pfeffer, L. M., and Donner, D. B. (1999). NF-kappaB activation by tumour necrosis factor requires the Akt serine-threonine kinase. *Nature* 401, 82–85. doi:10.1038/43466

Papandreou, I., Cairns, R. A., Fontana, L., Lim, A. L., and Denko, N. C. (2006). HIF-1 mediates adaptation to hypoxia by actively downregulating mitochondrial oxygen consumption. *Cell Metab.* 3, 187–197. doi:10.1016/j.cmet.2006.01.012

Pearce, E. L., and Pearce, E. J. (2013). Metabolic pathways in immune cell activation and quiescence. *Immunity* 38, 633–643. doi:10.1016/j.immuni.2013.04.005

Perry, F., Johnson, C., Aylward, B., and Arsenault, R. J. (2020). The differential phosphorylation-dependent signaling and glucose immunometabolic responses induced during infection by Salmonella enteritidis and Salmonella heidelberg in chicken macrophage-like cells. *Microorganisms* 8, 1041. doi:10.3390/microorganisms8071041

Perry, F., Lahaye, L., Santin, E., Johnson, C., Korver, D. R., Kogut, M. H., et al. (2022). Protected biofactors and antioxidants reduce the negative consequences of virus and cold challenge while enhancing performance by modulating immunometabolism through cytoskeletal and immune signaling in the jejunum. *Poult. Sci.* 101, 102172. doi:10.1016/j.psj.2022.102172

Piva, A., Pizzamiglio, V., Morlacchini, M., Tedeschi, M., and Piva, G. (2007). Lipid microencapsulation allows slow release of organic acids and natural identical flavors along the swine intestine. *J. Anim. Sci.* 85, 486–493. doi:10.2527/jas.2006-323

Romashkova, J. A., and Makarov, S. S. (1999). NF-kappaB is a target of AKT in anti-apoptotic PDGF signalling. *Nature* 401, 86–90. doi:10.1038/43474

Salminen, S., Collado, M. C., Endo, A., Hill, C., Lebeer, S., Quigley, E. M. M., et al. (2021). The International Scientific Association of Probiotics and Prebiotics (ISAPP) consensus statement on the definition and scope of postbiotics. *Nat. Rev. Gastroenterol. Hepatol.* 18, 649–667. doi:10.1038/s41575-021-00440-6

Sarbassov, D. D., Guertin, D. A., Ali, S. M., and Sabatini, D. M. (2005). Phosphorylation and regulation of akt/PKB by the rictor-mTOR complex. *Science* 307, 1098–1101. doi:10.1126/science.1106148

Semenza, G. L. (2013). HIF-1 mediates metabolic responses to intratumoral hypoxia and oncogenic mutations. *J. Clin. Invest.* 123, 3664–3671. doi:10.1172/JCI67230

Semenza, G. L. (2009). Regulation of cancer cell metabolism by hypoxia-inducible factor 1. *Semin. Cancer Biol.* 19, 12–16. doi:10.1016/j.semcancer.2008.11.009

Senftleben, U., Cao, Y., Xiao, G., Greten, F. R., Krähn, G., Bonizzi, G., et al. (2001). Activation by IKKalpha of a second, evolutionary conserved, NF-kappa B signaling pathway. *Science* 293, 1495–1499. doi:10.1126/science.1062677

Shimada, T., Kawai, T., Takeda, K., Matsumoto, M., Inoue, J., Tatsumi, Y., et al. (1999). IKK-i, a novel lipopolysaccharide-inducible kinase that is related to IkappaB kinases. *Int. Immunol.* 11, 1357–1362. doi:10.1093/intimm/11.8.1357

Suresh, G., Das, R. K., Kaur Brar, S., Rouissi, T., Avalos Ramirez, A., Chorfi, Y., et al. (2018). Alternatives to antibiotics in poultry feed: Molecular perspectives. *Crit. Rev. Microbiol.* 44, 318–335. doi:10.1080/1040841X.2017.1373062

Svihus, B. (2014). Function of the digestive system1 1Presented as a part of the informal nutrition symposium "from research measurements to application: Bridging the gap" at the poultry science association's annual meeting in san diego, California, july 22–25, 2013. *J. Appl. Poult. Res.* 23, 306–314. doi:10.3382/japr.2014-00937

Swaggerty, C. L., Arsenault, R. J., Johnson, C., Piva, A., and Grilli, E. (2020a). Dietary supplementation with a microencapsulated blend of organic acids and botanicals alters the kinome in the ileum and jejunum of Gallus gallus. *PLOS ONE* 15, e0236950. doi:10.1371/journal.pone.0236950

Swaggerty, C. L., Byrd, J. A., Arsenault, R. J., Perry, F., Johnson, C. N., Genovese, K. J., et al. (2022). A blend of microencapsulated organic acids and botanicals reduces necrotic enteritis via specific signaling pathways in broilers. *Poult. Sci.* 101, 101753. doi:10.1016/j.psj.2022.101753

Swaggerty, C. L., He, H., Genovese, K. J., Callaway, T. R., Kogut, M. H., Piva, A., et al. (2020b). A microencapsulated feed additive containing organic acids, thymol, and vanillin increases *in vitro* functional activity of peripheral blood leukocytes from broiler chicks. *Poult. Sci.* 99, 3428–3436. doi:10.1016/j.psj.2020.03.031

Szklarczyk, D., Gable, A. L., Nastou, K. C., Lyon, D., Kirsch, R., Pyysalo, S., et al. (2021). The STRING database in 2021: Customizable protein–protein networks, and functional characterization of user-uploaded gene/measurement sets. *Nucleic Acids Res.* 49, D605–D612. doi:10.1093/nar/gkaa1074

Trost, B., Kindrachuk, J., Määttänen, P., Napper, S., and Kusalik, A. (2013). Piika 2: An expanded, web-based Platform for analysis of kinome microarray data. *PLOS ONE* 8, e80837. doi:10.1371/journal.pone.0080837

Vander Heiden, M. G., Cantley, L. C., and Thompson, C. B. (2009). Understanding the Warburg effect: The metabolic requirements of cell proliferation. *Science* 324, 1029–1033. doi:10.1126/science.1160809

Vaupel, P., and Multhoff, G. (2021). Revisiting the Warburg effect: Historical dogma versus current understanding. *J. Physiol.* 599, 1745–1757. doi:10.1113/JP278810

Warden, S. M., Richardson, C., O'Donnell, J., Stapleton, D., Kemp, B. E., and Witters, L. A. (2001). Post-translational modifications of the beta-1 subunit of AMP-activated protein kinase affect enzyme activity and cellular localization. *Biochem. J.* 354, 275–283. doi:10.1042/0264-6021:3540275

Yadav, S., and Jha, R. (2019). Strategies to modulate the intestinal microbiota and their effects on nutrient utilization, performance, and health of poultry. *J. Anim. Sci. Biotechnol.* 10, 2. doi:10.1186/s40104-018-0310-9

Zeng, Z., Zhang, S., Wang, H., and Piao, X. (2015). Essential oil and aromatic plants as feed additives in non-ruminant nutrition: A review. *J. Anim. Sci. Biotechnol.* 6, 7. doi:10.1186/s40104-015-0004-5

Zhao, D., Farnell, M. B., Kogut, M. H., Genovese, K. J., Chapkin, R. S., Davidson, L. A., et al. (2022). From crypts to enteroids: Establishment and characterization of avian intestinal organoids. *Poult. Sci.* 101, 101642. doi:10.1016/j.psj.2021.101642

frontiers | Frontiers in Physiology

TYPE Opinion
PUBLISHED 05 July 2023
DOI 10.3389/fphys.2023.1228318



OPEN ACCESS

EDITED BY
Hai Lin,
Shandong Agricultural University, China

REVIEWED BY
Nima Emami,
Novozymes, United States

*CORRESPONDENCE
Sandra G. Velleman,
velleman.1@osu.edu

RECEIVED 24 May 2023
ACCEPTED 27 June 2023
PUBLISHED 05 July 2023

CITATION
Xu J and Velleman SG (2023), Critical role of the mTOR pathway in poultry skeletal muscle physiology and meat quality: an opinion paper.
*Front. Physiol.* 14:1228318.
doi: 10.3389/fphys.2023.1228318



# Critical role of the mTOR pathway in poultry skeletal muscle physiology and meat quality: an opinion paper

Jiahui Xu and Sandra G. Velleman*

Department of Animal Sciences, The Ohio State University, Wooster, OH, United States

KEYWORDS

**meat quality, mTOR, muscle growth, poultry, satellite cells, skeletal muscle**

Skeletal muscle is the major component of meat, and is primarily composed of muscle fibers bounded by multiple connective tissue layers (Velleman and McFarland, 2014). These connective tissue layers function as an essential support and functional system, incorporating components like blood vessels and extracellular matrix macromolecules. Consequently, muscle development and growth, morphological structure, and biochemistry are crucial aspects in the determination of meat yield and quality. The modern poultry industry has had one area of focus on selection for enhanced growth performance, specifically emphasizing increased body weight and skeletal muscle yield (Havenstein et al., 2007; Collins et al., 2014). Structural abnormalities, such as diminished connective tissue spacing and reduced capillary density resulting from excessive muscle fiber hypertrophy, have been observed in the breast muscle of modern rapid-growing poultry lines (Velleman et al., 2003; Joiner et al., 2014). The loss of connective tissue spacing and presence of oversized myofibers result in direct contact between muscle fibers, and this condition is correlated with a greater occurrence of muscle fiber degeneration (Wilson et al., 1990; Velleman et al., 2003). Furthermore, insufficient capillary supply in the breast muscle could limit the removal of anaerobic respiration byproducts, such as lactic acid. The residual lactic acid in the breast muscle can lead to a decrease in pH, potentially exacerbating muscle degeneration. In addition to the structural flaws, the breast muscle of modern fast-growing poultry breeds exhibits conditions such as Wooden Breast (Sihvo et al., 2014) and White Stripping (Soglia et al., 2018), which adversely affect the quality of the breast meat. Muscle growth and structure are primarily determined by muscle cell biology and biochemistry, which are influenced by signal transduction pathways. One of the key players involved in muscle function is the mechanistic target of rapamycin (mTOR) pathway, which is critical in regulating muscle hypertrophic growth and mass accretion in poultry (Vignale et al., 2015; Ma et al., 2018). This opinion paper will discuss how the mTOR pathway modulates skeletal muscle growth, structure, and biochemistry, and ultimately can affect poultry meat yield and quality.

Muscle fiber number is fixed by the time of hatch (Smith, 1963). Post-hatch muscle grows through the hypertrophy of existing muscle fibers. Accumulation of intracellular protein in existing muscle fibers is the most likely mechanism for post-hatch muscle hypertrophic growth. With regard to the molecular mechanisms, mTOR is a key regulator controlling muscle size and mass accretion in mammals and poultry (Bodine et al., 2001; Vignale et al., 2015). It has been broadly hypothesized that mTOR promotes myofiber hypertrophy by stimulating protein synthesis (Wang and Proud, 2006; Wang et al., 2015; You et al., 2019). A schematic illustration of possible mechanisms of mTOR pathway in skeletal muscle function is presented in Figure 1. Using mammalian models, the mTOR protein kinase has been found to function in two distinct multiprotein complexes: mTOR

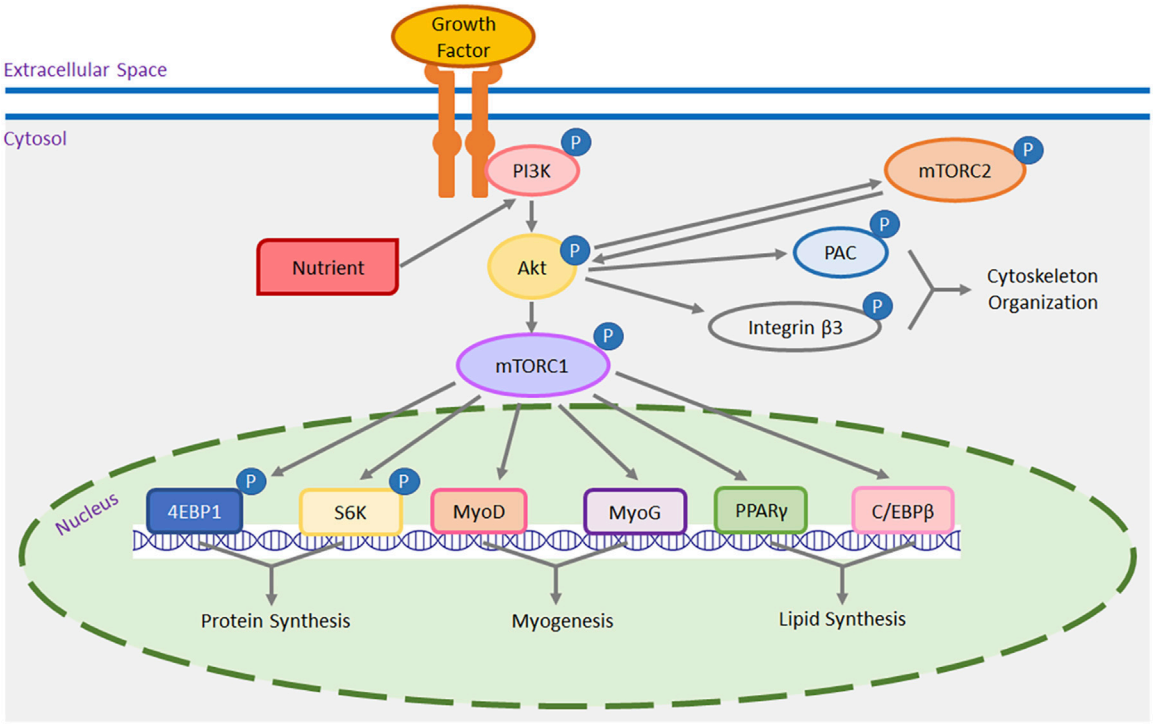


FIGURE 1
A schematic representation of the mTOR pathway in muscle cells. Both growth factors, through their receptors, and intracellular nutrients trigger the activation (or phosphorylation) of phosphoinositide 3 kinase (PI3K). Once activated, PI3K in turn activates protein kinase B (Akt) and mTOR complex 1 (mTORC1). Nutrients and growth factors, via the PI3K/Akt pathway, can also stimulate mTOR complex 2 (mTORC2), which, once activated, can further stimulate mTORC1 via Akt. Moreover, activated mTORC2 phosphorylates cytoplasmic p21-activated kinase (PAK) and integrin β3 via Akt, contributing to cytoskeleton organization and migration. Downstream targets of mTORC1 include but are not limited to p70 S6 kinase (S6K), eukaryotic initiation factor 4E binding protein 1 (4EBP1), myoblast determination factor 1 (MyoD), myogenin (MyoG), peroxisome proliferator-activated receptor-gamma (PPARγ), and CCAAT/enhancer-binding protein-beta (C/EBPβ). Both S6K and 4EBP1 are implicated in the initiation of gene expression for protein synthesis. MyoD and MyoG are myogenic transcriptional regulatory factors promoting myogenesis, while PPARγ and C/EBPβ are adipogenic factors that stimulate the transcription of genes involved in lipid synthesis.

complex 1 (mTORC1) and mTOR complex 2 (mTORC2) (Hara et al., 2002; Sarbassov et al., 2004). As an intracellular nutrient sensor (Tesseraud et al., 2006; Vignale et al., 2015), mTORC1 has been found to promote protein synthesis with the stimulation of intracellular nutrients including amino acids (Kop-Bozbay and Ocak, 2019), vitamins (Vignale et al., 2015), fatty acids (Yoon et al., 2011), and glucose (Patel et al., 2001) in birds and mammals. In addition to nutrients, extracellular growth factors also stimulate the activation of mTORC1 via specific transmembrane growth factor receptors (Rommel et al., 2001). Both nutrients and growth factors activate mTORC1 via the phosphoinositide 3 kinase (PI3K)/protein kinase B (Akt) signaling. For mTORC2, it can also be activated by nutrients (Tato et al., 2011) and growth factors (García-Martínez and Alessi, 2008) through the PI3K/Akt pathway in mammalian cells. Activated mTORC2 indirectly activates mTORC1 through Akt (Sarbassov et al., 2005; Moschella et al., 2013). Downstream mTOR effectors for protein synthesis are p70 S6 kinase (S6K) (Brown et al., 1995; Ohanna et al., 2005; Vignale et al., 2015) and eukaryotic initiation factor 4E binding protein 1 (4EBP1) (Hara et al., 1998; Wang et al., 2015). As the amount of intracellular protein directly determines the size of myofibers, both mTOR/S6K and mTOR/4EBP1 signaling plays an essential role in regulating the hypertrophic growth of poultry skeletal muscle (Zhang et al., 2014; Wang et al., 2015). Notably, using human models, Cuthbertson et al. (2006) reported that it is the myofibrillar proteins and not the sarcoplasmic proteins which promote hypertrophic growth of muscle fibers. Abou Sawan et al. (2018) also showed that mTORC1 increased muscle myofibrillar protein synthesis but not mitochondrial protein synthesis via the S6K and 4EBP1 in human muscle fibers. In avian species, the mTOR pathway may also promote muscle fiber hypertrophy and muscle mass accretion by upregulating myofibrillar proteins synthesis in an S6K- and 4EBP1-dependent manner. Future studies will be needed to test this hypothesis.

At the periphery of each muscle fiber, there exists a specific population of muscle stem cells known as satellite cells (Mauro, 1961). Satellite cells act as the exclusive cell reservoir for post-hatch muscle hypertrophy, and this occurs through satellite cell proliferation, differentiation, and donation of cell nuclei to existing muscle fibers (Moss and Leblond, 1971; Cardiasis and Cooper, 1975). In poultry, satellite cell mitotic activity peaks during the first week after hatch (Mozdziak et al., 1994; Halevy et al., 2000), after which it gradually diminishes, eventually reaching a mitotically quiescence state in mature muscle (Schultz and Lipton, 1982). With damage to muscle fibers (Bischoff, 1975; Snow, 1977),

the mitotically inactive satellite cells re-enter the cell cycle and repair the damaged muscle fibers. Numerous studies have suggested that mTORC1 promotes satellite cell myogenesis by inducing the expression of myogenic transcriptional factors such as myoblast determination factor 1 (MyoD) and myogenin (MyoG) (Han et al., 2008; Vignale et al., 2015; Xu et al., 2022a; Xu and Velleman, 2023) (Figure 1). In chicken breast muscle, impaired proliferation and differentiation with decreased expression of *mTOR, MyoD,* and *MyoG* were observed in the breast muscle satellite cells of a current faster-growing broiler chicken line compared to two historical chicken lines from 1990s (Xu and Velleman, 2023). Insufficient myogenesis by satellite cells may result in a higher incidence of myofiber degenerative and fibrotic myopathies like Wooden Breast, as satellite cells with impaired regeneration potential are unable to fully restore the necrotic myofibers to their original size (Velleman and Clark, 2015; Clark and Velleman, 2016; Velleman et al., 2018). In contrast, Wooden Breast has not been observed in modern faster-growing turkeys. This difference can be partially explained by increased satellite cell myogenesis facilitated by an enhanced mTOR/S6K pathway in turkeys (Xu et al., 2022a). The other complex, mTORC2, promotes mouse satellite cell myogenesis, primarily through the activation of Akt/mTORC1 signaling (Matheny Jr et al., 2012) (Figure 1). In addition, mTORC2-triggered Akt activation influences actin polymerization, which in turn affects cytoskeleton organization and cell migration through its downstream effectors including p21-activated kinase (PAK) (Zhou et al., 2003) and integrin β3 (Kirk et al., 2000) in mammals (Figure 1). Satellite cell alignment, a prerequisite for their fusion to form multinucleated myotubes, requires migration (Chazaud et al., 1998). Taken together, the mTOR pathway plays a multifaceted role in muscle biology; it not only directly regulates protein synthesis in muscle fibers but also modulates muscle hypertrophy and regeneration potential of damaged fibers by controlling the myogenic or regenerative potential and migration of satellite cells.

In addition to regulating muscle growth and regeneration, the mTOR pathway also governs the possible adipogenesis of muscle satellite cells. This is accomplished by regulating the expression of adipogenic regulatory factors like peroxisome proliferator-activated receptor-gamma (PPARγ) (Kim and Chen, 2004) and CCAAT/enhancer-binding protein-beta (C/EBPβ) (Kim et al., 2014) (Figure 1). As multipotential stem cells, satellite cells can spontaneously transdifferentiate to an adipocyte-like lineage and synthesize lipid content with appropriate extrinsic stimuli (Asakura et al., 2001; Shefer et al., 2004). As shown by Xu et al. (2021; 2022a), heat stress significantly increased the activity of the mTOR/S6K pathway, which is accompanied by increased lipid synthesis in turkey breast muscle satellite cells. Furthermore, knocking down the expression of *mTOR* significantly decreased lipid accumulation and suppressed the expression of both *PPARγ* and *C/EBPβ* in turkey satellite cells (Xu et al., 2022b). In in vivo studies, the increased intracellular lipid content has been associated with the increased intramuscular fat deposition in chicken breast muscle (Piestun et al., 2017; Patael et al., 2019), potentially influencing protein-to-fat ratio in poultry breast muscle. The increase in intramuscular fat depots may also be associated with fat-associated myopathies like White Striping.

Considering the crucial role of the mTOR pathway in skeletal muscle growth, structure, and physiology, numerous extrinsic factors have been investigated for their potential effects on mTOR activity. Nutrients such as phosphatidic acid (Yoon et al., 2011), vitamin D (Vignale et al., 2015) and leucine (Kop-Bozbay and Ocak, 2019) and specific growth factors like epidermal growth factor (EGF) (Cao et al., 2009) and insulin-like growth factor-1 (IGF-1) (Rommel et al., 2001) are well-known activators of the mTOR pathway in birds and mammals, which may in turn stimulates muscle protein synthesis. The mTOR pathway is also significantly influenced by various cellular stressors. For example, the mTOR pathway can sense and respond to thermal stress (Xu et al., 2022a) and oxygen stress (Chaillou and Lanner, 2016), subsequently adjusting protein synthesis in skeletal muscle. Nonetheless, the regulation of the mTOR pathway is tissue- and species-specific in poultry muscle, relying on a delicate balance of various factors. Different timing, intensity, or duration of these stimuli can also result in distinct cellular responses. Taking temperature effect as an example, Xu et al. (2022a) reported that cold stress (5°C colder than the control) inhibited the activity of the mTOR/S6K pathway in breast muscle satellite cells of one-week-old turkeys. However, an increase in mTOR activity was observed when newly hatched chickens were constantly challenged with chronic cold stress (5.3°–12.3°C colder than the control) during the first week after hatch in the chicken leg muscle (Nguyen et al., 2015). Comprehending how the extrinsic factors are involved in the regulation of the mTOR pathway is critical in optimizing poultry skeletal muscle growth and structure.

The mTOR pathway is undeniably critical in poultry skeletal muscle growth and physiology by stimulating myofiber protein accumulation (Wang and Proud, 2006) and regulating satellite cell myogenesis and adipogenesis (Xu et al., 2022a; b). These mTOR functions may have a direct impact on poultry meat quality. Gaining a deeper understanding of the mTOR pathway and its regulatory mechanisms will enable the poultry industry to develop strategies for optimizing poultry muscle growth and enhancing meat quality. For example, providing feed with higher vitamin D (Vignale et al., 2015), arginine (Yu et al., 2018), leucine (Kop-Bozbay and Ocak, 2019) might achieve the nutritional stimuli necessary for mTOR activity in poultry skeletal muscle. Introducing a heat stress with appropriate intensity and duration, particularly during the first week after hatch when satellite cells exhibit peak mitotic activity and temperature sensitivity (Mozdziak et al., 1994; Halevy et al., 2001), will significantly increase the activity of the mTOR pathway (Xu et al., 2022a), which in turn, will stimulate satellite cell myogenesis and protein synthesis, resulting in increased muscle mass accretion and preventing myofiber necrotic and fibrotic myopathies like Wooden Breast. Nevertheless, as indicated by Ma et al. (2018), it is vital to avoid chronic high-intensity heat stress to mitigate negative effects on mTOR activity. Furthermore, the elevation in mTOR activity induced by heat stress at an early age also promotes fat accumulation, particularly in the breast muscle satellite cells of rapid-growing poultry (Xu et al., 2022b). Increased intramuscular fat deposition could be associated with fat-associated myopathies like White Striping, impacting the quality of breast meat. As poultry breast muscle is a favored consumer source of high-protein and low-fat meat, fluctuating

between heat and cold stress in the first week post-hatch could potentially augment mTOR-mediated protein synthesis, while inhibiting mTOR-driven fat production. Continued research is necessary to discover the appropriate strategies of controlling the mTOR pathway in response to various stimuli, ultimately improving poultry skeletal muscle growth while producing a high-quality meat product.

## Author contributions

The paper represents the opinion of JX and SV and does not include new data. All authors contributed to the article and approved the submitted version.

## Conflict of interest

The authors declare that the research was conducted in the absence of any commercial or financial relationships that could be construed as a potential conflict of interest.

## Publisher's note

All claims expressed in this article are solely those of the authors and do not necessarily represent those of their affiliated organizations, or those of the publisher, the editors and the reviewers. Any product that may be evaluated in this article, or claim that may be made by its manufacturer, is not guaranteed or endorsed by the publisher.

## References


Abou Sawan, S., Van Vliet, S., Parel, J. T., Beals, J. W., Mazzulla, M., West, D. W., et al. (2018). Translocation and protein complex co-localization of mTOR is associated with postprandial myofibrillar protein synthesis at rest and after endurance exercise. *Physiol. Rep.* 6, e13628. doi:10.14814/phy2.13628

Asakura, A., Komaki, M., and Rudnicki, M. (2001). Muscle satellite cells are multipotential stem cells that exhibit myogenic, osteogenic, and adipogenic differentiation. *Differentiation* 68, 245–253. doi:10.1046/j.1432-0436.2001.680412.x

Bischoff, R. (1975). Regeneration of single skeletal muscle fibers *in vitro*. *Anat. Rec.* 182, 215–235. doi:10.1002/ar.1091820207

Bodine, S. C., Stitt, T. N., Gonzalez, M., Kline, W. O., Stover, G. L., Bauerlein, R., et al. (2001). Akt/mTOR pathway is a crucial regulator of skeletal muscle hypertrophy and can prevent muscle atrophy *in vivo*. *Nat. Cell Biol.* 3, 1014–1019. doi:10.1038/ncb1101-1014

Brown, E. J., Beal, P. A., Keith, C. T., Chen, J., Bum Shin, T., and Schreiber, S. L. (1995). Control of p70 s6 kinase by kinase activity of FRAP *in vivo*. *Nature* 377, 441–446. doi:10.1038/377441a0

Cao, C., Huang, X., Han, Y., Wan, Y., Birnbaumer, L., Feng, G. S., et al. (2009). Galpha(i1) and Galpha(i3) are required for epidermal growth factor-mediated activation of the Akt-mTORC1 pathway. *Sci. Signal.* 2, ra17. doi:10.1126/scisignal.2000118

Cardiasis, A., and Cooper, G. (1975). An analysis of nuclear numbers in individual muscle fibers during differentiation and growth: A satellite cell-muscle fiber growth unit. *J. Exp. Zool.* 191, 347–358. doi:10.1002/jez.1401910305

Chaillou, T., and Lanner, J. T. (2016). Regulation of myogenesis and skeletal muscle regeneration: Effects of oxygen levels on satellite cell activity. *FASEB J.* 30, 3929–3941. doi:10.1096/fj.201600757R

Chazaud, B., Christov, C., Gherardi, R. K., and Barlovatz-Meimon, G. (1998). *In vitro* evaluation of human muscle satellite cell migration prior to fusion into myotubes. *J. Muscle Res. Cell. Motil.* 19, 931–936. doi:10.1023/a:1005451725719

Clark, D., and Velleman, S. (2016). Spatial influence on breast muscle morphological structure, myofiber size, and gene expression associated with the wooden breast myopathy in broilers. *Poult. Sci.* 95, 2930–2945. doi:10.3382/ps/pew243

Collins, K., Kiepper, B., Ritz, C., Mclendon, B., and Wilson, J. (2014). Growth, livability, feed consumption, and carcass composition of the Athens Canadian Random Bred 1955 meat-type chicken versus the 2012 high-yielding Cobb 500 broiler. *Poult. Sci.* 93, 2953–2962. doi:10.3382/ps.2014-04224

Cuthbertson, D. J., Babraj, J., Smith, K., Wilkes, E., Fedele, M. J., Esser, K., et al. (2006). Anabolic signaling and protein synthesis in human skeletal muscle after dynamic shortening or lengthening exercise. *Am. J. Physiol.* 290, E731–E738. doi:10.1152/ajpendo.00415.2005

García-Martínez, J. M., and Alessi, D. R. (2008). mTOR complex 2 (mTORC2) controls hydrophobic motif phosphorylation and activation of serum-and glucocorticoid-induced protein kinase 1 (SGK1). *Biochem. J.* 416, 375–385. doi:10.1042/BJ20081668

Halevy, O., Geyra, A., Barak, M., Uni, Z., and Sklan, D. (2000). Early posthatch starvation decreases satellite cell proliferation and skeletal muscle growth in chicks. *J. Nutr.* 130, 858–864. doi:10.1093/jn/130.4.858

Halevy, O., Krispin, A., Leshem, Y., Mcmurtry, J. P., and Yahav, S. (2001). Early-age heat exposure affects skeletal muscle satellite cell proliferation and differentiation in chicks. *Am. J. Physiol. Regul. Integr. Comp. Physiol.* 281, R302–R309. doi:10.1152/ajpregu.2001.281.1.R302

Han, B., Tong, J., Zhu, M. J., Ma, C., and Du, M. (2008). Insulin-like growth factor-1 (IGF-1) and leucine activate pig myogenic satellite cells through mammalian target of rapamycin (mTOR) pathway. *Mol. Reprod. Dev.* 75, 810–817. doi:10.1002/mrd.20832

Hara, K., Maruki, Y., Long, X., Yoshino, K.-I., Oshiro, N., Hidayat, S., et al. (2002). Raptor, a binding partner of target of rapamycin (TOR), mediates TOR action. *Cell* 110, 177–189. doi:10.1016/s0092-8674(02)00833-4

Hara, K., Yonezawa, K., Weng, Q. P., Kozlowski, M. T., Belham, C., and Avruch, J. (1998). Amino acid sufficiency and mTOR regulate p70 S6 kinase and eIF-4E BP1 through a common effector mechanism. *J. Biol. Chem.* 273, 14484–14494. doi:10.1074/jbc.273.23.14484

Havenstein, G., Ferket, P., Grimes, J., Qureshi, M., and Nestor, K. (2007). Comparison of the performance of 1966-versus 2003-type turkeys when fed representative 1966 and 2003 Turkey diets: Growth rate, livability, and feed conversion. *Poult. Sci.* 86, 232–240. doi:10.1093/ps/86.2.232

Joiner, K. S., Hamlin, G. A., Lien, A. R., and Bilgili, S. F. (2014). Evaluation of capillary and myofiber density in the pectoralis major muscles of rapidly growing, high-yield broiler chickens during increased heat stress. *Avian Dis.* 58, 377–382. doi:10.1637/10733-112513-Reg.1

Kim, J. E., and Chen, J. (2004). Regulation of peroxisome proliferator–activated receptor-γ activity by mammalian target of rapamycin and amino acids in adipogenesis. *Diabetes* 53, 2748–2756. doi:10.2337/diabetes.53.11.2748

Kim, J. H., Kim, S. H., Song, S. Y., Kim, W. S., Song, S. U., Yi, T., et al. (2014). Hypoxia induces adipocyte differentiation of adipose-derived stem cells by triggering reactive oxygen species generation. *Cell Biol. Int.* 38, 32–40. doi:10.1002/cbin.10170

Kirk, R. I., Sanderson, M. R., and Lerea, K. M. (2000). Threonine phosphorylation of the β3 integrin cytoplasmic tail, at a site recognized by PDK1 and Akt/PKB *in vitro*, regulates Shc binding. *J. Biol. Chem.* 275, 30901–30906. doi:10.1074/jbc.M001908200

Kop-Bozbay, C., and Ocak, N. (2019). In ovo injection of branched-chain amino acids: Embryonic development, hatchability and hatching quality of Turkey poults. *J. Anim. Physiol. Anim. Nutr.* 103, 1135–1142. doi:10.1111/jpn.13111

Ma, B., He, X., Lu, Z., Zhang, L., Li, J., Jiang, Y., et al. (2018). Chronic heat stress affects muscle hypertrophy, muscle protein synthesis and uptake of amino acid in broilers via insulin like growth factor-mammalian target of rapamycin signal pathway. *Poult. Sci.* 97, 4150–4158. doi:10.3382/ps/pey291

Matheny, R. W., Jr, Lynch, C. M., and Leandry, L. A. (2012). Enhanced Akt phosphorylation and myogenic differentiation in PI3K p110β-deficient myoblasts is mediated by PI3K p110α and mTORC2. *Growth factors.* 30, 367–384. doi:10.3109/08977194.2012.734507

Mauro, A. (1961). Satellite cell of skeletal muscle fibers. *J. Cell Biol.* 9, 493–495. doi:10.1083/jcb.9.2.493

Moschella, P. C., Mckillop, J., Pleasant, D. L., Harston, R. K., Balasubramanian, S., and Kuppuswamy, D. (2013). mTOR complex 2 mediates Akt phosphorylation that requires PKCε in adult cardiac muscle cells. *Cell. Signal.* 25, 1904–1912. doi:10.1016/j.cellsig.2013.05.001

Moss, F., and Leblond, C. (1971). Satellite cells as the source of nuclei in muscles of growing rats. *Anat. Rec.* 170, 421–435. doi:10.1002/ar.1091700405

Mozdziak, P. E., Schultz, E., and Cassens, R. G. (1994). Satellite cell mitotic activity in posthatch Turkey skeletal muscle growth. *Poult. Sci.* 73, 547–555. doi:10.3382/ps.0730547

Nguyen, P., Greene, E., Ishola, P., Huff, G., Donoghue, A., Bottje, W., et al. (2015). Chronic mild cold conditioning modulates the expression of hypothalamic neuropeptide and intermediary metabolic-related genes and improves growth performances in young chicks. *PLoS One* 10, e0142319. doi:10.1371/journal.pone.0142319

Ohanna, M., Sobering, A. K., Lapointe, T., Lorenzo, L., Praud, C., Petroulakis, E., et al. (2005). Atrophy of S6K1−/− skeletal muscle cells reveals distinct mTOR effectors for cell cycle and size control. *Nat. Cell Biol.* 7, 286–294. doi:10.1038/ncb1231

Patael, T., Piestun, Y., Soffer, A., Mordechay, S., Yahav, S., Velleman, S. G., et al. (2019). Early posthatch thermal stress causes long-term adverse effects on pectoralis muscle development in broilers. *Poult. Sci.* 98, 3268–3277. doi:10.3382/ps/pez123

Patel, J., Wang, X., and Proud, C. G. (2001). Glucose exerts a permissive effect on the regulation of the initiation factor 4E binding protein 4E-BP1. *Biochem. J.* 358, 497–503. doi:10.1042/0264-6021:3580497

Piestun, Y., Patael, T., Yahav, S., Velleman, S. G., and Halevy, O. (2017). Early posthatch thermal stress affects breast muscle development and satellite cell growth and characteristics in broilers. *Poult. Sci.* 96, 2877–2888. doi:10.3382/ps/pex065

Rommel, C., Bodine, S. C., Clarke, B. A., Rossman, R., Nunez, L., Stitt, T. N., et al. (2001). Mediation of IGF-1-induced skeletal myotube hypertrophy by PI(3)K/Akt/mTOR and PI(3)K/Akt/GSK3 pathways. *Nat. Cell Biol.* 3, 1009–1013. doi:10.1038/ncb1101-1009

Sarbassov, D. D., Ali, S. M., Kim, D. H., Guertin, D. A., Latek, R. R., Erdjument-Bromage, H., et al. (2004). Rictor, a novel binding partner of mTOR, defines a rapamycin-insensitive and raptor-independent pathway that regulates the cytoskeleton. *Curr. Biol.* 14, 1296–1302. doi:10.1016/j.cub.2004.06.054

Sarbassov, D. D., Guertin, D. A., Ali, S. M., and Sabatini, D. M. (2005). Phosphorylation and regulation of Akt/PKB by the rictor-mTOR complex. *Science* 307, 1098–1101. doi:10.1126/science.1106148

Schultz, E., and Lipton, B. H. (1982). Skeletal muscle satellite cells: Changes in proliferation potential as a function of age. *Mech. Ageing Dev.* 20, 377–383. doi:10.1016/0047-6374(82)90105-1

Shefer, G., Wleklinski-Lee, M., and Yablonka-Reuveni, Z. (2004). Skeletal muscle satellite cells can spontaneously enter an alternative mesenchymal pathway. *J. Cell Sci.* 117, 5393–5404. doi:10.1242/jcs.01419

Sihvo, H. K., Immonen, K., and Puolanne, E. (2014). Myodegeneration with fibrosis and regeneration in the pectoralis major muscle of broilers. *Vet. Pathol.* 51, 619–623. doi:10.1177/0300985813497488

Smith, J. H. (1963). Relation of body size to muscle cell size and number in the chicken. *Poult. Sci.* 42, 283–290. doi:10.3382/ps.0420283

Snow, M. H. (1977). Myogenic cell formation in regenerating rat skeletal muscle injured by mincing. II. An autoradiographic study. *Anat. Rec.* 188, 201–217. doi:10.1002/ar.1091880206

Soglia, F., Baldi, G., Laghi, L., Mudalal, S., Cavani, C., and Petracci, M. (2018). Effect of white striping on Turkey breast meat quality. *Animal* 12, 2198–2204. doi:10.1017/S1751731117003469

Tato, I., Bartrons, R., Ventura, F., and Rosa, J. L. (2011). Amino acids activate mammalian target of rapamycin complex 2 (mTORC2) via PI3K/Akt signaling. *J. Biol. Chem.* 286, 6128–6142. doi:10.1074/jbc.M110.166991

Tesseraud, S., Abbas, M., Duchene, S., Bigot, K., Vaudin, P., and Dupont, J. (2006). Mechanisms involved in the nutritional regulation of mRNA translation: Features of the avian model. *Nutr. Res. Rev.* 19, 104–116. doi:10.1079/NRR2006120

Velleman, S. G., Anderson, J. W., Coy, C. S., and Nestor, K. E. (2003). Effect of selection for growth rate on muscle damage during Turkey breast muscle development. *Poult. Sci.* 82, 1069–1074. doi:10.1093/ps/82.7.1069

Velleman, S. G., and Clark, D. L. (2015). Histopathologic and myogenic gene expression changes associated with wooden breast in broiler breast muscles. *Avian Dis.* 59, 410–418. doi:10.1637/11097-042015-Reg.1

Velleman, S. G., Clark, D. L., and Tonniges, J. R. (2018). The effect of the wooden breast myopathy on sarcomere structure and organization. *Avian Dis.* 62, 28–35. doi:10.1637/11766-110217-Reg.1

Velleman, S. G., and McFarland, D. C. (2014). "Skeletal muscle," in *Sturkie's avian physiology: Six edition*. Editor C. G. Scanes (New York, NY: Academic Press), 379–402.

Vignale, K., Greene, E. S., Caldas, J. V., England, J. A., Boonsinchai, N., Sodsee, P., et al. (2015). 25-hydroxycholecalciferol enhances male broiler breast meat yield through the mTOR pathway. *J. Nutr. Sci.* 145, 855–863. doi:10.3945/jn.114.207936

Wang, X., Jia, Q., Xiao, J., Jiao, H., and Lin, H. (2015). Glucocorticoids retard skeletal muscle development and myoblast protein synthesis through a mechanistic target of rapamycin (mTOR)-signaling pathway in broilers (Gallus gallus domesticus). *Stress* 18, 686–698. doi:10.3109/10253890.2015.1083551

Wang, X., and Proud, C. G. (2006). The mTOR pathway in the control of protein synthesis. *Physiology* 21, 362–369. doi:10.1152/physiol.00024.2006

Wilson, B. W., Nieberg, P. S., Buhr, R. J., Kelly, B. J., and Shultz, F. T. (1990). Turkey muscle growth and focal myopathy. *Poult. Sci.* 69, 1553–1562. doi:10.3382/ps.0691553

Xu, J., Strasburg, G. M., Reed, K. M., and Velleman, S. G. (2021). Effect of temperature and selection for growth on intracellular lipid accumulation and adipogenic gene expression in Turkey pectoralis major muscle satellite cells. *Front. Physiol.* 12, 667814. doi:10.3389/fphys.2021.667814

Xu, J., Strasburg, G. M., Reed, K. M., and Velleman, S. G. (2022a). Thermal stress affects proliferation and differentiation of Turkey satellite cells through the mTOR/S6K pathway in a growth-dependent manner. *PLoS One* 17, e0262576. doi:10.1371/journal.pone.0262576

Xu, J., Strasburg, G. M., Reed, K. M., and Velleman, S. G. (2022b). Thermal stress and selection for growth affect myogenic satellite cell lipid accumulation and adipogenic gene expression through mechanistic target of rapamycin pathway. *J. Anim. Sci.* 100, skac001. doi:10.1093/jas/skac001

Xu, J., and Velleman, S. G. (2023). Effects of thermal stress and mechanistic target of rapamycin and wingless-type mouse mammary tumor virus integration site family pathways on the proliferation and differentiation of satellite cells derived from the breast muscle of different chicken lines. *Poult. Sci.* 102, 102608. doi:10.1016/j.psj.2023.102608

Yoon, M. S., Sun, Y., Arauz, E., Jiang, Y., and Chen, J. (2011). Phosphatidic acid activates mammalian target of rapamycin complex 1 (mTORC1) kinase by displacing FK506 binding protein 38 (FKBP38) and exerting an allosteric effect. *J. Biol. Chem.* 286, 29568–29574. doi:10.1074/jbc.M111.262816

You, J. S., Mcnally, R. M., Jacobs, B. L., Privett, R. E., Gundermann, D. M., Lin, K.-H., et al. (2019). The role of raptor in the mechanical load-induced regulation of mTOR signaling, protein synthesis, and skeletal muscle hypertrophy. *FASEB J.* 33, 4021–4034. doi:10.1096/fj.201801653RR

Yu, L., Gao, T., Zhao, M., Lv, P., Zhang, L., Li, J., et al. (2018). Effects of in ovo feeding of l-arginine on breast muscle growth and protein deposition in post-hatch broilers. *Animal* 12, 2256–2263. doi:10.1017/S1751731118000241

Zhang, R. P., Liu, H. H., Li, Q. Q., Wang, Y., Liu, J. Y., Hu, J.-W., et al. (2014). Gene expression patterns, and protein metabolic and histological analyses for muscle development in Peking duck. *Poult. Sci.* 93, 3104–3111. doi:10.3382/ps.2014-04145

Zhou, G. L., Zhuo, Y., King, C. C., Fryer, B. H., Bokoch, G. M., and Field, J. (2003). Akt phosphorylation of serine 21 on Pak1 modulates Nck binding and cell migration. *Mol. Cell. Biol.* 23, 8058–8069. doi:10.1128/MCB.23.22.8058-8069.2003

frontiers | Frontiers in Physiology

TYPE Original Research
PUBLISHED 11 July 2023
DOI 10.3389/fphys.2023.1218850



OPEN ACCESS

EDITED BY
Wu Shugeng,
Chinese Academy of Agricultural Sciences, China

REVIEWED BY
Tatiana Carlesso Santos,
State University of Maringá, Brazil
Mahmoud M. Alagawany,
Zagazig University, Egypt

*CORRESPONDENCE
E. A. Soumeh,
e.assadisoumeh@uq.edu.au
V. Jazi,
Jazi.vahid@gmail.com

RECEIVED 08 May 2023
ACCEPTED 03 July 2023
PUBLISHED 11 July 2023

CITATION
Ashayerizadeh O, Dastar B, Shams Shargh M, A. Soumeh E and Jazi V (2023), Effects of black pepper and turmeric powder on growth performance, gut health, meat quality, and fatty acid profile of Japanese quail. *Front. Physiol.* 14:1218850. doi: 10.3389/fphys.2023.1218850



# Effects of black pepper and turmeric powder on growth performance, gut health, meat quality, and fatty acid profile of Japanese quail

O. Ashayerizadeh[1], B. Dastar[1], M. Shams Shargh[1], E. A. Soumeh[2]* and V. Jazi[1]*

[1]Department of Animal and Poultry Nutrition, Faculty of Animal Science, Gorgan University of Agricultural Sciences and Natural Resources, Gorgan, Iran, [2]School of Agriculture and Food Sustainability, University of Queensland, Brisbane, QLD, Australia

In poultry production, the search for alternatives to in-feed antibiotics continues unabated. This study investigated the effects of dietary supplementation of black pepper and turmeric powder, separately or in combination, on the growth performance, gastrointestinal microbiota population, intestinal morphology, serum biochemical parameters, meat quality, and meat fatty acid profile in Japanese quails. Five hundred-day-old mixed-sex Japanese quail chicks were randomly assigned to one of five treatments: a control diet (CON); CON +0.2% antibiotic flavomycin as an antibiotic growth promoter (AGP); CON +0.5% turmeric powder (TUP); CON +0.5% black pepper powder (BPP); and CON +0.5% TUP, and 0.5% BPP (MIX). The findings showed that quail chicks fed AGP and TUP throughout the rearing period had better body weight gain ($p$ = 0.007) and feed conversion ratio ($p$ = 0.02) than the other treatments. The TUP, BPP, and MIX feeds reduced ($p$ = 0.005) abdominal fat percentage. The MIX group had a better breast muscle water-holding capacity ($p$ = 0.04) and lightness index ($p$ = 0.02) and lower ($p$ = 0.02) malondialdehyde concentration after 7 days of refrigerated storage. Feeding BPP, TUP, and MIX diets decreased ($p$ = 0.001) serum cholesterol concentration. Quail chicks fed the CON diet showed significantly higher coliform counts in the crop and ileum ($p$ < 0.001), whereas the lactic acid bacterial population was lower ($p$ = 0.008) in the ileum. Birds that received the MIX diet exhibited a higher ($p$ = 0.02) villus height to crypt depth ratio in the duodenum compared to the other groups. The tested feed additives increased ($p$ < 0.001) villus height in the jejunum and ileum compared to other groups. Feeding the TUP, BPP, and MIX diets reduced ($p$ < 0.001) total saturated fatty acid content and increased ($p$ = 0.004) total polyunsaturated fatty acid concentration, where the MIX diet had the best results. Overall, the present data indicate that supplementing the basal diet with turmeric powder enhances the growth performance of Japanese quails. In some respects, such as gut health and meat quality, combining turmeric powder and black pepper powder was more effective than using them independently.

KEYWORDS

**antibiotics as growth promoters, black pepper, gut health, phytogenic, turmeric**

# Introduction

The use of phytogenic feed additives (PFAs) in animal feeding has gained significant attention in recent years, particularly after the ban on antibiotics as growth promoters. PFAs are plant-derived substances and are utilized to improve livestock and poultry productivity. These additives encompass a wide range of herbs, spices, and their derivatives (Windisch et al., 2008). The bioactive compounds found in PFAs, such as polyphenols, organic acids, essential oils, terpenoids, and aldehydes, are known to possess antioxidant and antibacterial properties that can have a positive impact on animal productivity (Shirani et al., 2019). In addition, PFAs can stimulate blood circulation and promote the production of digestive secretions, including mucin, amylase, lipase, trypsin protease, and bile acid (Mohebodini et al., 2021). Previous studies have shown that PFAs can impact the gut microbiome (Barbarestani et al., 2020), improve lipid metabolism (Mohebodini et al., 2019), enhance intestinal mucosal morphology, strengthen the intestinal barrier function (Oso et al., 2019), and boost the immune system of broiler chickens (Pirgozliev et al., 2019). However, our knowledge about their applications in poultry nutrition is still somewhat limited.

Turmeric (*Curcuma longa*) is a spice that belongs to the Zingiberaceae family and is widely distributed in tropical and subtropical regions of the world, particularly in Asian countries (Amalraj et al., 2017). As a traditional herbal medicine, turmeric has been used for centuries to treat various ailments, including urinary tract infections, liver disorders, inflammation, menstrual disorders, and digestive issues (Salehi et al., 2019). Both *in vitro* and *in vivo* studies have demonstrated that turmeric possesses numerous biological and pharmacological properties, such as antioxidant, antibacterial, antifungal, anti-inflammatory, and immunomodulatory effects (Strimpakos and Sharma, 2008; Mirzaei et al., 2017). The pharmacological activity of turmeric is primarily attributed to the presence of various curcuminoid compounds, including curcumin, demethoxycurcumin, and bisdemethoxycurcumin (Salehi et al., 2019).

Black pepper (*Piper Nigrum*) is another significant, widely-used spice with therapeutic benefits. In traditional medicine, it is utilized to alleviate symptoms of dizziness, asthma, chronic indigestion, flu, fever, chills, and migraine (Gorgani et al., 2017). Piperine, the primary active compound found in black pepper, has been extensively researched in recent years due to its relatively low side effects and a broad range of physiological activities, including antioxidant, antimicrobial, anti-inflammatory, anticarcinogenic, and cholesterol-lowering effects (Vijayakumar and Nalini, 2006; Shityakov et al., 2019). Other benefits of piperine include promoting blood circulation, stimulating appetite, and producing saliva and digestive secretions in poultry (Ogbuewu et al., 2020). Although the pharmaceutical activities of turmeric and black pepper in humans and various experimental animals have been well-documented, there have been limited studies on the effects of these additives on poultry as natural growth promoters.

Given the pharmacological properties of turmeric and black pepper documented in previous *in vitro* studies, the current research postulated that these phytogenic products would work synergistically to enhance each other's beneficial effects. Therefore, the present study aimed to investigate the impact of turmeric and black pepper powder, either separately or in combination, on the growth performance, gastrointestinal microbial population, intestinal morphology, blood metabolites, meat quality, and fatty acid profile of Japanese quails. Additionally, the study sought to assess the potential of these additives as alternatives to antibiotics.

# Materials and methods

## Plant material and extraction procedures

Black pepper seeds and turmeric rhizomes were purchased from a local market in Gorgan, Iran. The samples were cleaned, dried, ground to a fine powder, and extracted with 80% ethanol by stirring for 1 h at room temperature. The extraction process was repeated thrice. The sample-to-solvent ratio was 1:10 (w/v). The extracts were filtered using Whatman No. 1 filter paper and concentrated using a vacuum rotary evaporator (Buchi, Switzerland). The final extracts were freeze-dried and stored at −18°C until use.

## Determination of total phenolic contents

The total phenolic content (TPC) of the samples was determined using the Folin–Ciocalteu method, as described by Singleton et al. (1999). Briefly, 50 µL of black pepper and turmeric extract (concentration of 1 mg/mL in methanol) was mixed with 3.95 mL distilled water and 250 µL of Folin–Ciocalteu, respectively. After 4 min, 750 µL of 20% sodium sulfite solution was added and the mixture was allowed to stand for 2 h at room temperature. The absorbance was measured at 760 nm using a UV/Visible Spectrophotometer. Results were expressed as mg Gallic acid equivalent/g of freeze-dried extract (mg GAE/g E).

## Determination of total flavonoid content

Total flavonoid contents (TFC) were determined according to the method described by Cottica. (2015). Briefly, 0.25 mL of 5% aluminum chloride (ethanolic) was mixed with 0.5 mL black pepper and turmeric extract (concentration of 1 mg/mL in methanol). Then, 4.25 mL of methanol was added to the mixture, and absorbance was read at 420 nm after 30 min at room temperature. Total flavonoids were expressed as mg Quercetin equivalent/g of freeze-dried extract (mg QE/g E).

## Antioxidant evaluation (DPPH free radical-scavenging assay)

The antioxidant capacity of the extracts was measured following the method described by Mensor et al. (2001) using the 1,1-diphenyl-2-picrylhydrazyl (DPPH). A volume of 200 µL of extracts (concentration of 1 mg/mL in methanol) was added to 80 µL 0.3 mM methanolic DPPH solution. The mixture was vortexed for 1 min and then allowed to stand in the dark for 30 min at room temperature. The absorbance of the solutions was measured at 517 nm using an ELISA reader (ELx800; BioTek Instruments, Winooski, VT, United States). The antioxidant activity (% inhibition) was calculated according to the following equation:

**TABLE 1 Ingredients and nutrient contents of the basal diet of Japanese quail.**

| Items | % |
|---|---|
| Ingredient | |
| Maize | 55.21 |
| Soybean meal | 23.69 |
| Maize gluten meal | 10 |
| Fish meal | 5.25 |
| Soybean oil | 2.84 |
| CaCO3 | 0.93 |
| Di-calcium phosphate | 0.84 |
| Salt | 0.23 |
| Vitamin premix[a] | 0.25 |
| Mineral premix[b] | 0.25 |
| $_{DL}$-methionine | 0.03 |
| $_{L}$-lysine | 0.36 |
| $_{L}$-threonine | 0.13 |
| Calculated composition | |
| Metabolize energy, kcal/kg | 2,900 |
| Crude protein, % | 24 |
| [c]SID-Lysine, % | 1.27 |
| SID-Methionine, % | 0.45 |
| SID-Methionine + cystine, % | 0.77 |
| SID-Arginine | 1.22 |
| SID-Threonine | 0.75 |
| Calcium, % | 0.80 |
| Phosphorus (available), % | 0.30 |
| Sodium, % | 0.15 |

[a]Supplied per kg of diet: 1.8 mg all-trans-retinyl acetate; 0.02 mg cholecalciferol; 8.3 mg alphatocopheryl acetate; 2.2 mg menadione; 2 mg pyridoxine HCl; 8 mg cyanocobalamin; 10 mg nicotine amid; 0.3 mg folic acid; 20 mg D-biotin; 160 mg choline chloride.
[b]Supplied per kg of diet: 32 mg Mn ($MnSO_4$_$H_2O$); 16 mg Fe ($FeSO_4$_$7H_2O$); 24 mg Zn (ZnO); 2 mg Cu ($CuSO_4$_$5H_2O$); 800 μg I (KI); 200 μg Co ($CoSO_4$); 60 μg Se ($NaSeO_3$).
[c]SID: standardised ileal digestibility.

$$\%\ \text{inhibition} = \left(1 - A_{\text{extract}} / A_{\text{control}}\right) \times 100$$

where $A_{control}$ represents absorbance of the methanol solution of DPPH without the sample, and $A_{sample}$ is absorbance of the methanol solution of DPPH with extract solution.

## Quails, experimental design, and diets

In a 35-day study, 500 1-day-old Japanese quails were procured from a local commercial hatchery. On arrival, quail chicks were weighed and randomly assigned to one of the five experimental diets with five replicate pens (20 birds per pen) in a completely randomized design. The birds were housed in wire-floored pens (60 cm × 55 cm × 40 cm) in an environmentally controlled room with continuous light and were allowed *ad libitum* access to feed and water throughout the experiment. Upon the arrival of the chicks, the temperature was set at 35°C for the first 3 days and then gradually decreased by 2.5°C per week until it reached 22.5°C. Nutritional requirements of the growing Japanese quails were adopted from NRC (1994) tables, and a basal diet was formulated (Table 1). The quail chicks were fed one of five experimental diets starting from day 1. These included: 1) a corn-soybean basal diet without feed additives (CON), 2) the basal diet with 0.2% antibiotic flavomycin added as an antibiotic growth promoter (AGP), 3) the basal diet with 0.5% turmeric powder added (TUP), 4) the basal diet with 0.5% black pepper powder added (BPP), and 5) the basal diet with a mixture of 0.5% turmeric powder and 0.5% black pepper powder added (MIX).

## Sampling and measurements

The individual body weight of quails was measured at d 1, 21, and 35, and the mean was calculated for each cage. Feed intake (FI) was recorded on a cage basis. The body weight gain (BWG), FI, and feed conversion ratio (feed: gain, FCR) were calculated for different periods (1–21, 21–35 days), and the total period (1–35 days).

On day 35, 2 birds with body weight close to the average of the cage were selected from each replicate cage. Blood samples were collected from the brachial vein into non-heparinized tubes and centrifuged at 2,500 g for 15 min at 4°C to obtain serum. The serum concentrations of aspartate aminotransferase (AST), alanine aminotransferase (ALT), alkaline phosphatase (ALP), total cholesterol, and triglycerides were determined using an automatic biochemical analyzer (Clima, Ral. Co, Spain), and commercial laboratory kits (Pars Azmoon Kits; Pars Azmoon, Tehran, Iran).

After blood sample collection, the same birds were euthanized by cervical dislocation to evaluate carcass characteristics, meat quality, the crop and ileum's microbial population, and the small intestine's morphological characteristics. After removing the feathers, carcass weight, breast, thighs, cloacal bursa, liver, spleen, heart, and abdominal fat were weighed. Then their weights were expressed as a percentage of live body weight.

For histological measurements, a 3 cm segment was first removed from the middle point of the duodenum, jejunum, and ileum; then flushed with distilled water and fixed in 10% neutral buffered formalin for 48 h. The fixed samples were dehydrated, cleared, and embedded in paraffin. Tissue samples (5 μm tickness) were cut by a microtome, stained with haematoxylin-eosin, and scanned using a light microscop. The morphological parameters including villus height (VH: from the top of the villus to the top of the lamina propria), crypt depth (CD: the depth of the invagination between adjacent villi), and villus width (VW: at the middle point of the villus) were measured on each slide. A total of 10 intact villi and crypts were randomly selected in each sample. The ratio of VH to CD was calculated. The ratio of VH to CD was calculated (Jazi et al., 2019). The villus surface area was calculated as 2π × (VW/2) × VH.

To estimate the lactic acid bacteria (LAB) and coliform count in crop and ileum sections, 1 g of crop and ileum contents (separately) was diluted serially in 0.9% sterile saline solution. Afterward, 100 μL of each dilution was plated onto MRS agar (Merck, Germany) and violet

red bile agar (Merck, Germany) plates to enumerate the LAB and coliforms, respectively. Plates were then incubated at 37°C for 24–48 h anaerobically (Jazi et al., 2018a). To measure pH, 1 g of each bird's fresh crop and ileum contents was collected, and the pH was measured using a portable pH meter as per the method by Shabani et al. (2019).

Breast meat samples of euthanized birds were also collected, cut into small pieces, and then stored in the refrigerator at 4°C in the dark for 7 days. The samples' pH value, malondialdehyde (MDA), meat color, and water-holding capacity (WHC) were analyzed for storage days 1 and 7. The pH value was determined in homogenates prepared by mixing 10 g of sample with 90 mL of distilled water, and a reading was taken with a digital pH meter (NWKbinar pH, K-21, Landsberg, Germany). The meat color of samples was assessed at three different locations across the muscles by using a Laovibond Tintometer Cam-System 500 (Amesbury, United Kingdom) and expressed as lightness (L*), redness (a*), and yellowness (b*). The water holding capacity was measured by centrifuging 1 g of the muscles placed on a round plastic plate in a tube for 4 min at 1,500 g and drying at 70°C (Castellini et al., 2002). The MDA level was measured by 2-TBA, the absorbance change at 532 nm was monitored by a spectrophotometer, and data were expressed as nanomole per mg of protein for muscle samples.

The breast muscle specimens were also evaluated for fatty acid analysis. First, the total lipids from thigh tissue were extracted using a chloroform and methanol solution to prepare fatty acid methyl esters. Then, fatty acid methyl esters were analyzed with a Hewlett-Packard 5,890 gas chromatograph equipped with an autosampler, a flame ionization detector, and a fused silica capillary column (30 m × 0.25 mm i.d; Chrompack, Middelburg, Netherlands). The initial oven temperature was 110°C, held for 1 min, then increased to 190°C at 150°C/min and held for 55 min, then increased to 230°C at 5°C/min and held for 5 min. Helium at 30 psi was used as the carrier gas at the flow rate of 0.5 mL/min. Identification of fatty acid methyl esters was made by comparing their retention times with the authentic external standards and obtained values were expressed as a percentage of fatty acid methyl esters or as g/100 g of sample (Apperson and Cherian, 2017).

## Statistical analysis

The Student's t-test was used to assess the TPC, TFC, and antioxidant capacity data, and the variability was expressed as standard error. Data obtained during the feeding period of quail chicks were checked for normality and then analyzed using the GLM procedures of SAS statistical software (SAS, 2010) version 9.4, as a completely randomized design. Tukey's test was used to compare significant differences among the means, and the level of probability less than 0.05 were considered statistically different. Each pen was the experimental unit for all variables studied.

# Results

## Estimation of bioactive compounds

Table 2 presents the mean TPC, TFC, and DPPH values in the black pepper and turmeric extracts. The methanol extract of turmeric was found to have a higher ($p < 0.001$) TPC (about 83.24%) and TFC (about 93.73%) than the black pepper extract. In addition, the turmeric extract showed higher ($p < 0.001$) DPPH radical scavenging activity (about 90%).

## Growth performance

The effects of dietary treatments on the growth performance of growing Japanese quails are presented in Table 3. The tested feed additives did not affect the FI during the starter period. However, the FI during the grower and entire experimental periods in birds fed the CON and BPP diets was lower ($p < 0.007$) than in the other treatments. Quail chicks fed diets supplemented with AGP and TUP had a higher ($p = 0.01$) BWG than those in the CON, BPP, and MIX groups during the starter period. In addition, BWG in the AGP and TUP groups was significantly greater than in the other treatments during the grower ($p = 0.003$) and entire experimental periods ($p = 0.007$). The FCR during the starter and grower periods was significantly better ($p = 0.02$) in birds fed the experimental diets than in the CON diet. During the entire rearing period, quail chicks fed AGP and TUP diets had better ($p = 0.02$) FCR than the other treatments. At all periods, birds fed AGP exhibited a lower FCR than those in the CON group. The results also showed that birds in the TUP group had a numerically lower FCR than those in the CON, BPP, and MIX groups.

## Carcass characteristics and meat quality

The effects of experimental diets on carcass characteristics and meat quality of Japanese quail are summarized in Table 4. The breast yield in birds fed with the CON diet was less ($p = 0.03$) than in the other groups. All the tested feed additives except AGP reduced ($p = 0.005$) abdominal fat percentage. However, the treatments did not affect the relative weights of the carcass, thigh, liver, spleen, cloacal bursa, and heart.

The breast muscle pH and WHC in the birds fed phytogenic additives, particularly in the MIX group, increased ($p = 0.04$; Table 4) after 7 days of refrigerated storage compared to the other groups. Diets supplemented with TUP and MIX decreased ($p = 0.02$) the lightness index in meat samples after 7 days of refrigerated storage compared to the other diets. In addition, after 7 days storage period, the MDA concentration in the MIX group was lower (Figure 1; $p = 0.02$) than in the CON and AGP groups. However, the experimental diets did not affect pH (1 day after storage), WHC (1 day after storage), lightness (1 day after storage), redness (one and 7 days after storage), yellowness (one and 7 days after storage), and the MDA concentration (1 day after storage) of the breast meat.

## Gut microbiota and pH

Table 5 depicts the effects of experimental diets on pH and microbial population in crop and ileum of Japanese quails. The coliform population was higher ($p < 0.001$) in the crop and ileum, while the LAB population was lower ($p = 0.008$) in the ileum section of birds fed the CON diet compared to the other groups. In addition, all the tested feed additives significantly reduced ($p < 0.001$) the

**TABLE 2 Total phenolic, flavonoid content, and antioxidant activity for black pepper and turmeric extracts.[a]**

| | TPC[b] | TFC[c] | DPPH[d] |
|---|---|---|---|
| Black pepper | 32.20 ± 2.03[b] | 19.79 ± 0.48[b] | 63.19 ± 0.90[b] |
| Turmeric | 192.18 ± 2.49[a] | 315.73 ± 2.45[a] | 76.83 ± 0.71[a] |
| *p*-value | <0.0001 | <0.0001 | <0.0001 |

[a]Results are reported as means of 6 replicates ± standard error on a dry weight basis.
[b]TPP, Total phenolic content (as mg gallic acid equivalent/g of freeze-dried extract).
[c]TFC, Total flavonoid content (as mg quercetin equivalent/g of freeze-dried extract).
[d]DPPH, Antioxidant activity evaluated by free radical scavenging activity (as % inhibition). DPPH, scavenging capability of vitamin C (as control) was 95.36%.

**TABLE 3 Effects of TUP, BPP, and MIX on growth performance of Japanese quails.**

| Item[b] | Treatment[a] | | | | | SEM | *p*-value |
|---|---|---|---|---|---|---|---|
| | CON | AGP | TUP | BPP | MIX | | |
| 1–21 days | | | | | | | |
| BWG, g | 90.10[b] | 102.55[a] | 100.36[ab] | 91.24[b] | 93.78[ab] | 2.56 | 0.013 |
| FI, g | 224.33 | 239.98 | 240.78 | 225.08 | 232.80 | 7.28 | 0.361 |
| FCR, g/g | 2.49[a] | 2.34[b] | 2.40[ab] | 2.46[ab] | 2.48[ab] | 0.03 | 0.020 |
| 21–35 days | | | | | | | |
| BWG, g | 70.27[b] | 83.37[a] | 79.27[ab] | 71.46[b] | 72.93[b] | 2.21 | 0.003 |
| FI, g | 318.23[b] | 360.48[a] | 352.82[ab] | 319.60[b] | 327.77[ab] | 8.52 | 0.007 |
| FCR, g/g | 4.53[a] | 4.32[b] | 4.45[ab] | 4.47[ab] | 4.49[ab] | 0.04 | 0.061 |
| 1–35 days | | | | | | | |
| BWG, g | 160.38[c] | 185.92[a] | 179.63[ab] | 162.71[c] | 166.72[bc] | 3.72 | 0.007 |
| FI, g | 542.56[b] | 600.48[a] | 593.60[ab] | 544.68[b] | 560.57[ab] | 12.17 | 0.009 |
| FCR, g/g | 3.38[a] | 3.22[b] | 3.30[ab] | 3.35[a] | 3.36[a] | 0.02 | 0.015 |

[a–c]Means with different superscripts in each row are statistically different ($p < 0.05$).
Data represent means of 5 replicates of 20 quails per treatment.
[a]CON, control; AGP, antibiotic growth promoter; TP, turmeric powder; BPP, black pepper powder; MIX, TP plus BPP.
[b]BWG, body weight gain; FI, feed intake; FCR, feed conversion ratio.

pH of the ileum. Diets containing TUP and MIX showed the best performance in improving the microbiota balance. However, the treatment groups did not affect the pH and LAB population in the crop.

## Intestinal morphology

The morphological characteristics of the small intestine in growing Japanese quails are presented in Table 6. The VH to CD ratio in the duodenum was greater ($p = 0.02$) in the birds fed the tested additives, particularly the MIX diet, than in the CON diet. In the jejunum and ileum, the VH and VH to CD ratios were increased ($p < 0.05$) by supplementation with AGP, TUP, BPP, and MIX compared to the CON diet. In addition, the tested feed additives, particularly MIX and AGP, reduced ($p = 0.02$) CD in the jejunum. However, gut morphology assessments did not reveal any other differences in the morphometric parameters in the birds fed dietary supplements' duodenum, jejunum, and ileum.

## Serum biochemical parameters

Data on blood serum biochemistry are shown in Table 7. Feeding quails with experimental diets including TUP, BPP, and MIX decreased ($p = 0.001$) serum concentration of cholesterol compared to the CON diet. Dietary treatments did not affect triglycerides, ALP, ALT, and AST serum concentrations.

## Fatty acid profile

The effect of the experimental diets on fatty acid content in the breast muscle of Japanese quails is shown in Table 8. Birds fed diets containing phytogenic products (TUP, BPP, and in particular MIX) had higher ($p < 0.05$) contents of C16:1, C18:1, C18:2, C20:5, MUFA, PUFA, and PUFA/SFA ratio and lower ($p < 0.001$) concentrations of C16:0 and SFA compared to the CON diet. The ratio of hypocholesterolaemic to hypercholesterolaemic

**TABLE 4 Effects of TUP, BPP, and MIX on carcass characteristics and meat quality of breast muscle in Japanese quails at 35 days of age.**

| Item[b] | Treatment[a] | | | | | SEM | *p*-value |
|---|---|---|---|---|---|---|---|
| | CON | AGP | TUP | BPP | MIX | | |
| Carcass, % LBW | 69.41 | 70.66 | 69.54 | 70.26 | 69.88 | 0.72 | 0.730 |
| Breast, % LBW | 24.05$^{b}$ | 26.37$^{a}$ | 25.40$^{ab}$ | 25.12$^{ab}$ | 25.31$^{ab}$ | 0.41 | 0.025 |
| Thigh, % LBW | 17.74 | 18.17 | 18.07 | 17.64 | 17.82 | 0.83 | 0.981 |
| Abdominal fat, % LBW | 1.17$^{ab}$ | 1.64$^{a}$ | 0.63$^{b}$ | 0.74$^{b}$ | 0.59$^{b}$ | 0.14 | 0.005 |
| Liver, % LBW | 3.03 | 2.96 | 2.84 | 3.00 | 3.20 | 0.21 | 0.830 |
| Spleen, % LBW | 0.05 | 0.05 | 0.04 | 0.05 | 0.05 | 0.01 | 0.675 |
| Cloacal bursa, % LBW | 0.15 | 0.16 | 0.15 | 0.17 | 0.18 | 0.01 | 0.321 |
| Heart, % LBW | 0.81 | 0.72 | 0.63 | 0.88 | 0.94 | 0.86 | 0.698 |
| $pH_{1\ d}$ | 6.09 | 6.11 | 6.16 | 6.18 | 6.15 | 0.01 | 0.123 |
| $pH_{7\ d}$ | 5.97$^{c}$ | 5.95$^{c}$ | 6.13$^{ab}$ | 6.10$^{b}$ | 6.20$^{a}$ | 0.01 | 0.012 |
| $WHC_{1\ d}$,% | 66.81 | 66.54 | 66.94 | 67.26 | 67.39 | 0.02 | 0.104 |
| $WHC_{7\ d}$,% | 61.94$^{b}$ | 61.63$^{b}$ | 62.42$^{ab}$ | 62.50$^{ab}$ | 63.25$^{a}$ | 0.01 | 0.033 |
| $L^*_{1\ d}$ | 45.47 | 45.59 | 44.34 | 45.38 | 44.04 | 0.28 | 0.365 |
| $L^*_{7\ d}$ | 48.04$^{a}$ | 48.12$^{a}$ | 46.53$^{b}$ | 47.20$^{ab}$ | 46.12$^{b}$ | 0.33 | 0.015 |
| $a^*_{1\ d}$ | 6.21 | 6.18 | 6.30 | 6.59 | 6.61 | 0.19 | 0.401 |
| $a^*_{7\ d}$ | 7.05 | 7.22 | 7.87 | 7.70 | 7.98 | 0.22 | 0.687 |
| $b^*_{1\ d}$ | 25.76 | 25.89 | 25.63 | 25.14 | 25.80 | 0.45 | 0.614 |
| $b^*_{7\ d}$ | 27.05 | 27.13 | 26.33 | 26.90 | 25.92 | 0.50 | 0.321 |

[a-c]Means with different superscripts in each row are statistically different ($p < 0.05$).
Data are means of 5 replicate pens, 2 birds per pen.
[a]CON, control; AGP, antibiotic growth promoter; TUP, turmeric powder; BPP, black pepper powder; MIX, TUP plus BPP.
[b]LBW, live body weight; WHC, water holding capacity; L*, lightness; a*, redness; b*, yellowness.

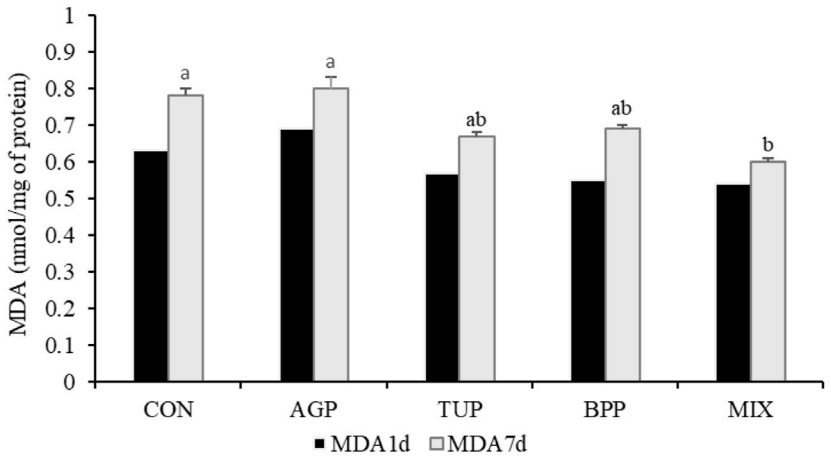


FIGURE 1
Effects of TUP, BPP, and MIX on malondialdehyde (MDA) concentration of breast muscle in Japanese quails at 35 days of age. Data are means of 5 replicate pens, 2 birds per pen. CON, control; AGP, antibiotic growth promoter; TUP, turmeric powder; BPP, black pepper powder; MIX, TUP plus BPP. MDA1d and MDA7d, the content of malondialdehyde 1 and 7 days after storage. Bars with different letters (a, b) statistically differ ($p < 0.05$).

**TABLE 5 Effects of TUP, BPP, and MIX on gastrointestinal microbiota composition and pH value in Japanese quails at 35 days of age.**

| Item | Treatment[a] | | | | | SEM | *p*-value |
|---|---|---|---|---|---|---|---|
| | CON | AGP | TUP | BPP | MIX | | |
| Crop | | | | | | | |
| pH | 5.05 | 5.06 | 4.97 | 4.91 | 5.05 | 0.06 | 0.484 |
| LAB[b] | 7.72 | 7.69 | 8.06 | 7.99 | 7.92 | 0.09 | 0.071 |
| Coliforms | 6.36$^{a}$ | 5.01$^{b}$ | 5.74$^{ab}$ | 5.63$^{ab}$ | 5.52$^{b}$ | 0.19 | <.001 |
| Ileum | | | | | | | |
| pH | 6.67$^{a}$ | 6.30$^{days}$ | 6.43$^{bc}$ | 6.50$^{b}$ | 6.37$^{cd}$ | 0.03 | <.001 |
| LAB | 7.08$^{b}$ | 7.55$^{a}$ | 7.56$^{a}$ | 7.27$^{ab}$ | 7.50$^{a}$ | 0.08 | 0.008 |
| Coliforms | 7.11$^{a}$ | 5.98$^{b}$ | 6.12$^{b}$ | 6.60$^{ab}$ | 6.14$^{b}$ | 0.19 | <.001 |

[a-d]Means with different superscripts in each row are statistically different ($p < 0.05$).
Data are means of 5 replicate pens, 2 birds per pen.
[a]CON, control; AGP, antibiotic growth promoter; TUP, turmeric powder; BPP, black pepper powder; MIX, TUP plus BPP.
[b]LAB, lactic acid bacteria.

**TABLE 6 Effects of TUP, BPP, and MIX on intestinal morphometric analysis in Japanese quails at 35 days of age.**

| Item | Treatment[a] | | | | | SEM | *p*-value |
|---|---|---|---|---|---|---|---|
| | CON | AGP | TUP | BPP | MIX | | |
| Duodenum | | | | | | | |
| Villus height (VH), μm | 776.89 | 806.26 | 769.97 | 784.85 | 825.67 | 24.10 | 0.242 |
| Crypt depth (CD), μm | 117.15 | 104.01 | 113.50 | 112.02 | 104.38 | 5.65 | 0.191 |
| VH:CD | 5.88$^{b}$ | 7.03$^{ab}$ | 6.79$^{ab}$ | 6.68$^{ab}$ | 7.83$^{a}$ | 0.36 | 0.022 |
| Villus width, μm | 141.20 | 153.73 | 145.10 | 152.17 | 153.12 | 11.08 | 0.793 |
| Villus surface area, mm$^2$ | 0.35 | 0.37 | 0.35 | 0.34 | 0.39 | 0.03 | 0.540 |
| Jejunum | | | | | | | |
| Villus height (VH), μm | 610.02$^{c}$ | 655.48$^{a}$ | 629.82$^{b}$ | 624.12$^{bc}$ | 628.08$^{b}$ | 3.81 | <.001 |
| Crypt depth (CD), μm | 120.84$^{a}$ | 111.30$^{b}$ | 113.44$^{ab}$ | 119.67$^{ab}$ | 111.06$^{b}$ | 2.12 | 0.015 |
| VH:CD | 5.05$^{c}$ | 5.89$^{a}$ | 5.56$^{ab}$ | 5.22$^{bc}$ | 5.65$^{ab}$ | 0.10 | 0.001 |
| Villus width, μm | 159.88 | 159.78 | 161.07 | 160.33 | 160.27 | 4.20 | 0.990 |
| Villus surface area, mm$^2$ | 0.30 | 0.33 | 0.32 | 0.31 | 0.31 | 0.09 | 0.474 |
| Ileum | | | | | | | |
| Villus height (VH), μm | 429.16$^{c}$ | 495.66$^{a}$ | 494.04$^{a}$ | 436.80$^{b}$ | 488.18$^{a}$ | 5.38 | <.001 |
| Crypt depth (CD), μm | 105.58 | 112.62 | 114.76 | 110.69 | 113.72 | 2.61 | 0.162 |
| VH:CD | 4.07 | 4.40 | 4.31 | 4.20 | 4.29 | 0.07 | 0.063 |
| Villus width, μm | 91.34 | 88.13 | 89.96 | 80.80 | 88.65 | 5.90 | 0.746 |
| Villus surface area, mm$^2$ | 0.12 | 0.13 | 0.14 | 0.11 | 0.13 | 0.01 | 0.425 |

[a-d]Means with different superscripts in each row are statistically different ($p < 0.05$).
Data are means of 5 replicate pens, 2 birds per pen.
[a]CON, control; AGP, antibiotic growth promoter; TUP, turmeric powder; BPP, black pepper powder; MIX, TUP plus BPP.

**TABLE 7 Effects of TUP or/and BPP on serum biochemical parameters in Japanese quails at 35 days of age.**

| Item[b] | Treatment[a] | | | | | SEM | *p*-value |
|---|---|---|---|---|---|---|---|
| | CON | AGP | TUP | BPP | MIX | | |
| Cholesterol, mg/dL | 131.25$^{a}$ | 128.25$^{ab}$ | 109.50$^{c}$ | 115.75$^{c}$ | 117.75$^{bc}$ | 2.54 | 0.001 |
| Triglycerides, mg/dL | 67.60 | 79.80 | 63.40 | 63.00 | 63.80 | 7.15 | 0.495 |
| ALP, U/L | 366.10 | 390.63 | 375.10 | 379.02 | 334.41 | 24.31 | 0.563 |
| ALT, U/L | 6.06 | 6.39 | 6.21 | 6.16 | 6.03 | 0.39 | 0.972 |
| AST, U/L | 136.81 | 143.06 | 136.40 | 138.14 | 136.53 | 3.42 | 0.621 |

[a-c]Means with different superscripts in each row are significantly different ($p < 0.05$).
Data are means of 5 replicate pens, 2 birds per pen.
[a]CON, control; AGP, antibiotic growth promoter; TUP, turmeric powder; BPP, black pepper powder; MIX, TUP, plus BPP.
[b]ALP, alkaline phosphatase; ALT, alanine aminotransferase; AST, aspartate aminotransferase.

**TABLE 8 Effects of TUP or/and BPP on the fatty acid profile of breast muscle in Japanese quails at 35 days of age.**

| Fatty acid (%) | Treatment[a] | | | | | SEM | *p*-value |
|---|---|---|---|---|---|---|---|
| | CON | AGP | TUP | BPP | MIX | | |
| C14:0 | 0.60 | 0.62 | 0.64 | 0.66 | 0.61 | 0.01 | 0.376 |
| C16:0 | 26.33$^{a}$ | 24.34$^{ab}$ | 23.43$^{b}$ | 23.73$^{b}$ | 22.40$^{b}$ | 0.37 | <.001 |
| C18:0 | 9.25 | 9.16 | 8.64 | 8.99 | 8.64 | 0.10 | 0.178 |
| C20:0 | 0.67 | 0.65 | 0.68 | 0.74 | 0.72 | 0.01 | 0.438 |
| C16:1 n-7 | 3.47$^{b}$ | 4.40$^{ab}$ | 4.61$^{a}$ | 4.57$^{a}$ | 4.63$^{a}$ | 0.14 | 0.021 |
| C18:1 n-9 | 31.39$^{ab}$ | 31.17$^{b}$ | 32.27$^{ab}$ | 32.02$^{ab}$ | 32.52$^{a}$ | 0.15 | 0.031 |
| C18:2 n-6 | 16.84$^{b}$ | 17.86$^{ab}$ | 17.91$^{ab}$ | 17.71$^{ab}$ | 18.33$^{a}$ | 0.14 | 0.010 |
| C18:3 n-3 | 0.79 | 0.81 | 0.83 | 0.86 | 0.84 | 0.01 | 0.139 |
| C18:3 n-6 | 0.35 | 0.34 | 0.35 | 0.36 | 0.37 | 0.01 | 0.810 |
| C20:1 n-9 | 0.65 | 0.66 | 0.71 | 0.65 | 0.70 | 0.01 | 0.734 |
| C20:2 n-6 | 0.42 | 0.44 | 0.45 | 0.42 | 0.48 | 001 | 0.231 |
| C20:3 n-3 | 0.10 | 0.28 | 0.24 | 0.09 | 0.27 | 0.05 | 0.716 |
| C20:3 n-6 | 2.23 | 2.25 | 2.20 | 2.61 | 2.17 | 0.05 | 0.080 |
| C20:4 n-6 | 2.59 | 2.80 | 2.76 | 2.41 | 2.77 | 0.04 | 0.092 |
| C20:5 n-3 | 0.72$^{a}$ | 0.69$^{ab}$ | 0.68$^{ab}$ | 0.61$^{b}$ | 0.72$^{a}$ | 0.01 | 0.021 |
| C22:5 n-3 | 0.64 | 0.64 | 0.69 | 0.71 | 0.72 | 0.01 | 0.102 |
| C22:6 n-3 | 2.65 | 2.84 | 2.79 | 2.80 | 3.03 | 0.04 | 0.159 |
| Saturated fatty acid (SFA) | 36.86$^{a}$ | 34.78$^{ab}$ | 33.41$^{bc}$ | 34.13$^{bc}$ | 32.38$^{c}$ | 0.39 | <.001 |
| Monounsaturated fatty acid (MUFA) | 35.11$^{b}$ | 35.57$^{ab}$ | 36.88$^{a}$ | 36.60$^{ab}$ | 37.16$^{a}$ | 0.23 | 0.006 |
| Polyunsaturated fatty acid (PUFA) | 28.02$^{b}$ | 29.64$^{a}$ | 29.70$^{a}$ | 29.26$^{ab}$ | 30.43$^{a}$ | 0.23 | 0.004 |
| PUFA/SFA | 0.76$^{b}$ | 0.85$^{ab}$ | 0.89$^{a}$ | 0.86$^{a}$ | 0.94$^{a}$ | 0.01 | <.001 |
| n-6/n-3[b] | 4.59 | 4.49 | 4.48 | 4.64 | 4.32 | 0.06 | 0.611 |
| H/H[c] | 2.08$^{c}$ | 2.27$^{bc}$ | 2.41$^{ab}$ | 2.34$^{abc}$ | 2.56$^{a}$ | 0.04 | 0.001 |

[a-c]Means with different superscripts in each row are significantly different ($p < 0.05$).
Data are means of 5 replicate pens, 2 birds per pen.
[a]CON, control; AGP, antibiotic growth promoter; TUP, turmeric powder; BPP, black pepper powder; MIX, TUP, plus BPP.
[b]n-6/n-3, total omega 6 to total omega 3 fatty acid ratio.
[c]H/H, hypocholesterolaemic to hypercholesterolaemic fatty acid ratio.

(H/H) fatty acid increased ($p$ = 0.001) in response to dietary TUP and MIX. However, no significant differences were found between the treatment groups in the contents of C14:0, C18:0, C20:0, C18:3 n-3, C18:3 n-6, C20:1, C20:2, C20:2 n-3, C20:2 n-6, C20:4, C20:5, C20:6, and n-3: n-6 ratio in the breast muscle.

## Discussion

The use of PFAs has become increasingly popular in the post-antibiotic era due to their various biological properties, including antibacterial, antioxidant, and anti-inflammatory effects. Phenolic and flavonoid compounds, which are secondary metabolites of plants, are primarily responsible for their antioxidant and antimicrobial activities. In the current study, turmeric extract's phenolic and flavonoid contents were higher than black pepper extract's, resulting in higher DPPH scavenging activity for turmeric. The feeding trial results indicated that quail chicks fed diets supplemented with AGP and TUP had higher body weight gain and lower FCR than the other groups. However, adding BPP to the experimental diets did not enhance growth performance at any trial stage. Likewise, Khan and Ahmad (2022) reported that TUP at a 0.1% inclusion rate increased BWG and reduced FCR in broiler chickens. Yarru et al. (2009) also suggested adding TUP at a 0.5% inclusion rate to diets to improve BWG in aflatoxin-exposed broiler chickens. Furthermore, prior research has demonstrated that adding different PFAs to broiler diets, such as *Pulicaria gnaphalodes* powder and *Achyrabthes japonica* extract, can improve BWG, FCR, nutrient digestibility, gut microbiota, and intestinal morphology (Shirani et al., 2019; Park and Kim, 2020). Plant extracts, spices, and herbs can improve nutrient digestion in poultry by stimulating various digestive functions, such as appetite, saliva secretion, bile acid secretion, and digestive enzyme activity, including lipase, amylase, and protease (Jang et al., 2007; Oso et al., 2019). These outcomes can ultimately contribute to improved growth performance. The improved growth performance in birds fed the TUP diet in the present study was associated with the higher concentrations of phenolic and flavonoid compounds in turmeric extract. Nevertheless, some studies on PFAs in poultry diets have yielded inconsistent results regarding growth performance, such as the report by Jang et al. (2007). The lack of impact of diets containing BPP on growth performance in the current study is likely due to factors like inclusion dosage, BPP composition, active ingredient concentrations, and their biological activity.

In terms of carcass characteristics, breast yield was found to be higher in birds fed AGP, TUP, and MIX than in the other groups, indicating the growth-promoting effect of these feed additives. Furthermore, the present study's findings demonstrate that using herbal additives (TUP, BPP, and MIX) can reduce abdominal fat in Japanese quails. Similarly, previous studies have demonstrated that dietary supplementation with 100–300 mg/kg turmeric rhizome extract reduces abdominal fat in broiler chickens (Wang et al., 2015). Xie et al. (2019) investigated the effect of curcumin (the primary constituent of turmeric) on the lipid metabolism of broiler chickens and found that curcumin could reduce abdominal fat by decreasing hepatic and plasma lipid concentration and regulating the expression of genes associated with lipogenesis and lipolysis, such as acetyl-CoA carboxylase. According to other studies, active substances present in medicinal plants can also reduce abdominal fat by inhibiting the synthesis of adipose tissue through the modulation of fatty acid transportation (Shirani et al., 2019).

Meat pH is a significant factor that affects meat quality attributes such as color and WHC. A decrease in postmortem pH can result in protein denaturation, leading to paleness and decreased WHC of the meat. The data from this study indicated that the MIX treatment increased the meat sample pH value after 7 days of refrigerated storage compared to the CON and AGP treatments. The WHC of meat is another critical parameter that indicates the muscle tissue's ability to retain moisture and directly affects meat taste and tenderness. A lower WHC reflects losses in the meat's nutritional value through released exudates, resulting in tougher and less flavorful meat (Cao et al., 2012). The simultaneous inclusion of TUP and BPP in the diet and their synergistic effect can control oxidation reactions in meat to maintain water storage space between myofibrils and increase WHC in meat (Huff-Lonergan and Lonergan, 2005). Rajput et al. (2014) also reported that natural antioxidants, such as carotenoids in curcumin, can improve meat's WHC by modulating the redox state and enhancing the antioxidant capacity in muscle. Meat color is a crucial criterion related to meat freshness and quality, affecting consumer acceptance of meat. It is evaluated by determining the lightness, redness, and yellowness (Niu et al., 2017). According to Jiang et al. (2014), consumers prefer redness; a lower yellowness index indicates less pale meat. In the present study, diets supplemented with TUP and MIX decreased the lightness index in meat samples after 7 days of refrigerated storage compared to the other diets. Niu et al. (2017) suggested that the decrease in the lightness index might be related to the increased antioxidant activity of PFAs, which protects cells from damage and prevents cell juice extravasation, ultimately decreasing light reflection.

The MDA concentration in tissue indirectly mirrors lipid peroxidation, which is the outcome of attenuated antioxidant protection (Jazi et al., 2020). Long-term storage is one of the reasons for the increased lipid peroxidation in meat after slaughter (Aziza et al., 2010). In the current study, lower MDA content in breast muscle during 7 days of storage at 4°C was observed when quails were fed the MIX diet. Thus, the simultaneous inclusion of TUP and BPP may provide a more efficient free radical scavenging activity in birds. Similarly, improvements in the lipid peroxidation of meat have been reported in several studies when herbal additives rich in phenolic compounds or flavonoids were added to the diet (Aziza et al., 2010; Cao et al., 2012).

The current study found that the tested feed additives reduced pH and coliforms in the crop and ileum while increasing the LAB population in the ileum of birds. The growth inhibition of coliforms by TUP and BPP was similar to that of AGP. Curcumin possesses high antibacterial activity against *Clostridium difficile*, as shown by an *in vitro* study by Mody et al. (2020). Additionally, the administration of curcumin in humans has been reported to markedly shift the ratio of beneficial and pathogenic bacteria by enhancing the population of *lactobacilli*, *bifidobacteria*, and butyrate-producing bacteria and decreasing the number of *enterococci* and *enterobacteria*, as

reported by Zam (2018). Moreover, several *in vivo* studies have demonstrated the potent antibacterial activity of black pepper essential oil against pathogenic *Escherichia coli* and *Staphylococcus*. (Zhang et al., 2017; Abdallah and Abdolla, 2018). Some studies with Japanese quails (Mehri et al., 2015) and broiler chickens (Chowdhury et al., 2018) indicate *in vivo* antibacterial activity of different PFAs (peppermint and cinnamon) against intestinal pathogenic microbes such as coliform and *E. coli*. One of the critical features of PFAs is their hydrophobicity, allowing them to easily enter the bacterial cell membrane, leading to cell membrane disintegration, leakage of intracellular material, reduction of proton force, and, eventually, death of the bacterial cell (Zeng et al., 2015; Barbarestani et al., 2020). Therefore, reducing the population of pathogenic bacteria, such as coliforms within the gastrointestinal tract, may increase the number of beneficial bacteria, such as LAB. Another possible explanation for the positive effect of PFAs on the growth of beneficial bacteria is that LAB can metabolize phenolic compounds as nutritional substrates, suggesting the prebiotic-like impact of phenolic compounds (Iqbal et al., 2020).

Intestinal epithelial integrity and structure play an important role in nutrient digestion, absorption, and overall gut health (Soumeh et al., 2019). Intestinal villi are the leading site for absorption of nutrients; therefore, longer villi may indicate a greater surface area, which in turn can enhance nutrient absorption capacity, while deeper crypt may suggest fast cellular turnover and regeneration processes of tissue due to damage that is induced by pathogens (Jazi et al., 2018b). Therefore, VH: CD can reflect digestive and absorptive capacities. The present study showed that the MIX treatment group had a higher VH: CD ratio in the duodenum, while the AGP, TUP, and MIX groups had higher VH and VH: CD ratio in the jejunum. The tested feed additives increased the ileum's VH compared to the control group. Improving the intestinal mucosal structure in response to dietary PFAs may be linked to an increased population of beneficial bacteria, which can produce antibacterial compounds and compete with harmful pathogens like coliforms. This can prevent their colonization and minimize their negative impact on the intestinal structure (Jazi et al., 2017). Feeding broiler chickens with PFAs may also stimulate mucus secretion into the intestine, which can act as a dynamic protective surface and prevent the adherence of pathogens to intestinal epithelial cells (Cornick et al., 2015; Zeng et al., 2015). Furthermore, the antioxidant activity of PFAs may protect villi from oxidative stress caused by digestive processes (Zeng et al., 2015). The present study found that combining TUP and BPP in the diet improved the population of gastrointestinal microbiota and intestinal morphology more effectively, indicating synergistic effects between TUP and BPP.

The serum concentrations of cholesterol and triglycerides can reflect lipid metabolism (Sharifi et al., 2023). The current study revealed that the tested feed additives reduced the concentration of cholesterol. Kim and Kim (2010) reported a significant reduction in serum cholesterol levels in rats fed an excessive fat diet supplemented with curcumin, possibly due to increased expression of cholesterol 7α-hydroxylase, a rate-limiting enzyme in bile acid formation from cholesterol. Xie et al. (2019) suggested that curcumin reduces cholesterol by inhibiting ATP-citrate lyase, a key enzyme in fatty acid synthesis that converts citrate to acetyl CoA. Piperine, the active compound in black pepper, is known to reduce plasma and liver cholesterol by changing cholesterol transporter proteins and reducing lipogenic gene expression (Tunsophon and Chootip, 2016). Shirani et al. (2019) suggested that the hypocholesterolemic effect of PFAs may result from the active ingredient's inhibitory effects on the 3-hydroxy-3-methyl glutaryl-CoA enzyme, a key enzyme for cholesterol biosynthesis. Serum levels of ALT, ALP, and AST serve as indicators of liver health and functionality, as their concentrations increase when liver cells are destroyed (Mohebodini et al., 2019). However, in the present study, the experimental treatments did not affect the concentrations of these enzymes and therefore had no negative impact on the liver.

Researchers have recently focused on modifying fatty acid compounds in poultry meat, as the level of SFA are correlated to hypercholesterolemia and coronary heart disease (Ahmed et al., 2015; Shirani et al., 2019). Our results demonstrated that dietary supplementation with TUP, BPP, and MIX increased the concentrations of total MUFA, PUFA, and PUFA/SFA ratio while decreasing total SFA content. However, the MIX diet had a more pronounced effect on the meat fatty acid profile, possibly due to the synergistic effects. Similar observations were made in broiler chickens fed phytogenic products containing TUP by Daneshyar et al. (2011). It has been suggested that palmitic acid (C16:0) often raises blood cholesterol levels, while oleic acid (C18:1) has the opposite effect on blood cholesterol. Additionally, PUFA may decrease abdominal fat deposition by enhancing the expression of acyl-CoA oxidase (the main enzyme of the beta-oxidation process) (Crespo and Esteve-Garcia, 2001; 2002). The decrease in SFA in the meat of birds may be related to an increase in the amount of oleic acid (C18:1) and MUFA, given that stearic acid (C18:0) is converted to oleic acid (C18:1) more rapidly (Ahmed et al., 2015). In addition, the enhanced PUFA concentration may be due to the improvement of the antioxidant defense system, which could protect PUFA oxidation and cause the production of stable products (Mohebodini et al., 2021). The PUFA: SFA and n-6: n-3 ratios are typically used to assess the nutritional value of meat. Ahmed et al. (2015) suggested that meat with a PUFA: SFA ratio less than 0.4 and n-6: n-3 ratio greater than 5 is considered unfavorable because they may increase cholesterolemia. In the current study, although the n-6: n-3 ratio was not affected by the experimental treatments, the PUFA: SFA ratio in birds fed the additives was higher than the minimum recommended values, indicating a positive effect of the tested PFAs on meat quality. In addition to the above indices, a more comprehensive approach to the nutritional evaluation of meat could involve using indices based on the functional effects of fatty acids, such as the HH ratio (Santos-Silva et al., 2002). The highest HH index values were recorded in birds fed the MIX diet, indicating a better nutritional value of meat in this group. Therefore, these findings suggest that consuming these meats may lower humans' risk of coronary disease.

The present study indicates that the simultaneous application of TUP and BPP to improve growth performance is ineffective. However, TUP alone can result in improvements in BWG and FCR. Additionally, because the simultaneous inclusion of TUP and BPP can positively affect the population of gastrointestinal microbiota and intestinal morphology, their combination may be more effective under stressful conditions. Combining TUP and BPP

in the diet also improves breast meat quality and shelf life, indicating the synergistic effects between TUP and BPP.

## Data availability statement

The raw data supporting the conclusion of this article will be made available by the authors, without undue reservation.

## Ethics statement

The animal study was reviewed and approved by the Institutional Animal Care and Use Committee at the Gorgan University of Agriculture Sciences and Natural Resources, Gorgan, Iran.

## Author contributions

The authors listed have made a substantial, direct, and intellectual contribution to the work and approved it for publication.

## Funding

This work is funded by the Gorgan University of Agricultural Sciences and Natural Resources.

## Conflict of interest

The authors declare that the research was conducted in the absence of any commercial or financial relationships that could be construed as a potential conflict of interest.

## Publisher's note

All claims expressed in this article are solely those of the authors and do not necessarily represent those of their affiliated organizations, or those of the publisher, the editors and the reviewers. Any product that may be evaluated in this article, or claim that may be made by its manufacturer, is not guaranteed or endorsed by the publisher.

## References

Abdallah, E. M., and Abdalla, W. E. (2018). Black pepper fruit (*Piper nigrum* L) as antibacterial agent: A mini-review. *J. Bacteriol. Mycol. Open Access* 6, 141–145. doi:10.15406/jbmoa.2018.06.00192

Ahmed, S. T., Islam, M. M., Bostami, A. R., Mun, H. S., Kim, Y. J., and Yang, C. J. (2015). Meat composition, fatty acid profile and oxidative stability of meat from broilers supplemented with pomegranate (*Punica granatum L*) by-products. *Food Chem.* 188, 481–488. doi:10.1016/j.foodchem.2015.04.140

Amalraj, A., Pius, A., Gopi, S., and Gopi, S. (2017). Biological activities of curcuminoids, other biomolecules from turmeric and their derivatives–A review. *Tradit. Complement. Med.* 7, 205–233. doi:10.1016/j.jtcme.2016.05.005

Apperson, K. D., and Cherian, G. (2017). Effect of whole flax seed and carbohydrase enzymes on gastrointestinal morphology, muscle fatty acids, and production performance in broiler chickens. *Poult. Sci.* 96, 1228–1234. doi:10.3382/ps/pew371

Aziza, A. E., Quezada, N., and Cherian, G. (2010). Antioxidative effect of dietary Camelina meal in fresh, stored, or cooked broiler chicken meat. *Poult. Sci.* 89, 2711–2718. doi:10.3382/ps.2009-00548

Barbarestani, S. Y., Jazi, V., Mohebodini, H., Ashayerizadeh, A., Shabani, A., and Toghyani, M. (2020). Effects of dietary lavender essential oil on growth performance, intestinal function, and antioxidant status of broiler chickens. *Livest. Sci.* 233, 103958. doi:10.1016/j.livsci.2020.103958

Cao, F. L., Zhang, X. H., Yu, W. W., Zhao, L. G., and Wang, T. (2012). Effect of feeding fermented Ginkgo biloba leaves on growth performance, meat quality, and lipid metabolism in broilers. *Poult. Sci.* 91, 1210–1221. doi:10.3382/ps.2011-01886

Castellini, C., Mugnai, C. A. N. D., and Dal Bosco, A. (2002). Effect of organic production system on broiler carcass and meat quality. *Meat Sci.* 60, 219–225. doi:10.1016/S0309-1740(01)00124-3

Chowdhury, S., Mandal, G. P., Patra, A. K., Kumar, P., Samanta, I., Pradhan, et al. (2018). Different essential oils in diets of broiler chickens: 2. Gut microbes and morphology, immune response, and some blood profile and antioxidant enzymes. *Anim. Feed Sci. Tech.* 236, 39–47. doi:10.1016/j.anifeedsci.2017.12.003

Cornick, S., Tawiah, A., and Chadee, K. (2015). Roles and regulation of the mucus barrier in the gut. *Tissue Barriers* 3, e982426. doi:10.4161/21688370.2014.982426

Cottica, S. M., Sabik, H., Antoine, C., Fortin, J., Graveline, N., Visentainer, J. V., et al. (2015). Characterization of Canadian propolis fractions obtained from two-step sequential extraction. *LWT - Food Sci. Technol.* 60, 609–614. doi:10.1016/j.lwt.2014.08.045

Crespo, N., and Esteve-Garcia, E. (2001). Dietary fatty acid profile modifies abdominal fat deposition in broiler chickens. *Poult. Sci.* 80, 71–78. doi:10.1093/ps/80.1.71

Crespo, N., and Esteve-Garcia, E. (2002). Dietary linseed oil produces lower abdominal fat deposition but higher de novo fatty acid synthesis in broiler chickens. *Poult. Sci.* 81, 1555–1562. doi:10.1093/ps/81.10.1555

Daneshyar, M., Ghandkanlo, M. A., Bayeghra, F. S., Farhangpajhoh, F., and Aghaei, M. (2011). Effects of dietary turmeric supplementation on plasma lipoproteins, meat quality and fatty acid composition in broilers. *S. Afr. J. Anim.* 41, 420–428. doi:10.4314/sajas.v41i4.13

Gorgani, L., Mohammadi, M., Najafpour, G. D., and Nikzad, M. (2017). Piperine—the bioactive compound of black pepper: From isolation to medicinal formulations. *Compr. Rev. Food Sci. Food Saf.* 16, 124–140. doi:10.1111/1541-4337.12246

Huff-Lonergan, E., and Lonergan, S. M. (2005). Mechanisms of water-holding capacity of meat: The role of postmortem biochemical and structural changes. *Meat Sci.* 71, 194–204. doi:10.1016/j.meatsci.2005.04.022

Iqbal, Y., Cottrell, J. J., Suleria, H. A., and Dunshea, F. R. (2020). Gut microbiota-polyphenol interactions in chicken: A review. *Animals* 10, 1391. doi:10.3390/ani10081391

Jang, I. S., Ko, Y. H., Kang, S. Y., and Lee, C. Y. (2007). Effect of a commercial essential oil on growth performance, digestive enzyme activity and intestinal microflora population in broiler chickens. *Anim. Feed Sci. Tech.* 134, 304–315. doi:10.1016/j.anifeedsci.2006.06.009

Jazi, V., Ashayerizadeh, A., Toghyani, M., Shabani, A., and Tellez, G. (2018b). Fermented soybean meal exhibits probiotic properties when included in Japanese quail diet in replacement of soybean meal. *Poult. Sci.* 97, 2113–2122. doi:10.3382/ps/pey071

Jazi, V., Boldaji, F., Dastar, B., Hashemi, S. R., and Ashayerizadeh, A. (2017). Effects of fermented cottonseed meal on the growth performance, gastrointestinal microflora population and small intestinal morphology in broiler chickens. *Br. Poult. Sci.* 58, 402–408. doi:10.1080/00071668.2017.1315051

Jazi, V., Farahi, M., Khajali, F., Abousaad, S., Ferket, P., and Assadi Soumeh, E. (2020). Effect of dietary supplementation of whey powder and *Bacillus subtilis* on growth performance, gut and hepatic function, and muscle antioxidant capacity of Japanese quail. *J. Anim. Physiol. Anim. Nutr.* 104, 886–897. doi:10.1111/jpn.13323

Jazi, V., Foroozandeh, A. D., Toghyani, M., Dastar, B., and Koochaksaraie, R. R. (2018a). Effects of *Pediococcus acidilactici*, mannan-oligosaccharide, butyric acid and their combination on growth performance and intestinal health in young broiler chickens challenged with *Salmonella* Typhimurium. *Poult. Sci.* 97, 2034–2043. doi:10.3382/ps/pey035

Jazi, V., Mohebodini, H., Ashayerizadeh, A., Shabani, A., and Barekatain, R. (2019). Fermented soybean meal ameliorates Salmonella Typhimurium infection in young broiler chickens. *Poult. Sci.* 98, 5648–5660. doi:10.3382/ps/pez338

Jiang, S. Q., Jiang, Z. Y., Zhou, G. L., Lin, Y. C., and Zhemg, C. T. (2014). Effects of dietary isoflavone supplementation on meat quality and oxidative stability during storage in lingnan yellow broilers. *J. Integr. Agric.* 13, 387–393. doi:10.1016/S2095-3119(13)60386-X

Khan, K., and Ahmad, N. (2022). Using cinnamon (*Cinnamomum zeylanicum*) and turmeric (*Curcuma longa* L) powders as an antibiotic growth promoter substitution in broiler chicken's diets. *Anim. Biotechnol.* 1, 1–8. doi:10.1080/10495398.2022.2157282

Kim, M., and Kim, Y. (2010). Hypocholesterolemic effects of curcumin via up-regulation of cholesterol 7a-hydroxylase in rats fed a high fat diet. *Nutr. Res. Pract.* 4, 191–195. doi:10.4162/nrp.2010.4.3.191

Mehri, M., Sabaghi, V., and Bagherzadeh-Kasmani, F. (2015). Mentha piperita (*peppermint*) in growing Japanese quails diet: Performance, carcass attributes, morphology and microbial populations of intestine. *Anim. Feed Sci. Tech.* 207, 104–111. doi:10.1016/j.anifeedsci.2015.05.021

Mensor, L. L., Menezes, F. S., Leitão, G. G., Reis, A. S., Santos, T. C. D., Coube, C. S., et al. (2001). Screening of Brazilian plant extracts for antioxidant activity by the use of DPPH free radical method. *Phytother. Res.* 15, 127–130. doi:10.1002/ptr.687

Mirzaei, H., Shakeri, A., Rashidi, B., Jalili, A., Banikazemi, Z., and Sahebkar, A. (2017). Phytosomal curcumin: A review of pharmacokinetic, experimental and clinical studies. *Biomed. Pharmacother.* 85, 102–112. doi:10.1016/j.biopha.2016.11.098

Mody, D., Athamneh, A. I., and Seleem, M. N. (2020). Curcumin: A natural derivative with antibacterial activity against *Clostridium difficile*. *J. Glob. Antimicrob. Resist* 21, 154–161. doi:10.1016/j.jgar.2019.10.005

Mohebodini, H., Jazi, V., Ashayerizadeh, A., Toghyani, M., and Tellez-Isaias, G. (2021). Productive parameters, cecal microflora, nutrient digestibility, antioxidant status, and thigh muscle fatty acid profile in broiler chickens fed with *Eucalyptus globulus* essential oil. *Poult. Sci.* 100, 100922. doi:10.1016/j.psj.2020.12.020

Mohebodini, H., Jazi, V., Bakhshalinejad, R., Shabani, A., and Ashayerizadeh, A. (2019). Effect of dietary resveratrol supplementation on growth performance, immune response, serum biochemical indices, cecal microflora, and intestinal morphology of broiler chickens challenged with *Escherichia coli*. *Livest. Sci.* 229, 13–21. doi:10.1016/j.livsci.2019.09.008

Niu, Y., Wan, X. L., Zhang, X. H., Zhao, L. G., He, J. T., Zhang, J. F., et al. (2017). Effect of supplemental fermented Ginkgo biloba leaves at different levels on growth performance, meat quality, and antioxidant status of breast and thigh muscles in broiler chickens. *Poult. Sci.* 96, 869–877. doi:10.3382/ps/pew313

NRC (1994). *Nutrient requirements of poultry*. 9th rev. Washington, DC, USA: Natl. Acad. Press.

Ogbuewu, I. P., Okoro, V. M., and Mbajiorgu, C. A. (2020). Meta-analysis of the influence of phytobiotic (pepper) supplementation in broiler chicken performance. *Trop. Anim. Health Prod.* 6, 17–30. doi:10.1007/s11250-019-02118-3

Oso, A. O., Suganthi, R. U., Reddy, G. M., Malik, P. K., Thirumalaisamy, G., Awachat, V. B., et al. (2019). Effect of dietary supplementation with phytogenic blend on growth performance, apparent ileal digestibility of nutrients, intestinal morphology, and cecal microflora of broiler chickens. *Poult. Sci.* 98, 4755–4766. doi:10.3382/ps/pez191

Park, J. H., and Kim, I. H. (2020). Effects of dietary *Achyranthes japonica* extract supplementation on the growth performance, total tract digestibility, cecal microflora, excreta noxious gas emission, and meat quality of broiler chickens. *Poult. Sci.* 99, 463–470. doi:10.3382/ps/pez533

Pirgozliev, V., Mansbridge, S. C., Rose, S. P., Lillehoj, H. S., and Bravo, D. (2019). Immune modulation, growth performance, and nutrient retention in broiler chickens fed a blend of phytogenic feed additives. *Poult. Sci.* 98, 3443–3449. doi:10.3382/ps/pey472

Rajput, N., Ali, S., Naeem, M., Khan, M. A., and Wang, T. (2014). The effect of dietary supplementation with the natural carotenoids curcumin and lutein on pigmentation, oxidative stability and quality of meat from broiler chickens affected by a coccidiosis challenge. *Br. Poult. Sci.* 55, 501–509. doi:10.1080/00071668.2014.925537

Salehi, B., Stojanović-Radić, Z., Matejić, J., Sharifi-Rad, M., Kumar, N. V. A., Martins, N., et al. (2019). The therapeutic potential of curcumin: A review of clinical trials. *Eur. J. Med. Chem.* 163, 527–545. doi:10.1016/j.ejmech.2018.12.016

Santos-Silva, J., Bessa, R. J. B., and Santos-Silva, F. J. L. P. S. (2002). Effect of genotype, feeding system and slaughter weight on the quality of light lambs: II. Fatty acid composition of meat. *Livest. Prod. Sci.* 77, 187–194. doi:10.1016/S0301-6226(02)00059-3

SAS (2010). *SAS user's guide. Statistics. Version 9.3ed*. Cary, NC: SAS Inst. Inc.

Shabani, A., Jazi, V., Ashayerizadeh, A., and Barekatain, R. (2019). Inclusion of fish waste silage in broiler diets affects gut microflora, cecal short-chain fatty acids, digestive enzyme activity, nutrient digestibility, and excreta gas emission. *Poult. Sci.* 98, 4909–4918. doi:10.3382/ps/pez244

Sharifi, F., Jazi, V., and Assadi Soumeh, E. (2023). Elecampane rhizome extract alleviates methotrexate-induced hepatotoxicity and nephrotoxicity in male rats. *Adv. Tradit. Med.* 2023. doi:10.1007/s13596-023-00679-1

Shirani, V., Jazi, V., Toghyani, M., Ashayerizadeh, A., Sharifi, F., and Barekatain, R. (2019). *Pulicaria gnaphalodes* powder in broiler diets: Consequences for performance, gut health, antioxidant enzyme activity, and fatty acid profile. *Poult. Sci.* 98, 2577–2587. doi:10.3382/ps/pez010

Shityakov, S., Bigdelian, E., Hussein, A. A., Hussain, M. B., Tripathi, Y. C., Khan, M. U., et al. (2019). Phytochemical and pharmacological attributes of piperine: A bioactive ingredient of black pepper. *Eur. J. Med. Chem.* 176, 149–161. doi:10.1016/j.ejmech.2019.04.002

Singleton, V. L., Orthofer, R., and Lamuela-Raventós, R. M. (1999). [14] Analysis of total phenols and other oxidation substrates and antioxidants by means of folin-ciocalteu reagent. *Meth. Enzymol.* 299, 152–178. doi:10.1016/S0076-6879(99)99017-1

Soumeh, E. A., Mohebodini, H., Toghyani, M., Shabani, A., Ashayerizadeh, A., and Jazi, V. (2019). Synergistic effects of fermented soybean meal and mannan-oligosaccharide on growth performance, digestive functions, and hepatic gene expression in broiler chickens. *Poult. Sci.* 98, 6797–6807. doi:10.3382/ps/pez409

Strimpakos, A. S., and Sharma, R. A. (2008). Curcumin: Preventive and therapeutic properties in laboratory studies and clinical trials. *Antioxid. Redox Signal* 10, 511–545. doi:10.1089/ars.2007.1769

Tunsophon, S., and Chootip, K. (2016). Comparative effects of piperine and simvastatin in fat accumulation and antioxidative status in high fat-induced hyperlipidemic rats. *Can. J. Physiol. Pharmacol.* 94, 1344–1348. doi:10.1139/cjpp-2016-0193

Vijayakumar, R. S., and Nalini, N. (2006). Piperine, an active principle from Piper nigrum, modulates hormonal and apolipoprotein profiles in hyperlipidemic rats. *J. Basic. Clin. Physiol. Pharmacol.* 17, 71–86. doi:10.1515/JBCPP.2006.17.2.71

Wang, D., Huang, H., Zhou, L., Li, W., Zhou, H., Hou, G., et al. (2015). Effects of dietary supplementation with turmeric rhizome extract on growth performance, carcass characteristics, antioxidant capability, and meat quality of Wenchang broiler chickens. *Ital. J. Anim. Sci.* 14, 3870. doi:10.4081/ijas.2015.3870

Windisch, W., Schedle, K., Plitzner, C., and Kroismayr, A. (2008). Use of phytogenic products as feed additives for swine and poultry. *J. Anim. Sci.* 86, E140–E148. doi:10.2527/jas.2007-0459

Xie, Z., Shen, G., Wang, Y., and Wu, C. (2019). Curcumin supplementation regulates lipid metabolism in broiler chickens. *Poult. Sci.* 98, 422–429. doi:10.3382/ps/pey315

Yarru, L. P., Settivari, R. S., Gowda, N. K. S., Antoniou, E., Ledoux, D. R., and Rottinghaus, G. E. (2009). Effects of turmeric (*Curcuma longa*) on the expression of hepatic genes associated with biotransformation, antioxidant, and immune systems in broiler chicks fed aflatoxin. *Poult. Sci.* 88, 2620–2627. doi:10.3382/ps.2009-00204

Zam, W. (2018). Gut microbiota as a prospective therapeutic target for curcumin: A review of mutual influence. *J. Nutr. Metab.* 2018, 1367984. doi:10.1155/2018/1367984

Zeng, Z., Xu, X., Zhang, Q., Li, P., Zhao, P., Li, Q., et al. (2015). Effects of essential oil supplementation of a low-energy diet on performance, intestinal morphology and microflora, immune properties and antioxidant activities in weaned pigs. *Anim. Sci. J.* 86, 279–285. doi:10.1111/asj.12277

Zhang, J., Ye, K. P., Zhang, X., Pan, D. D., Sun, Y. Y., and Cao, J. X. (2017). Antibacterial activity and mechanism of action of black pepper essential oil on meat-borne *Escherichia coli*. *Front. Microbiol.* 7, 2094. doi:10.3389/fmicb.2016.02094

frontiers | Frontiers in Physiology

TYPE Review
PUBLISHED 31 August 2023
DOI 10.3389/fphys.2023.1260987



OPEN ACCESS

EDITED BY
Xiaofei Wang,
Tennessee State University, United States

REVIEWED BY
Nima Emami,
Novozymes, United States
Stephen T. Kinsey,
University of North Carolina Wilmington, United States

*CORRESPONDENCE
Nabeel Alnahhas,
nabeel.alnahhas@fsaa.ulaval.ca

RECEIVED 18 July 2023
ACCEPTED 21 August 2023
PUBLISHED 31 August 2023

CITATION
Alnahhas N, Pouliot E and Saucier L (2023), The hypoxia-inducible factor 1 pathway plays a critical role in the development of breast muscle myopathies in broiler chickens: a comprehensive review.
*Front. Physiol.* 14:1260987.
doi: 10.3389/fphys.2023.1260987



# The hypoxia-inducible factor 1 pathway plays a critical role in the development of breast muscle myopathies in broiler chickens: a comprehensive review

Nabeel Alnahhas[1]*, Eric Pouliot[2] and Linda Saucier[1,3,4]

[1]Department of Animal Science, Faculty of Agricultural and Food Sciences, Université Laval, Quebec, QC, Canada, [2]Olymel S.E.C./L.P, Boucherville, QC, Canada, [3]Institute of Nutrition and Functional Foods, Université Laval, Quebec, QC, Canada, [4]Swine and Poultry Infectious Diseases Research Center, Université de Montréal, Saint-Hyacinthe, QC, Canada

In light of the increased worldwide demand for poultry meat, genetic selection efforts have intensified to produce broiler strains that grow at a higher rate, have greater breast meat yield (BMY), and convert feed to meat more efficiently. The increased selection pressure for these traits, BMY in particular, has produced multiple breast meat quality defects collectively known as breast muscle myopathies (BMM). Hypoxia has been proposed as one of the major mechanisms triggering the onset and occurrence of these myopathies. In this review, the relevant literature on the causes and consequences of hypoxia in broiler breast muscles is reviewed and discussed, with a special focus on the hypoxia-inducible factor 1 (HIF-1) pathway. Muscle fiber hypertrophy induced by selective breeding for greater BMY reduces the space available in the *perimysium* and *endomysium* for blood vessels and capillaries. The hypoxic state that results from the lack of circulation in muscle tissue activates the HIF-1 pathway. This pathway alters energy metabolism by promoting anaerobic glycolysis, suppressing the tricarboxylic acid cycle and damaging mitochondrial function. These changes lead to oxidative stress that further exacerbate the progression of BMM. In addition, activating the HIF-1 pathway promotes fatty acid synthesis, lipogenesis, and lipid accumulation in myopathic muscle tissue, and interacts with profibrotic growth factors leading to increased deposition of matrix proteins in muscle tissue. By promoting lipidosis and fibrosis, the HIF-1 pathway contributes to the development of the distinctive phenotypes of BMM, including white striations in white striping–affected muscles and the increased hardness of wooden breast–affected muscles.

KEYWORDS

**wooden breast, white striping, spaghetti meat, hypoxia, HIF-1, broiler chickens**

## 1 Introduction

Poultry meat is increasingly popular, and is increasingly consumed worldwide. According to the OECD (2022), meat consumption has been shifting toward poultry meat, and this trend is expected to continue in the long term. The popularity of poultry meat can be explained in high-income countries by consumer preference for white meat that is seen as a healthier choice than red meat. In low- and middle-income countries, this trend is

mainly driven by the lower price of poultry meat than for other meat-producing animal species (OECD, 2022). In addition, poultry meat production and consumption are not subjected to traditional or religious restrictions.

In response to this increased popularity and to the growing world population, poultry meat production has been constantly increasing since the 1960s. In 2020, poultry meat accounted for 32% of worldwide meat production, slightly behind pork (36%) and well above meat produced from other species. Poultry meat production is projected to increase by 16% and to account for nearly half of all meat consumed between 2020 and 2031 (OECD, 2022).

The ability of the poultry industry to meet this increasing demand is based on its capacity to develop broiler strains with improved growth rates, higher feed efficiencies, and greater meat yield. This is achieved mainly by genetic selection, improved management, and optimized nutritional strategies. Early studies comparing strains of broiler chickens over time showed that genetic selection accounted for 80%–90% of achieved progress in broiler performances, while improved nutritional and feeding strategies accounted only for 10%–20% of this progress (Havenstein et al., 2003a; Havenstein et al., 2003b). In a more recent study, Zuidhof et al. (2014) compared broiler strains from 1957, 1978, and 2005 and showed that broiler growth rate had increased by 400% between 1957 and 2005 with a 50% reduction in feed conversion ratio. This study also showed an increase of 79% and 85% in the yield of the *Pectoralis major* muscle over this same period in male and female broilers, respectively. In modern commercial broiler chickens, such as Ross 308 weighing 2.6 kg, breast meat accounts for 25.1% and 27.2% of body weight in male and female broilers, respectively.

As it will be discussed in the following sections, the increased development of the pectoral muscles in commercial strains of broiler chickens has not been without consequences for the quality of broiler breast meat. In fact, multiple breast meat quality defects have emerged in recent years including breast muscle myopathies (BMM) of non-infectious origin such as white striping (WS), wooden breast (WB), and spaghetti meat (SM). These myopathies, which are moderately to highly (50%–65%) determined by genetics (Alnahhas et al., 2016; Lake et al., 2021), are associated with significant negative economic consequences for the poultry industry (Kuttappan et al., 2016; Barbut, 2019), and research is underway to develop strategies to reduce their occurrence and severity.

This review will summarize the available literature on the role of hypoxia in the development of BMM and will specifically elucidate the relationship between the hypoxia-inducible factor 1 (HIF-1) pathway and the development of the pathological changes associated with BMM. In Section 2, a brief overview of the characteristics of the *P. major* muscle is presented. In Section 3, the major structural and biochemical changes associated with selection for increased BMY are briefly discussed. The histopathological and biochemical characteristics of myopathic muscles are briefly described in Section 4. Sections 5 and 6 discuss the role of the HIF-1 pathway in the development of the histopathological and biochemical characteristics observed in myopathic muscles. The role of hypoxia in inducing apoptosis in myopathic muscles is discussed in Section 7. A summary of the most probable cascade of events between the activation of the HIF-1 pathway and the development of the phenotypic characteristics of BMM is presented in Section 8. Finally, conclusions and research perspectives are presented in Section 9.

## 2 A brief overview of the pectoral muscles in broiler chickens

The pectoral muscles in avian species are skeletal muscles that are responsible for producing the mechanical force required for flight. This section will focus on the *P. major* muscle, the target of breast muscles myopathies. The primary role of this muscle is to produce the force necessary for wing downstrokes, in contrast to the *P. minor* muscle, which powers wing upstrokes (Cao and Jin, 2020).

In terms of structure, the *P. major* muscle, similar to other skeletal muscles, is composed of striated muscle fibers. These fibers are individually surrounded by a thin collagen layer called the *endomysium*. Individual muscle fibers aggregate to form muscle bundles, and each bundle is surrounded by a collagen layer called the *perimysium*. Muscle bundles combine to form whole muscles, which are surrounded by a third dense layer of collagen called the *epimysium* (Kranen et al., 2000; Velleman, 2020). The structural integrity of these layers of connective tissue is critical for the maintenance of muscle structure, and blood vessels and capillaries supplying muscle tissue with nutrients and oxygen run through the *perimysium* and *endomysium*, respectively (Kranen et al., 2000; Velleman, 2015).

Microscopically, a muscle fiber is composed of a succession of sarcomeres, the smallest structural and functional units in skeletal muscles. In normal *P. major* muscle, sarcomere lengths vary between 1.6 and 1.8 µm (Soglia et al., 2020). Sarcomeres are composed of thin and thick myofilaments, called actin and myosin myofilaments, respectively. These proteins represent the contractile fraction of muscle proteins (Mudalal et al., 2014). Muscle contraction is produced when actin filaments slide past myosin filaments, shortening the sarcomeres, which in turn leads to muscle fiber contraction (Squire, 2016). The cytoplasm of muscle fibers that fill the space between myofilaments is called the *sarcoplasm* and contains the sarcoplasmic fraction of muscle proteins. Anaerobic glycolysis, the main pathway that generates the necessary chemical energy to power muscle contraction, takes place in the sarcoplasm where glycogen reserves are stored and glycolytic enzymes are located (Xu and Becker, 1998; Meléndez-Morales et al., 2009).

Muscle fibers can be generally classified as type I and type II. Type II muscle fibers can be further classified into type IIA and type IIB (Talbot and Maves, 2016). The *P. major* muscle in commercial broiler chickens is entirely composed of the latter fiber type (Verdiglione and Cassandro, 2013). Compared with type I, type IIB muscle fibers have a larger diameter, faster contractile speeds, lower concentrations of myoglobin, and greater glycogen reserves (Huo et al., 2022). Metabolically, Type IIB muscle fibers have reduced numbers of mitochondria and large glycolytic reserves, which means anaerobic glycolysis is the main energy (*i.e.,* ATP) production pathway in this muscle (Velleman, 2020; Huo et al., 2022). This type of muscle fiber is adapted to short and intense bursts of activity, in contrast to type I fibers that are more adapted to less intense but longer periods of activity (Meléndez-Morales et al., 2009). Broilers are mostly kept in closed poultry houses (limiting the

possibility of flight), which is likely the reason for the shift of their breast muscle fibers from type I, which is observed in the breast of their common ancestor the red jungle fowl (*Gallus gallus spadiceuse*), to type IIB fibers, which are observed in the breast muscles of modern broiler strains (Lokman et al., 2016). Selecting broilers for increased BMY is also a contributing factor to this switch in muscle fiber type as it has been previously shown that the mitochondrial content of the *P. major* muscle of broiler chickens was negatively correlated (−0.27, $p = 0.037$) with BMY (Reverter et al., 2017). Evidence suggests that in type IIB myofibers, centralized nuclei can be observed during growth in normal breast muscles (Rosser et al., 2002). According to these authors, this intermyofibrillar distribution of nuclei is an adaptation that allows muscle fibers to meet their requirements in protein synthesis during hypertrophic growth. This centralized position of nuclei coupled with the shift of mitochondria toward the periphery of myofibers during hypertrophic growth (Belichenko et al., 2004) indicate that type IIB myofibers are susceptible to becoming hypoxic at their core as the diffusion distance from blood capillaries increases due to increased myofiber diameter while demand for oxygen is simultaneously increasing due to the high metabolic rate of broiler chickens.

During embryogenesis, muscle development is achieved by the formation of embryonic myoblasts that fuse together to form myotubes, which later become mature muscle fibers (Yablonka-Reuveni, 1995; Greene et al., 2023). At hatch, the number of muscle fibers is fixed, and post-hatch muscle growth is achieved through the increase in muscle fibers size or myofiber hypertrophy (Remignon et al., 1995; Geiger et al., 2018). Muscle satellite cells are adult stem cells or precursor cells that are also formed during embryogenesis and located peripherally between the basal lamina and the sarcoplasmic membrane (or the sarcolemma) of muscle fibers (Daughtry et al., 2017). These cells provide the nuclei required for the hypertrophy of muscle fibers by fusing with them, and they also play a critical role in muscle repair (*i.e.,* regenerative myogenesis) after injury (Geiger et al., 2018; Velleman, 2023). Under normal conditions, satellite cells remain in a quiescent state in their niches. When stimulated, they activate and start proliferating to increase their number and to maintain their populations. They then differentiate to form new myofibers that replace degenerated muscle tissue (Velleman, 2015; 2020). In skeletal muscles, satellite cells need to be within 21 µm of blood capillaries to actively regenerate muscle fibers (Christov et al., 2007).

In summary, the *P. major* muscle in broiler chickens is composed of fast-twitch, hypertrophic, glycolytic muscle fibers using anaerobic glycolysis as the main energy production pathway. In case of injury or damage, satellite cells are activated to repair the damaged muscle tissue, which requires the presence of blood capillaries in the niches of these cells.

# 3 Consequences of muscle fiber hypertrophy in the *Pectoralis major* muscle

Genetic selection for increased growth rate and BMY is known to operate by increasing the diameter of muscle fibers. For instance, Geiger et al. (2018) compared two genetic lines of broiler chickens that were divergently selected over 58 generations for higher or lower body weight (BW), which is positively correlated with the growth of the *P. major* muscle (Alnahhas et al., 2014; Alnahhas et al., 2016). In the study of Geiger et al. (2018), the cross-sectional area of muscle (CSA) fibers in the *P. major* muscle from the line selected for increased BW was twice as large ($p < 0.001$) as that of the line selected for lower BW. In another study, Orlowski et al. (2021) compared the histomorphological traits of the *P. major* muscle at the 5th generation in two broiler lines divergently selected for greater (HBY4) or lower (LBY4) percent breast yield at 4 days of age. These authors showed that the diameter of muscle fibers of the *P. major* from the HBY4 line was significantly larger than that of the LBY4 line at day 56 (54.29 ± 1.13 vs. 45.39 ± 0.92 µm, $p < 0.0001$) while the number of muscle fibers in this muscle was not significantly different between the two lines. Finally, Koomkrong et al. (2015) compared a native Thai breed that did not undergo selection to a commercial strain of broiler chickens. These authors also reported a significantly greater diameter of muscle fiber in the *P. major* muscle of the commercial strain compared with that of the native breed (52.31 ± 1.83 vs. 33.31 ± 2.20 µm, $p = 0.003$). These findings provide further evidence that muscle fiber hypertrophy in broiler breast muscles is the primary driver of post-hatch growth, and it is mainly induced by selective breeding for increased BW and BMY.

## 3.1 Muscle fiber hypertrophy is associated with decreased muscle capillary density

One consequence of myofiber hypertrophy is the decrease in connective tissue spaces, especially in the *perimysium* and *endomysium* (Velleman et al., 2003; Velleman, 2019). As mentioned earlier, muscle blood capillaries run through these layers of connective tissue. Thus, a reduction in their spaces leads to reduced muscle capillary density. For instance, Joiner et al. (2014) evaluated the histomorphology of the *P. major* muscle from standard (2.5 kg) and heavy (3.5 kg) broilers and reported a significant increase in the diameter of muscle fibers (+18%) that was associated with a significant decrease in the average number of capillaries (−22.9%) and blood vessels (−43.9%) in the heavy broilers compared to the standard broilers. More recently, Pampouille et al. (2019) compared the histological characteristics of a normal *P. major* muscle from a slow-growing genetic line (similar to the French Label Rouge) to normal *P. major* muscle from a fast-growing commercial line of broiler chickens and showed that increased growth rate and BMY were associated with a 121% ($p < 0.001$) increase in muscle fiber size coupled with a 34% ($p < 0.001$) decrease in the number of blood capillaries. Yalcin et al. (2019) also compared slow- and fast-growing commercial broilers at market age and reported a 48% increase ($p < 0.05$) in myofiber area that was associated with a 14.9% decrease in the capillary density in the *P. major* muscle of the fast-compared to the slow-growing strain. The reduced capillary density of the *P. major* muscle in fast-growing and high-yielding broiler strains is the primary factor predisposing this muscle to the development of BMM as it will be discussed in the following sections.

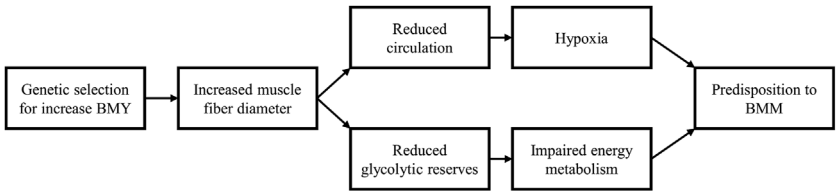


FIGURE 1
Consequences of muscle fiber hypertrophy. Genetic selection for increased breast meat yield (BMY) operates by increasing muscle fiber diameter. Myofiber hypertrophy leads to a decrease in the interstitial spaces (*perimysium* and *endomysium*) in which blood vessels and capillaries are found, resulting in a reduced density of the vascular network. Myofiber hypertrophy is also associated with decreased energy or glycogen content in muscle tissue. The reduced capillary density and decreased glycogen reserves predispose the *Pectoralis major* muscle to the development of breast muscle myopathies.

### 3.2 Muscle fiber hypertrophy is associated with decreased muscle energy reserves

Another consequence of genetic selection for increased BW and BMY is decreased energy (glycogen) reserves in the *P. major* muscle. In an earlier study, Berri et al. (2001) compared an experimental and a commercial line to their respective control lines in terms of glycolytic potential at 6 weeks of age. These authors showed a significant ($p < 0.05$) decrease in the glycolytic potential from 128 to 87 µM/g in the *P. major* muscle from the selected commercial line compared with its non-selected control line. In a later study, Berri et al. (2007) investigated the histological and metabolic characteristics of the *P. major* muscle of male birds from a commercial grand-parental line of broiler chickens at 6 weeks of age. In this study, muscle fibers were grouped into five categories based on their CSA ranging from 1,260 to 2,443 µm$^2$ before comparing their metabolic characteristics. Findings from this work demonstrated that muscle energy reserves, as measured by the glycolytic potential, decreased significantly from 111.6 to 102.4 µM/g with increased muscle fiber CSA.

In summary (Figure 1), increased muscle fiber diameter reduces the capillary density and glycogen storage in the *P. major* muscle compromising its functioning and predisposing it to the occurrence of BMM.

## 4 Breast muscle myopathies (BMM)

Selective breeding for increased BW and BMY has resulted in structural and metabolic changes in the *P. major* muscle. These changes have led to the emergence of a new category of non-infectious myopathies collectively called breast muscle myopathies (Petracci and Cavani, 2012; Petracci et al., 2015; Kuttappan et al., 2016; Barbut, 2019). The three most commonly known and studied myopathies are WS, WB, and SM. These myopathies were first reported in 2009, 2014, and 2016 by Bauermeister et al. (2009), Sihvo et al. (2014) and by Sirri et al. (2016), respectively. In this section, we will briefly describe the pathological changes associated with these myopathies in the *P. major* muscle before we described the role of hypoxia in the development of these changes in the following sections.

### 4.1 Macroscopic description of myopathic muscles

BMM have very distinctive visual and textural characteristics. White striping (WS, Figure 2A) can be described as the appearance of white striations running parallel to the direction of muscle fibers on the ventral (skin) side of the *P. major* muscle (Kuttappan et al., 2012). The thickness of these striations and the muscle surface they cover depend on the severity of this myopathy. In mild to moderate forms, the thickness of the striations is usually less than 1 mm and cover the cranial part of muscle surface, while in severe cases, their thickness is greater than 1 mm and cover the entire ventral surface of the muscle (Kuttappan et al., 2012; Khalil et al., 2021).

Wooden breast (WB, Figure 2B), as its name implies, is characterized by increased muscle hardness. In the mild forms of WB, this hardness is rather focal and limited to the cranial part of the *P. major* muscle, while in severe cases, it diffuses toward the caudal part of the muscle leading to extensive hardness of the entire muscle accompanied by bulges and petechiae covered with a thin viscous layer of clear or turbid material (Sihvo et al., 2014).

Spaghetti meat (SM, Figure 2C) is described as the loss of cohesiveness in the tissue of the *P. major* muscle (Sirri et al., 2016). In its moderate forms, it is characterized by a moderate loss of cohesiveness on the cranioventral part of the muscle leading to a loose muscle tissue that can fold relatively easily when pinched. In its severe forms, extended superficial lacerations of muscle tissue can be observed on the cranioventral surface of the muscle (Sirri et al., 2016). In addition, muscle bundles are separated and appear as thin mushy fibers that resemble spaghetti, hence the name (Baldi et al., 2021).

### 4.2 Microscopic description of myopathic muscles

BMM are characterized by multiphasic degenerative processes that induce regenerative and anti-inflammatory responses from muscle tissue. In the case of WS, Kuttappan et al. (2013) reported muscle fiber degeneration, lysis, and loss of cross-striation in the *P. major* muscle of 45-day-old commercial broiler chickens. They also reported multifocal edema and infiltration of lymphocytes and macrophages in the interstitial spaces of these muscles. Signs of muscle tissue regeneration such as variability in

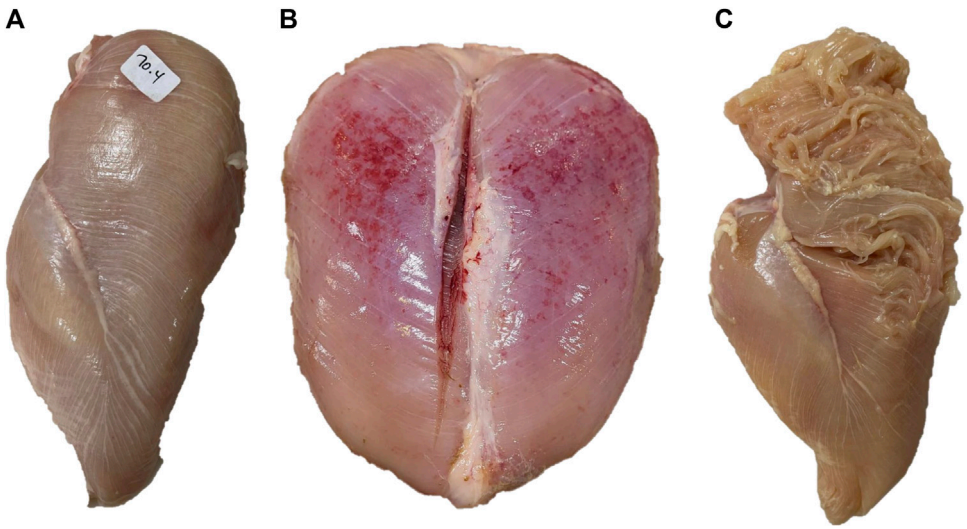


FIGURE 2
Examples of breast muscles exhibiting severe white striping **(A)**, wooden breast **(B)** and spaghetti meat **(C)**. Severe white striping is characterized by the occurrence of white striations with a diameter greater than 1 mm, running in parallel to the direction of muscle fibers, covering the entire ventral surface of the muscle. Severe wooden breast is associated with increased muscle hardness from the cranial to the caudal end of the *Pectoralis major* muscle, coupled with petechia. Severe spaghetti meat is associated with disintegration and separation of muscle bundles appearing like spaghetti.

muscle fiber size, nuclear rowing and the presence of multinucleated cells were also reported in this study. One of the distinctive features of WS is increased lipid deposition (lipidosis) within the connective tissue, leading to the appearance of the characteristic phenotype of white striations on the surface of the muscle (Alnahhas et al., 2016; Baldi et al., 2018).

WB-affected *P. major* muscles exhibit similar histopathological changes to those observed in WS. For instance, Sihvo et al. (2014) reported multifocal degeneration of muscle fibers, loss of cross-striation, and infiltration of inflammatory cells including macrophages and heterophils within and around the degenerated muscle fibers in the *P. major* muscle from 5 to 6-week-old commercial broiler chickens. These authors also reported the presence of muscle fibers of variable diameters and centralized nuclei, which are signs of regeneration of damaged muscle tissue. One of the most important characteristics of WB is the diffuse thickening of the interstitial spaces with a variable amount of collagen-rich connective tissue or fibrosis (Sihvo et al., 2014). This replacement of muscle tissue by fibrous connective tissue leads to the increased hardness of the *P. major* muscle that can be detected by palpation (Velleman et al., 2017).

SM also presents histopathological changes similar to those associated with WS and WB. According to Baldi et al. (2018), SM-affected *P. major* muscles are very soft and stringy, particularly in the cranioventral part. These authors reported extensive myofiber degeneration accompanied by inflammatory cell infiltration, lipidosis in damaged muscle tissue, and regeneration of fibers with variable diameters. The distinctive characteristics of SM are the compromised (*i.e.,* very thin) connective tissue of the *perimysium* and *endomysium,* and the numerous longitudinally split myofibers that give this myopathy its specific phenotype (Baldi et al., 2018).

The histopathological changes associated with BMM are more pronounced in the cranial and middle part of the *P. major* muscle (Che et al., 2022), and are mostly focused in the superficial layer (0.5–1.2 cm from the ventral surface) of this muscle in WS (Baldi et al., 2018) and in both the superficial and deep (from 1.5 to 2.5 cm from the ventral surface) layers of the muscle in WB (Soglia et al., 2017).

## 4.3 Protein, lipid, and collagen content of myopathic muscles

The histopathological changes associated with BMM induce changes in the chemical composition of the *P. major* muscle. Gratta et al. (2019) investigated the effect of WS and WB on the proximate composition of the *P. major* muscle from 49-day-old commercial broiler chickens. In this study, protein content was similar in WS-affected fillets and normal fillets (23.2% vs. 23.9%, $p > 0.05$) while the protein content in WB was significantly lower than in normal fillets (21.4% vs. 23.9%, $p < 0.05$). Baldi et al. (2019) analyzed the proximate composition of the superficial and deep layers of normal and myopathic *P. major* muscles from 46-day-old commercial broiler chickens. Compared with normal fillets, WB- and SM-affected fillets had significantly ($p < 0.001$) lower protein content (20.5, 21.0, and 22.9% for WB, SM, and normal, respectively) in the superficial layer, while in the deep layer, only SM-affected fillets had a lower protein content than unaffected muscles (21.6% vs. 23.0%, $p < 0.001$). In both layers, the protein content of WS-affected fillets was not significantly different from normal fillets (22.0% vs. 22.9% and 22.5% vs. 23.0%, respectively, for the two layers). Fillets affected with any of the three myopathies had significantly ($p < 0.05$) greater lipid content in the superficial layer than normal fillets (1.51, 2.05, 2.12, and 1.84% for normal, WS, WB,

and SM, respectively). In this study, the same trend ($p < 0.05$) was also found in the deep layer of the *P. major* muscle (1.59, 1.84, 1.80, and 1.83% of lipid for normal, WS, WB, and SM, respectively). Taken together, these findings indicate a more extensive degenerative process that can reach the deep layers of the *P. major* muscle in the case of WB and SM, but it tends to be more focused in the superficial layer in the case of WS in line with the above-reported histopathological changes.

In skeletal muscles, collagen is one of the main building blocks of the connective tissue that maintains the structural integrity of these muscles (Sanden et al., 2021). As previously mentioned, BMM are associated with fibrosis, where degenerated or necrotic muscle tissue is replaced by fibrous collagen-rich tissue, resulting in the development of the BMM phenotypes such as muscle hardness in WB-affected fillets. There are two types of collagen fibrils in skeletal muscles: type I and type III. This latter type is predominant in muscles during early growth stages and after injuries (Velleman, 2020). In myopathic muscles, the distribution of type III collagen was found to vary between WS- and WB-affected muscles (Mazzoni et al., 2020). Using immunohistochemistry on breast muscle samples from 45-days-old fast-growing broilers, these authors showed that the connective tissue of WS-affected muscle was strongly reactive for collagen type III while a weak immunoreactivity to this collagen fibril type was found in the perimysium and endomysium of WB-affected muscles. Multiple studies have investigated changes in collagen content in myopathic muscles. In their work, Soglia et al. (2016a) compared fillets from 52-day-old commercial broilers exhibiting WB, WS, or both (WB + WS) with normal fillets and reported a significant ($p < 0.001$) increase in collagen content in (WB + WS)–affected fillets compared with normal fillets (1.09 < 1.18 < 1.26%, respectively for normal, WB, and WB + WS). Geronimo et al. (2022) compared the ratio of collagen-to-protein between normal and WB-affected *P. major* muscles from 47-day-old commercial broilers and saw a significant increase in this ratio in the WB-affected muscles compared with normal muscle (7.15 vs. 5.18, $p < 0.05$). Findings from these two studies clearly showed that with increased severity of WB, muscle tissue is replaced by fibrous tissue, which explains the increased hardness of WB-affected muscles. This statement is also supported by the work of Ferreira et al. (2020) who used fluorescent Western blotting to analyze the relative expression of collagen protein in the *P. major* muscle sampled from a high-yielding strain of broiler chickens at the age of 43 days, scoring them as normal, mild, and severe with respect to WB. These authors found that the relative expression of collagen protein increased ($p = 0.001$) with the severity of WB (3-fold increase from normal to severe) at 43 days of age. Evidence suggests that different changes in the structural organization of muscle collagen could lead to the development of phenotypically distinctive myopathies. For instance, Sanden et al. (2021) combined differential staining and Fourier Transform Infrared (FTIR) microspectroscopy to study changes in the collagen structure of the *P. major* muscle from 32-day-old commercial broilers exhibiting WB and SM. In cross-sections of the muscle stained with picrosirius red, the *perimysium* of myopathic muscles was heterogeneously stained, and it exhibited gaps and short threads oriented in different directions. This is in contrast to the *perimysium* of normal muscles, which appeared as compact and continuous strings with evenly sized, parallelly aligned, and tightly packed bundles of collagen. Furthermore, the matrix was denser and more intensely stained in WB-affected muscles than in SM-affected muscles. According to Sanden et al. (2021), these changes suggest alterations in the structure and organization of collagen fiber in myopathic muscles. An interesting finding from this study was that collagen from SM-affected muscles was rich in loosely bound *a*-helices, while WB-affected fillets had more triple helical and *ß*-sheet structures. This could explain the difference between their distinctive phenotypes of structural disintegration or extreme hardness, respectively.

In summary, the development of BMM is associated with the replacement of muscle tissue by increased amounts of lipids and disorganized connective tissue, which contributes to the development of their characteristic phenotypes.

## 4.4 Biochemical characteristics of myopathic muscles

The hypertrophic growth of breast muscles of fast-growing and high-yielding strains of broiler chickens is associated with a decrease in glycogen reserves (Berri et al., 2007; Abasht et al., 2016), resulting in a higher ultimate pH of breast meat in severe cases of BMM (Mudalal et al., 2015). Baldi et al. (2020) conducted a study that aimed to elucidate the mechanisms underlying the higher ultimate pH in WB-affected *P. major* muscles sampled from 48-day-old commercial broilers. As expected, muscle glycogen levels were lower ($p < 0.001$) in WB-affected muscles compared with normal muscles at 15 min *post-mortem*. The ultimate pH (pHu) is almost completely determined by the glycolytic potential (GP) of the *P. major* muscle at death as measured by the GP at 15 min *post-mortem*, and these two parameters (GP and pHu) were found to be almost perfectly negatively correlated at the genetic level (Le Bihan-Duval et al., 2008). Consequently, in the study of Baldi et al. (2020), the lower GP at 15 min *post-mortem* led to a significantly higher ($p < 0.001$) pHu in WB-affected muscles at 24 h *post-mortem*, which could be attributed to an earlier cessation of *post-mortem* acidification caused by the lower initial (at death) glycogen content in WB-affected muscles. Additionally, in WB-affected muscles, Zhao et al. (2020) reported a 2.8-fold ($p < 0.02$) and 3.5-fold ($p < 0.004$) increase in the mRNA and protein expression of monocarboxylate transporter 4 (*MTC4*) in WB-affected muscles compared with normal muscles. This translates to an increase in lactate exportation from the cell (Zhao et al., 2020), which could also contribute to the higher pHu in WB-affected muscles. In their study, Baldi et al. (2020) suggested multiple hypotheses to explain the changes in *post-mortem* energy metabolism in myopathic muscles. One of the hypotheses suggested an impaired mitochondrial function based on the significantly ($p < 0.001$) lower ATP levels found in WB-affected muscles at 15 min *post-mortem*. In a recent study, Li et al. (2022) examined the effect of WB severity on the activity of citrate synthase, a major enzyme in the tricarboxylic acid cycle (TCA) and a marker of mitochondrial activity. In support of the hypothesis of Baldi et al. (2020), Li et al. (2022) showed a significant ($p < 0.05$) decrease in the activity of this enzyme from 2.7 μmol/(mLmin) in normal *P. major* muscle to 1.8 μmol/

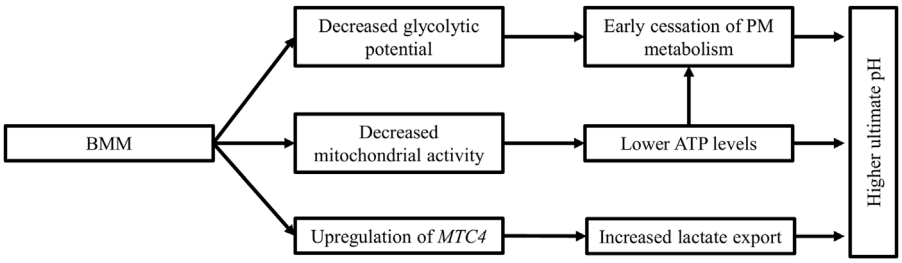


FIGURE 3
Biochemical changes in myopathic muscles. Breast muscle myopathies are associated with a higher ultimate pH than unaffected muscles. The increase in ultimate pH can be explained by the lower glycolytic reserves in these muscles at death, coupled with decreased mitochondrial activity, leading to lower ATP levels and early cessation of *post-mortem* acidification. The lower lactate level in myopathic muscles is the result of the upregulation of the monocarboxylate transporter 4 (*MTC4*), which increases lactate export from cells.

(mLmin) in severely affected muscles. This finding, coupled with the observed deterioration of mitochondrial ultrastructure (Sihvo et al., 2018; Hosotani et al., 2020), could also contribute to the higher pHu in WB-affected muscles. This mitochondrial damage may potentially reduce *in vivo* ATP synthesis, resulting in rapid ATP depletion and in the cessation of *post-mortem* metabolism shortly after death.

To summarize (Figure 3), myopathic muscles are characterized by a deficient energy reserve and perturbated energy production leading to early cession of *post-mortem* acidification and subsequently a higher ultimate pH in the *P. major* muscle.

# 5 Hypoxia induces the development of breast muscle myopathies

The immediate consequences of the reduced density of the capillary network in the *P. major* muscle (see section 3.1) and the subsequent reduction in circulation are hypoxia, lower nutrient supply, and accumulation of metabolic waste in muscle tissue which are all factors that predispose muscles for the development of BMM.

Hypoxia is now largely accepted as a trigger of the development of BMM (Zambonelli et al., 2016; Boerboom et al., 2018; Greene et al., 2019; Emami et al., 2021). In their study, Greene et al. (2019) used diffused reflectance spectroscopy to measure oxygen saturation in the *P. major* muscle of WB-affected and unaffected commercial broilers. These authors found a significant decrease in oxygen saturation in the thickest part of the severely WB-affected muscles, which is indicative of a hypoxic condition. Emami et al. (2021) placed random-bred modern broilers in hypobaric chambers to simulate high altitude (*i.e.,* lower oxygen) conditions from 2 to 6 weeks of age. In this study, the total incidence of WB in the birds kept under high altitude conditions was 3.3-fold higher than that of birds kept under low altitude conditions (90.41% vs. 27.69%) at similar BW. These two studies provided experimental evidence confirming the critical role of hypoxia in the development of BMM.

Under hypoxic conditions, the HIF-1 pathway, a major regulator of oxygen homeostasis, is upregulated (Greene et al., 2019). In this section, the consequences of the upregulation of this pathway on the development of BMM will be examined after a brief overview of the HIF-1 pathway.

## 5.1 Overview of the hypoxia-inducible factor 1 (HIF-1) pathway

HIF-1 (Figure 4) is a heterodimeric transcription factor consisting of two subunits: the *a* (HIF-1α) and *ß* (HIF-1β) subunits (Ziello et al., 2007). In contrast to HIF-1β, which is constitutively expressed, HIF-1α is oxygen sensitive or oxygen regulated (Masoud and Li, 2015).

Under normoxic conditions, HIF-1α is continuously synthesized, but it has a very short lifespan as cells continuously degrade HIF-1α protein (Weidemann and Johnson, 2008). The *a* subunit of HIF-1 has a degradation domain called the oxygen-dependent degradation domain (Huang et al., 1998). This domain has two proline residues ($Pro^{402}$ and $Pro^{564}$) that are hydroxylated under normoxic conditions by a group of oxygen-dependent enzymes called prolyl-4-hydroxylases or PHD (Kant et al., 2013). The hydroxylation of these two proline residues lead to the binding of the von Hippel–Lindau tumor suppressor protein (pVHL), the substrate recognition component of an E3 ubiquitin ligase, to the HIF-1α protein (Haase, 2009). The pVHL protein tags the cytoplasmic HIF-1α protein for ubiquitination and subsequently for rapid proteasomal degradation (Haase, 2009). Thus, when oxygen is available in the cells, the HIF-1 transcription factor cannot be formed, and consequently, hypoxia-inducible genes are not transcribed.

Under hypoxic conditions, the hydroxylation of the proline residues on the cytoplasmic HIF-1α protein cannot take place, because PHD enzymes are oxygen-dependent and are suppressed during the absence of oxygen (Jaakkola et al., 2001). The persisting HIF-1α protein in the cytoplasm can then be translocated to the nucleus to form the HIF-1 heterodimer with the HIF-1β subunit. This transactivating complex can then bind to hypoxia-responsive elements (HRE) in hypoxia-inducible genes (HIG), leading to their enhanced transcription (Weidemann and Johnson, 2008).

As a major transcription factor, HIF-1 not only regulates oxygen homeostasis, but it is also involved in energy metabolism, including glycolysis, oxidative phosphorylation and fatty acid metabolism (Weidemann and Johnson, 2008; Kierans and Taylor, 2021), angiogenesis, apoptosis, and several other pathways of importance to BMM (Malila et al., 2019; Marchesi et al., 2019). Finally, HIF-1 is involved in the regulation of mitochondrial mass, size, distribution, and morphology (Thomas and Ashcroft, 2019)

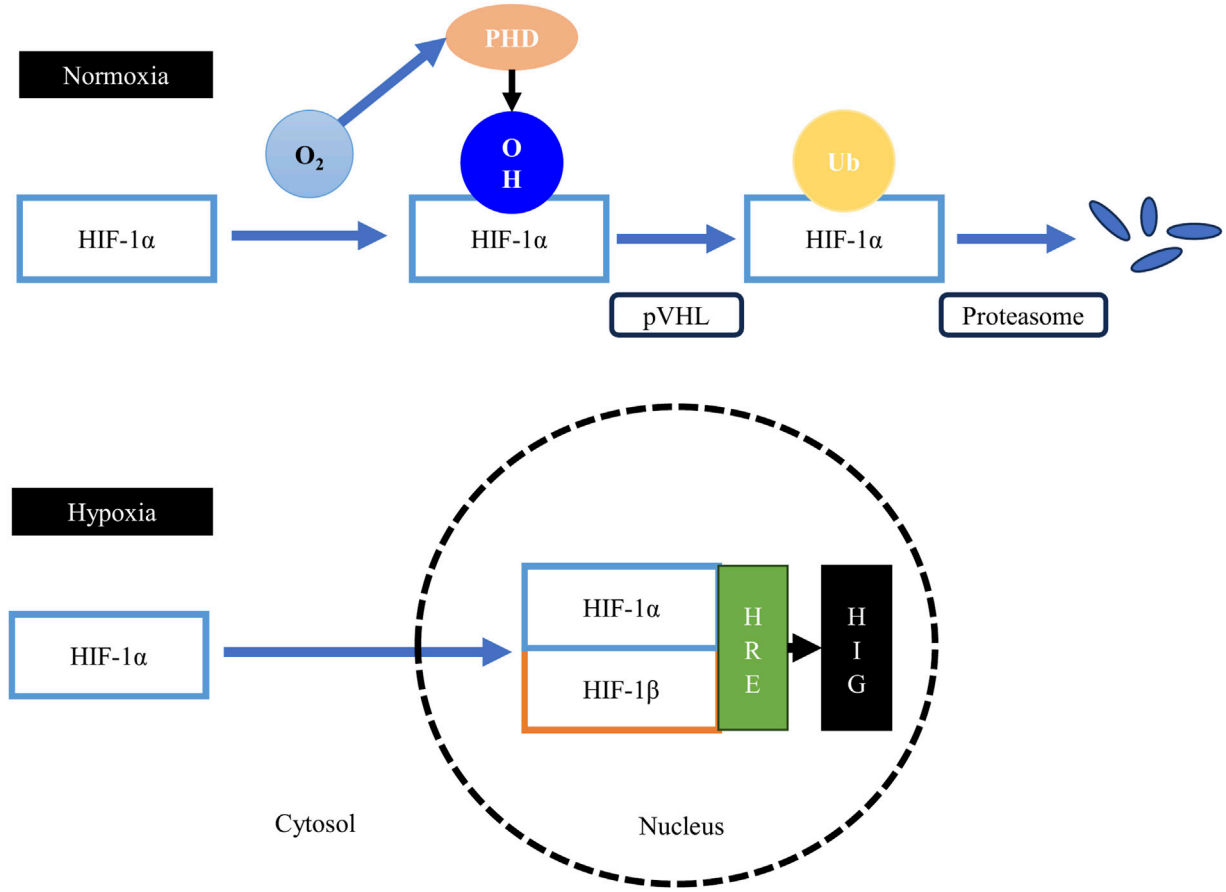


FIGURE 4
The hypoxia-inducible factor 1 (HIF-1) pathway. Under normoxic conditions, the proline residues on the HIF-1α subunit are hydroxylated by the oxygen-dependent prolyl-4-hydroxylases (PHD), leading to the binding of the von Hippel–Lindau tumor suppressor protein (pVHL), the substrate recognition component of an E3 ubiquitin ligase, to the HIF-1α protein. The pVHL protein tags the sarcoplasmic HIF-1α protein for ubiquitination and subsequent rapid proteasomal degradation. Therefore, formation of the HIF-1 heterodimer is obstructed, suppressing the transcription of hypoxia-inducible genes (HIG). Under hypoxic conditions, the activity of the prolyl-4-hydroxylases is suppressed, which allows the stabilization of the HIF-1α subunit and its subsequent translocation to the nucleus to form the HIF-1 heterodimer with the HIF-1β subunit. The heterodimer then binds to the hypoxia-responsive elements (HRE), upregulating the expression of HIG.

and also in the regulation of mitochondrial dynamics (Hosotani et al., 2020).

## 5.2 *HIF-1α* is upregulated in myopathic muscles

Hypoxia plays a key role in the development of BMM. In this context, multiple studies have reported an upregulation of the HIF-1 pathway in muscles exhibiting one or more myopathies. In their study, Marchesi et al. (2019) analyzed the whole transcriptome of WS-affected *P. major* muscles from 42-day-old commercial broiler chickens using the RNA-Seq technology. Among the differentially expressed genes detected in this study, *HIF-1α* was upregulated (>1.2-fold) in WS-affected muscles when compared with normal muscles. Using droplet digital PCR, the mRNA expression of *HIF-1α* was investigated in normal and myopathic muscles exhibiting WS or WS + WB from 6-week-old broilers with medium- or heavy-weight carcasses (Malila et al., 2019). This study also demonstrated an approximate 4-fold increase in the expression of *HIF-1α* in the myopathic muscles compared with normal muscles. In a different study, the expression of *HIF-1α* at the mRNA and protein levels was measured in WB-affected muscles sampled from 56-day-old broilers using RT-qPCR and Western blotting, respectively (Greene et al., 2019). These authors confirmed the increased expression of *HIF-1α* at the mRNA level in the myopathic muscles compared with unaffected muscles, and further showed a significant increase in its expression at the protein level.

Taken together, these findings provide further evidence for the critical role of hypoxia in the occurrence of BMM and highlight the key role of the HIF-1 pathway in the development of these myopathies.

## 5.3 Hypoxia alters energy metabolism in myopathic muscles

The HIF-1 pathway plays a key role in the adaptation of cells to hypoxia by promoting a shift in their energy metabolism from mitochondrial respiration toward anaerobic glycolysis (Kierans and

Taylor, 2021). As discussed previously, the *P. major* muscle of broiler chickens is entirely composed of type IIB myofibers (Verdiglione and Cassandro, 2013), in which anaerobic glycolysis is the predominant energy production pathway. This is important to highlight because, in skeletal muscles, the expression of *HIF-1α* varies according to muscle fiber type. At the mRNA level, the expression of *HIF-1α* in mouse glycolytic muscles (composed of type IIB myofibers) was 3-fold higher than that in oxidative muscles (composed of type I myofibers), while at the protein level, the expression of HIF-1α was 8- to 10-fold higher in the glycolytic than in the oxidative muscles (Pisani and Dechesne, 2005). Thus, glycolytic muscles are expected to have a degree of hypoxia under physiological conditions that favor anaerobic glycolysis over aerobic phosphorylation. However, in the case of BMM, a pronounced lack of oxygenation is observed when compared with unaffected breast muscles which alters energy metabolism.

### 5.3.1 Hypoxia further promotes anaerobic glycolysis in myopathic muscles

Myopathic muscles have lower glycogen content than normal muscles (Abasht et al., 2016; Baldi et al., 2020). One hypothesis to explain this finding is chronic hypoxia. With age (*i.e.,* increased muscle growth and development), the diameter of muscle fibers increases while the number of capillaries decreases, which leads to a lower myofiber surface area being exposed to capillaries, subsequently reducing oxygen supply (Sihvo et al., 2018) and increasing the diffusion distance of critical micronutrients from the capillaries to the myofibers (Joiner et al., 2014). Under such conditions, hypoxia can further stimulate anaerobic glycolysis as birds grow to meet muscle energy requirements, which consequently depletes the glycolytic reserves as birds reach market age and dysregulates *post-mortem* energy metabolism (see section 4.4). The hypothesis of chronic hypoxia is supported by findings from the literature showing that the expression of *HIF-1α* increased ($p < 0.05$) progressively with age from 21 to 42 days in the *P. major* muscle of fast-growing broiler chickens (Young and Rasmussen, 2020; Malila et al., 2022).

In myopathic muscles, stimulated anaerobic glycolysis is associated with increased conversion of pyruvate to lactate which is also mediated by HIF-1α. For instance, the increase in the mRNA expression of *HIF-1α* (2.0-fold) has been shown to be associated with an increase (1.5-fold) in the mRNA expression of the gene encoding pyruvate dehydrogenase kinase 1 (*PDK1*) in WB-affected muscles from 7-week-old commercial broilers (Thanatsang et al., 2020). Under hypoxic conditions, *HIF-1α* directly activates the gene encoding the PDK1 enzyme, which in turn inactivates pyruvate dehydrogenase through phosphorylation. This results in reduced conversion of pyruvate to acetyl-CoA to limit oxygen consumption while continuing to fulfill cellular energetic requirements (Kim et al., 2006). Concomitantly, *HIF-1α* upregulates the expression of lactate dehydrogenase (*LDH*), which mediates the conversion of pyruvate to lactate (Cui et al., 2017). Accordingly, the abundance of LDH in myopathic muscles exhibiting WB/WS has been confirmed at the protein level using SDS-PAGE (Zambonelli et al., 2016), and pyruvate concentration was found to be significantly lower in WB-affected muscles than in unaffected muscles (Abasht et al., 2016). Paradoxically, lactate levels in WB-affected muscles have been shown to decrease rather than increase (Abasht et al., 2016; Baldi et al., 2020). As mentioned before, *HIF-1α* upregulates the monocarboxylate transporter 4 (*MCT4*) responsible for lactate export from cells under hypoxic conditions (Ullah et al., 2006). In WB-affected muscles, the expression of *MTC4* is significantly upregulated at both the mRNA and protein levels (Zhao et al., 2020), which can partly explain the lower lactate levels and the subsequently higher pHu in myopathic muscles (Baldi et al., 2020).

### 5.3.2 Hypoxia inhibits the TCA cycle in myopathic muscles

Under normoxic conditions, pyruvate is transported from the sarcoplasm to the mitochondria where it is used to produce acetyl-CoA (Martínez-Reyes and Chandel, 2020). Acetyl-CoA is then used in the TCA cycle to generate electrons that are transported in the form of NADH and $FADH_2$ to the electron transport chain (ETC). These electrons establish a proton gradient across the inner mitochondrial membrane, which is then used by ATP synthase to produce ATP (Taylor and Scholz, 2022). As discussed in the previous section, by increasing PDK1 levels, HIF-1α inhibits the TCA cycle by reducing the conversion of pyruvate to acetyl-CoA. Furthermore, myopathic muscles affected by WS or WB have been shown to contain elevated levels of fumarate, malate, and citrate (Abasht et al., 2016; Boerboom et al., 2018). These TCA intermediates play a regulatory role in the HIF-1 pathway and have been found to inhibit the prolyl-4-hydroxylases (Koivunen et al., 2007). As mentioned earlier, the inhibition of these enzymes leads to the stabilization of the *a*-subunit of HIF-1 in the sarcoplasm and subsequently its translocation into the nucleus to form the HIF-1 complex with the *ß* subunit. In turn, this enhances the transcription of hypoxia-responsive genes and pathways, including *PDK1*, which further reduces the conversion of pyruvate to acetyl-CoA and inhibits the TCA cycle to reduce oxygen consumption and enhance cell survivability. This could partly explain the lower ATP levels reported in WB-affected muscles at 15 min *post-mortem* (Baldi et al., 2020).

In summary (Figure 5), activation of the HIF-1 pathway in myopathic muscles can lead to reduced glycogen content in the *P. major* muscle at market age, inhibition of the TCA cycle, increased conversion of pyruvate to lactate and increased export of lactate from cells, resulting in higher pHu in these muscles.

## 5.4 Hypoxia alters lipid metabolism in myopathic muscles

Myopathic breast muscles are also characterized by dysregulated lipid metabolism (Liu et al., 2022; Boerboom et al., 2023), which causes increased lipid accumulation in muscle tissue (Alnahhas et al., 2016; Baldi et al., 2019). Hypoxia can contribute to lipid accumulation in myopathic muscles through increased fatty acid synthesis, adipogenesis, and lipid accumulation. With regard to fatty acid synthesis, the upregulation of *HIF-1α* under hypoxic conditions has been shown to downregulate the expression of myogenic regulatory factors, including *Pax7* (paired box-7) and *Myf5* (myogenic factor-5), and to upregulate the expression of lipogenic factors, including *ACCα* (acetyl-CoA carboxylase) and *FAS* (fatty acid synthase), at the mRNA and protein level in WB-affected muscles (*in vivo*) and in satellite cells (*in vitro*) from broiler

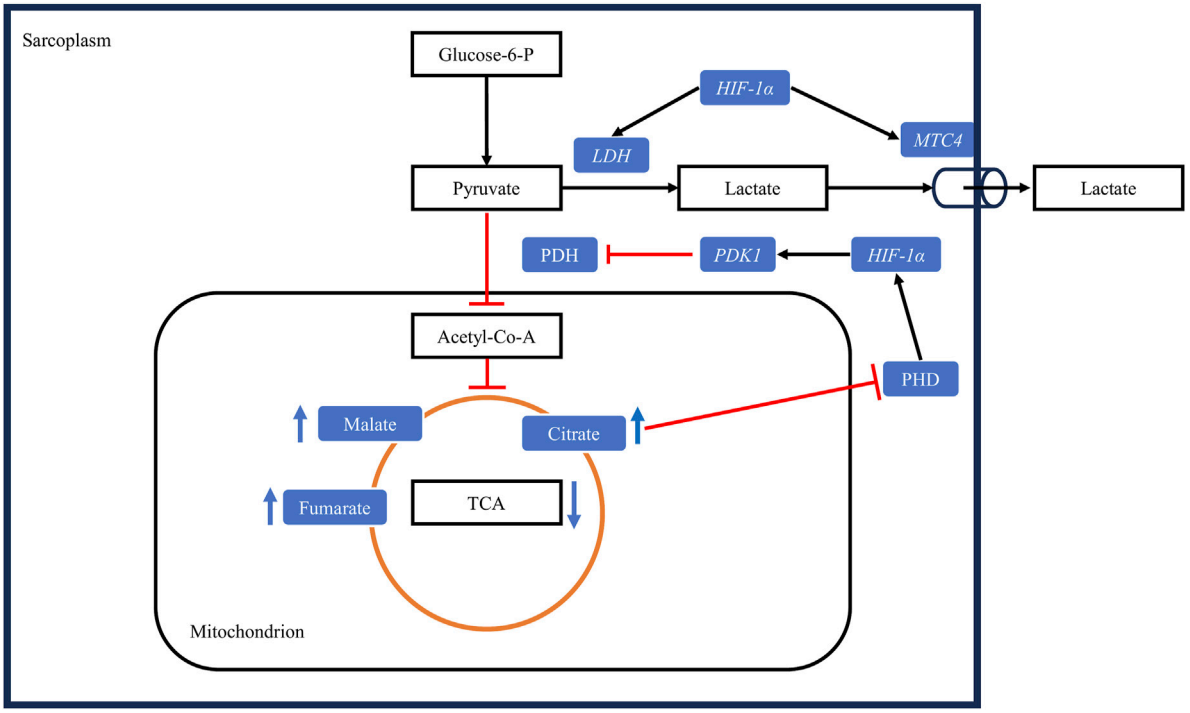


FIGURE 5
Hypoxia alters muscle energy metabolism through the upregulation of the HIF-1 pathway. Under hypoxic conditions, *HIF-1α* upregulates pyruvate dehydrogenase kinase 1 (*PDK1*), leading to the inactivation of the enzyme pyruvate dehydrogenase (PDH) through phosphorylation. Consequently, the conversion of pyruvate to acetyl-CoA is decreased. Concurrently, *HIF-1α* upregulates lactate dehydrogenase (*LDH*), increasing the conversion of pyruvate to lactate, and upregulates the monocarboxylate transporter 4 (*MTC4*), promoting lactate export from cells. The decrease in the conversion of pyruvate to acetyl-CoA slows the tricarboxylic acid cycle (TCA), leading to the accumulation of its intermediates. These intermediates downregulate the activity of prolyl-4-hydroxylases (PHD), further upregulating the HIF-1 pathway by allowing the stabilization of HIF-1α protein in the sarcoplasm. Black arrows: upregulation, blunt red arrows: downregulation.

breast muscles (Emami et al., 2021). ACCα is a major rate-limiting enzyme in the biosynthesis of long-chain fatty acids, as it catalyzes the carboxylation of acetyl-CoA to form malonyl-CoA (Tian et al., 2010), which is then used by FAS to synthesize long-chain fatty acids. In normal breast muscles, fatty acid synthesis is almost nonexistent, because these muscles lack the enzymes required for this process, particularly FAS (Cui et al., 2012). Thus, elevated expression levels of *ACCα* and *FAS* in satellite cells under hypoxic conditions suggest that these cells switched from their myogenic program to a lipogenic program, leading to increased fatty acid synthesis and accumulation in hypoxic muscles (Emami et al., 2021). This statement is supported by findings from metabolomic studies showing significantly higher levels of long-chain fatty acids in WB-affected (Abasht et al., 2016) and WS-affected (Boerboom et al., 2018) muscles.

Lipid accumulation involves the peroxisome proliferator-activated receptor gamma (PPARγ), which is a ligand-dependent transcription factor, a master regulator of adipogenesis, and an active modulator of lipid metabolism (Ma et al., 2018). The expression of the *PPARγ* gene was upregulated in WB-affected muscles from 7-week-old commercial broiler chickens (Lake et al., 2019). These authors argued that the increased expression of this gene could induce a pathological deposition of lipids in WB-affected muscles, promoting lipid accumulation in myopathic muscles. In a more recent study, the expression of *PPARγ* was investigated *in vitro* using satellite cells from the breast muscles of a random-bred line and from a modern line of broiler chickens (Velleman et al., 2022). These authors showed that the expression level of *PPARγ* was significantly higher in the modern line than in the random-bred line. More importantly, they showed that knocking down *PPARγ* was associated with reduced lipid accumulation in satellite cells from both lines during the proliferation phase of these cells, which supported the role of this gene in lipid accumulation in myopathic muscles. Hypoxia was shown to upregulate *PPARγ* in a human hepatocellular carcinoma cell line (Zhao et al., 2014) and in cardiomyocytes (Krishnan et al., 2009) through activation of the HIF-1 pathway. Therefore, it could be argued that lipid accumulation in myopathic muscles could be caused in part by the upregulation of *PPARγ* by the HIF-1 pathway in these muscles but further research is required to confirm this in broiler breast muscles. Furthermore, the upregulation of the HIF-1 pathway can enhance lipogenesis by increasing the expression of fatty acid binding proteins or FABPs (Mylonis et al., 2019). The expression of genes encoding FABP3 and FABP4 was also shown to be upregulated in WB-affected muscles (Lake et al., 2019). FABPs are a family of proteins that act as lipid chaperones, actively facilitating lipid transport to specific compartments of the cell and their storage in lipid droplets (Furuhashi and Hotamisligil, 2008). Mice deficient in FABP3 exhibited severely inhibited uptake of long-chain fatty acids in the heart and skeletal muscles (Binas

10.3389/fphys.2023.1260987

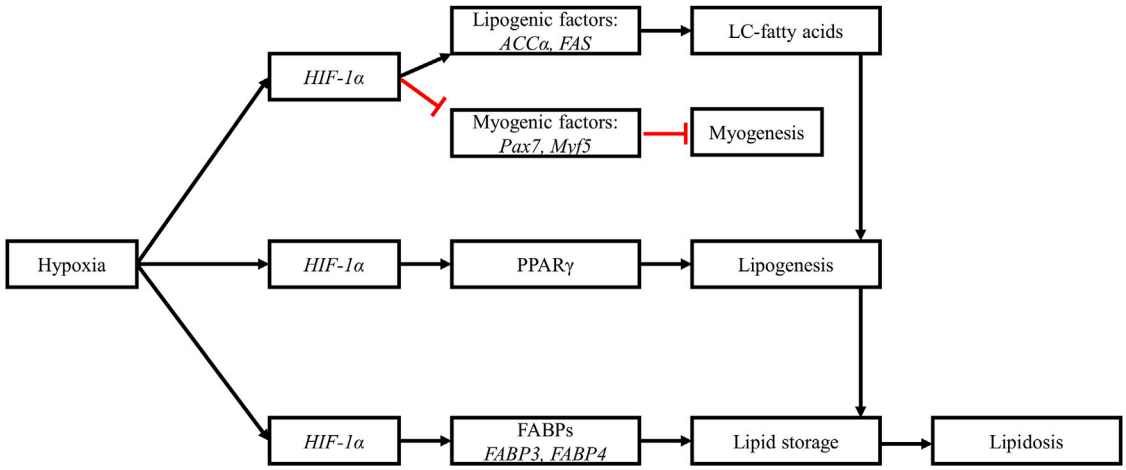


FIGURE 6
Hypoxia alters muscle lipid metabolism. Upregulation of *HIF-1α* downregulates myogenic factors while upregulating lipogenic factors. The increased expression of acetyl-CoA carboxylase *a* (*ACCα*) and fatty acid synthase (*FAS*) promotes the synthesis of long-chain fatty acids in myopathic muscles. The upregulation of *HIF-1α* is also associated with increased expression of peroxisome proliferator-activated receptor gamma (*PPARγ*), leading to increased adipogenesis and accumulation of lipids in myopathic muscles. Hypoxia also upregulates the expression of fatty acid binding proteins (FABPs), further stimulating lipogenesis and lipid storage in muscle tissues. These hypoxia-induced changes are responsible for the observed lipidosis in myopathic muscles. Black arrows: upregulation, blunt red arrows: downregulation.

et al., 1999). An upregulation of this gene through HIF-1α could thus contribute to lipid accumulation in myopathic muscles.

To summarize (Figure 6), through the activation of the HIF-1 pathway, hypoxia upregulates pathways involved in fatty acid synthesis, lipogenesis and in lipid storage, which results in pathological lipid accumulation in myopathic breast muscles.

## 5.5 Hypoxia and fibrosis in myopathic muscles

As discussed earlier, BMM are characterized by the necrosis and degeneration of muscle fibers and the infiltration of the damaged muscle tissue by inflammatory cells. The degeneration and inflammation of the *P. major* muscle induce an increased deposition of extracellular matrix (ECM) proteins, leading to fibrosis, which is a microscopic characteristic of WB and WS (Kuttappan et al., 2013; Soglia et al., 2016a; Velleman, 2020). In a study that used proteomic data from WB-affected muscles of 52-day-old broiler chickens, an analysis of the upstream regulators of this myopathy showed that the transforming growth factor β1 (TGF-β1) was activated (Bottje et al., 2021). This cytokine is one of three members of TGF-β family, which is involved in a wide range of cellular events and is known to promote fibrosis in skeletal muscles (Delaney et al., 2017). TGF-β1 produces its cellular effects by binding to its receptor TβRII. This dimer then phosphorylates the TβRI receptor. This phosphorylated receptor in turn phosphorylates SMAD2 and SMAD3, two members of the SMAD signaling pathway (Schmierer and Hill, 2007). Consequently, the activated SMAD2 and SMAD3 form a complex with SMAD4, which promotes the translocation of the complex to the nucleus to induce the expression of their target genes, including genes that encode proteins of the ECM such as fibronectin and collagen (Delaney et al., 2017). A recent study investigated the mechanisms underlying the fibrosis of WB-affected muscles sampled from commercial broilers at 6 weeks of age (Xing et al., 2021). These authors showed that the expression of all three members of the TGF-β family was significantly increased in WB-affected muscles compared with unaffected muscles at both the mRNA and protein levels. Consequently, the expression of fibronectin and collagen was also significantly increased in WB-affected muscles at the mRNA and protein levels. The deposition of large amounts of connective tissue fibers in a parallel and highly packed fashion in the interstitial spaces gives WB-affected muscles their characteristic hardness (Velleman, 2020).

Hypoxia has been recently shown to increase the expression of collagen genes (*Col1A1* and *Col1A2*) and proteins (Col1) in chicken primary myoblasts contributing to fibrosis (Greene et al., 2023). Hypoxia can contribute to fibrosis in two ways (Figure 7). It has been shown to activate the TGF-β1/SMAD signaling pathway through HIF-1α signaling, leading to increased collagen deposition in human epidermal fibroblasts (Mingyuan et al., 2018). Furthermore, HIF-1α signaling act synergistically with TGF-β1 to increase the expression of the connective tissue growth factor (CTGF) in myotubes of different models of skeletal muscles (Valle-Tenney et al., 2020). CTGF is a potent profibrotic growth factor that increases the expression of the ECM components, thus contributing to fibrosis (Vial et al., 2008). The expression of this growth factor was significantly higher in WB-affected than in unaffected muscles (Xing et al., 2021). Thus, it can be argued that under hypoxic conditions in myopathic muscles, HIF-1α can interact with TGF-β1, leading to increased expression of CTGF, which in turn increases secretion of the ECM components including fibronectin and collagen. The increased deposition of these components in the *perimysium* and *endomysium* produces the form of fibrosis that characterizes myopathic breast muscles. Further research is needed to better understand the pathways by which hypoxia contributes to fibrosis in broiler breast muscle.

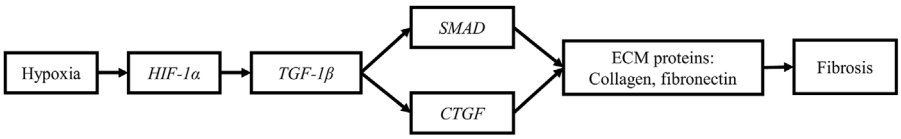


FIGURE 7
Hypoxia promotes fibrosis in myopathic muscles. The upregulation of *HIF-1α* promotes the synthesis and deposition of extracellular matrix (ECM) proteins (collagen and fibronectin) in myopathic muscles through its interaction with the transforming growth factor β1/SMAD signaling pathway and its upregulation of connective tissue growth factor (CTGF).

# 6 Hypoxia alters mitochondrial morphology, dynamics, and functions in myopathic muscles

In muscles composed of type IIB myofibers, such as *P. major*, mitochondria have a small size (0.15 vs. 0.35 $\mu m^2$ in type I), an ellipsoid shape, and are sparsely distributed among myofibrils (Hosotani et al., 2021). According to these authors, individual mitochondria from type IIB myofibers exhibited fewer interconnections and formed less extensive networks than mitochondria from type I myofibers. With age, mitochondria in the *P. major* muscle shift their position from the center of myofibers to the zone adjacent to blood capillaries as an adaptation to decreased blood flow and increased diffusion distances which facilitates access to oxygen (Belichenko et al., 2004).

In myopathic muscles, mitochondria exhibit hyperplasia and they aggregate in large numbers (up to 40 mitochondria) between myofibrils (Sihvo et al., 2018). These mitochondria also exhibit morphological changes including vacuolation, swollen matrix, loss of cristae, and irregular shape (Sihvo et al., 2018; Hosotani et al., 2020; Pan et al., 2021). These studies suggested that changes in mitochondrial morphology were associated with the hypoxic state of myopathic muscles.

## 6.1 Hypoxia stimulates mitochondrial fission and fusion in myopathic muscles

Mitochondria are highly dynamic organelles that undergo fission (*i.e.,* division of one mitochondrion into two daughter mitochondria) and fusion (*i.e.,* one mitochondrion produced by a fusion of two mitochondria) to maintain their shape, size, and cellular distribution (Tilokani et al., 2018; Chen et al., 2022). These processes are fundamental in allowing mitochondria to respond to cellular stress conditions and to help cells adapt to such conditions (Wang et al., 2022).

Hypoxia, through the activation of the HIF-1 pathway, has been associated with changes in the expression of genes regulating mitochondrial dynamics to protect mitochondria from oxidative stress (Li et al., 2019). In a recent study of WB-affected muscles sampled from 50-day-old commercial broilers, the expression of *HIF-1α* was positively correlated ($r = 0.33$, $p = 0.049$) with dynamin-related protein 1 (*DRP1*), a gene involved in mitochondrial fission (Hosotani et al., 2020). The promotion of mitochondrial fission by upregulating *DRP1* helps segregate mitochondria impaired by hypoxia-induced cellular stress. This enables their selective elimination to maintain mitochondrial function which is essential for cell survival (Li et al., 2019; Wang et al., 2022).

Mitochondrial fusion also helps in alleviating stress because it combines the contents of partially damaged mitochondria, which limits excessive mitochondrial clearance (Youle and van der Bliek, 2012). This process is regulated by genes including mitofusion (*MFN*) 1 and 2 (Tilokani et al., 2018). Proteins encoded by *MFN1* and *MFN2* maintain mitochondrial networks by binding mitochondria together and initiating the fusion of their outer membrane (Lugus et al., 2011). In WB-affected muscles, the expression of *HIF-1α* was not directly correlated with that of *MFN1* or *MFN2*; however, *HIF-1α* upregulation induced an upregulation of the *VEGF-A* gene encoding the vascular endothelial growth factor A (Hosotani et al., 2020), an essential mediator of skeletal muscle angiogenesis and a well-known transcriptional target of HIF-1 (Rodriguez-Miguelez et al., 2015). The upregulation of *VEGF-A* also upregulates *MFN1* and *MFN2* (Lugus et al., 2011; Rodriguez-Miguelez et al., 2015). This relationship was observed in WB-affected muscles, where the expression of *VEGF-A* was significantly correlated with that of *MFN1* ($r = 0.68$, $p < 0.0001$) and *MFN2* ($r = 0.75$, $p < 0.0001$) (Hosotani et al., 2020) suggesting an indirect stimulation of mitochondrial fusion by HIF-1.

Therefore, the upregulation of the HIF-1 pathway in myopathic muscles seems to directly stimulate mitochondrial fission and indirectly stimulate mitochondrial fusion. Both mechanisms reduce cellular stress while eliminating defective mitochondria to reduce the risk of muscle tissue damage or to limit further progression of myopathies. However, under persistent cellular stress, these mechanisms could be overwhelmed, leading to the above-described changes in mitochondrial morphology. The subsequent mitochondrial damage can also contribute to the dysregulated energy metabolism in myopathic muscles (see Section 4.4 and Section 5.3).

## 6.2 Hypoxia induces an oxidative stress in myopathic muscles

The mitochondrial respiratory chain is a major source of reactive oxygen species or ROS (Murphy, 2009). These molecules are produced during muscle contraction and their role depends on their concentration and on the duration of cellular components exposure to these molecules. Under high concentrations and long exposure times, ROS pose significant danger to mitochondria and other cellular components. Under low concentrations and short

exposure times, ROS are signaling molecules that regulate multiple physiological processes in skeletal muscles (Barbieri and Sestili, 2012). In broiler breast muscles, superoxide, a primary ROS, is formed at complex I and complex III of the, ETC (Hakamata et al., 2020). Superoxide is formed when electrons leak from these complexes and are transferred to molecular oxygen (Murphy, 2009). Excessive amounts of superoxide undergo dismutation by superoxide dismutase (SOD), generating hydrogen peroxide (Wang et al., 2018), which is another member of the ROS family. Hydrogen peroxide is then converted to water and oxygen by glutathione peroxidase or catalase (Kozakowska et al., 2015).

The mitochondrial damage reported in myopathic muscles, coupled with the metabolic shift toward further anaerobic glycolysis, can lead to decreased mitochondrial respiratory activity, highlighted by lower citrate synthase activity (Pan et al., 2021; Li et al., 2022) and lower mitochondrial membrane potential reported in myopathic muscles (Pan et al., 2021). As the respiratory chain is slowed, the likelihood of electron leakage and transfer to molecular oxygen increases, which can increase the production of superoxide (Thomas and Ashcroft, 2019). According to the phenomenon of ROS-induced ROS release, the production of a small amount of ROS by a small number of mitochondria can propagate to other mitochondria via the mitochondrial network, leading to increased mitochondrial ROS production and eventually promote ROS production from non-mitochondrial sources (Park et al., 2011). This could partly explain the significantly higher levels of ROS reported in WB-affected (+15%, $p < 0.01$) muscles (Pan et al., 2021) and in WS-affected (+57%, $p < 0.001$) muscles (Salles et al., 2019) compared with unaffected muscles.

The elevated levels of ROS induce a response from the antioxidant defense system in myopathic muscles. Compared with unaffected muscles, muscles moderately affected by WS exhibited a significant increase in the activity of SOD, glutathione peroxidase, and catalase (Salles et al., 2019; Carvalho et al., 2021). Under persistent oxidative stress, the antioxidant defense system becomes overwhelmed by oxidative damage coupled with depletion of antioxidant molecules (Abasht et al., 2016), resulting in the decreased activity of the antioxidant enzymes in muscles severely affected by this myopathy (Salles et al., 2019; Carvalho et al., 2021). A similar response of antioxidant enzymes has also been reported in WB-affected muscles (Praud et al., 2020; Pan et al., 2021). The response of the antioxidant defense system to increased ROS production in myopathic muscles is partly mediated by the nuclear factor erythroid 2-related factor 2 (Nrf2) pathway (Pan et al., 2021). Nrf2, a master transcriptional regulator responsible for cellular redox hemostasis, is sequestered in the cytoplasm by Kelch-like ECH-associated protein 1 (Keap1) and is rapidly degraded by the Cullin 3 ubiquitin–proteasomal system under physiological conditions (Surai et al., 2019; Gao et al., 2021). Under oxidative stress conditions, Nrf2 dissociates from Keap1 and is translocated to the nucleus (Bellezza et al., 2018). In the nucleus, Nrf2 binds either directly to antioxidant response elements (ARE) or indirectly to ARE-like sequences within the Nrf2 promotor, which leads to the upregulation of genes involved in the antioxidant defense system, including genes encoding SOD, catalase, and glutathione peroxidase (Gao et al., 2021). Hypoxia, through the upregulation of *HIF-1α*, upregulates Nrf2 expression at the protein level and its binding to ARE leading to an upregulation of genes encoding antioxidant enzymes in mouse skeletal muscles (Ji et al., 2018). Therefore, the upregulation of the Nrf2 pathway and the subsequent upregulation of genes encoding for SOD and glutathione peroxidase evidenced in WB-affected muscles (Pan et al., 2021) can be attributed to hypoxia and to the hypoxia-induced oxidative stress in these muscles.

### 6.3 Hypoxia-induced oxidative damage in myopathic muscles

The increased production of ROS in myopathic muscles due to hypoxia results in a concomitant increase of lipid peroxidation, as well as protein and DNA oxidation products. The thiobarbituric acid–reactive substances (TBA-RS) index is a widely used method to assay secondary products of lipid peroxidation (Sammari et al., 2023). Using this method, multiple studies have reported significantly increased levels of malondialdehyde (MDA) in WS- (Carvalho et al., 2021; Pereira et al., 2022) and WB-affected muscles, indicating elevated levels of lipid peroxidation (Soglia et al., 2019; Pan et al., 2021; Li et al., 2022). Carbonyl and thiol groups in muscle and meat are widely used markers of protein oxidation (Soglia et al., 2016b). In myopathic muscles, proteins are exposed not only to ROS but also to other pro-oxidant molecules, such as lipid peroxidation products. Consequently, proteins in these muscles undergo oxidation as seen through their significantly elevated levels of carbonyl and thiol groups (Carvalho et al., 2021; Li et al., 2022). Other markers of lipid peroxidation and protein oxidative damage have also been reported in the literature. For instance, eicosanoids, including 15-HETE and 15-KETE (both metabolites of arachidonic acid), were shown to be among top metabolites differentiating WB-affected from unaffected muscles (Abasht et al., 2016). In this same study, 1-methylhistidine, an indicator of skeletal muscle oxidative stress, and 3-methylhistidine, a known marker of protein breakdown, were also shown to be present in higher quantities in WB-affected than unaffected muscles.

In summary (Figure 8), under hypoxic conditions, lipid accumulation increases in myopathic muscles, and energy metabolism is shifted away from the TCA cycle to reduce oxygen consumption. These changes, coupled with altered mitochondrial functions, lead to increased ROS production. When the antioxidant defense system becomes overwhelmed by persistent ROS exposure, oxidative damage develops. This is often manifested by elevated levels of products and markers of lipid peroxidation and protein oxidation. Hypoxia-induced oxidative stress can therefore contribute to the initiation and progression of the pathological changes underlying BMM.

## 7 Hypoxia-induced apoptosis in myopathic muscles

Breast muscle growth increases with age leading to increased muscle fiber diameter and decreased myofiber area to blood capillary (Sihvo et al., 2018). These changes in muscle histology are associated with increased myofiber necrosis and degeneration due to ischemia and hypoxia (Joiner et al., 2014). Radaelli et al. (2017) evaluated muscle fiber

10.3389/fphys.2023.1260987

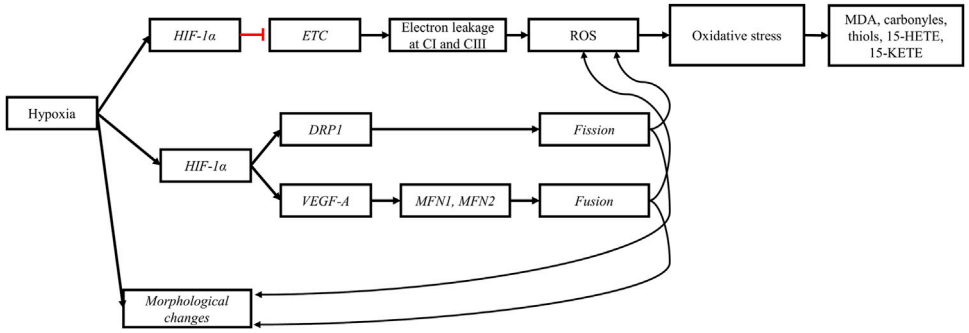


FIGURE 8
Hypoxia impairs mitochondrial morphology and functions. The perturbation of the tricarboxylic acid cycle (TCA) induced by the upregulation of *HIF-1α* slows the electron transport chain (ETC.), increasing the probability of electron leakage at complex I (CI) and III (CIII). The leaked electrons bind to molecular oxygen to form reactive oxygen species (ROS). High concentrations of ROS and prolonged exposure of cellular components to ROS lead to oxidative stress and subsequently to lipid peroxidation and protein oxidation. The products from oxidative damage (MDA, carbonyls, thiols, 15-HETE, and 15-KETE) accumulate in myopathic muscles. Furthermore, the upregulation of *HIF-1α* upregulates genes responsible for mitochondrial fission (*DRP1*) and fusion (*VEGF-A*, *MFN1*, and *MFN2*). The stimulation of mitochondrial dynamics is a response mechanism aiming to alleviate cellular stress and eliminate defective mitochondria induced by hypoxia. Black arrows: upregulation, blunt red arrows: downregulation.

degeneration in the *P. major* muscle of commercial strains of broiler chickens and showed that the percentage of myofibers with signs of degeneration increased from 28.1% at 21 days to 96.6% at 46 days while the number of nuclei showing signs of apoptotic processes increased from 0.44 at 21 days to 8.45 per examined field at 46 days. Interestingly, increase in the apoptotic and degenerative processes in the *P. major* muscle reported in this study coincided with the previously reported increase in the expression of *HIF-1α* in this muscle from 21 to 42 days (Young and Rasmussen, 2020; Malila et al., 2022) which provided further support for the key role of hypoxia in triggering the histopathological changes that characterize myopathic muscles. In skeletal muscles, caspases are one of the major regulators of apoptotic signaling (Quadrilatero et al., 2011), and they are activated under hypoxic conditions. In a recent study, Greene et al. (2023) assessed the mRNA levels of genes encoding for caspase-1, cappase-3 and caspase-9 in chicken primary myoblasts culture that was exposed to hypoxia for 0, 8 and 24 h. The mRNA level of genes encoding all three proteases increased significantly after 24 h under hypoxic conditions (1% $O_2$, 5% $CO_2$ and 94% $N_2$). These authors further showed that the protein level of caspase-3 evaluated by Western blotting was significantly increased after 24 h under hypoxic conditions. Caspase-9 is an initiator caspase that promotes the downstream activation of caspase-3 which is an executioner or effector caspase responsible for the ultimate degradation of cellular content (Sendoel and Hengartner, 2014). Damage to DNA and stress of the sarcoplasmic reticulum, which both have been reported in myopathic muscles (Radaelli et al., 2017; Greene et al., 2023), are considered two of the most important signaling pathways upregulating the apoptotic activity of caspases (Quadrilatero et al., 2011). Once activated, effector caspases dismantle cellular components that could induce inflammation to prevent further damage to muscle tissue (Fink and Cookson, 2005). However, the specific role of the caspase signaling pathway in the development of BMM phenotypes requires further research.

To summarize (Figure 9), the damaged nuclei and stressed sarcoplasmic reticulum associated with hypoxia in myopathic muscles activate the caspase pathway leading to apoptosis in response to myofiber necrosis.

## 8 The big picture

The continually increasing worldwide demand for poultry meat necessitates the development of broiler strains that allow the industry to meet the increasing demand while reducing the effect of broiler production on the environment.

Genetic selection is one of the most important tools used by the industry to create and develop fast-growing and high-yielding strains of broiler chickens. The increased selection pressure to continuously improve broiler BMY leads to increased muscle fiber hypertrophy in the pectorals of these birds, reducing the capillary density of these muscles, and inducing an ischemic and hypoxic states. Hypoxia activates and upregulates the HIF-1 pathway (Figure 10). This transcription factor upregulates the expression of numerous hypoxia-responsive genes, leading to an upregulation of anaerobic glycolysis and lipogenesis, a downregulation of the TCA cycle, a slowdown of the, ETC, and an increase of pro-oxidant molecules coupled with a decrease of antioxidant molecules. The pro-oxidant molecules target lipids and proteins in the cell membrane and in cellular organelles, leading to their oxidation and the further release of pro-oxidant molecules, inducing further oxidative damage and overwhelming the antioxidant defense system.

Ischemia and hypoxia-induced oxidative stress can then initiate the multiphasic degenerative process in muscle tissue. In response to necrosis and inflammation, satellite cells are activated to repair the necrotic damage once inflammatory cells infiltrate the damaged muscle tissue and clean the zone from necrotic debris. Under the persistent hypoxic state, the caspase signaling pathway is upregulated initiating apoptosis as an attempt to control inflammation. In addition, satellite cells

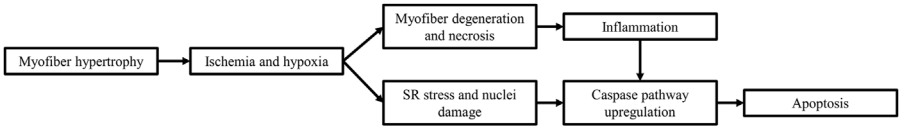


FIGURE 9
Hypoxia and ischemia stimulate apoptosis in myopathic muscles. The ischemic and hypoxic state of myopathic muscle is responsible for necrosis and myofiber degeneration, inducing an inflammatory response in affected muscles. Moreover, hypoxia stresses the sarcoplasmic reticulum (SR) and damages the nuclei of affected muscle tissue. The inflammation, SR stress, and nuclei damage upregulate the caspase signaling pathway, ultimately dismantling cellular proteins, and leading to apoptosis as a response mechanism to limit further damage to muscle tissue.

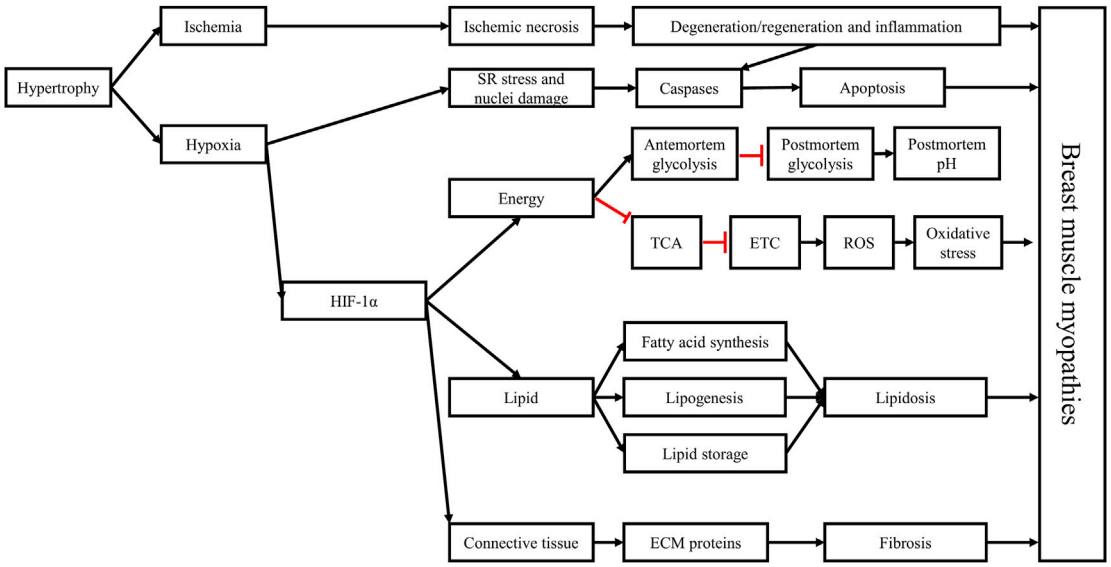


FIGURE 10
Hypoxia plays a critical role in the development of breast muscle myopathies through the activation of the hypoxia-inducible factor 1 (HIF-1) pathway. The hypertrophic growth of breast muscles is associated with decreased capillary density, leading to decreased circulation (ischemia) and oxygenation (hypoxia) in muscle tissue, coupled with lower nutrient supply. The histopathological changes associated with breast muscle myopathies, including necrosis, myofiber degeneration, and inflammation, are consequences of the ischemic and hypoxic states. Hypoxia can stress the sarcoplasmic reticulum and damage the nuclei, leading to the activation of the caspase signaling pathway, triggering apoptosis. Moreover, HIF-1α can further stimulate antemortem anaerobic glycolysis in the *Pectoralis major* muscle, depleting glycogen reserves by the time birds reach market age, contributing to the early cessation of *post-mortem* acidification in this muscle which explain the higher ultimate pH in these muscles. Furthermore, HIF-1α slows the TCA cycle and impedes mitochondrial function, leading to increased ROS production and accumulation, triggering a state of oxidative stress in the muscle and damaging its cellular components. HIF-1α also alters lipid metabolism in the *Pectoralis major* muscle, leading to increased synthesis of long-chain fatty acids, lipogenesis, and lipid storage, ultimately causing lipidosis. Finally, by interacting with the TGF-β1/SMAD pathway and with the connective tissue growth factor, HIF-1α increases the deposition of extracellular matrix (ECM) proteins in muscle tissue, leading to fibrosis. These structural and metabolic changes trigger the onset and development of breast muscle myopathies and give them their distinctive phenotypes. Black arrows: upregulation, blunt red arrows: downregulation.

change their program and instead of differentiating to myoblasts to form new myotubes that replace damaged muscle fibers, they become lipogenic, resulting in the increased synthesis of fatty acids and fat deposition in muscle tissue. Simultaneously, hypoxia acts synergistically with the transforming growth factor β1 to upregulate the connective tissue growth factor, which in turn inhibits myogenesis and increases the expression of the extracellular matrix proteins, leading to fibrosis. Lipidosis and fibrosis replace muscle tissue with fat and connective tissue, resulting in the distinctive phenotypic characteristics of BMM.

## 9 Conclusions and perspectives

Hypoxic and oxidative damages resulting from the reduced capillary density in the *P. major* muscle are critical determinants of the onset and progression of BMM. Although an important progress has been achieved on understanding the role of hypoxia in the development of BMM, further research is needed to better understand the relationship between the HIF-1 pathway and other pathways involved in the occurrence of BMM. In particular, the interaction between HIF-1 and the TGF-β family requires further investigation in relation with fibrosis

and the development of the specific and distinct phenotypes of BMM. More research is also required to confirm the relationship between HIF-1 and PPARγ and the consequences of this relationship for pathological lipid storage in muscle tissue. In addition, research is needed to advance our understanding of the role of the caspase signaling pathway in the development of BMM under hypoxic stress. In terms of solutions for BMM, future research should focus on developing strategies to improve both the vasculature and the antioxidant status of breast muscles to limit the occurrence and severity of these myopathies. In the past, developmental problems caused by genetic selection were mostly resolved by genetic selection, with leg deformities and ascites being prime examples of the role of genetic selection in resolving genetic issues. Given that BMM are moderately to highly determined by genetics, genetic selection would be highly efficient in reducing their occurrence or at least their severity. However, given the genetic and phenotypic positive association between BMM and increased BMY, selecting directly against these myopathies could reduce BMY, which is undesirable. Consequently, research is needed to identify new selection criteria in relation to muscle structure (*e.g.*, capillary density, ratio of muscle fiber number to blood capillaries, width of interstitial spaces, density and organization of connective tissue) and in relation to muscle content of naturally occurring antioxidant molecules (*e.g.*, histidine-containing dipeptides including carnosine and anserine and their derivatives). Research is also needed to test the feasibility of selection for such criteria and the efficacy of the selection process in reducing the occurrence and severity of BMM with limited impact on BMY. However, because of the pyramidal organization of broiler breeding schemes, results from this approach would not be available in the short term; therefore, other approaches need to be developed in parallel to the genetic selection-based approach. Embryonic manipulations (*e.g.*, acclimatization to lower oxygen levels during the critical phase of development of the pectoral muscles) and the use of *in ovo* feeding with substances that upregulate the expression of angiogenic genes during embryogenesis could be explored. Nutritional strategies to improve the antioxidant status of breast muscle using naturally occurring antioxidants (*e.g.*, carnosine) should also be further explored. Finally, the reduction of the occurrence and severity of BMM with limited undesirable consequences for economically important traits would probably require a combination of genetic selection with improved nutritional and managerial strategies.

## Author contributions

NA: Conceptualization, Funding acquisition, Writing–original draft. EP: Conceptualization, Funding acquisition, Writing–review and editing. LS: Conceptualization, Funding acquisition, Writing–review and editing.

## Funding

The authors declare financial support was received for the research, authorship, and/or publication of this article. This review was supported by the MAPAQ Research Chair on meat quality and safety–Musculo (https://musculo.fsaa.ulaval.ca/) funded by the Agri-Food Innovation Partnership Program, under the Canadian Agricultural Partnership, an agreement between the governments of Canada and Quebec (Ministère de l'Agriculture des Pêcheries et de l'Alimentation du Québec MAPAQ), and by Olymel S.E.C./L.P.

## Conflict of interest

Author EP was employed by the company Olymel S.E.C./L.P.

The remaining authors declare that the research was conducted in the absence of any commercial or financial relationships that could be construed as a potential conflict of interest.

## Publisher's note



## References

Abasht, B., Mutryn, M. F., Michalek, R. D., and Lee, W. R. (2016). Oxidative stress and metabolic perturbations in wooden breast disorder in chickens. *Plos One* 11 (4), e0153750. doi:10.1371/journal.pone.0153750

Alnahhas, N., Berri, C., Boulay, M., Baéza, E., Jégo, Y., Baumard, Y., et al. (2014). Selecting broiler chickens for ultimate pH of breast muscle: analysis of divergent selection experiment and phenotypic consequences on meat quality, growth, and body composition traits. *J. Anim. Sci.* 92 (9), 3816–3824. doi:10.2527/jas.2014-7597

Alnahhas, N., Berri, C., Chabault, M., Chartrin, P., Boulay, M., Bourin, M. C., et al. (2016). Genetic parameters of white striping in relation to body weight, carcass composition, and meat quality traits in two broiler lines divergently selected for the ultimate pH of the pectoralis major muscle. *BMC Genet.* 17, 61. doi:10.1186/s12863-016-0369-2

Baldi, G., Soglia, F., Laghi, L., Tappi, S., Rocculi, P., Tavaniello, S., et al. (2019). Comparison of quality traits among breast meat affected by current muscle abnormalities. *Food Res. Int.* 115, 369–376. doi:10.1016/j.foodres.2018.11.020

Baldi, G., Soglia, F., Mazzoni, M., Sirri, F., Canonico, L., Babini, E., et al. (2018). Implications of white striping and spaghetti meat abnormalities on meat quality and histological features in broilers. *Animal* 12 (1), 164–173. doi:10.1017/s1751731117001069

Baldi, G., Soglia, F., and Petracci, M. (2021). Spaghetti meat abnormality in broilers: current understanding and future research directions. *Front. Physiol.* 12 (715), 684497. doi:10.3389/fphys.2021.684497

Baldi, G., Yen, C. N., Daughtry, M. R., Bodmer, J., Bowker, B. C., Zhuang, H., et al. (2020). Exploring the factors contributing to the high ultimate pH of broiler pectoralis major muscles affected by wooden breast condition. *Front. Physiol.* 11, 343. doi:10.3389/fphys.2020.00343

Barbieri, E., and Sestili, P. (2012). Reactive oxygen species in skeletal muscle signaling. *J. Signal Transduct.* 2012, 982794. doi:10.1155/2012/982794

Barbut, S. (2019). Recent myopathies in broiler's breast meat fillets. *Worlds Poult. Sci. J.* 75 (4), 559–582. doi:10.1017/s0043933919000436

Bauermeister, L., Morey, A., Moran, E., Singh, M., Owens, C., and McKee, S. (2009). Occurrence of white striping in chicken breast fillets in relation to broiler size. *Poult. Sci.* 88, 33. Suppl 1. doi:10.3382/ps.2012-03001

Belichenko, V. M., Korostishevskaya, I. M., Maximov, V. F., and Shoshenko, C. A. (2004). Mitochondria and blood supply of chicken skeletal muscle fibers in ontogenesis. *Microvasc. Res.* 68 (3), 265–272. doi:10.1016/j.mvr.2004.06.005

Bellezza, I., Giambanco, I., Minelli, A., and Donato, R. (2018). Nrf2-Keap1 signaling in oxidative and reductive stress. *Biochimica Biophysica Acta (BBA) - Mol Cell. Res* 1865 (5), 721–733. doi:10.1016/j.bbamcr.2018.02.010

Berri, C., Le Bihan-Duval, E., Debut, M., Sante-Lhoutellier, V., Baeza, E., Gigaud, V., et al. (2007). Consequence of muscle hypertrophy on characteristics of Pectoralis major muscle and breast meat quality of broiler chickens. *J. Anim. Sci.* 85 (8), 2005–2011. doi:10.2527/jas.2006-398

Berri, C., Wacrenier, N., Millet, N., and Le Bihan-Duval, E. (2001). Effect of selection for improved body composition on muscle and meat characteristics of broilers from experimental and commercial lines. *Poult. Sci.* 80 (7), 833–838. doi:10.1093/ps/80.7.833

Binas, B., Danneberg, H., McWhir, J., Mullins, L., and Clark, A. J. (1999). Requirement for the heart-type fatty acid binding protein in cardiac fatty acid utilization. *Faseb J.* 13 (8), 805–812. doi:10.1096/fasebj.13.8.805

Boerboom, G. M., Navarro-Villa, A., and van Kempen, T. A. T. G. (2023). Metabolomic analysis of wooden breast myopathy shows a disturbed lipid metabolism. *Metabolites* 13 (1), 20. doi:10.3390/metabo13010020

Boerboom, G., van Kempen, T., Navarro-Villa, A., and Perez-Bonilla, A. (2018). Unraveling the cause of white striping in broilers using metabolomics. *Poult. Sci.* 97 (11), 3977–3986. doi:10.3382/ps/pey266

Bottje, W. G., Lassiter, K. R., Kuttappan, V. A., Hudson, N. J., Owens, C. M., Abasht, B., et al. (2021). Upstream regulator analysis of wooden breast myopathy proteomics in commercial broilers and comparison to feed efficiency proteomics in pedigree male broilers. *Foods* 10 (1), 104. doi:10.3390/foods10010104

Cao, T., and Jin, J.-P. (2020). Evolution of flight muscle contractility and energetic efficiency. *Front. Physiol.* 11, 1038. doi:10.3389/fphys.2020.01038

Carvalho, L. M., Delgado, J., Madruga, M. S., and Estévez, M. (2021). Pinpointing oxidative stress behind the white striping myopathy: depletion of antioxidant defenses, accretion of oxidized proteins and impaired proteostasis. *J. Sci. Food Agric.* 101 (4), 1364–1371. doi:10.1002/jsfa.10747

Che, S., Wang, C., Iverson, M., Varga, C., Barbut, S., Bienzle, D., et al. (2022). Characteristics of broiler chicken breast myopathies (spaghetti meat, woody breast, white striping) in Ontario, Canada. *Poult. Sci.* 101 (4), 101747. doi:10.1016/j.psj.2022.101747

Chen, T.-H., Koh, K.-Y., Lin, K. M.-C., and Chou, C.-K. (2022). Mitochondrial dysfunction as an underlying cause of skeletal muscle disorders. *Int. J. Mol. Sci.* 23 (21), 12926. doi:10.3390/ijms232112926

Christov, C., Chrétien, F., Abou-Khalil, R., Bassez, G., Vallet, G., Authier, F. J., et al. (2007). Muscle satellite cells and endothelial cells: close neighbors and privileged partners. *Mol. Biol. Cell.* 18 (4), 1397–1409. doi:10.1091/mbc.e06-08-0693

Cui, H. X., Zheng, M. Q., Liu, R. R., Zhao, G. P., Chen, J. L., and Wen, J. (2012). Liver dominant expression of fatty acid synthase (FAS) gene in two chicken breeds during intramuscular-fat development. *Mol. Biol. Rep.* 39 (4), 3479–3484. doi:10.1007/s11033-011-1120-8

Cui, X. G., Han, Z. T., He, S. H., Wu, X. D., Chen, T. R., Shao, C. H., et al. (2017). HIF1/2α mediates hypoxia-induced LDHA expression in human pancreatic cancer cells. *Oncotarget* 8 (15), 24840–24852. doi:10.18632/oncotarget.15266

Daughtry, M. R., Berio, E., Shen, Z., Suess, E. J. R., Shah, N., Geiger, A. E., et al. (2017). Satellite cell-mediated breast muscle regeneration decreases with broiler size. *Poult. Sci.* 96 (9), 3457–3464. doi:10.3382/ps/pex068

Delaney, K., Kasprzycka, P., Ciemerych, M. A., and Zimowska, M. (2017). The role of TGF-β1 during skeletal muscle regeneration. *Cell. Biol. Int.* 41 (7), 706–715. doi:10.1002/cbin.10725

Emami, N. K., Cauble, R. N., Dhamad, A. E., Greene, E. S., Coy, C. S., Velleman, S. G., et al. (2021). Hypoxia further exacerbates woody breast myopathy in broilers via alteration of satellite cell fate. *Poult. Sci.* 101167, 101167. doi:10.1016/j.psj.2021.101167

Ferreira, T. Z., Kindlein, L., Flees, J. J., Shortnacy, L. K., Vieira, S. L., Nascimento, V. P., et al. (2020). Characterization of pectoralis major muscle satellite cell population heterogeneity, macrophage density, and collagen infiltration in broiler chickens affected by wooden breast. *Front. Physiol.* 11, 529. doi:10.3389/fphys.2020.00529

Fink, S. L., and Cookson, B. T. (2005). Apoptosis, pyroptosis, and necrosis: mechanistic description of dead and dying eukaryotic cells. *Infect. Immun.* 73 (4), 1907–1916. doi:10.1128/iai.73.4.1907-1916.2005

Furuhashi, M., and Hotamisligil, G. S. (2008). Fatty acid-binding proteins: role in metabolic diseases and potential as drug targets. *Nat. Rev. Drug Discov.* 7 (6), 489–503. doi:10.1038/nrd2589

Gao, L., Wang, H. J., Tian, C., and Zucker, I. H. (2021). Skeletal muscle Nrf2 contributes to exercise-evoked systemic antioxidant defense via extracellular vesicular communication. *Exerc Sport Sci. Rev.* 49 (3), 213–222. doi:10.1249/jes.0000000000000257

Geiger, A. E., Daughtry, M. R., Gow, C. M., Siegel, P. B., Shi, H., and Gerrard, D. E. (2018). Long-term selection of chickens for body weight alters muscle satellite cell behaviors. *Poult. Sci.* 97 (7), 2557–2567. doi:10.3382/ps/pey050

Geronimo, B. C., Prudencio, S. H., and Soares, A. L. (2022). Biochemical and technological characteristics of wooden breast chicken fillets and their consumer acceptance. *JFST* 59 (3), 1185–1192. doi:10.1007/s13197-021-05123-3

Gratta, F., Fasolato, L., Birolo, M., Zomeno, C., Novelli, E., Petracci, M., et al. (2019). Effect of breast myopathies on quality and microbial shelf life of broiler meat. *Poult. Sci.* 98 (6), 2641–2651. doi:10.3382/ps/pez001

Greene, E., Flees, J., Dadgar, S., Mallmann, B., Orlowski, S., Dhamad, A., et al. (2019). Quantum blue reduces the severity of woody breast myopathy via modulation of oxygen homeostasis-related genes in broiler chickens. *Front. Physiol.* 10, 1251. doi:10.3389/fphys.2019.01251

Greene, E. S., Maynard, C., Mullenix, G., Bedford, M., and Dridi, S. (2023). Potential role of endoplasmic reticulum stress in broiler woody breast myopathy. *Am. J. Physiol. Cell. Physiol.* 324 (3), C679–C693. doi:10.1152/ajpcell.00275.2022

Haase, V. H. (2009). The VHL tumor suppressor: master regulator of hif. *Curr. Pharm. Des.* 15 (33), 3895–3903. doi:10.2174/138161209789649394

Hakamata, Y., Toyomizu, M., and Kikusato, M. (2020). Differences in breast muscle mitochondrial respiratory capacity, reactive oxygen species generation, and complex characteristics between 7-week-old meat- and laying-type chickens. *J. Poult. Sci.* 57 (4), 319–327. doi:10.2141/jpsa.0190133

Havenstein, G. B., Ferket, P. R., and Qureshi, M. A. (2003a). Carcass composition and yield of 1957 versus 2001 broilers when fed representative 1957 and 2001 broiler diets. *Poult. Sci.* 82 (10), 1509–1518. doi:10.1093/ps/82.10.1509

Havenstein, G. B., Ferket, P. R., and Qureshi, M. A. (2003b). Growth, livability, and feed conversion of 1957 versus 2001 broilers when fed representative 1957 and 2001 broiler diets. *Poult. Sci.* 82 (10), 1500–1508. doi:10.1093/ps/82.10.1500

Hosotani, M., Kametani, K., Ohno, N., Hiramatsu, K., Kawasaki, T., Hasegawa, Y., et al. (2021). The unique physiological features of the broiler pectoralis major muscle as suggested by the three-dimensional ultrastructural study of mitochondria in type IIb muscle fibers. *J. Vet. Med. Sci.* 83 (11), 1764–1771. doi:10.1292/jvms.21-0408

Hosotani, M., Kawasaki, T., Hasegawa, Y., Wakasa, Y., Hoshino, M., Takahashi, N., et al. (2020). Physiological and pathological mitochondrial clearance is related to pectoralis major muscle pathogenesis in broilers with wooden breast syndrome. *Front. Physiol.* 11, 579. doi:10.3389/fphys.2020.00579

Huang, L. E., Gu, J., Schau, M., and Bunn, H. F. (1998). Regulation of hypoxia-inducible factor 1alpha is mediated by an O2-dependent degradation domain via the ubiquitin-proteasome pathway. *PNAS* 95 (14), 7987–7992. doi:10.1073/pnas.95.14.7987

Huo, W., Weng, K., Li, Y., Zhang, Y., Zhang, Y., Xu, Q., et al. (2022). Comparison of muscle fiber characteristics and glycolytic potential between slow- and fast-growing broilers. *Poult. Sci.* 101 (3), 101649. doi:10.1016/j.psj.2021.101649

Jaakkola, P., Mole, D. R., Tian, Y. M., Wilson, M. I., Gielbert, J., Gaskell, S. J., et al. (2001). Targeting of HIF-alpha to the von Hippel-Lindau ubiquitylation complex by O2-regulated prolyl hydroxylation. *Science* 292 (5516), 468–472. doi:10.1126/science.1059796

Ji, W., Wang, L., He, S., Yan, L., Li, T., Wang, J., et al. (2018). Effects of acute hypoxia exposure with different durations on activation of Nrf2-ARE pathway in mouse skeletal muscle. *PLoS One* 13 (12), e0208474. doi:10.1371/journal.pone.0208474

Joiner, K. S., Hamlin, G. A., Lien, A. R., and Bilgili, S. F. (2014). Evaluation of capillary and myofiber density in the pectoralis major muscles of rapidly growing, high-yield broiler chickens during increased heat stress. *Avian Dis.* 58 (3), 377–382. doi:10.1637/10733-112513-Reg.1

Kant, R., Bali, A., Singh, N., and Jaggi, A. S. (2013). Prolyl 4 hydroxylase: A critical target in the pathophysiology of diseases. *Korean J. Physiol. Pharmacol.* 17 (2), 111–120. doi:10.4196/kjpp.2013.17.2.111

Khalil, S., Saenbungkhor, N., Kesnava, K., Sivapirunthep, P., Sitthigripong, R., Jumanee, S., et al. (2021). Effects of guanidinoacetic acid supplementation on productive performance, pectoral myopathies, and meat quality of broiler chickens. *Animals* 11 (11), 3180. doi:10.3390/ani11113180

Kierans, S. J., and Taylor, C. T. (2021). Regulation of glycolysis by the hypoxia-inducible factor (HIF): implications for cellular physiology. *J. Physiol.* 599 (1), 23–37. doi:10.1113/JP280572

Kim, J. W., Tchernyshyov, I., Semenza, G. L., and Dang, C. V. (2006). HIF-1-mediated expression of pyruvate dehydrogenase kinase: A metabolic switch required for cellular adaptation to hypoxia. *Cell. Metab.* 3 (3), 177–185. doi:10.1016/j.cmet.2006.02.002

Koivunen, P., Hirsilä, M., Remes, A. M., Hassinen, I. E., Kivirikko, K. I., and Myllyharju, J. (2007). Inhibition of hypoxia-inducible factor (HIF) hydroxylases by citric acid cycle intermediates: possible links between cell metabolism and stabilization of hif. *J. Biol. Chem.* 282 (7), 4524–4532. doi:10.1074/jbc.M610415200

Koomkrong, N., Theerawatanasirikul, S., Boonkaewwan, C., Jaturasitha, S., and Kayan, A. (2015). Breed-related number and size of muscle fibres and their response to carcass quality in chickens. *Ital. J. Anim. Sci.* 14 (4), 4145. doi:10.4081/ijas.2015.4145

Kozakowska, M., Pietraszek-Gremplewicz, K., Jozkowicz, A., and Dulak, J. (2015). The role of oxidative stress in skeletal muscle injury and regeneration: focus on antioxidant enzymes. *J. Muscle Res. Cell. Motil.* 36 (6), 377–393. doi:10.1007/s10974-015-9438-9

Kranen, R. W., Lambooij, E., Veerkamp, C. H., Van Kuppevelt, T. H., and Veerkamp, J. H. (2000). Haemorrhages in muscles of broiler chickens. *Worlds Poult. Sci. J.* 56 (2), 93–126. doi:10.1079/WPS20000009

Krishnan, J., Suter, M., Windak, R., Krebs, T., Felley, A., Montessuit, C., et al. (2009). Activation of a HIF1alpha-PPARgamma axis underlies the integration of glycolytic and lipid anabolic pathways in pathologic cardiac hypertrophy. *Cell. Metab.* 9 (6), 512–524. doi:10.1016/j.cmet.2009.05.005

Kuttappan, V. A., Hargis, B. M., and Owens, C. M. (2016). White striping and woody breast myopathies in the modern poultry industry: A review. *Poult. Sci.* 95 (11), 2724–2733. doi:10.3382/ps/pew216

Kuttappan, V. A., Lee, Y. S., Erf, G. F., Meullenet, J. F., McKee, S. R., and Owens, C. M. (2012). Consumer acceptance of visual appearance of broiler breast meat with varying degrees of white striping. *Poult. Sci.* 91 (5), 1240–1247. doi:10.3382/ps.2011-01947

Kuttappan, V. A., Shivaprasad, H. L., Shaw, D. P., Valentine, B. A., Hargis, B. M., Clark, F. D., et al. (2013). Pathological changes associated with white striping in broiler breast muscles. *Poult. Sci.* 92 (2), 331–338. doi:10.3382/ps.2012-02646

Lake, J. A., Dekkers, J. C. M., and Abasht, B. (2021). Genetic basis and identification of candidate genes for wooden breast and white striping in commercial broiler chickens. *Sci. Rep.* 11 (1), 6785. doi:10.1038/s41598-021-86176-4

Lake, J. A., Papah, M. B., and Abasht, B. (2019). Increased expression of lipid metabolism genes in early stages of wooden breast links myopathy of broilers to metabolic syndrome in humans. *Genes* 10 (10), 746. doi:10.3390/genes10100746

Le Bihan-Duval, E., Debut, M., Berri, C. M., Sellier, N., Santé-Lhoutellier, V., Jégo, Y., et al. (2008). Chicken meat quality: genetic variability and relationship with growth and muscle characteristics. *BMC Genet.* 9, 53. doi:10.1186/1471-2156-9-53

Li, B., Dong, X., Puolanne, E., and Ertbjerg, P. (2022). Effect of wooden breast degree on lipid and protein oxidation and citrate synthase activity of chicken pectoralis major muscle. *LWT* 154, 112884. doi:10.1016/j.lwt.2021.112884

Li, H.-S., Zhou, Y.-N., Li, L., Li, S.-F., Long, D., Chen, X.-L., et al. (2019). HIF-1α protects against oxidative stress by directly targeting mitochondria. *Redox Biol.* 25, 101109. doi:10.1016/j.redox.2019.101109

Liu, R., Kong, F., Xing, S., He, Z., Bai, L., Sun, J., et al. (2022). Dominant changes in the breast muscle lipid profiles of broiler chickens with wooden breast syndrome revealed by lipidomics analyses. *J. Anim. Sci. Biotechnol.* 13 (1), 93. doi:10.1186/s40104-022-00743-x

Lokman, I., Jawad, H. S., Goh, Y., Sazili, A., Noordin, M., and Zuki, A. (2016). Morphology of breast and thigh muscles of Red Jungle Fowl (Gallus gallus spadiceus), Malaysian village chicken (Gallus gallus domesticus) and commercial broiler chicken. *Int. J. Poult. Sci.* 15 (4), 144–150. doi:10.3923/ijps.2016.144.150

Lugus, J. J., Ngoh, G. A., Bachschmid, M. M., and Walsh, K. (2011). Mitofusins are required for angiogenic function and modulate different signaling pathways in cultured endothelial cells. *J. Mol. Cell. Cardiol.* 51 (6), 885–893. doi:10.1016/j.yjmcc.2011.07.023

Ma, X., Wang, D., Zhao, W., and Xu, L. (2018). Deciphering the roles of PPARγ in adipocytes via dynamic change of transcription complex. *Front. Endocrinol. (Lausanne)* 9, 473. doi:10.3389/fendo.2018.00473

Malila, Y., Thanatsang, K., Arayamethakorn, S., Uengwetwanit, T., Srimarut, Y., Petracci, M., et al. (2019). Absolute expressions of hypoxia-inducible factor-1 alpha (HIF1A) transcript and the associated genes in chicken skeletal muscle with white striping and wooden breast myopathies. *PLoS One* 14 (8), e0220904. doi:10.1371/journal.pone.0220904

Malila, Y., Thanatsang, K. V., Sanpinit, P., Arayamethakorn, S., Soglia, F., Zappaterra, M., et al. (2022). Differential expression patterns of genes associated with metabolisms, muscle growth and repair in Pectoralis major muscles of fast- and medium-growing chickens. *PLoS One* 17 (10), e0275160. doi:10.1371/journal.pone.0275160

Marchesi, J. A. P., Ibelli, A. M. G., Peixoto, J. O., Cantao, M. E., Pandolfi, J. R. C., Marciano, C. M. M., et al. (2019). Whole transcriptome analysis of the pectoralis major muscle reveals molecular mechanisms involved with white striping in broiler chickens. *Poult. Sci.* 98 (2), 590–601. doi:10.3382/ps/pey429

Martínez-Reyes, I., and Chandel, N. S. (2020). Mitochondrial TCA cycle metabolites control physiology and disease. *Nat. Commun.* 11 (1), 102. doi:10.1038/s41467-019-13668-3

Masoud, G. N., and Li, W. (2015). HIF-1α pathway: role, regulation and intervention for cancer therapy. *Acta Pharm. Sin. B* 5 (5), 378–389. doi:10.1016/j.apsb.2015.05.007

Mazzoni, M., Soglia, F., Petracci, M., Sirri, F., Lattanzio, G., and Clavenzani, P. (2020). Fiber metabolism, procollagen and collagen type III immunoreactivity in broiler pectoralis major affected by muscle abnormalities. *Animals* 10 (6), 1081. doi:10.3390/ani10061081

Meléndez-Morales, D., de Paz-Lugo, P., and Meléndez-Hevia, E. (2009). Glycolysis activity in flight muscles of birds according to their physiological function. An experimental model *in vitro* to study aerobic and anaerobic glycolysis activity separately. *Mol. Cell. Biochem.* 328 (1-2), 127–135. doi:10.1007/s11010-009-0082-9

Mingyuan, X., Qianqian, P., Shengquan, X., Chenyi, Y., Rui, L., Yichen, S., et al. (2018). Hypoxia-inducible factor-1α activates transforming growth factor-β1/Smad signaling and increases collagen deposition in dermal fibroblasts. *Oncotarget* 9 (3), 3188–3197. doi:10.18632/oncotarget.23225

Mudalal, S., Lorenzi, M., Soglia, F., Cavani, C., and Petracci, M. (2015). Implications of white striping and wooden breast abnormalities on quality traits of raw and marinated chicken meat. *Animal* 9 (4), 728–734. doi:10.1017/s175173111400295x

Mudalal, S., Babini, E., Cavani, C., and Petracci, M. (2014). Quantity and functionality of protein fractions in chicken breast fillets affected by white striping. *Poult. Sci.* 93 (8), 2108–2116. doi:10.3382/ps.2014-03911

Murphy, M. P. (2009). How mitochondria produce reactive oxygen species. *Biochem. J.* 417 (1), 1–13. doi:10.1042/bj20081386

Mylonis, I., Simos, G., and Paraskeva, E. (2019). Hypoxia-inducible factors and the regulation of lipid metabolism. *Cells* 8 (3), 214. doi:10.3390/cells8030214

OECD (2022). *OECD-FAO agricultural outlook 2022-2031*. Paris, France: OECD. doi:10.1787/19991142

Orlowski, S. K., Dridi, S., Greene, E. S., Coy, C. S., Velleman, S. G., and Anthony, N. B. (2021). Histological analysis and gene expression of satellite cell markers in the pectoralis major muscle in broiler lines divergently selected for percent 4-day breast yield. *Front. Physiol.* 12, 712095. doi:10.3389/fphys.2021.712095

Pampouille, E., Hennequet-Antier, C., Praud, C., Juanchich, A., Brionne, A., Godet, E., et al. (2019). Differential expression and co-expression gene network analyses reveal molecular mechanisms and candidate biomarkers involved in breast muscle myopathies in chicken. *Sci. Rep.* 9 (1), 14905. doi:10.1038/s41598-019-51521-1

Pan, X., Zhang, L., Xing, T., Li, J., and Gao, F. (2021). The impaired redox status and activated nuclear factor-erythroid 2-related factor 2/antioxidant response element pathway in wooden breast myopathy in broiler chickens. *Anim. Biosci.* 34 (4), 652–661. doi:10.5713/ajas.19.0953

Park, J., Lee, J., and Choi, C. (2011). Mitochondrial network determines intracellular ROS dynamics and sensitivity to oxidative stress through switching inter-mitochondrial messengers. *PLoS One* 6 (8), e23211. doi:10.1371/journal.pone.0023211

Pereira, M. R., Mello, J. L. M., Oliveira, R. F., Villegas-Cayllahua, E. A., Cavalcanti, E. N. F., Fidelis, H. A., et al. (2022). Effect of freezing on the quality of breast meat from broilers affected by White Striping myopathy. *Poult. Sci.* 101 (2), 101607. doi:10.1016/j.psj.2021.101607

Petracci, M., and Cavani, C. (2012). Muscle growth and poultry meat quality issues. *Nutrients* 4 (1), 1–12. doi:10.3390/nu4010001

Petracci, M., Mudalal, S., Soglia, F., and Cavani, C. (2015). Meat quality in fast-growing broiler chickens. *Worlds Poult. Sci. J.* 71 (2), 363–374. doi:10.1017/S0043933915000367

Pisani, D. F., and Dechesne, C. A. (2005). Skeletal muscle HIF-1alpha expression is dependent on muscle fiber type. *J. Gen. Physiol.* 126 (2), 173–178. doi:10.1085/jgp.200509265

Praud, C., Jimenez, J., Pampouille, E., Couroussé, N., Godet, E., Le Bihan-Duval, E., et al. (2020). Molecular phenotyping of white striping and wooden breast myopathies in chicken. *Front. Physiol.* 11, 633. doi:10.3389/fphys.2020.00633

Quadrilatero, J., Alway, S. E., and Dupont-Versteegden, E. E. (2011). Skeletal muscle apoptotic response to physical activity: potential mechanisms for protection. *Appl. Physiol. Nutr. Metab.* 36 (5), 608–617. doi:10.1139/h11-064

Radaelli, G., Piccirillo, A., Birolo, M., Bertotto, D., Gratta, F., Ballarin, C., et al. (2017). Effect of age on the occurrence of muscle fiber degeneration associated with myopathies in broiler chickens submitted to feed restriction. *Poult. Sci.* 96 (2), 309–319. doi:10.3382/ps/pew270

Remignon, H., Gardahaut, M. F., Marche, G., and Ricard, F. H. (1995). Selection for rapid growth increases the number and the size of muscle fibres without changing their typing in chickens. *J. Muscle Res. Cell. Motil.* 16 (2), 95–102. doi:10.1007/bf00122527

Reverter, A., Okimoto, R., Sapp, R., Bottje, W. G., Hawken, R., and Hudson, N. J. (2017). Chicken muscle mitochondrial content appears co-ordinately regulated and is associated with performance phenotypes. *Biol. Open* 6 (1), 50–58. doi:10.1242/bio.022772

Rodriguez-Miguelez, P., Lima-Cabello, E., Martínez-Flórez, S., Almar, M., Cuevas, M. J., and González-Gallego, J. (2015). Hypoxia-inducible factor-1 modulates the expression of vascular endothelial growth factor and endothelial nitric oxide synthase induced by eccentric exercise. *J. Appl. Physiol.* 118 (8), 1075–1083. doi:10.1152/japplphysiol.00780.2014

Rosser, B. W. C., Dean, M. S., and Bandman, E. (2002). Myonuclear domain size varies along the lengths of maturing skeletal muscle fibers. *Int. J. Dev. Biol.* 46 (5), 747–754. doi:10.1387/ijdb.12216987

Salles, G. B. C., Boiago, M. M., Silva, A. D., Morsch, V. M., Gris, A., Mendes, R. E., et al. (2019). Lipid peroxidation and protein oxidation in broiler breast fillets with white striping myopathy. *J. Food Biochem.* 43 (4), e12792. doi:10.1111/jfbc.12792

Sammari, H., Askri, A., Benahmed, S., Saucier, L., and Alnahhas, N. (2023). A survey of broiler breast meat quality in the retail market of Quebec. *Can. J. Anim. Sci.* 0 (0), 1–14. doi:10.1139/cjas-2023-0001

Sanden, K. W., Böcker, U., Ofstad, R., Pedersen, M. E., Høst, V., Afseth, N. K., et al. (2021). Characterization of collagen structure in normal, wooden breast and spaghetti meat chicken fillets by FTIR microspectroscopy and histology. *Foods* 10 (3), 548. doi:10.3390/foods10030548

Schmierer, B., and Hill, C. S. (2007). TGFbeta-SMAD signal transduction: molecular specificity and functional flexibility. *Nat. Rev. Mol. Cell. Biol.* 8 (12), 970–982. doi:10.1038/nrm2297

Sendoel, A., and Hengartner, M. O. (2014). Apoptotic cell death under hypoxia. *Physiol. (Bethesda)* 29 (3), 168–176. doi:10.1152/physiol.00016.2013

Sihvo, H. K., Immonen, K., and Puolanne, E. (2014). Myodegeneration with fibrosis and regeneration in the pectoralis major muscle of broilers. *Vet. Pathol.* 51 (3), 619–623. doi:10.1177/0300985813497488

Sihvo, H. K., Airas, N., Linden, J., and Puolanne, E. (2018). Pectoral vessel density and early ultrastructural changes in broiler chicken wooden breast myopathy. *J. Comp. Pathol.* 161, 1–10. doi:10.1016/j.jcpa.2018.04.002

Sirri, F., Maiorano, G., Tavaniello, S., Chen, J., Petracci, M., and Meluzzi, A. (2016). Effect of different levels of dietary zinc, manganese, and copper from organic or inorganic sources on performance, bacterial chondronecrosis, intramuscular collagen characteristics, and occurrence of meat quality defects of broiler chickens. *Poult. Sci.* 95 (8), 1813–1824. doi:10.3382/ps/pew064

Soglia, F., Gao, J. X., Mazzoni, M., Puolanne, E., Cavani, C., Petracci, M., et al. (2017). Superficial and deep changes of histology, texture and particle size distribution in broiler wooden breast muscle during refrigerated storage. *Poult. Sci.* 96 (9), 3465–3472. doi:10.3382/ps/pex115

Soglia, F., Mudalal, S., Babini, E., Di Nunzio, M., Mazzoni, M., Sirri, F., et al. (2016a). Histology, composition, and quality traits of chicken Pectoralis major muscle affected by wooden breast abnormality. *Poult. Sci.* 95 (3), 651–659. doi:10.3382/ps/pev353

Soglia, F., Petracci, M., and Ertbjerg, P. (2016b). Novel DNPH-based method for determination of protein carbonylation in muscle and meat. *Food Chem.* 197, 670–675. doi:10.1016/j.foodchem.2015.11.038

Soglia, F., Petracci, M., and Puolanne, E. (2020). Sarcomere lengths in wooden breast broiler chickens. *Ital. J. Anim. Sci.* 19 (1), 569–573. doi:10.1080/1828051x.2020.1761271

Soglia, F., Silva, A. K., Liao, L. M., Laghi, L., and Petracci, M. (2019). Effect of broiler breast abnormality and freezing on meat quality and metabolites assessed by 1H-NMR spectroscopy. *Poult. Sci.* 98 (12), 7139–7150. doi:10.3382/ps/pez514

Squire, J. M. (2016). Muscle contraction: sliding filament history, sarcomere dynamics and the two huxleys. *Glob. Cardiol. Sci. Pract.* 2016 (2), e201611. doi:10.21542/gcsp.2016.11

Surai, P. F., Kochish, I. I., Fisinin, V. I., and Kidd, M. T. (2019). Antioxidant defence systems and oxidative stress in poultry biology: an update. *Antioxidants* 8 (7), 235. doi:10.3390/antiox8070235

Talbot, J., and Maves, L. (2016). Skeletal muscle fiber type: using insights from muscle developmental biology to dissect targets for susceptibility and resistance to muscle disease. *Wiley Interdiscip. Rev. Dev. Biol.* 5 (4), 518–534. doi:10.1002/wdev.230

Taylor, C. T., and Scholz, C. C. (2022). The effect of HIF on metabolism and immunity. *Nat. Rev. Nephrol.* 18 (9), 573–587. doi:10.1038/s41581-022-00587-8

Thanatsang, K. V., Malila, Y., Arayamethakorn, S., Srimarut, Y., Tatiyaborworntham, N., Uengwetwanit, T., et al. (2020). Nutritional properties and oxidative indices of broiler breast meat affected by wooden breast abnormality. *Animals* 10 (12), 2272. doi:10.3390/ani10122272

Thomas, L. W., and Ashcroft, M. (2019). Exploring the molecular interface between hypoxia-inducible factor signalling and mitochondria. *Cell. Mol. Life Sci.* 76 (9), 1759–1777. doi:10.1007/s00018-019-03039-y

Tian, J., Wang, S., Wang, Q., Leng, L., Hu, X., and Li, H. (2010). A single nucleotide polymorphism of chicken acetyl-CoA carboxylase A gene associated with fatness traits. *Anim. Biotechnol.* 21 (1), 42–50. doi:10.1080/10495390903347009

Tilokani, L., Nagashima, S., Paupe, V., and Prudent, J. (2018). Mitochondrial dynamics: overview of molecular mechanisms. *Essays Biochem.* 62 (3), 341–360. doi:10.1042/ebc20170104

Ullah, M. S., Davies, A. J., and Halestrap, A. P. (2006). The plasma membrane lactate transporter MCT4, but not MCT1, is up-regulated by hypoxia through a HIF-1alpha-dependent mechanism. *J. Biol. Chem.* 281 (14), 9030–9037. doi:10.1074/jbc.M511397200

Valle-Tenney, R., Rebolledo, D. L., Lipson, K. E., and Brandan, E. (2020). Role of hypoxia in skeletal muscle fibrosis: synergism between hypoxia and tgf-β signaling upregulates ccn2/ctgf expression specifically in muscle fibers. *Matrix Biol.* 87, 48–65. doi:10.1016/j.matbio.2019.09.003

Velleman, S. G., Clark, D. L., and Tonniges, J. R. (2017). Fibrillar collagen organization associated with broiler wooden breast fibrotic myopathy. *Avian Dis.* 61 (4), 481–490. doi:10.1637/11738-080217-Reg.1

Velleman, S. G., Coy, C. S., and Abasht, B. (2022). Effect of expression of PPARG, DNM2L, RRAD, and LINGO1 on broiler chicken breast muscle satellite cell function. *CBPA* 268, 111186. doi:10.1016/j.cbpa.2022.111186

Velleman, S. G., Coy, C. S., Anderson, J. W., Patterson, R. A., and Nestor, K. E. (2003). Effect of selection for growth rate and inheritance on posthatch muscle development in turkeys. *Poult. Sci.* 82 (9), 1365–1372. doi:10.1093/ps/82.9.1365

Velleman, S. G. (2020). Pectoralis major (breast) muscle extracellular matrix fibrillar collagen modifications associated with the wooden breast fibrotic myopathy in broilers. *Front. Physiol.* 11, 461. doi:10.3389/fphys.2020.00461

Velleman, S. G. (2019). Recent developments in breast muscle myopathies associated with growth in poultry. *Annu. Rev. Anim. Biosci.* 7, 289–308. doi:10.1146/annurev-animal-020518-115311

Velleman, S. G. (2015). Relationship of skeletal muscle development and growth to breast muscle myopathies: A review. *Avian Dis.* 59 (4), 525–531. doi:10.1637/11223-063015-Review.1

Velleman, S. G. (2023). Satellite cell-mediated breast muscle growth and repair: the impact of thermal stress. *Front. Physiol.* 14, 1173988. doi:10.3389/fphys.2023.1173988

Verdiglione, R., and Cassandro, M. (2013). Characterization of muscle fiber type in the pectoralis major muscle of slow-growing local and commercial chicken strains. *Poult. Sci.* 92 (9), 2433–2437. doi:10.3382/ps.2013-03013

Vial, C., Zúñiga, L. M., Cabello-Verrugio, C., Cañón, P., Fadic, R., and Brandan, E. (2008). Skeletal muscle cells express the profibrotic cytokine connective tissue growth factor (CTGF/CCN2), which induces their dedifferentiation. *J. Cell. Physiol.* 215 (2), 410–421. doi:10.1002/jcp.21324

Wang, S., Tan, J., Miao, Y., and Zhang, Q. (2022). Mitochondrial dynamics, mitophagy, and mitochondria-endoplasmic reticulum contact sites crosstalk under hypoxia. *Front. Cell. Dev. Biol.* 10, 848214. doi:10.3389/fcell.2022.848214

Wang, Y., Branicky, R., Noë, A., and Hekimi, S. (2018). Superoxide dismutases: dual roles in controlling ros damage and regulating ros signaling. *J. Cell. Biol.* 217 (6), 1915–1928. doi:10.1083/jcb.201708007

Weidemann, A., and Johnson, R. S. (2008). Biology of HIF-1alpha. *Cell. Death Differ.* 15 (4), 621–627. doi:10.1038/cdd.2008.12

Xu, K. Y., and Becker, L. C. (1998). Ultrastructural localization of glycolytic enzymes on sarcoplasmic reticulum vesticles. *J. Histochem Cytochem* 46 (4), 419–427. doi:10.1177/002215549804600401

Xing, T., Zhao, Z. R., Zhao, X., Xu, X. L., Zhang, L., and Gao, F. (2021). Enhanced transforming growth factor-beta signaling and fibrosis in the pectoralis major muscle of broiler chickens affected by wooden breast myopathy. *Poult. Sci.* 100 (3), 100804. doi:10.1016/j.psj.2020.10.058

Yablonka-Reuveni, Z. (1995). Myogenesis in the chicken: the onset of differentiation of adult myoblasts is influenced by tissue factors. *Basic Appl. Myol.* 5 (1), 33–41.

Yalcin, S., Şahin, K., Tuzcu, M., Bilgen, G., Özkan, S., Izzetoğlu, G. T., et al. (2019). Muscle structure and gene expression in pectoralis major muscle in response to deep pectoral myopathy induction in fast- and slow-growing commercial broilers. *Br. Poult. Sci.* 60 (3), 195–201. doi:10.1080/00071668.2018.1430351

Youle, R. J., and van der Bliek, A. M. (2012). Mitochondrial fission, fusion, and stress. *Science* 337 (6098), 1062–1065. doi:10.1126/science.1219855

Young, J. F., and Rasmussen, M. K. (2020). Differentially expressed marker genes and glycogen levels in pectoralis major of Ross308 broilers with wooden breast syndrome indicates stress, inflammation and hypoxic conditions. *Food Chem. Mol. Sci.* 1, 100001. doi:10.1016/j.fochms.2020.100001

Zambonelli, P., Zappaterra, M., Soglia, F., Petracci, M., Sirri, F., Cavani, C., et al. (2016). Detection of differentially expressed genes in broiler pectoralis major muscle affected by White Striping - wooden Breast myopathies. *Poult. Sci.* 95 (12), 2771–2785. doi:10.3382/ps/pew268

Zhao, D., Kogut, M. H., Genovese, K. J., Hsu, C. Y., Lee, J. T., and Farnell, Y. Z. (2020). Altered expression of lactate dehydrogenase and monocarboxylate transporter involved in lactate metabolism in broiler wooden breast. *Poult. Sci.* 99 (1), 11–20. doi:10.3382/ps/pez572

Zhao, Y.-Z., Liu, X.-L., Shen, G.-M., Ma, Y.-N., Zhang, F.-L., Chen, M.-T., et al. (2014). Hypoxia induces peroxisome proliferator-activated receptor γ expression via HIF-1-dependent mechanisms in HepG2 cell line. *Arch. Biochem. Biophys.* 543, 40–47. doi:10.1016/j.abb.2013.12.010

Ziello, J. E., Jovin, I. S., and Huang, Y. (2007). Hypoxia-Inducible Factor (HIF)-1 regulatory pathway and its potential for therapeutic intervention in malignancy and ischemia. *Yale J. Biol. Med.* 80 (2), 51–60.

Zuidhof, M. J., Schneider, B. L., Carney, V. L., Korver, D. R., and Robinson, F. E. (2014). Growth, efficiency, and yield of commercial broilers from 1957, 1978, and 2005. *Poult. Sci.* 93 (12), 2970–2982. doi:10.3382/ps.2014-04291

frontiers | Frontiers in Physiology

TYPE Original Research
PUBLISHED 16 November 2023
DOI 10.3389/fphys.2023.1288809



OPEN ACCESS

EDITED BY
Francesca Soglia,
University of Bologna, Italy

REVIEWED BY
Tomohide Takaya,
Shinshu University, Japan
Wei Guo,
University of Wisconsin-Madison,
United States

*CORRESPONDENCE
Jessica D. Starkey,
jessica.starkey@auburn.edu

RECEIVED 04 September 2023
ACCEPTED 27 October 2023
PUBLISHED 16 November 2023

CITATION
Gregg CR, Hutson BL, Flees JJ, Starkey CW and Starkey JD (2023), Effect of standard and physiological cell culture temperatures on *in vitro* proliferation and differentiation of primary broiler chicken *pectoralis major* muscle satellite cells. *Front. Physiol.* 14:1288809. doi: 10.3389/fphys.2023.1288809



# Effect of standard and physiological cell culture temperatures on *in vitro* proliferation and differentiation of primary broiler chicken *pectoralis major* muscle satellite cells

Caroline R. Gregg, Brittany L. Hutson, Joshua J. Flees, Charles W. Starkey and Jessica D. Starkey*

Department of Poultry Science, Auburn University, Auburn, AL, United States

Culture temperatures for broiler chicken cells are largely based on those optimized for mammalian species, although normal broiler body temperature is typically more than 3°C higher. The objective was to evaluate the effects of simulating broiler peripheral muscle temperature, 41°C, compared with standard temperature, 38°C, on the *in vitro* proliferation and differentiation of primary muscle-specific stem cells (satellite cells; SC) from the *pectoralis major* (PM) of broiler chickens. Primary SC cultures were isolated from the PM of 18-day-old Ross 708 × Yield Plus male broilers. SC were plated in triplicate, 1.8-cm$^2$, gelatin-coated wells at 40,000 cells per well. Parallel plates were cultured at either 38°C or 41°C in separate incubators. At 48, 72, and 96 h post-plating, the culture wells were fixed and immunofluorescence-stained to determine the expression of the myogenic regulatory factors Pax7 and MyoD as well as evaluated for apoptosis using a TUNEL assay. After 168 h in culture, plates were immunofluorescence-stained to visualize myosin heavy chain and Pax7 expression and determine myotube characteristics and SC fusion. Population doubling times were not impacted by temperature ($p \geq 0.1148$), but culturing broiler SC at 41°C for 96 h promoted a more rapid progression through myogenesis, while 38°C maintained primitive populations ($p \leq 0.0029$). The proportion of apoptotic cells increased in primary SC cultured at 41°C ($p \leq 0.0273$). Culturing at 41°C appeared to negatively impact fusion percentage ($p < 0.0001$) and tended to result in the formation of thinner myotubes ($p = 0.061$) without impacting the density of differentiated cells ($p = 0.7551$). These results indicate that culture temperature alters primary broiler PM SC myogenic kinetics and has important implications for future *in vitro* work as well as improving our understanding of how thermal manipulation can alter myogenesis patterns during broiler embryonic and post-hatch muscle growth.

KEYWORDS

**broiler chicken, muscle satellite cell, cell culture temperature, myogenic regulatory factor, apoptosis, myogenesis**

# 1 Introduction

Hypertrophic growth of post-mitotic muscle fibers in young animals relies on populations of resident, muscle-specific stem cells, or satellite cells (SC; White et al., 2010). SC are capable of proliferating and fusing with existing muscle fibers to increase DNA content and allow for growth by expanding the potential for protein synthesis (Hall and Ralston, 1989). There is growing interest in evaluating SC isolated from the *pectoralis major* (PM) of modern broiler chickens *in vitro* to better understand broiler muscle growth, as well as develop practical methods to optimize meat yield. However, *in vitro* research on SC from current broiler strains is limited, and cell culture conditions are not well established in the existing literature. Many avian SC experimental protocols have been adapted from early work culturing murine SC (Bischoff, 1986), where the physiological body temperature of the donor animal is typically between 37°C and 38°C. Many researchers have adopted this range as a standard culture temperature for chicken SC (Matsuda et al., 1983; Halevy et al., 2004; Geiger et al., 2018; Tompkins et al., 2021). Yet, the average core body temperature of modern broilers is closer to 41°C (Giloh et al., 2012; Peebles et al., 2021), so this widely used standard cell culture temperature may not be reproducing physiological conditions of the broiler SC niche *in vivo*.

Increasing culture temperature above 38°C appears to increase both proliferation and differentiation of chicken SC (Harding et al., 2016). However, it is worth noting that the previously mentioned experiment was conducted with passaged SC isolated from broilers over 25 years ago (McFarland et al., 1997) that likely differ greatly from modern broiler strains, given the extensive genetic selection for muscle growth. Considering recent evidence that culture temperature impacts SC function in cells from fast-growing turkeys differently compared to cells from their heritage strain counterparts (Xu et al., 2022; Xu et al., 2023), evaluating SC from modern broilers may provide an updated understanding of the influence of temperature. In mammalian species, culturing SC continuously at temperatures above their respective physiological body temperature suppresses proliferation in primary swine cells (Park et al., 2023) and reduces myotube diameter in primary human cultures (Yamaguchi et al., 2010). Therefore, comparing the effects of a standard cell culture temperature versus a temperature that is closer to that of peripheral broiler muscle on SC proliferation and differentiation could help establish optimal culture conditions to properly evaluate modern broiler SC in future work. It was hypothesized that primary SC isolated from broiler chicken PM would have improved proliferation and greater SC fusion when cultured at 41°C.

# 2 Materials and methods

All procedures regarding live birds were approved by the Auburn University Institutional Animal Care and Use Committee (PRN 2020-3767).

## 2.1 Primary cell isolation

Primary muscle cell cultures were isolated from the pooled PM of 18-day-old Ross 708 × Yield Plus male broilers ($n = 6$ per replicate isolation). The broilers were reared on a common corn- and soybean meal-based diet formulated to meet or exceed primary breeder nutrient specifications in floor pens in an environmentally controlled facility (Charles C. Miller Jr. Poultry Research and Education Center, Auburn, AL, United States). Lighting and temperature were established according to primary breeder recommendations. Prior to muscle harvest and immediately following euthanasia via electrocution, a thermometer was inserted approximately 2–3 cm into a small opening cut in the center of the PM within a sterile environment. The average PM internal temperature of all birds harvested ($n = 18$) was 41.14 ± 0.08°C. PM was harvested, trimmed of excess fat, and briefly stored in Dulbecco's modified Eagle's medium (DMEM; Thermo Fisher, Waltham, MA, Cat. 10567022) with 1% antibiotic/antimycotic (AB/AM; Thermo Fisher, Waltham, MA, Cat. 15240112) + 0.1% gentamicin (Thermo Fisher, Waltham, MA, Cat. 15710064) at room temperature. PM tissue was pooled and chopped using a bullet chopper to a uniform consistency. SC isolation methods were adapted from Yablonka-Reuveni et al. (1987). Tissue was digested in 0.2% collagenase type 1 (Sigma-Aldrich, St. Louis, MO, Cat. C0130) in DMEM for 1 h with mechanical inversion every 5 min. Tissue was rinsed with phosphate-buffered saline (PBS) + 1% AB/AM + 0.1% gentamycin and then resuspended in PBS and vigorously shaken. The suspended tissue was centrifuged at 500 × g for 5 min, and then the cell-containing supernatant was collected and centrifuged at 1,500 × g for 5 min to obtain a cell pellet. This process was repeated three times to maximize cell yield, and the resulting cell pellets were resuspended in low-glucose DMEM (Thermo Fisher, Waltham, MA, Cat. 10567014) with 5% horse serum (Millipore Sigma, Burlington, MA, Cat. H1270) + 3% AB/AM + 0.3% gentamicin, pooled, and then passed through a 40-μM filter (Sigma-Aldrich, St. Louis, MO, Cat. SCNY00040). A density centrifugation step to remove muscle debris was conducted by layering the cell suspension over 20% Percoll (Cytiva, Marlborough, MA, Cat. 17089101) in Minimum Essential Medium (MEM; Thermo Fisher, Waltham, MA, Cat. 11090081) and centrifuged at 1,700 × g for 5 min in 15-mL conical tubes that were previously coated with horse serum. The remaining muscle debris layer was removed from the top of the tube and discarded, and cells were collected from the lower fraction. Cells were rinsed in MEM and resuspended in DMEM with 10% horse serum + 10% DMSO (Millipore Sigma, Burlington, MA, Cat. D2650) + 3% AB/AM + 0.3% gentamicin for long-term cryopreservation in liquid nitrogen until further analysis. Three replicate isolations were conducted to obtain three independent pools of cells from different birds of the same flock on the same day.

## 2.2 Cell culture

Upon removal from liquid nitrogen storage, vials of primary SC were briefly thawed in a water bath and rinsed in low-glucose DMEM. Live cells were quantified using the Countess™ 3 Automated Cell Counter (Invitrogen, Waltham, MA) via trypan blue dye exclusion staining (Invitrogen, Waltham, MA, Cat. T10282). Cells were diluted in proliferation media, as described in Flees et al. (2022), consisting of low-glucose DMEM with 10% chicken serum (Millipore Sigma, Burlington, MA, Cat. C5405) + 5% horse serum + 1% antibiotic/antimycotic + 0.1%

gentamicin to achieve 40,000 live cells per well in triplicate on 24-well, gelatin-coated, tissue culture plates. The plates were incubated in one of two tri-gas Heracell™ 160i incubators (Thermo Fisher, Waltham, MA, Cat. 51033557) with 18% oxygen and 5% carbon dioxide set at either 38 or 41°C. For the proliferation and TUNEL assays, parallel plates were removed after 48, 72, and 96 h in culture. The final plates used for the differentiation assay were changed to differentiation media at 96 h post-plating consisting of low-glucose DMEM + 5% horse serum + 1% antibiotic/antimycotic + 0.1% gentamicin. The final parallel plates were removed after an additional 72 h or 168 h post-plating. The media were refreshed every 48 h. The experiment was replicated three times with replicate pools of cells from different birds of the same flock isolated on the same day.

## 2.3 Proliferation

The expression of myogenic regulatory factor (MRF) at 48, 72, and 96 h post-plating was determined using indirect immunofluorescence staining adapted from Day et al. (2007). In brief, cultures were rinsed with PBS before fixation in 4% paraformaldehyde (Santa Cruz Biotechnology, Dallas, TX, Cat. Sc-281692) for 10 min, followed by 15 min of permeabilization with 0.2% Triton X-100 (Thermo Fisher, Waltham, MA, Cat. A16046). Nonspecific binding was blocked using 3% bovine serum albumin (MP Biomedicals, Irvine, CA, Cat. 08810032) in PBS. Primary antibodies against the MRF paired box 7 (Pax7; Developmental Studies Hybridoma Bank, Iowa City, IA) and myogenic determination factor 1 (MyoD; Santa Cruz Biotechnology, Dallas, TX, Cat. sc-377460) were applied, followed by goat anti-mouse IgG1 Alexa Fluor 488 and IgG2b Alexa Fluor 546 (Invitrogen, Waltham, MA, Cat. A-21121 and A-21143). A 4′,6-diamidino-2-phenylindole (DAPI; MP Biomedicals, Santa Ana, CA, Cat. 0215757410) nuclear counterstain was applied to label all cell nuclei. Five random fields per culture well were captured using a Nikon ECLIPSE® Ti2 inverted fluorescence microscopy system at ×200 magnification. The Taxonomy tool in NIS-Elements software was used to enumerate populations of Pax7+:MyoD-, Pax7+:MyoD+, Pax7+:MyoD+, and MRF+ (Pax7+:MyoD-, Pax7+:MyoD+, and Pax7+:MyoD+) nuclei. Populations were set as a proportion of total nuclei as well as reported on a $mm^2$ basis. Population data were used to calculate doubling time using the following formula adapted from Li et al. (2011), where $t$ = time in h, Nt = final cell count, and Ni = initial cell count.

$$DT = \frac{t}{\log_2\left(\frac{Nt}{Ni}\right)}.$$

## 2.4 Apoptosis

The incidence of late-stage apoptotic cells was determined at 48, 72, and 96 h post-plating on parallel plates using a Click-iT™ TUNEL Alexa Fluor Imaging Assay (Invitrogen, Waltham, MA, Cat. C10245) to identify DNA fragmentation associated with cell death. Extra culture wells were plated to serve as a positive control with DNase I treatment as per the manufacturer's recommendations. A DAPI nuclear counterstain was applied to label all cell nuclei. Following completion of the assay protocol, five random fields per culture well were captured using a Nikon ECLIPSE® Ti2 inverted fluorescence microscopy system at ×200 with the Taxonomy tool in NIS-Elements software to determine cells that were TUNEL-positive per $mm^2$ as well as on a proportion of total nuclei.

## 2.5 Differentiation

At 168 h post-plating, indirect immunofluorescence staining was used to evaluate myogenic cell differentiation and fusion. The same protocol as the proliferation assay was employed using primary antibodies against Pax7 and myosin heavy chain (MHC; Developmental Studies Hybridoma Bank, Iowa City, IA) followed by goat anti-mouse IgG1 Alexa Fluor 488 and IgG2b Alexa Fluor 546 with a DAPI nuclear counterstain. Five representative fields per well were captured using a Nikon ECLIPSE® Ti2 inverted fluorescence microscopy system at ×200 magnification. NIS-Elements software was used to analyze all images. Myotube boundaries were determined by MHC expression, and myotube width was measured in μm perpendicular to the widest point using the Length 3D tool in NIS-Elements. When myotubes branched off one another, each branch was considered a new myotube. The number of width measurements obtained per image was used to quantify the density of myotubes per $mm^2$ as well as the coefficient of variation among the widths. The myotube area was quantified as a proportion of MHC expression to the total image area using the Binary feature of NIS-Elements software as previously described by Murphy et al. (2011) and Ferreira et al. (2020), with thresholds set for each image. Finally, SC fusion was determined using the Taxonomy tool in NIS-Elements to classify nuclei as either internal or external to the myotubes and calculated as a proportion of internal to total nuclei. The density of cells expressing Pax7 was also determined.

## 2.6 Statistical analysis

MRF heterogeneity and apoptosis data during proliferation were analyzed by time point, and doubling time, myotube characteristics, and fusion data were analyzed as a one-way analysis of variance using the generalized linear mixed model GLIMMIX procedure in SAS version 9.4 (PC version 9.4, SAS Inst. Inc., Cary, NC, United States). Culture temperature was the main effect. Culture well ($n$ = 9 per treatment, assay, and time point) served as the experimental unit. The PDIFF option in SAS was used to perform all possible pairwise least square mean comparisons at $p < 0.05$. The Satterthwaite adjustment was used to correct the degrees of freedom. Proportional data were analyzed using the events/experiments syntax with a binomial distribution, and both continuous and proportional data were analyzed using an R-side covariance structure. Significant differences were declared when $p \leq 0.05$ and tendencies when $0.0501 \leq p \leq 0.10$.

# 3 Results

## 3.1 Proliferation

Heterogeneity of Pax7+:MyoD-, Pax7-:MyoD+, and Pax7+:MyoD+ SC populations after 48, 72, and 96 h in culture are reported in Table 1.

10.3389/fphys.2023.1288809

**TABLE 1 Effect of culture temperature on myogenic regulatory factor heterogeneity during proliferation of primary broiler chicken *pectoralis major* satellite cells.**

| Cell population[1] | Time post-plating, h | | | | | | | | | | | |
|---|---|---|---|---|---|---|---|---|---|---|---|---|
| | 48 | | | | 72 | | | | 96 | | | |
| | Temperature, °C | | SEM[2] | *p*-value | Temperature, °C | | SEM | *p*-value | Temperature, °C | | SEM | *p*-value |
| | 38 | 41 | | | 38 | 41 | | | 38 | 41 | | |
| Density, cells per mm$^2$ | | | | | | | | | | | | |
| Pax7+:MvoD- | 4 | 3 | 0 | 0.4818 | 11 | 12 | 1 | 0.3063 | 23$^a$ | 14$^b$ | 2 | 0.0008 |
| Pax7-:MyoD+ | 25$^b$ | 37$^a$ | 3 | 0.0078 | 77$^b$ | 114$^a$ | 11 | 0.0204 | 99$^b$ | 152$^a$ | 12 | 0.0029 |
| Pax7+:MyoD+ | 77$^a$ | 53$^b$ | 5 | 0.0006 | 115 | 108 | 11 | 0.6747 | 184$^a$ | 117$^b$ | 15 | 0.0016 |
| MRF+ | 106 | 93 | 7 | 0.2119 | 202 | 235 | 22 | 0.3117 | 307 | 284 | 26 | 0.5292 |
| Total nuclei | 121 | 108 | 8 | 0.2602 | 221 | 264 | 24 | 0.2041 | 356 | 378 | 30 | 0.6003 |
| Relative density, % of total nuclei | | | | | | | | | | | | |
| Pax7+:MvoD- | 2.99 | 2.95 | 0.35 | 0.9387 | 4.86 | 4.71 | 0.37 | 0.7533 | 6.60$^a$ | 3.81$^b$ | 0.27 | <0.0001 |
| Pax7-:MyoD+ | 21.04$^b$ | 34.25$^a$ | 1.35 | <0.000 | 34.66$^b$ | 43.23$^a$ | 1.40 | <0.0001 | 27.89$^b$ | 40.24$^a$ | 1.52 | <0.0001 |
| Pax7+:MyoD+ | 64.03[1] | 49.47$^b$ | 1.40 | <0.000 | 51.89$^a$ | 40.96$^b$ | 1.32 | <0.0001 | 51.83$^a$ | 31.08$^b$ | 1.68 | <0.0001 |
| MRF+ | 87.96 | 86.57 | 0.92 | 0.2656 | 91.47$^a$ | 88.88$^b$ | 0.83 | 0.0304 | 86.3$^a$ | 75.12$^b$ | 1.68 | <0.0001 |

[1]Total nuclei describes every nuclei expressing the 4′,6-diamidino-2-phenylindole counterstain regardless of the status of other target proteins; MRF+ describes a combination of cells positive for Pax7, MyoD, or both Pax7 and MyoD.
[2]SEM = highest standard error of the pairwise mean comparisons.
[a,b]Means within the same row with different superscripts differ $p \leq 0.05$.

The density of total nuclei in the cultures was similar among temperatures at every time point ($p \geq 0.2041$; Table 1). After 48 h in culture, 41°C conditions increased the density of Pax7-:MyoD+ ($p = 0.0078$; Table 1) and reduced the density of Pax7+:MyoD+ populations per mm$^2$ ($p = 0.0006$; Table 1), which was reflected in the proportional data. After 72 h, only the density of the Pax7-:MyoD+ population was increased in wells cultured at 41°C per mm$^2$ ($p = 0.0204$; Table 1), and the relative densities of Pax7-:MyoD+, Pax7+:MyoD+, and MRF + populations were altered by temperature ($p \leq 0.0304$; Table 1). The heterogeneity of proliferative SC populations was the most impacted by temperature after 96 h, where increasing to physiological temperature reduced the density of Pax7+:MyoD- and Pax7+:MyoD+ cells ($p \leq 0.0016$; Table 1) and increased the density of Pax7-:MyoD+ cells by approximately 150% ($p < 0.0001$; Table 1). Diminished Pax7+ expression at 41°C after 96 h is shown in Figure 1. At 96 h, the relative densities as a proportion of the total nuclei of all populations quantified were altered by temperature ($p < 0.0001$; Table 1). The MRF heterogeneity of SC populations was altered over time in culture (Figure 2). Across all time points, the density of MRF+ nuclei as well as total nuclei was similar across treatments ($p > 0.5292$; Table 1). Finally, the doubling time of all populations measured was not impacted by culture temperature ($p > 0.1148$; Table 2).

## 3.2 Apoptosis

Cell apoptosis was measured during proliferation time points (48, 72, and 96 h post-plating) using a TUNEL assay to detect the presence of double-stranded DNA breaks that are characteristic of cells undergoing apoptosis. The results of this assay are shown in Table 3. Representative images showing a TUNEL-positive cell accompanied by images of positive control cells treated with DNase I are shown in Figure 3. The number of apoptotic cells per mm$^2$ increased when cultured at 41°C after 48 and 96 h in culture compared with 38°C ($p \leq 0.0491$; Table 3). In addition, 41°C incubation consistently increased the relative density of apoptotic cells ($p \leq 0.0302$; Table 3) and diminished the relative density of normal cells ($p \leq 0.0273$; Table 3) as a proportion of total nuclei at 48, 72, and 96 h post-plating. Regardless of treatment, apoptosis numerically reduced over time in culture from 48 to 96 h.

## 3.3 Differentiation

SC differentiation was measured by visualizing MHC expression to determine the formation of myotubes in culture. DAPI+ nuclei that were inside the MHC boundaries were considered internal or fused cells, and those that were not overlapping with MHC were considered external or unfused cells. The expression of Pax7 was also determined. The percentage of fused myonuclei was greater in primary cultures grown at 38°C ($p < 0.0001$; Table 4). Interestingly, when internal nuclei were expressed on a mm$^2$ basis, the density of fused nuclei was similar among treatments ($p = 0.7551$; Figure 4). The difference in fusion percentage appears to originate from a greater density of external nuclei at 41°C ($p < 0.0001$; Table 4), which was more than double the external nuclei present in cultures at 38°C. The density and proportion of Pax7+ SC populations were increased at 38°C ($p < 0.0001$; Table 4). The width

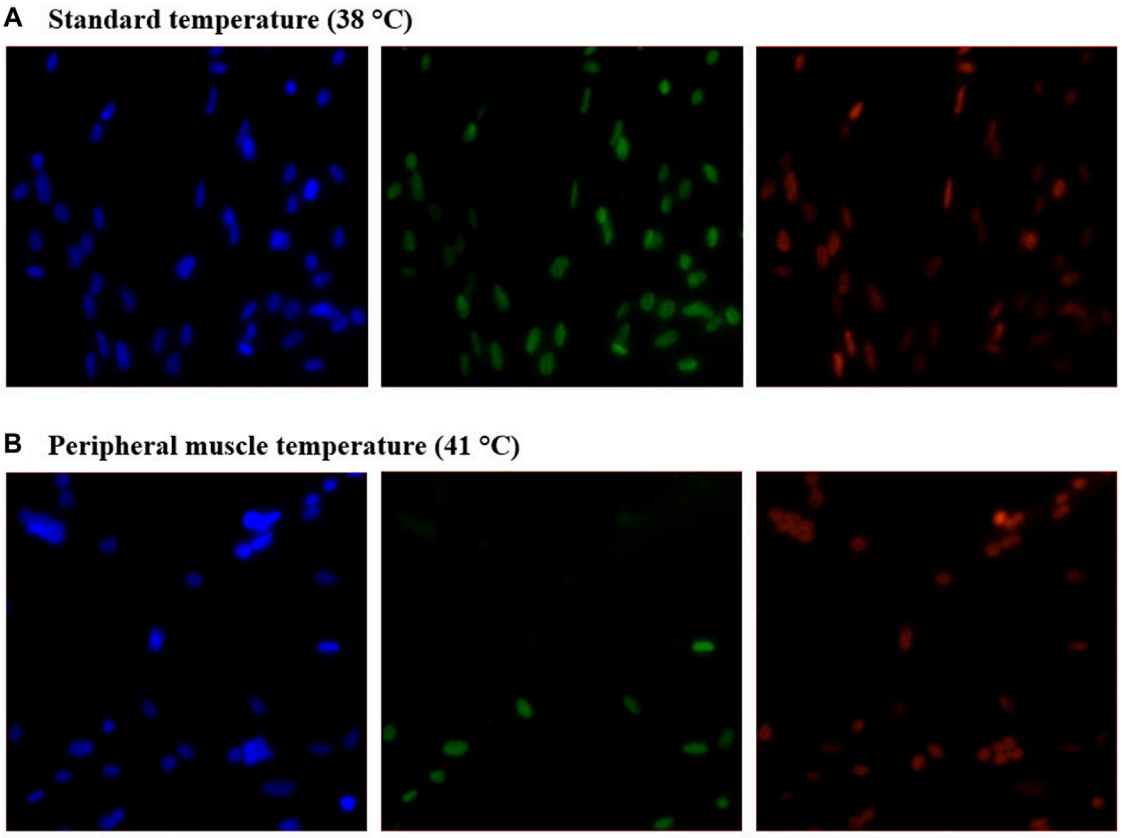


FIGURE 1
Effect of culture temperature on myogenic regulatory factor expression in primary broiler chicken *pectoralis major* satellite cell cultures after 96 h. Representative inverted fluorescence images of 4′,6-diamidino-2-phenylindole-stained nuclei (blue; left) and Pax7 (green; center) and MyoD (red; right) protein expression in cultures grown at 38°C **(A)** or 41°C **(B)**.

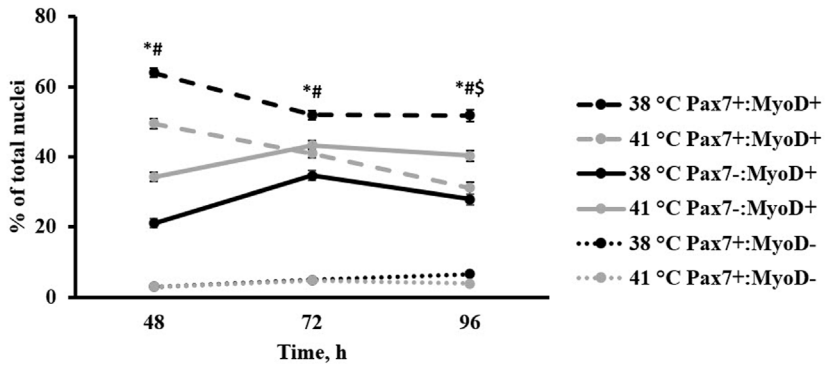


FIGURE 2
Effect of culture temperature on primary broiler chicken *pectoralis major* satellite cell myogenic regulatory factor heterogeneity over time. $n$ = 9 wells per treatment of either 38 or 41°C incubation were immunofluorescence-stained to detect Pax7 and MyoD expression at 48, 72, and 96 h post-plating. Populations are presented as a percentage of total nuclei. Total nuclei describes every nucleus expressing the 4′,6-diamidino-2-phenylindole counterstain regardless of the status of other target proteins. Error bars represent the highest standard error of the pairwise mean comparison. Least square means accompanied by a * signify that the proportion of Pax7+:MyoD+ cells differs ($p < 0.05$) between 38°C and 41°C, # signify that the proportion of Pax7-:MyoD+ cells differs ($p < 0.05$) between 38°C and 41°C, and $ signify that the proportion of Pax7+:MyoD- cells differs ($p < 0.05$) between 38°C and 41°C.

**TABLE 2 Effect of culture temperature on population doubling time from 48 to 96 h post-plating of primary broiler chicken *pectoralis major* satellite cells.**

| Cell population | Temperature, ˚C | | SEM[1] | *p*-value |
|---|---|---|---|---|
| | 38 | 41 | | |
| Population doubling time, h | | | | |
| Pax7+:MyoD- | 24.28 | 31.08 | 31.08 | 0.5284 |
| Pax7-:MyoD+ | 29.97 | 23.69 | 4.58 | 0.3466 |
| Pax7+:MyoD+ | 45.16 | 58.46 | 7.30 | 0.2156 |
| MRF+ | 34.00 | 31.98 | 2.25 | 0.5347 |
| Total nuclei | 32.17 | 28.09 | 1.73 | 0.1148 |

[1]SEM = highest standard error of the pairwise mean comparisons.

of all myotubes was measured at the widest section of each myotube, and every new branch was considered its own myotube. Representative IF images of myotubes can be visualized in Figure 5. While the number of myotubes per mm$^2$ was similar ($p$ = 0.6111; Table 4), 41˚C conditions tended to result in thinner myotubes ($p$ = 0.0736; Table 4) that covered less total area of the culture well ($p$ = 0.0806; Table 4). Myotubes appeared to be more consistent in width when cultured at 41˚C and had a lower standard deviation ($p$ = 0.0174; Table 4), but differences in the coefficient of variation among widths were not detected ($p$ = 0.5248; Table 4).

# 4 Discussion

Alterations to the MRF heterogeneity of SC populations at 48, 72, and 96 h post-plating indicate an overall shift in proliferative myogenic cell activity as culture temperature changes. While the MRF Pax7 and MyoD are both generally considered to be expressed during myoblast proliferation (Cornelison and Wold, 1997; Bentzinger et al., 2012), Pax7 expression is associated with primitive SC populations during early activation (Seale et al., 2000). MyoD expression is upregulated as the cell progresses toward commitment to the myogenic fate (Berkes and Tapscott, 2005) and appears to be required for differentiation, serving as the molecular switch from proliferation to differentiation (Cornelison et al., 2000). Based on the increased presence of Pax7+:MyoD- cells when culturing at 38˚C during both proliferation and differentiation assays, this temperature may better retain a robust Pax7+:MyoD population or a population of SC either in the early stages of myogenesis or undergoing self-renewal. Based on the results of the differentiation assay, the observed increase in Pax7 expression at 38˚C continued to 168 h post-plating. Culturing at 41˚C advanced cells through the myogenic program faster as the presence of cells expressing MyoD was enhanced at that temperature (Figure 2). These data suggest that culturing primary broiler SC at physiological muscle temperature promoted a more rapid progression toward myogenic differentiation. However, in disagreement with the original hypothesis, total cell proliferation did not appear to be impacted by these culture temperatures as the densities of total nuclei and nuclei expressing one or more MRF remained similar over time. This was also reflected by similarities in the doubling time of all populations measured among temperatures between 48 and 96 h. It should be noted that proliferative capability was not altered during the proliferation time points between 48 and 96˚h, but total nuclei was distinctly increased at 168 h post-plating at 41˚C. This could mean proliferation was impacted by temperature but occurring later than expected, thus warranting further analysis in the future. Hayashi and Yonekura (2019) reported an increase in the differentiation of C2C12 mouse myoblasts with a 2˚C increase in culture temperature above physiological temperature with thermal stimulation at later time points compared with higher temperature during the first few days of culture only. This suggests a temporal component to the impact of temperature on myogenic cells and may help explain the increase in nuclei in cultures that occurred between 96 and 168 h observed here.

Given that the peripheral muscle temperature of the PM harvested for the primary cultures utilized in this experiment was 41˚C, it was

**TABLE 3 Effect of culture temperature on apoptosis during proliferation of primary broiler chicken *pectoralis major* satellite cells.**

| Cell population[1] | Time post-plating, h | | | | | | | | | | | |
|---|---|---|---|---|---|---|---|---|---|---|---|---|
| | 48 | | | | 72 | | | | 96 | | | |
| | Temperature, ˚C | | SEM[2] | *p*-value | Temperature, ˚C | | SEM | *p*-value | Temperature, ˚C | | SEM | *p*-value |
| | 38 | 41 | | | 38 | 41 | | | 38 | 41 | | |
| Density, cells per mm$^2$ | | | | | | | | | | | | |
| Normal | 97 | 92 | 8 | 0.6431 | 248 | 226 | 18 | 0.3804 | 368 | 342 | 29 | 0.5401 |
| Apoptotic | 7$^b$ | 10$^a$ | 1 | 0.0491 | 11 | 13 | 1 | 0.1713 | 10$^b$ | 13$^a$ | 1 | 0.0255 |
| Relative density, % of total nuclei | | | | | | | | | | | | |
| Normal | 93.23$^a$ | 90.60$^b$ | 0.69 | 0.0045 | 95.92$^a$ | 94.64$^b$ | 0.45 | 0.0302 | 97.45$^a$ | 96.27$^b$ | 0.30 | 0.0030 |
| Apoptotic | 6.79$^a$ | 9.36$^b$ | 0.68 | 0.0051 | 4.08$^b$ | 5.39$^a$ | 0.45 | 0.0273 | 2.54$^b$ | 3.76 | 0.31 | 0.0026 |

[1]Total nuclei describes every nuclei expressing the 4′,6-diamidino-2-phenylindole counterstain regardless of the cell status; normal describes nuclei not indicating double-stranded DNA breaks; apoptotic describes nuclei that were fluorescent under the TUNEL assay to denote apoptosis.
[2]SEM = highest standard error of the pairwise mean comparisons.
[a,b]Means within the same row with different superscripts differ $p \leq 0.05$.

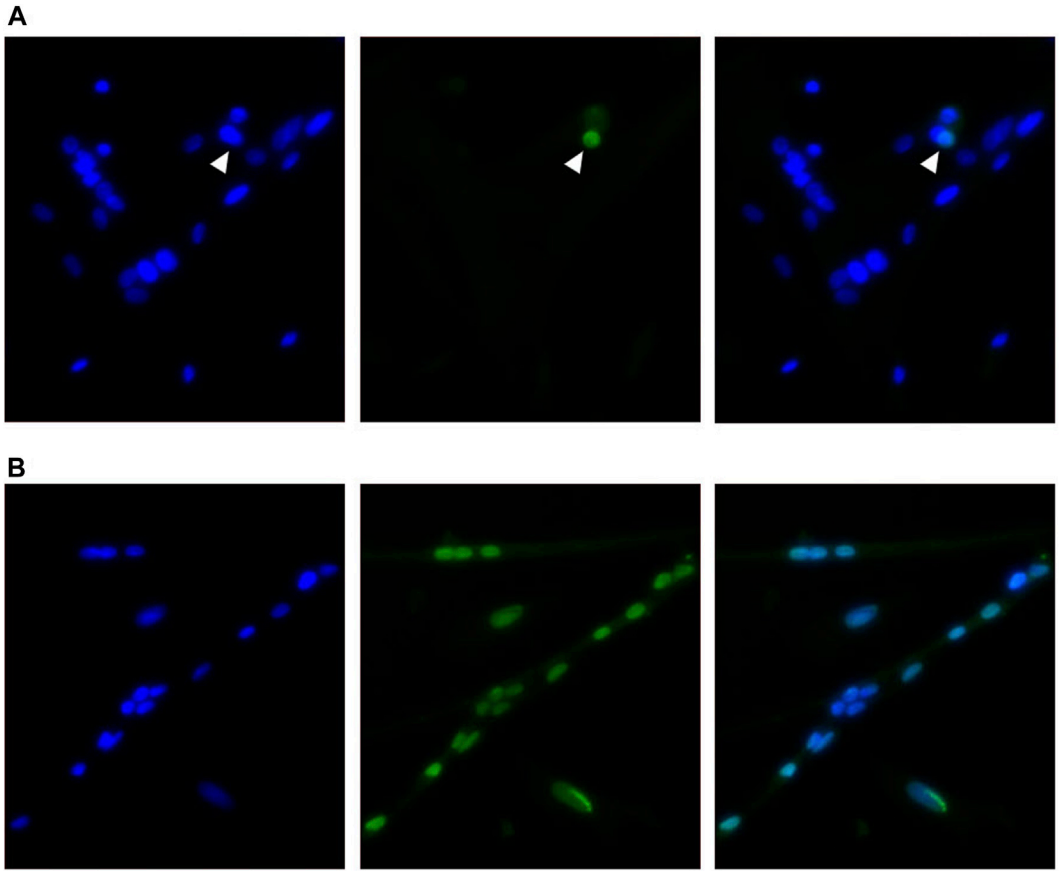


FIGURE 3
Representative inverted fluorescence images showing a TUNEL-positive nuclei indicated with an arrow among normal nuclei **(A)** in primary broiler *pectoralis major* satellite cell cultures with a corresponding positive control image **(B)** after DNase I treatment. Images show 4′,6-diamidino-2-phenylindole-stained nuclei (blue; left), TUNEL assay (green; center), and merged channels (right).

hypothesized that culturing the cells at 41°C would better support proliferation and differentiation than the standard 38°C culture temperature since the increased temperature better replicates physiological conditions. This hypothesis was formulated based on observations by Harding et al. (2016) who reported increased DNA and creatine kinase content in broiler SC cultured at 43°C compared with a 38°C control temperature, indicating that increasing culture temperature improves cell proliferation and differentiation. These results were mirrored by a similar study with SC isolated from turkey PM that found that increasing culture temperature from 38°C to 41°C increased DNA content as well as resulted in the formation of wider myotubes (Clark et al., 2016). Furthermore, Xu et al. (2021) also reported increased proliferation and differentiation of turkey SC, but they also highlighted elevated gene expression of MyoD with increased culture temperature, which was consistent with observations from the present study. Researchers have previously attempted to relate the impact of elevated culture temperature on broiler SC to the impact of heat stress on muscle growth in the bird, yet the culture conditions they consider to be thermal stress may be better replicating the normal, physiological SC environment.

The results obtained from the present experiment appear to contradict the past literature as well as lead to a partial rejection of the original hypothesis as total cell proliferation was not impacted by temperature between the typical proliferation time points of 48 and 96 h post-plating, but MRF expression and fusion percentage were altered. One potential reason for the discrepancy between the results of this experiment and those reported previously may be the genetic difference between the cells from donor birds in the previous studies compared with cells from modern broilers presented here. Given that cells used for previously mentioned experiments originated from broilers and turkeys over two decades ago (McFarland et al., 1997; Velleman et al., 2000), it is possible that the rigorous selection pressure on increasing PM yield has altered the SC populations in modern broilers and turkeys since then. It has been demonstrated that the heat production of broilers has changed over time, as demonstrated by increasing heat production in modern *ad libitum*-fed broiler breeder hens compared with earlier genetic lines (Carney et al., 2022), and this may contribute to SC populations in modern broilers responding differently to temperature than their predecessor strains as the cellular environment and metabolism of the muscle evolve. The previous *in vitro* work was also conducted using SC after multiple passages, which would result in a highly selected population of SC that are less representative of the resident SC population *in vivo*. In addition, donor bird age may

**TABLE 4 Effect of culture temperature on myonuclear fusion and myotube characteristics of primary broiler chicken *pectoralis major* satellite cells after 168 h in culture.**

| Variable[1] | Temperature, °C | | SEM[2] | *p*-value |
|---|---|---|---|---|
| | 38 | 41 | | |
| Nuclei per mm$^2$ | 1272$^b$ | 2017$^a$ | 153 | 0.0009 |
| Internal per mm$^2$ | 819 | 860 | 94 | 0.7551 |
| External per mm$^2$ | 453$^b$ | 1156$^a$ | 91 | <0.0001 |
| Pax7+ per mm$^2$ | 398$^a$ | 144$^b$ | 33 | <0.0001 |
| Pax7+, % of total nuclei | 31.32$^a$ | 7.15$^b$ | 1.89 | <0.0001 |
| Fusion, % of total nuclei | 64.37$^a$ | 42.66$^b$ | 2.72 | <0.0001 |
| Number of myotubes per mm$^2$ | 64 | 67 | 3 | 0.6111 |
| Average myotube width, µm | 32$^x$ | 24$^y$ | 3 | 0.0736 |
| Myotube width standard deviation, µm | 32$^a$ | 18$^b$ | 4 | 0.0174 |
| Myotube width coefficient of variation, % | 75.09 | 72.27 | 3.31 | 0.5248 |
| Myotube area, % | 41.59$^x$ | 33.58$^y$ | 3.22 | 0.0806 |

[1]Total nuclei describes every nucleus expressing the 4′,6-diamidino-2-phenylindole counterstain regardless of the status of other target proteins; internal nuclei were located within an area expressing the myosin heavy chain (MHC) protein; external nuclei did not overlap with MHC expression; myotube width was measured at the widest section of every new myotube branch as denoted by MHC expression; myotube area denotes the proportion of the culture well expressing MHC.
[2]SEM = highest standard error of the pairwise mean comparisons.
[a,b]Means within the same row with different superscripts differ $p \leq 0.05$.
[x,y]Means within the same row with different superscripts describe a tendency $0.10 > p < 0.05$.

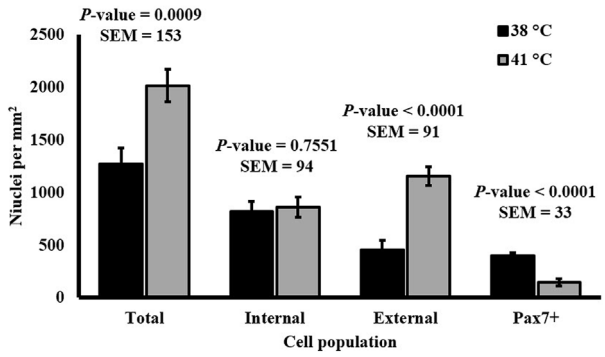


FIGURE 4
Effect of culture temperature on the density of nuclei relative to myotubes in primary broiler chicken *pectoralis major* satellite cell cultures after 168 h. *n* = 9 wells per treatment of either 38°C or 41°C incubation were immunofluorescence-stained to detect Pax7 and myosin heavy chain (MHC) expression. Total nuclei describes every nucleus expressing the 4′,6-diamidino-2-phenylindole counterstain regardless of the status of other target proteins; internal nuclei were located within an area expressing MHC protein; external nuclei did not overlap with MHC expression. Error bars represent the highest standard error of the pairwise mean comparison. [a,b]Bars with different superscripts within a cell population differ $p \leq 0.05$.

also impact how cells respond to temperature and aid in explaining the inconsistency in findings. Sarais et al. (2023) reported that the gene expression of SC from younger pigs with an undeveloped thermoregulation capacity responded to heat and cold stress *in vitro* differently than their older, developed counterparts. Therefore, the age of donor broilers and their capability to thermoregulate may also impact how SC function when cultured in different temperature environments.

Apoptosis was also evaluated at these time points and appeared to increase in cells cultured at a higher temperature. These results are in agreement with previous literature that found increased markers of apoptosis in cultured chicken SC at 41°C compared with 37°C (Siddiqui et al., 2020b) and at 43°C compared with 38°C (Harding et al., 2015). However, the proportion of apoptotic cells observed was overall higher than expected, which may be attributed to the use of freshly isolated (i.e., non-passaged) primary cultures that underwent minimal purification or selection apart from density gradient centrifugation. The TUNEL assay in the present study was conducted on parallel plates separate from MRF evaluation, so it was unfortunately impossible to determine whether apoptotic cells were also expressing myogenic markers and the exact cell populations more affected by apoptosis in the primary culture may be different than the proliferative SC populations of interest. The increase in apoptosis observed during proliferation time points was likely not detrimental for primary broiler SC at 41°C as total cells per mm$^2$ were increased by 168 h post-plating in cultures grown at a higher temperature. Analysis of cell death during differentiation time points at these culture temperatures should be conducted to aid in understanding this observation.

Observing a similar density of fused cells across temperature treatments indicates a similar SC fusion capacity (Figure 4). The substantial difference in the densities of unfused cells raises questions about the identity of external cell populations. Culturing at 41°C may increase the proliferation of alternative cell populations without impacting the extent of SC fusion. It is impossible to determine whether all external cells were myogenic in nature as only the expression of Pax7 was assessed, and evaluating a more complete MRF panel would be needed. However, the relative density of cells

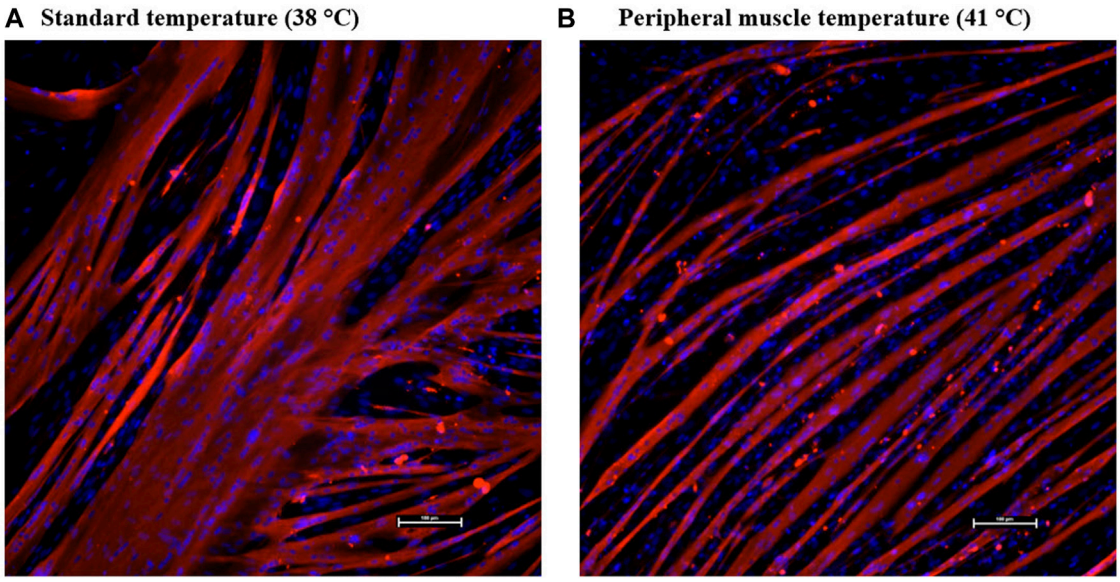


FIGURE 5
Effect of culture temperature on myotube formation in primary broiler chicken *pectoralis major* satellite cell cultures after 168 h. Representative inverted fluorescence images at ×200 magnification of myosin heavy chain-defined myotubes (red) and 4′,6-diamidino-2-phenylindole-stained nuclei (blue) in cultures grown at 38°C **(A)** or 41°C **(B)**. The scale bar depicts 100 μm.

expressing Pax7 was diminished at 41°C, indicating a reduction in primitive SC populations. It is possible that the unfused cell populations were myogenic in nature and capable of proliferation, but the increased temperature had prevented myotube fusion. It is also possible that these cells were non-myogenic populations like fibro/adipogenic progenitors, as primary muscle cultures likely contain non-myogenic progenitor populations. This is supported by a previous study comparing 37°C–41°C culture temperature on broiler fibroblasts that observed greater fibroblast proliferation at 41°C based on cell cycle analysis (Siddiqui et al., 2020a) and observations of improved chicken fibroblast *in vitro* adherence at 41°C (Kim et al., 2022). The external cells in the present study may have also been adipogenic in nature, as Harding et al. (2015) observed increased expression of adipogenic genes in broiler SC cultures grown at higher temperatures. This may be further supported by observations of diminished myofiber diameter and increased lipid content in cultured SC isolated from young broilers reared under continuous heat stress conditions compared with commercial conditions (Piestun et al., 2017). Further investigation is needed to characterize the identity and lineage of all progenitor cell types present in primary broiler PM cultures in response to altering temperatures.

Visually, myotubes cultured at physiological muscle temperature were formed and arranged differently than those at the standard lower temperature. The representative images in Figure 5 display a more regular alignment of thinner myotubes at 41°C, while those at the standard lower temperature appeared to be thicker and more variable. This was confirmed by quantifying myotube width and area. Myotubes at 41°C tended to be thinner and more consistent in shape and size than those cultured at 38°C. The lower culture temperature appeared to produce thicker myotubes that take up more total area of the culture well. The appearance of larger myotubes may explain the use of a temperature that is lower than the physiological culture temperature in previous literature, as thicker myotubes may be perceived as more desirable for *in vitro* experiments. With the retention of a robust Pax7+:MyoD- population and genesis of thicker myotubes promoting the fusion of a greater proportion of cells present, SC cultured at a lower temperature appeared to retain a more primitive status for longer, thus better replicating embryonic myogenesis (Sieiro-Mosti et al., 2014) despite being isolated from post-hatch broilers. The industry standard temperature for broiler egg incubation is typically 37.5°C. This has been shown to result in eggshell temperatures between 38°C and 39°C that were strongly correlated with embryo temperatures during later stages of incubation (Agyekum et al., 2022) and embryo temperatures between 37.5°C and 38°C during earlier stages (Tejeda et al., 2021). It has been previously established that the proliferation capacity of SC is greater in younger animals (Schultz and Lipton, 1982), and these results may reveal that placing SC from mature muscle into an embryonic-simulating environment enhanced the population of cells expressing transcription factors indicative of early proliferation. Moreover, these *in vitro* observations may serve to highlight and explain changes in broiler muscle growth following thermal manipulations during embryogenesis.

The results of embryonic thermal manipulation on post-hatch broiler performance are not consistent in the current literature. During the early stages of embryogenesis, increasing incubation temperature above the industry standard did not alter broiler body weight and breast yield in one study (Wall et al., 2022) but increased body weight and breast yield of similarly aged broilers in another (Janisch et al., 2015). While increasing temperature during incubation during late-stage development has been found to reduce broiler body weight (Piestun et al., 2008; Piestun et al., 2015), increased temperature on embryonic days 16–18 has also been observed to improve the reservoir of myogenic cells, increasing Pax7 expression and PM yield (Piestun et al., 2009). A high eggshell temperature during development

has also been found to improve breast meat yield without impacting the overall growth performance (Molenaar et al., 2011). These data support the theory that pre-hatch thermal manipulation can alter muscle growth as increased temperature *in vitro* impacted broiler SC heterogeneity and myotube characteristics. The tendency for a reduction in myotube width with a similar density of fused nuclei when culturing at a higher temperature (Table 4; Figure 4) suggests that temperature may impact the density of myonuclei per fiber. When applied *in vivo*, these potential changes could lead to long-term alterations in mature muscle hypertrophy. Previously, thermal manipulation during critical points in myogenesis was found to increase the total muscle fiber number in turkeys (Maltby et al., 2004), and increasing temperature of cultured bovine SC altered myosin heavy chain isoform expression, implying that temperature may also alter the fiber type during development (Kim and Kim, 2023). Differences in myotube width observed in the present study may help understand how increased temperature during embryonic myogenesis changes SC differentiation patterns that could lead to increased fiber number. Further investigation to elucidate the mechanisms through which temperature impacts broiler PM SC function is warranted.

In conclusion, incubation of primary broiler chicken PM SC at 38°C and 41°C impacted MRF heterogeneity and myotube formation. Previous literature evaluating the impact of culturing broiler SC at temperatures above 38°C referred to elevated temperatures as thermal stress conditions and attempted to relate this to potential impacts of heat stress in post-hatch broiler muscle (Harding et al., 2015; Harding et al., 2016; Siddiqui et al., 2020b). However, a culture temperature closer to 41°C may better replicate the physiological environment of broiler SC, which stresses the importance of avoiding misrepresentations of *in vitro* experimental results when applying conclusions back to *in vivo* myogenesis. Furthermore, the observed shift in SC heterogeneity and changes in myotube characteristics may help understand the mechanism through which thermal manipulation during embryonic myogenesis can influence broiler muscle yield.

## Data availability statement

The raw data supporting the conclusion of this article will be made available by the authors, without undue reservation.

## Ethics statement

The animal study was approved by the Auburn University Institutional Animal Care and Use Committee. The study was conducted in accordance with the local legislation and institutional requirements.

## Author contributions

CG: data curation, formal analysis, investigation, writing–original draft, and writing–review and editing. BH: investigation and writing–review and editing. JF: investigation, methodology, and writing–review and editing. CS: funding acquisition, investigation, resources, supervision, and writing–review and editing. JS: conceptualization, funding acquisition, investigation, methodology, project administration, resources, supervision, and writing–review and editing.

## Funding

The authors declare that financial support was received for the research, authorship, and/or publication of this article. This work was supported by the United States Department of Agriculture National Institute of Food and Agriculture (USDA-NIFA) Competitive Grant Nos 2018-67017-27556 and 2020-67015-30824 awarded to JS, the USDA Hatch Program funds, and the Alabama Agricultural Experiment Station.

## Acknowledgments

The sarcomeric myosin (MF20) and Pax7 (PAX7) antibody hybridoma cell lines developed by D. A. Fischman and A. Kawakami, respectively, were obtained from the Developmental Studies Hybridoma Bank, created by the NICHD of the NIH and maintained at The University of Iowa, Department of Biology, Iowa City, IA, United States.

## Conflict of interest

The authors declare that the research was conducted in the absence of any commercial or financial relationships that could be construed as a potential conflict of interest.

## Publisher's note



## References

Agyekum, G., Okai, M. A., Tona, J. K., Donkoh, A., and Hamidu, J. A. (2022). Impact of incubation temperature profile on chick quality, bone, and immune system during the late period of incubation of Cobb 500 broiler strain. *Poult. Sci.* 101 (9), 101999. doi:10.1016/j.psj.2022.101999

Bentzinger, C. F., Wang, Y. X., and Rudnicki, M. A. (2012). Building muscle: molecular regulation of myogenesis. *Cold Spring Harb. Perspect. Biol.* 4 (2), a008342. doi:10.1101/cshperspect.a008342

Berkes, C. A., and Tapscott, S. J. (2005). MyoD and the transcriptional control of myogenesis. *Semin. Cell Dev. Biol.* 16 (4-5), 585–595. doi:10.1016/j.semcdb.2005.07.006

Bischoff, R. (1986). Proliferation of muscle satellite cells on intact myofibers in culture. *Dev. Biol.* 115 (1), 129–139. doi:10.1016/0012-1606(86)90234-4

Carney, V. L., Anthony, N. B., Robinson, F. E., Reimer, B. L., Korver, D. R., Zuidhof, M. J., et al. (2022). Evolution of maternal feed restriction practices over 60 years of selection for broiler productivity. *Poult. Sci.* 101 (10), 101957. doi:10.1016/j.psj.2022.101957

Clark, D. L., Coy, C. S., Strasburg, G. M., Reed, K. M., and Velleman, S. G. (2016). Temperature effect on proliferation and differentiation of satellite cells from turkeys with different growth rates. *Poult. Sci.* 95 (4), 934–947. doi:10.3382/ps/pev437

Cornelison, D., Olwin, B. B., Rudnicki, M. A., and Wold, B. J. (2000). MyoD−/− satellite cells in single-fiber culture are differentiation defective and MRF4 deficient. *Dev. Biol.* 224 (2), 122–137. doi:10.1006/dbio.2000.9682

Cornelison, D., and Wold, B. J. (1997). Single-cell analysis of regulatory gene expression in quiescent and activated mouse skeletal muscle satellite cells. *Dev. Biol.* 191 (2), 270–283. doi:10.1006/dbio.1997.8721

Day, K., Shefer, G., Richardson, J. B., Enikolopov, G., and Yablonka-Reuveni, Z. (2007). Nestin-GFP reporter expression defines the quiescent state of skeletal muscle satellite cells. *cells. Dev. Biol.* 304 (1), 246–259. doi:10.1016/j.ydbio.2006.12.026

Flees, J. J., Starkey, C. W., and Starkey, J. D. (2022). Effect of different basal culture media and sera type combinations on primary broiler chicken muscle satellite cell heterogeneity during proliferation and differentiation. *Animals (Basel)* 12 (11). doi:10.3390/ani12111425

Ferreira, T. Z., Kindlein, L., Flees, J. J., Shortnacy, L. K., Vieira, S. L., Nascimento, V. P., et al. (2020). Characterization of Pectoralis major muscle satellite cell population heterogeneity, macrophage density, and collagen infiltration in broiler chickens affected by Wooden Breast. *Front. Physiol.* 11, 529. doi:10.3389/fphys.2020.00529

Geiger, A. E., Daughtry, M. R., Gow, C. M., Siegel, P. B., Shi, H., and Gerrard, D. E. (2018). Long-term selection of chickens for body weight alters muscle satellite cell behaviors. *Poult. Sci.* 97 (7), 2557–2567. doi:10.3382/ps/pey050

Giloh, M., Shinder, D., and Yahav, S. (2012). Skin surface temperature of broiler chickens is correlated to body core temperature and is indicative of their thermoregulatory status. *Poult. Sci.* 91 (1), 175–188. doi:10.3382/ps.2011-01497

Halevy, O., Piestun, Y., Allouh, M. Z., Rosser, B. W., Rinkevich, Y., Reshef, R., et al. (2004). Pattern of Pax7 expression during myogenesis in the posthatch chicken establishes a model for satellite cell differentiation and renewal. *Dev. Dyn.* 231 (3), 489–502. doi:10.1002/dvdy.20151

Hall, Z. W., and Ralston, E. (1989). Nuclear domains in muscle cells. *Cell* 59 (5), 771–772. doi:10.1016/0092-8674(89)90597-7

Harding, R. L., Clark, D. L., Halevy, O., Coy, C. S., Yahav, S., and Velleman, S. G. (2015). The effect of temperature on apoptosis and adipogenesis on skeletal muscle satellite cells derived from different muscle types. *Physiol. Rep.* 3 (9), e12539. doi:10.14814/phy2.12539

Harding, R. L., Halevy, O., Yahav, S., and Velleman, S. G. (2016). The effect of temperature on proliferation and differentiation of chicken skeletal muscle satellite cells isolated from different muscle types. *Physiol. Rep.* 4 (8), e12770. doi:10.14814/phy2.12770

Hayashi, S., and Yonekura, S. (2019). Thermal stimulation at 39°C facilitates the fusion and elongation of C2C12 myoblasts. *Anim. Sci. J.* 90 (8), 1008–1017. doi:10.1111/asj.13227

Janisch, S., Sharifi, A. R., Wicke, M., and Krischek, C. (2015). Changing the incubation temperature during embryonic myogenesis influences the weight performance and meat quality of male and female broilers. *Poult. Sci.* 94 (10), 2581–2588. doi:10.3382/ps/pev239

Kim, S. H., Kim, C. J., Lee, E. Y., Son, Y. M., Hwang, Y. H., and Joo, S. T. (2022). Optimal pre-plating method of chicken satellite cells for cultured meat production. *Food Sci. Anim. Resour.* 42 (6), 942–952. doi:10.5851/kosfa.2022.e61

Kim, W. S., and Kim, J. (2023). Exploring the impact of temporal heat stress on skeletal muscle hypertrophy in bovine myocytes. *J. Therm. Biol.* 117, 103684. doi:10.1016/j.jtherbio.2023.103684

Li, J., Gonzalez, J. M., Walker, D. K., Hersom, M. J., Ealy, A. D., and Johnson, S. E. (2011). Evidence of heterogeneity within bovine satellite cells isolated from young and adult animals. *J. Anim. Sci.* 89 (6), 1751–1757. doi:10.2527/jas.2010-3568

Maltby, V., Somaiya, A., French, N. A., and Stickland, N. C. (2004). In ovo temperature manipulation influences post-hatch muscle growth in the Turkey. *Br. Poult. Sci.* 45 (4), 491–498. doi:10.1080/00071660412331286190

Matsuda, R., Spector, D. H., and Strohman, R. C. (1983). Regenerating adult chicken skeletal muscle and satellite cell cultures express embryonic patterns of myosin and tropomyosin isoforms. *Dev. Biol.* 100 (2), 478–488. doi:10.1016/0012-1606(83)90240-3

McFarland, D. C., Gilkerson, K. K., Pesall, J. E., Ferrin, N. H., and Wellenreiter, R. H. (1997). *In vitro* characteristics of myogenic satellite cells derived from the pectoralis major and biceps femoris muscles of the chicken. *Cytobios* 91 (364), 45–52.

Molenaar, R., Hulet, R., Meijerhof, R., Maatjens, C. M., Kemp, B., and van den Brand, H. (2011). High eggshell temperatures during incubation decrease growth performance and increase the incidence of ascites in broiler chickens. *Poult. Sci.* 90 (3), 624–632. doi:10.3382/ps.2010-00970

Murphy, M. M., Lawson, J. A., Mathew, S. J., Hutcheson, D. A., and Kardon, G. (2011). Satellite cells, connective tissue fibroblasts and their interactions are crucial for muscle regeneration. *Development* 138 (17), 3625–3637. doi:10.1242/dev.064162

Park, J., Lee, J., and Shim, K. (2023). Effects of heat stress exposure on porcine muscle satellite cells. *J. Therm. Biol.* 114, 103569. doi:10.1016/j.jtherbio.2023.103569

Peebles, E. D., Oliveira, T. F. B., Kim, E. J., Olojede, O. C., Elliott, K. E. C., Lindsey, L. L., et al. (2021). Research Note: effects of the in ovo injection of organic zinc, manganese, and copper and posthatch holding time before placement on broiler body temperature during grow out. *Poult. Sci.* 100 (2), 755–759. doi:10.1016/j.psj.2020.10.048

Piestun, Y., Harel, M., Barak, M., Yahav, S., and Halevy, O. (2009). Thermal manipulations in late-term chick embryos have immediate and longer term effects on myoblast proliferation and skeletal muscle hypertrophy. *J. Appl. Physiol. (1985)* 106(1), 233–240. doi:10.1152/japplphysiol.91090.2008

Piestun, Y., Patael, T., Yahav, S., Velleman, S. G., and Halevy, O. (2017). Early posthatch thermal stress affects breast muscle development and satellite cell growth and characteristics in broilers. *Poult. Sci.* 96 (8), 2877–2888. doi:10.3382/ps/pex065

Piestun, Y., Shinder, D., Ruzal, M., Halevy, O., Brake, J., and Yahav, S. (2008). Thermal manipulations during broiler embryogenesis: effect on the acquisition of thermotolerance. *Poult. Sci.* 87 (8), 1516–1525. doi:10.3382/ps.2008-00030

Piestun, Y., Yahav, S., and Halevy, O. (2015). Thermal manipulation during embryogenesis affects myoblast proliferation and skeletal muscle growth in meat-type chickens. *Poult. Sci.* 94 (10), 2528–2536. doi:10.3382/ps/pev245

Sarais, F., Metzger, K., Hadlich, F., Kalbe, C., and Ponsuksili, S. (2023). Transcriptomic response of differentiating porcine myotubes to thermal stress and donor piglet age. *Int. J. Mol. Sci.* 24 (17), 13599. doi:10.3390/ijms241713599

Schultz, E., and Lipton, B. H. (1982). Skeletal muscle satellite cells: changes in proliferation potential as a function of age. *Mech. Ageing Dev.* 20 (4), 377–383. doi:10.1016/0047-6374(82)90105-1

Seale, P., Sabourin, L. A., Girgis-Gabardo, A., Mansouri, A., Gruss, P., and Rudnicki, M. A. (2000). Pax7 is required for the specification of myogenic satellite cells. *Cell* 102 (6), 777–786. doi:10.1016/s0092-8674(00)00066-0

Siddiqui, S. H., Subramaniyan, S. A., Kang, D., Park, J., Khan, M., Choi, H. W., et al. (2020a). Direct exposure to mild heat stress stimulates cell viability and heat shock protein expression in primary cultured broiler fibroblasts. *Cell Stress Chaperones* 25 (6), 1033–1043. doi:10.1007/s12192-020-01140-x

Siddiqui, S. H., Subramaniyan, S. A., Kang, D., Park, J., Khan, M., and Shim, K. (2020b). Modulatory effect of heat stress on viability of primary cultured chicken satellite cells and expression of heat shock proteins *ex vivo*. *Anim. Biotechnol.* 32, 774–785. doi:10.1080/10495398.2020.1757460

Sieiro-Mosti, D., De La Celle, M., Pele, M., and Marcelle, C. (2014). A dynamic analysis of muscle fusion in the chick embryo. *Development* 141 (18), 3605–3611. doi:10.1242/dev.114546

Tejeda, O. J., Meloche, K. J., and Starkey, J. D. (2021). Effect of incubator tray location on broiler chicken growth performance, carcass part yields, and the meat quality defects wooden breast and white striping. *Poult. Sci.* 100 (2), 654–662. doi:10.1016/j.psj.2020.10.035

Tompkins, Y. H., Su, S., Velleman, S. G., and Kim, W. K. (2021). Effects of 20(S)-hydroxycholesterol on satellite cell proliferation and differentiation of broilers. *Poult. Sci.* 100 (2), 474–481. doi:10.1016/j.psj.2020.10.032

Velleman, S. G., Liu, X., Nestor, K. E., and McFarland, D. C. (2000). Heterogeneity in growth and differentiation characteristics in male and female satellite cells isolated from Turkey lines with different growth rates. *Comp. Biochem. Physiology Part A Mol. Integr. Physiology* 125 (4), 503–509. doi:10.1016/s1095-6433(00)00178-1

Wall, B. L., Rueda, M. S., Davis, J. D., Purswell, J. L., Starkey, C. W., and Starkey, J. D. (2022). "Evaluation of thermal variation during early-stage incubation on broiler chicken growth performance, carcass characteristics, and the breast meat quality defects, Wooden Breast and White Striping," in *Poultry science association annual meeting* (Texas): San Antonio).

White, R. B., Bierinx, A. S., Gnocchi, V. F., and Zammit, P. S. (2010). Dynamics of muscle fibre growth during postnatal mouse development. *BMC Dev. Biol.* 10, 21. doi:10.1186/1471-213X-10-21

Xu, J., Strasburg, G. M., Reed, K. M., Bello, N. M., and Velleman, S. G. (2023). Differential effects of temperature and mTOR and Wnt-planar cell polarity pathways on syndecan-4 and CD44 expression in growth-selected Turkey satellite cell populations. *PLoS One* 18 (2), e0281350. doi:10.1371/journal.pone.0281350

Xu, J., Strasburg, G. M., Reed, K. M., and Velleman, S. G. (2021). Response of Turkey pectoralis major muscle satellite cells to hot and cold thermal stress: effect of growth selection on satellite cell proliferation and differentiation. *Comp. Biochem. Physiol. A Mol. Integr. Physiol.* 252, 110823. doi:10.1016/j.cbpa.2020.110823

Xu, J., Strasburg, G. M., Reed, K. M., and Velleman, S. G. (2022). Temperature and growth selection effects on proliferation, differentiation, and adipogenic potential of Turkey myogenic satellite cells through Frizzled-7-mediated Wnt planar cell polarity pathway. *Front. Physiol.* 13, 892887. doi:10.3389/fphys.2022.892887

Yablonka-Reuveni, Z., Quinn, L. S., and Nameroff, M. (1987). Isolation and clonal analysis of satellite cells from chicken pectoralis muscle. *Dev. Biol.* 119 (1), 252–259. doi:10.1016/0012-1606(87)90226-0

Yamaguchi, T., Suzuki, T., Arai, H., Tanabe, S., and Atomi, Y. (2010). Continuous mild heat stress induces differentiation of mammalian myoblasts, shifting fiber type from fast to slow. *Am. J. Physiol. Cell Physiol.* 298 (1), C140–C148. doi:10.1152/ajpcell.00050.2009

frontiers | Frontiers in Physiology

TYPE Original Research
PUBLISHED 22 November 2023
DOI 10.3389/fphys.2023.1275922



OPEN ACCESS

EDITED BY
Francesca Soglia,
University of Bologna, Italy

REVIEWED BY
Jessye Wojtusik,
Omaha's Henry Doorly Zoo and Aquarium, United States
Mustafa Hitit,
Kastamonu University, Türkiye

*CORRESPONDENCE
Kahina S. Boukherroub,
kahina@umn.edu

RECEIVED 10 August 2023
ACCEPTED 08 November 2023
PUBLISHED 22 November 2023

CITATION
Kosonsiriluk S, Reed KM, Noll SL, Wileman BW, Studniski MM and Boukherroub KS (2023), Prolonged repeated inseminations trigger a local immune response and accelerate aging of the uterovaginal junction in turkey hens.
*Front. Physiol.* 14:1275922.
doi: 10.3389/fphys.2023.1275922



# Prolonged repeated inseminations trigger a local immune response and accelerate aging of the uterovaginal junction in turkey hens

Sunantha Kosonsiriluk[1], Kent M. Reed[2], Sally L. Noll[1], Ben W. Wileman[3], Marissa M. Studniski[3] and Kahina S. Boukherroub[1]*

[1]Department of Animal Science, University of Minnesota, Saint Paul, MN, United States, [2]Department of Veterinary and Biomedical Sciences, University of Minnesota, Saint Paul, MN, United States, [3]Select Genetics, Willmar, MN, United States

Artificial insemination is a standard practice in the turkey breeder industry to ensure the production of fertile eggs. Even though hens are inseminated on a weekly basis, their fertility tends to decline after a few weeks of production. Avian species have a specialized structures called sperm storage tubules (SSTs), located in the uterovaginal junction (UVJ) of the oviduct. The ability of SSTs to store sperm is directly correlated with the fertility of the hen. The objective of the study was to examine changes in the transcriptome of the turkey hen's UVJ in response to the presence of sperm at three key stages of production. We hypothesized that repeated and prolonged exposure to sperm would alter the transcriptome of the UVJ. Samples were collected from virgin hens prior to the onset of lay, as well as from sham-inseminated (extender only) and semen-inseminated hens at early lay, peak lay, and late lay. Gene expression profiling of the UVJ was examined, and a differential expression analysis was conducted through pairwise comparisons between semen- and sham-inseminated groups at each production stage and across production stages. In the early laying stage, no significant gene expression changes were found between semen- and sham-inseminated groups. However, at peak lay, genes related to lipid biosynthesis, Wnt signaling, cell proliferation, and O-glycan biosynthesis were upregulated in the semen group, while the immune response and cytokine-cytokine receptor interaction were downregulated. In the late lay stage, the transcription pathway was upregulated in the semen group, whereas the translation pathway was downregulated. The local immune response that was suppressed during peak lay was increased at the late laying stage. In the semen-inseminated group, the UVJ exhibited advanced aging at the late laying stage, evidenced by reduced telomere maintenance and translation processes. The results from this study provide valuable insights into the alteration of the UVJ function in response to the presence of sperm at different stages of production and throughout the production cycle. Targeting the modulation of local immune response and addressing aging processes after peak production could potentially prevent or delay the decline in fertility of turkey breeder hens.

KEYWORDS

**aging, avian, immune response, insemination, reproductive tract, transcriptomics, turkey, uterovaginal junction**

# 1 Introduction

Turkey breeder operations heavily rely on artificial insemination as a crucial method for producing fertile eggs that will eventually hatch and give rise to meat-producing turkeys. However, maintaining optimal fertility in turkey hens has proven to be a complex challenge. Hens reach peak production at around 6–8 weeks of lay, then fertility starts to gradually decline. Previous attempts to enhance fertility through increased insemination frequency and varying sperm insemination quantities have yielded minimal improvements (Bakst, 1988). The decline in fertility observed in avian species can be attributed to various factors, including hormonal imbalances, disease and immune-related factors, environmental influences, the timing of insemination, and the selection of sperm within the vaginal tract (Assersohn et al., 2021). One critical aspect affecting fertility is the storage of sperm in the hen's reproductive tract.

Sperm can be stored in the reproductive tract for several weeks, primarily in tubular invaginations of the surface epithelium at the uterovaginal junction (UVJ) region, known as sperm storage tubules (SSTs) (Holt, 2011). The UVJ plays a pivotal role in sperm selection, and its function is directly correlated with the fertility of avian species. Studies have shown that the number of spermatozoa residing in the SSTs positively correlates with the number of spermatozoa embedded in the perivitelline layer of oviductal eggs, thus improving the fertility of birds (Brillard and Bakst, 1990; Santos et al., 2013). Additionally, high-fertility line hens exhibit more SSTs, higher numbers of stored sperm, and longer sperm storage durations compared to low-fertility line hens, supporting the importance of SSTs in fertility (Brillard et al., 1998; Yang et al., 2021a).

Spermatozoa are considered foreign to the female immune system and promptly stimulate a local immune response in the reproductive tract for elimination. During mating, immune-modulatory genes are expressed in the UVJ of chickens (Atikuzzaman et al., 2015), leading to the recruitment of immune cell populations to the UVJ, potentially impacting sperm survivability (Das et al., 2005). Previous studies have highlighted the critical role of suppressing local immunity in the UVJ against sperm for successful sperm survival and storage in laying hens (Das et al., 2009) and transforming growth factor β (TGFβ) has been implicated in this mechanism (Das et al., 2006).

Beyond the immune-related factors, various other elements contribute to sperm survival and storage in the SSTs of birds. Fatty acids have been found to influence sperm survival, maintenance, and motility in the SSTs (Huang et al., 2016). Additionally, several proteins, including carbonic anhydrase (Holm et al., 1996; Holm et al., 2000), avidin (Foye-Jackson et al., 2011), and aquaporins (Zaniboni and Bakst, 2004) play crucial roles in supporting the function of SSTs. While these findings provide valuable insights into the sperm storage function, there remain many factors that are not fully understood. Further research is needed to comprehensively explore the mechanisms behind sperm storage and its regulation in the UVJ of avian species.

Recent studies have used transcriptomics to explore the sperm storage function of the SSTs in chickens, shedding light on the comprehensive information about sperm storage in the UVJ (Han et al., 2019; Yang et al., 2020; Yang et al., 2021a; Yang et al., 2021b; Yang et al., 2023). However, it is crucial to acknowledge that turkey breeder reproduction is different from commercial chicken layers. The production lifespan of turkey breeder hens is approximately 28 weeks, unlike commercial chicken layers that produce eggs regularly for 2–3 years (El-Sabrout et al., 2022). This difference in the production cycle between the two species may indicate distinct mechanisms of reproductive tract development, maintenance, and regression. Additionally, sperm storage capacity and duration in the SSTs can vary significantly among avian species (Birkhead and Møller, 1992), and there is a substantial difference in the number of SSTs observed between chicken and turkey breeders (Bakst et al., 2010).

Recent transcriptomic studies on turkey focusing on the SSTs have provided valuable insights into the mechanism of SSTs in sperm storage (Brady et al., 2022). However, to gain a comprehensive understanding of the sperm storage process, it is imperative to conduct a transcriptomic study encompassing the entire turkey UVJ tissue. This approach allows for the exploration of integrated functions among various cell populations, including epithelial (both ciliated and non-ciliated), goblet, fibroblasts, muscle, SST, and immune cells located within the UVJ. Gaining insights into how these components work collectively will provide valuable insight into fertility dynamics in turkey breeder hens. In this study, we characterize transcriptomic changes in the turkey UVJ in response to repeated insemination across the production cycle. We hypothesized that prolonged exposure to sperm leads to alterations in the UVJ transcriptome, contributing to a decline in fertility among turkey breeder hens.

# 2 Methods

## 2.1 Experimental animals

Twenty-eight turkey breeder hens (*Meleagris gallopavo*) were generously donated by a turkey breeding company that collaborated with this study. The experimental birds were randomly selected from a parent stock breeder flock. A sample log of experimental birds was maintained to coordinate group assignment. The hens were provided with a conventional diet containing 12% protein during the pre-production phase and 18% protein during egg production. Water was available *ad libitum*. At 29 weeks of age, the hens were photo-stimulated with a light schedule of 14.5 h of light and 9.5 h of darkness. Beginning at 31 weeks of age, the hens were inseminated using 2 million fresh sperm diluted 1:1 with the extender, Turkey A1 Diluent with gentamicin (Southeast Poultry Health Services, Polkton, NC). Raw semen was collected to 16 milliliters (mL) by vacuum suction into 20 mL syringes pre-filled with an 8 mL extender. The viability of sperm was more than 85%, and the motility was 4.5 or greater on a scale of 5. Insemination was carried out three times in the first week and once per week throughout the 27 weeks production lifespan. The sham-inseminated groups were inseminated with the extender, following the same schedule as the flock insemination. Four virgin birds were collected 24 h before the first insemination. Semen- and sham-inseminated birds ($n$ = 4/group) were collected at early lay (2 days after the first insemination), peak

lay (8 weeks after the first insemination), and late lay (27 weeks after the first insemination). The protocol used in this study was approved by the University of Minnesota Institutional Animal Care and Use Committee.

## 2.2 UVJ tissue collection

Hens were humanely euthanized with assisted mechanical cervical dislocation. The lower reproductive tract was removed and dissected from the uterus to the vaginal opening. The UVJ tissue was dissected and divided horizontally into 1 $cm^2$ sections. One tissue section was snap-frozen in liquid nitrogen and stored at −80°C for RNA extraction and another section was fixed in 10% neutral-buffered formalin (NBF) for histology and group confirmation using hematoxylin and eosin (H&E) stain.

## 2.3 Tissue processing and H&E staining

UVJ tissues were fixed overnight at the room temperature in 10% NBF and processed through dehydration, clearing, and infiltration with paraffin using an Epredia STP 120 spin tissue processor (Epredia, Kalamazoo, MI). The tissues were embedded in paraffin blocks, sectioned at 5 µm, and mounted on charged slides (VWR International, Radnor, PA). H&E staining included deparaffinization and rehydration of tissues through a series of 100% xylene, a mixture of 50% xylene and 50% ethanol, 100% ethanol, 75% ethanol, and distilled water. Tissues were stained with hematoxylin, Gill III (Sigma-Aldrich, St. Louis, MO) for 2 min, then the slides were quickly dipped twice in acidic alcohol (0.1% HCl in 75% ethanol) and rinsed with several changes of distilled water until the water became clear. Tissues were immersed in 75% ethanol and stained with eosin for 2 min. Tissues were then dehydrated through a series of 75% ethanol, 100% ethanol, a mixture of 50% xylene and 50% ethanol, and 100% xylene. Tissues were mounted with mounting medium, and coverslips were applied. Tissues were observed under a light microscope to confirm the histology of the UVJ. The presence or absence of sperm in the SST was examined to confirm the assignment of semen- and sham-inseminated groups, respectively.

## 2.4 RNA extraction, cDNA library construction, and sequencing

Total RNA was extracted using the RNeasy Midi Kit and treated with DNase (Qiagen, Germantown, MD, United States) following the manufacturer's protocol. The samples were submitted to the University of Minnesota Genomics Center for quantity and quality assessment using the RiboGreen assay (Thermo Fisher Scientific, Waltham, MA, United States) and TapeStation 4200 (Agilent, Santa Clara, CA, United States), respectively. Sample RNA integrity numbers ranged from 8.0 to 9.4 and these were processed through cDNA library construction. Indexed libraries were constructed with the TruSeq Stranded mRNA Sample Preparation Kit (Illumina, Inc., San Diego, CA, United States) and size-selected for approximately 200 bp inserts. The libraries were multiplexed and sequenced on the Illumina NovaSeq 6000 platform using 150 PE flow cell to produce 51 bp paired-end reads.

## 2.5 Transcriptomic data analysis

Sequence processing and mapping were conducted as described in Reed et al. (2022) using the turkey genome (UMD 5.1, ENSEMBL Annotation 104). Gene IDs were determined as described in Reed et al. (2022). Raw read counts were uploaded to the integrated Differential Expression and Pathway analysis (iDEP) version 0.96 which is a web-based tool available at http://bioinformatics.sdstate.edu/idep96/ (Ge et al., 2018). In the pre-processing step, data were normalized using the cpm function in edgeR. Genes that were expressed at <0.5 counts per million (CPM) in a library were filtered out. Normalized counts were transformed using edgeR log2(CPM+c), with a pseudo count $c = 4$ added to all counts before transformation. The transformed data were used for exploratory data analysis including clustering and principal component analysis (PCA). K-means clustering analysis was performed using gene expression pattern across samples of the top 2000 most variable genes. Differentially expressed genes (DEGs) were determined through pairwise comparisons between semen- and sham-insemination at early lay, peak lay, and late lay and across production cycle in both groups using DESeq2 (Love et al., 2014). For all comparisons, false discovery rate (FDR) < 0.05 and fold-change > |1.5| were considered statistically significant.

Enrichment analysis was performed using DEGs from each pairwise comparison. The Database for Annotation, Visualization and Integrated Discovery (DAVID) Functional Annotation Tool (Huang et al., 2009; Sherman et al., 2022) was used for gene ontology (GO) analysis and Kyoto Encyclopedia of Genes and Genomes (KEGG) pathway enrichment. The annotation summary results of each comparison were used to create enrichment bubble plots (http://www.bioinformatics.com.cn/srplot). Pathway analysis was performed using Parametric Gene Set Enrichment Analysis (PGSEA) (Jambusaria et al., 2018). KEGG pathway diagrams (Kanehisa et al., 2017) were used to visualize gene expression data using Pathview (Luo and Brouwer, 2013). The transcriptome data have been deposited with the National Center for Biotechnology Information (NCBI) Sequence Read Archive (SRA) database, BioProject ID PRJNA1003625.

# 3 Results

## 3.1 The presence of sperm in the SST of semen inseminated UVJ tissues

The histology of UVJ tissues was examined to validate the accuracy of collected samples. The presence of sperm demonstrated successful semen insemination in semen-inseminated groups. The key distinguishing feature of UVJ tissue from the adjacent uterus and vagina tissues is the presence of SSTs. It is noteworthy that SSTs were consistently observed in all samples collected and that the presence of sperm was exclusively found in the SSTs of the semen-inseminated groups of all stages of production. This finding confirms successful

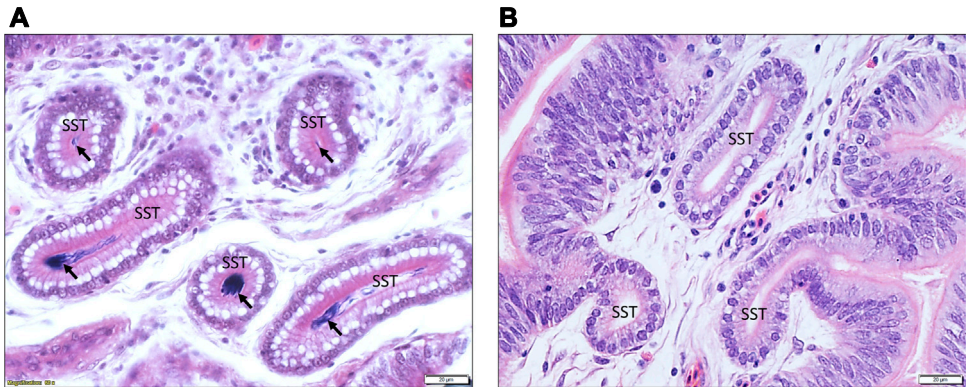


FIGURE 1
An illustrative example of the histology of the UVJ tissue containing SST stained with hematoxylin and eosin. **(A)** Arrows indicate sperm present in the SST of UVJ tissues from a semen-inseminated bird. **(B)** Sperm are lacking in the SST of UVJ tissues in a sham-inseminated bird.

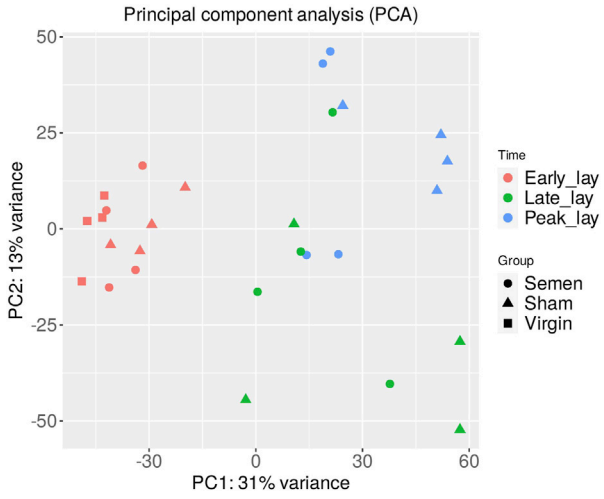


FIGURE 2
Principal component analysis (PCA) of the UVJ samples. A PCA plot of RNA-seq normalized read counts data shows clusters of samples based on their similarity. Samples with similar characteristics appear close to each other and samples with dissimilar characteristics are farther apart. Groups are denoted by different shapes and sampling times by color.

tissue collection, semen insemination, and the validity of our group assignments. Figure 1 provides an illustrative example of H&E stained UVJ tissues, showcasing sperm presence in the SSTs from semen-inseminated birds (Figure 1A) and the absence of sperm in the SSTs from sham-inseminated birds (Figure 1B).

## 3.2 Gene expression data clustering according to stages of production

A total of 750 million paired-end sequence reads were generated across the 28 samples (7 groups × $n = 4$ per group). The average number of reads per library was 26.8 million, with consistently high-quality reads (Q values ranging from 36.1 to 36.2). After filtration, 14,828 genes out of the 17,970 total expressed genes were used for the subsequent PCA. The results of the PCA (Figure 2) revealed distinct clusters representing semen, sham, and virgin samples during early lay, well-separated from the clusters of samples obtained during peak lay and late lay. This striking separation underscores the significant influence of the production stage on the overall gene expression patterns in the UVJ.

To further explore the dynamic changes in gene expression over the stages of production, we utilized a hierarchical clustering heatmap based on the 1,200 most variable genes (Figure 3). These findings provided insights into the shifts in gene expression profiles as hens entered peak production. Although the clustering of peak lay and late lay samples showed some heterogeneity, the observed variations in gene expression may be indicative of distinct reproductive performances among individual hens.

The analysis of K-means clustering of the 2,000 most variable genes across all samples is visually depicted in Figure 4. To better understand the functional implications, we identified enriched GO biological process pathways for each cluster, summarized in Table 1. The key findings from the clustering analysis are: Cluster B: during early lay, there was a robust effect of cell cycle and cell division. These effects were reduced as hens reached peak lay and continued to late lay. Cluster C: pathways related to ion transport and fibroblast growth factor were significantly enriched during peak lay, particularly in the sham group. Cluster D: pathways associated with cell communication, signaling, and response to stimulus showed increased activity during peak lay and late lay, notably in the sham groups. The identification of these dynamic gene expression pathways provides insights into the underlying molecular mechanisms that influence avian reproduction throughout the stages of production.

## 3.3 The presence of sperm alters UVJ transcriptome during peak lay and late lay

To investigate the influence of sperm on the UVJ transcriptome across the stages of production, we identified DEGs in the comparison between semen-inseminated and sham-inseminated birds (Supplementary Table S1). The number of DEGs identified at a threshold of FDR < 0.05 and fold-change > |1.5| between semen

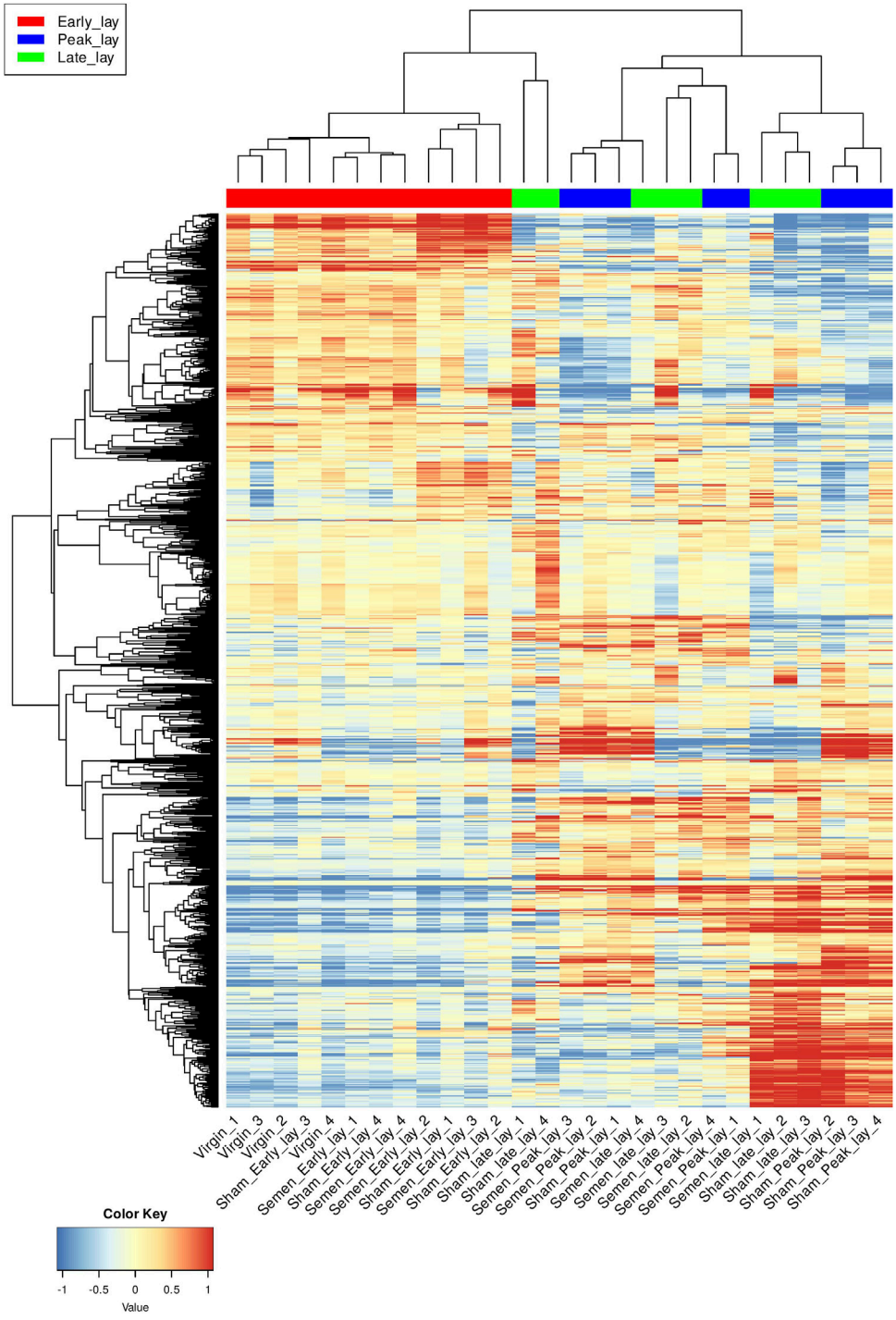


FIGURE 3
Hierarchical clustering of the UVJ samples. A hierarchical clustering heatmap based on 1,200 most variable genes of transformed data. Each row represents a gene and each column represents a sample. Genes were grouped based on expression level and samples were grouped based on similarity of gene expression profile. The color key indicates gene expression values.

and sham birds across the stages of production are given in Table 2. As shown in Figure 5A, DEGs between semen and sham birds at peak lay and late lay were relatively unique, with limited overlapping genes, indicating distinct responses of the UVJ to sperm in each production stage. However, no significant expression changes were observed between semen and sham at early lay.

The enriched GO terms, KEGG pathways, and UniProt Knowledgebase (UniPortKB) keywords of DEGs between semen and sham comparison at peak lay and late lay are shown in Figure 6. Notably enrichment analysis of the DEGs during peak lay, found the ion transport pathway was enriched, with some genes being upregulated in the semen group and others downregulated

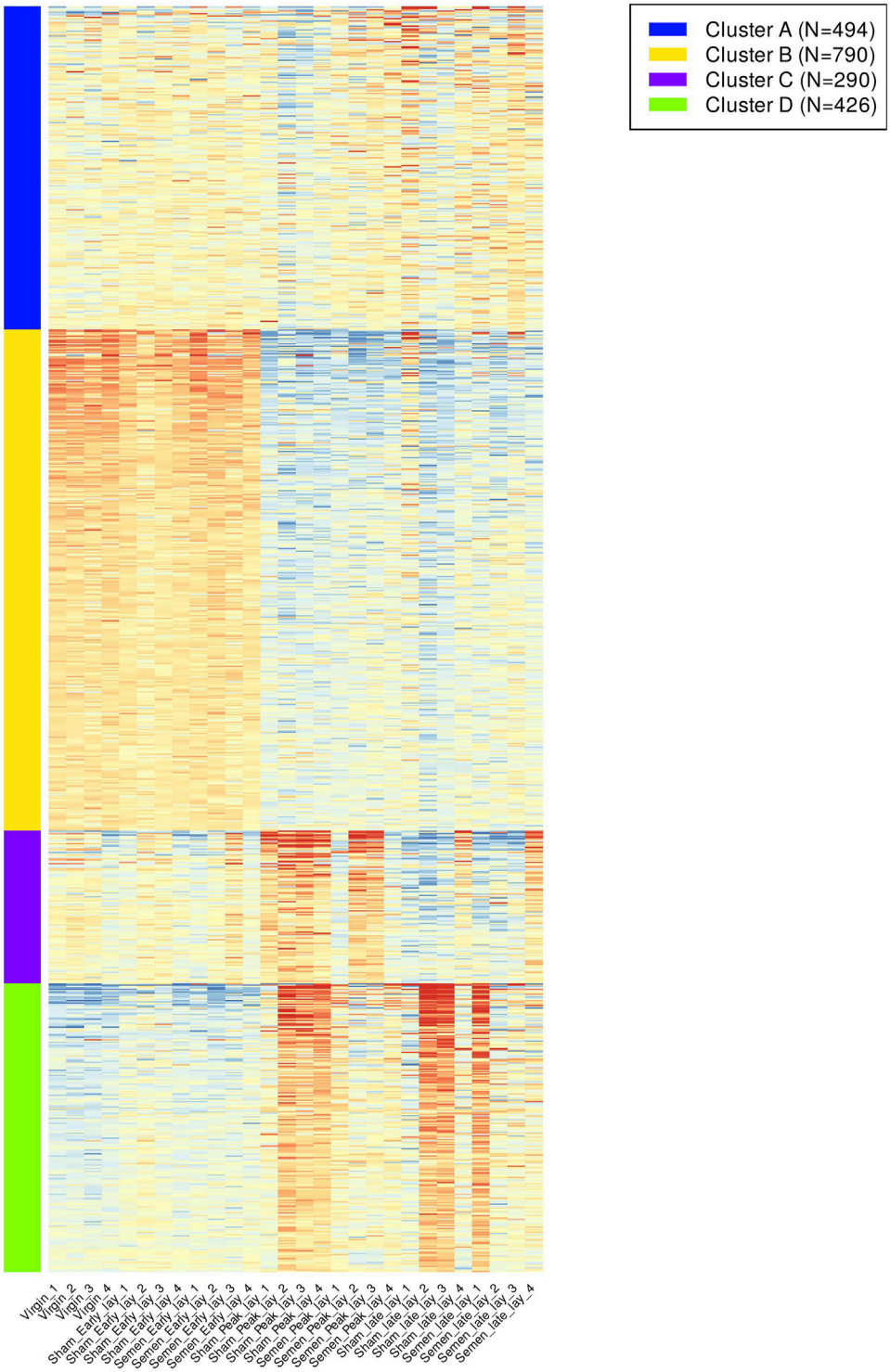


FIGURE 4
K-means clustering of gene expression pattern and enriched pathways across samples. A heatmap of the top 2,000 most variable genes across all samples were grouped according to their expression pattern. Different color bars depicted different clusters.

(Figures 6A, B). Additionally, lipid biosynthesis and metabolism, Wnt signaling pathway, regulation of epithelial cell proliferation, and O-glycan biosynthesis were enriched and upregulated (Figure 6A). In contrast, the immune response and cytokine-cytokine receptor interaction were enriched but downregulated in semen-inseminated birds at peak lay (Figure 6B). Noteworthy, pro-inflammatory cytokine receptors including interleukin 1 receptor like 1 (*IL1RL1*), C-C motif chemokine receptor 7 (*CCR7*), tumor necrosis factor receptor superfamily member 6b (*TNFRSF6B*), Fas cell surface death receptor (*FAS*), and prolactin receptor (*PRLR*)

10.3389/fphys.2023.1275922

**TABLE 1 Enriched gene ontology (GO) terms for biological process of K-means clustering with their significant values and number of genes presented in each pathway.**

| Cluster | Pathways | nGenes | adj.Pval |
|---|---|---|---|
| A | G protein-coupled receptor signaling pathway | 31 | 2.1E-03 |
| | Morphogenesis of an epithelial bud | 5 | 2.3E-03 |
| | Morphogenesis of an epithelial fold | 5 | 3.0E-03 |
| | Prostate gland morphogenesis | 5 | 4.0E-03 |
| B | Cell cycle process | 55 | 6.8E-10 |
| | Mitotic cell cycle process | 42 | 6.8E-10 |
| | Nuclear chromosome segregation | 26 | 7.0E-10 |
| | Cell cycle | 68 | 8.2E-10 |
| | Chromosome segregation | 27 | 1.6E-09 |
| | Mitotic cell cycle | 45 | 2.6E-09 |
| | Nuclear division | 30 | 6.6E-09 |
| | Mitotic nuclear division | 25 | 9.9E-09 |
| | Organelle fission | 30 | 8.3E-08 |
| | Mitotic sister chromatid segregation | 18 | 1.1E-07 |
| | Sister chromatid segregation | 19 | 4.8E-07 |
| | Attachment of spindle microtubules to kinetochore | 7 | 1.4E-04 |
| | DNA-dependent DNA replication | 13 | 2.3E-04 |
| | DNA replication initiation | 7 | 2.3E-04 |
| | Centromere complex assembly | 6 | 1.1E-03 |
| C | Ion transport | 37 | 1.1E-05 |
| | Transport | 63 | 1.3E-03 |
| | Cation transport | 26 | 1.3E-03 |
| | Ion transmembrane transport | 26 | 1.3E-03 |
| | Establishment of localization | 64 | 1.3E-03 |
| | Transmembrane transport | 34 | 1.3E-03 |
| | Fibroblast growth factor receptor signaling pathway | 7 | 1.6E-03 |
| | Cellular response to fibroblast growth factor stimulus | 7 | 2.3E-03 |
| | Response to fibroblast growth factor | 7 | 2.3E-03 |
| | Ureteric bud development | 6 | 2.5E-03 |
| | Mesonephros development | 6 | 2.5E-03 |
| | Mesonephric epithelium development | 6 | 2.5E-03 |
| | Mesonephric tubule development | 6 | 2.5E-03 |
| | Kidney morphogenesis | 5 | 4.6E-03 |
| | Sodium ion transport | 8 | 5.6E-03 |
| D | Ion transport | 43 | 7.2E-04 |
| | Multicellular organismal process | 94 | 7.2E-04 |
| | G protein-coupled receptor signaling pathway | 28 | 9.9E-04 |
| | Transmembrane transport | 46 | 9.9E-04 |

(Continued on following page)

**TABLE 1 (*Continued*) Enriched gene ontology (GO) terms for biological process of K-means clustering with their significant values and number of genes presented in each pathway.**

| Cluster | Pathways | nGenes | adj.Pval |
|---|---|---|---|
| | Cell communication | 104 | 1.6E-03 |
| | Signaling | 103 | 1.6E-03 |
| | Response to stimulus | 126 | 3.5E-03 |
| | Signal transduction | 94 | 5.7E-03 |
| | Regulation of membrane potential | 12 | 5.7E-03 |
| | Sulfate assimilation | 3 | 8.9E-03 |

**TABLE 2 Summary of gene expression and differential expressed genes (DEGs) of the UVJ between semen- and sham-insemination and across stages of production at FDR < 0.05 and fold-change > |1.5|.**

| Comparison | Groups | Total expressed genes | Common genes | Unique genes by group | DEGs | Up/Down genes |
|---|---|---|---|---|---|---|
| Treatment (Semen vs. sham) | Early lay | 15,395 | 14,888 | 282/225 | 0 | 0/0 |
| | Peak lay | 15,252 | 14,661 | 288/303 | 428 | 225/203 |
| | Late lay | 15,242 | 14,647 | 232/363 | 649 | 464/185 |
| Production stage | | | | | | |
| Virgin vs. early lay | Sham | 15,433 | 14,898 | 263/272 | 13 | 5/8 |
| Early lay vs. peak lay | Sham | 15,426 | 14,693 | 477/256 | 2,495 | 1,615/880 |
| | Semen | 15,367 | 14,710 | 403/254 | 1,295 | 895/400 |
| Peak lay vs. late lay | Sham | 15,251 | 14,577 | 372/302 | 1,205 | 546/659 |
| | Semen | 15,288 | 14,686 | 278/324 | 52 | 16/36 |

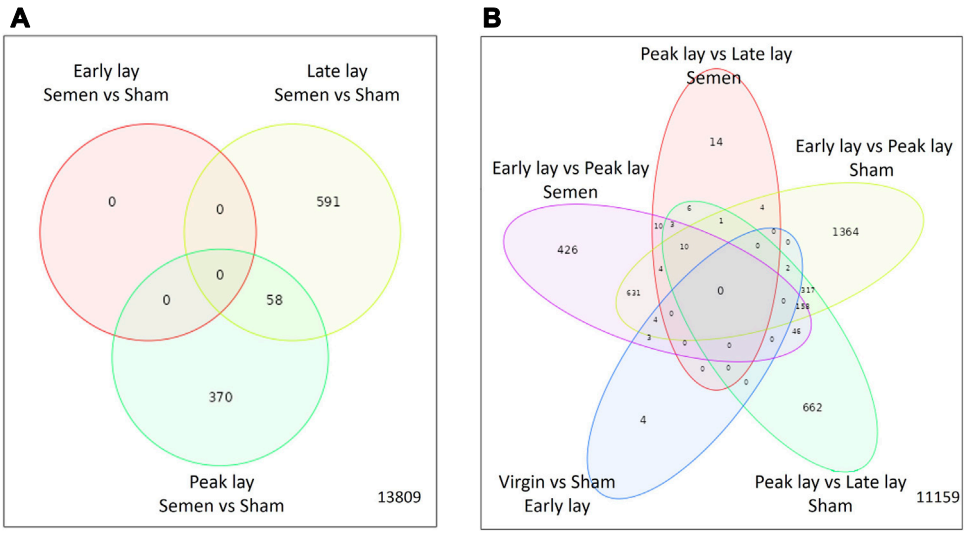


FIGURE 5
Characterization of differentially expressed genes in the UVJ. Venn diagrams show the number of common and unique differentially expressed genes in the semen vs. sham comparison at early lay, peak lay, and late lay **(A)** and among production stages comparisons in semen- and sham-inseminated groups **(B)**.

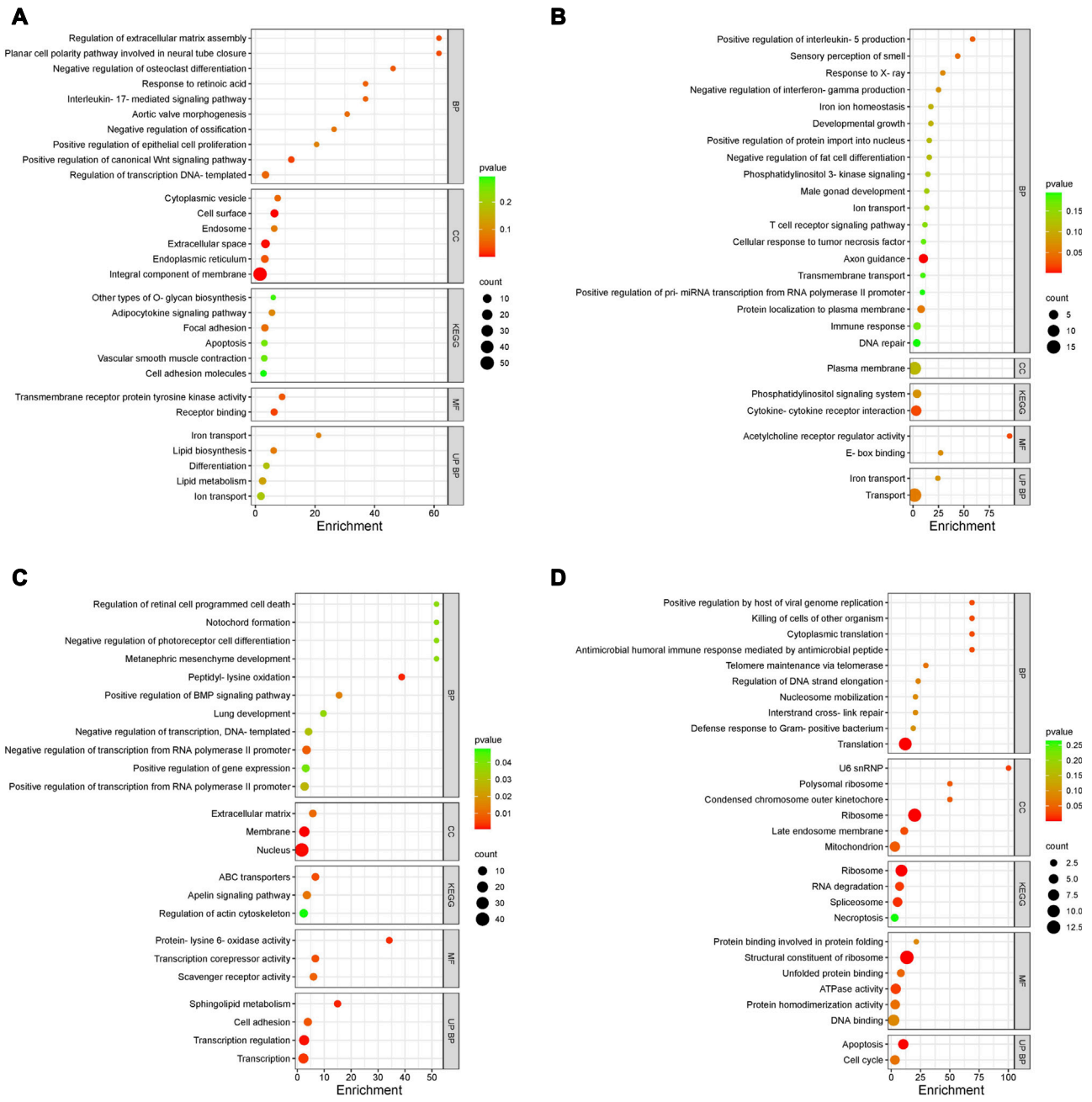


FIGURE 6
Enriched Gene Ontology (GO) terms of DEGs in the uterovaginal junction between semen vs. sham at peak lay and late lay. An enrichment bubble plot of upregulated **(A,C)** and downregulated **(B,D)** DEGs in semen group at peak lay and late lay, respectively. *P* values are represented by colors, gene counts are represented by bubble size. Abbreviations: BP, Biological process; CC, Cellular component; KEGG, Kyoto Encyclopedia of Genes and Genomes; MF, Molecular function; UP BP, UniProt biological process. Bubble plots were plotted by https://www.bioinformatics.com.cn/en, a free online platform for data analysis and visualization.

were significantly downregulated in the semen-inseminated hens at peak lay (Supplementary Table S1).

During late lay, the UVJ exhibited an imbalance between transcription and translation. Specifically, genes upregulated in the semen group were enriched for GO terms related to transcription, while downregulated genes were enriched for GO terms related to translation compared to the sham group. The PGSEA analysis of the top 30 pathways (Figure 7) revealed significant downregulation in pathways associated with translation, protein synthesis, and modification in the semen group at late lay, compared to the sham group during the same stage of production. Additionally, telomere maintenance *via* telomerase and the cell cycle were enriched and downregulated in the semen group (Figure 6D). Genes related to the ribosome, ribosome biogenesis, and proteasome were downregulated in the semen group (Figures 8A–C). In contrast, the C-type lectin receptor

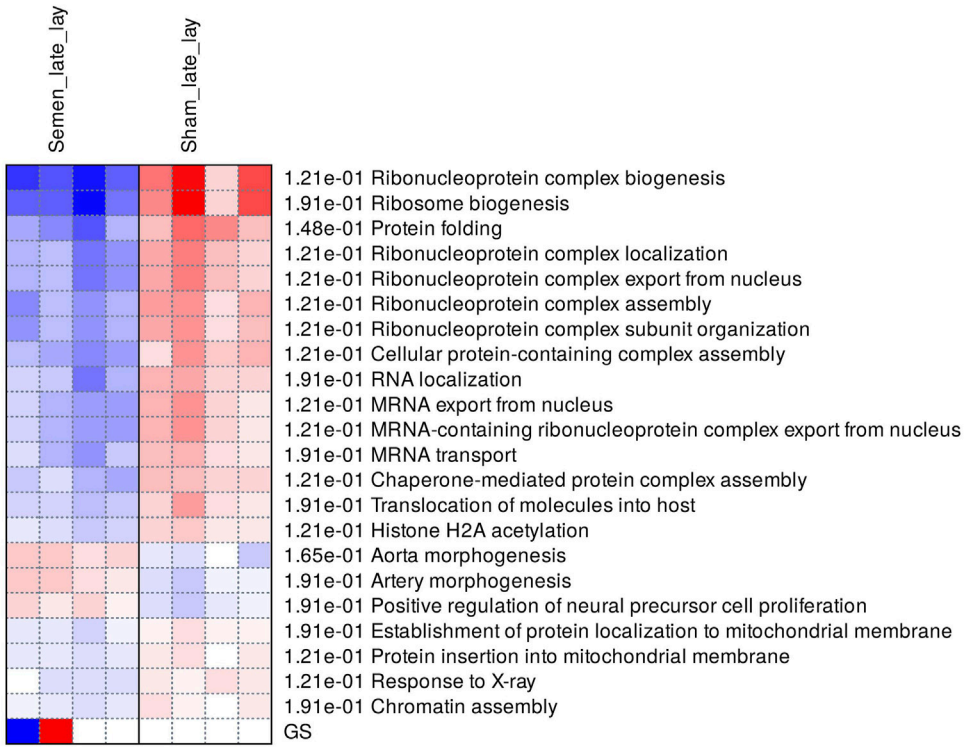


FIGURE 7
Enriched pathways of differentially expressed genes between semen- and sham-inseminated birds at late lay. A heatmap visualization of the top 30 enriched pathways reveal numerous ribosome-related and translation pathways in a downregulated direction in the semen group. Red and blue indicate activated and suppressed pathways, respectively.

signaling pathway (Figure 9A) and the extracellular matrix (ECM)-receptor interaction pathways (Figure 9B) were enriched and upregulated in the semen group compared to the sham group during late lay.

## 3.4 Transcriptomic alterations in the UVJ across the stages of production

To explore the transcriptomic changes throughout the production stages, we conducted a total of five pairwise comparisons. Specifically, we evaluated the transcriptomic alterations between early lay and peak lay, and between peak lay and late lay, in both semen and sham groups. Additionally, we made a comparison between virgin and sham groups at early lay. Table 2 summarizes the total number of DEGs from each pairwise comparison at different stages of production.

During the transition from early lay to peak lay, numerous DEGs were shared between the semen and sham groups. These genes are associated with reproductive development from early to peak lay, irrespective of the presence of sperm (Figure 5B). The sham groups exhibited the greatest number of DEGs during this transition, followed by the semen groups. A drastic decrease in DEGs was observed in semen groups from peak lay to late lay when compared to sham groups during the same period. Moreover, only a small number of genes were differentially expressed when comparing virgin and sham at early lay (Table 2).

Next, we examined the enriched GO terms for biological processes in the sham group during the transition from early lay to peak lay. This analysis revealed a decline in processes related to cell cycle, cell division, extracellular matrix organization, and cell adhesion, along with an increase in ion and transmembrane transports, cellular, ion, and chemical homeostasis, and endoplasmic reticulum stress (Table 3). Similar GO terms were enriched in the downregulated genes observed in the semen group during the same transition period.

At late lay, the enriched GO terms in the sham group indicated an upregulation of processes related to microtubule-based movement and transport, along with cilium assembly, organization, and movement (Table 4). Conversely, the nucleoside biphosphate and thioester metabolic processes were enriched and downregulated in the semen group at late lay. These findings provide insights into the dynamic changes in gene expression patterns and shed light on the biological processes and pathways involved in the UVJ during different stages of production.

# 4 Discussion

In this study, we investigated the transcriptomic changes in the UVJ in response to repeated insemination throughout the production cycle of female turkey breeders. Our objective was to identify the factors contributing to declining fertility following prolonged and repeated insemination as hens advanced through their production cycles. It is important to note that our study did not include virgin controls at each

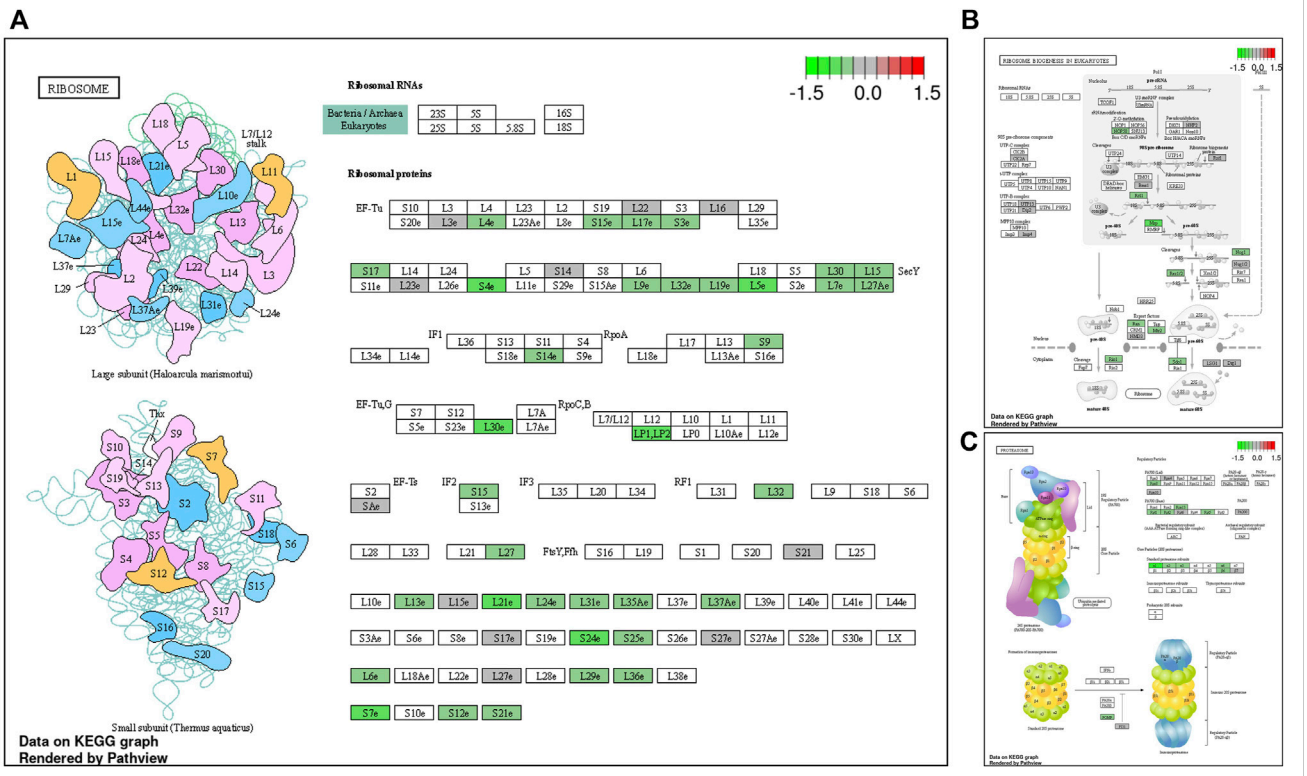


FIGURE 8
Enriched Kyoto Encyclopedia of Genes and Genomes (KEGG) pathway diagrams of downregulated differentially expressed genes between semen- and sham-inseminated birds at late lay. KEGG pathway diagrams illustrate downregulation of genes in the ribosome **(A)** ribosome biogenesis **(B)**, proteasome **(C)** pathways in the semen group at late lay. Fold-change (log2) cutoff in color code: bright red indicates most upregulated, bright green, most downregulated.

time point, which represents a limitation in our experimental design. The conclusions and discussions drawn were primarily grounded in the comparison between semen-inseminated and sham-inseminated groups, both within various stages of production and across different production stages. In our study, we found that the transcriptome of the UVJ undergoes dynamic remodeling at the beginning of laying period. Robust gene expression mapping to the processes of cell cycle and cell division were dominant in early lay groups (virgin, sham, and semen), while these processes declined as hens progressed towards peak lay and remained suppressed during late lay. This suggests that the UVJ tissue undergoes essential modifications at the start of the laying period to prepare for forthcoming active egg-laying. Additionally, once hens entered their peak production phase, we observed a significant upregulation in ion transport and epithelium development in the UVJ. These processes appear to exert their roles during the peak lay phase of egg production. Ion transport is crucial for maintaining the ionic balance and proper functioning of the reproductive tract (Atikuzzaman et al., 2015; Yang et al., 2021a). Epithelium development is likely involved in optimizing the structure and function of the UVJ to support the high reproductive demands during peak production (Yang et al., 2023).

Although previous evidence indicated that the UVJ responds to sperm as early as 24 h after mating (Atikuzzaman et al., 2015), our study did not observe significant transcriptomic alterations in the UVJ between semen and sham groups at 48 h after the first insemination. The lack of changes could be attributed to species divergence, experimental conditions, and differences in technology used. However, we did observe a substantial number of genes differentially expressed in sham birds from early lay to peak lay. Notable effects in cell cycle process, cell division, and extracellular matrix organization during early lay demonstrate the development of the reproductive tract in preparation for the approaching increase in reproductive performance. We observed upregulation of genes in ion and transmembrane transport pathways of sham-inseminated hens entering peak lay. Interestingly, these favorable arrangements occurred naturally alongside the production cycle, regardless of the presence of sperm. We speculate that changes in reproductive hormones across the production stages contribute to the fundamental transformation of the UVJ tissue, and the presence of sperm further enhances tissue modification.

The role of fatty acids in sperm survival in the SST has been reported for the hen oviduct (Huang et al., 2016). Lipid synthesis and metabolism are altered in the transcriptome of the avian UVJ suggesting a role of sperm maintenance in the SST (Han et al., 2019; Yang et al., 2021a; Yang et al., 2021b; Brady et al., 2022). In our study, we observed upregulation of lipid biosynthesis and metabolism in the semen-inseminated birds compared to sham-inseminated birds during peak lay, including key genes such as 1-acylglycerol-3-phosphate O-acyltransferase 2 (*AGPAT2*), acyl-CoA synthetase bubblegum family member 2 (*ACSBG2*), diacylglycerol kinase beta (*DGKG*), ELOVL fatty acid elongase 2 (*ELOVL2*), fatty acid 2-hydroxylase (*FA2H*), and lipase G, endothelial type (*LIPG*) (Supplementary Table S1). The transition in lipid biosynthesis and metabolism of the UVJ during peak lay was

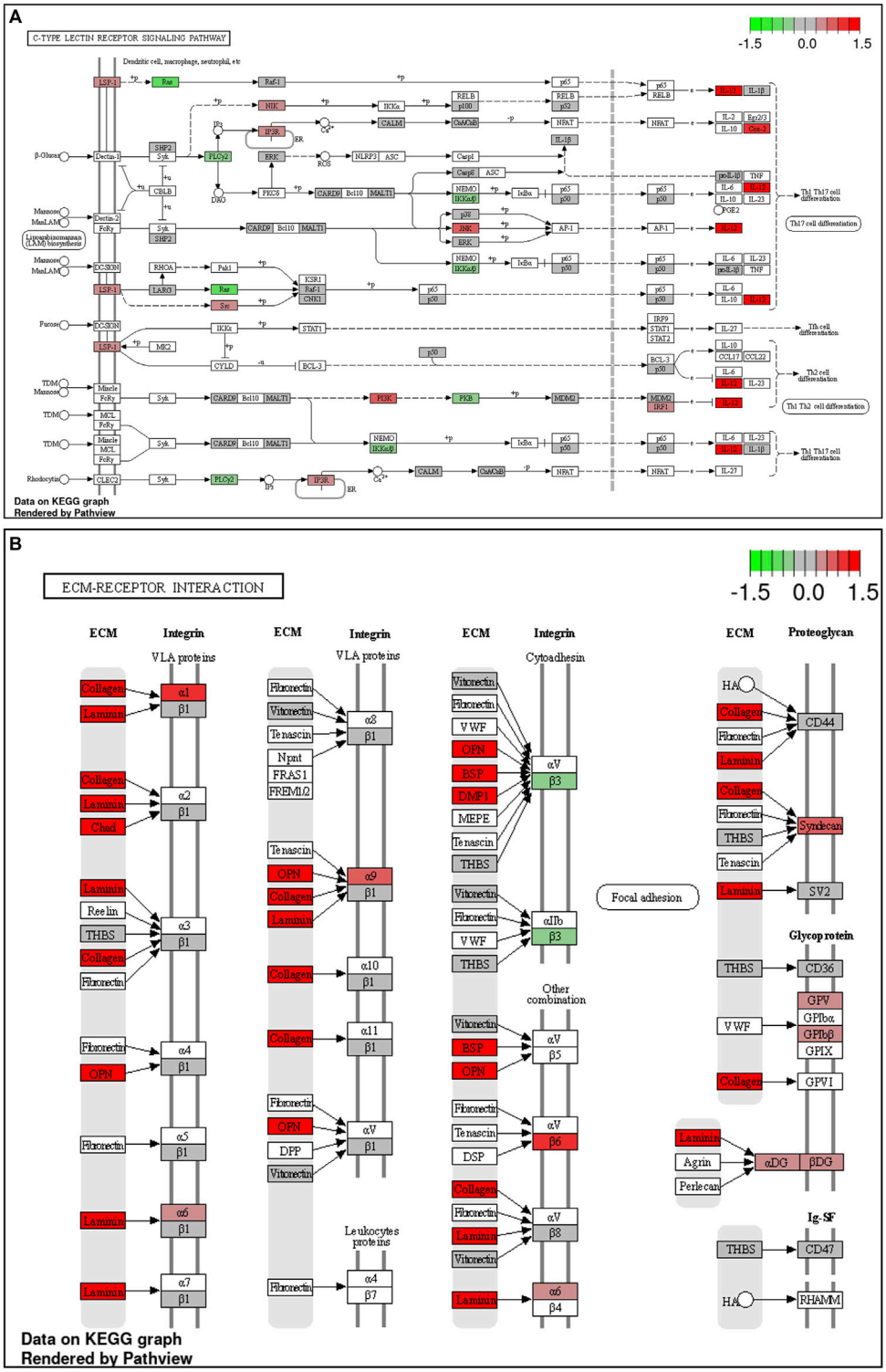


FIGURE 9
Enriched Kyoto Encyclopedia of Genes and Genomes (KEGG) pathways of upregulated differentially expressed genes between semen- and sham-inseminated birds at late lay. KEGG pathway diagrams illustrate upregulation of genes in the C-type lectin receptor signaling **(A)** and extracellular matrix (ECM)-receptor interaction **(B)** pathways in the semen group at late lay. Fold-change (log2) cutoff in color code: bright red indicates most upregulated, bright green, most downregulated.

**TABLE 3 Enriched pathways of differentially expressed genes of sham-inseminated hens at peak lay compared to early lay.**

| Direction | Pathways | nGenes | adj.Pval |
|---|---|---|---|
| Downregulated | Extracellular structure organization | 26 | 3.8e-05 |
| | Extracellular matrix organization | 25 | 4.2e-05 |
| | External encapsulating structure organization | 25 | 4.2e-05 |
| | Cell cycle | 93 | 2.2e-04 |
| | Attachment of spindle microtubules to kinetochore | 9 | 3.3e-04 |
| | Cell cycle process | 69 | 4.4e-04 |
| | Nuclear chromosome segregation | 27 | 4.4e-04 |
| | Mitotic cell cycle | 56 | 5.4e-04 |
| | Nuclear division | 34 | 8.8e-04 |
| | Microtubule-based process | 67 | 9.3e-04 |
| | Chromosome segregation | 28 | 1.0e-03 |
| | Cell adhesion | 78 | 1.0e-03 |
| | Biological adhesion | 78 | 1.0e-03 |
| | Organelle fission | 36 | 1.0e-03 |
| | Movement of cell or subcellular component | 103 | 2.1e-03 |
| Upregulated | Response to endoplasmic reticulum stress | 23 | 5.7e-06 |
| | Ion transport | 77 | 4.2e-05 |
| | Protein targeting to ER | 9 | 4.2e-05 |
| | Transport | 165 | 1.4e-04 |
| | Establishment of localization | 169 | 1.4e-04 |
| | Establishment of protein localization to endoplasmic reticulum | 9 | 1.4e-04 |
| | Inorganic ion homeostasis | 30 | 1.7e-04 |
| | Ion homeostasis | 31 | 2.6e-04 |
| | Cation homeostasis | 29 | 2.6e-04 |
| | Cellular homeostasis | 32 | 4.7e-04 |
| | Cellular ion homeostasis | 25 | 6.4e-04 |
| | Chemical homeostasis | 39 | 6.4e-04 |
| | Cellular chemical homeostasis | 29 | 6.4e-04 |
| | Transmembrane transport | 79 | 6.4e-04 |
| | Protein localization to endoplasmic reticulum | 9 | 6.4e-04 |

triggered by the presence of sperm and seminal plasma, as the levels of these genes did not increase in sham comparisons between early lay and peak lay. Notably, a prominent upregulation of *ELOVL2* in semen-inseminated birds at peak lay perhaps marks a crucial role of its function in fertility. ELOVL2 catalyzes the first and rate-limiting reaction that constitutes the long-chain fatty acid elongation cycle (Zhang et al., 2016). Although studies on its function in female reproduction are lacking, several studies have demonstrated its fundamental role in male fertility in mammals (Zadravec et al., 2011; Olia Bagheri et al., 2021; Castellini et al., 2022; Liu et al., 2022).

Regulation of pH also plays a role in sperm survival and activity in the UVJ of birds (Holm et al., 1996; Holm and Wishart, 1998). In our studies, we observed an increase in *CA4* expression from virgin to early lay to peak lay in both sham and semen groups (Supplementary Table S2). The level further elevated only in the semen group at late lay. Carbonic anhydrases (CA) have long been studied for their roles in sperm motility and fertility in both male and female reproductive tracts of mammals and birds (Harris and Goto, 1984; Holm et al., 1996; Holm et al., 2000; Wandernoth et al., 2010; Wandernoth et al., 2015). We believe that CA4 plays a fundamental role in turkey UVJ, but its levels may not directly reflect fertility rates.

The avian innate immune system plays a dual role in the reproductive tract. It protects against microbial challenges, and at the same time, it establishes tolerance for sperm to support successful

**TABLE 4 Enriched pathways of differentially expressed genes of sham-inseminated hens at late lay compared to peak lay.**

| Direction | Pathways | nGenes | adj.Pval |
|---|---|---|---|
| Upregulated | Microtubule-based process | 52 | 5.4e-11 |
| | Cilium organization | 30 | 1.6e-10 |
| | Microtubule-based movement | 29 | 1.2e-08 |
| | Cell projection assembly | 31 | 1.2e-08 |
| | Cilium assembly | 26 | 1.2e-08 |
| | Cilium movement | 17 | 1.2e-08 |
| | Axoneme assembly | 12 | 3.8e-08 |
| | Plasma membrane bounded cell projection assembly | 30 | 3.8e-08 |
| | Cell projection organization | 50 | 6.1e-07 |
| | Microtubule cytoskeleton organization | 31 | 6.1e-07 |
| | Microtubule bundle formation | 12 | 7.6e-07 |
| | Organelle assembly | 35 | 1.6e-06 |
| | Plasma membrane bounded cell projection organization | 47 | 2.9e-06 |
| | Microtubule-based transport | 13 | 6.9e-05 |
| | Determination of left/right symmetry | 11 | 7.8e-05 |

reproduction. In our study, we observed both immune activation and suppression pathways during the comparison of semen and sham groups at peak lay. An upregulation of antimicrobial peptides, including beta-defensin 2 (*THP2*) and cathelicidin-3 (*LOC104911326*) were noted in the semen group at peak lay (Supplementary Table S1). Antimicrobial peptides play a crucial role in protecting the reproductive tract from potential microbial threats. Simultaneously, we observed a downregulation of several pro-inflammatory cytokine and chemokine receptors in the semen-inseminated hens at peak lay. Pro-inflammatory cytokines and chemokines are essential in initiating immune responses and local inflammatory responses (Staeheli et al., 2001). These down-regulations appear to counterbalance the potential increase in cytokines and chemokines, aiming to attenuate local inflammation that could be triggered by foreign bodies, such as sperm. The suppression of the UVJ immune response is essential for sperm survival and storage, as it helps create a favorable environment for sperm within the reproductive tract. The decrease in cytokine-cytokine receptor interaction during peak lay may contribute to the improved survival and storage of sperm, ultimately reflecting a higher reproductive performance of the hen during this phase of the production cycle. However, as the production cycle progresses towards late lay, the expression pattern of these genes is reversed. We observed an upregulation of genes in the same immune families between semen groups at late lay compared to peak lay, indicating a rise in UVJ immune responses to sperm. This change was not observed in comparison to sham groups during the same time periods, illustrating the variation in local immune responses to sperm across different stages of production. These immune responses could be a crucial factor in determining the reproductive efficiency of turkey hens.

Several studies have reported an increase in transforming growth factor β and its receptor expression after insemination in avian species (Das et al., 2006; Atikuzzaman et al., 2015; Yang et al., 2023), suggesting a positive correlation of their expression with fertility (Gu et al., 2017). We also found an increase in *TGFB2* and its receptor in the semen group at peak lay with lower expression at late lay. Previous studies have suggested that TGF-β may suppress anti-sperm immune responses and protect sperm in the SST in chickens (Das et al., 2006). There is also evidence that TGF-β maintains tolerance to sperm cells in the murine epididymis (Voisin et al., 2020). Further investigation of TGF-β roles in the avian UVJ could enhance our understanding of sperm tolerance and the evasion of immune responses by the female reproductive tract.

In aging brains of mice and fish, a progressive reduction in the correlation between protein and mRNA levels is noted, often attributed to reduced proteasome activity (Kelmer Sacramento et al., 2020). Similar findings in roundworms and yeast indicate age-related degradation of ribosome function, leading to impaired protein synthesis and disrupted cellular processes (Stein et al., 2022). The transcriptomic analysis of semen-inseminated hens during late lay revealed a distinct pattern: an increase in transcription but a decrease in translation processes, indicating a potential reduction in overall protein synthesis. This pattern is reminiscent of a characteristic of aging, where there is often an observed loss of protein homeostasis. A downregulation of genes related to ribosomes, ribosome biogenesis, the proteasome, and protein export pathways observed in the UVJ of semen-inseminated hens at late lay implies the UVJ experiences advanced aging-like impairments, resembling the characteristics of aging in terms of altered protein synthesis, similar to what has been observed in the brains of aging mice and fish, which did not occur in the sham birds at the same production stage. These findings indicate that the UVJ exposed to repeated insemination exhibits characteristics of advanced aging, including loss of organelle function and telomere maintenance. Several recent studies have demonstrated an association of ribosome disruption and aging, adding to the relevance of our findings (Gonskikh and Polacek, 2017; Turi et al., 2019; Skariah and Todd, 2021; Stein et al., 2022).

Taken together, our study highlights that the transcriptome of the turkey UVJ undergoes dynamic alterations in response to laying status and the frequency and duration of semen exposure. Tissue remodeling occurs at the start of lay, preparing the UVJ to function as a sperm storage site. Local immune suppression appears to promote sperm survival and storage during peak lay, which coincides with the peak fertility period. At the late production stage, when hens had experienced prolonged repeated insemination, the UVJ exhibited a loss of protein homeostasis, resembling aging-like impairment. This was accompanied by an increase in immune responses, which could potentially lead to a loss of proper UVJ function and a favorable environment for sperm storage. To further explore possibilities to prevent or delay the destruction of the UVJ, we plan to investigate immune responses and reproductive aging at the single-cell level, aiming to gain deeper insights into the underlying mechanisms responsible for these phenomena. Understanding these mechanisms may provide potential strategies to maintain the UVJ's functionality and slow fertility decline in turkey hens.

## Data availability statement

The datasets presented in this study can be found in online repositories. The names of the repository/repositories and accession number(s) can be found below: (NCBI) BioProject: PRJNA1003625.

## Ethics statement

The animal studies were approved by University of Minnesota Institutional Animal Care and Use Committee. The studies were conducted in accordance with the local legislation and institutional requirements. Written informed consent was obtained from the owners for the participation of their animals in this study.

## Author contributions

SK: Conceptualization, Formal Analysis, Investigation, Methodology, Project administration, Resources, Validation, Visualization, Writing–original draft, Writing–review and editing. KR: Conceptualization, Data curation, Formal Analysis, Software, Supervision, Writing–review and editing. SN: Conceptualization, Methodology, Supervision, Writing–review and editing. BW: Conceptualization, Methodology, Project administration, Resources, Supervision, Writing–review and editing. MS: Conceptualization, Investigation, Project administration, Resources, Writing–review and editing. KB: Conceptualization, Funding acquisition, Investigation, Methodology, Project administration, Resources, Supervision, Validation, Writing–review and editing.

## Funding

The authors declare financial support was received for the research, authorship, and/or publication of this article. This work was financially supported by the Minnesota State Legislature through the Rapid Agricultural Response Fund, project no. AES00RR256 to KB.

## Acknowledgments

The authors thank the University of Minnesota Genomics Center for RNA sequencing service. Dr. Juan Abrahante, University of Minnesota Informatics Institute for RNA-seq data processing. Dr. Milena Saqui-Salces for histology guidance.

## Conflict of interest

Authors BW and MS were employed by the company Select Genetics.

The remaining authors declare that the research was conducted in the absence of any commercial or financial relationships that could be construed as a potential conflict of interest.

The authors declared that they were an editorial board member of Frontiers, at the time of submission. This had no impact on the peer review process and the final decision.

## Publisher's note



## Supplementary material

The Supplementary Material for this article can be found online at: https://www.frontiersin.org/articles/10.3389/fphys.2023.1275922/full#supplementary-material

**SUPPLEMENTARY TABLE S1**
Summary of differentially expressed genes of semen and sham comparison across production cycle and among production cycle in semen and sham groups.

**SUPPLEMENTARY TABLE S2**
Mean quality-trimmed RNAseq read counts of UVJ tissues from virgin birds, sham- and semen-inseminated birds sampling at early lay, peak lay, and late lay.

## References

Assersohn, K., Brekke, P., and Hemmings, N. (2021). Physiological factors influencing female fertility in birds. *R. Soc. Open Sci.* 8, 202274. doi:10.1098/rsos.202274

Atikuzzaman, M., Mehta Bhai, R., Fogelholm, J., Wright, D., and Rodriguez-Martinez, H. (2015). Mating induces the expression of immune- and pH-regulatory genes in the utero-vaginal junction containing mucosal sperm-storage tubuli of hens. *Reproduction* 150, 473–483. doi:10.1530/REP-15-0253

Bakst, M. R. (1988). Turkey hen fertility and egg production after artificial insemination and multiple oviduct eversion during the pre-laying period. *J. Reprod. Fertil.* 83, 873–877. doi:10.1530/jrf.0.0830873

Bakst, M. R., Donoghue, A. M., Yoho, D. E., Moyle, J. R., Whipple, S. M., Camp, M. J., et al. (2010). Comparisons of sperm storage tubule distribution and number in 4 strains of mature broiler breeders and in Turkey hens before and after the onset of photostimulation. *Poult. Sci.* 89, 986–992. doi:10.3382/ps.2009-00481

Birkhead, T. R., and Møller, A. P. (1992). Numbers and size of sperm storage tubules and the duration of sperm storage in birds: a comparative study. *Biol. J. Linn. Soc.* 45, 363–372. doi:10.1111/j.1095-8312.1992.tb00649.x

Brady, K., Krasnec, K., and Long, J. A. (2022). Transcriptome analysis of inseminated sperm storage tubules throughout the duration of fertility in the domestic Turkey, *Meleagris gallopavo*. *Poult. Sci.* 101, 101704. doi:10.1016/j.psj.2022.101704

Brillard, J. P., and Bakst, M. R. (1990). Quantification of spermatozoa in the sperm-storage tubules of Turkey hens and the relation to sperm numbers in the perivitelline layer of eggs. *Biol. Reprod.* 43, 271–275. doi:10.1095/biolreprod43.2.271

Brillard, J. P., Beaumont, C., and Scheller, M. F. (1998). Physiological responses of hens divergently selected on the number of chicks obtained from a single insemination. *J. Reprod. Fertil.* 114, 111–117. doi:10.1530/jrf.0.1140111

Castellini, C., Mattioli, S., Moretti, E., Cotozzolo, E., Perini, F., Dal Bosco, A., et al. (2022). Expression of genes and localization of enzymes involved in polyunsaturated fatty acid synthesis in rabbit testis and epididymis. *Sci. Rep.* 12, 2637. doi:10.1038/s41598-022-06700-y

Das, S. C., Isobe, N., Nishibori, M., and Yoshimura, Y. (2006). Expression of transforming growth factor-β isoforms and their receptors *in utero*-vaginal junction of hen oviduct in presence or absence of resident sperm with reference to sperm storage. *Reproduction* 132, 781–790. doi:10.1530/rep.1.01177

Das, S. C., Isobe, N., and Yoshimura, Y. (2009). Changes in the expression of interleukin-1beta and lipopolysaccharide-induced TNF factor in the oviduct of laying hens in response to artificial insemination. *Reproduction* 137, 527–536. doi:10.1530/REP-08-0175

Das, S. C., Nagasaka, N., and Yoshimura, Y. (2005). Changes in the localization of antigen presenting cells and T cells in the utero-vaginal junction after repeated artificial insemination in laying hens. *J. Reprod. Dev.* 51, 683–687. doi:10.1262/jrd.17027

El-Sabrout, K., Aggag, S., and Mishra, B. (2022). Advanced practical strategies to enhance table egg production. *Sci. (Cairo)* 2022, 1393392. doi:10.1155/2022/1393392

Foye-Jackson, O. T., Long, J. A., Bakst, M. R., Blomberg, L. A., Akuffo, V. G., Silva, M. V. B., et al. (2011). Oviductal expression of avidin, avidin-related protein-2, and progesterone receptor in Turkey hens in relation to sperm storage: effects of oviduct tissue type, sperm presence, and Turkey line. *Poult. Sci.* 90, 1539–1547. doi:10.3382/ps.2010-01159

Ge, S. X., Son, E. W., and Yao, R. (2018). iDEP: an integrated web application for differential expression and pathway analysis of RNA-Seq data. *BMC Bioinforma.* 19, 534. doi:10.1186/s12859-018-2486-6

Gonskikh, Y., and Polacek, N. (2017). Alterations of the translation apparatus during aging and stress response. *Mech. Ageing Dev.* 168, 30–36. doi:10.1016/j.mad.2017.04.003

Gu, L., Sun, C., Gong, Y., Yu, M., and Li, S. (2017). Novel copy number variation of the TGFβ3 gene is associated with TGFβ3 gene expression and duration of fertility traits in hens. *PLoS One* 12, e0173696. doi:10.1371/journal.pone.0173696

Han, J., Ahmad, H. I., Jiang, X., and Liu, G. (2019). Role of genome-wide mRNA-seq profiling in understanding the long-term sperm maintenance in the storage tubules of laying hens. *Trop. Anim. Health Prod.* 51, 1441–1447. doi:10.1007/s11250-019-01821-5

Harris, G. C., and Goto, K. (1984). Carbonic anhydrase activity of the reproductive tract tissues of aged male fowls and its relationship to semen production. *J. Reprod. Fertil.* 70, 25–30. doi:10.1530/jrf.0.0700025

Holm, L., Ridderstråle, Y., and Knutsson, P. G. (1996). Localisation of carbonic anhydrase in the sperm storing regions of the domestic hen oviduct. *Acta Anat. (Basel)* 156, 253–260. doi:10.1159/000147853

Holm, L., Ruziwa, S. D., Dantzer, V., and Ridderstråle, Y. (2000). Carbonic anhydrase in the utero-vaginal junction of immature and mature ostriches. *Br. Poult. Sci.* 41, 244–249. doi:10.1080/713654906

Holm, L., and Wishart, G. J. (1998). The effect of pH on the motility of spermatozoa from chicken, Turkey and quail. *Anim. Reprod. Sci.* 54, 45–54. doi:10.1016/s0378-4320(98)00142-0

Holt, W. V. (2011). Mechanisms of sperm storage in the female reproductive tract: an interspecies comparison. *Reproduction Domest. Animals* 46, 68–74. doi:10.1111/j.1439-0531.2011.01862.x

Huang, A., Isobe, N., Obitsu, T., and Yoshimura, Y. (2016). Expression of lipases and lipid receptors in sperm storage tubules and possible role of fatty acids in sperm survival in the hen oviduct. *Theriogenology* 85, 1334–1342. doi:10.1016/j.theriogenology.2015.12.020

Huang, D. W., Sherman, B. T., and Lempicki, R. A. (2009). Systematic and integrative analysis of large gene lists using DAVID bioinformatics resources. *Nat. Protoc.* 4, 44–57. doi:10.1038/nprot.2008.211

Jambusaria, A., Klomp, J., Hong, Z., Rafii, S., Dai, Y., Malik, A. B., et al. (2018). A computational approach to identify cellular heterogeneity and tissue-specific gene regulatory networks. *BMC Bioinforma.* 19, 217. doi:10.1186/s12859-018-2190-6

Kanehisa, M., Furumichi, M., Tanabe, M., Sato, Y., and Morishima, K. (2017). KEGG: new perspectives on genomes, pathways, diseases and drugs. *Nucleic Acids Res.* 45, D353-D361–D361. doi:10.1093/nar/gkw1092

Kelmer Sacramento, E., Kirkpatrick, J. M., Mazzetto, M., Baumgart, M., Bartolome, A., Di Sanzo, S., et al. (2020). Reduced proteasome activity in the aging brain results in ribosome stoichiometry loss and aggregation. *Mol. Syst. Biol.* 16, e9596. doi:10.15252/msb.20209596

Liu, J., Li, W., Weng, X., Yue, X., and Li, F. (2022). Composition of fatty acids and localization of SREBP1 and ELOVL2 genes in cauda epididymides of Hu sheep with different fertility. *Animals* 12, 3302. doi:10.3390/ani12233302

Love, M. I., Huber, W., and Anders, S. (2014). Moderated estimation of fold change and dispersion for RNA-seq data with DESeq2. *Genome Biol.* 15, 550. doi:10.1186/s13059-014-0550-8

Luo, W., and Brouwer, C. (2013). Pathview: an R/Bioconductor package for pathway-based data integration and visualization. *Bioinformatics* 29, 1830–1831. doi:10.1093/bioinformatics/btt285

Olia Bagheri, F., Alizadeh, A., Sadighi Gilani, M. A., and Shahhoseini, M. (2021). Role of peroxisome proliferator-activated receptor gamma (PPARγ) in the regulation of fatty acid metabolism related gene expressions in testis of men with impaired spermatogenesis. *Reprod. Biol.* 21, 100543. doi:10.1016/j.repbio.2021.100543

Reed, K. M., Mendoza, K. M., Strasburg, G. M., and Velleman, S. G. (2022). Transcriptome response of proliferating muscle satellite cells to thermal challenge in commercial Turkey. *Front. Physiol.* 13, 970243. doi:10.3389/fphys.2022.970243

Santos, T. C., Murakami, A. E., Oliveira, C. L., and Giraldelli, N. (2013). Sperm-egg interaction and fertility of Japanese breeder quails from 10 to 61 weeks. *Poult. Sci.* 92, 205–210. doi:10.3382/ps.2012-02536

Sherman, B. T., Hao, M., Qiu, J., Jiao, X., Baseler, M. W., Lane, H. C., et al. (2022). DAVID: a web server for functional enrichment analysis and functional annotation of gene lists (2021 update). *Nucleic Acids Res.* 50, W216–W221. doi:10.1093/nar/gkac194

Skariah, G., and Todd, P. K. (2021). Translational control in aging and neurodegeneration. *Wiley Interdiscip. Rev. RNA* 12, e1628. doi:10.1002/wrna.1628

Staeheli, P., Puehler, F., Schneider, K., Göbel, T. W., and Kaspers, B. (2001). Cytokines of birds: conserved functions—a largely different look. *J. Interferon & Cytokine Res.* 21, 993–1010. doi:10.1089/107999001317205123

Stein, K. C., Morales-Polanco, F., van der Lienden, J., Rainbolt, T. K., and Frydman, J. (2022). Ageing exacerbates ribosome pausing to disrupt cotranslational proteostasis. *Nature* 601, 637–642. doi:10.1038/s41586-021-04295-4

Turi, Z., Lacey, M., Mistrik, M., and Moudry, P. (2019). Impaired ribosome biogenesis: mechanisms and relevance to cancer and aging. *Aging (Albany NY)* 11, 2512–2540. doi:10.18632/aging.101922

Voisin, A., Damon-Soubeyrand, C., Bravard, S., Saez, F., Drevet, J. R., and Guiton, R. (2020). Differential expression and localisation of TGF-β isoforms and receptors in the murine epididymis. *Sci. Rep.* 10, 995. doi:10.1038/s41598-020-57839-5

Wandernoth, P. M., Mannowetz, N., Szczyrba, J., Grannemann, L., Wolf, A., Becker, H. M., et al. (2015). Normal fertility requires the expression of carbonic anhydrases II and IV in sperm. *J. Biol. Chem.* 290, 29202–29216. doi:10.1074/jbc.M115.698597

Wandernoth, P. M., Raubuch, M., Mannowetz, N., Becker, H. M., Deitmer, J. W., Sly, W. S., et al. (2010). Role of carbonic anhydrase IV in the bicarbonate-mediated activation of murine and human sperm. *PLOS ONE* 5, e15061. doi:10.1371/journal.pone.0015061

Yang, L., Cai, J., Rong, L., Yang, S., and Li, S. (2023). Transcriptome identification of genes associated with uterus-vagina junction epithelial folds formation in chicken hens. *Poult. Sci.* 102, 102624. doi:10.1016/j.psj.2023.102624

Yang, L., Li, S., Mo, C., Zhou, B., Fan, S., Shi, F., et al. (2021b). Transcriptome analysis and identification of age-associated fertility decreased genes in hen uterovaginal junction. *Poult. Sci.* 100, 100892. doi:10.1016/j.psj.2020.12.005

Yang, L., Li, S., Zhao, Q., Chu, J., Zhou, B., Fan, S., et al. (2021a). Transcriptomic and metabolomic insights into the variety of sperm storage in oviduct of egg layers. *Poult. Sci.* 100, 101087. doi:10.1016/j.psj.2021.101087

Yang, L., Zheng, X., Mo, C., Li, S., Liu, Z., Yang, G., et al. (2020). Transcriptome analysis and identification of genes associated with chicken sperm storage duration. *Poult. Sci.* 99, 1199–1208. doi:10.1016/j.psj.2019.10.021

Zadravec, D., Tvrdik, P., Guillou, H., Haslam, R., Kobayashi, T., Napier, J. A., et al. (2011). ELOVL2 controls the level of n-6 28:5 and 30:5 fatty acids in testis, a prerequisite for male fertility and sperm maturation in mice. *J. Lipid Res.* 52, 245–255. doi:10.1194/jlr.M011346

Zaniboni, L., and Bakst, M. R. (2004). Localization of aquaporins in the sperm storage tubules in the Turkey oviduct. *Poult. Sci.* 83, 1209–1212. doi:10.1093/ps/83.7.1209

Zhang, J. Y., Kothapalli, K. S. D., and Brenna, J. T. (2016). Desaturase and elongase limiting endogenous long chain polyunsaturated fatty acid biosynthesis. *Curr. Opin. Clin. Nutr. Metab. Care* 19, 103–110. doi:10.1097/MCO.0000000000000254

frontiers | Frontiers in Physiology

TYPE Original Research
PUBLISHED 14 December 2023
DOI 10.3389/fphys.2023.1296342



OPEN ACCESS

EDITED BY
Kent M. Reed,
University of Minnesota Twin Cities, United States

REVIEWED BY
Stephen T. Kinsey,
University of North Carolina Wilmington, United States
Nima Emami,
Novozymes, United States

*CORRESPONDENCE
Zehava Uni,
zehava.uni@mail.huji.ac.il

RECEIVED 18 September 2023
ACCEPTED 04 December 2023
PUBLISHED 14 December 2023

CITATION
Dayan J, Melkman-Zehavi T, Goldman N, Soglia F, Zampiga M, Petracci M, Sirri F, Braun U, Inhuber V, Halevy O and Uni Z (2023), In-ovo feeding with creatine monohydrate: implications for chicken energy reserves and breast muscle development during the pre-post hatching period.
*Front. Physiol.* 14:1296342.
doi: 10.3389/fphys.2023.1296342



# In-ovo feeding with creatine monohydrate: implications for chicken energy reserves and breast muscle development during the pre-post hatching period

Jonathan Dayan[1], Tal Melkman-Zehavi[1], Noam Goldman[2], Francesca Soglia[3], Marco Zampiga[3], Massimiliano Petracci[3], Federico Sirri[3], Ulrike Braun[4], Vivienne Inhuber[4], Orna Halevy[1] and Zehava Uni[1]*

[1]Department of Animal Science, The Robert H. Smith Faculty of Agriculture, Food, and Environment, The Hebrew University of Jerusalem, Rehovot, Israel, [2]Koret School of Veterinary Medicine, The Robert H. Smith Faculty of Agriculture, Food, and Environment, The Hebrew University of Jerusalem, Rehovot, Israel, [3]Department of Agricultural and Food Sciences, Alma Mater Studiorum—University of Bologna, Cesena, Italy, [4]Alzchem Trostberg GmbH, Trostberg, Germany

The most dynamic period throughout the lifespan of broiler chickens is the pre-post-hatching period, entailing profound effects on their energy status, survival rate, body weight, and muscle growth. Given the significance of this pivotal period, we evaluated the effect of in-ovo feeding (IOF) with creatine monohydrate on late-term embryos' and hatchlings' energy reserves and post-hatch breast muscle development. The results demonstrate that IOF with creatine elevates the levels of high-energy-value molecules (creatine and glycogen) in the liver, breast muscle and yolk sac tissues 48 h post IOF, on embryonic day 19 ($p < 0.03$). Despite this evidence, using a novel automated image analysis tool on day 14 post-hatch, we found a significantly higher number of myofibers with lower diameter and area in the IOF creatine group compared to the control and IOF NaCl groups ($p < 0.004$). Gene expression analysis, at hatch, revealed that IOF creatine group had significantly higher expression levels of myogenin (MYOG) and insulin-like growth factor 1 (IGF1), related to differentiation of myogenic cells ($p < 0.01$), and lower expression of myogenic differentiation protein 1 (MyoD), related to their proliferation ($p < 0.04$). These results imply a possible effect of IOF with creatine on breast muscle development through differential expression of genes involved in myogenic proliferation and differentiation. The findings provide valuable insights into the potential of pre-hatch enrichment with creatine in modulating post-hatch muscle growth and development.

KEYWORDS

**in-ovo feeding, creatine, glycogen, breast muscle, myogenic genes, proliferation, differentiation, broiler chicken**

# 1 Introduction

Meat-type chickens (broilers) have undergone intense selective breeding since the 1950s, aiming to achieve higher growth rates, better feed conversion, and increased meat yield. Consequently, modern broilers reach marketing weight in just 35–42 days (Havenstein et al., 2003a; Havenstein et al., 2003b; Zuidhof et al., 2014; Givisiez et al., 2020). This means that the 21-day of embryonic development (i.e., incubation period) and the early days post-hatch represent about 50% of the entire lifespan of modern broilers, hence, being of great importance to the production of poultry.

Throughout the broiler's lifespan, the pre-to post-hatching period constructs the most dynamic period transitioning from late-term embryo to hatchling and growing chick (Uni and Ferket, 2004; Moran, 2007; De Oliveira et al., 2008). During this period, the skeletal muscle system switches from the second wave of myogenesis, starting at embryonic day (E) 8 until hatch, to the third wave of myogenesis, starting at E17 and continuing through post-hatch growth (Chal and Pourquié, 2017; Halevy and Velleman, 2022). The second myogenic wave is sustained essentially by cell fusion and adding myonuclei from proliferating Pax7+ progenitors (Otto et al., 2006; White et al., 2010). This is achieved by various factors, among them are Myogenic determination factor 1 (MyoD), which has a key role in myogenic commitment and lineage of the muscle progenitors (Davis et al., 1987), and Myogenin (MYOG) that acts downstream to MyoD and is crucial for terminal differentiation which includes the fusion of myoblasts to myotubes (Hasty et al., 1993; Zammit, 2017). During the third myogenic wave, MyoD is also involved in maintaining the pool of adult muscle stem cells -the satellite cells-, a subset of Pax7+ progenitors (Relaix et al., 2004; Gros et al., 2005; Kassar-Duchossoy et al., 2005; Zammit et al., 2006), which are the only source of new myoblasts required for the third myogenic wave. Muscle growth during the third myogenic wave is attributed primarily to myofiber hypertrophy (increased diameter of existing fibers through protein deposition) and to the proliferation and differentiation of satellite cells that either fuse to existing fibers or synthesize new myotubes (Hartley et al., 1992; Gokhin et al., 2008; Sparrow and Schöck, 2009). Two key factors involved in myoblast proliferation, terminal differentiation, and muscle hypertrophy in broilers are Insulin-like growth factor 1 (IGF1) and MYOG (Halevy et al., 2001; Halevy et al., 2004).

In order to promote muscle growth of embryos and hatchlings, energy supply is attained through egg nutrients (yolk and albumen) and later through exogenous nutrition (Moran, 2007; Uni et al., 2012). The transition from embryo to hatchling includes a dramatic change in energy metabolism, as towards hatch, the embryo switches from chorioallantoic to pulmonary respiration (De Oliveira et al., 2008; Cogburn et al., 2018), and energy production switches from oxidation of yolk derived lipids to anaerobic catabolism, by glycogenolysis and by gluconeogenesis (Tazawa et al., 1983; Decuypere et al., 2001). By the time the embryo hatches, its energy reserves are exploited, as almost all glycogen stores are depleted (Uni and Ferket, 2004; Uni et al., 2005; De Oliveira et al., 2008; Yadgary and Uni, 2012; Dayan et al., 2023a). Consequently, gluconeogenesis becomes the dominant pathway for energy provision supplied primarily by breast muscle protein degradation for amino acids (Donaldson, 1995; Keirs et al., 2002). This highlights the significance of the first exogenic feeding to support muscle development and integrity (Noy and Sklan, 1999; Halevy et al., 2000; Halevy et al., 2003; Bigot et al., 2003; Uni and Ferket, 2004; Kornasio et al., 2011).

This study investigates whether the elevation of late-term embryos' energy stores will provide a jumpstart for breast muscle development and growth. For this aim, the method of in-ovo feeding (IOF), by inserting 0.6 mL of 1.5% creatine monohydrate solution into the embryo's amniotic fluid three to 4 days before hatch, was applied according to Uni and Ferket (2003). The potential of creatine is derived from its high energetic value, with the possibility of rapid ATP provision through the creatine/phosphocreatine system (Bessman and Carpenter, 1985; Wyss and Kaddurah-Daouk, 2000). In chickens, creatine was shown to play a major role in energy metabolism, pivotal for the energetic status of hatchlings and their post-hatch performance (Zhang et al., 2016; Zhao et al., 2017a; Zhao et al., 2017b; Melo et al., 2022; Dayan et al., 2023a; Firman et al., 2023). Here, we provide an inclusive view of creatine and glycogen dynamics during the pre-to post-hatching period and in response to IOF with creatine in three essential tissues, breast muscle, liver, and yolk sac (YS) tissue, which are involved in energy supply and demand. To evaluate the effects of energy enhancement on early post-hatch breast muscle development, a novel, high-precision image analysis tool for histological evaluation was applied. In addition, we explored a possible mechanism underlying how energy status may modulate muscle development through differential expression of four genes involved in myoblast proliferation and differentiation (IGF1, MYOG, MyoD, and proliferating cell nuclear antigen- PCNA).

# 2 Materials and methods

## 2.1 In-ovo feeding calibration test

Fertile eggs ($n$ = 220; mean weight = 62.7 g, SD = 3.6 g) from 39-week-old broiler hens (Cobb 500) were purchased from a commercial breeder farm (Y. Brown and Sons Ltd., Hod Hasharon, Israel). Eggs were incubated in a Petersime hatchery at the Faculty of Agriculture of the Hebrew University under standard conditions (37.8°C and 56% relative humidity). On E10, eggs were candled, and unfertilized or dead embryo eggs were removed. Eggs were divided into two treatment groups: the control group (non-injected) and the IOF creatine group [injection volume of 0.6 mL with amount per embryo of 9 mg creatine monohydrate (Alzchem Trostberg GmbH, Germany) and 3 mg NaCl]. On E17.5, amniotic fluid (amnion) enrichment by in-ovo feeding (IOF) was performed according to the procedure developed by Uni and Ferket (2003). Eggs were injected according to treatments, and IOF was performed using a 21-gauge needle. The site of injection was verified in a pre-test designed to ensure that the IOF solution reached the amnion successfully (Figure 1). Once the IOF procedure was completed, all eggs were transferred to hatching trays, and hatchability was monitored. At hatch day, 24 male chicks per group were sampled and the rest were transferred to brooders at the Faculty of Agriculture of the Hebrew University and reared according to the breeder recommendations (Cobb-Vantress). During the 3-day rearing period, chicks were fed a standard commercial starter diet (formulated by Brown feed mill, Kaniel, Israel) with *ad-libitum*

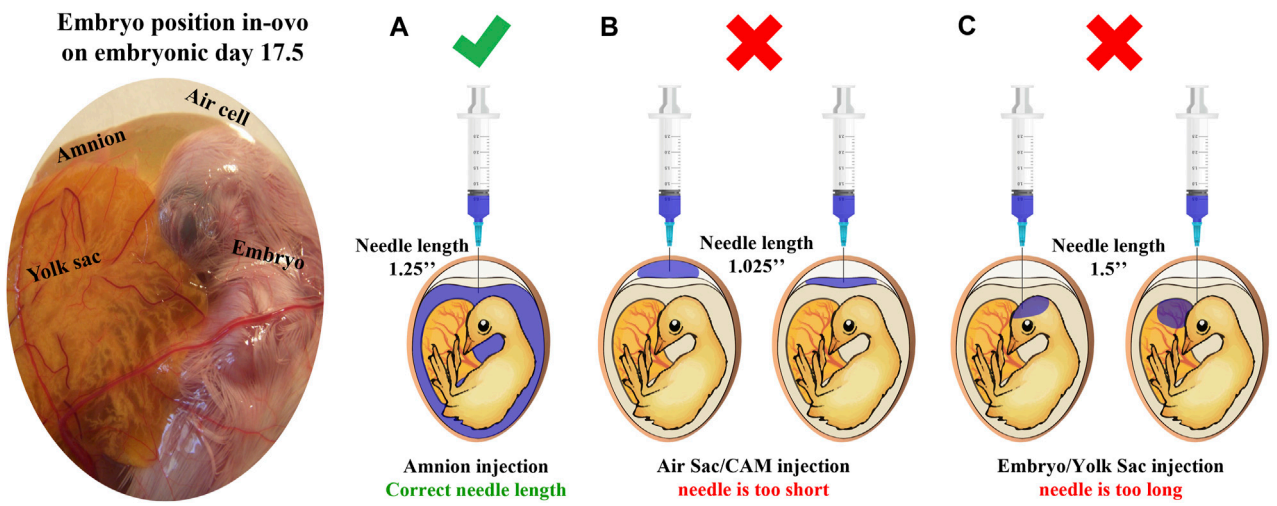


FIGURE 1
Site of injection test illustration. This test is designed to verify that the IOF solution reaches the amnion successfully. First, the amnion is identified by candling; next, needles in estimated lengths are chosen, and a sample of eggs is injected with 1 mL of coomassie blue dye ($n$ = 20 eggs/examined needle). After cooling, eggs are opened to confirm successful injection with the correct needle. **(A)** A successful injection; only the amnion is stained. **(B)** An unsuccessful injection, the needle is too short, and the staining solution is found on top of the embryo reaching the air sac or chorioallantoic membrane. **(C)** An unsuccessful injection, the needle is too long, and the staining solution is found in embryonic tissues or yolk sacs.

access to water and feed. Tissue sampling was performed on day of hatch and day 3 post-hatch. On each sampling day, 24 birds/treatment were randomly selected and euthanized by cervical dislocation, the body and breast muscle weights were recorded. Breast muscle (*Pectoralis major and Pectoralis minor*) percentage was calculated relative to body weight.

## 2.2 In-ovo feeding with creatine monohydrate-mode of action

Fertile eggs ($n$ = 330; mean weight = 62.46 g, SD = 4.4 g) from 33-week-old broiler hens (Cobb 500) were purchased from a commercial breeder farm (Y. Brown and Sons Ltd., Hod Hasharon, Israel). Eggs' incubation and handling were the same as described above. On E17.5, IOF was performed, and eggs were divided into three treatment groups: control group (non-injected), IOF NaCl group (injection volume: 0.6 mL with amount per embryo of 3 mg NaCl), and IOF creatine group [injection volume of 0.6 mL with amount per embryo of 9 mg creatine monohydrate (Alzchem Trostberg GmbH, Germany) and 3 mg NaCl]. After completion of the IOF procedure, all eggs were transferred to hatching trays, and hatchability was monitored. At hatch day, six male chicks per group were sampled and the rest were transferred to brooders at the Faculty of Agriculture of the Hebrew University at hatch and reared according to the breeder recommendations (Cobb-Vantress). During the 14-day rearing period, chicks were fed a standard commercial starter diet (formulated by Brown feed mill, Kaniel, Israel) with *ad-libitum* access to water and feed. Tissue sampling was performed on E17, E19, hatch day, day 1, day 3, day 6, and day 14. On each sampling day, six embryos/birds were randomly selected and euthanized by cervical dislocation. The following parameters were recorded: body weight, YS tissue weight (according to Yadgary et al., 2010), liver weight, and breast muscle weight. The relative weights of the liver, breast muscle, and YS tissue were calculated as a percent of body weight. Liver, YS tissue, and breast muscle (*Pectoralis major*) samples were collected to determine creatine and glycogen content (E17—day 1). In addition, breast muscle samples were collected for histology (day 14) and the evaluation of expression levels of myogenic genes (E17—day 6).

## 2.3 Analysis of creatine and glycogen energy resources

Tissue samples (approximately 500–1,500 mg per tissue) were collected, placed in liquid nitrogen, and kept at −80°C until further processing. Next, samples were lyophilized and examined for their creatine and glycogen content by Swiss-BioQuant-AG (Reinach, Switzerland). The concentrations of creatine and glycogen (mg/g dry weight tissue) were determined, and the total amount (mg) was calculated in order to demonstrate the full capacity of energy storage in each tissue as previously described (Yadgary and Uni, 2012; Dayan et al., 2023a).

## 2.4 Evaluation of muscle histomorphology

Muscle sampling for histology was performed as previously described by Halevy et al. (2004). Briefly, muscle samples (approximately 0.5 cm × 0.5 cm × 1 cm) were removed from the superficial region of the proximal half of the left *Pectoralis major* muscle. The muscle samples were fixed in 3.7% formaldehyde in PBS at pH 7.4 (Sigma-Aldrich, Rehovot, Israel) for 24 h. Then, samples were dehydrated, cleared, and embedded in paraffin. Cross sections of 4–6 µm thick were cut, deparaffinized in Histochoice clearing agent (Sigma-Aldrich St. Louis, MO), rehydrated, and stained with

**TABLE 1** In-ovo feeding calibration test.

| Day | Treatment | Hatchability (%) | Body weight (g) | Breast muscle weight (g) | Breast muscle % |
|---|---|---|---|---|---|
| Hatch | Control | 93.6 (N hatched = 88/94) | 47.42 ± 0.55 | 1.81 ± 0.06 | 3.81 ± 0.10 |
| | IOF Creatine | 95.5 (N hatched = 86/90) | 47.30 ± 0.63 | 1.99 ± 0.06* | 4.21 ± 0.12* |
| Day 3 | Control | — | 87.85 ± 1.6 | 6.57 ± 0.21 | 7.48 ± 0.19 |
| | IOF Creatine | — | 82.99 ± 1.49 | 6.17 ± 0.17 | 7.43 ± 0.15 |

Comparison of hatchability (%), body weight (g), breast muscle weight (g), and breast muscle percent (relative to body weight) between control chicks and chicks that were in-ovo feeding (IOF) with creatine. Each IOF-treated embryo was injected with 0.6 mL of 1.5% creatine monohydrate (9 mg/embryo) dissolved in 0.5% NaCl (3 mg). Asterisk denotes means that are significantly different between treatments at each time point, as derived from Student's t-test ($p \leq 0.05$). For data of body weight, breast muscle weight, and breast muscle percent, $n = 24$ per treatment and day.

Picrosirius Red Fast Green staining to differentiate between myofibers (stained in green) and connective tissue (stained in red). After drying, samples were mounted on cover glass using DPX slide mounting medium (Sigma-Aldrich St. Louis, MO). Finally, images were captured using an EVOS FL Auto-inverted microscope. Images are comprised of 12 stitched fields of ×60 magnification.

The automated image analysis workflow was developed and performed as described by Dayan et al. (2023b). Briefly, the workflow for Fiji software is based on PT-BIOP, Cellpose wrapper, and MorphoLibJ plugin. Image processing included detecting myofibers and converting label masks to regions of interest (ROIs). The morphological analysis included extracting myofiber metrics from the ROIs; the lesser diameter (μm) and cross-sectional area ($\mu m^2$) were measured, and the number of myofibers per $mm^2$ was calculated.

## 2.5 Analysis of mRNA expression

Tissue samples were collected, placed in liquid nitrogen, and refrigerated at −80°C until further processing. Total RNA was isolated from 100 mg of tissue (YS tissue, liver, and breast muscle) using TRI-Reagent (Sigma-Aldrich, St. Louis, MO) according to the manufacturer's protocol. RNA concentration was determined using a NanoDrop ND-1000 instrument (Thermo Fisher Scientific, Wilmington, DE). Total RNA was treated with DNase using a Turbo DNA-free Kit according to the manufacturer's protocol (Ambion; Thermo Fisher Scientific, Wilmington, DE). cDNA was created from 1 μg of DNA-free RNA using the qPCRBIO cDNA synthesis kit according to the manufacturer's protocol (PCRBIOSYSTEMS, London, United Kingdom). Relative mRNA expression was evaluated using gene-specific primers (Table 1): IGF1, involved in the induction of muscle cell differentiation and hypertrophy; MYOG, myogenic regulatory factor; MyoD, myogenic regulatory factor; PCNA, a marker for dividing cells, correlated with S phase in DNA replication; β-actin a housekeeping cytoskeletal protein, and HPRT, an enzyme in the purine synthesis in salvage pathway, also a housekeeping gene (Dayan et al., 2023a). Primer sequences were designed using Primer-BLAST software (Ye et al., 2012) based on published cDNA sequences purchased from Sigma-Aldrich (Rehovot, Israel). PCR products were validated by gel electrophoresis in 1.5% agarose gel. Real-time quantitative polymerase chain reactions (qPCR) were conducted in triplicate in a Roche Light cycler 96 (Roche Molecular Systems, Inc., Pleasanton, CA). Each reaction (20 μL) included 3 μL of cDNA sample diluted in ultrapure water in a ratio of 1:20 (UPW, Biological Industries, Beit HaEmek, Israel), 4 μM of each primer, and Platinum SYBR Green qPCR super mix-UDG (Thermo Fisher Scientific, Wilmington, DE). Reaction conditions were: preincubation at 95°C for 60 s followed by 40 cycles of a 2-step amplification cycle of 95°C for 10 s and 60°C for 30 s. The procedure was finalized with a melting curve generated in the following conditions: 95°C for 60 s, 65°C for 60 s, and 97°C for 1 s. Relative mRNA expression was calculated by subtracting the housekeeping gene's geometric mean of cycle threshold (Ct) values from sample Ct (Pfaffl, 2007; Dayan et al., 2023a).

## 2.6 Statistical analysis

For the IOF calibration test, at each time point, differences between treatments were evaluated using Student's *t*-test and considered significant with a *p*-value lower than or equal to 0.05 ($p \leq 0.05$).

For the IOF "mode of action" test, differences between treatments at each time point were evaluated by one-way ANOVA analysis, followed by Tukey's HSD test. Differences were considered significant with a *p*-value lower than or equal to 0.05 ($p \leq 0.05$).

All values are presented as mean ± standard error mean (SEM). All statistical analyses were performed using JMP-pro 16 software (SAS Institute Inc., Cary, NC).

# 3 Results

## 3.1 In-ovo feeding calibration test

In order to examine the feasibility of creatine injection into broiler embryos, the site of injection and hatching performance test was performed. The IOF solution was designed based on solubility, osmolality (mmol/kg), and pH levels of the amniotic fluid (Omede et al., 2017). Our results prove that when correctly injected with a needle of appropriate length (Figure 1), IOF of creatine in a concentration of 1.5% will not affect embryonic mortality, as hatchability of the IOF creatine group was 95.5% compared to 93.6% of the non-injected control (Table 1). Furthermore, on the day of hatch, IOF creatine hatchlings had significantly higher breast muscle weight with a percentage of 4.2% compared to 3.8% in the

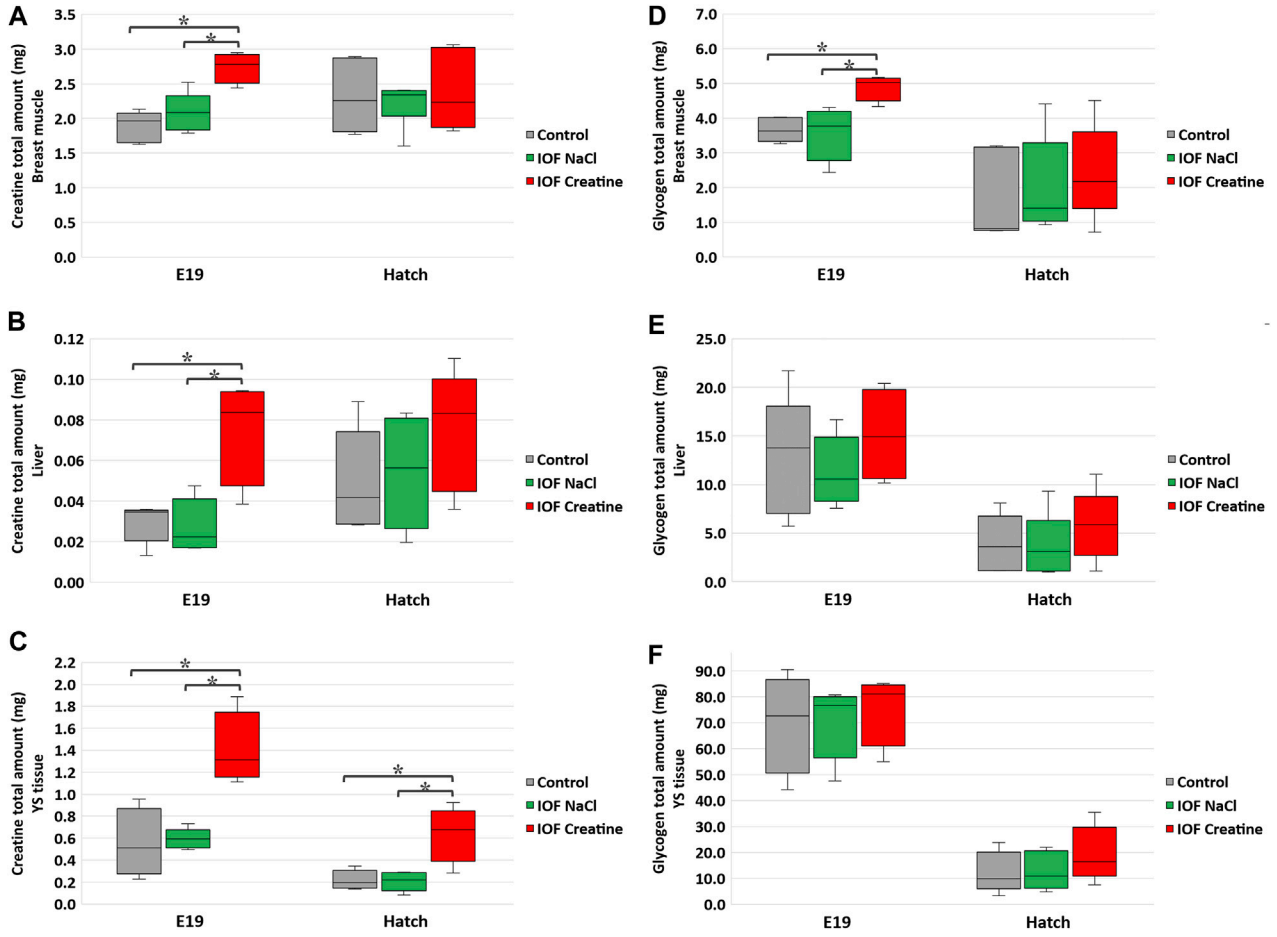


FIGURE 2
Creatine **(A–C)** and glycogen **(D–F)** levels per tissue on E19 and at hatch day of the Control, IOF NaCl, and IOF Creatine treatment groups. Levels are presented as total tissue creatine amount (mg) in breast muscle **(A, D)**, liver **(B, E)**, and YS tissue **(C, F)**. Asterisks denotes means that are significantly different between treatments at each time point, as derived from Tukey's HSD test ($p \leq 0.05$), $n = 6$ per treatment and day.

control group ($p < 0.02$). On day 3 post-hatch, no significant differences were shown.

## 3.2 In-ovo feeding with creatine monohydrate-mode of action

Once optimal conditions were found, and a positive effect of IOF with creatine was observed on breast muscle weight and percentage, a "mode-of-action" experiment was done. In this experiment, the specific effects of creatine enrichment were examined on: (1) energy resources in three key tissues (breast muscle, liver, and YS tissue) and 2) breast muscle histological and molecular parameters during the critical days' pre-to post-hatch [E17-D14]. To this purpose, three treatment groups were selected: control (non-injected), IOF creatine (injection volume: 0.6 mL; 9 mg/embryo of creatine monohydrate and 3 mg of NaCl), and IOF NaCl (injection volume: 0.6 mL; 3 mg/embryo of NaCl). As previously observed for the calibration test, hatchability was not affected by IOF as it ranged between 94.8% in the NaCl group to 95.04% in IOF creatine and 95.4% in the control group.

The total amount (mg) of creatine and glycogen were calculated in order to demonstrate the full capacity of energy storage in each examined tissue as previously described (Yadgary and Uni, 2012; Dayan et al., 2023a). Our results show that on E19, 48 h post-IOF, creatine levels were 45% higher, and glycogen levels were 30% higher ($p < 0.03$) in the breast muscle of the IOF creatine group compared to control and NaCl groups (Figures 2A, D). Analysis of liver and YS tissues on the same day revealed an even higher difference with more than 140% creatine amount ($p < 0.01$) compared to the control and NaCl groups (Figures 2B, C). As for liver and YS tissue glycogen, no significant differences were observed between treatments (Figures 2E, F). At hatch (Figure 2C), YS tissue creatine amount remained significantly higher in the IOF creatine group with over 180% difference ($p < 0.004$). Overall, between E19 and the day of hatch, in all treatments a significant reduction in glycogen amount in the breast muscle, liver, and YS tissue was observed ($p < 0.01$).

Breast muscle percentage was similar in all groups on day 14 post-hatch (16.32% ± 0.33%, 16.49% ± 0.31%, and 16.11% ± 0.79% in control, IOF NaCl, and IOF creatine groups, respectively). To gain further understating of these results we evaluated breast

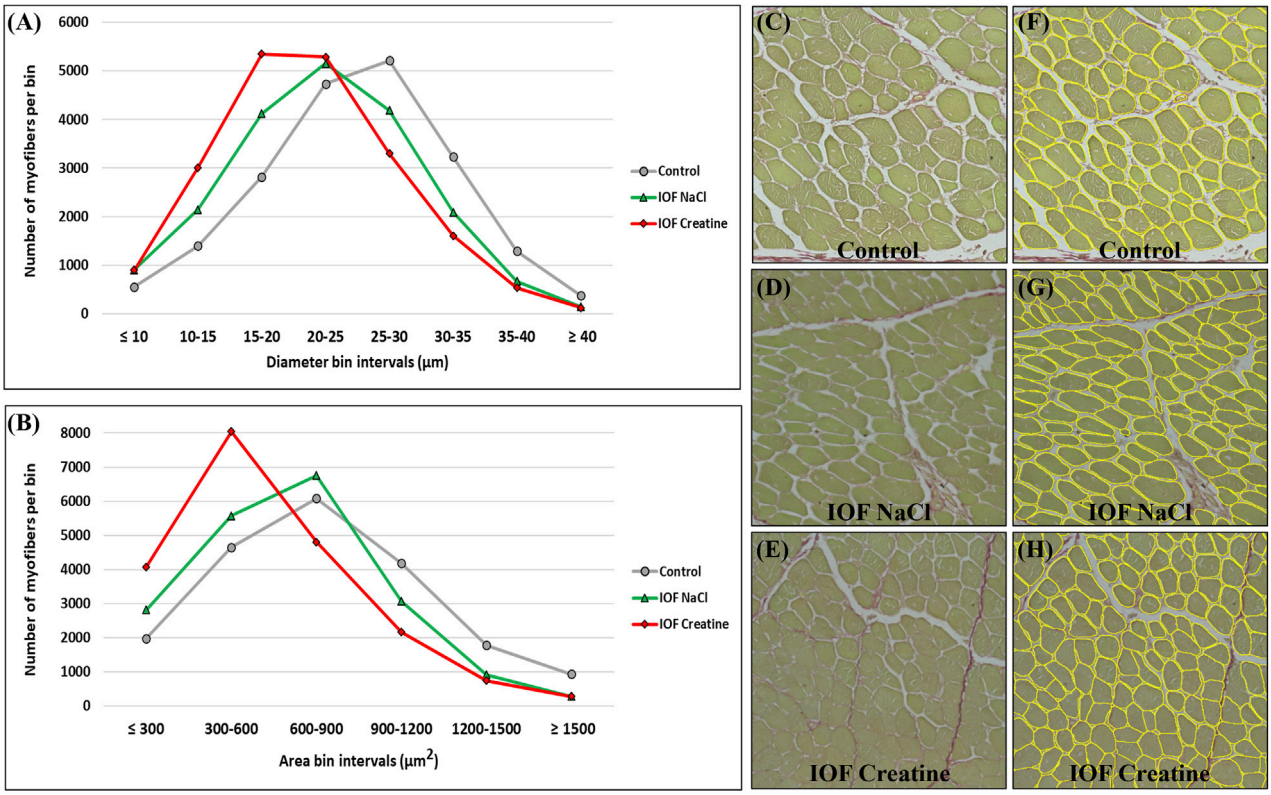


FIGURE 3
Myofiber distribution in the breast muscle (*pectoralis major*) of 14-day-old broiler. Myofibers are clustered in bin intervals where **(A)** displays the diameter distribution in intervals of 5 µm and **(B)** presents the area distribution in intervals of 300 µm$^2$. **(C–H)** A representative field of original sirius red fast green stained images from the control **(C, F)**, IOF NaCl **(D, G)**, and IOF Creatine **(E, H)** treatments. Images were generated using an EVOS FL Auto-inverted microscope with ×60 magnification and are comprised of 12 stitched fields. Measurements were performed using Fiji ImageJ with Cellpose and MorphoLibJ plugins.

**TABLE 2 Histomorphological analysis of the Control, IOF creatine, and IOF NaCl groups.**

| Treatment | Number of myofibers | Myofiber diameter (µm) | Myofiber area (µm$^2$) | Number of myofibers per mm$^2$ |
|---|---|---|---|---|
| Control | 19,610 | 24.97 ± 0.053$^a$ | 787.21 ± 2.84$^a$ | 1,268.52 ± 38.12$^c$ |
| IOF NaCl | 19,415 | 22.43 ± 0.052$^b$ | 667.13 ± 2.39$^b$ | 1,494.34 ± 42.58$^b$ |
| IOF Creatine | 20,103 | 21.14 ± 0.049$^c$ | 577.38 ± 2.36$^c$ | 1797.83 ± 105.38$^a$ |

Summary of morphological analysis and comparison between the Control, IOF, creatine, and IOF, NaCl treatment groups in the pectoral muscle of a 14-day-old broiler. Myofiber diameter and area are presented as mean size ± standard error mean. The number of myofibers per mm$^2$ was calculated for each image. The number of counted myofibers was normalized with the total myofiber area. Superscript letters denote the means that are significantly different between treatments, as derived from Tukey's HSD, test ($p \leq 0.05$), $n = 84$ (four birds per treatment and 7 images per bird). Images comprised of 12 stitched fields of ×60 magnification were generated using an EVOS FL, Auto-inverted microscope.

muscle myofibers' histomorphology on day 14 post-hatch. To that end, a novel deep learning-based automated image analysis tool was applied according to Dayan et al. (2023b). Figures 3C–H shows representative images and the automated identification of myofibers. This enabled us to analyze tens of thousands of myofibers relatively quickly; 19,610, 19,415, and 20,103 for control, IOF NaCl, and IOF creatine treatments, respectively. Our results show that the average myofiber size of the IOF creatine group was significantly smaller ($p < 0.0001$) as the diameter and area were 21.4 and 577.4 µm$^2$, respectively, compared to 22.4 µm, 667.1 µm$^2$ of the IOF NaCl group and 24.9 µm, 787.2 µm$^2$ of the control group (Table 2). Figures 3A, B presents the distribution of myofibers' diameter and area, displaying a distinct Gaussian curve for the IOF creatine group with the highest rate of smaller myofibers. As expected, an opposing trend was demonstrated for the number of myofibers per mm$^2$ (Table 2), with a significantly higher number of myofibers in the IOF creatine group compared to the control and the IOF NaCl groups ($p < 0.004$).

At the molecular level, the evaluation of the "mode of action" on muscle development during the pre-to post-hatching period E17-D6 was performed by examining four genes involved in myoblast proliferation and differentiation; IGF1, MYOG, MyoD, and PCNA (Table 3). In order to evaluate the expression levels of these genes, in each timepoint, data were subjected to one-way ANOVA analysis followed by Tukey's HSD test. For IGF1 and MYOG genes (Figures 4A, B), at hatch, significantly higher

10.3389/fphys.2023.1296342

**TABLE 3** Primers used for real-time PCR gene expression analysis.

| Target[a] | Accession number | Primer F (5′-3′) | Primer R (5′-3′) | Amplicon size | References |
|---|---|---|---|---|---|
| IGF1 | NM_001004384.2 | GTATGTGGAGACAGAGGCTTC | TTGGCATATCAGTGTGGC | 193 | Kornasio et al. (2009) |
| MYOG | D90157.1 | GCGGAGGCTGAAGAAGGT | AGGCGCTCGATGTACTGG | 123 | Chen et al. (2018) |
| MyoD | NM_204214.3 | GACGGCATGATGGAGTACAG | GCTTCAGCTGGAGGCAGTA | 200 | Harding et al. (2016) |
| PCNA | NM_204170.3 | GTGCAAAAGACGGTGTGA | ACCTCAGAGCAAAAGTCAGC | 147 | Primer Blast |
| HPRT | NM_204848 | AAGTGGCCAGTTTGTTGGTC | GTAGTCGAGGGCGTATCCAA | 110 | Boo et al. (2020) |
| β-actin | NM_205518.1 | AATGGCTCCGGTATGTGCAA | GGCCCATACCAACCATCACA | 112 | Primer Blast |

[a]Insulin-like growth factor 1 (IGF1), involved in the induction of muscle cell differentiation and hypertrophy; Myogenin (MYOG), myogenic regulatory factor; Myogenic differentiation protein 1 (MyoD), myogenic regulatory factor; Proliferating cell nuclear antigen (PCNA), a marker for dividing cells; hypoxanthine phosphoribosyl transferase 1 (HPRT) is an enzyme in the purine synthesis in salvage pathway and a housekeeping gene, and; β-actin, a housekeeping cytoskeletal protein.

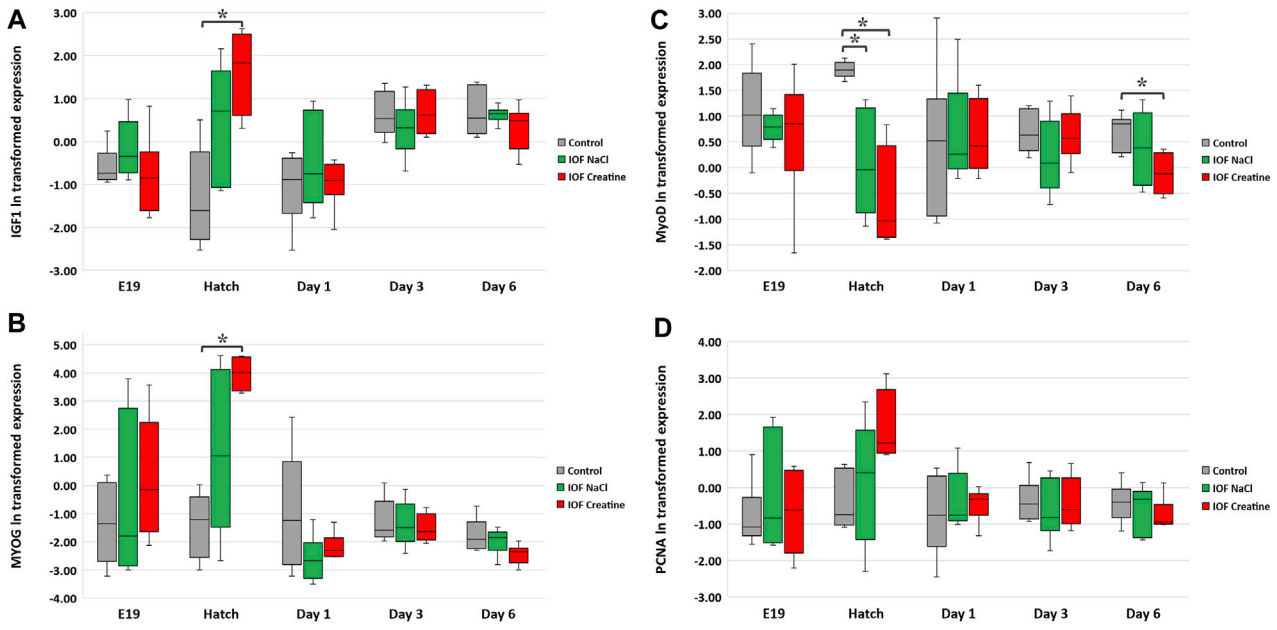


FIGURE 4
Expression analysis of breast muscle genes: **(A)** IGF1, **(B)** MYOG, **(C)** MyoD, and **(D)** PCNA. According to the heterogeneity of variance in embryonic exponential growth, logarithmic (ln) transformation was carried out for the data. Expression is normalized to GEOMEAN of HPRT, β-actin, and is relative to expression on E17 (before IOF). Asterisks denote means that are significantly different between treatments at each time point, as derived from Tukey's HSD test ($p \leq 0.05$), $n = 6$ per treatment and day.

expression levels were found in the IOF creatine group, compared to the control ($p < 0.01$). For the expression of MyoD (Figure 4C), significant differences were found at hatch and on day 6, with higher expression levels in the control group compared to the IOF creatine group ($p < 0.04$). As for the expression of PCNA, although not significant, a trend for higher expression levels is shown in the IOF creatine group at hatch.

# 4 Discussion

The pre-to post-hatching period is recognized as the most dynamic phase throughout the lifespan of broilers, with profound effects on their energy status, survival rate, body weight, post-hatch muscle growth, and the onset of growth-related myopathies (Christensen et al., 1999; Collin et al., 2007; Leksrisompong et al., 2007; Moran, 2007; De Oliveira et al., 2008; Kornasio et al., 2011; Oviedo-Rondón et al., 2020). Given the significance of this critical period, there is a growing interest in exploring the effectiveness of IOF as a potential strategy for optimizing the transition from late-term embryo to hatchling and growing chick (Oliveira et al., 2023). In addition, the selection of meat-type chicken lines for increased growth and muscle development has been accompanied by a significant decrease in muscle energy reserves (Berri et al., 2001). In this study, we evaluated the effect of the IOF with creatine on the energy levels of late-term embryos and hatchlings and post-hatch breast muscle development. We provide an inclusive view of the high-energy value molecules of creatine and glycogen simultaneously in the breast muscle, liver, and YS tissue. The results demonstrate that IOF with creatine elevates high-energy-value molecules in all tissues. On day 14 post-hatch, despite the evidence of highest energy levels post-IOF in the IOF creatine group,

the mean myofiber diameter and area are lower than those found in the other groups. Gene expression analysis implies a possible effect of creatine enrichment by IOF on early post-hatch breast muscle development through differential expression of myogenic-related genes.

An ongoing controversy still exists about the exact method to perform IOF, sometimes leading to different results; clear descriptions are missing in many of the published studies where IOF was used (Oliveira et al., 2023). However, the present study provides a comprehensive view of the IOF procedure, including the site of the injection test designed to confirm the successful delivery of the injected solution to the embryo's amniotic fluid (Uni and Ferket, 2003; Uni et al., 2005). Figure 1 illustrates the embryo's position within the egg on E17.5 and outlines the verification process for optimal needle length. As for the timing of IOF, E17.5 marks the optimal time for injection due to the embryo's favorable positioning, which facilitates relatively easy access to the amniotic fluid. Additionally, IOF at this stage ensures rapid delivery of the solution to the embryo's intestine, as it coincides with the onset of rapid swallowing of the amniotic fluid (Romanoff, 1960). In terms of the effect on muscle development, E17.5 is just between the critical transition period from the second to the third wave of myogenesis (Stockdale, 1992), suggesting that this timing may offer an opportunity for modulatory effects on muscle development and growth (Kornasio et al., 2011). In addition, our study demonstrates the feasibility of creatine injection via IOF, and when performed correctly, IOF will not cause higher embryonic mortality. Indeed, hatchability was similar in all treatments. Moreover, the results revealed that IOF with creatine significantly increased breast muscle weight and percentage at day of hatch, corresponding with previous reports by Zhao et al. (2017a,b).

Creatine was shown to maintain an available energy supply in late-term embryos and hatchlings (Dayan et al., 2023a). This evidence and our present findings of higher creatine amount in the breast muscle, liver, and YS tissue in IOF creatine embryos and hatchlings, suggest their improved energy status. Moreover, in accordance with previous studies, it is suggested that the surplus of breast muscle's creatine and glycogen in the IOF creatine group has slowed down breast muscle catabolism for energy provision towards hatch through protein mobilization and amino acid supply for the gluconeogenic pathway (Uni et al., 2005; Foye et al., 2006; De Oliveira et al., 2008; Kornasio et al., 2011). It can be concluded that the higher levels of creatine and glycogen have contributed to a higher breast muscle weight and percentage at hatch.

To further understand the similar values of breast muscle percentage found on day 14 post-hatch, the hypertrophy of breast myofibers has been evaluated by an automated image analysis tool (Dayan et al., 2023b). This tool enables us to analyze a large number of data sets, with maximal coverage for each examined cross-section, producing a better representation of the examined samples, while providing rapid and high-precision results. Distribution analysis of myofiber diameter and area exhibited the typical Gaussian curve, similar to that reported in previous publications (Halevy et al., 2006; Piestun et al., 2009; Piestun et al., 2011; Piestun et al., 2017; Patael et al., 2019). Surprisingly, despite the evidence of the highest energy levels on E19 and hatch, the IOF creatine group had significantly smaller myofibers with lower mean myofiber diameter and area on day 14. Our findings of decreased myofiber size following the treatment of IOF with creatine differ from those reported by Zhao et al. (2017b) and Firman et al. (2023). Zhao et al. (2017b) used creatine pyruvate, a different creatine source, which has a lower bioavailability compared to the creatine monohydrate used in our study (Deldicque et al., 2007a; Jäger et al., 2007).

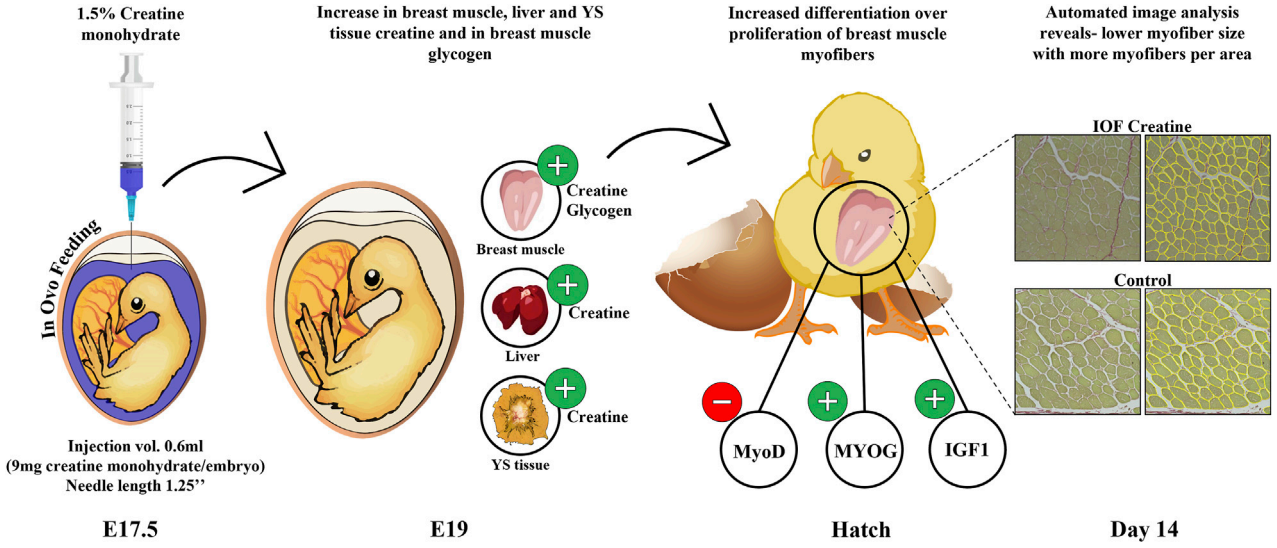


FIGURE 5
Graphical illustration demonstrating the effect of IOF with creatine monohydrate on energy resources (creatine and glycogen) of chicken embryos and the mode of effect on muscle growth during the pre-to post-hatch period. Our study shows an increase in creatine levels in breast muscle, liver, and YS tissue and in glycogen levels in breast muscle towards hatch. This in turn may influence gene expression changes in the IOF creatine group at hatch with modulatory effects on muscle development through differentiation over-proliferation of breast muscle cells. This is shown in reduced MyoD expression over increased MYOG and IGF1 expression and in reduced myofiber size in IOF creatine group compared to control.

Firman et al. (2023) applied a different IOF protocol with injection on E14 compared to injection on E17.5 in our study. Together, the previous and our present findings emphasize the importance of IOF timing and formulation of injected solution.

The higher bioavailability of creatine monohydrate used in our study may explain the rapid elevation of IGF1 and MYOG gene levels and consequently acceleration of muscle cell differentiation. Indeed, results from Deldicque et al. (2007b) and Fernyhough et al. (2010) point toward the role of creatine in accelerating the differentiation rate of myogenic cell lines *in vitro*. This is achieved by activating the p38 and the ERK1/2 mitogen-activated protein kinase (MAPK) as well as the phosphatidylinositol 3-kinase (PI3K) pathways that are known to be key signaling cascades in the differentiation process of myoblasts (Gredinger et al., 1998; Zester et al., 1999; Li, 2000; Li and johnson, 2006). In addition, a previous study showed an induction of IGF1 levels and higher breast muscle percentage in response to dietary guanidinoacetate—a creatine precursor—in broilers (Michiels et al., 2012). IGF1 and MYOG, were shown to be involved in myoblast proliferation, terminal differentiation, and muscle hypertrophy in broilers (Halevy et al., 2001; Halevy et al., 2004). An opposing trend is shown for MyoD expression with the lowest gene expression levels found in the IOF creatine group at hatch. MyoD has a key role in myogenic commitment and lineage of muscle progenitors and is also involved in the proliferation of satellite cells which serve as a pool for newly synthesized myotubes post hatch (Relaix et al., 2004; Gros et al., 2005; Kassar-Duchossoy et al., 2005). Overall, it is plausible that the energy boost achieved by IOF with creatine monohydrate has accelerated the differentiation of myogenic cells while slowing down their proliferation, resulting in premature differentiation with smaller size myofibers on day 14 post-hatch. These findings could be speculated as early signs for developmental abnormalities in the breast muscle (Halevy and Velleman, 2022). Additional analyses such as for collagen and fat accumulation as well as overall morphometry at later time points will shed more light on this speculation.

In summary, our study provides important insights into the optimal procedure for IOF (Figure 1). Moreover, as seen in Figure 5, this study demonstrates that in-ovo creatine monohydrate enrichment of late-term embryos promotes their energy levels towards hatch and modulates early post-hatch muscle development through altered expression of myogenic-related genes. This is implied by higher expression levels of IGF1 and MYOG genes, related to differentiation of myogenic cells, and lower expression of MyoD, related to their proliferation. Thus, resulting in a significantly higher number of myofibers per area with smaller size on day 14 post-hatch. Altogether, the scope of this study exhibits a short-term potential of IOF with highly bioavailable creatine molecule in modulating post-hatch muscle growth and development. Therefore, it is important to examine the long-term effects as well as the formulation of IOF for its potential applications to overcome the current challenges related to muscle development and abnormalities in commercial broiler production.

## Data availability statement

The original contributions presented in the study are included in the article/Supplementary Material, further inquiries can be directed to the corresponding author.

## Ethics statement

The animal study was approved by the Hebrew University Institutional Animal Care and Use Committee (IACUC), approval number: AG-20-16298. The study was conducted in accordance with the local legislation and institutional requirements.

## Author contributions

JD: Conceptualization, Formal Analysis, Methodology, Writing–original draft, Writing–review and editing. TM-Z: Methodology, Writing–review and editing. NG: Writing–review and editing, Methodology, Software. FS: Writing–review and editing, Conceptualization. MZ: Conceptualization, Writing–review and editing. MP: Conceptualization, Writing–review and editing. FS: Conceptualization, Writing–review and editing. UB: Writing–review and editing, Funding acquisition. VI: Funding acquisition, Writing–review and editing. OH: Writing–review and editing, Supervision. ZU: Conceptualization, Supervision, Writing–review and editing.

## Funding

The authors declare financial support was received for the research, authorship, and/or publication of this article. Alzchem Trostberg GmbH provided the creatine monohydrate and a partial funding for this study. The funder was not involved in study design, experimental methodologies, analysis, interpretation of data, the writing of this article or the decision to submit it for publication.

## Conflict of interest

Authors UB and VI were employed by Alzchem Trostberg GmbH.

The remaining authors declare that the research was conducted in the absence of any commercial or financial relationships that could be construed as a potential conflict of interest.

## Publisher's note

All claims expressed in this article are solely those of the authors and do not necessarily represent those of their affiliated organizations, or those of the publisher, the editors and the reviewers. Any product that may be evaluated in this article, or claim that may be made by its manufacturer, is not guaranteed or endorsed by the publisher.

## Supplementary material

The Supplementary Material for this article can be found online at: https://www.frontiersin.org/articles/10.3389/fphys.2023.1296342/full#supplementary-material

# References


Berri, C., Wacrenier, N., Millet, N., and Le Bihan-Duval, E. (2001). Effect of selection for improved body composition on muscle and meat characteristics of broilers from experimental and commercial lines. *Poult. Sci.* 80, 833–838. doi:10.1093/ps/80.7.833

Bessman, S. P., and Carpenter, C. L. (1985). The creatine-creatine phosphate energy shuttle. *Annu. Rev. Biochem.* 54 (1), 831–862. doi:10.1146/annurev.bi.54.070185.004151

Bigot, K., Mignon-Grasteau, S., Picard, M., and Tesseraud, S. (2003). Effects of delayed feed intake on body, intestine, and muscle development in neonate broilers. *Poult. Sci.* 82, 781–788. doi:10.1093/ps/82.5.781

Boo, S. Y., Tan, S. W., Alitheen, N. B., Ho, C. L., Omar, A. R., and Yeap, S. K. (2020). Identification of reference genes in chicken intraepithelial lymphocyte natural killer cells infected with very-virulent infectious bursal disease virus. *Sci. Rep.* 10 (1), 8561. doi:10.1038/s41598-020-65474-3

Chal, J., and Pourquié, O. (2017). Making muscle: skeletal myogenesis *in vivo* and *in vitro*. *Development* 144, 2104–2122. doi:10.1242/dev.151035

Chen, R., Zhuang, S., Chen, Y. P., Cheng, Y. F., Wen, C., and Zhou, Y. M. (2018). Betaine improves the growth performance and muscle growth of partridge shank broiler chickens via altering myogenic gene expression and insulin-like growth factor-1 signaling pathway. *Poult. Sci.* 97, 4297–4305. doi:10.3382/ps/pey303

Christensen, V., Donaldson, W., Nestor, K., and McMurtry, J. (1999). Effects of genetics and maternal dietary iodide supplementation on glycogen content of organs within embryonic turkeys. *Poult. Sci.* 78 (6), 890–898. doi:10.1093/ps/78.6.890

Cogburn, L. A., Trakooljul, N., Chen, C., Huang, H., Wu, C. H., Carré, W., et al. (2018). Transcriptional profiling of liver during the critical embryo-to-hatchling transition period in the chicken (Gallus gallus). *BMC Genomics* 19 (1), 695. doi:10.1186/s12864-018-5080-4

Collin, A., Berri, C., Tesseraud, S., Rodón, F. E. R., Skiba-Cassy, S., Crochet, S., et al. (2007). Effects of thermal manipulation during early and late embryogenesis on thermotolerance and breast muscle characteristics in broiler chickens. *Poult. Sci.* 86 (5), 795–800. doi:10.1093/ps/86.5.795

Davis, R. L., Weintraub, H., and Lassar, A. B. (1987). Expression of a single transfected cDNA converts fibroblasts to myoblasts. *Cell.* 51, 987–1000. doi:10.1016/0092-8674(87)90585-X

Dayan, J., Goldman, N., Waiger, D., Melkman-Zehavi, T., Halevy, O., and Uni, Z. (2023b). A deep learning-based automated image analysis for histological evaluation of broiler pectoral muscle. *Poult. Sci.* 102 (8), 102792. doi:10.1016/j.psj.2023.102792

Dayan, J., Melkman-Zehavi, T., Reicher, N., Braun, U., Inhuber, V., Mabjeesh, S. J., et al. (2023a). Supply and demand of creatine and glycogen in broiler chicken embryos. *Front. Physiol.* 14, 1079638. doi:10.3389/fphys.2023.1079638

Decuypere, E., Tona, K., Bruggeman, V., and Bamelis, F. (2001). The day-old chick: a crucial hinge between breeders and broilers. *World's Poult. Sci. J.* 57 (2), 127–138. doi:10.1079/WPS20010010

Deldicque, L., Décombaz, J., Zbinden Foncea, H., Vuichoud, J., Poortmans, J. R., and Francaux, M. (2007a). Kinetics of creatine ingested as a food ingredient. *Eur. J. Appl. Physiol.* 102, 133–143. doi:10.1007/s00421-007-0558-9

Deldicque, L., Theisen, D., Bertrand, L., Hespel, P., Hue, L., and Francaux, M. (2007b). Creatine enhances differentiation of myogenic $C_2C_{12}$ cells by activating both p38 and Akt/PKB pathways. *Am. J. Physiol. Cell. Physiol.* 293, C1263–C1271. doi:10.1152/ajpcell.00162.2007

De Oliveira, J. E., Uni, Z., and Ferket, P. R. (2008). Important metabolic pathways in poultry embryos prior to hatch. *World's Poult. Sci. J.* 64 (4), 488–499. doi:10.1017/S0043933908000160

Donaldson, W. E. (1995). *Carbohydrate, hatchery stressors affect poult survival*. Feedstuffs (USA).

Fernyhough, M. E., Bucci, L. R., Feliciano, J., and Dodson, M. V. (2010). The effect of nutritional supplements on muscle-derived stem cells *in vitro*. *Int. J. Stem Cells* 3, 63–67. doi:10.15283/ijsc.2010.3.1.63

Firman, C.-A. B., Inhuber, V., Cadogan, D. J., Van Wettere, W. H. E. J., and Forder, R. E. A. (2023). Effect of in ovo creatine monohydrate on hatchability, post-hatch performance, breast muscle yield and fiber size in chicks from young breeder flocks. *Poult. Sci.* 102, 102447. doi:10.1016/j.psj.2022.102447

Foye, O. T., Uni, Z., and Ferket, P. R. (2006). Effect of in ovo feeding egg white protein, β-hydroxy-β-methylbutyrate, and carbohydrates on glycogen status and neonatal growth of turkeys. *Poult. Sci.* 85 (7), 1185–1192. doi:10.1093/ps/85.7.1185

Givisiez, P. E. N., Moreira Filho, A. L. B., Santos, M. R. B., Oliveira, H. B., Ferket, P. R., Oliveira, C. J. B., et al. (2020). Chicken embryo development: metabolic and morphological basis for in ovo feeding technology. *Poult. Sci.* 99, 6774–6782. doi:10.1016/j.psj.2020.09.074

Gokhin, D. S., Ward, S. R., Bremner, S. N., and Lieber, R. L. (2008). Quantitative analysis of neonatal skeletal muscle functional improvement in the mouse. *J. Exp. Biol.* 211, 837–843. doi:10.1242/jeb.014340

Gredinger, E., Gerber, A. N., Tamir, Y., Tapscott, S. J., and Bengal, E. (1998). Mitogen-activated protein kinase pathway is involved in the Differentiation of Muscle Cells. *J. Biol. Chem.* 273, 10436–10444. doi:10.1074/jbc.273.17.10436

Gros, J., Manceau, M., Thomé, V., and Marcelle, C. (2005). A common somitic origin for embryonic muscle progenitors and satellite cells. *Nature* 435, 954–958. doi:10.1038/nature03572

Halevy, O., Geyra, A., Barak, M., Uni, Z., and Sklan, D. (2000). Early post-hatch starvation decreases satellite cell proliferation and skeletal muscle growth in chicks. *J. Nutr.* 130, 858–864. doi:10.1093/jn/130.4.858

Halevy, O., Krispin, A., Leshem, Y., McMurtry, J. P., and Yahav, S. (2001). Early-age heat exposure affects skeletal muscle satellite cell proliferation and differentiation in chicks. *Am. J. Physiol. Regul. Int. Comp. Physiol.* 281, R302–R309. –R309. doi:10.1152/ajpregu.2001.281.1.R302

Halevy, O., Nadel, Y., Barak, M., Rozenboim, I., and Sklan, D. (2003). Early post hatch feeding stimulates satellite cell proliferation and skeletal muscle growth in Turkey poults. *J. F. Nutr.* 133, 1376–1382. doi:10.1093/jn/133.5.1376

Halevy, O., Piestun, Y., Allouh, M. Z., Rosser, B. W. C., Rinkevich, Y., Reshef, R., et al. (2004). Pattern of Pax7 expression during myogenesis in the post-hatch chicken establishes a model for satellite cell differentiation and renewal. *Dev. Dyn.* 231, 489–502. doi:10.1002/dvdy.20151

Halevy, O., and Velleman, S. G. (2022). *Skeletal muscle" in* sturkie's avian Physiology. Elsevier, 565–589. doi:10.1016/B978-0-12-819770-7.00024-4

Halevy, O., Yahav, S., and Rozenboim, I. (2006). Enhancement of meat production by environmental manipulations in embryo and young broilers. *World's Poult. Sci. J.* 62, 485–497. doi:10.1017/S0043933906001103

Harding, R. L., Halevy, O., Yahav, S., and Velleman, S. G. (2016). The effect of temperature on proliferation and differentiation of chicken skeletal muscle satellite cells isolated from different muscle types. *Physiol. Rep.* 4, e12770. doi:10.14814/phy2.12770

Hartley, R. S., Bandman, E., and Yablonka-Reuveni, Z. (1992). Skeletal muscle satellite cells appear during late chicken embryogenesis. *Dev. Biol.* 153, 206–216. doi:10.1016/0012-1606(92)90106-Q

Hasty, P., Bradley, A., Morris, J. H., Edmondson, D. G., Venuti, J. M., Olson, E. N., et al. (1993). Muscle deficiency and neonatal death in mice with a targeted mutation in the myogenin gene. *Nature* 364, 501–506. doi:10.1038/364501a0

Havenstein, G., Ferket, P., and Qureshi, M. (2003a). Carcass composition and yield of 1957 versus 2001 broilers when fed representative 1957 and 2001 broiler diets. *Poul. Sci.* 82 (10), 1509–1518. doi:10.1093/ps/82.10.1509

Havenstein, G., Ferket, P., and Qureshi, M. (2003b). Growth, livability, and feed conversion of 1957 versus 2001 broilers when fed representative 1957 and 2001 broiler diets. *Poult. Sci.* 82 (10), 1500–1508. doi:10.1093/ps/82.10.1500

Jäger, R., Harris, R. C., Purpura, M., and Francaux, M. (2007). Comparison of new forms of creatine in raising plasma creatine levels. *J. Int. Soc. Sports Nutr.* 4, 17. doi:10.1186/1550-2783-4-17

Kassar-Duchossoy, L., Giacone, E., Gayraud-Morel, B., Jory, A., Gomès, D., and Tajbakhsh, S. (2005). Pax3/Pax7 mark a novel population of primitive myogenic cells during development. *Genes. Dev.* 19, 1426–1431. doi:10.1101/gad.345505

Keirs, R. W., Peebles, E. D., Hubbard, S. A., and Whitmarsh, S. K. (2002). Effects of supportive gluconeogenic substances on the early performance of Broilers under adequate brooding conditions. *J. Appl. Poult. Res.* 11, 367–372. doi:10.1093/japr/11.4.367

Kornasio, R., Halevy, O., Kedar, O., and Uni, Z. (2011). Effect of in ovo feeding and its interaction with timing of first feed on glycogen reserves, muscle growth, and body weight. *Poult. Sci.* 90, 1467–1477. doi:10.3382/ps.2010-01080

Kornasio, R., Riederer, I., Butler-Browne, G., Mouly, V., Uni, Z., and Halevy, O. (2009). Beta-hydroxy-beta-methylbutyrate (HMB) stimulates myogenic cell proliferation, differentiation and survival via the MAPK/ERK and PI3K/Akt pathways. *Biochim. Biophys. Acta - Mol. Cell. Res.* 1793, 755–763. doi:10.1016/j.bbamcr.2008.12.017

Leksrisompong, N., Romero-Sanchez, H., Plumstead, P. W., Brannan, K. E., and Brake, J. (2007). Broiler incubation. 1. Effect of elevated temperature during late incubation on body weight and organs of chicks. *Poult. Sci.* 86 (12), 2685–2691. doi:10.3382/ps.2007-00170

Li, J., and Johnson, S. E. (2006). ERK2 is required for efficient terminal differentiation of skeletal myoblasts. *Biochem. Biophys. Res. Comm.* 345, 1425–1433. doi:10.1016/j.bbrc.2006.05.051

Li, Y., Jiang, B., Ensign, W. Y., Vogt, P. K., and Han, J. (2000). Myogenic differentiation requires signalling through both phosphatidylinositol 3-kinase and p38 MAP kinase. *Cell. Signal.* 12, 751–757. doi:10.1016/S0898-6568(00)00120-0

Melo, L. D., Cruz, F. G. G., Rufino, J. P. F., Melo, R. D., Feijó, J. D. C., Andrade, P. G. C. D., et al. (2022). In ovo feeding of creatine monohydrate increases performances of hatching and development in breeder chicks. *Anim. Biotech.* 34, 2979–2989. doi:10.1080/10495398.2022.2126368

Michiels, J., Maertens, L., Buyse, J., Lemme, A., Rademacher, M., Dierick, N. A., et al. (2012). Supplementation of guanidinoacetic acid to broiler diets: effects on

performance, carcass characteristics, meat quality, and energy metabolism. *Poult. Sci.* 91, 402–412. doi:10.3382/ps.2011-01585

Moran, E. T. (2007). Nutrition of the developing embryo and hatchling. *Poult. Sci.* 86 (5), 1043–1049. doi:10.1093/ps/86.5.1043

Noy, Y., and Sklan, D. (1999). Different types of early feeding and performance in chicks and poults. *J. Appl. Poult. Res.* 8, 16–24. doi:10.1093/japr/8.1.16

Oliveira, G. D. S., McManus, C., Salgado, C. B., and Dos Santos, V. M. (2023). Bibliographical mapping of research into the relationship between in ovo injection practice and hatchability in poultry. *Vet. Sci.* 10, 296. doi:10.3390/vetsci10040296

Omede, A. A., Bhuiyan, M. M., Lslam, A. F., and Iji, P. A. (2017). Physico-chemical properties of late-incubation egg amniotic fluid and a potential in ovo feed supplement. *Asian-Australasian J. Anim. Sci.* 30, 1124–1134. doi:10.5713/ajas.16.0677

Otto, A., Schmidt, C., and Patel, K. (2006). Pax3 and Pax7 expression and regulation in the avian embryo. *Anat. Embryol.* 211, 293–310. doi:10.1007/s00429-006-0083-3

Oviedo-Rondón, E. O., Velleman, S. G., and Wineland, M. J. (2020). The role of incubation conditions in the onset of avian myopathies. *Front. Physiol.* 11, 545045. doi:10.3389/fphys.2020.545045

Patael, T., Piestun, Y., Soffer, A., Mordechay, S., Yahav, S., Velleman, S. G., et al. (2019). Early post-hatch thermal stress causes long-term adverse effects on pectoralis muscle development in broilers. *Poult. Sci.* 98, 3268–3277. doi:10.3382/ps/pez123

Pfaffl, M. W. (2007). *"Relative quantification" in real-time PCR*. Abingdon, UK: Taylor & Francis, 89–108.

Piestun, Y., Halevy, O., Shinder, D., Ruzal, M., Druyan, S., and Yahav, S. (2011). Thermal manipulations during broiler embryogenesis improves post-hatch performance under hot conditions. *J. Therm. Biol.* 36, 469–474. doi:10.1016/j.jtherbio.2011.08.003

Piestun, Y., Harel, M., Barak, M., Yahav, S., and Halevy, O. (2009). Thermal manipulations in late-term chick embryos have immediate and longer-term effects on myoblast proliferation and skeletal muscle hypertrophy. *J. Appl. Physiol.* 106, 233–240. doi:10.1152/japplphysiol.91090.2008

Piestun, Y., Patael, T., Yahav, S., Velleman, S. G., and Halevy, O. (2017). Early post-hatch thermal stress affects breast muscle development and satellite cell growth and characteristics in broilers. *Poult. Sci.* 96, 2877–2888. doi:10.3382/ps/pex065

Relaix, F., Rocancourt, D., Mansouri, A., and Buckingham, M. (2004). Divergent functions of murine Pax3 and Pax7 in limb muscle development. *Genes. Dev.* 18, 1088–1105. doi:10.1101/gad.301004

Romanoff, A. L. (1960). *The avian embryo*. New York, NY: Wiely.

Sparrow, J. C., and Schöck, F. (2009). The initial steps of myofibril assembly: integrins pave the way. *Nat. Rev. Mol. Cell. Biol.* 10, 293–298. doi:10.1038/nrm2634

Stockdale, F. E. (1992). Myogenic cell lineages. *Dev. Biol.* 154, 284–298. doi:10.1016/0012-1606(92)90068-R

Tazawa, H., Visschedijk, A. H. J., Wittmann, J., and Piiper, J. (1983). Gas exchange, blood gases and acid-base status in the chick before, during and after hatching. *Resp. Physiol.* 53, 173–185. doi:10.1016/0034-5687(83)90065-8

Uni, Z., and Ferket, P. R. (2003). *Enhancement of development of oviparous species by in ovo feeding*. USA: Patent US6592878B2.

Uni, Z., Ferket, P. R., Tako, E., and Kedar, O. (2005). In ovo feeding improves energy status of late-term chicken embryos. *Poult. Sci.* 84 (95), 764–770. doi:10.1093/ps/84.5.764

Uni, Z., and Ferket, R. P. (2004). Methods for early nutrition and their potential. *World's Poult. Sci. J.* 60 (1), 101–111. doi:10.1079/WPS20038

Uni, Z., Yadgary, L., and Yair, R. (2012). Nutritional limitations during poultry embryonic development. *J. App. Poult. Res.* 21, 175–184. doi:10.3382/japr.2011-00478

White, R. B., Biérinx, A.-S., Gnocchi, V. F., and Zammit, P. S. (2010). Dynamics of muscle fibre growth during postnatal mouse development. *BMC Dev. Biol.* 10, 21. doi:10.1186/1471-213X-10-21

Wyss, M., and Kaddurah-Daouk, R. (2000). Creatine and creatinine metabolism. *Physiol. Rev.* 80, 1107–1213. doi:10.1152/physrev.2000.80.3.1107

Yadgary, L., Cahaner, A., Kedar, O., and Uni, Z. (2010). Yolk sac nutrient composition and fat uptake in late-term embryos in eggs from young and old broiler breeder hens. *Poul. Sci.* 89 (11), 2441–2452. doi:10.3382/ps.2010-00681

Yadgary, L., and Uni, Z. (2012). Yolk sac carbohydrate levels and gene expression of key gluconeogenic and glycogenic enzymes during chick embryonic development. *Poult. Sci.* 91 (2), 444–453. doi:10.3382/ps.2011-01669

Ye, J., Coulouris, G., Zaretskaya, I., Cutcutache, I., Rozen, S., and Madden, T. L. (2012). Primer-BLAST: a tool to design target-specific primers for polymerase chain reaction. *BMC Bioinforma.* 13 (1), 134. doi:10.1186/1471-2105-13-134

Zammit, P. S. (2017). Function of the myogenic regulatory factors Myf5, MyoD, Myogenin and MRF4 in skeletal muscle, satellite cells and regenerative myogenesis. *Seminars Cell. & Dev. Biol.* 72, 19–32. doi:10.1016/j.semcdb.2017.11.011

Zammit, P. S., Partridge, T. A., and Yablonka-Reuveni, Z. (2006). The skeletal muscle satellite cell: the stem cell that came in from the cold. *J. Histoch. Cytochem.* 54, 1177–1191. doi:10.1369/jhc.6R6995.2006

Zetser, A., Gredinger, E., and Bengal, E. (1999). p38 mitogen-activated protein kinase pathway promotes skeletal muscle differentiation. Participation of the Mef2c transcription factor. *J. Biol. Chem.* 274, 5193–5200. doi:10.1074/jbc.274.8.5193

Zhang, L., Zhu, X. D., Wang, X. F., Li, J. L., Gao, F., and Zhou, G. H. (2016). Individual and combined effects of in-ovo injection of creatine monohydrate and glucose on somatic characteristics, energy status, and post-hatch performance of broiler embryos and hatchlings. *Poult. Sci.* 95 (10), 2352–2359. doi:10.3382/ps/pew130

Zhao, M. M., Gao, T., Zhang, L., Li, J. L., Lv, P. A., Yu, L. L., et al. (2017a). Effects of in ovo feeding of creatine pyruvate on the hatchability, growth performance and energy status in embryos and broiler chickens. *Animal* 11, 1689–1697. doi:10.1017/S1751731117000374

Zhao, M. M., Gao, T., Zhang, L., Li, J. L., Lv, P. A., Yu, L. L., et al. (2017b). In ovo feeding of creatine pyruvate alters energy reserves, satellite cell mitotic activity and myogenic gene expression of breast muscle in embryos and neonatal broilers. *Poult. Sci.* 96, 3314–3323. doi:10.3382/ps/pex150

Zuidhof, M. J., Schneider, B. L., Carney, V. L., Korver, D. R., and Robinson, F. E. (2014). Growth, efficiency, and yield of commercial broilers from 1957, 1978, and 2005. *Poult. Sci.* 93 (12), 2970–2982. doi:10.3382/ps.2014-04291

frontiers | Frontiers in Physiology

TYPE Original Research
PUBLISHED 08 January 2024
DOI 10.3389/fphys.2023.1305168



OPEN ACCESS

EDITED BY
Servet Yalcin,
Ege University, Türkiye

REVIEWED BY
John Even Schjenken,
The University of Newcastle, Australia
Dayal Nitai Das,
National Dairy Research Institute (Southern Regional Station), India

*CORRESPONDENCE
Kristen Brady,
kristen.brady@usda.gov

†These authors have contributed equally to this work

RECEIVED 30 September 2023
ACCEPTED 18 December 2023
PUBLISHED 08 January 2024

CITATION
Brady K, Krasnec K, Hanlon C and Long JA (2024), Turkey hen sperm storage tubule transcriptome response to artificial insemination and the presence of semen. *Front. Physiol.* 14:1305168. doi: 10.3389/fphys.2023.1305168



# Turkey hen sperm storage tubule transcriptome response to artificial insemination and the presence of semen

Kristen Brady[1]*, Katina Krasnec[2†], Charlene Hanlon[3†] and Julie A. Long[1]

[1]Animal Biosciences and Biotechnology Laboratory, Beltsville Agricultural Research Center, Agricultural Research Service, United States Department of Agriculture, Beltsville, MD, United States, [2]Mouse Genetics and Gene Modification Section, Comparative Medicine Branch, National Institute of Allergy and Infectious Diseases, NIH, Bethesda, MD, United States, [3]Department of Poultry Science, Auburn University, Auburn, AL, United States

**Introduction:** Sperm storage within the uterovaginal junction (UVJ) of avian species occurs in specialized structures termed sperm storage tubules (SSTs) and allows for prolonged storage of semen, though the molecular mechanisms involved in semen preservation are not well understood. Little work has been done examining how function of the SSTs is impacted by insemination and by semen present in the SSTs.

**Methods:** Transcriptome analysis was performed on isolated SSTs from turkey hens receiving no insemination (control), sham-insemination, or semen-insemination at three timepoints (D1, D30, and D90 post-insemination). Bioinformatic and functional annotation analyses were performed using CLC Genomics Workbench, Database for Annotation, Visualization, and Integrated Discovery (DAVID), and Ingenuity Pathway Analysis (IPA). Pairwise comparisons and k-medoids cluster analysis were utilized to decipher differential expression profiles in the treatment groups.

**Results:** The SST transcriptome of the semen inseminated group exhibited the greatest differences within the group, with differences detectable for up to 90 days post insemination, while control and sham-inseminated groups were more similar. In the semen-inseminated samples, upregulation of pathways relating to classical and non-classical reproductive signaling, cytoskeletal remodeling, physiological parameters of the local UVJ environment, and cellular metabolism was observed. In the sham-inseminated samples, upregulation of immune pathways and non-reproductive endocrine hormones was observed.

**Discussion:** This work provides insights into the molecular level changes of the SST in response to insemination as well as to the presence of semen. Results from this study may have direct implications on fertility rates as well as potential strategies for avian semen cryopreservation protocols.

KEYWORDS

**Turkey, sperm storage tubule, fertility, artificial insemination, transcriptome**

# 1 Introduction

Avian species are capable of prolonged sperm storage in the female reproductive tract due to specialized tubular glands that invaginate the mucosal folds of the uterovaginal junction (UVJ), referred to as sperm storage tubules (SST). SST differentiation immediately precedes sexual maturation, with simple columnar epithelium as the primary site responsible for prolonged fertility following a single artificial insemination or natural mating interaction (Christensen, 1981; Bakst, 1994). In avian species, duration of fertility from a single artificial insemination corresponds to the number and size of the SST present in the UVJ and varies across species. The turkey hen has been shown to possess up to 30,566 elongated SST, capable of storing sperm for up to 70 days compared to the domestic chicken, which has only up to 4,893 shorter SST, capable of storing sperm for only 21 days (Birkhead and Møller, 1992; Bakst et al., 2010). Despite stark differences in SST numbers between avian species correlated with duration of fertility, SST number does not differ between low fertility and high fertility hens within the same flock, indicating that SST functional differences are responsible for downstream differences in flock fertility rates. Further, knowledge of how SST preserve sperm function for an extended period could be exploited to improve current semen cryopreservation procedures. Semen cryopreservation has not yet proven to be economically feasible in the poultry industry, as fertility rates have been reported to decline dramatically after only 6 h of storage at 4°C (Long and Conn, 2012). The development of greater understanding of the changes occurring *in vivo* during sperm storage provides an opportunity to simulate the SST environment for the cryopreservation of semen in the poultry industry.

SST function encompasses sperm entry into the SST, sperm maintenance within the SST, and sperm release from the SST. SST selectivity acts as a significant barrier for sperm entry into the SST, with only approximately one percent of all inseminated sperm being stored. Overall, most of the sperm is expelled from the reproductive tract or triggers an immunological response, leaving only high-quality sperm to be selected for subsequent fertilization (Brillard, 1993). Within the SST, spermatozoa arrange in parallel bundles with the heads pointed at the blind end of the tubules (Bobr et al., 1964; Tingari and Lake, 1973). While in the SST, spermatozoa are maintained in a quiescent state, with a lowered rate of metabolism due to immotility (Bakst, 1987; Holm et al., 2000). SST release mechanisms have been widely investigated in regard to the timing of oviposition and ovulation, as sperm must reach the infundibulum of the oviduct shortly after follicle ovulation occurs. An initial hypothesis regarding the mechanical stimulation of release following the egg passing through the UVJ (Van Krey et al., 1967; Mero and Ogasawara, 1970) has been previously disputed by Bobr et al. (1964), who determined that spermatozoa were released around the time of follicle ovulation. This was further supported by Ito et al. (2011), who demonstrated that exogenous progesterone was able to stimulate SST sperm release. This work suggests that SST release is coordinated to occur immediately prior to the time of ovulation (Das et al., 2006).

Several studies have also investigated oviductal immunological response in virgin, sham-inseminated, and semen-inseminated layer hens. Compared to virgin hens, repeated inseminations with semen led to a reduction in fertility rates. This is suggested to be a consequence of swollen SST with a thinned epithelial layer and elevated lymphocyte populations, indicating that repeated artificial insemination (AI) will break down SST over time and reduce their functionality over the course of a breeding cycle (Das et al., 2005b). Bakst (1987) determined that virgin and sperm-inseminated hens displayed a similar number of intraepithelial lymphocytes during the later stages of the laying cycle (52 weeks), a signal that SST immune response may be inevitable regardless of sperm presence. It was proposed that this response may be triggered as the hen ages by an autoimmune reaction to an estrogen-dependent factor associated with SST (Bakst, 1987). Recently, estrogen receptor alpha (ERα) mRNA in the UVJ was observed to decline following repeat AI hens in comparison to virgin hens (Das et al., 2006). Thus, estrogen is unlikely to be the sole component of this immunological response due to changes in UVJ responsivity to this hormone in the presence of sperm. While the overall intraepithelial lymphocyte populations are elevated with age, regardless of insemination status, further investigation into lymphocytes determined that both $CD4^+$ and $CD8^+$ T cells were upregulated following repeated AI. T cell upregulation demonstrates a more robust cell-mediated immune response along with the capacity to stimulate macrophages, B cells, and plasma cells, that correspond to lower fertility rates (Das et al., 2005a). Interestingly, while these cell types were also present in the oviductal mucosal tissue of laying hens undergoing repeated AI (Zheng et al., 1998; 2001), elevated levels of antibody-producing plasma cells were found in the SST epithelium of infertile turkey hens (Van Krey et al., 1987). While the strong immune reaction in response to repeated AI has been identified, it remains unclear how immunity impacts SST filling and release rates, and if this response is directly linked to declining fertility.

We have previously characterized the SST transcriptome throughout the first 90 days of the production cycle following a single post-lay insemination. Through that characterization, we have identified genes involved in immune response, hormone signaling, ion homeostasis, sperm motility, and cytoskeletal reorganization that are hypothesized to play a critical role in the declining fertility rates with flock age (Brady et al., 2022). However, it remains unclear if these expression changes are the result of the presence of semen or the mechanical process of AI. To fully elucidate these differences, this study examined the transcriptomic profiles between virgin (non-inseminated), sham-inseminated, and semen-inseminated turkey hens over the course of fertility to identify the impact of sperm in comparison to mechanisms of insemination on genomic regulation and activity. The turkey industry relies exclusively on AI to produce poults used for subsequent meat production. Further investigation is necessary to differentiate SST response to the act of AI and to the presence of semen. Aside from a direct impact on flock fertility rates, a deeper understanding of SST function could also have implications on poultry semen cryopreservation protocols.

# 2 Materials and methods

## 2.1 Bird husbandry and insemination

All procedures in this study were approved by the Institutional Animal Care and Use Committee of the Beltsville Animal Research

Center, United States Department of Agriculture. Commercial lines of turkey hens and toms were obtained for this study (Hendrix Genetics, Kitchener, Ontario, Canada) and housed separately. Hens were placed in individual cages to monitor egg production, and toms were kept in floor pens ($n$ = 8–10 toms per pen). A ratio of 4 hens per tom was maintained throughout the study. All hens were housed under non-stimulatory photoperiods of 6L:18D to maintain the reproductive system in an immature state. At 27 weeks of age (woa), hens were photostimulated with 14L:10D to encourage the initiation of sexual maturation, inducing egg production. Toms were initially housed under 12L:12D until 28 woa, during which they were also photostimulated with 14L:10D to stimulate testicular maturation and semen production. As per the industry standard, all birds were provided *ad libitum* access to feed and water throughout the study.

Hens were randomly allocated to one of three treatments ($n$ = 3 per group): no insemination (control), sham-insemination with 50 µL of Beltsville Turkey Semen Extender (Continental, Delavan, WI) only, or semen-insemination with a dose of $2.5 \times 10^8$ sperm per hen + Beltsville Turkey Semen Extender in a 1:1 ratio totaling 50 µL. For the semen-inseminated group, toms were milked twice per week, simulating the conditions of the industry. This preparation began at 30 woa to familiarize the males with the abdominal message method (Burrows and Quinn, 1935) and to determine the quality of the semen through previously established screening techniques at 31 and 32 woa (Long and Kulkarni, 2004). All semen determined to be acceptable and passing the quality check were pooled at 32 woa to ensure the same pool of semen was used in all AI for the study. Two pre-lay inseminations were performed at 8 and 11 days post-photostimulation. Two weeks post-photostimulation (29 woa), a single, post-lay insemination occurred, referred to as D0.

## 2.2 UVJ tissue and SST isolation

At D1, D30, and D90, representing the days post-AI (D0), turkey hens were euthanized via pentobarbital sodium and phenytoin sodium injection (390:50 mg). Each treatment group contained 3 replicates per time point. Following euthanasia, the UVJ was dissected from the oviduct of the hen, as previously outlined by Bakst (1992). The UVJ was excised from the vagina and shell gland, and a longitudinal incision was made to display the mucosal folds known to contain SST. This region underwent microscopic analysis to identify the specific location of SST, with SST-containing regions excised. Each region was embedded in optimal cutting temperature compound (Tissue Tek, Leica Microsystems, Buffalo Grove, IL) in 25 × 20 × 5 mm cryomolds before snap freezing in liquid nitrogen and storage at −80°C. This entire procedure, from euthanasia to freezing, was conducted within 20 min. SST were isolated from the UVJ using methods previously described by Brady et al. (2022). Snap-frozen blocks were sectioned using a Lecia CM1860 cryostat at a thickness of 10 µm and positioned onto PEN membrane 2 µm slides (Leica Microsystems). Following staining with Nuclear Fast Red (Sigma-Aldrich, Inc., St. Louis, MO), individual SST structures were visualized at ×10 magnification and isolated using the Leica LMD7 (Lecia Microsystems). These structures were removed from the surrounding UVJ via laser capture microdissection techniques outlined by Brady et al. (2022) and stored at −80°C until RNA isolation. On average, 317.26 ± 11.62 SST were isolated from each slide, and the average surface area was 1,953,668.81 ± 516,597.16 µm$^2$.

## 2.3 RNA isolation, quality assessment and sequencing

RNA isolation, quality assessment, and sequencing were performed as previously described (Brady et al., 2022). Isolated SST total RNA was extracted using the RNeasy Plus Micro Kit (Qiagen) according to the provided protocol as well as on-column deoxyribonuclease digestion. The RNA purity and concentration were determined using the Tapestation RNA HS Assay (Agilent, Santa Clara, CA, United States) and the Qubit RNA HS assay (Thermo Fisher Scientific, Carlsbad, CA, United States), respectively. RNA integrity number (RIN) values were determined using a Bioanalyzer 2100 (Agilent, Santa Clara, CA, United States), with an average RIN value of 8.0 ± 0.1. Libraries were constructed with the SMARTer Stranded RNA-Seq Kit (Takara Bio Inc., San Jose, CA, United States), then quantified using KAPA SYBR FAST qPCR (Roche Diagnostics, Basel, Switzerland), and quality was determined through the Tapestation RNA HS Assay (Agilent, Santa Clara, CA, United States). Sequencing was performed using the Illumina HiSeq platform according to Illumina protocols and paired end-reads of 2 × 150 bp were generated. Images were produced by the base calling pipeline using RTA 1.18.64.0 and were stored as FASTQ files.

## 2.4 Bioinformatic analysis of sequencing data

All sequencing files (Bioproject: PRJNA1022824; Biosamples: SAMN37628532- SAMN37628544, SAMN37628829- SAMN37628838, SAMN37629530- SAMN37629533) were submitted to the NIH Short Read Archive (https://www.ncbi.nlm.nih.gov/sra). Bioinformatic analysis was conducted using CLC Genomics Workbench 20.0 (Qiagen; https://digitalinsights.qiagen.com). The quality of sequence reads (raw and trimmed) was verified using FastQC (http://www.bioinformatics.babragam.ac.uk/projects/fastqc/) (Andrews, 2010) to determine sequencing read artifacts, including sites with a low-quality Phred score (<20), with reads falling below this threshold trimmed. Removal of low-quality reads was performed using the trimming tool of the CLC Genomics Workbench platform. Reads that passed quality control were aligned to the most recent *Meleagris gallopavo* reference genome (Turkey_5.1; NCBI annotation release 103: https://www.ncbi.nlm.nih.gov/datasets/genome/GCF_000146605.3/). Differentially expressed genes (DEGs) were determined using CLC Genomic Workbench, with cutoffs of a $q$-value of <0.05, an absolute fold change greater than 1.5, and an FPKM value greater than 1 (Liu and Di, 2020). DEGs were determined through pairwise comparisons between control and sham-inseminated treatment groups and between sham-inseminated and semen-inseminated treatment groups at D1, D30, and D90 timepoints. Additionally, k-medoids cluster analysis was performed at each timepoint to determine genes with expression profiles peaking in control, sham-inseminated, and semen-inseminated SST samples. Features used for clustering were restricted to genes with expression levels significantly impacted by treatment at each given timepoint. Lastly, a one-way ANOVA was performed to determine genes statistically impacted by treatment at each timepoint.

**TABLE 1** Primer sequences used for confirmation of gene expression results obtained from RNA sequencing.

| Gene | Forward | Reverse |
|---|---|---|
| *SCD* | CAATGCCACCTGGCTAGTGA | GGTGGAGTAGTCGTAGGGGA |
| *SPARC* | AAGTGCACCTTGGAGGGAAC | GCGCTTCTCATTCTCGTGGA |
| *SERPINB5* | AAGCTACGTTTTGCCTGGGT | TCAGGGGTGAGTGCCTTTTC |
| *KCNMB1* | CAGCCTCAGGACAAGAGGTC | GTGAAGAGGAGGCCTTTGGG |
| *SPINT4* | ATTTCTGCACGGTCACTCCC | CGCGTTGTAGAAGAAGCGGAT |
| *CYGB* | GGAGAACCTCAACGACCCAG | CACGTGGGTGTAGATGAGGG |
| *UBB* | TCAAGCAAGATGCACAGCAC | TTTCAACATACAGATCAGCAG |
| *TUBB3* | CAGTTTTGGGAGGTGATCAGCGA | CCCGCTCTGACCGAAAATGA |
| *BTUBB* | TTGGCCCACTATTTCGACCT | GTCACAGCTCTCACACTCGT |

Over-represented gene ontology (GO) biological processes, cellular components, and molecular functions as well as KEGG pathways were identified using Database for Annotation, Visualization, and Integrated Discovery (DAVID), utilizing *Meleagris gallopavo* as the species to include any avian-specific mechanisms (Huang et al., 2009a; Huang et al., 2009b). DEGs were also analyzed with Ingenuity Pathway Analysis (IPA) to determine significant networks and upstream regulators (Qiagen; https://www.qiagen bioinformatics.com/products/ingenuity-pathway-analysis; Kramer et al., 2014). All three time points were examined individually using the core analysis function and then evaluated using the comparison analysis function of IPA. Generated networks with a network score of 35 or higher were considered significant. An absolute z-score greater than 2 and a $p$-value <0.05 was considered significantly activated or inhibited for the analysis of upstream gene regulators. Though very extensive, the knowledge base of IPA is currently human/mouse centric, which could exclude avian specific mechanisms occurring in SST.

## 2.5 RNA-seq gene expression validation

Reverse transcription (RT) was performed on 10 ng of all RNA-extracted samples using SuperScript III (Thermo Fisher Scientific, Waltham, MA, United States) and an anchored dT primer (Integrated DNA Technologies, Skokie, IL, United States), according to the manufacturer protocols. A negative control sample without reserve transcriptase was also prepared from pooled RNA to control for any genomic DNA contamination (no RT). RT-qPCR was conducted on 6 randomly selected DEGs to determine expression profiles. All primers (Integrated DNA Technologies, Skokie, IL, United States) were designed using primer BLAST software (NCBI, Bethesda, MD, United States) (Table 1). Primer pairs were validated as previously described (Brady et al., 2019; Brady et al., 2022). Briefly, dissociation curve analysis and gel electrophoresis were conducted for each primer pair to ensure amplification of a single PCR product of expected size and was absent from the no RT and water controls (Brady et al., 2022). Primer pairs were also validated for amplification efficiencies and sequencing of the resulting PCR product (Brady et al., 2019). Amplification was performed using the CFX Connect Real-Time PCR System (Bio-Rad, Hercules, CA, United States), using 1 µL of cDNA, 0.6 µL of each of the forward and reverse primers (final concentration in PCR reaction of 0.4 µm), 7.5 µL of 2X iTaq Universal SYBR Green Supermix (Bio-Rad, Hercules, CA), and 5.3 µL of nuclease-free water. The PCR cycling conditions were as follows: initial denaturation at 95°C for 3 min followed by 40 cycles of 95°C for 15 s, 60°C for 30 s, and 72°C for 30 s. Data were normalized to the average mean of the housekeeping genes, *TUBB3, UBB,* and *BTUBB* (Livak and Schmittgen, 2001), and the $2^{-\Delta\Delta Ct}$ method was used. Housekeeping genes were selected based on expression levels across the experimental groups in the RNA sequencing dataset and housekeeping gene mRNA levels resulting from RT-qPCR were confirmed to be insignificant between experimental groups through statistical analysis prior to normalization. Levels of mRNA for each gene are presented relative to the average of the control treatment group for each timepoint. SAS v9.4 (SAS Institute, Cary, NC, United States) was used to perform a Pearson's correlation comparing the $\log_2$ fold change values obtained through RT-qPCR and RNA sequencing.

# 3 Results

A total of 2.7 billion reads were obtained across the 27 samples sequenced, with an average read count of 99 ± 5.9 million reads per sample (Supplementary Figures S1A). Following quality assessment and trimming, a total of 2.4 billion reads remained, with an average read count of 88 ± 5.2 million reads per sample. On average, 86.31% ± 0.45% of reads mapped in pairs, 2.01% ± 0.13% of reads mapped in broken pairs, and 11.68% ± 0.41% of reads did not map to the turkey genome (Supplementary Figures S1B). No significant differences were identified between experimental treatments or timepoints related to reads obtained, trimmed read counts, or read mapping ($p > 0.05$).

At day 1 (D1), a total of 677 DEGs were identified as statistically significant due to treatment. Cluster analysis revealed a total of 104 DEGs upregulated in control samples, 248 DEGs upregulated in sham samples, and 325 DEGs upregulated in experimental samples (Figure 1). SST isolated from control hens exhibited increased expression for genes associated with ion channel activity, thyroid/parathyroid hormone activity, cell proliferation, and proteolysis.

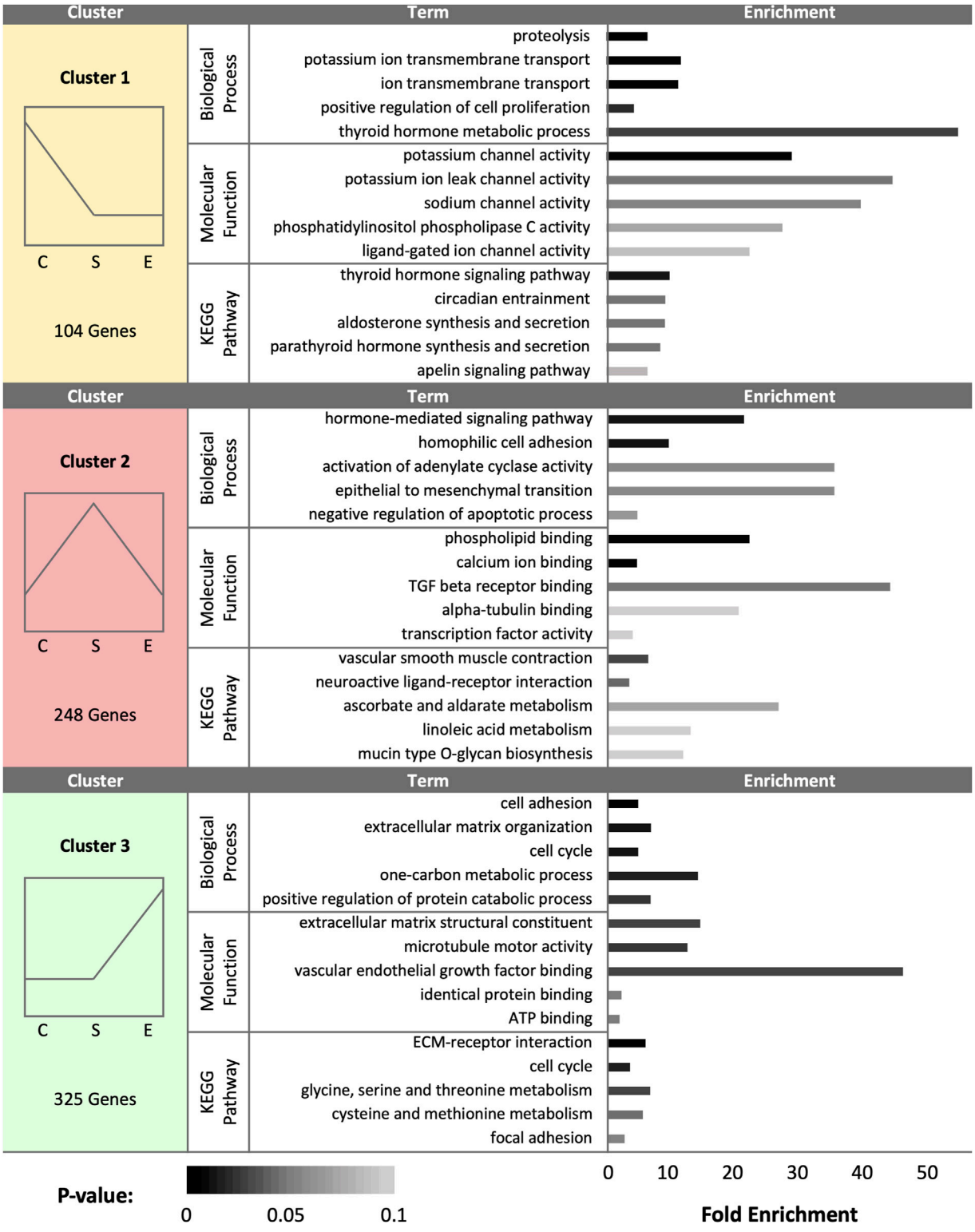


FIGURE 1
K-medoids cluster analysis of sperm storage tubules (SSTs) isolated from: control, sham-inseminated, and semen-inseminated at 1-day post-insemination (D1). The k-medoids cluster analysis tool from CLC Genomics (Qiagen, Valencia, CA) was used to identify genes exhibiting peak expression in treatment group. Genes included in the analysis were differentially expressed due to treatment ($q < 0.05$). Left panels show the expression profile and number of genes in each cluster (C = control, S = sham-insemination, E = semen-insemination). Right panels show enriched gene ontology (GO) term biological processes and molecular functions as well as KEGG pathway enrichment generated from Database for Annotation, Visualization, and Integrated Discovery (DAVID).

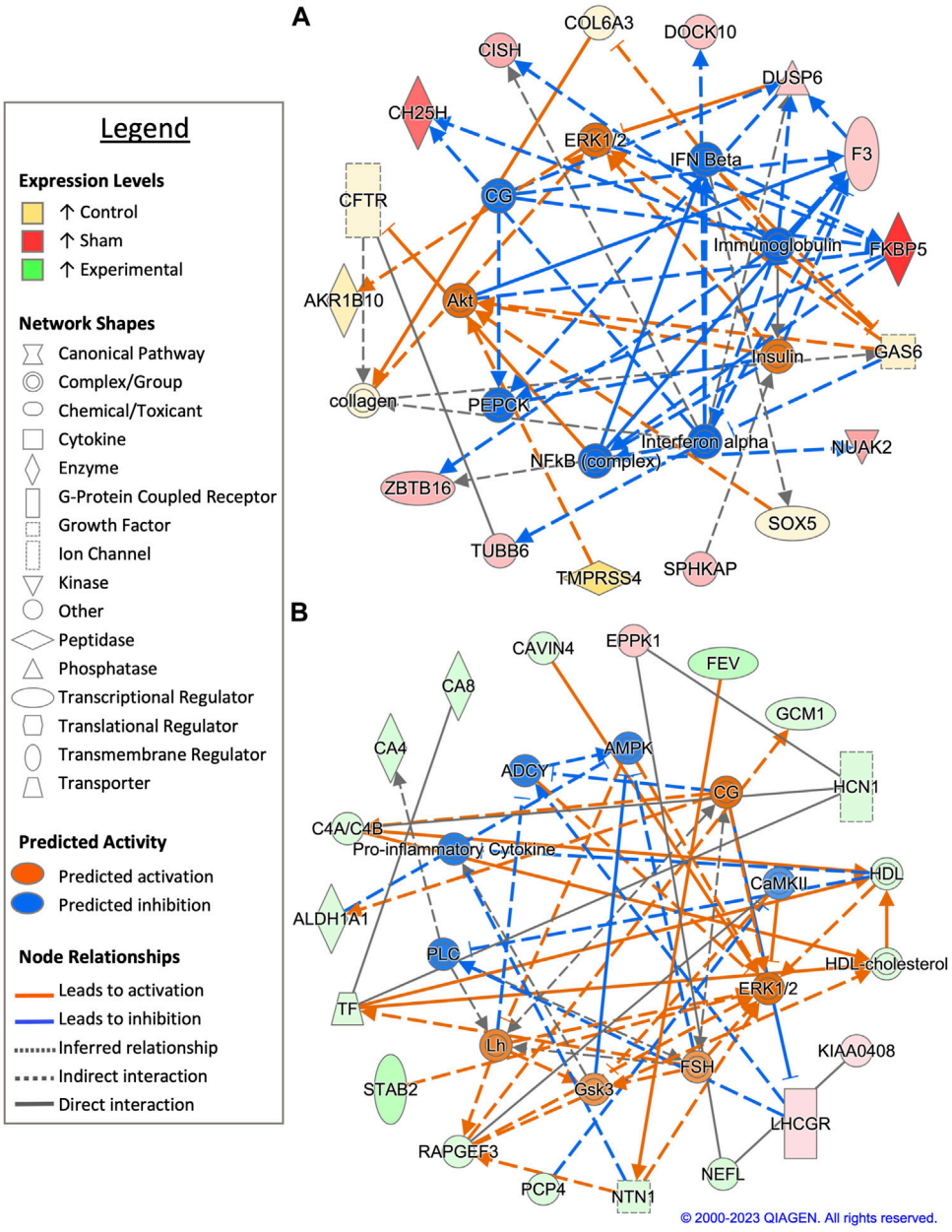


FIGURE 2
Network analysis of sperm storage tubules (SSTs) isolated at 1 day post insemination (D1). The core analysis tool from Ingenuity Pathway Analysis (IPA) (Qiagen, Valencia, CA) was used to biologically interpret differentially expressed genes (DEGs). Copyright permission from Qiagen has been obtained for use of the images presented. **(A)** The top network generated through pathway analysis of DEGs between control and sham-inseminated hens (FPKM > 1, $q$-value < 0.05, |fold change| > 1.5). **(B)** The top network generated through pathway analysis of DEGs between sham-inseminated and semen-inseminated hens (FPKM > 1, $q$-value < 0.05, |fold change| > 1.5).

Pathway enrichment in control hen samples was related to thyroid/parathyroid signaling, circadian entrainment, aldosterone signaling, and apelin signaling. SST isolated from sham-inseminated hens displayed upregulation of genes related to hormone response, cell adhesion, epithelial cell differentiation, and transcription factor activity. Pathway enrichment in sham-inseminated hen samples was related to muscle contraction, ligand-receptor interaction, metabolic networks, and mucin type o-glycan biosynthesis. SST isolated from semen-inseminated hens exhibited enriched gene expression linked to ECM organization, one-carbon and protein metabolism, cell division, and vascular endothelial growth factor binding. Pathway enrichment in semen-inseminated hen samples was related to amino acid metabolism, cell cycle, ECM-receptor interaction, and focal adhesion.

Pairwise comparison between control and sham-inseminated SST at D1 generated a total of 49 DEGs, a majority of which were involved in immune response and regulation of cell proliferation (Figure 2A; Supplementary Table S1). Within the top generated

10.3389/fphys.2023.1305168

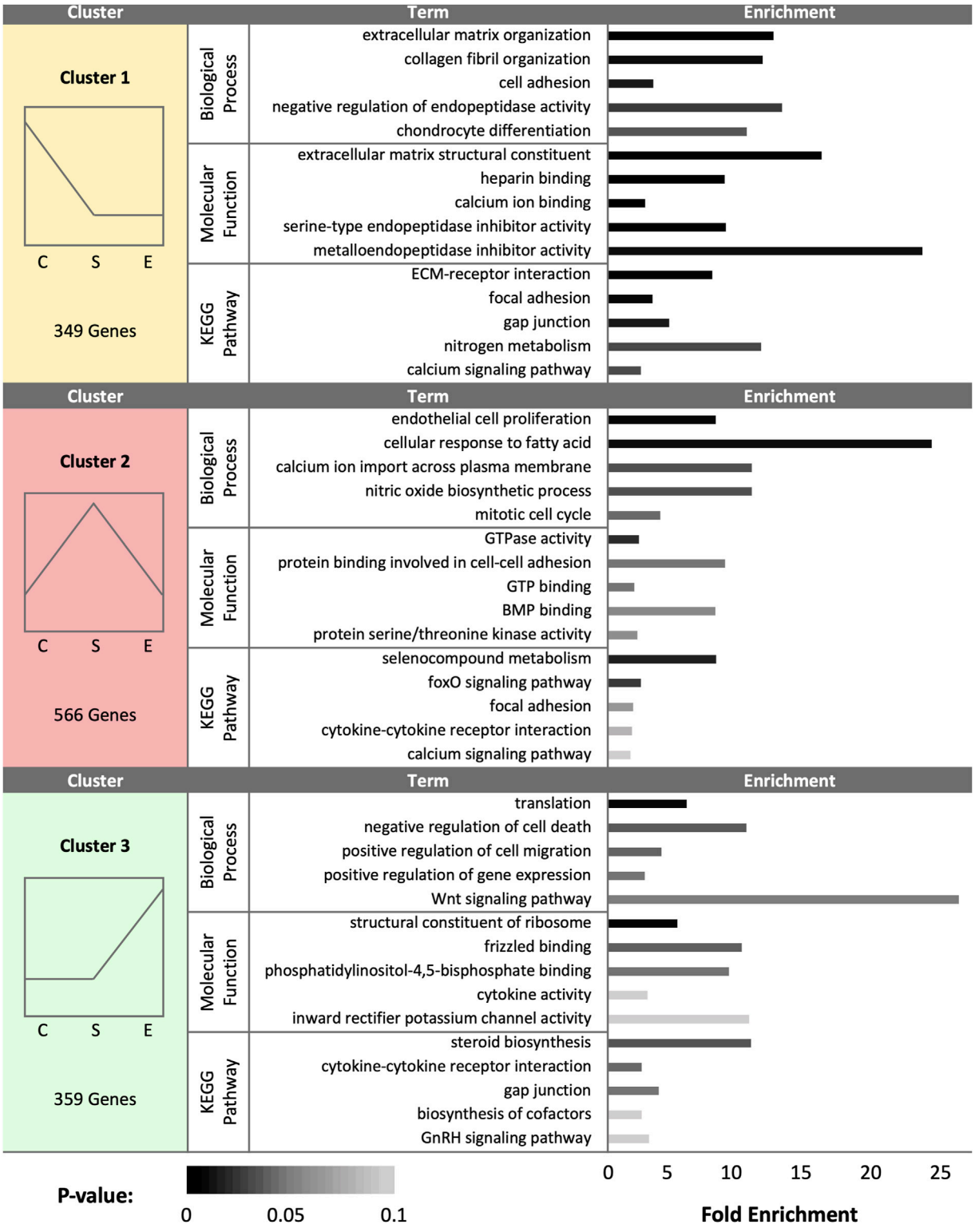


FIGURE 3
K-medoids cluster analysis of sperm storage tubules (SSTs) isolated from: control, sham-inseminated, and semen-inseminated at 30-days post-insemination (D30). The k-medoids cluster analysis tool from CLC Genomics (Qiagen, Valencia, CA) was used to identify genes exhibiting peak expression in treatment group. Genes included in the analysis were differentially expressed due to treatment ($q < 0.05$). Left panels show the expression profile and number of genes in each cluster (C = control, S = sham-insemination, E = semen-insemination). Right panels show enriched gene ontology (GO) term biological processes and molecular functions as well as KEGG pathway enrichment generated from Database for Annotation, Visualization, and Integrated Discovery (DAVID).

network, key immune drivers, such as immunoglobulin, interferon alpha and beta, and nuclear factor kappa B (NFκB), were identified as upstream regulators, with predicted increased expression in sham-inseminated samples, leading to elevated cytokine inducible SH2 containing protein (*CISH*), FKBP prolyl isomerase 5 (*FKBP5*), and dual specificity phosphatase 6 (*DUSP6*) expression in sham-inseminated samples. These regulators are also predicted to lead to increased cell proliferation in control samples, including growth arrest specific 6 (*GAS6*) expression in control samples. In addition to the predicted regulators identified in the top generated network, upstream analysis identified eight potential regulators exhibiting significant activity with roles in immune function (*NOD2*, DUB, caspase) as well as thyroid hormone (*NKX2-1*), hypothalamo-pituitary gonadal axis (progesterone), and insulin signaling (*SPRY4*) (Supplementary Table S2). GO analysis of DEGs from the pairwise comparison between control and sham-inseminated SST at D1 showed enrichment of B cell chemotaxis, cartilage development, and chondrocyte differentiation biological processes (Supplementary Table S3).

Examination of sham-inseminated and semen-inseminated SST at D1 using a pairwise comparison identified a total of 185 DEGs (Supplementary Table S1). The top network constructed was composed of DEGs with functional roles in angiogenesis, innervation, and cytoskeletal structure (Figure 2B). The genes, stabilin 2 (*STAB2*) and rap guanine nucleotide exchange factor 3 (*RAPGEF3*), both showed increased expression in semen-inseminated samples and play roles in angiogenesis. Additionally, neurofilament light chain (*NEFL*) and netrin 1 (*NTN1*) also showed increased expression in semen-inseminated samples and play roles in innervation and cytoskeletal maintenance. Upstream regulators with classical reproductive functions, such as luteinizing hormone (LH) and follicle stimulating hormone (FSH), were predicted to be increased in semen-inseminated samples, while upstream regulators with immune functions, such as pro-inflammatory cytokine and calmodulin-dependent protein kinase II (CaMKII), were predicted to be increased in sham-inseminated samples. Upstream analysis also identified 90 potential regulators exhibiting significant activity, with one regulator, spalt like transcription factor 4 (*SALL4*), also exhibiting increased expression in semen-inseminated samples when compared to sham-inseminated samples (Supplementary Table S2). GO analysis of DEGs from the pairwise comparison between sham-inseminated and semen-inseminated SST at D1 showed enrichment of cell adhesion, angiogenesis, negative regulation of cell migration, and breakdown of glycolytic intermediates (Supplementary Table S3).

At day 30 (D30), a total of 1,274 DEGs were identified as statistically significant due to treatment group. Cluster analysis revealed a total of 349 DEGs upregulated in control samples, 566 DEGs upregulated in sham samples, and 359 DEGs upregulated in experimental samples (Figure 3). Control hen SSTs exhibited upregulation of genes associated with ECM organization, calcium and heparin binding, endopeptidase inhibitor activity, cell adhesion, and collagen production. In control hen samples, enriched pathways included ECM-receptor interaction, focal adhesion, gap junction formation, nitrogen metabolism, and calcium signaling. Sham-inseminated SSTs showed enriched gene expression linked to endothelial cell proliferation, calcium ion transport, fatty acid cellular response, nitric oxide biosynthesis, and BMP binding. In sham-inseminated hen samples, enriched pathways included cytokine-receptor interaction, selenocompound metabolism, focal adhesion, and foxO and calcium signaling. Semen-inseminated SSTs exhibited increased mRNA levels for genes related to translation, Wnt signaling, potassium channel and cytokine activity, and cell viability. In semen-inseminated hen samples, enriched pathways included steroid and cofactor biosynthesis, cytokine receptor interaction, gap junction formation, and GnRH signaling.

Pairwise comparison between control and sham-inseminated SSTs at D30 identified a total of 59 DEGs, some of which were involved in immune response and insulin responsiveness (Figure 4A; Supplementary Table S1). Specifically, immune associated genes such as interleukin-1 (IL1) and immunoglobulin G (IgG) were predicted to have increased expression in sham-inseminated and control samples, respectively, leading to increased interleukin 17 receptor D (*IL17RD*) expression in sham-inseminated samples, while increased CD34 molecule (*CD34*) expression was identified in control samples. Additionally, insulin activity was also predicted to be increased in control samples (also seen at D1), with downstream metabolic targets, such as adiponectin, C1Q and collagen domain containing (*ADIPOQ*) and protein phosphatase 1 (*PP1*) exhibited increased expression in control samples. Upstream analysis also identified 53 potential regulators exhibiting significant activity, with regulators such as ADAM metallopeptidase with thrombospondin type 1 motif 1 (*ADAMTS1*) and androgen receptor (*AR*) playing key roles in extracellular matrix remodeling and reproductive signaling, respectively (Supplementary Table S2). GO analysis of DEGs from the pairwise comparison between control and sham-inseminated SST at D30 showed enrichment of cell redox homeostasis and selenocompound metabolism (Supplementary Table S3).

When sham-inseminated and semen-inseminated SSTs were compared at D30 through a pairwise analysis, a total of 769 DEGs were identified (Supplementary Table S1). The top network constructed comprised of DEGs with functional roles in anti-apoptotic functions, fatty acid synthesis, and metabolism (Figure 4B). Increased anti-apoptotic gene expression, including tyrosine 3-monooxygenase/tryptophan 5-monooxygenase activation protein eta/gamma (*YWHAH*/*YWHAG*) and yes-associated protein 1 (*YAP1*) with predicted upstream regulation by class I phosphoinositide 3-kinases (PI3K class I), were seen in sham-inseminated samples. Gene expression in sham-inseminated samples was indicative of fatty acid synthesis, potentially driven by upstream regulator cytochrome-c oxidase, with ATP citrate lyase (*ACLY*) and fatty acid synthase (*FASN*) exhibiting increased expression in sham-inseminated samples. Within semen-inseminated samples, upregulation of succinyl-CoA:glutarate-CoA transferase (*SUGCT*), was identified, which plays a role in fatty acid metabolism. Both pairwise comparisons identified genes upregulated in sham-inseminated samples related to: 1) thyroid hormone metabolism and signaling from deiodinase 2 (*DIO2*) and thyroid hormone receptor beta (*THRB*); 2) cellular stress with ectodermal-neural cortex 1 (*ENC1*), growth arrest and DNA damage inducible gamma (*GADD45G*), coiled-coil-helix-coiled-coil-helix domain containing 4 (*CHCHD4*), and DDB1 and CUL4 associated factor 12 (*DCAF12*); and 3) cell cycle dynamics from tousled like kinase 1 (*TLK1*) and tubulin beta 4B class IVb

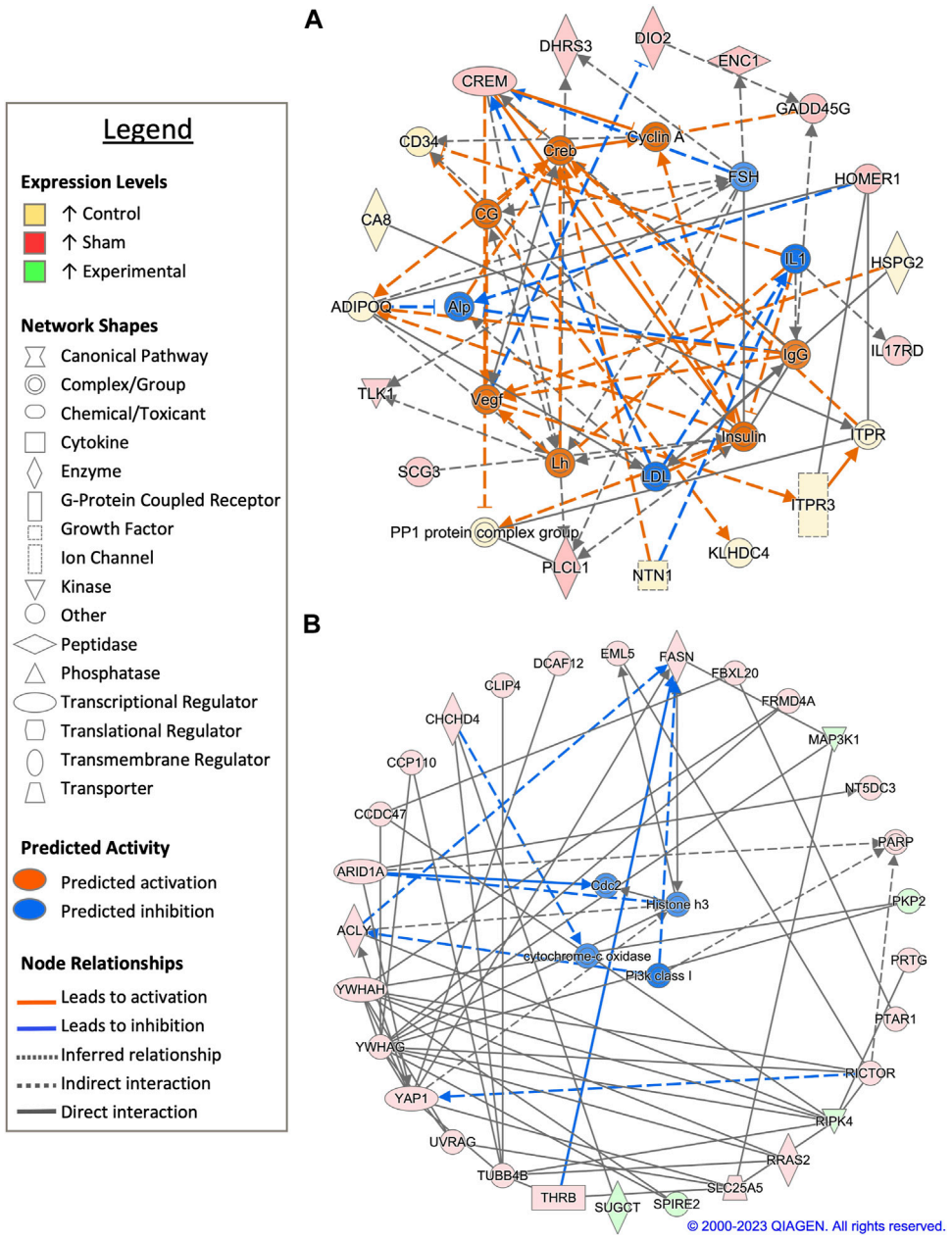


FIGURE 4
Network analysis of sperm storage tubules (SSTs) isolated at 30-days post insemination (D30). The core analysis tool from Ingenuity Pathway Analysis (IPA) (Qiagen, Valencia, CA) was used to biologically interpret differentially expressed genes (DEGs). Copyright permission from Qiagen has been obtained for use of the images presented. **(A)** The top network generated through pathway analysis of DEGs between control and sham-inseminated hens (FPKM > 1, $q$-value < 0.05, |fold change| > 1.5). **(B)** The top network generated through pathway analysis of DEGs between sham-inseminated and semen-inseminated hens (FPKM > 1, $q$-value < 0.05, |fold change| > 1.5).

(*TUBB4B*) as well as potential upstream regulation by cyclin-dependent protein kinase Cdk1/Cdc2 (*CDC2*). Upstream analysis also identified 312 potential regulators exhibiting significant activity, with 12 potential regulators exhibiting increased expression in sham-inseminated samples and 2 potential regulators exhibiting increased expression in semen-inseminated samples (Supplementary Table S2). GO analysis of DEGs from the pairwise comparison between sham-inseminated and semen-inseminated SST at D30 showed enrichment signal transduction, cellular response to fatty acid, ECM organization, and bleb assembly biological processes. In addition, glycosaminoglycan biosynthesis, calcium signaling, selenocompound metabolism, and ECM-receptor interaction KEGG pathways also showed enrichment (Supplementary Table S3).

At day 90 (D90), a total of 532 DEGs were identified as statistically significant due to treatment group. Cluster analysis revealed a total of 178 DEGs upregulated in control samples, 202 DEGs upregulated in sham samples, and 152 DEGs

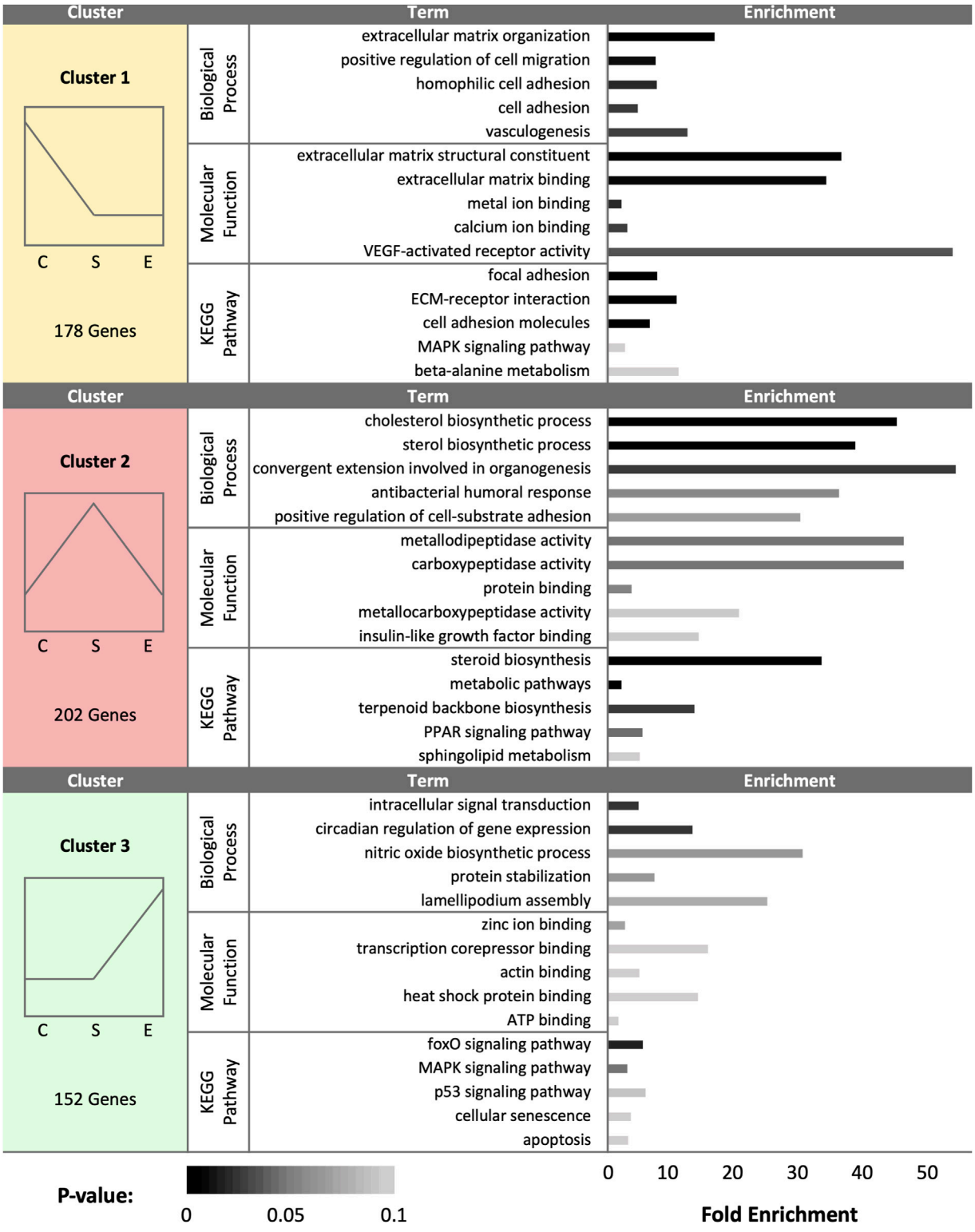


FIGURE 5
K-medoids cluster analysis of sperm storage tubules (SSTs) isolated from: control, sham-inseminated, and semen-inseminated at 90-days post-insemination (D90). The k-medoids cluster analysis tool from CLC Genomics (Qiagen, Valencia, CA) was used to identify genes exhibiting peak expression in treatment group. Genes included in the analysis were differentially expressed due to treatment ($q < 0.05$). Left panels show the expression profile and number of genes in each cluster (C = control, S = sham-insemination, E = semen-insemination). Right panels show enriched gene ontology (GO) term biological processes and molecular functions as well as KEGG pathway enrichment generated from Database for Annotation, Visualization, and Integrated Discovery (DAVID).

10.3389/fphys.2023.1305168

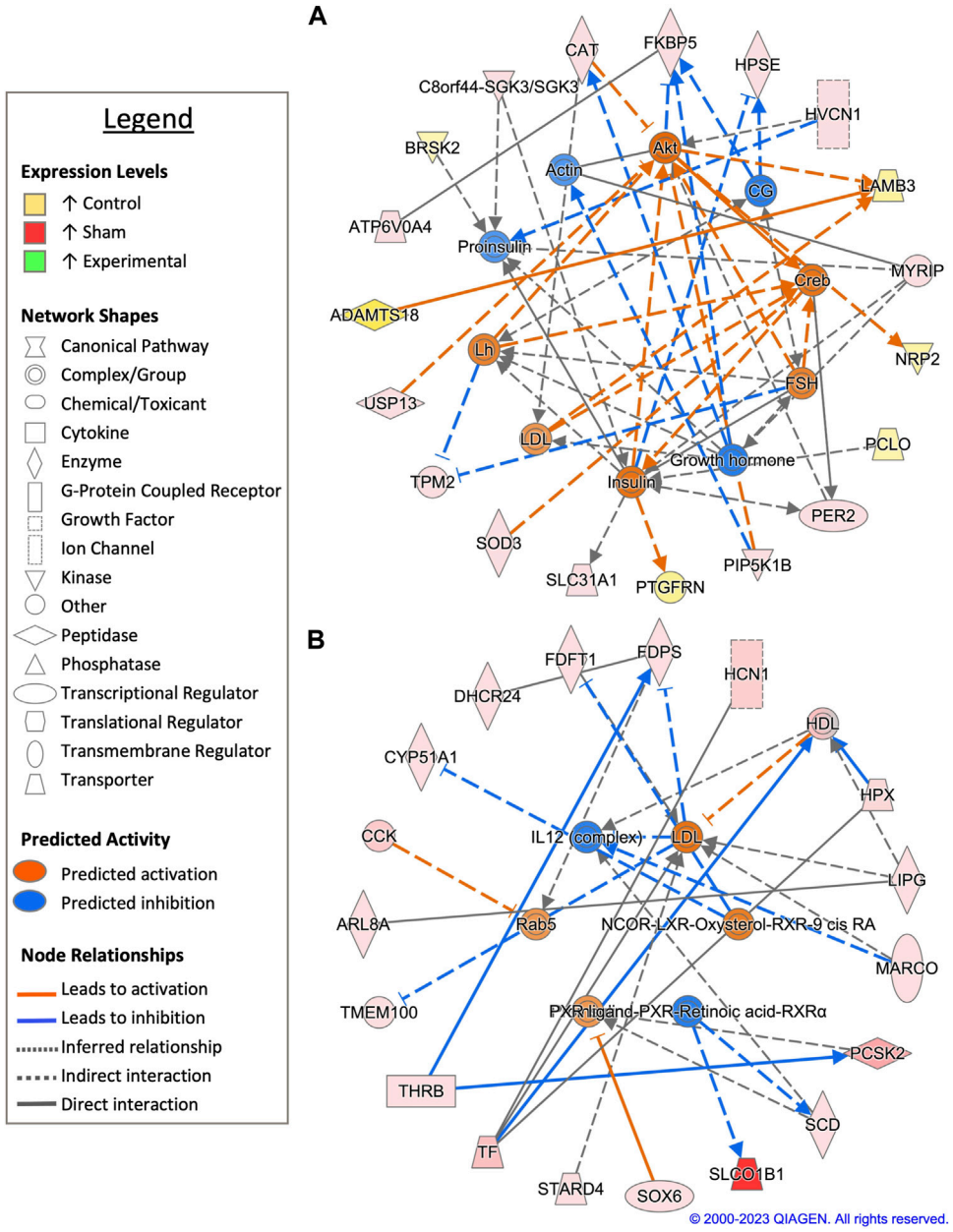


FIGURE 6
Network analysis of sperm storage tubules (SSTs) isolated at 90-days post insemination (D90). The core analysis tool from Ingenuity Pathway Analysis (IPA) (Qiagen, Valencia, CA) was used to biologically interpret differentially expressed genes (DEGs). Copyright permission from Qiagen has been obtained for use of the images presented. **(A)** The top network generated through pathway analysis of DEGs between control and sham-inseminated hens (FPKM > 1, $q$-value < 0.05, |fold change| > 1.5). **(B)** The top network generated through pathway analysis of DEGs between sham-inseminated and semen-inseminated hens (FPKM > 1, $q$-value < 0.05, |fold change| > 1.5).

upregulated in experimental samples (Figure 5). In control hens, enriched gene expression associated with ECM organization, cell adhesion and migration, vasculogenesis, and metal and calcium binding were identified. The pathway enrichment in control hen SSTs was identified as related to cell adhesion, ECM receptor interaction, MAPK signaling, and alanine metabolism. The sham-inseminated hen samples exhibited gene upregulation related to cholesterol and sterol biosynthesis, cell adhesion, peptidase activity, insulin-like growth factor binding, and humoral immune response. Pathway enrichment in sham-inseminated hen SSTs was identified as related to steroid biosynthesis, metabolic pathways, and PPAR signaling. Lastly, the semen-inseminated hen samples had increased expression levels for genes linked to nitric oxide biosynthesis, lamellipodium assembly, circadian gene regulation, and protein stabilization, along with zinc ion, corepressor, actin, heat shock protein, and ATP binding. Pathway enrichment in semen-inseminated hen SSTs was associate with foxO, MAPK, and p53 signaling as well as cellular senescence and apoptosis.

Pairwise comparison between control and sham-inseminated SSTs at D90 generated a total of 118 DEGs, which were involved in

extracellular matrix organization and insulin responsiveness (Figure 6A; Supplementary Table S1). A cytoskeletal upstream regulator, actin, was predicted to have increased expression along with cytoskeletal genes, heparanase (*HPSE*) and beta-tropomyosin (*TPM2*), in sham-inseminated samples. Conversely, in control samples, upregulation of basement membrane proteins and extracellular matrix degradation metalloproteinases, laminin subunit beta 3 (*LAMB3*) and ADAM metallopeptidase with thrombospondin type 1 motif 18 (*ADAMTS18*), was observed. Similar to the D30 timepoint, insulin activity was predicted to increase in control samples, with downstream targets such as BR serine/threonine kinase 2 (*BRSK2*) and prostaglandin F2 receptor inhibitor (*PTGFRN*) exhibiting increased expression levels in control samples. Upstream analysis identified 63 potential regulators exhibiting significant activity, with several regulators involved in immune function (NfkB-RelA, *PTPN13*, *ICOS*) (Supplementary Table S2). GO analysis of DEGs from the pairwise comparison between control and sham-inseminated SST at D90 showed enrichment of intracellular signal transduction and cell adhesion molecules (Supplementary Table S3).

In a pairwise comparison of sham-inseminated and semen-inseminated SSTs at D90, a total of 108 DEGs were identified (Supplementary Table S1). The top network identified in analysis was comprised of DEGs with roles in immune function, thyroid hormone signaling, and cholesterol metabolism (Figure 6B). The upstream immune regulator interleukin 12 (IL12), was predicted to have increased expression in sham-inseminated, along with increased expression of macrophage receptor with collagenous structure (*MARCO*). Thyroid hormone signaling genes, such as *THRB* and solute carrier organic anion transporter family member 1B1 (*SLCO1B1*) exhibited upregulation in sham-inseminated samples, like those at the D30 timepoint. Several genes with roles in cholesterol metabolism exhibited increased expression in the sham-inseminated samples, including cytochrome P450 family 51 subfamily A member 1 (*CYP51A1*), 24-dehydrocholesterol reductase (*DHCR24*), farnesyl-diphosphate farnesyltransferase 1 (*FDFT1*), farnesyl diphosphate synthase (*FDPS*), high density lipoprotein (*HDL*), and StAR related lipid transfer domain containing 4 (*STARD4*). Low density lipoprotein (LDL) was predicted to be activated in semen-inseminated samples. Like the D30 timepoint, both pairwise comparisons showed sham-inseminated samples had upregulation of genes related to cellular stress, namely, catalase (*CAT*), superoxide dismutase 3 (*SOD3*), and hemopexin (*HPX*). Upstream analysis identified 129 potential regulators exhibiting significant activity, with several regulators involved in fatty acid metabolism (*ELOVL3*, *SCD*), glycolysis/gluconeogenesis (*ACSS2*, *PGK1*), and insulin signaling (*HRAS*, *INSR*, *RPTOR*, *SREBF1*) (Supplementary Table S2). GO analysis of DEGs from the pairwise comparison between sham-inseminated and semen-inseminated SST at D90 showed enrichment of lipid metabolism and steroid biosynthesis (Supplementary Table S3).

Upstream analysis revealed 10 predicted upstream regulators based upon DEGs between sham-inseminated and semen-inseminated pairwise comparisons that were common to more than one timepoint, with one of the predicted upstream regulators, insulin, also appearing in pairwise comparisons between control and sham inseminated samples as well. Dihydrotestosterone (*DHT*), signal transducer and activator of transcription 6 (*STAT6*), tumor necrosis factor (*TNF*), and vascular endothelial growth factor A (*VEGFA*) were identified as upstream regulators at the D1 and D30 timepoints, while beta-estradiol, high mobility group 20A (*HMG20A*), insulin, and L-glutamic acid were identified as upstream regulators at the D30 and D90 timepoints. In total, these regulators had 60 downstream targets that exhibited differential expression between sham-inseminated and semen-inseminated samples, with considerable target overlap between regulators (Figure 7). Downstream targets were associated with the following biological pathways: steroid biosynthesis, calcium signaling, cholesterol biosynthesis, fatty acid biosynthesis, cell adhesion, fibroblast and endothelial cell proliferation, plasminogen activation, angiogenesis, insulin-like and vascular endothelial growth factor receptor signaling, and extracellular matrix organization (Supplementary Figure S2).

RT-qPCR was performed on six randomly selected genes using all treatment groups, timepoints, and replicates to assess the reliability of results obtained through RNA sequencing. For each gene analyzed, the $\log_2$ fold change obtained through RT-qPCR showed strong correlation with the $\log_2$ fold change obtained through RNA sequencing (Supplementary Figures S3), with the $R_2$ ranging from 0.7992 for *KCNMB1* to 0.8867 for *SPARC* and an average $R_2$ of 0.85 for the six genes examined.

# 4 Discussion

Previous analysis of the SST transcriptome demonstrated temporal changes throughout the duration of fertility (Brady et al., 2022). In the current study, it has now been established that the SST transcriptome is also impacted by the presence of semen and the act of insemination. Between the treatment groups, comparisons between control and sham-inseminated hens yielded fewer DEGs, while more stark differences were observed in comparisons between sham-inseminated and semen-inseminated hens. Transcriptome differences, particularly in the semen-inseminated group, were measurable for up to 90 days post-insemination. Analysis of the DEGs acquired through analysis revealed upregulation of pathways relating to classical and non-classical reproductive signaling, cytoskeletal remodeling, physiological parameters of the local UVJ environment, and cellular metabolism in semen-inseminated samples. In contrast, sham-inseminated samples were observed to have upregulation of immune pathways and non-reproductive endocrine hormones.

Classical reproductive signaling was noted in each comparison across the three timepoints. It has been previously established that SST function is regulated by steroid hormones, such as progesterone and estradiol, that target sperm-release and sperm storage duration (Ito et al., 2011; Yang et al., 2020). Less is known about direct gonadotropin stimulation on SST function. In the Japanese quail, receptors for LH, FSH, progesterone, and estradiol have been detected in the UVJ, with expression levels increasing leading up to the initiation of egg lay (Khillare et al., 2018). Expression of LH and FSH receptors, coupled with the predicted upstream regulation of LH and FSH in the current dataset, indicates that gonadotropins may act directly on SST, in addition to acting indirectly through stimulation of follicular steroid hormone production. In the analysis, LH and FSH were predicted to be activated at

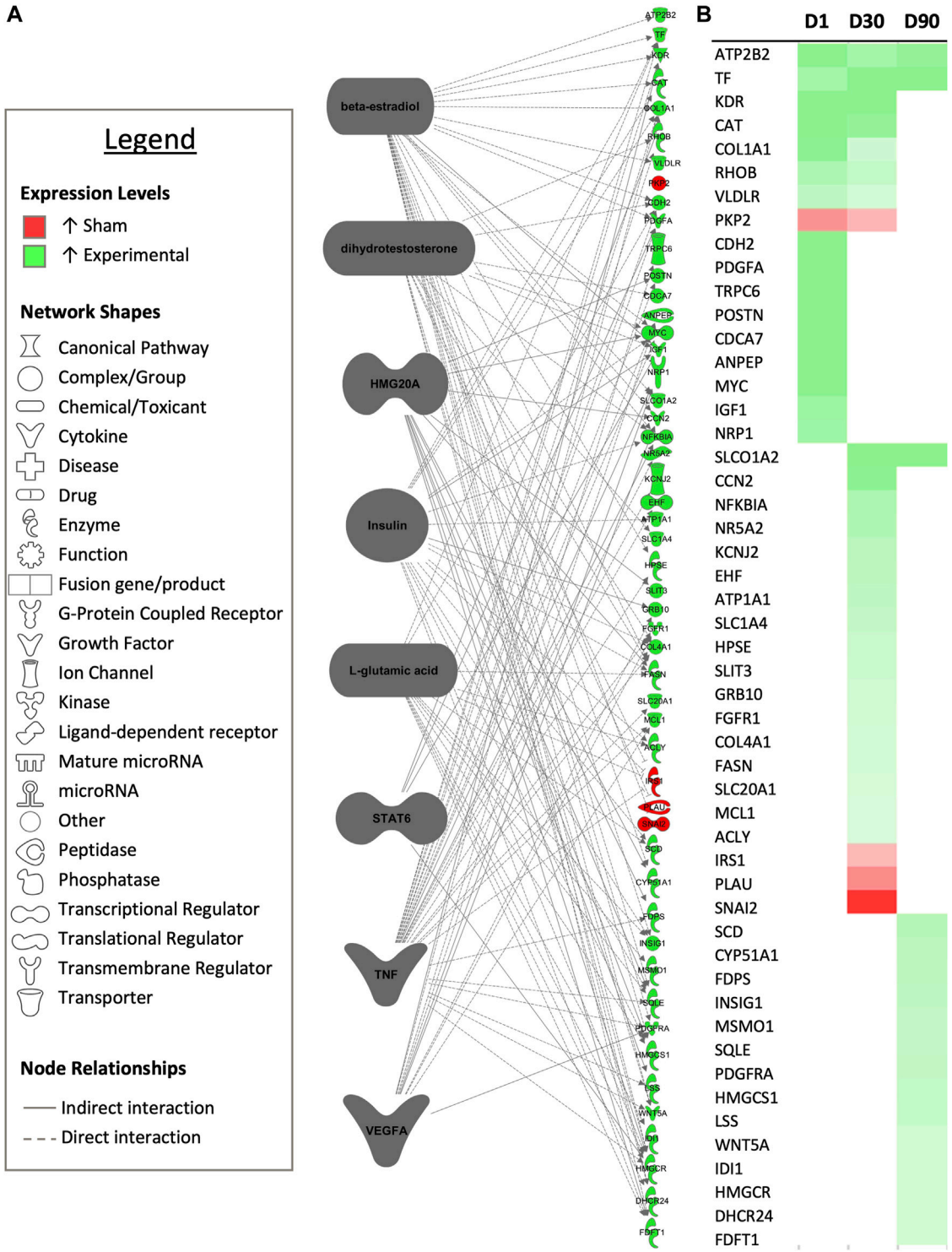


FIGURE 7
Common upstream regulators occurring multiple timepoints. **(A)** Common predicted upstream regulators for each experimental timepoint from the core analysis tool of Ingenuity Pathway Analysis (Qiagen, Valencia, CA) are presented. Only upstream regulators with significant predicted activity (|z-score| > 2, $p < 0.05$) are represented. Downstream targets exhibiting differential expression between sham-inseminated and semen-inseminated samples are presented (FPKM > 1, $q$-value < 0.05, |fold change| > 1.5). **(B)** Heat map expression profiles for each target gene 1-day (D1), 30-days (D30), and 90-days (D90) post-insemination. Green represents increased expression in semen-inseminated samples, while red represents higher expression in sham-inseminated samples.

D1 in semen-inseminated samples, but not predicted to be active until D30 and D90 timepoints in control hens. Within the cluster analysis at D1, GO term and KEGG pathway enrichment included hormone-mediated signaling pathway and activation of adenylate cyclase activity, both related to *FSHR* and *LHCGR* expression, in the sham-inseminated group. These D1 pathway results indicate that the act of insemination, rather than the presence of semen, can modulate SST gonadotropin responsiveness. Sustained gonadotropin responsiveness is evident at the D30 timepoint in semen-inseminated hens, with GO term and KEGG pathway enrichment including GnRH signaling and steroid hormone biosynthesis. Within the pairwise comparisons at each timepoint, upstream regulators related to steroid hormone signaling, such as estrogen receptors 1 and 2 (*ESR1* and *ESR2*), beta-estradiol, progesterone receptor (*PGR*), and progesterone, were predicted to have significant activity in the comparisons between sham-inseminated and semen-inseminated samples. In addition to direct action of gonadotropins on SST function, the predicted upstream regulators also indicate indirect regulation of gonadotropins on SST function through steroid hormone signaling.

Non-classical aspects of reproductive signaling were also observed, including androgen regulation and calcium signaling. Increased circulating androgens have been associated with hibernation related sperm storage in turtles and with sperm storage in bats (Roy and Krishna, 2010; Liu et al., 2016). In avian species, androgen derivatives have been identified in the serum metabolome of hens with increased sperm storage capacities (Yang et al., 2021). In the current dataset, dihydrotestosterone was identified as a potential upstream regulator common to both the D1 and D30 timepoints, indicating that androgen regulation may be responsible for downstream gene expression differences seen between the sham-inseminated and semen-inseminated hens. Upstream analysis through pairwise comparisons of sham-inseminated and semen-inseminated samples also predicted androgen receptor (AR) and testosterone to have significant activity, further supporting the role of androgens in SST function. Additionally, calcium signaling and ion binding appeared in the enrichment analysis of control and sham-inseminated samples at each timepoint. Calcium stimulates sperm motility and respiration (Ashizawa et al., 1992) *in vitro;* however, with calcium signaling and ion binding enrichment not seen in semen-inseminated samples, one could speculate that calcium regulation may be required for prolonged sperm storage. On the other hand, calcium ions have been visualized in SSTs with co-localization with sperm cells (Riou et al., 2017). Calcium involvement in sperm storage is further complicated by vast calcium mobilization to the oviduct for egg formation. Further studies are necessary to examine the role of both androgens and calcium in SST function.

Apart from reproductive hormones, other endocrine hormones were identified as upstream regulators, specifically thyroid hormone and insulin. Within the sham-inseminated treatment, upregulation of thyroid hormone receptors, deiodinases, and transporters was observed at multiple timepoints. The role of thyroid hormone regulation on egg lay initiation and cessation has been well characterized; but recently, the impact of thyroid hormone treatment on broiler breeder UVJ gene expression has been distinguished. Thyroid hormone treatment decreased expression of carbonic anhydrase, avidin-related protein 2, and TGF beta, which play key roles in SST function (Hatami et al., 2018; Saemi et al., 2018). Upregulation of thyroid hormone related genes in the sham-inseminated hens may serve to downregulate key SST functions when sperm are not present. The alteration of circulating thyroid hormones in chickens through inhibition of thyroid hormone synthesis is reported to increase fertility rates (Marks, 1969; Elnagar et al., 2005). Downregulation of thyroid hormone receptors, deiodinases, and transporters in the semen-inseminated group compared with the sham-inseminated group suggest that the presence of semen may modulate SST receptiveness to circulating thyroid hormones. Insulin was found as a predicted upstream regulator in the pairwise comparisons made between control and sham-inseminated hens at each timepoint. In addition, insulin receptor repressor, *SPRY4* exhibited increased expression in semen-inseminated samples at D1. Circulating insulin levels have been associated with decreased fertility levels (Chen et al., 2006) and insulin receptor expression was found to increase with age in chickens, correlating to decreased fertility levels (Yang et al., 2021). Circulating insulin levels are regulated, in part by estradiol levels, with estradiol decreasing insulin levels (Jaccoby et al., 1995). With estradiol identified as a possible upstream regulator of semen-inseminated gene expression, increased estradiol levels could also decrease circulating insulin and/or insulin signaling in the semen-inseminated hens.

Formation and maintenance of SSTs throughout the laying cycle involves cytoskeletal remodeling and extracellular matrix organization, including actin microfilament formation and chondrocyte proliferation (Mendonca et al., 2019; Nabil et al., 2022). Cytoskeletal remodeling and extracellular matrix organization regulate other physiological processes, such as angiogenesis, that are important for nutrient delivery. Cluster analysis identified numerous GO terms and KEGG pathways associated with cytoskeletal remodeling and extracellular matrix organization were identified in all three treatment groups at the D30 and D90 timepoints. However, these terms are enriched only in the semen-inseminated group at D1. Further, pairwise comparisons of sham-inseminated and semen-inseminated samples resulted in DEGs with enrichment in angiogenesis and fibroblast proliferation biological processes at D1. Upregulation of cytoskeletal genes was also previously identified in semen-inseminated SSTs compared to sham-inseminated samples (Long et al., 2003). Within the turkey industry, pre-lay inseminations are utilized to increase SST filling rates and increase early fertility rate (Brillard and Bakst, 1990). Results from this study suggest that the presence of semen accelerates SST development at this early timepoint and could explain why pre-lay insemination strategies lead to improved SST function. Signaling of Wnt has been previously implicated in SST structure in poultry (Yang et al., 2023), and in this analysis, Wnt signaling shows extensive enrichment in semen-inseminated samples at the D30 timepoint.

The local UVJ environment is dictated by nutrient availability and transport, oxidative status, and pH. In this analysis, *HMG20A* and *VEGFA* were identified as potential upstream regulators in multiple comparisons between sham-inseminated and semen-inseminated samples (*HMG20A* at D30/D90 and *VEGFA* at D1/D30), with vascular endothelial growth factor binding highly enriched in semen-inseminated samples at D1. The *HMG20A* gene regulates epithelial cell characteristics, while *VEGFA* is a key regulator of angiogenesis (Silva and Mooney, 2010; Rivero et al., 2015). Both epithelial cell function and angiogenesis could have profound effects on nutrient availability the local SST environment, ultimately impacting sperm storage capabilities. Ion transport of

calcium, iron, potassium, sodium, zinc, and selenium was enriched across both treatments and timepoints. In particular, transferrin, an iron transporter, was upregulated in the semen-inseminated samples at the D1 timepoint and has been shown to be associated with sperm storage in poultry (Matsuzaki et al., 2020; Kubota et al., 2023). In addition to nutrient availability, the local SST environment is also impacted by pH and reactive oxygen species (ROS). The carbonic anhydrase activity in SSTs has been associated with pH maintenance, and multiple carbonic anhydrases were identified as upregulated in the semen-inseminated group (Han et al., 2019). Oxidative stress generates ROS, leading to cellular and DNA damage and several oxidative stress genes (*CAT, HPX, ENC1*) exhibited upregulation in the sham-insemination group across the different timepoints. The presence of ROS in tissue that store sperm is associated with decreased sperm quality and fertility potential in chickens (Kheawkanha et al., 2023), with selenium supplementation mitigating the ROS damage (Chauychu-Noo et al., 2021). Additional work is required to determine critical components of the local UVJ environment that are necessary for prolonged sperm storage success.

Lastly, immune response is directly related to sperm storage capabilities. It has been previously established that mating and artificial insemination upregulate immune related genes in SSTs (Atikuzzaman et al., 2015; Brady et al., 2022). In this analysis, upregulation of immune related genes as well as predicted upstream regulators with immune functions was seen in the sham-inseminated samples compared to control samples. Pairwise comparisons between control and sham-inseminated samples identified several immune related upstream regulators at D1 (*NOD2*, DUB, caspase), D30 (*CHUK*, *CXCR5*, *IL10RB*, *TRIM32*), and D90 (NfkB-RelA, *PTPN13*, *ICOS*) timepoints, indicating that the immune response is sustained to some degree for an extended period. When sham-inseminated and semen-inseminated samples were compared, sham-inseminated samples still exhibited higher expression of immune related genes and regulators. This could be indicative that the presence of semen in the SST may reduce the localized oviduct immune response to increase or preserve semen viability within the avian reproductive tract. Heightened immune responses were also seen in subfertile chicken oviduct fluid, with increased immunoglobulin receptor proteins, resulting in greater immune responsiveness (Riou et al., 2019). Additionally, two of the predicted upstream regulators identified in multiple comparisons, STAT6 and TNF, are known regulators of immune function (Kowssar et al., 2013; Rohde et al., 2018). Further research is needed to elucidate the different types of immune response to the act of insemination and to the presence of sperm.

From this study, the presence of semen 1) increased classical and non-classical reproductive signaling, 2) accelerated cytoskeletal remodeling, 3) buffered physiological parameters of the local UVJ environment, and 4) upregulated cellular metabolism. Conversely, the act of insemination 1) upregulated immune pathways and 2) increased non-reproductive endocrine hormones, such as thyroid hormone and insulin. Additional research is needed to further validate the upstream regulators predicted through this study and determine the role of these regulators on SST functionality. This study has laid the groundwork to characterize the transcriptome changes due to artificial insemination that will potentially aid in optimization in turkey hen insemination and *in vitro* semen storage protocols.

## Data availability statement

The datasets presented in this study can be found in online repositories. The names of the repository/repositories and accession number(s) can be found below: https://www.ncbi.nlm.nih.gov/bioproject, PRJNA1022824 https://www.ncbi.nlm.nih.gov/, Biosamples: SAMN37628532- SAMN37628544, SAMN37628829-SAMN37628838, SAMN37629530- SAMN37629533.

## Ethics statement

The animal study was approved by Institutional Animal Care and Use Committee of the Beltsville Animal Research Center, United States Department of Agriculture. The study was conducted in accordance with the local legislation and institutional requirements.

## Author contributions

KB: Data curation, Formal Analysis, Investigation, Methodology, Resources, Software, Validation, Visualization, Writing–original draft. KK: Conceptualization, Data curation, Methodology, Writing–review and editing. CH: Formal Analysis, Writing–original draft, Writing–review and editing. JL: Conceptualization, Investigation, Methodology, Project administration, Writing–review and editing.

## Funding

The author(s) declare financial support was received for the research, authorship, and/or publication of this article. This research was funded by the in-house USDA-ARS CRIS project number 8042-31000-111-00D to KB and JL.

## Conflict of interest

The authors declare that the research was conducted in the absence of any commercial or financial relationships that could be construed as a potential conflict of interest.

## Publisher's note



## Supplementary material

The Supplementary Material for this article can be found online at: https://www.frontiersin.org/articles/10.3389/fphys.2023.1305168/full#supplementary-material

**SUPPLEMENTARY FIGURE S1**
Mapping and fragment statistics of control (C), sham-inseminated (S), and semen-inseminated (E) sperm storage tubules (SST) at 1-day (D1), 30-days (D30), and 90-days (D90) post-insemination. **(A)** Raw reads obtained for each sample. **(B)** Percentage of reads mapped in pairs, reads mapped in broken pairs, and reads not mapped.

**SUPPLEMENTARY FIGURE S2**
Functional annotation analysis of target genes of upstream regulators common to more than one pairwise comparison. Enriched gene ontology (GO) term biological processes and molecular functions as well as KEGG pathway enrichment generated from Database for Annotation, Visualization, and Integrated Discovery (DAVID) for target genes of the upstream regulators common to more than one pairwise comparison.

**SUPPLEMENTARY FIGURE S3**
Confirmation by RT-qPCR of gene expression results obtained through RNA sequencing. Pearson's correlation analysis of log2 fold changes obtained through RNA sequencing and RT-qPCR for **(A)** cytoglobin (CYGB), **(B)** serine peptidase inhibitor, kunitz type 4 (SPINT4), **(C)** potassium calcium-activated channel subfamily M regulatory beta subunit 1 (KCNMB1), **(D)** serpin family B member 5 (SERPINB5), **(E)** secreted protein acidic and cysteine rich (SPARC), and **(F)** stearoyl-CoA desaturase (SCD) in control **(C)**, sham-inseminated (S), and semen-inseminated **(E)** sperm storage tubules (SST) at 1-day (D1), 30-days (D30), and 90-days (D90) post-insemination.

**SUPPLEMENTARY TABLE S1**
Differential expression output obtained from CLC Genomics Workbench for each pairwise comparison. Differentially expressed genes (DEGs) are highlighted in yellow and meet the following conditions: $q < 0.05$, |fold change|>1.5, and FPKM>1.

**SUPPLEMENTARY TABLE S2**
Upstream analysis output for each pairwise comparison obtained from Ingenuity Pathway Analysis. Upstream regulators listed meet the following conditions: |z-score|>2 and $p < 0.05$.

**SUPPLEMENTARY TABLE S3**
Gene ontology (GO) and KEGG pathway analysis for each pairwise comparison. Listed terms and pathways meet the following conditions: gene count>2 and $p < 0.05$.

# References

Andrews, S. (2010). FastQC: a quality control tool for high throughput sequence data. Available online at: http://www.bioinformatics.babraham.ac.uk/projects/fastqc/.

Ashizawa, K., Hashiguchi, A., and Tsuzuki, Y. (1992). Intracellular free Ca2+ concentration in fowl spermatozoa and its relationship to motility and respiration in spermatozoa. *Reproduction* 96 (1), 395–405. doi:10.1530/jrf.0.0960395

Atikuzzaman, M., Bhai, R. M., Fogelholm, J., Wright, D., and Rodriguez-Martinez, H. (2015). Mating induces the expression of immune-and pH-regulatory genes in the utero-vaginal junction containing mucosal sperm-storage tubuli of hens. *Reproduction* 150 (6), 473–483. doi:10.1530/REP-15-0253

Bakst, M. R. (1987). Anatomical basis of sperm-storage in the avian oviduct. *Scanning Microsc.* 1, 1257–1266.

Bakst, M. R. (1992). Observations on the Turkey oviductal sperm-storage tubule using differential interference contrast microscopy. *J. Reproduction Fertil.* 95, 877–883. doi:10.1530/jrf.0.0950877

Bakst, M. R. (1994). Fate of fluorescent stained sperm following insemination: new light on oviducal sperm transport and storage in the Turkey. *Biol. Reproduction* 50, 987–992. doi:10.1095/biolreprod50.5.987

Bakst, M. R., Donoghue, A. M., Yoho, D. E., Moyle, J. R., Whipple, S. M., Camp, M. J., et al. (2010). Comparisons of sperm storage tubule distribution and number in 4 strains of mature broiler breeders and in Turkey hens before and after the onset of photostimulation. *Poult. Sci.* 89, 986–992. doi:10.3382/ps.2009-00481

Birkhead, T. R., and Møller, A. P. (1992). Numbers and size of sperm storage tubules and the duration of sperm storage in birds: a comparative study. *Biol. J. Linn. Soc.* 45, 363–372. doi:10.1111/j.1095-8312.1992.tb00649.x

Bobr, L. W., Ogasawara, F. X., and Lorenz, F. W. (1964). Distribution of spermatozoa in the oviduct and fertility in domestic birds. *J. Reproduction Fertil.* 8, 49–58. doi:10.1530/jrf.0.0080049

Brady, K., Krasnec, K., and Long, J. A. (2022). Transcriptome analysis of inseminated sperm storage tubules throughout the duration of fertility in the domestic Turkey, *Meleagris gallopavo*. *Poult. Sci.* 101, 101704. doi:10.1016/j.psj.2022.101704

Brady, K., Porter, T. E., Liu, H.-C., and Long, J. A. (2019). Characterization of gene expression in the hypothalamo-pituitary-gonadal axis during the preovulatory surge in the Turkey hen. *Poult. Sci.* 1–9. doi:10.3382/ps/pez437

Brillard, J. P. (1993). Sperm storage and transport following natural mating and artificial insemination. *Poult. Sci.* 72, 923–928. doi:10.3382/ps.0720923

Brillard, J. P., and Bakst, M. R. (1990). Quantification of spermatozoa in the sperm-storage tubules of Turkey hens and the relation to sperm numbers in the perivitelline layer of eggs. *Biol. Reprod.* 43, 271–275. doi:10.1095/biolreprod43.2.271

Burrows, W. H., and Quinn, J. P. (1935). A method of obtaining spermatozoa from the domestic fowl. *Poult. Sci.* 14, 251–253. doi:10.3382/ps.0140251

Chauychu-Noo, N., Thananurak, P., Boonkum, W., Vongpralub, T., and Chankitisakul, V. (2021). Effect of organic selenium dietary supplementation on quality and fertility of cryopreserved chicken sperm. *Cryobiology* 98, 57–62. doi:10.1016/j.cryobiol.2020.12.008

Chen, S. E., McMurtry, J. P., and Walzem, R. L. (2006). Overfeeding-induced ovarian dysfunction in broiler breeder hens is associated with lipotoxicity. *Poult. Sci.* 85 (1), 70–81. doi:10.1093/ps/85.1.70

Christensen, V. L. (1981). Effect of insemination intervals on oviducal sperm storage in turkeys. *Poult. Sci.* 60, 2150–2156. doi:10.3382/ps.0602150

Das, S. C., Nagasaka, N., and Yoshimura, Y. (2005a). Changes in the localization of antigen presenting cells and T cells in the utero-vaginal junction after repeated artificial insemination in laying hens. *J. Reproduction Dev.* 51, 683–687. doi:10.1262/jrd.17027

Das, S. C., Nagasaka, N., and Yoshimura, Y. (2006). Changes in the expression of estrogen receptor mRNA in the utero-vaginal junction containing sperm storage tubules in laying hens after repeated artificial insemination. *Theriogenology* 65, 893–900. doi:10.1016/j.theriogenology.2005.07.004

Das, S. C., Nagaska, N., and Yoshimura, Y. (2005b). Effects of repeated artificial insemination on the structure and function of oviductal sperm storage tubules in hens. *J. Poult. Sci.* 42, 39–47. doi:10.2141/JPSA.42.39

Elnagar, S. A., Khalil, H. M., Hanafy, M. M., and El-Sheikh, A. M. H. (2005). Thyroid hormone and hens reproductive performance of two local strains. *Egypt Poult. Sci.* 25 (1), 147–165.

Han, J., Ahmad, H. I., Jiang, X., and Liu, G. (2019). Role of genome-wide mRNA-seq profiling in understanding the long-term sperm maintenance in the storage tubules of laying hens. *Trop. animal health Prod.* 51 (6), 1441–1447. doi:10.1007/s11250-019-01821-5

Hatami, M., Ansari Pirsaraei, Z., Akhlaghi, A., and Deldar, H. (2018). Effect of long-term oral administration of extra thyroxine on oviductal expression of carbonic anhydrase and avidin-related protein-2 genes in broiler breeder hens. *J. Livest. Sci. Technol.* 6 (2), 67–72. doi:10.22103/jlst.2018.11741.1228

Holm, L., Ekwall, H., Wishart, G., and Ridderstråle, Y. (2000). Localization of calcium and zinc in the sperm storage tubules of chicken, quail and Turkey using X-ray microanalysis. *J. Reproduction Fertil.* 118, 331–336. doi:10.1530/reprod/118.2.331

Huang, daW., Sherman, B. T., and Lempicki, R. A. (2009). Bioinformatics enrichment tools: paths toward the comprehensive functional analysis of large gene lists. *Nucleic acids Res.* 37 (1), 1–13. doi:10.1093/nar/gkn923

Huang, daW., Sherman, B. T., and Lempicki, R. A. (2009). Systematic and integrative analysis of large gene lists using DAVID bioinformatics resources. *Nat. Protoc.* 4 (1), 44–57. doi:10.1038/nprot.2008.211

Ito, T., Yoshizaki, N., Tokumoto, T., Ono, H., Yoshimura, T., Tsukada, A., et al. (2011). Progesterone is a sperm-releasing factor from the sperm-storage tubules in birds. *Endocrinology* 152, 3952–3962. doi:10.1210/en.2011-0237

Jaccoby, S., Arnon, E., Snapir, N., and Robinzon, B. (1995). Effects of estradiol and tamoxifen on feeding, fattiness, and some endocrine criteria in hypothalamic obese hens. *Pharmacol. Biochem. Behav.* 50 (1), 55–63. doi:10.1016/0091-3057(94)00251-d

Kheawkanha, T., Chankitisakul, V., Thananurak, P., Pimprasert, M., Boonkum, W., and Vongpralub, T. (2023). Solid storage supplemented with serine of rooster semen enhances higher sperm quality and fertility potential during storage at 5° C for up to 120 h. *Poult. Sci.* 102 (6), 102648. doi:10.1016/j.psj.2023.102648

Khillare, G. S., Sastry, K. V. H., Agrawal, R., Saxena, R., Mohan, J., and Singh, R. P. (2018). Expression of gonadotropin and sex steroid hormone receptor mRNA in the utero-vaginal junction containing sperm storage tubules of oviduct during sexual maturation in Japanese quail. *General Comp. Endocrinol.* 259, 141–146. doi:10.1016/j.ygcen.2017.11.015

Kowsar, R., Hambruch, N., Liu, J., Shimizu, T., Pfarrer, C., and Miyamoto, A. (2013). Regulation of innate immune function in bovine oviduct epithelial cells in culture: the homeostatic role of epithelial cells in balancing Th1/Th2 response. *J. Reproduction Dev.* 59 (5), 470–478. doi:10.1262/jrd.2013-036

Krämer, A., Green, J., Pollard, J., Jr, and Tugendreich, S. (2014). Causal analysis approaches in ingenuity pathway analysis. *Bioinforma. Oxf. Engl.* 30 (4), 523–530. doi:10.1093/bioinformatics/btt703

Kubota, S., Pasri, P., Okrathok, S., Jantasaeng, O., Rakngam, S., Mermillod, P., et al. (2023). Transcriptome analysis of the uterovaginal junction containing sperm storage tubules in heat-stressed breeder hens. *Poult. Sci.* 102 (8), 102797. doi:10.1016/j.psj.2023.102797

Liu, C. H., and Di, Y. P. (2020). "Analysis of RNA sequencing data using CLC genomics Workbench," in *61–113 in molecular toxicology protocols: methods in molecular biology*. Editors P Keohavong, K P Singh, and W Gao. 3rd ed. (New York, NY: Humana Press).

Liu, T., Chu, X., Huang, Y., Yang, P., Li, Q., Hu, L., et al. (2016). Androgen-related sperm storage in oviduct of Chinese Soft-Shelled Turtle *in vivo* during annual cycle. *Sci. Rep.* 6, 20456. doi:10.1038/srep20456

Livak, K. J., and Schmittgen, T. D. (2001). Analysis of relative gene expression data using real-time quantitative PCR and the 2(-Delta Delta C(T)) Method. *Methods* 25, 402–408. doi:10.1006/meth.2001.1262

Long, E. L., Sonstegard, T. S., Long, J. A., Van Tassell, C. P., and Zuelke, K. A. (2003). Serial analysis of gene expression in Turkey sperm storage tubules in the presence and absence of resident sperm. *Biol. Reproduction* 69 (2), 469–474. doi:10.1095/biolreprod.102.015172

Long, J. A., and Conn, T. L. (2012). Use of phosphatidylcholine to improve the function of Turkey semen stored at 4°C for 24 hours. *Poult. Sci.* 91, 1990–1996. doi:10.3382/ps.2011-02028

Long, J. A., and Kulkarni, G. (2004). An effective method for improving the fertility of glycerol-exposed poultry semen. *Poult. Sci.* 83, 1594–1601. doi:10.1093/ps/83.9.1594

Marks, H. L. (1969). Fertility of chickens fed thiouracil prior to maturity. *Poult. Sci.* 48 (5), 1612–1618. doi:10.3382/ps.0481612

Matsuzaki, M., Mizushima, S., Dohra, H., and Sasanami, T. (2020). Expression of transferrin and albumin in the sperm-storage tubules of Japanese quail and their possible involvement in long-term sperm storage. *J. Poult. Sci.* 57 (1), 88–96. doi:10.2141/jpsa.0190049

Mendonca, T., Cadby, A. J., and Hemmings, N. (2019). Sperm gatekeeping: 3D imaging reveals a constricted entrance to zebra finch sperm storage tubules. *Biophysical J.* 117 (11), 2180–2187. doi:10.1016/j.bpj.2019.10.038

Mero, K. N., and Ogasawara, F. X. (1970). Dimensions of uterovaginal sperm-storage tubules of the chicken and their possible significance in sperm release. *Poult. Sci.* 49, 1304–1308. doi:10.3382/ps.0491304

Nabil, T. M., Hassan, R. M., Mahmoud, H. H., Tawfiek, M. G., and Moawad, U. K. (2022). Histomorphology and histochemistry of the oviduct in laying Turkey hens with emphasis on the sperm host glands. *Adv. Anim. Vet. Sci.* 10 (5), 1076–1089. doi:10.17582/journal.aavs/2022/10.5.1076.1089

Riou, C., Brionne, A., Cordeiro, L., Harichaux, G., Gargaros, A., Labas, V., et al. (2019). Proteomic analysis of uterine fluid of fertile and subfertile hens before and after insemination. *Reprod. Camb. Engl.* 158 (4), 335–356. doi:10.1530/REP-19-0079

Riou, C., Cordeiro, L., and Gérard, N. (2017). Eggshell matrix proteins OC-116, OC-17 and OCX36 in hen's sperm storage tubules. *Animal reproduction Sci.* 185, 28–41. doi:10.1016/j.anireprosci.2017.07.022

Rivero, S., Ceballos-Chavez, M., Bhattacharya, S. S., and Reyes, J. C. (2015). HMG20A is required for SNAI1-mediated epithelial to mesenchymal transition. *Oncogene* 34 (41), 5264–5276. doi:10.1038/onc.2014.446

Rohde, F., Schusser, B., Hron, T., Farkašová, H., Plachý, J., Härtle, S., et al. (2018). Characterization of chicken tumor necrosis factor-α, a long missed cytokine in birds. *Front. Immunol.* 9, 605. doi:10.3389/fimmu.2018.00605

Roy, V. K., and Krishna, A. (2010). Evidence of androgen-dependent sperm storage in female reproductive tract of Scotophilus heathi. *General Comp. Endocrinol.* 165 (1), 120–126. doi:10.1016/j.ygcen.2009.06.012

Saemi, F., Zare Shahneh, A., Zhandi, M., Akhlaghi, A., and Ansari Pirsaraei, Z. (2018). TGF-β4 and HSP70 responses in breeder hens treated with thyroxine. *Animal reproduction Sci.* 198, 82–89. doi:10.1016/j.anireprosci.2018.09.004

Silva, E. A., and Mooney, D. J. (2010). Effects of VEGF temporal and spatial presentation on angiogenesis. *Biomaterials* 31 (6), 1235–1241. doi:10.1016/j.biomaterials.2009.10.052

Tingari, M. D., and Lake, P. E. (1973). Ultrastructural studies on the uterovaginal sperm-host glands of the domestic hen, *Gallus domesticus*. *J. Reproduction Fertil.* 34, 423–431. doi:10.1530/jrf.0.0340423

Van Krey, H. P., Ogasawara, F. X., and Pangborn, J. (1967). Light and electron microscopic studies of possible sperm gland emptying mechanisms. *Poult. Sci.* 46, 69–78. doi:10.3382/ps.0460069

Van Krey, H. P., Schuppin, G. T., Denbow, D. M., and Hulet, R. M. (1987). Turkey breeder hen infertility associated with plasma cells in the uterovaginal sperm storage glands. *Theriogenology* 27, 913–921. doi:10.1016/0093-691x(87)90213-5

Yang, L., Cai, J., Rong, L., Yang, S., and Li, S. (2023). Transcriptome identification of genes associated with uterus–vagina junction epithelial folds formation in chicken hens. *Poult. Sci.* 102 (6), 102624. doi:10.1016/j.psj.2023.102624

Yang, L., Li, S., Mo, C., Zhou, B., Fan, S., Shi, F., et al. (2021). Transcriptome analysis and identification of age-associated fertility decreased genes in hen uterovaginal junction. *Poult. Sci.* 100 (3), 100892. doi:10.1016/j.psj.2020.12.005

Yang, L., Zheng, X., Mo, C., Li, S., Liu, Z., Yang, G., et al. (2020). Transcriptome analysis and identification of genes associated with chicken sperm storage duration. *Poult. Sci.* 99 (2), 1199–1208. doi:10.1016/j.psj.2019.10.021

Zheng, W. M., Nishibori, M., Isobe, N., and Yoshimura, Y. (2001). An *in situ* hybridization study of the effects of artificial insemination on the localization of cells expressing MHC class II mRNA in the chicken oviduct. *Reproduction* 122, 581–586. doi:10.1530/rep.0.1220581

Zheng, W. M., Yoshimura, Y., and Tamura, T. (1998). Effects of age and gonadal steroids on the localization of antigen-presenting cells, and T and B cells in the chicken oviduct. *J. Reproduction Fertil.* 114, 45–54. doi:10.1530/jrf.0.1140045

frontiers | Frontiers in Physiology

TYPE Original Research
PUBLISHED 15 February 2024
DOI 10.3389/fphys.2024.1358682



OPEN ACCESS

EDITED BY
Servet Yalcin,
Ege University, Türkiye

REVIEWED BY
Felix Kwame Amevor,
Sichuan Agricultural University, China
Birendra Mishra,
University of Hawaii at Manoa, United States

*CORRESPONDENCE
Zhaozheng Yin,
yzhzh@zju.edu.cn

RECEIVED 20 December 2023
ACCEPTED 05 February 2024
PUBLISHED 15 February 2024

CITATION
Huang Y, Li S, Tan Y, Xu C, Huang X and Yin Z (2024), Identification and functional analysis of ovarian lncRNAs during different egg laying periods in Taihe Black-Bone Chickens. *Front. Physiol.* 15:1358682. doi: 10.3389/fphys.2024.1358682



# Identification and functional analysis of ovarian lncRNAs during different egg laying periods in Taihe Black-Bone Chickens

Yunyan Huang, Shibao Li, Yuting Tan, Chunhui Xu, Xuan Huang and Zhaozheng Yin*

College of Animal Science, Zhejiang University, Hangzhou, China

**Introduction:** Long non-coding RNA (lncRNA) refers to a category of non-coding RNA molecules exceeding 200 nucleotides in length, which exerts a regulatory role in the context of ovarian development. There is a paucity of research examining the involvement of lncRNA in the regulation of ovary development in Taihe Black-Bone Chickens. In order to further investigate the egg laying regulation mechanisms of Taihe Black-Bone Chickens at different periods, transcriptome analysis was conducted on the ovarian tissues at different laying periods.

**Methods:** This study randomly selected ovarian tissues from 12 chickens for RNA-seq. Four chickens were selected for each period, including the early laying period (102 days, Pre), the peak laying period (203 days, Peak), and the late laying period (394 days, Late). Based on our previous study of mRNA expression profiles in the same ovarian tissue, we identified three differentially expressed lncRNAs (DE lncRNAs) at different periods and searched for their cis- and trans-target genes to draw an lncRNA-mRNA network.

**Results and discussion:** In three groups of ovarian tissues, we identified 136 DE lncRNAs, with 8 showing specific expression during the early laying period, 10 showing specific expression during the peak laying period, and 4 showing specific expression during the late laying period. The lncRNA-mRNA network revealed 16 pairs of lncRNA-target genes associated with 7 DE lncRNAs, and these 14 target genes were involved in the regulation of reproductive traits. Furthermore, these reproductive-related target genes were primarily associated with signaling pathways related to follicle and ovary development in Taihe Black-Bone Chickens, including cytokine-cytokine receptor interaction, TGF-beta signaling pathway, tyrosine metabolism, ECM-receptor interaction, focal adhesion, neuroactive ligand-receptor interaction, and cell adhesion molecules (CAMs). This study offers valuable insights for a comprehensive understanding of the influence of lncRNAs on poultry reproductive traits.

KEYWORDS

**long non-coding RNA, Taihe Black-Bone Chicken, ovary, egg production, RNA-seq**

## 1 Introduction

Chickens are one of the primary domesticated poultry in China, serving as a significant source of meat and egg-related products (Zhang et al., 2022). In recent years, the improvement in living standards has increased the demand for chicken meat and eggs. However, current production levels often fall short of domestic demand (Iannotti et al.,

2014). On the other hand, one of the primary goals in egg laying chicken breeding is achieving high egg production, which plays a crucial role in enhancing production efficiency. Currently, low egg production rates are also one of the key factors hindering the development of the poultry industry (Mu et al., 2021; Chomchuen et al., 2022).

The ovary is the primary organ within a hen's body responsible for producing eggs. It contains numerous small follicles. A follicle consists of both the oocyte and follicular cells, including granulosa cells and theca cells. The interactions among these components form a complex system (Li et al., 2011). Follicle development represents the basic functional unit of the ovary and is a finely regulated process. Follicle development is influenced by both the hypothalamus-pituitary-gonad (HPG) axis and environmental factors. Within the HPG axis (Sun et al., 2021), various hormones are secreted, including follicle-stimulating hormone (FSH), luteinizing hormone (LH) and inhibin (Mishra et al., 2020). FSH's primary role is to stimulate follicular development within the ovary, promoting follicle maturation and ultimately leading to oocyte development and ovulation (Ghanem and Johnson, 2019). LH induces ovulation by triggering the release of matured follicles from the ovary and promoting the formation of the corpus luteum to maintain its function. Inhibin, on the other hand, inhibits the secretion of FSH and LH from the pituitary gland, helping to maintain an appropriate number of follicles within the ovary. These hormones work in harmony, regulating the hen's sexual maturation, follicular development, ovulation, and reproductive cycles (Zhao et al., 2018). Normal HPG axis function is of utmost importance for the reproductive health of chickens, while the health and normal function of the ovary are essential for hen's reproduction and the production of high-quality eggs.

Long non-coding RNAs (lncRNAs) are a class of RNA molecules that typically exceed 200 nucleotides in length and unlike protein-coding RNAs, do not encode proteins. They have long been overlooked as transcripts with no apparent function (Bonasio and Shiekhattar, 2014). However, in recent years, with the advancement of next-generation sequencing technologies in the field of genetics, researchers have discovered that lncRNAs play significant biological roles in the ovary (Zhang et al., 2020). For instance, lncRNAs are involved in regulating the development and maturation of ovarian follicles, influencing the proliferation, differentiation, and apoptosis of follicular cells, thus impacting follicular growth and development (Zhao et al., 2020). LncRNAs also affect the quality of eggs by regulating chromatin structure and epigenetic modifications in oocytes, which are crucial for normal fertilization and embryo development (Minarovits et al., 2016). Furthermore, lncRNAs can modulate hormone sensitivity in the ovary, affecting signaling pathways such as FSH and LH, thereby influencing follicular development and ovulation. Some lncRNAs are associated with the occurrence and progression of ovarian cancer. They may play roles in cancer cell proliferation, invasion, and metastasis, making them potential biomarkers or therapeutic targets for cancer. Additionally, lncRNAs in the ovary may regulate immune responses, influencing ovarian inflammation and autoimmune ovarian diseases (Ren et al., 2015). Recently, it has been discovered that lncRNAs can promote granulosa cell apoptosis in ducks and participate in lncRNA-miRNA-mRNA co-expression networks, potentially affecting duck follicles (Wu et al., 2021). Whole-genome sequencing of ovarian tissues from different developmental stages of Hu sheep revealed that lncRNA target genes may be involved in follicle development, steroid hormone-mediated signaling pathways, steroid hormone biosynthesis, gonadotropin responses and insulin-like growth factor receptor binding (Shabbir et al., 2021). Using confocal transmission electron microscopy and RNA-Seq, Macaulay et al. (2014) discovered that granulosa cells surrounding bovine oocytes transport a significant amount of nutrients and substances, including mRNA and lncRNA. Brown et al. (2014), in their research on *Drosophila* ovaries, also found a substantial presence of promoter-associated antisense lncRNAs, which may regulate the transcriptional activation of their homologous genes, playing a crucial role in early embryonic development before implantation. Additionally, non-additive lncRNAs MSTRG.6475.20 and MSTRG17017.1, along with their non-additive target genes (*GNAQ*, *CACNA1C*, and *TGFB1*), were discovered in the molecular mechanisms of chicken hybrid advantage, involving the gonadotropin-releasing hormone (GnRH) signaling pathway and female gonad development (Wang et al., 2022).

Taihe Black-Bone Chicken, originating from Taihe County in Jiangxi Province, China, boasts a rich history of breeding. It is not only recognized in traditional medicine for its unique medicinal and culinary properties but also holds a high ornamental value, thus contributing significantly to its economic importance (Mi et al., 2018). However, Taihe Black-Bone Chickens have low egg production performance, and systematic breeding work started relatively late. The breeding potential has not yet been fully explored, reflecting the problem of insufficient production performance faced by local breeds. According to our previous work, 1,167 Taihe Black-Bone Chicken breeding core group hens were used as experimental subjects, and egg production data were systematically recorded. It was found that Taihe Black-Bone Chickens have a longer early laying period and lower egg production rate. They enter the peak laying period for a longer time, and the egg production rate reaches the highest at about 72.49% at 30 weeks of age. The egg production peak maintains a rate of 70% between 30 and 32 weeks of age, only 3 weeks, after which the egg production rate rapidly declines. In this study, we collected ovarian tissues from Taihe Black-Bone Chickens at three distinct laying periods: the early laying period (102 days, Pre), the peak laying periods (203 days, Peak) and the late laying period (394 days, Late). To identify differentially expressed lncRNAs (DE lncRNAs) across these periods, we conducted lncRNA sequencing on ovarian tissues. Additionally, we performed functional enrichment analysis using Gene Ontology (GO) and the Kyoto Encyclopedia of Genes and Genomes (KEGG) to uncover the regulatory roles of DE lncRNAs in ovarian development. These findings offer novel insights into enhancing the ovarian development of Taihe Black-Bone Chickens and provide new prospects for increasing their egg production rate.

# 2 Materials and methods

## 2.1 Ethics approval

Our study was carried out in compliance with the ARRIVE guidelines (AVMA Guidelines for the Euthanasia of Animals: 2020 Edition). All animal care and experimental procedures were

approved by the Institutional Animal Care and Use Committee of Zhejiang University (protocol code ZJU14814 and 23 May 2022 of approval). All research work strictly adhered to the experimental animal welfare and ethical guidelines of Zhejiang University (ZJU).

## 2.2 Animal

Taihe Black-Bone Chickens were obtained from the Poultry Breeding Center of Jiangxi Taihe Livestock Company (Taihe county, Jiangxi province, China). All chickens were subjected to identical rearing conditions. Four chickens were randomly selected from each age group at 102 days (Pre), 203 days (Peak), and 394 days (Late), and chickens were euthanized by cervical dislocation after $CO_2$ inhalation (inhaled 40%). In the ovaries, mixed samples of small white follicles, large white follicles, and follicular stroma were collected after removal of the follicular fluid. The samples were rapidly frozen by immersion in liquid nitrogen.

## 2.3 RNA extraction

Total RNA from each ovarian tissue was separately extracted using Trizol reagent (Invitrogen, Shanghai solarbio Bioscience & Technology Co., Shanghai, China). Subsequently, the integrity of RNA and DNA contamination were assessed through 1.2% agarose gel electrophoresis. Finally, RNA concentration was determined using the Nanodrop 2000 instrument. Qualified samples were sent to Beijing Novogene Corporation (Beijing, China) for RNA sequencing.

## 2.4 Library construction, sequencing, and transcript assembly

The lncRNA library construction was performed as required, and the library was qualified by Illumina. The raw data (Raw Reads) obtained by the high-throughput sequencing platform Illumina sequencing after quality control and removed from low quality, contaminated, and containing sequences including adaptors (Clean Reads) were used for subsequent analysis. Alignment analysis of the reference genome for the filtered reads using HISAT2 (Pertea et al., 2016). The results of the HISAT2 alignment were spliced using StringTie (Pertea et al., 2015) to obtain the smallest set of transcripts possible, and the transcripts were quantified.

## 2.5 Distribution and identification of LncRNAs

Novel lncRNA classification criteria are as follows: 1) Selection of transcripts containing at least two exons. 2) Transcripts with a length greater than 200 base pairs. 3) Filtering transcripts that overlap with annotated exon regions in the database using Cuffcompare software. Transcripts that overlap with exon regions of annotated spliced transcripts in the database are subsequently annotated as lncRNAs. 4) Retention of transcripts with an expression level calculated as FPKM value greater than or equal to 0.5. 5) Using the Coding-Non-Coding Index (CNCI), Coding Potential Calculator (CPC) (Kong et al., 2007) and Pfam Scan (Pfamsca), we predicted the potential protein-coding ability of each transcript (Sun et al., 2013). During the preprocessing stage, low-quality reads, removal of 3′ adapter/insert tags, elimination of 5′ adapter contaminants and filtering out reads containing poly-A/T/G/C were performed using Illumina Casava (version 1.8) To obtain clean readings from raw data (Finn et al., 2014). Clean reads of lengths between 18 and 30 nucleotides were further filtered for downstream analysis.

## 2.6 Screening for the differentially expressed lncRNAs

Based on the transcriptome splicing results, using the Cuffmerge software to get the combined transcript set, according to the structure of lncRNA and the functional characteristics of encoding protein, set up a series of stringent filtering criteria through five steps: filtering by exon count, transcript length, known transcript annotation, transcript expression, and coding potential. Follow this with cross-analysis using CPC2, CNCI and PFAM for subsequent analysis. Use the StringTie software (Kovaka et al., 2019) to quantify transcripts such as mRNA, lncRNA, and TUCP, obtaining FPKM information for each transcript in each sample. Perform differential analysis using a filtering approach, with threshold criteria set at $|\log2 \text{(fold change)}| > 2$ and q-value $< 0.05$ for selecting differentially expressed transcripts.

## 2.7 Target gene (cis and trans) prediction analysis

There are various mechanisms of lncRNA regulating target genes. In this study, two methods were used to predict lncRNA target genes: 1) co-location: positional correlation target gene analysis, predicting cis target genes according to the positional relationship between lncRNA and mRNA, and the screening range was within 100 k. 2) co-expression: expression correlation target gene analysis predicts the trans target gene according to the expression correlation between lncRNA and mRNA, and the screening conditions are that the absolute value of Pearson correlation coefficient is greater than 0.95 and the $p$-value is $< 0.05$.

## 2.8 Differential expression analysis of lncRNA target genes, functional enrichment analysis, and the construction of lncRNA-mRNA networks

To study the biological processes of the differentially expressed lncRNAs' cis- and trans-target genes that were filtered, GO term and KEGG pathway enrichment analyses were conducted. Gene Ontology (GO) is an international standardized classification system for gene functions (Young

TABLE 1 Primer sequences.

| Name | Primer-F | Primer-R | Product length (bp) |
|---|---|---|---|
| LARGE1-OT3 | GCAAGTCATGTAGAAGCCGC | AGGCTGAGATGCTTTGGGAT | 131 |
| LINC5957 | CCCAAGCAGAATGCTGAGAC | TGGGTGGGTGAAATGACTGG | 124 |
| ENSGALT00000093358 | AGCCGGATATCTACGGAGCA | GTGGTATGGTGCCTCTCCTG | 92 |
| LINC8942 | TCCCTCTGGGAGTACATGGC | TCCCTCCAAGGATGTTGCCT | 136 |
| ENSGALG00000006958-AS3 | GAAGATGCCACCGGAACCA | CTCACCTCTGAACGAGGCAT | 91 |
| LINC7964 | TCCAGGACTGCCCATGAAAC | TCACTGACAACGTGGGATGG | 104 |
| STMN2 | ACGTCTCCAAGAAAAGGAGAGG | GGGTCACATCCACCATTGCT | 100 |
| GAL | TACCTACTTGGGCCACATGC | CATCAGCCAGTGGTCTTCCA | 130 |
| INHBB | CTTCGCCGAGACAGACGAT | GGCTGGCTTGAACGACAAAC | 98 |
| EXFABP | CTGAACGAGATGAGGACGCT | ATTTCCCTGCAACCTCGCTC | 109 |
| VCAN | GGACAAAGAGTTGAACGGCA | ACAACATCTTGATCCCAGGTT | 84 |
| PLAU | ACCCAAATGGAAGGAGCAGG | GCCACATGTACGCTCACACT | 101 |
| β-actin | CAGCCAGCCATGGATGATGA | ACCAACCATCACACCCTGAT | 185 |

et al., 2010). GO enrichment analysis was performed on the differentially expressed lncRNAs' target genes. KEGG (Kyoto Encyclopedia of Genes and Genomes) is a major public database for pathways (Kanehisa et al., 2008) and pathway enrichment analysis, using KOBAS (2.0) with an FDR of 0.05. Based on our previous report on mRNA expression profiles in the same ovarian tissue, differentially expressed genes related to poultry breeding traits and their corresponding specific lncRNAs were selected from the predicted target genes. A lncRNA-mRNA network was constructed using Cytoscape V3.5.1.

## 2.9 Protein-protein interaction analysis

First, we identified lncRNA-regulated mRNAs during different periods. Based on the GO and KEGG pathway enrichment of the mRNAs, we explored the interaction relationships among these genes in the STRING database. Utilizing the extracted relationships from the database, we unveiled the mRNA network and imported the interaction data into Cytoscape software for visualizing the interaction network. This analysis aims to infer the role of lncRNAs in the ovaries.

## 2.10 Validation of lncRNAs and mRNAs by RT-qPCR

Randomly selected six differentially expressed lncRNAs and mRNAs for validation by RT-qPCR, using β-actin as the internal reference. Primer sequences were provided in Table 1. Total cDNA was synthesized using the ReverTra Ace qPCR Master Mix (TOYOBO), qPCR was performed on the 7900 HT Sequence Detection System (ABI, United States). The efficiency of PCR was estimated by four points of serial dilutions of cDNA. The primer concentration in each reaction system was 0.3 μM. The $2^{(-\Delta\Delta Ct)}$ method was employed to calculate the relative expression levels of the genes. Data obtained were analyzed using GraphPad Prism 3.8. The Student's t-test ($p < 0.05$) was used for mean comparisons. All results were presented in bar charts.

# 3 Results

## 3.1 Overview of sequencing data

To identify DE lncRNAs, we analyzed a total of 12 cDNA libraries representing 3 different physiological stages of chicken ovaries, with four biological replicates for each stage. The RNA sequencing generated a total of 224.03 Gb of data. In the sequencing libraries, each sample had an average of 94,062,415 raw reads. After removing low-quality reads and adapter fragments, there were an average of 91,814,733.83 clean reads and 862,827,885.42 mapped reads. The average Q20 content was 96.97%, demonstrating high data quality for Illumina sequencing. Over 92.67% of the clean reads could be accurately mapped to the chicken reference genome. The GC content of the reads from the 12 samples ranged from 89.69% to 91.85%, with a percentage of less than 50% (Table 2). The result indicates that the quality of the sequencing data is sufficiently high to proceed with further analysis.

## 3.2 The identified lncRNAs

After filtering and potential coding assessment steps, a total of 26,056 candidate lncRNA transcripts were identified, comprising 17,186 known lncRNAs and 8,870 novel lncRNAs. These transcripts were used for further analysis. To gain a deeper understanding of the functional roles of lncRNAs in chicken ovaries, we conducted a genomic background analysis based on

10.3389/fphys.2024.1358682

TABLE 2 Summary statistics for sequence quality and alignment information.

| Sample | Raw reads | Clean reads | Q20 (%) | Q30 (%) | GC Pct (%) | Total mapped | Uniquely mapped |
|---|---|---|---|---|---|---|---|
| Late1 | 91,303,490 | 89,513,990 | 96.86 | 91.59 | 46.33 | 84,088,885 (93.94%) | 81,637,435 (91.2%) |
| Late2 | 101,718,054 | 99,544,712 | 96.88 | 91.76 | 46.94 | 93,360,531 (93.79%) | 90,319,483 (90.73%) |
| Late3 | 89,284,248 | 87,474,918 | 96.94 | 91.77 | 46.7 | 82,186,244 (93.95%) | 79,133,106 (90.46%) |
| Late5 | 88,621,544 | 86,565,784 | 96.41 | 90.51 | 47.18 | 80,218,421 (92.67%) | 77,715,574 (89.78%) |
| Pre25 | 104,413,870 | 101,823,504 | 97.07 | 92.12 | 46.86 | 95,666,581 (93.95%) | 92,680,183 (91.02%) |
| Pre26 | 93,332,334 | 90,510,302 | 97.08 | 92.05 | 45.56 | 85,418,005 (94.37%) | 83,532,973 (92.29%) |
| Pre28 | 90,282,166 | 88,758,264 | 97.09 | 92.09 | 46.6 | 83,593,248 (94.18%) | 81,077,877 (91.35%) |
| Pre29 | 93,306,348 | 90,256,188 | 97.03 | 92 | 45.51 | 84,848,360 (94.01%) | 82,708,657 (91.64%) |
| Peak10 | 92,547,334 | 90,696,320 | 97.06 | 92.09 | 47.45 | 85,154,842 (93.89%) | 81,684,877 (90.06%) |
| Peak11 | 86,443,334 | 83,522,870 | 96.88 | 91.57 | 46.61 | 78,938,778 (94.51%) | 76,717,770 (91.85%) |
| Peak12 | 103,790,790 | 101,415,404 | 97.12 | 92.21 | 47.15 | 95,446,885 (94.11%) | 91,569,791 (90.29%) |
| Peak9 | 93,705,468 | 91,694,550 | 97.21 | 92.38 | 47.38 | 86,472,645 (94.31%) | 82,238,961 (89.69%) |

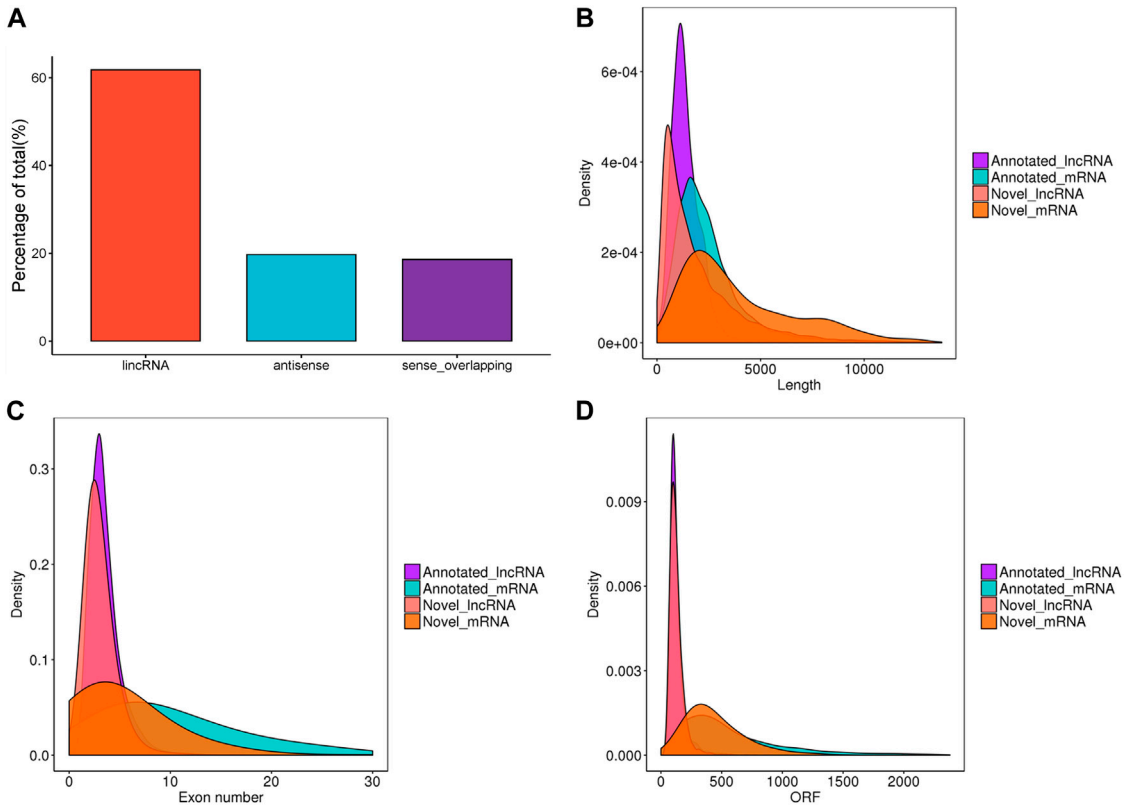


FIGURE 1
Characteristics of lncRNAs identified in the ovaries of Taihe Black-Bone Chickens. **(A)** Distribution of lncRNA type; **(B)** lncRNA and mRNA transcripts length; **(C)** lncRNA and mRNA exon number; **(D)** lncRNA and mRNA ORF length.

their positional relationships with known mRNAs. Among them, we identified 61.8% lincRNA, 19.7% antisense, and 18.6% sense-overlapping (Figure 1A). As shown in Figures 1B–D, the exon number, transcript length, and expression levels of lncRNAs and mRNAs were calculated and plotted. The results showed that the overall trend of lncRNA length was consistent (Figure 1B), most of the exons of lncRNAs were less than 10, significantly lower than that of mRNAs (Figure 1C). The average ORF length of

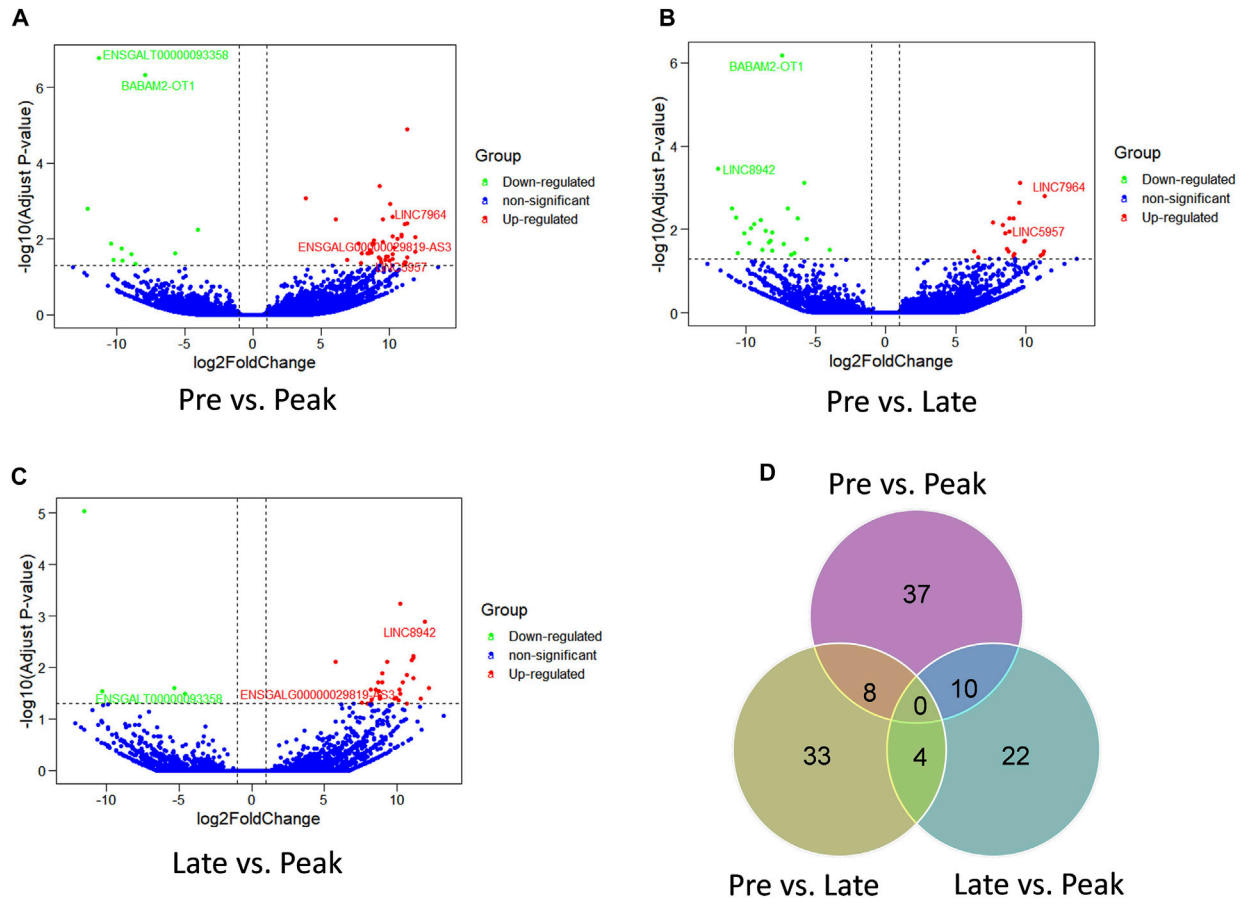


FIGURE 2
Comparison of expression level and the differential expression of lncRNAs in three groups. **(A)** The volcano plot of lncRNAs in Pre vs. Peak; **(B)** the volcano plot of lncRNAs in Pre vs. Late; **(C)** The volcano plot of lncRNAs in Late vs. Peak. **(D)** Venn diagram of DE lncRNAs of the three groups.

lncRNA was less than that of mRNA (Figure 1D), which suggested that lncRNAs played a crucial role in transcription and post-transcription regulation.

## 3.3 LncRNAs differential expression analysis

The comparison of lncRNA expression levels were estimated through FPKM. RNA sequencing detected a total of 136 lncRNAs as differentially expressed in the three comparison groups. 55 lncRNAs were differentially expressed (44 upregulated, 11 downregulated) (Figure 2A) in Pre vs. Peak, 45 lncRNAs (21 upregulated, 24 downregulated) in Pre vs. Late (Figure 2B) and 36 lncRNAs (32 upregulated, 4 downregulated) in Late vs. Peak respectively (Figure 2C). To further analyze the interactions between DE lncRNAs, Venn maps were constructed using 55, 45 and 36 lncRNAs differentially expressed in Pre vs. Peak, Pre vs. Late, and Late vs. Peak, respectively (Figure 2D). We did not detect any commonly differentially expressed lncRNAs in the three control groups, but we identified lncRNAs that were specifically differentially expressed in each of the two control groups. Including 8 lncRNAs specifically expressed during the early laying period, 10 lncRNAs specifically expressed during the peak laying period and 4 lncRNAs expressed during the late laying period.

## 3.4 Functional enrichment analysis of differentially expressed lncRNAs target genes

In total, 453 trans-target genes and 445 cis-target genes were identified against the 136 DE lncRNAs. To further interpret the role of particular signaling pathways in ovarian development, we conducted biological functional analysis of the target genes of 136 lncRNAs derived from three control groups. The figures (Figure 3) displayed the top 30 enriched Gene Ontology (GO) items for target genes in each of the three control groups. The GO results for target genes at different laying period suggested significant associations between cellular components, biological processes, and molecular functions with ovarian development and hormone production. During the early laying period, the predominant biological processes included cell signaling, ovarian follicle development, and germ cell development. In terms of molecular functions, there was significant enrichment in receptor ligand activity. Cellular

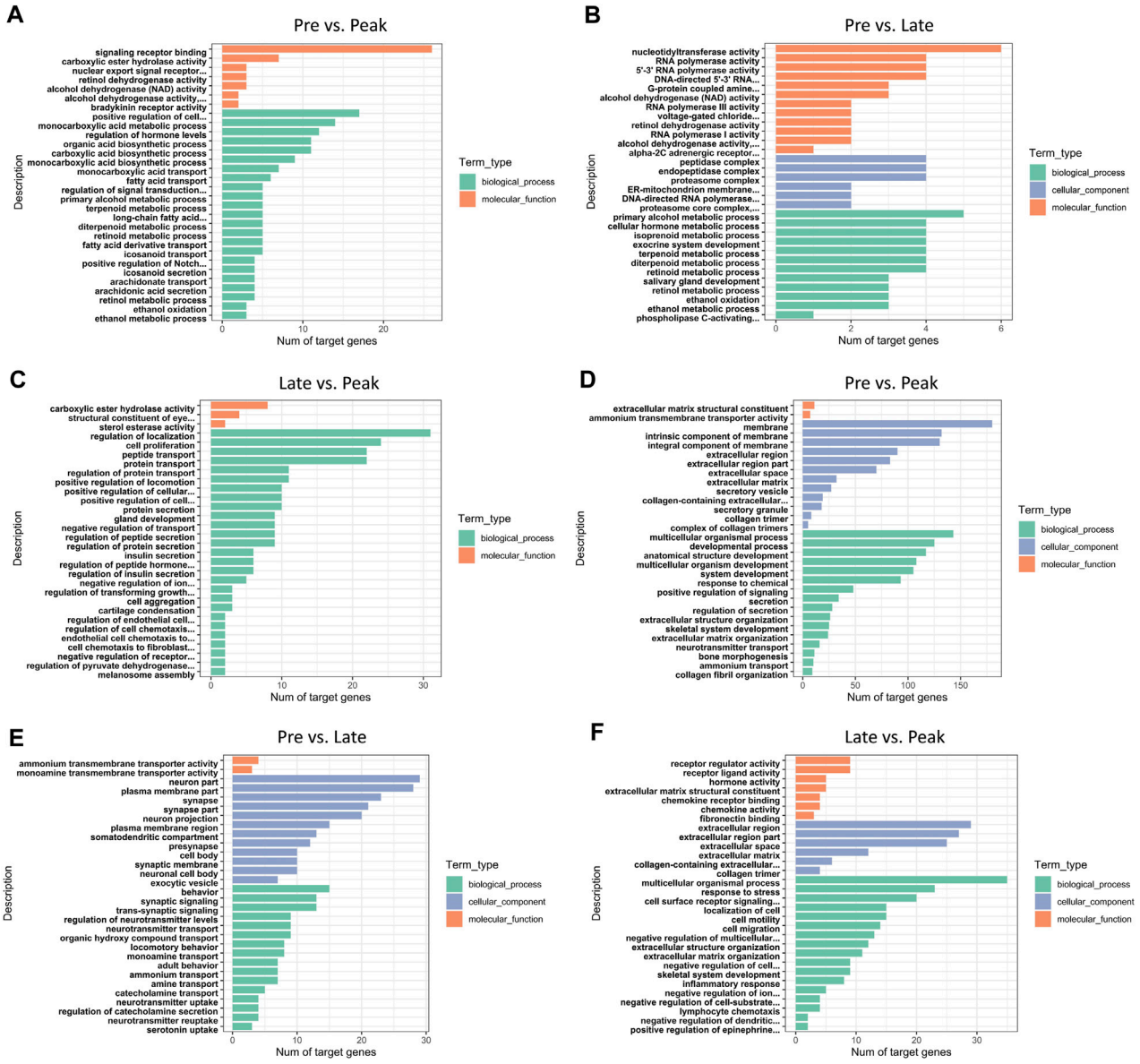


FIGURE 3
GO annotation of DE lncRNAs' cis target genes for the top 30 items in **(A)** Pre vs. Peak, **(B)** Pre vs. Late, and **(C)** Late vs. Peak. GO annotation of DE lncRNAs' trans target genes for the top 30 items in **(D)** Pre vs. Peak, **(E)** Pre vs. Late, and **(F)** Late vs. Peak.

components showed notable enrichment in secretory vesicle, secretory granule, and extracellular region part (Supplementary Table S1). Furthermore, during the peak laying period, GO enrichment projects were similar to the early laying period. However, target genes regulated by lncRNAs specifically expressed during the egg laying peak also involved biological processes such as cell migration, regulation of blood vessel morphogenesis, enzyme-linked receptor protein signaling pathway, and regulation of insulin secretion. Cellular components were significantly enriched in extracellular matrix and collagen trimer (Supplementary Tables S2, S3). In the late laying period, GO items were mainly enriched in processes such as positive regulation of nitrogen compound metabolic process and cellular glucose homeostasis (Supplementary Table S4).

In the KEGG enrichment analysis, the target genes of DE lncRNAs were significantly enriched in 38 pathways ($p < 0.05$) in Pre vs. Peak, including glycolysis/gluconeogenesis, fatty acid degradation, tyrosine metabolism, and ECM-receptor interaction (Figures 4A, D). In Pre vs. Late, the target genes were significantly enriched to 19 pathways ($p < 0.05$). These included fatty acid degradation, tyrosine metabolism, proteasome and neuroactive ligand-receptor interaction (Figures 4B, E). In Late vs. Peak, they were significantly enriched to 18 pathways ($p < 0.05$), including arachidonic acid metabolism, MAPK signaling pathway, regulation of actin cytoskeleton, and TGF-beta signaling pathway, al (Figures 4C, F). Pathways in the top 20 of the *p*-values are shown in Figure 4. After organizing and analyzing the data, we observed that target genes regulated by various specifically expressed lncRNAs were

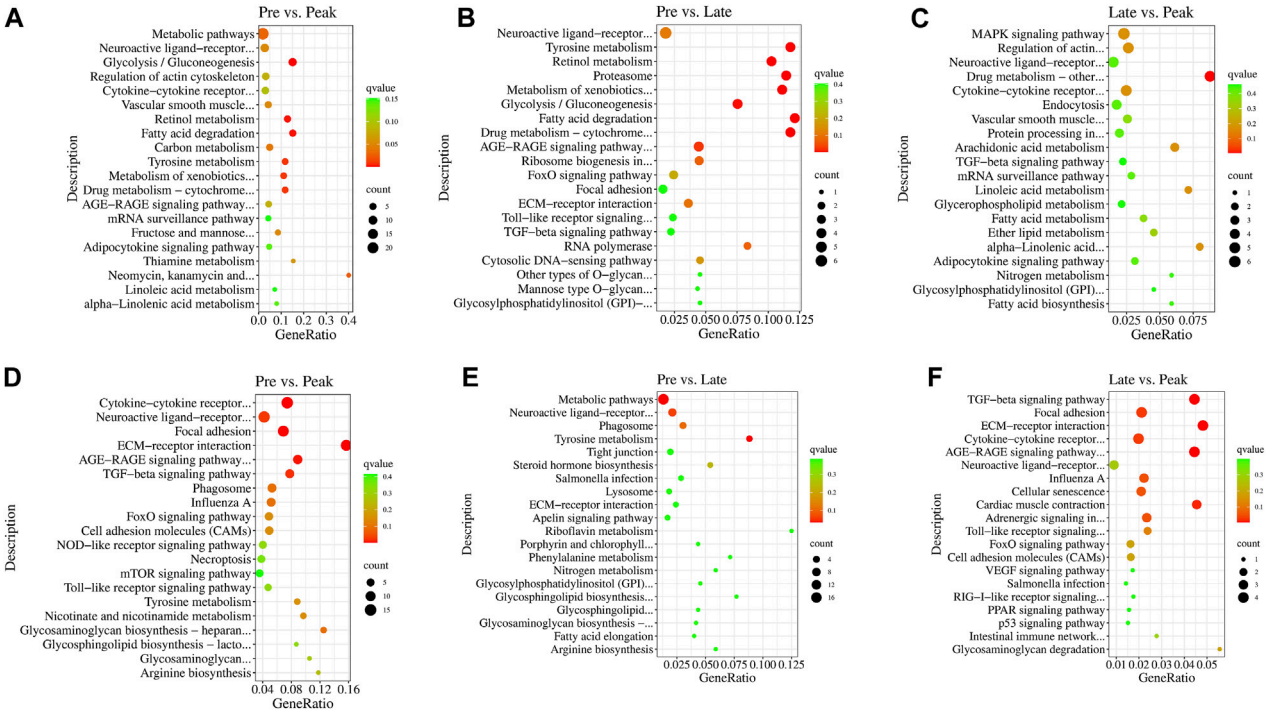


FIGURE 4
The 20 most significant KEGG pathways of DE lncRNAs' cis target genes in **(A)** Pre vs. Peak, **(B)** Pre vs. Late, and **(C)** Late vs. Peak. The 20 most significant KEGG pathways of DE lncRNAs' trans target genes in **(D)** Pre vs. Peak, **(E)** Pre vs. Late, and **(F)** Late vs. Peak.

involved in multiple pathways related to ovary and follicle development. The development of different parts of the ovary is characterized by a series of events influencing sexual maturation. This finding holds significant implications for understanding the function of relevant lncRNAs in the regulation of ovarian development. During the early laying period, enrichment was observed in pathways such as cytokine-cytokine receptor interaction, TGF-beta signaling pathway, and tyrosine metabolism. In the peak laying period, enrichment was observed in pathways in ECM-receptor interaction, focal adhesion, neuroactive ligand-receptor interaction, cell adhesion molecules (CAMs), cytokine-cytokine receptor interaction, and TGF-beta signaling pathway. These pathways align with GO terms related to oocyte cell development. From the results of KEGG pathway enrichment analysis, we infer that lncRNAs may influence these pathways by regulating mRNA during ovarian development processes. The identified pathways are crucial for understanding the intricate regulatory mechanisms involved in the development of the ovary, particularly in relation to oocyte cell development.

## 3.5 LncRNA-mRNA network

Among the 22 lncRNAs specifically expressed during different laying period, we identified that a total of 9 lncRNAs exhibit trans-regulation of the expression of 134 target genes (Figure 5A), while 17 lncRNAs exhibited cis-regulation of 100 target genes (Figure 5B), forming a complex regulatory network. From this, we infer that lncRNAs play a crucial regulatory role in ovarian mRNAs. Through differential analysis and functional analysis of these target genes, we identified 7 lncRNAs that regulated the expression of differentially expressed genes (DEGs) associated with ovarian growth and development. Based on the role of DEGs in ovarian development, we selected a total of 16 lncRNA-mRNA pairs to construct the lncRNA-mRNA network (Figure 5C). During the early laying period, LINC5957 and LINC7964 jointly trans-regulated the expression levels of stathmin-like 2 (*STMN2*), synaptosome-associated protein 25 (*SNAP25*), and LINC5957 also trans-regulated Dopamine β-hydroxylase (*DBH*). BABAM2-OT1 trans-regulated anti-Müllerian hormone (*AMH*). LARGE1-OT3 trans-regulated phenylethanolamine N-methyltransferase (*PNMT*). These target genes were enriched in cytokine-cytokine receptor interaction, TGF-beta signaling pathway, and tyrosine metabolism, and participate in follicle development. During the peak laying period, ENSGALT00000093358 trans-regulated the expression levels of inhibin subunit beta B(INHBB), relaxin-3 (*RLN3*), versican (*VCAN*), secretogranin II (*SCG2*), secreted protein, acidic and rich in cysteine (*SPARC*), collagen family members *COL5A2*, *COL4A1*, and *COL4A2*. The downregulated ENSGALG00000029819-AS3 positively regulated the expression level of secretogranin II (*SCG2*). These target genes were involved in oocyte cell development, oogenesis, ECM-receptor interaction, focal adhesion, neuroactive ligand-receptor interaction, CAMs, cytokine-cytokine receptor interaction, and TGF-beta signaling pathway. During the late laying period, LINC8942 trans-regulated the expression of *NHLH2*. It is evident that these lncRNAs participate in the regulation of ovarian growth and development by targeting mRNAs.

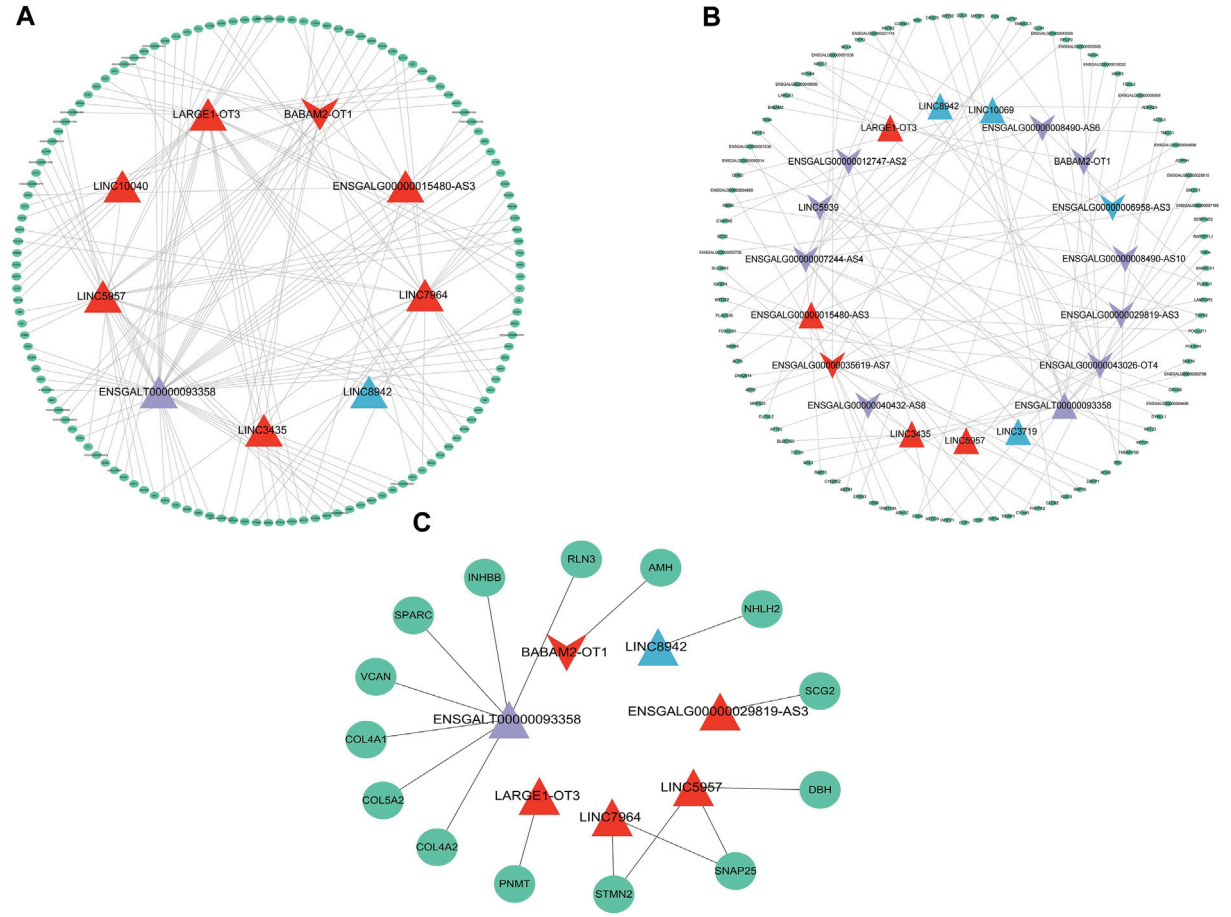


FIGURE 5
The lncRNA-mRNA interaction network depicting mRNAs regulated by specially expressed lncRNAs with specific expression during various periods. **(A)** mRNAs regulated in trans, **(B)** mRNAs regulated in cis, **(C)** mRNAs related to ovarian development. The triangles and inverted triangle exhibit upregulated and downregulated lncRNAs: red exhibits in the early laying period; purple exhibits during the peak laying period; blue exhibits during the late laying period. The green ellipses exhibit target genes.

## 3.6 Protein–protein interaction between mRNAs regulated by lncRNAs with temporal specificity in different periods

Based on the enrichment analysis of GO and KEGG pathways for target genes, we conducted a protein-protein interaction network analysis for mRNAs regulated by lncRNAs with specific expression during different laying periods. This approach provides insight into potential functional networks of mRNAs that regulate ovarian growth and development. We identified key genes, such as *SNAP25*, *STMN2*, *DBH*, and *PNMT*, as central hub genes in the protein-protein interaction network during the early laying period (highly correlated in the candidate module, with the top 40% connectivity, Figure 6A). Similarly, during the peak laying period, *COL4A2*, *COL4A1*, *COL5A2*, *SPARC*, and other key genes were identified as central hub genes in the protein-protein interaction network (highly correlated in the candidate module, with the top 40% connectivity, Figure 6B). Previous studies have reported the crucial roles of these genes in regulating ovarian growth and development. It is noteworthy that these hub genes exhibit differential expression during different laying periods, suggesting that they may play distinct roles at different periods of ovarian development. These findings provide clues for a more in-depth understanding of the precise roles of these key genes in the ovarian development process and offer important directions for future research.

Finally, we conducted RT-qPCR analysis to assess the expression levels of the six lncRNAs and six mRNAs across various laying periods. As depicted in Figure 7, the qPCR expression results aligned with the trends observed in the RNA-seq data, offering valuable insights for the potential functional validation of these molecules in our subsequent experiments.

# 4 Discussion

Egg production is a crucial indicator for assessing poultry fertility, and it significantly influences the production efficiency and profitability of the layer chicken industry (Mu et al., 2021). The laying process is governed by ovarian function and is stimulated by specific peptides or hormones secreted by the HPG axis, promoting the maturation and ovulation of follicles (Tilly and

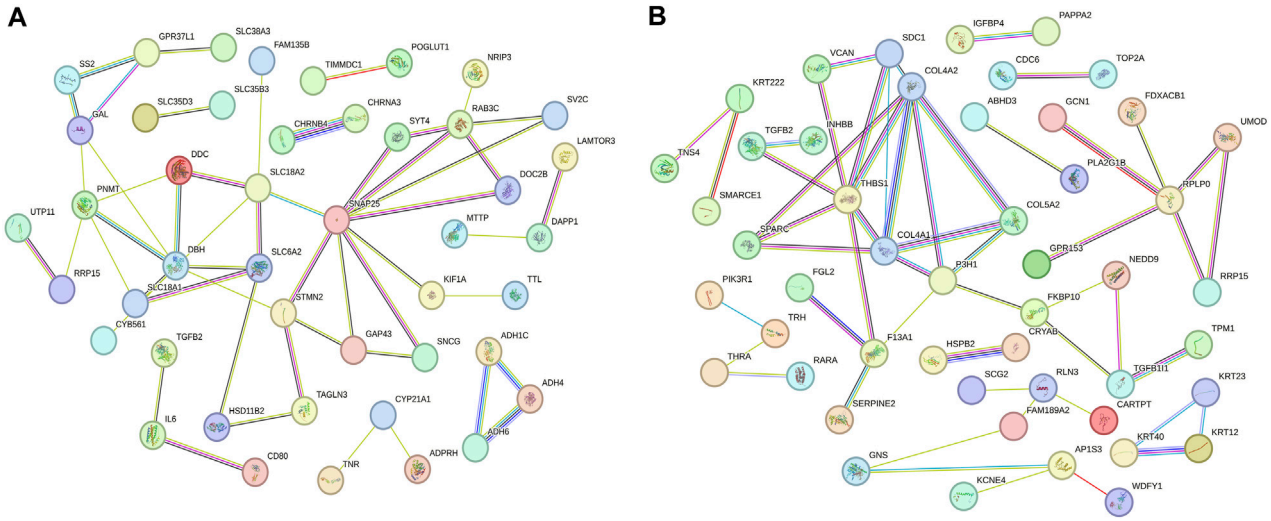


FIGURE 6
Protein–protein interaction network of mRNAs regulated by lncRNAs specifically expressed across various periods. **(A)** The early laying period, **(B)** the peak laying period.

Johnson, 1990; Onagbesan et al., 2009). In recent years, an increasing amount of research has shown that lncRNAs play a significant role in wide-ranging biological processes (Liu et al., 2018). Researchers have found that lncRNAs participate in various reproductive processes in animals. Including pregnancy (Nakagawa et al., 2014), gonadotropin responses (Li et al., 2013), oocyte maturation (Li et al., 2015), and placental formation (Gao et al., 2012). In order to gain a better understanding of the physiological characteristics of Taihe Black-Bone Chickens and enhance their reproductive capabilities, this study conducted an in-depth analysis of the expression patterns of ovarian lncRNAs during the developmental process. Therefore, this study constructed 12 ovarian cDNA libraries from three different laying periods and assessed the expression of lncRNAs using Illumina high-throughput sequencing. The aim is to study functional lncRNAs associated with egg laying characteristics.

This study marks the first report of the expression profile of lncRNAs in the ovaries of Taihe Black-Bone Chickens. Specifically, we identified a total of 136 differentially expressed lncRNAs across three distinct laying periods, uncovering lncRNAs that exhibited stage-specific expression patterns (Figure 2). When comparing the characteristics of lncRNAs with mRNAs, we observed that lncRNAs had fewer exons, transcripts, and shorter open reading frame lengths, and their abundance was lower than that of mRNAs, consistent with findings in other species (Tilgner et al., 2012). The lncRNAs identified in this study exhibited similar characteristics to those found in previous research, indicating the reliability of their detection in this study.

In this study, we observed some lncRNAs with stage-specific expression patterns regulated the expression of target genes related to ovarian development (Figure 8). In the GO analysis during the early laying period, these target genes were enriched in items such as follicle development, germ cell development, and hormone synthesis (Supplementary Table S1). In the KEGG analysis, the target genes were predominantly enriched in the pathways of Cytokine-cytokine receptor interaction, TGF-beta signaling pathway, and Tyrosine metabolism (Figures 4D, E). Cytokine-cytokine receptor interaction is a biological pathway involved in regulating immune and inflammatory processes. It plays a role in immune cell regulation in ovarian tissue to ensure a normal immune response. This pathway is also related to the regulation of ovarian hormones, affecting processes like follicle development, egg maturation, and ovulation. TGF-beta signaling pathway plays a crucial role in the proliferation, differentiation, and survival of granulosa cells and follicular wall cells (Han et al., 2022). Additionally, it regulates the selection and release of follicles. The target gene *AMH* is significantly enriched in both pathways. Anti-Müllerian hormone (*AMH*) belongs to the transforming growth factor-beta super family and is mainly secreted by granulosa cells. It inhibits the activation of primordial follicles in the early stages of ovarian follicle development, preventing the depletion of the follicle pool. Research indicates that during the follicle selection stage, *AMH* significantly decreases (Xu J. et al., 2016). Additionally, different concentrations of *AMH* treatment have varying effects on follicular development and steroidogenesis in the reproductive organs of laying hens (Huang et al., 2021). *AMH* exhibited high specific expression in the early laying period (Supplementary Tables S5, S6) and was inversely regulated by downregulated BABAM2-OT1. This regulation contributes to maintaining the reserve of follicles and preventing their premature development.

Tyrosine metabolism plays an essential role in ovarian function and physiological processes, especially in hormone synthesis, neural regulation, and antioxidant defense. Tyrosine is a crucial precursor molecule for hormone biosynthesis. In the ovaries, tyrosine is involved in the synthesis of progesterone and catecholamine hormones. The target genes enriched in this pathway include *PNMT* and *DBH*. Dopamine β-hydroxylase (*DBH*) and phenylethanolamine N-methyltransferase (*PNMT*) are key enzymes in the biosynthesis of catecholamines, with *PNMT* being responsible for a crucial step in the biosynthesis of catecholamine

10.3389/fphys.2024.1358682

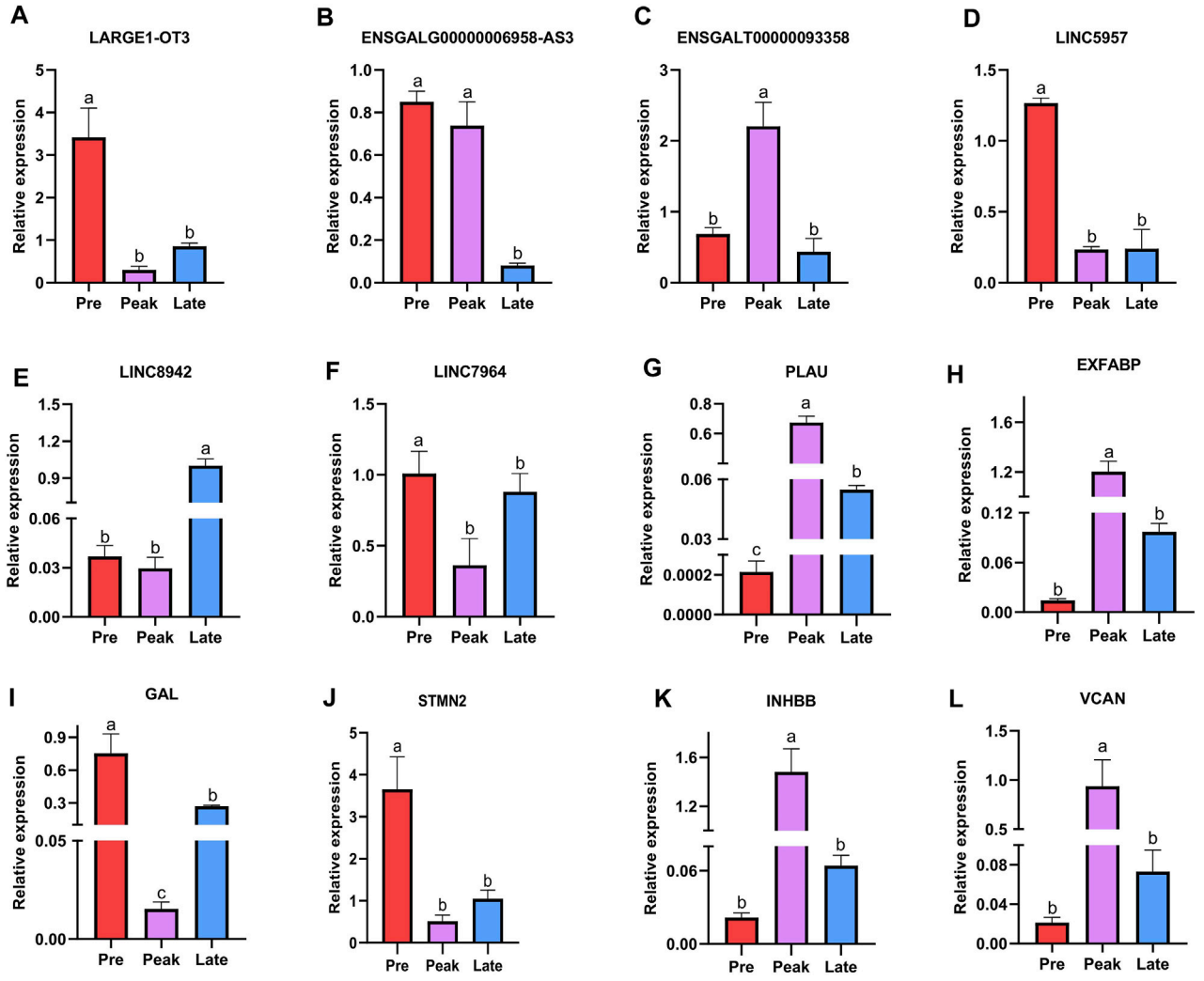


FIGURE 7
Validation of six differentially expressed lncRNAs and six differentially expressed mRNAs was performed by qPCR. The letters on the column diagram indicate significant ($p < 0.05$) differences at different stages. **(A–F)** represents lncRNA, and **(G–L)** represents mRNA.

neurotransmitters. Its primary function is to convert the precursor molecule phenylethanolamine into norepinephrine. Moreover, studies suggest that *DBH* regulates reproductive activity in geese through the HPG axis. In the ovaries of high-egg-producing Yangzhou geese, the expression level of *DBH* is higher than in low-egg-producing counterparts. It is speculated that a higher egg production requires the release of more hormones for ovulation, and a higher expression level of *DBH* ensures an adequate hormone secretion (Xu Q. et al., 2016). The upregulated LARGE1-OT3 inversely regulated *PNMT*, *PNMT* was highly expressed in the early laying period of the ovaries (Supplementary Tables S5, S6), while *DBH* was upregulated in Pre vs. Late (Supplementary Table S6) and was inversely regulated by the upregulated LINC5957. It is evident that LARGE1-OT3 and LINC5957, by regulating the expression of *PNMT* and *DBH*, contribute to maintaining neurotransmitter balance and hormone levels in the early laying period of the ovaries.

Furthermore, the specific high expression of *STMN2* and *SNAP25* during the early laying period has captured our attention (Supplementary Tables S5, S6). These two target genes were hub genes in protein-protein interaction networks (Figure 6A), and we infer that they play crucial roles in the ovaries of Taihe Black-bone Chickens during the early laying period. Stathmin 2 (*STMN2*) is a gene encoding a member of the stathmin family. Stathmins are a protein family that regulates the dynamic stability of microtubules, influencing ovarian cell mitosis, migration, and infiltration, and regulating intracellular signal transduction. Reports suggest that the expression of *STMN2* in the hypothalamus and pituitary of native Taiwanese chickens influences the number of eggs at 50 weeks of age and the laying rate after the first egg (Chen et al., 2007). These findings emphasize the significant role of *STMN2* in the chicken ovaries. Synaptosome-associated protein 25 (*SNAP25*) is one of the key proteins involved in the fusion of neuronal synaptic vesicles, participating in the process of neurotransmitter release (Shimada et al., 2007). It may be involved in neurotransmitter release in ovarian tissue, regulating cell communication and signal transduction within

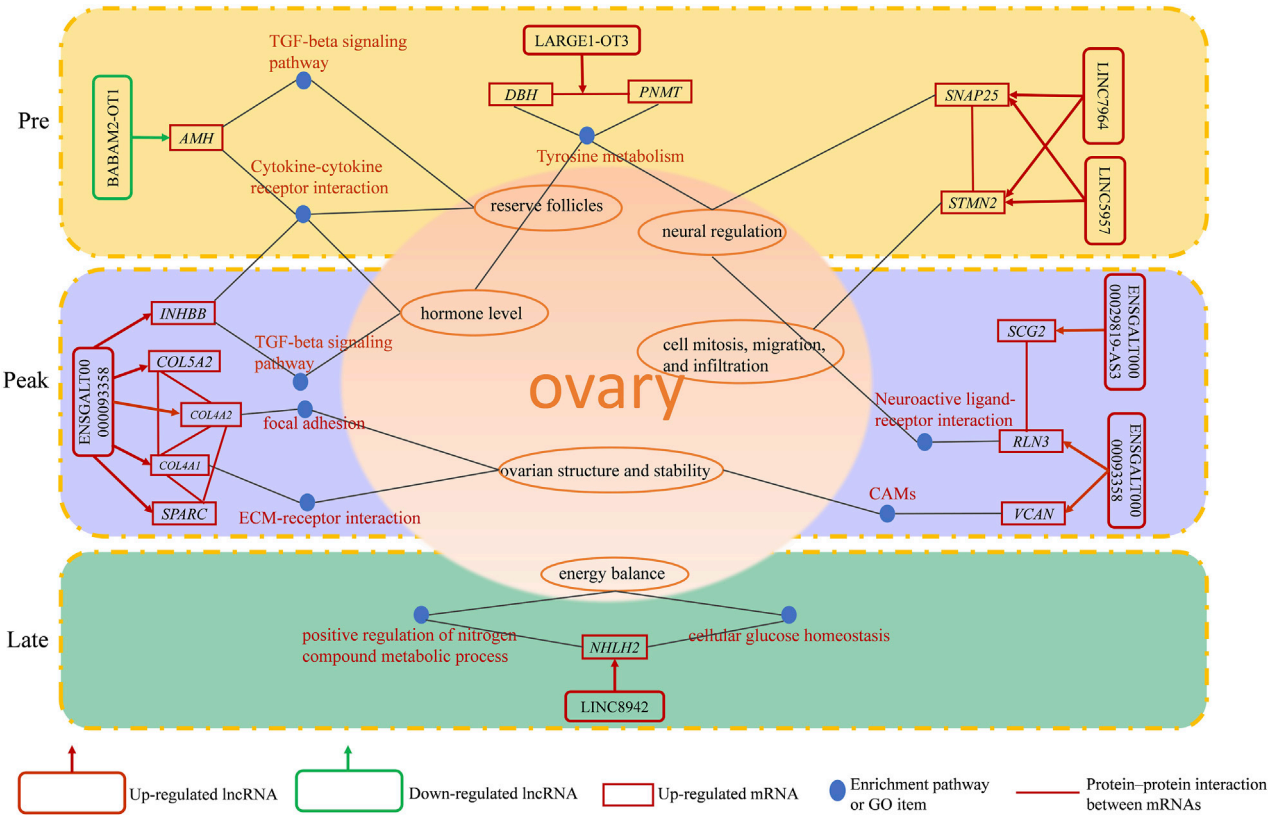


FIGURE 8
A schematic diagram of the regulatory role of identified lncRNAs in ovarian function.

the ovaries. The upregulated LINC5957 and LINC7964 collectively inversely regulated *STMN2* and *SNAP25*, impacting the overall functionality of ovarian tissue.

During the peak laying period, ENSGALT00000093358 was the most upregulated specific lncRNA. It inversely regulated the expression of *INHBB*, *RLN3*, *VCAN*, *COL4A1*, *COL4A2*, *COL5A2*, and *SPARC*, while the downregulated ENSGALG00000029819-AS3 positively regulated the expression level of *SCG2*. These target genes were involved in biological processes such as ovarian cell migration, regulation of vascular morphogenesis, enzyme-linked receptor protein signaling pathway, insulin secretion regulation, as well as cellular components like follicular wall extracellular matrix and collagen trimer, according to the GO analysis (Supplementary Tables S2, S3). In KEGG analysis of the target genes, we found that ECM-receptor interaction is a crucial cell signaling pathway, consistent with the results of the GO analysis. As known, the ovarian follicular wall of hens mainly consists of the extracellular matrix (ECM), and the ability of the ECM to guide cell proliferation, differentiation, and function highlights its critical role in normal ovarian function reconstruction. Focal adhesion is a cellular structure that connects cells to the ECM, achieved by the binding of receptors on the cell membrane to the ECM (Huang et al., 2022). ECM-receptor interaction may participate in the interaction between granulosa cells and the follicular wall, influencing the formation and maturation of follicles. *COL4A1* and *COL4A2*, two crucial genes, are enriched in these pathways. *COL4A1* and *COL4A2* encode collagen proteins (collagen type IV alpha 1 chain and collagen type IV alpha 2 chain, respectively). In the ovaries, these genes are involved in the structure and function of the extracellular matrix (ECM) and interactions with cells (Tang et al., 2019). *COL4A1* was specifically highly expressed during the high-production period, and *COL4A2* and *COL5A2* were upregulated in Peak vs. Pre (Supplementary Table S5). Additionally, upregulated secreted protein, acidic and rich in cysteine (*SPARC*) in Peak vs. Pre (Supplementary Table S5), was a hub gene in the protein-protein interaction network during the peak laying period and is involved in the regulation of the extracellular matrix (Figure 6B; Supplementary Table S2). Therefore, ENSGALT00000093358 may maintain ovarian structure and stability by regulating these target genes.

Neuroactive ligand-receptor interaction is a biological pathway involving the interaction between neurotransmitters and their receptors. There are neurons present in ovarian tissue that may release neurotransmitters, interacting with corresponding receptors and influencing hormone secretion and physiological effects in the ovary, participating in reproductive regulation. *RLN3* is significantly enriched in this pathway and is highly expressed during the peak egg-laying period. Relaxin-like peptides, such as *RLN3*, are produced in granulosa cells post-ovulation and play a role in promoting egg laying, impacting the oviduct and ovary (Ghanem and Johnson, 2021). Additionally, in the protein-protein interaction network, we observed an interaction between *RLN3* and *SCG2* (Figure 6B).

Secretogranin II (*SCG2*) is a protein involved in neurosecretion, particularly associated with the secretion granules of neuroendocrine cells. *SCG2* was upregulated in Peak vs. Late (Supplementary Table S7). In the ovaries of Taihe Black-bone Chickens, these two target genes may influence ovarian function through neural regulation, affecting the laying rate during the peak laying period. CAMs are glycoproteins on the cell membrane that facilitate adhesion of different types of ovarian cells, coordinating interactions between oocytes and supporting cells within the follicle (Heffner et al., 2020). Versican (*VCAN*) was significantly enriched in CAMs and was highly expressed during the peak laying period, promoting follicle maturation. *INHBB* (Inhibin subunit beta B) is a glycoprotein hormone belonging to the transforming growth factor-beta superfamily, known to simultaneously affect apoptosis and steroidogenesis in primary granulosa cells (M'Baye et al., 2015). High expression of *INHBB* during the peak laying period (Supplementary Tables S5, S7), along with its enrichment in the Cytokine-cytokine receptor interaction and TGF-beta signaling pathway, suggests its role in regulating hormone secretion and maintaining reproductive system balance through a feedback mechanism. Therefore, based on the functional analysis of target genes, it is inferred that during the peak laying period, the lncRNAs ENSGALT00000093358 and ENSGALG00000029819-AS3, which show specific expression, may play crucial regulatory roles in target genes associated with ovarian development, participating in the regulation of ovarian follicle development and maturation.

In our analysis of the late laying period ovarian-specific lncRNAs expression, the upregulation of LINC8942 caught our attention as it was found to exhibit trans regulation of *NHLH2* expression. *NHLH2* is a member of the basic helix-loop-helix (*bHLH*) transcription factor family. The GO items of this target gene was significantly enriched in positive regulation of nitrogen compound metabolic process and cellular glucose homeostasis (Supplementary Table S4), suggesting that *NHLH2* participates in the regulation of ovarian glucose metabolism and energy balance. In addition, in a study on mouse gonadal development, *NHLH2* was found to be necessary for the migration of embryonic GnRH neurons, and migration defects could potentially impact gonadal development (Good and Braun, 2013). This target gene was downregulated in Pre vs. Late (Supplementary Table S6). Consequently, it can be inferred that LINC8942 may influence the late laying period egg production by regulating genes associated with gonadal development and energy metabolism. Despite our observations, the underlying mechanisms need further investigation

## 5 Conclusion

In this study, we conducted RNA-seq analysis on Taihe Black-Bone Chicken ovaries at different laying periods. We identified 136 DE lncRNAs. Among these, 8 were specific to early laying periods, 10 to peak laying periods, and 4 to late laying periods. Seven stage-specific DE lncRNAs regulated 14 target genes associated with ovarian development. During the early laying period, upregulated lncRNAs (LINC5957, LINC7964) co-trans-regulated *STMN2*, *SNAP25*, and cis-regulated *DBH*. LARGE1-OT3 cis-regulated *PNMT*. The downregulated DE lncRNA BABAM2-OT1 trans-regulated *AMH*. Upregulated ENSGALT00000093358 trans-regulated *INHBB*, *RLN3*, *VCAN*, *SPARC*, *COL5A2*, *COL4A1*, *COL4A2*, while upregulated ENSGALG00000029819-AS3 cis-regulated *SCG2* in the peak laying period. LINC8942 trans-regulated *NHLH2* in the late laying period. These target genes are involved in follicular development, oocyte-related signaling pathways (tyrosine metabolism, CAMs, neuroactive ligand-receptor interactions, focal adhesion, cytokine-cytokine receptor interactions, TGF-beta signaling pathway). This study provides a foundation for further research on the impact of lncRNAs on reproductive characteristics of Taihe Black-Bone Chickens. Future studies can explore functional roles of these lncRNAs and use genetic modification to enhance chicken reproductive performance and ovarian health. Comparative analysis with other species can yield insights into avian reproductive biology.

## Data availability statement

The sequence data were submitted to the NCBI SRA database under the accession number PRJNA889190.

## Ethics statement

The animal study was approved by Institutional Animal Care and Use Committee of Zhejiang University. The study was conducted in accordance with the local legislation and institutional requirements.

## Author contributions

YH: Data curation, Methodology, Writing–original draft. SL: Methodology, Writing–original draft. YT: Validation, Visualization, Writing–original draft. CX: Methodology, Software, Visualization, Writing–original draft. XH: Formal Analysis, Investigation, Writing–original draft. ZY: Writing–review and editing.

## Funding

The authors declare financial support was received for the research, authorship, and/or publication of this article. This research was funded by Major Scientific and Technological cooperation between Zhejiang University and Taihe County Government, grant number 2021-KYY-517102-0023, and the Zhejiang Provincial "Fourteenth Five Year Plan" major scientific and technological special projects in agriculture, grant number 2021C02068-11.

## Acknowledgments

We thank Taihe Aoxin Black-Bone silky fowl Development Co., Ltd., for providing all the experimental chickens.

## Conflict of interest

The authors declare that the research was conducted in the absence of any commercial or financial relationships that could be construed as a potential conflict of interest.

## Publisher's note

All claims expressed in this article are solely those of the authors and do not necessarily represent those of their affiliated organizations, or those of the publisher, the editors and the reviewers. Any product that may be evaluated in this article, or claim that may be made by its manufacturer, is not guaranteed or endorsed by the publisher.

## Supplementary material

The Supplementary Material for this article can be found online at: https://www.frontiersin.org/articles/10.3389/fphys.2024.1358682/full#supplementary-material

## References

Bonasio, R., and Shiekhattar, R. (2014). Regulation of transcription by long noncoding RNAs. *Annu. Rev. Genet.* 48, 433–455. doi:10.1146/annurev-genet-120213-092323

Brown, J. B., Boley, N., Eisman, R., May, G. E., Stoiber, M. H., Duff, M. O., et al. (2014). Diversity and dynamics of the Drosophila transcriptome. *Nature* 512 (7515), 393–399. doi:10.1038/nature12962

Chen, C. F., Shiue, Y. L., Yen, C. J., Tang, P. C., Chang, H. C., and Lee, Y. P. (2007). Laying traits and underlying transcripts, expressed in the hypothalamus and pituitary gland, that were associated with egg production variability in chickens. *Theriogenology* 68 (9), 1305–1315. doi:10.1016/j.theriogenology.2007.08.032

Chomchuen, K., Tuntiyasawasdikul, V., Chankitisakul, V., and Boonkum, W. (2022). Genetic evaluation of body weights and egg production traits using a multi-trait animal model and selection Index in Thai native synthetic chickens (kaimook e-san2). *Anim. (Basel)* 12 (3), 335. doi:10.3390/ani12030335

Finn, R. D., Bateman, A., Clements, J., Coggill, P., Eberhardt, R. Y., Eddy, S. R., et al. (2014). Pfam: the protein families database. *Nucleic Acids Res.* 42, D222–D230. doi:10.1093/nar/gkt1223

Gao, W. L., Liu, M., Yang, Y., Yang, H., Liao, Q., Bai, Y., et al. (2012). The imprinted H19 gene regulates human placental trophoblast cell proliferation via encoding miR-675 that targets Nodal Modulator 1 (NOMO1). *RNA Biol.* 9 (7), 1002–1010. doi:10.4161/rna.20807

Ghanem, K., and Johnson, A. L. (2019). Response of hen pre-recruitment ovarian follicles to follicle stimulating hormone, *in vivo*. *Gen. Comp. Endocrinol.* 270, 41–47. doi:10.1016/j.ygcen.2018.10.004

Ghanem, K., and Johnson, A. L. (2021). Proteome profiling of chicken ovarian follicles immediately before and after cyclic recruitment. *Mol. Reprod. Dev.* 88 (8), 571–583. doi:10.1002/mrd.23522

Good, D. J., and Braun, T. (2013). NHLH2: at the intersection of obesity and fertility. *Trends Endocrinol. Metab.* 24 (8), 385–390. doi:10.1016/j.tem.2013.04.003

Han, S., Wang, J., Cui, C., Yu, C., Zhang, Y., Li, D., et al. (2022). Fibromodulin is involved in autophagy and apoptosis of granulosa cells affecting the follicular atresia in chicken. *Poult. Sci.* 101 (1), 101524. doi:10.1016/j.psj.2021.101524

Heffner, K., Hizal, D. B., Majewska, N. I., Kumar, S., Dhara, V. G., Zhu, J., et al. (2020). Expanded Chinese hamster organ and cell line proteomics profiling reveals tissue-specific functionalities. *Sci. Rep.* 10 (1), 15841. doi:10.1038/s41598-020-72959-8

Huang, S. J., Purevsuren, L., Jin, F., Zhang, Y. P., Liang, C. Y., Zhu, M. Q., et al. (2021). Effect of anti-müllerian hormone on the development and selection of ovarian follicle in hens. *Poult. Sci.* 100 (3), 100959. doi:10.1016/j.psj.2020.12.056

Huang, X., Zhou, W., Cao, H., Zhang, H., Xiang, X., and Yin, Z. (2022). Ovarian transcriptomic analysis of ninghai indigenous chickens at different egg-laying periods. *Genes (Basel)* 13 (4), 595. doi:10.3390/genes13040595

Iannotti, L. L., Lutter, C. K., Bunn, D. A., and Stewart, C. P. (2014). Eggs: the uncracked potential for improving maternal and young child nutrition among the world's poor. *Nutr. Rev.* 72 (6), 355–368. doi:10.1111/nure.12107

Kanehisa, M., Araki, M., Goto, S., Hattori, M., Hirakawa, M., Itoh, M., et al. (2008). KEGG for linking genomes to life and the environment. *Nucleic Acids Res.* 36, D480–D484. doi:10.1093/nar/gkm882

Kong, L., Zhang, Y., Ye, Z. Q., Liu, X. Q., Zhao, S. Q., Wei, L., et al. (2007). CPC: assess the protein-coding potential of transcripts using sequence features and support vector machine. *Nucleic Acids Res.* 35, W345–W349. doi:10.1093/nar/gkm391

Kovaka, S., Zimin, A. V., Pertea, G. M., Razaghi, R., Salzberg, S. L., and Pertea, M. (2019). Transcriptome assembly from long-read RNA-seq alignments with StringTie2. *Genome Biol.* 20 (1), 278. doi:10.1186/s13059-019-1910-1

Li, J., Cao, Y., Xu, X., Xiang, H., Zhang, Z., Chen, B., et al. (2015). Increased new lncRNA-mRNA gene pair levels in human cumulus cells correlate with oocyte maturation and embryo development. *Reprod. Sci.* 22 (8), 1008–1014. doi:10.1177/1933719115570911

Li, W., Notani, D., Ma, Q., Tanasa, B., Nunez, E., Chen, A. Y., et al. (2013). Functional roles of enhancer RNAs for oestrogen-dependent transcriptional activation. *Nature* 498 (7455), 516–520. doi:10.1038/nature12210

Li, W. L., Liu, Y., Yu, Y. C., Huang, Y. M., Liang, S. D., and Shi, Z. D. (2011). Prolactin plays a stimulatory role in ovarian follicular development and egg laying in chicken hens. *Domest. Anim. Endocrinol.* 41 (2), 57–66. doi:10.1016/j.domaniend.2011.03.002

Liu, K. S., Li, T. P., Ton, H., Mao, X. D., and Chen, Y. J. (2018). Advances of long noncoding RNAs-mediated regulation in reproduction. *Chin. Med. J. Engl.* 131 (2), 226–234. doi:10.4103/0366-6999.222337

Macaulay, A. D., Gilbert, I., Caballero, J., Barreto, R., Fournier, E., Tossou, P., et al. (2014). The gametic synapse: RNA transfer to the bovine oocyte. *Biol. Reprod.* 91 (4), 90. doi:10.1095/biolreprod.114.119867

M'Baye, M., Hua, G., Khan, H. A., and Yang, L. (2015). RNAi-mediated knockdown of INHBB increases apoptosis and inhibits steroidogenesis in mouse granulosa cells. *J. Reprod. Dev.* 61 (5), 391–397. doi:10.1262/jrd.2014-158

Mi, S., Shang, K., Jia, W., Zhang, C. H., Li, X., Fan, Y. Q., et al. (2018). Characterization and discrimination of Taihe black-boned silky fowl (Gallus gallus domesticus Brisson) muscles using LC/MS-based lipidomics. *Food Res. Int.* 109, 187–195. doi:10.1016/j.foodres.2018.04.038

Minarovits, J., Banati, F., Szenthe, K., and Niller, H. H. (2016). Epigenetic regulation. *Adv. Exp. Med. Biol.* 879, 1–25. doi:10.1007/978-3-319-24738-0_1

Mishra, S. K., Chen, B., Zhu, Q., Xu, Z., Ning, C., Yin, H., et al. (2020). Transcriptome analysis reveals differentially expressed genes associated with high rates of egg production in chicken hypothalamic-pituitary-ovarian axis. *Sci. Rep.* 10 (1), 5976. doi:10.1038/s41598-020-62886-z

Mu, R., Yu, Y. Y., Gegen, T., Wen, D., Wang, F., Chen, Z., et al. (2021). Transcriptome analysis of ovary tissues from low- and high-yielding Changshun green-shell laying hens. *BMC Genomics* 22 (1), 349. doi:10.1186/s12864-021-07688-x

Nakagawa, S., Shimada, M., Yanaka, K., Mito, M., Arai, T., Takahashi, E., et al. (2014). The lncRNA Neat1 is required for corpus luteum formation and the establishment of pregnancy in a subpopulation of mice. *Development* 141 (23), 4618–4627. doi:10.1242/dev.110544

Onagbesan, O., Bruggeman, V., and Decuypere, E. (2009). Intra-ovarian growth factors regulating ovarian function in avian species: a review. *Anim. Reprod. Sci.* 111 (2-4), 121–140. doi:10.1016/j.anireprosci.2008.09.017

Pertea, M., Kim, D., Pertea, G. M., Leek, J. T., and Salzberg, S. L. (2016). Transcript-level expression analysis of RNA-seq experiments with HISAT, StringTie and Ballgown. *Nat. Protoc.* 11 (9), 1650–1667. doi:10.1038/nprot.2016.095

Pertea, M., Pertea, G. M., Antonescu, C. M., Chang, T. C., Mendell, J. T., and Salzberg, S. L. (2015). StringTie enables improved reconstruction of a transcriptome from RNA-seq reads. *Nat. Biotechnol.* 33 (3), 290–295. doi:10.1038/nbt.3122

Ren, C., Li, X., Wang, T., Wang, G., Zhao, C., Liang, T., et al. (2015). Functions and mechanisms of long noncoding RNAs in ovarian cancer. *Int. J. Gynecol. Cancer* 25 (4), 566–569. doi:10.1097/igc.0000000000000413

Shabbir, S., Boruah, P., Xie, L., Kulyar, M. F., Nawaz, M., Yousuf, S., et al. (2021). Genome-wide transcriptome profiling uncovers differential miRNAs and lncRNAs in ovaries of Hu sheep at different developmental stages. *Sci. Rep.* 11 (1), 5865. doi:10.1038/s41598-021-85245-y

Shimada, M., Yanai, Y., Okazaki, T., Yamashita, Y., Sriraman, V., Wilson, M. C., et al. (2007). Synaptosomal-associated protein 25 gene expression is hormonally regulated during ovulation and is involved in cytokine/chemokine exocytosis from granulosa cells. *Mol. Endocrinol.* 21 (10), 2487–2502. doi:10.1210/me.2007-0042

Sun, L., Luo, H., Bu, D., Zhao, G., Yu, K., Zhang, C., et al. (2013). Utilizing sequence intrinsic composition to classify protein-coding and long non-coding transcripts. *Nucleic Acids Res.* 41 (17), e166. doi:10.1093/nar/gkt646

Sun, X., Chen, X., Zhao, J., Ma, C., Yan, C., Liswaniso, S., et al. (2021). Transcriptome comparative analysis of ovarian follicles reveals the key genes and signaling pathways implicated in hen egg production. *BMC Genomics* 22 (1), 899. doi:10.1186/s12864-021-08213-w

Tang, J., Hu, W., Chen, S., Di, R., Liu, Q., Wang, X., et al. (2019). The genetic mechanism of high prolificacy in small tail han sheep by comparative proteomics of ovaries in the follicular and luteal stages. *J. Proteomics* 204, 103394. doi:10.1016/j.jprot.2019.103394

Tilgner, H., Knowles, D. G., Johnson, R., Davis, C. A., Chakrabortty, S., Djebali, S., et al. (2012). Deep sequencing of subcellular RNA fractions shows splicing to be predominantly co-transcriptional in the human genome but inefficient for lncRNAs. *Genome Res.* 22 (9), 1616–1625. doi:10.1101/gr.134445.111

Tilly, J. L., and Johnson, A. L. (1990). Effect of several growth factors on plasminogen activator activity in granulosa and theca cells of the domestic hen. *Poult. Sci.* 69 (2), 292–299. doi:10.3382/ps.0690292

Wang, Y., Yuan, J., Sun, Y., Li, Y., Wang, P., Shi, L., et al. (2022). Genetic basis of sexual maturation heterosis: insights from ovary lncRNA and mRNA repertoire in chicken. *Front. Endocrinol. (Lausanne)* 13, 951534. doi:10.3389/fendo.2022.951534

Wu, Y., Xiao, H., Pi, J., Zhang, H., Pan, A., Pu, Y., et al. (2021). LncRNA lnc_13814 promotes the cells apoptosis in granulosa cells of duck by acting as apla-miR-145-4 sponge. *Cell Cycle* 20 (9), 927–942. doi:10.1080/15384101.2021.1911102

Xu, J., Bishop, C. V., Lawson, M. S., Park, B. S., and Xu, F. (2016a). Anti-Müllerian hormone promotes pre-antral follicle growth, but inhibits antral follicle maturation and dominant follicle selection in primates. *Hum. Reprod.* 31 (7), 1522–1530. doi:10.1093/humrep/dew100

Xu, Q., Song, Y., Liu, R., Chen, Y., Zhang, Y., Li, Y., et al. (2016b). The dopamine β-hydroxylase gene in Chinese goose (Anas cygnoides): cloning, characterization, and expression during the reproductive cycle. *BMC Genet.* 17, 48. doi:10.1186/s12863-016-0355-8

Young, M. D., Wakefield, M. J., Smyth, G. K., and Oshlack, A. (2010). Gene ontology analysis for RNA-seq: accounting for selection bias. *Genome Biol.* 11 (2), R14. doi:10.1186/gb-2010-11-2-r14

Zhang, R., Wesevich, V., Chen, Z., Zhang, D., and Kallen, A. N. (2020). Emerging roles for noncoding RNAs in female sex steroids and reproductive disease. *Mol. Cell Endocrinol.* 518, 110875. doi:10.1016/j.mce.2020.110875

Zhang, Y., Zhang, J., Chang, X., Qin, S., Song, Y., Tian, J., et al. (2022). Analysis of 90 Listeria monocytogenes contaminated in poultry and livestock meat through whole-genome sequencing. *Food Res. Int.* 159, 111641. doi:10.1016/j.foodres.2022.111641

Zhao, D., Leghari, I. H., Li, J., Mi, Y., and Zhang, C. (2018). Isolation and culture of chicken growing follicles in 2- and 3-dimensional models. *Theriogenology* 111, 43–51. doi:10.1016/j.theriogenology.2018.01.012

Zhao, Z., Zou, X., Lu, T., Deng, M., Li, Y., Guo, Y., et al. (2020). Identification of mRNAs and lncRNAs involved in the regulation of follicle development in goat. *Front. Genet.* 11, 589076. doi:10.3389/fgene.2020.589076

frontiers | Frontiers in Physiology

TYPE Original Research
PUBLISHED 06 March 2024
DOI 10.3389/fphys.2024.1368382



OPEN ACCESS

EDITED BY
Sandra G. Velleman,
The Ohio State University, United States

REVIEWED BY
Servet Yalcin,
Ege University, Türkiye
Rie Henriksen,
Linköping University, Sweden

*CORRESPONDENCE
Lisa Hildebrand,
lisa.hildebrand@fli.de

RECEIVED 10 January 2024
ACCEPTED 13 February 2024
PUBLISHED 06 March 2024

CITATION
Hildebrand L, Gerloff C, Winkler B, Eusemann BK, Kemper N and Petow S (2024), Japanese quails (*Cortunix Japonica*) show keel bone damage during the laying period—a radiography study.
*Front. Physiol.* 15:1368382.
doi: 10.3389/fphys.2024.1368382



# Japanese quails (*Cortunix Japonica*) show keel bone damage during the laying period—a radiography study

Lisa Hildebrand[1]*, Christoph Gerloff[1], Birthe Winkler[1], Beryl Katharina Eusemann[2], Nicole Kemper[3] and Stefanie Petow[1]

[1]Institute of Animal Welfare and Animal Husbandry, Friedrich-Loeffler-Institut, Celle, Germany, [2]Institute of Animal Hygiene and Public Veterinary Services, Faculty of Veterinary Medicine, Leipzig University, Leipzig, Germany, [3]Institute for Animal Hygiene, Animal Welfare and Farm Animal Behaviour, University of Veterinary Medicine Hannover, Hannover, Germany

Keel bone damage is an important welfare issue in laying hens and can occur with a high prevalence of up to 100% of hens within one flock. Affected hens suffer from pain. Although multiple factors contribute to the prevalence and severity of keel bone damage, selection for high laying performance appears to play a key role. With up to 300 eggs/year, Japanese quails show a high laying performance, too, and, thus, may also show keel bone damage. However, to our knowledge, there are no scientific results on keel bone damage in Japanese quails to date. Therefore, the aim of this study was to assess whether keel bone fractures and deviations occur in Japanese quails and to obtain more detailed information about the development of their keel bone during the production cycle. A group of 51 female quails were radiographed at 8, 10, 15, 19, and 23 weeks of age. The X-rays were used to detect fractures and deviations and to measure the lateral surface area, length, and radiographic density of the keel bone. In addition, the length of the caudal cartilaginous part of the keel bone was measured to learn more about the progress of ossification. At 23 weeks of age, quails were euthanized and their macerated keel bones assessed for fractures and deviations. Both keel bone deviations and keel bone fractures were detected in the Japanese quails. In the 23rd week of age, 82% of the quails had a deviated keel bone as assessed after maceration. Furthermore, there was a decrease in radiographic density, lateral surface area, and length of the keel bone between weeks of age 8 and 19. This could indicate a general loss of bone substance and/or demineralization of the keel bone. Our study shows that keel bone damage is not only a problem in laying hens but also affects female Japanese quails.

KEYWORDS

**keel bone damage, Japanese quails, animal welfare, keel bone fracture, keel bone deviation, radiography, keel bone deformities, ossification**

## 1 Introduction

Keel bone damage is one of the most important animal welfare issues in chicken laying hens (Jinman, 2013; Nielsen et al., 2023). The prevalence of fractures can reach up to 100% of hens within one flock (Käppeli et al., 2011; Baur et al., 2020; Thøfner et al., 2021) and affected hens experience pain (Nasr et al., 2012; Nasr et al., 2013; Riber et al., 2018).

Furthermore, they are restricted in their mobility and have a lower laying performance (Nasr et al., 2013; Rufener et al., 2019). Thus, keel bone damage has economic effects as well.

The term "Keel bone damage" includes both, keel bone fractures and keel bone deviations. A keel bone deviation is defined as an abnormal shape of the keel bone that is not due to a fracture and varies from the perfect two-dimensional shape of the keel bone (Casey-Trott et al., 2015).

Keel bone fractures are shown as "sharp bends, shearing, and/or fragmented sections of the keel bone" (Casey-Trott et al., 2015). In terms of location, the majority of fractures are found in the caudal third of the keel (Baur et al., 2020; Habig et al., 2021; Kittelsen et al., 2021). Since ossification of the avian sternum proceeds from cranial to caudal, this portion is usually still cartilage at the onset of lay (Wang et al., 2021).

Radiography is a versatile tool to assess keel bone damage. It enables the comparison of different hens as well as longitudinal studies of the same animals (Eusemann et al., 2018a). Besides a high sensitivity and specificity for the detection of fractures, it also offers further possibilities to measure other keel bone parameters. As conducted by Eusemann et al. (2018a), X-ray pictures can be used to measure and calculate the proportion of deviated keel bone area (POD) and thereby quantify the severity of deviations. Another method to quantify keel bone damage on X-ray images is rating it using a tagged visual analog scale as introduced by Rufener et al. (2018) for fractures and Jung et al. (2022) for deviations. Furthermore, Fleming et al. (2000) established a method to assess the bone density of the humerus and tibiotarsus *in vivo* by including an aluminum step wedge on the X-ray picture. This method, which has later been adapted to measure the radiographic density of the keel bone (Eusemann et al., 2020), allows the investigation of the radiographic density at different time points in a longitudinal study. A lower bone density has been linked to more severe keel bone deviations in caged layers and is also associated with pathological fractures through osteoporosis (Dobbs et al., 1999; Habig et al., 2021). In addition, egg-laying hens were found to have a lower radiographic density of the keel bone compared to non-egg-laying hens (Eusemann et al., 2020).

Shortly before the onset of lay, estradiol-17ß, together with androgens, induces the formation of medullary bone (Dacke, 1979; Dacke et al., 1993; Whitehead, 2004). In histologic images, this bone structure can be seen as basophil short spicules extending from the endosteal surface of the cortical and trabecular bone to the medullary cavity (Wilson and Duff 1990; Bloom et al., 1958). This non-structural type of bone serves as a labile calcium source and shows rapid reduction and new formation throughout the egg-laying cycle (Bloom et al., 1941; Bloom et al., 1958; Whitehead, 2004; Kerschnitzki et al., 2014). Loss of structural bone has been linked to the formation of medullary bone by Wilson and Thorp (1998). The authors found a loss of trabecular bone after inducing medullary bone formation in male fowl through estradiol treatment and could also show that a treatment of female fowl with the estrogen receptor modulator Tamoxifen prevented both, formation of medullary bone and loss of trabecular bone. In another study conducted by Dacke et al. (1993), medullary bone recovery during a calcium deficiency was accompanied by a loss of cortical bone. However, there are other studies in which a negative effect of estrogen treatment on cortical bone could not be confirmed (Squire et al., 2017; Eusemann et al., 2022).

Habig et al. (2021) found a higher prevalence of keel bone fractures in high-performing layer lines than in low-performing layer lines. This was also the case within brown layer lines in a study by Eusemann et al. (2018a). A link between keel bone fractures and egg-laying activity is also made by Eusemann et al. (2020). They showed that laying hens prevented from egg-laying through a Deslorelin acetate releasing implant had fewer keel bone fractures than control hens without an implant. This was also the case in hens that additionally received an estrogen releasing implant. Those hens did not lay eggs but built medullary bone. In a study conducted by Kittelsen et al. (2021), the authors found significantly fewer keel bone fractures in red jungle fowl hens compared to White Leghorn hens, a selected laying breed. Red jungle fowl is the non-domesticated species of our laying hens that has never been selected for high laying performance.

This suggests that other species that have been selected for high laying performance may also suffer from keel bone damage. Japanese quails have been domesticated since at least the 12th century (Kovach, 1974) and selected for egg production since 1910 (Yamashina, 1961). As a result, Japanese quails can show a laying performance of 250–300 eggs per year and attain sexual maturity at five to 6 weeks (Yamashina, 1961; Gerken and Mills, 1993). Thus, it is possible that keel bone damage may be an animal welfare problem in Japanese quail hens, too.

The aim of our study was to investigate whether female Japanese quails show keel bone damage and to characterize the keel bone throughout their laying period using radiographic imaging.

# 2 Animals, materials, and methods

## 2.1 Ethical statement

The animal experiment was approved by the competent authority (Lower Saxony State Office for Consumer Protection and Food Safety; no. 33.9-42502-04-13/1096). The competent authority had been informed about certain changes done in the experimental procedure. The quails in the experiment were kept and managed following the general requirements laid down in the German Animal Welfare Act (Tierschutzgesetz, TierSchG) and according to the Directive 2010/63/EU. The animals were daily controlled for health and welfare problems.

## 2.2 Birds and housing conditions

For the experiment, 119 Japanese quails of a layer strain were bred and raised at the Institute of Animal Welfare and Animal Husbandry of the Friedrich-Loeffler-Institut in Celle, Germany. All animals descended from a parent line kept in our facility and hatched on the same day.

After hatching, the quails were moved to a barn compartment of 24 $m^2$ where they were kept in a floor housing system littered with sand. The maximum stocking density amounted to five animals per square meter in the first 4 weeks of age The barn compartment was cleaned as required and the sand was replaced every 3 weeks.

A heating lamp was placed above the middle of the area to provide extra warmth for the first 2 weeks and then removed. In the first week, the quails were kept at a compartment temperature of 35°C–38°C. From day 6 to day 18, the temperature decreased continuously until reaching 18°C and then remained constant for the remainder of the experiment.

The pen was equipped with two nipple drinking troughs and two feed dispensers that provided feed *ad libitum*. The animals received quail diets of the Friedrich-Loeffler-Institut. For the first 3 weeks of age, they were fed quail chick feed (11,37 MJ AMEN/kg, 272 g/kg crude protein, 37 g/kg crude fat, 12,0 g/kg Ca, 8.5 g/kg P), from weeks four to six feed for quail pullets (11,84 MJ AMEN/kg, 213 g/kg crude protein, 40 g/kg crude fat, 11,0 g/kg Ca, 7.4 g/kg P). Thereafter, they received a complete feed for laying hens (11.2 M J AMEN/kg, 155 g/kg crude protein, 52,4 g/kg crude fat, 35 g/kg Ca, 5.5 g/kg P).

After hatching, the light duration was reduced from 24 h on the first day to 16 h on the 25th day and then remained constant for the remainder of the experiment.

In the fifth week of age, the male quails, which can be recognized by their feathering at this stage, were captured and removed from the compartment. The remaining 51 female quails were marked with individual wing tags. From there on, the maximum stocking density in the barn was 2.13 animals per square meter. Unfortunately, some of the hens died during the experiment so that at the end, there were 41 hens left and the number of hens differed between examination dates. *Post mortem* dissection revealed a wide range of causes of death including enteritis, salpingitis, pneumonia, dystocia and injuries from cannibalism and accidents. The numbers of hens that were included in the analysis of each parameter at a certain examination date are given in the results section.

## 2.3 Methods

During the experimental period, the quails were investigated five times. The first three dates were set according to the course of the laying period. The first session took place in their eighth week of age as Japanese quails normally start laying between their fifth and seventh weeks of age. The second session was conducted in week 10 when quails reach their maximum of laying performance. In week 15, when the laying performance is still high, the third investigation took place. The last two investigations were performed with an interval of 4 weeks in the 19th and 23rd week of age to ensure the detection of fractures before complete healing. At each of these dates, body weight was recorded and X-rays were taken of all hens. After the last examination at 23 weeks of age, the hens were killed and keel bones were macerated to verify the radiographic findings.

Additionally, a histological analysis of Japanese quail keel bones was conducted to gain more information about the structure and composition of the bone in laying quails, especially about the presence of medullary bone in the keel bone.

### 2.3.1 Examination of general condition and body weight

At each of the above mentioned dates, the birds were caught in their barn compartment and transported to the examination room in boxes. They were separately unloaded from the box and weighed with a precision scale IP65 (Sartorius, Göttingen, Germany), The general health status was visually assessed, and the footpads were examined to determine the occurrence of pododermatitis before continuing with the X-ray.

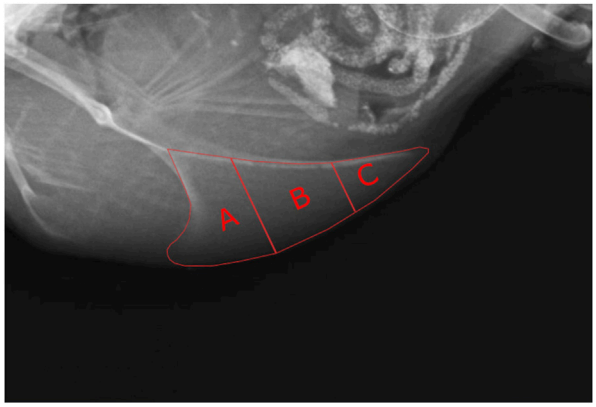


FIGURE 1
Subdivision of the keel bone into sections for the detection of fractures. **(A)** = cranial section, **(B)** = middle section, **(C)** = caudal section.

### 2.3.2 Radiographic examination

Radiographs were taken with the X-ray generator WDT Blueline 1040 HF (Wirtschaftsgenossenschaft Deutscher Tierärzte eG, Garbsen, Germany), the digital flat panel detector Thales Piximum 2430 EZ wireless (Thales Electron Devices S.A., Velizy-Villacoublay, France), and a laptop, which was transported in an X-ray case Leonardo DR mini (Oehm and Rehbein GmbH, Rostock, Germany).

For the X-ray, the quails were fixated upside down in a home-built rack. A left latero-lateral radiography was taken with 50.0 kV at 2 mAs. As conducted by Eusemann et al. (2020), a home-built 2 cm * 17.8 cm aluminum step wedge was positioned on the flat panel detector and radiographed with each bird. The 17 steps of the step wedge decreased by 0.25 cm each step and were used to determine the radiographic density of the keel bone on the X-ray image (see below).

### 2.3.3 Radiographic evaluation

Each X-ray picture was examined for fractures, deviations, radiographic density, total lateral surface area, and length of the keel bone as well as the length of the caudal cartilaginous part of the keel bone (Supplementary Material 1).

To gain more information about the location of the fractures within the keel bone, it was divided into three sections from cranial to caudal as conducted by Baur et al. (2020) excluding the labeling of the apices (Figure 1). Afterward, the number of fractures in each section was counted.

A tagged visual analog scale developed for keel bone deviations in laying hens by Jung et al. (2022) was used to rate the severity of deviations displayed on the X-ray pictures. The rating was conducted by a single observer who had completed the online training supplied by Jung et al. (2022) before.

Due to blurry images and tilting five radiographs had to be excluded from evaluation for radiographic density, lateral surface

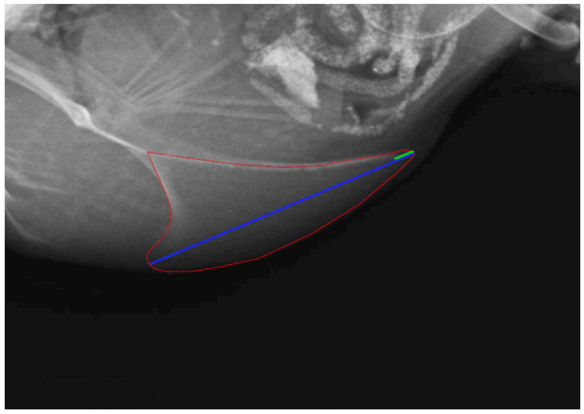

FIGURE 2
Measurement of the lateral surface area (red), the length (blue) and the cartilaginous portion of the keel bone (green).

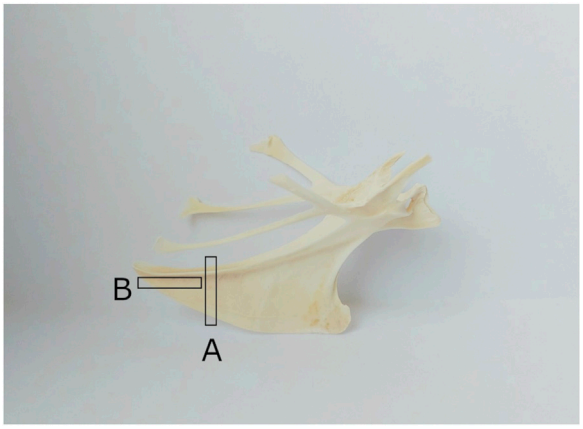


FIGURE 3
Cutting of the keel bone for transversal and horizontal sections ((**A**) for transversal sections, **(B)** for horizontal sections).

area, and length of the keel bone. For the measurement of the lateral surface area and length of the keel bone as well as the length of the cartilaginous part, the software Axio Vision 4.8 (Carl Zeiss Microscopy GmbH, Jena, Germany) was used. The lateral surface area was measured by encircling the keel bone, including the caudal cartilaginous part, and the length by drawing a straight line from the most cranio-ventral part to the most caudal part of the carina. The length of the cartilaginous part was also measured along that line (Figure 2). Area and lengths were then calculated with the help of a given scaling. For the measurement of the radiographic density, the aluminum step wedge provided the data to generate a calibration curve with a third polynomial function. An individual calibration curve was created for each radiograph. Then the area of the keel bone without the cartilaginous part was encircled and the software ImageJ (Version 1.52; Rasband, W; National Institute of Health, Bethesda, Maryland, United States) was used to transfer the mean gray value of the area into mm of aluminum equivalent as described by Eusemann et al. (2020). Further, to validate that the scaling of the X-ray pictures did not differ between the dates of examination, the width of the aluminum step wedge was measured and compared.

### 2.3.4 Recording laying performance, egg weight, and eggshell weight

From the beginning of the experiment onwards, the number of eggs was counted at the same time every day at group level (Supplementary Material 2). If there were days on which the eggs were not collected, the number of eggs found on the following day was equally between the days. One day per week, the eggs of the day were weighed and their shell weight was determined (Supplementary Material 3). For this purpose, each egg was weighed on an electronic analysis scale Kern PCB 100-3 (Kern & Sohn GmbH, Balingen, Germany) and cut open with dissection scissors (Carl Roth GmbH &Co-KG, Karlsruhe, Germany) along the center to divide the egg into two-halves. The inner components were completely collected in a beaker (Carl Roth GmbH & Co. KG, Karlsruhe, Germany). The two-halves of the eggshell were numbered and placed in a paper egg tray with their inner surface towards the opened part of the tray. Afterward, the tray was placed in a compartment drier (Memmert UF750plus; Memmert GmbH u. Co. KG, Schwabach, Germany) for 24 h at 45°C to completely remove water containing components like yolk and egg white. Finally, the egg shells were removed from the egg tray using a pair of tweezers (Carl Roth GmbH & Co. KG, Schwabach, Germany) and weighed on an electronic analysis scale (Kern PCB 100-3; Kern & Sohn GmbH, Balingen, Germany).

### 2.3.5 Maceration of the keel bones

For the maceration, the sternum was separated from the surrounding tissue using scissors (Wirtschaftsgenossenschaft deutscher Tierärzte eG, Gabsen, Germany) and a scalpel (Wirtschaftsgenossenschaft deutscher Tierärzte eG, Gabsen, Germany). It was then placed into a 1 L beaker (Carl Roth GmbH & Co.KG, Karlsruhe, Germany) and covered with a solution, which was made of 85% water, 10% Biozym SE (Spinnrad GmbH, Bad Segeberg, Germany), and 5% Biozym F (Spinnrad GmbH, Bad Segeberg, Germany). The beaker was then placed in a compartment drier (Memmert UF750plus; Memmert GmbH u. Co. KG, Schwabach, Germany) at 60 °C overnight (approximately 15–18 h). Afterward, the solution was poured through a strainer and the remaining tissue was removed from the bones. This procedure was then repeated one more time and finally the sternum was placed in a compartment drier at 35°C–45 °C overnight for drying. They were then stored in labeled containers until evaluation.

At the evaluation, two observers assessed the macerated keel bones for the absence or presence of keel bone deviation. The sensitivity was calculated by dividing the number of animals that showed keel bone deviation on both, X-ray image at 23 weeks of age and macerated keel bone by the total number of animals that showed deviation on their macerated keel bone. The specificity was determined by dividing the number of animals that showed neither a deviation on the X-ray image at 23 weeks of age nor on the macerated keel bone, by the number of animals without deviation on their macerated keel bone.

### 2.3.6 Histological analysis

For the histological analysis of the quail keel bone, samples of ten 20-week-old female Japanese quails were used. These quails were not

identical to the quails that were radiographed. Instead, they had been part of another study and we received their keel bones as part of an organ sharing initiative. After separation from the muscles, pieces for transversal and horizontal sections were cut from each keel bone. For the transversal section, a piece of 3–4 mm in thickness was cut from the caudal third of the keel bone. For the horizontal section, a piece of 3–4 mm in thickness was cut from the caudal part of the keel bone parallel to the corpus of the sternum (Figure 3). The pieces were then decalcified for 6 weeks in buffered ethylene-diamine tetra acetic acid (EDTA; Carl Roth GmbH + Co. KG, Karlsruhe, Germany). Afterward, they were washed in tap water, dehydrated through an ascending alcohol series, and embedded in paraffin wax (Surgipath Paraplast plus, Leica, Illinois, United States). Finally, the sections were cut at 5 µm with a rotary microtome (Microm HM 355 S, Thermo Fisher Scientific™ Inc., Waltham, Massachusetts, United States), mounted on a slide covered with poly-l-lysine (Thermo Fisher Scientific Inc., Waltham, Massachusetts, United States), and stained with hematoxylin and eosin (Hematoxylin solution acc. to Delafield, Carl Roth GmbH + Co. KG, Karlsruhe, Germany) In order to assess how the medullary bone is distributed in the keel bone of laying female quails, horizontal and longitudinal sections of the keel bone were examined at ×2.5 and ×20 magnification with a light microscope (Axio Imager 2, Carl Zeiss AG, Oberkochen, Germany).

### 2.3.7 Statistical analysis

Statistical analysis was performed with RStudio 2023.03.0 and Excel (Version 1808; Microsoft, Redmond, Washington, United States).

The length of the cartilaginous part of the keel bone was calculated as the percentage of the total keel bone length. For the length of the cartilaginous part (log-transformed), body weight, radiographic density, keel bone length, keel bone lateral surface area, and the score of the deviation (log-transformed), mixed models with week of age as fixed effect were created using the nlme package and an ANOVA was performed. The animal was included as a random factor to take the repeated measures into account. The residuals were controlled for normal distribution by visual examination using q-q-plots and histograms. Post-hoc analysis was performed using Tukey's HSD tests.

As there were animal losses throughout the study (see 2.2), the daily egg-laying rate was calculated by dividing the number of eggs by the number of hens. As quails are reported to enter full lay between the eighth and ninth week of age (Gerken and Mills, 1993), only the laying rates from week 10 to week 23 were considered in order to assess whether there were any changes in laying performance throughout the laying period. As conducted before, a mixed model with the week of age as fixed and the animal as random effect was created. The residuals were visually controlled for normal distribution and Tukey's HSD tests were performed for post-hoc analysis.

The relative weight of the eggshell was calculated by dividing the weight of the eggshell by the weight of the whole egg. To assess changes during the laying period, a linear model with week of age as a fixed effect was created and an ANOVA was performed.

# 3 Results

## 3.1 Body weight

The body weight was significantly influenced by age ($F_{4,161}$ = 13.31, $p < 0.0001$). There was a significant increase in body weight between weeks 8 and 10 (z = 4.53, $p < 0.0001$). From week 10 onwards, no significant changes in body weight could be detected. However, there was a trend of an increase (z = 2.71, $p = 0.067$) between weeks 19 and 23. For more detailed information, the weight data can be found in Supplementary Material 1.

## 3.2 Laying rate and eggshell weight

The daily egg-laying rate can be viewed in Figure 4. There were strong fluctuations between the days. The egg-laying rate first inclined in week 7 and then seemed to reach a plateau in week 10. Statistical analysis revealed that during the time between weeks 10 and 23 there were significant differences between the weeks ($F_{13}$ = 2.95, $p = 0.0015$) with the egg-laying rate being significantly lower in week 20 compared to weeks 13 (z = −4.4, $p = 0.003$), 14 (z = −2.79, $p = 0.0033$), 15 (z = −4.11, $p = 0.0086$), 17 (z = −4.13, $p = 0.008$), and 18 (z = −4.04, $p = 0.0111$) and tending to be lower compared to weeks 11 (z = −3.6, $p = 0.0509$), 12 (z = −3,58, $p = 0.0532$), and 16 (z = −3.43, $p = 0.0884$).

There was no significant effect of week of age on the relative eggshell weight.

## 3.3 Fractures

Throughout the experiment, fractures were seen in a total of three animals. There were only single fractures, no multiple fractures. In terms of location, two of the fractures were found in the caudal third (section C; Figure 5) and one in the cranial third (section A) of the keel bone. The fractures in section C were present in weeks 8 and 15, respectively. There was no callus formation visible at the subsequent dates of examination. The fracture in section A was first detected in week 19 with callus formation in week 23.

## 3.4 Deviations

In the X-ray pictures, deviations were scored with a maximum of 2 out of 10 which indicates minor deviation. The overall average score was 0.27 ± 0.42. Statistical analysis showed significant changes with age ($F_{4,161}$ = 11.56, $p < 0.0001$): A significantly higher deviation score was seen from week 15 onwards compared to week 8 (z = 3.82, $p = 0.0014$) and in week 23 compared to week 10 (z = 4.33, $p = 0.0001$). Prevalence of deviation varied between 19.6% and 55.8% during the study when assessed with radiography while maceration revealed that 82.1% of the keel bones were deviated (Table 1). Compared to the outcome of the maceration, the sensitivity and specificity of the radiography for detecting keel bone deviation were 56.25% and 57.14%, respectively.

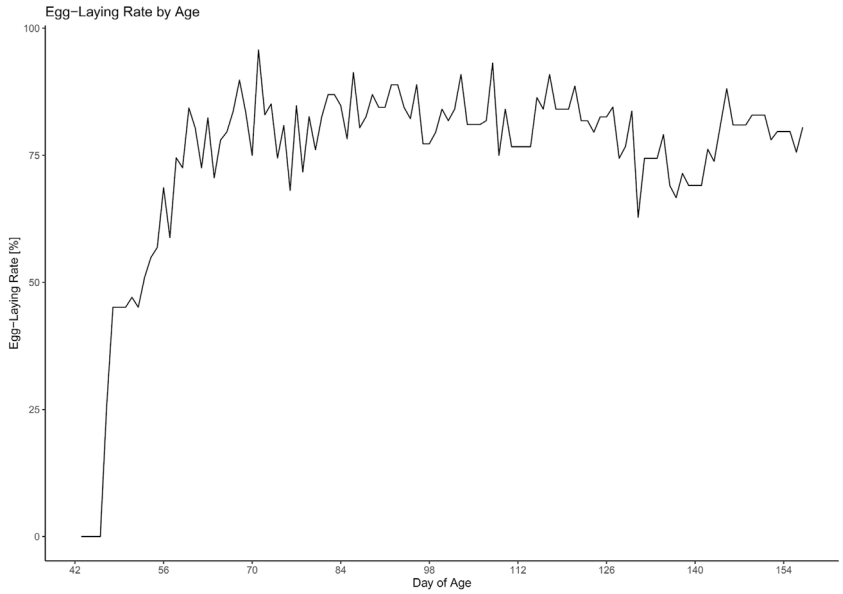


FIGURE 4
Development of the egg-laying rate throughout the experiment.

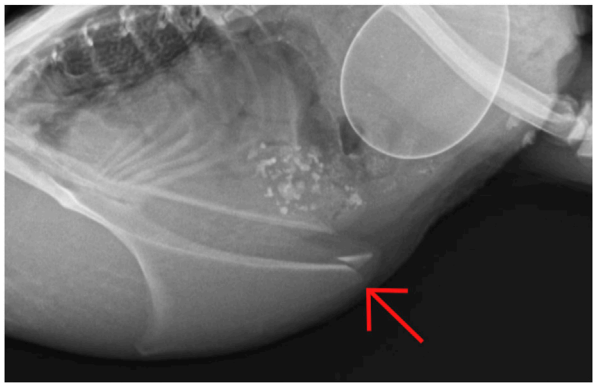

FIGURE 5
Keel bone fracture in section C (caudal third) at 15 weeks of age.

## 3.5 Lateral surface area, length, and ossification of the keel bone

Both, the length ($F_{4,161}$ = 85.27, $p$ < 0.0001) and the lateral surface area ($F_{4,161}$ = 69.83, $p$ < 0.0001) of the keel bone were significantly influenced by age.

The lateral surface area of the keel bone gradually decreased between the eighth and the 10th (z = −9.4, $p$ < 0.0001) and the 10th and the 15th week of age (z = −4.58, $p$ < 0.0001), then increased between the 19th and 23rd week of age (z = 5.3, $p$ < 0.0001) (Figure 6). Likewise, the length of the keel bone decreased between weeks 8 and 10 (z = −9.47, $p$ < 0.0001) and weeks 10 and 15 (z = −6.3, $p$ < 0.0001) and then leveled off (Figure 7).

The mean of the absolute and relative length of the cartilaginous part of the keel bone as well as the maximum and minimum and the percentage of animals whose keel bones were fully ossified can be viewed in Table 2. Statistical analysis showed a significant effect of age on the relative length of the cartilaginous part ($F_{4,161}$ = 280.73, $p$ < 0.0001) with a decrease between weeks 8 and 10 (z = −23.35, $p$ < 0.0001) and weeks 10 and 15 (z = −3.57, $p$ = 0.0035). From week 19 onwards, no cartilage component could be identified anymore.

## 3.6 Radiographic density of the keel bone

The radiographic density of the keel bone was significantly influenced by age ($F_{4,161}$ = 18.84, $p$ < 0.0001). There was a significant decrease between weeks 10 and 15 (z = −4.76, $p$ < 0.0001). In contrast, there were no significant changes in

TABLE 1 Keel bone deviations: Severity scores and prevalence throughout the experiment.

| | Week 8 | Week 10 | Week 15 | Week 19 | Week 23 | *Post mortem* dissection |
|---|---|---|---|---|---|---|
| Ø Score of deviation | 0.1 ± 0.32 | 0.2 ± 0.35 | 0.3 ± 0.43 | 0.3 ± 0.44 | 0.4 ± 0.55 | - |
| Minimum score of deviation | 0 | 0 | 0 | 0 | 0 | - |
| Maximum score of deviation | 2 | 2 | 2 | 2 | 2 | - |
| Prevalence [%] | 19.6 | 41.3 | 55.8 | 53.7 | 48.6 | 82.1 |

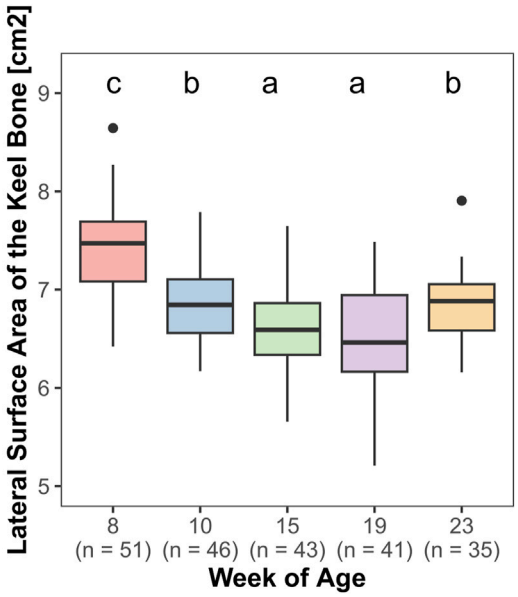


FIGURE 6
Lateral surface area of the keel bone.

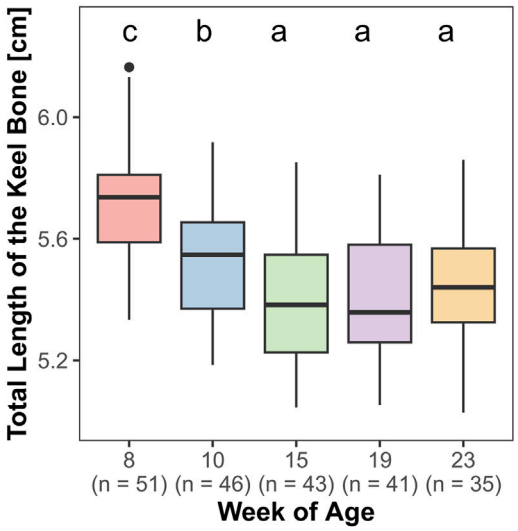


FIGURE 7
Total length of the keel bone.

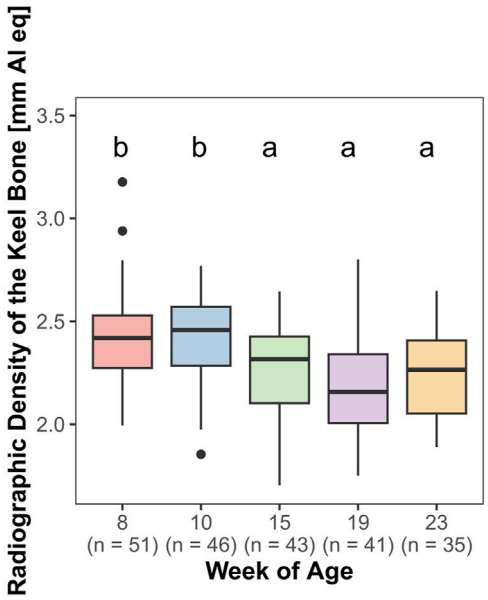


FIGURE 8
Radiographic density of the keel bone.

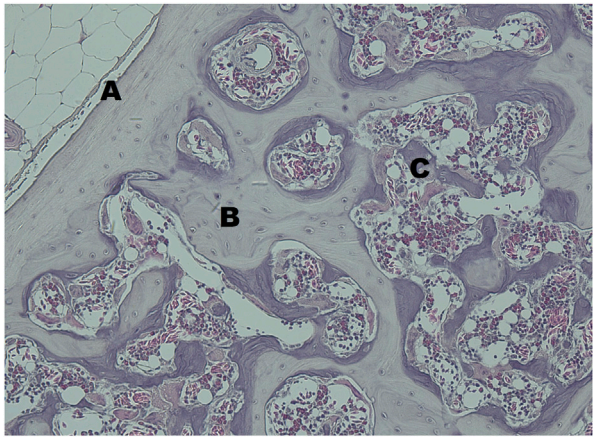


FIGURE 9
The transversal section of the keel bone of a female quail at 20 Weeks of age stained with haematoxylin and eosin at ×20 magnification. **(A)** cortical bone, **(B)** trabecular bone in bright violet, **(C)** medullary bone, in dark violet.

**TABLE 2** Progress of ossification: Length of the cartilaginous part and percentage of animals with fully ossified keel bones.

| | Week 8 | Week 10 | Week 15 | Week 19 | Week 23 |
|---|---|---|---|---|---|
| Ø Length of the cartilaginous part of the keel bone [cm] | 0.53 ± 0.18 | 0.08 ± 0.11 | 0.01 ± 0.03 | 0 | 0 |
| Ø Relative length of the cartilaginous part of the complete keel bone [%] | 9.3 ± 3.2 | 1.4 ± 2 | 0.1 ± 0.6 | 0 | 0 |
| Minimum length of the cartilaginous part of the keel bone [cm] | 0 | 0 | 0 | 0 | 0 |
| Maximum length of the cartilaginous part of the keel bone [cm] | 0.89 | 0.36 | 0.17 | 0 | 0 |
| Percentage of animals with fully ossified keel bones [%] | 5.9 | 63 | 95.3 | 100 | 100 |

radiographic density between weeks 8 and 10 and weeks 15–23 (Figure 8).

### 3.7 Histological analysis

All examined keel bones contained basophile short spicules, which were identified as medullary bone (Figure 9). They were detectable in both, transversal and horizontal sections, and were located on the endosteal surface of the cancellous, i.e., trabecular bone.

## 4 Discussion

Our results clearly show that both, keel bone fractures and deviations occur in Japanese quail. In addition, we observed changes in the radiographic density, length, and lateral surface area of the keel bone during the laying period.

### 4.1 Laying performance, eggshell weight, and body weight

The rather strong variation of the egg-laying rate between the individual days is probably due to the fact that quails were not provided with nests and laid their eggs in the sand. Therefore, it cannot be guaranteed that all eggs were found on the same day. It has to be taken into account, that the number of eggs found in the sand may differ from the number of eggs that were actually laid. Between weeks 10 and 23, there was a significantly lower laying rate in week 20 than in other weeks. Even if no signs of illness or increased mortality were reported, it cannot be fully excluded that this reduction in performance was caused by stress or other external factors. In addition, we can not completely eliminate that fewer eggs were found in the sand this week due to management errors. However, another explanation for the decrease in laying performance could be that more animals showed physiological clutch pauses during this period (Aggrey et al., 1993).

Analysis of the relative weight of the eggshell showed no significant effect of age. This is in contrast to findings in laying hens (Silversides and Scott, 2001) where the relative weight of the eggshell declines in progress of the laying period. A possible explanation for the different findings could be the shorter production and observation period in the present study.

The significant increase in body weight between weeks 8 and 10 suggests that the quails are still growing at that age and therefore gain body mass. This is supported by the fact that the ossification of the keel bone is not completed in the majority of animals at that age. Another reason for the increase could be the incline in laying activity. When hens enter lay, this is accompanied by an increase in the weight of the reproductive organs (Kwakkel et al., 1995).

### 4.2 Keel bone fractures and ossification

Overall, keel bone fractures were detected in three out of the 51 animals, which equals 5.9%. Two out of these three fractures were located in the caudal third of the keel. This matches the findings of Baur et al. (2020) in laying hens, where 77% of keel bone fractures occurred in the caudal third of the keel. In contrast to laying hens that frequently show multiple fractures (Thøfner et al., 2021), only single fractures were found in Japanese quail in the present study.

Even if these numbers seem to be relatively low compared to the number of fractures in laying hens, where keel bone fractures can affect up to 100% of the animals in a flock (Thøfner et al., 2020), it has to be taken into account that the quails were observed for a shorter period and more fractures could have occurred if they had been observed for a longer period. Depending on the author, production periods for laying quails last from 24 up to 40 weeks (Lukanov et al., 2018; Damme et al., 2021). Also, it has to be taken into account that due to the animal losses not all 51 quails were observed until the end of the study.

There may also be a reduced risk for traumatic fractures through collisions and falls since quails do not roost. This would be consistent with the relationship between accessible height and keel bone fractures in laying hens described by Wilkins et al. (2011) and laying hens in floor housing showing fewer keel bone fractures than those kept in aviaries (Jung et al., 2019).

However, the lower number of keel bone fractures could also be explained by differences in the calcium metabolism between quail and laying hens. Even if quails and laying hens show a similarly high laying performance in terms of egg number, the absolute and relative content of calcium is higher in chicken eggshells (Navarro and Murillo, 1976; Ajala et al., 2018; Kalbarczyk et al., 2022). Furthermore, in contrast to chicken, domesticated Japanese quail lay their eggs in the afternoon (Yamashina, 1961). Andrade et al. (2023) observed that most parts of quail eggshell are secreted during the day and, thus, suggest that the calcium source from the medullary bone has less importance in quail than in commercial laying hens, which lay most eggs in the morning and therefore their eggshell is formed at night, when no calcium is absorbed from food (van de Velde et al., 1984; Samiullah et al., 2016).

Another factor that could contribute to a lower prevalence of keel bone fractures is the earlier completion of ossification of the keel bone in Japanese quail as observed in our study. Buckner et al. (1949) showed that in New Hampshire chicken, at 20 weeks of age (i.e., at the onset of lay) 50% of the keel bone was still cartilage and complete ossification of the keel was not reached before 35–40 weeks of age. In contrast, the average cartilaginous part of the quail keel at 8 weeks of age, when the quails started to lay, was 9.3% and all keels were fully ossified at 19 weeks of age. Also, the lack of significant changes in body weight from the 10th week onwards suggests that the quails are fully grown at that point. In laying hens, fractures of the caudal part of the keel bone often show an appearance similar to greenstick fractures (Thøfner et al., 2020). In humans, greenstick fractures are bending fractures that occur in the calcified cartilage of pediatric patients before complete ossification (Kittleson and Whitehouse, 1966). As the ossification of the keel bone is further progressed at the onset of lay in Japanese quail, they may be less likely to experience greenstick fractures.

The presence of keel bone fractures in Japanese quail proves that this condition is not restricted to chicken but also affects quail and could affect other bird species (e.g., ducks, geese) that are used for egg production as well if they show an increased laying rate compared to the wild type. As in chickens, high laying

performance may contribute to the appearance of keel bone fractures in female Japanese quail, too. Our results also point out the ossification of the keel at the onset of lay as a key factor for the development of caudal keel bone fractures. As laying hens with keel bone fractures experience pain (Nasr et al., 2012; 2013), quails with keel bone fractures are most likely to experience pain as well. Thus, keel bone fractures in laying quail should be kept in mind as a potential animal welfare problem and included in welfare protocols for this species.

## 4.3 Keel bone deviations

When assessed with radiography, 60.8% of the 51 quails showed deviations at one or several examination dates. The percentage of deviated keel bones that were discovered through maceration at the end of the experiment was 82.1%. These results are similar to the prevalence of deviations found in laying hens (Eusemann et al., 2018a; Jung et al., 2022). Due to the rather low sensitivity and specificity of radiography in this study, X-ray examination does not seem to be an adequate tool for detecting keel bone deviations in Japanese quail. In laying hens, it has been shown to be a useful tool for assessing keel bone deviations by some authors while others found a rather low sensitivity of 60%, too (Tracy et al., 2019). Keel bone deviations may be difficult to detect with radiography in Japanese quail as they are less severe than the ones found in laying hens. The Japanese quails in the present study showed an average score of 0.27 with a maximum of 2 out of 10 while laying hens were scored with an average score of 2.48 and a maximum of 10 out of 10 (Jung et al., 2022). During perching, high peak forces impact the keel bone of laying hens (Pickel et al., 2011). As quails do not use perches and, thus, do not experience the same kind of peak force on their keel bone, they are likely to develop fewer and less severe sagittal deviations than laying hens. Since only lateral X-ray pictures were taken, sagittal deviations were easier to detect than transversal ones. However, it was not possible to evaluate postero-anterior radiographs in former studies due to the small ventral surface of the keel bone and projections with other body parts (Eusemann et al., 2018a). Thus, no postero-anterior radiographs were taken in the present study. As the sagittal deviations in the present study were rather slight and barely exceeded a straight line, it was not practicable to measure the proportion of deviated keel bone area (POD) in the X-ray images as it was done by Eusemann et al. (2018a).

Our results show that the prevalence of keel bone deviations in Japanese quail is comparable to that in laying hens, even if they are less severe. A possible common factor is rearing in the absence of ultraviolet-B (UV-B) radiation. Both, quails and laying hens, are usually reared inside a barn without access to the full spectrum of sunlight. Doyle (1925) already described a bend of the keel bone as a symptom of rickets in mature chickens that occurs when young chickens are housed inside. UV-B plays a major role in the synthesis of Vitamin D3. Vitamin D3 activates the calcium-binding proteins in the intestine (Bar et al., 1976). Although dietary Vitamin D3 is supplemented, UV-B radiation has been shown to have a better effect on the bone health of young chicks compared to dietary supplementation of Vitamin D3 (Edwards, 2003). The high prevalence of keel bone deviations in both, laying hens and Japanese quail, emphasizes the need of further investigation on the cause and impact of deviations on the animals. Furthermore, our study indicates that radiography is not sensitive enough to detect all keel bone deviations in quails and should therefore be supplemented with another technique such as palpation or maceration.

## 4.4 Radiographic density, lateral surface area, and length of the keel bone

There was a significant decrease in radiographic density between the 10th and 15th weeks of age. At this time, the quails reached their laying maximum. Therefore both, the loss of bone mass due to the high calcium demand for eggshell formation and a shift in bone composition in favor of medullary bone are conceivable. In a study by Eusemann et al. (2018b), radiographic density initially increased until week 33 but then stayed constant throughout the study in untreated laying hens. This is in contrast to our study. However, non-egg-laying hens showed higher radiographic density values compared to control hens (Eusemann et al., 2020), supporting the hypothesis that radiographic density may be negatively influenced by eggshell formation. In humeri, the bone mineral density has been shown to be linked to the breaking strength of the bone (Fleming et al., 2000). Toscano et al. (2018) showed that a greater bone mineral density provides a protective effect at low collision energies, but increases the possibility of severe fractures at high collision energies. It should be kept in mind that the *in vivo* assessment of radiographic density may be influenced by other factors such as feathers, skin, and muscles and not by the actual density of the bone alone. However, these factors were approximately the same in our study at all times and in all animals. Therefore, in our opinion, it cannot be assumed that this had an effect on the results.

Both, the length and the lateral surface area of the keel bone, decreased between the 8th and 19th week of age and then increased again until the 23rd week of age. It is possible that there is a loss of bone substance due to the calcium demand for eggshell formation. A decrease in keel bone area throughout the laying period has been noticed in laying hens before and was the reason for Eusemann et al. (2018a) to establish the "Proportion of deviated keel bone area, POD" to observe the area of deviation in proportion to the overall area of the keel bone.

The increase in keel bone length and area between weeks 19 and 23 could indicate a recovery of the bone substance. A decrease in new fractures for older birds, which could indicate a recovery of bone substance, too, has also been reported for laying hens (Jung et al., 2019; Baur et al., 2020).

The recovery of bone substance could also be due to the decrease in laying performance in week 20, which might stand for laying pauses. Further studies would have to show if this possible recovery is reproducible.

## 4.5 Conclusion

In our study Japanese quails suffered from keel bone damage. Furthermore, we could observe changes in keel bone features such as length, radiographic density, and lateral surface area, which could indicate loss of bone substance/mineralization throughout the laying period. In our opinion, further research is required to gain more information about the extent of keel bone damage in layer quails and the effect of their high laying performance on bone quality. It should also be investigated in further studies whether the damage to the

sternum has the same aetiology as in laying hens and whether there are other parallels in this clinical picture.

## Data availability statement

The original contributions presented in the study are included in the article/Supplementary Material, further inquiries can be directed to the corresponding author.

## Ethics statement

The animal study was approved by the Lower Saxony State Office for Consumer Protection and Food Safety. The study was conducted in accordance with the local legislation and institutional requirements.

## Author contributions

LH: Writing–original draft, Writing–review and editing. CG: Formal Analysis, Visualization, Writing–review and editing. BW: Investigation, Writing–review and editing. BE: Writing–review and editing, Validation. NK: Writing–review and editing. SP: Conceptualization, Investigation, Writing–review and editing, Supervision, Data Curation.

## Funding

The author(s) declare financial support was received for the research, authorship, and/or publication of this article. All costs were covered by budget resources of the Friedrich-Loeffler-Institut.

## Acknowledgments

We thank the staff of our animal husbandry facility for taking care of the Japanese quails and Silke Werner, Gabriele Kirchhof, Franziska Suerborg and Elaine Ibold for their technical assistance. Furthermore, we thank Lars Schrader for his support and the helpful comments on our manuscript.

## Conflict of interest

The authors declare that the research was conducted in the absence of any commercial or financial relationships that could be construed as a potential conflict of interest.

The author(s) declared that they were an editorial board member of Frontiers, at the time of submission. This had no impact on the peer review process and the final decision.

## Publisher's note



## Supplementary material

The Supplementary Material for this article can be found online at: https://www.frontiersin.org/articles/10.3389/fphys.2024.1368382/full#supplementary-material

## References

Aggrey, S. E., Nichols, C. R., and Cheng, K. M. (1993). Multiphasic analysis of egg production in Japanese quail. *Poult. Sci.* 72, 2185–2192. doi:10.3382/ps.0722185

Ajala, E. O., Eletta, O., Ajala, M. A., and Oyeniyi, S. K. (2018). Characterization and Evaluation of chicken eggshell for use as a bio-resource. *Arid Zone J. Eng. Technol. Environ.* 14, 26–40.

Andrade, K. G., Cruz, F. K., Nascimento, M. C., Iwaki, L. C., and Santos, T. C. (2023). Daily egg-cycle in Japanese quail: serum biochemistry, bones, and oviduct changes. *Braz. J. Poult. Sci.* 25. doi:10.1590/1806-9061-2021-1599

Bar, A., Dubrov, D., Eisner, U., and Hurwitz, S. (1976). Calcium-binding protein and calcium absorption in the laying quail (*Coturnix coturnix* japonica). *Poult. Sci.* 55, 622–628. doi:10.3382/ps.0550622

Baur, S., Rufener, C., Toscano, M. J., and Geissbühler, U. (2020). Radiographic evaluation of keel bone damage in laying hens-morphologic and temporal observations in a longitudinal study. *Front. veterinary Sci.* 7, 129. doi:10.3389/fvets.2020.00129

Bloom, M. A., Domm, L. V., Nalbandov, A. V., and Bloom, W. (1958). Medullary bone of laying chickens. *Am. J. Anatomie* 102, 411–453. doi:10.1002/aja.1001020304

Bloom, W., Bloom, M. A., and McLean, F. C. (1941). Calcification and ossification. Medullary bone changes in the reproductive cycle of female pigeons. *Anatomical Rec.* 81, 443–475. doi:10.1002/ar.1090810404

Buckner, G. D., Insko, W. M., Henry, A. H., and Wachs, E. F. (1949). Rate of growth and calcification of the sternum of male and female New Hampshire chickens having crooked keels. *Poult. Sci.* 28, 289–292. doi:10.3382/ps.0280289

Dacke, C. G. (1979). *Calcium regulation in sub-mammalian vertebrates*. London: Academic Press.

Dacke, C. G., Arkle, S., Cook, D. J., Wormstone, I. M., Jones, S., Zaidi, M., et al. (1993). Medullary bone and avian calcium regulation. *J. Exp. Biol.* 184, 63–88. doi:10.1242/jeb.184.1.63

Damme, K., Golze, M., and Schreiter, R. (2021). *Haltung von Spezialgefügel*. Frankfurt: DLG kompakt.

Dobbs, M. B., Bruckwalter, J., and Saltzmann, C. (1999). Osteoporosis: the increasing role of the orthopaedist. *Iowa Orthop. J.* 19, 43–52.

Doyle, L. P. (1925). Rickets in mature chickens. *Poult. Sci.* 4, 146–150. doi:10.3382/ps.0040146

Edwards, H. M. (2003). Effects of u.v. irradiation of very young chickens on growth and bone development. *Br. J. Nutr.* 90, 151–160. doi:10.1079/bjn2003860

Eusemann, B. K., Baulain, U., Schrader, L., Thöne-Reineke, C., Patt, A., and Petow, S. (2018a). Radiographic examination of keel bone damage in living laying hens of different strains kept in two housing systems. *PloS one* 13 (e0194974). doi:10.1371/journal.pone.0194974

Eusemann, B. K., Patt, A., Schrader, L., Weigend, S., Thöne-Reineke, C., and Petow, S. (2020). The role of egg production in the etiology of keel bone damage in laying hens. *Front. veterinary Sci.* 7, 81. doi:10.3389/fvets.2020.00081

Eusemann, B. K., Sharifi, A. R., Patt, A., Reinhard, A. K., Schrader, L., Thöne-Reineke, C., et al. (2018b). Influence of a sustained release Deslorelin acetate implant on reproductive Physiology and associated traits in laying hens. *Front. physiology* 9, 1846. doi:10.3389/fphys.2018.01846

Eusemann, B. K., Ulrich, R., Sanchez-Rodriguez, E., Benavides-Reyes, C., Dominguez-Gasca, N., Rodriguez-Navarro, A. B., et al. (2022). Bone quality and composition are influenced by egg production, layer line, and oestradiol-17ß in laying hens. *Avian pathology J. W.V.P.A* 51, 267–282. doi:10.1080/03079457.2022.2050671

Fleming, R. H., McCormack, H. A., and Whitehead, C. C. (2000). Prediction of breaking strength in osteoporotic avian bone using digitized fluoroscopy, a low cost radiographic technique. *Calcif. tissue Int.* 67, 309–313. doi:10.1007/s002230001120

Gerken, M., and Mills, A. D. (1993). "Welfare of domestic quail," in *Proceedings of the fourth European symposium on poultry welfare*. Editors C. J. Savory and H. O. Hughes (Potters Bar, England), 158–176.

Habig, C., Henning, M., Baulain, U., Jansen, S., Scholz, A. M., and Weigend, S. (2021). Keel bone damage in laying hens-its relation to bone mineral density, body growth rate and laying performance. *Animals* 11, 1546. doi:10.3390/ani11061546

Jinman, P. (2013). *FAWC advice on keel bone fractures in laying hens*.

Jung, L., Niebuhr, K., Hinrichsen, L. K., Gunnarsson, S., Brenninkmeyer, C., Bestman, M., et al. (2019). Possible risk factors for keel bone damage in organic laying hens. *Animal* 13, 2356–2364. doi:10.1017/S175173111900003X

Jung, L., Rufener, C., and Petow, S. (2022). A tagged visual analog scale is a reliable method to assess keel bone deviations in laying hens from radiographs. *Front. veterinary Sci.* 9, 937119. doi:10.3389/fvets.2022.937119

Kalbarczyk, M., Szcześ, A., Kantor, I., May, Z., and Sternik, D. (2022). Synthesis and characterization of calcium phosphate materials derived from eggshells from different poultry with and without the eggshell membrane. *Materials* 15, 934. doi:10.3390/ma15030934

Käppeli, S., Gebhardt-Henrich, S. G., Fröhlich, E., Pfulg, A., and Stoffel, M. H. (2011). Prevalence of keel bone deformities in Swiss laying hens. *Br. Poult. Sci.* 52, 531–536. doi:10.1080/00071668.2011.615059

Kerschnitzki, M., Zander, T., Zaslansky, P., Fratzl, P., Shahar, R., and Wagermaier, W. (2014). Rapid alterations of avian medullary bone material during the daily egg-laying cycle. *Bone* 69, 109–117. doi:10.1016/j.bone.2014.08.019

Kittelsen, K. E., Gretarsson, P., Jensen, P., Christensen, J. P., Toftaker, I., Moe, R. O., et al. (2021). Keel bone fractures are more prevalent in White Leghorn hens than in Red Jungle fowl hens-A pilot study. *PloS one* 16, e0255234. doi:10.1371/journal.pone.0255234

Kittleson, A. C., and Whitehouse, W. M. (1966). Stress, greenstick and impaction fractures. *Radiologic Clin. N. Am.* 4, 277–288. doi:10.1016/S0033-8389(22)02893-7

Kovach, J. K. (1974). The behaviour of Japanese quail: review of literature from a bioethological perspective. *Appl. Anim. Ethol.* 1, 77–102. doi:10.1016/0304-3762(74)90010-8

Kwakkel, R. P., van Esch, J. A., Ducro, B. J., and Koops, W. J. (1995). Onset of lay related to multiphasic growth and body composition in White Leghorn pullets provided *ad libitum* and restricted diets. *Poult. Sci.* 74, 821–832. doi:10.3382/ps.0740821

Lukanov, H., Genchev, A., and Kolev, P. (2018). Comparative investigarion of egg production in W, GG and GI Japanese quail populations. *TJS* 16, 334–343. doi:10.15547/tjs.2018.04.011

Nasr, M. A. F., Murrell, J., and Nicol, C. J. (2013). The effect of keel fractures on egg production, feed and water consumption in individual laying hens. *Br. Poult. Sci.* 54, 165–170. doi:10.1080/00071668.2013.767437

Nasr, M. A. F., Nicol, C. J., and Murrell, J. (2012). Do laying hens with keel bone fractures experience pain? *PloS one* 7, e42420. doi:10.1371/journal.pone.0042420

Navarro, M. P., and Murillo, A. (1976). Calcium balance in the quail (*Coturnix coturnix* japonica). 1, Influence of sex and diethylstilbestrol. *Poult. Sci.* 55, 2201–2209. doi:10.3382/ps.0552201

Nielsen, S., Alvarez, J., Bicout, D., Calistri, P., Canali, E., Drewe, J., et al. (2023). Welfare of laying hens on farm. *efsa J.* 21. doi:10.2903/j.efsa.2023.7789

Pickel, T., Schrader, L., and Scholz, B. (2011). Pressure load on keel bone and foot pads in perching laying hens in relation to perch design. *Poult. Sci.* 90, 715–724. doi:10.3382/ps.2010-01025

Riber, A. B., Casey-Trott, T. M., and Herskin, M. S. (2018). The influence of keel bone damage on welfare of laying hens. *Front. veterinary Sci.* 5, 6. doi:10.3389/fvets.2018.00006

Rufener, C., Baur, S., Stratmann, A., and Toscano, M. J. (2018). A reliable method to assess keel bone fractures in laying hens from radiographs using a tagged visual analogue scale. *Front. veterinary Sci.* 5, 124. doi:10.3389/fvets.2018.00124

Rufener, C., Baur, S., Stratmann, A., and Toscano, M. J. (2019). Keel bone fractures affect egg laying performance but not egg quality in laying hens housed in a commercial aviary system. *Poult. Sci.* 98, 1589–1600. doi:10.3382/ps/pey544

Samiullah, S., Roberts, J., and Chousalkar, K. (2016). Oviposition time, flock age, and egg position in clutch in relation to brown eggshell color in laying hens. *Poult. Sci.* 95, 2052–2057. doi:10.3382/ps/pew197

Silversides, F. G., and Scott, T. A. (2001). Effect of storage and layer age on quality of eggs from two lines of hens. *Poult. Sci.* 80, 1240–1245. doi:10.1093/ps/80.8.1240

Squire, M. E., Veglia, M. K., Drucker, K. A., Brazeal, K. R., Hahn, T. P., and Watts, H. E. (2017). Estrogen levels influence medullary bone quantity and density in female house finches and pine siskins. *General Comp. Endocrinol.* 246, 249–257. doi:10.1016/j.ygcen.2016.12.015

Thøfner, I., Hougen, H. P., Villa, C., Lynnerup, N., and Christensen, J. P. (2020). Pathological characterization of keel bone fractures in laying hens does not support external trauma as the underlying cause. *PloS one* 15, e0229735. doi:10.1371/journal.pone.0229735

Thøfner, I. C. N., Dahl, J., and Christensen, J. P. (2021). Keel bone fractures in Danish laying hens: prevalence and risk factors. *PloS one* 16, e0256105. doi:10.1371/journal.pone.0256105

Toscano, M., Booth, F., Richards, G., Brown, S., Karcher, D., and Tarlton, J. (2018). Modeling collisions in laying hens as a tool to identify causative factors for keel bone fractures and means to reduce their occurrence and severity. *PloS one* 13, 0200025. doi:10.1371/journal.pone.0200025

Tracy, L. M., Temple, S. M., Bennett, D. C., Sprayberry, K. A., Makagon, M. M., and Blatchford, R. A. (2019). The reliability and accuracy of palpation, radiography, and sonography for the detection of keel bone damage. *Animals* 9. doi:10.3390/ani9110894

van de Velde, J. P., Vermeiden, J. P. W., Touw, J. J. A., and Veldhuijzen, J. P. (1984). Changes in activity of chicken medullary bone cell populations in relation to the egg-laying cycle. *Metabolic Bone Deseases Relat. Res.* 5, 191–193. doi:10.1016/0221-8747(84)90029-8

Wang, Y., Wu, K., Gan, X., Ouyang, Q., Wu, Q., Liu, H., et al. (2021). The pattern of duck sternal ossification and the changes of histological structure and gene expression therein. *Poult. Sci.* 100, 101112. doi:10.1016/j.psj.2021.101112

Whitehead, C. C. (2004). Overview of bone biology in the egg-laying hen. *Poult. Sci.* 83, 193–199. doi:10.1093/ps/83.2.193

Wilkins, L. J., McKinstry, J. L., Avery, N. C., Knowles, T. G., Brown, S. N., Tarlton, J., et al. (2011). Influence of housing system and design on bone strength and keel bone fractures in laying hens. *Veterinary Rec.* 169, 414. doi:10.1136/vr.d4831

Wilson, S., and Thorp, B. H. (1998). Estrogen and cancellous bone loss in the fowl. *Calcif. tissue Int.* 62, 506–511. doi:10.1007/s002239900470

Yamashina, H. (1961). Quail breeding in Japan. *J. Bombay Nat. Hist. Soc.* 58, 216–222.

# Frontiers in Physiology

**Understanding how an organism's components work together to maintain a healthy state**

The second most-cited physiology journal, promoting a multidisciplinary approach to the physiology of living systems - from the subcellular and molecular domains to the intact organism and its interaction with the environment.

---

## Discover the latest Research Topics

See more →

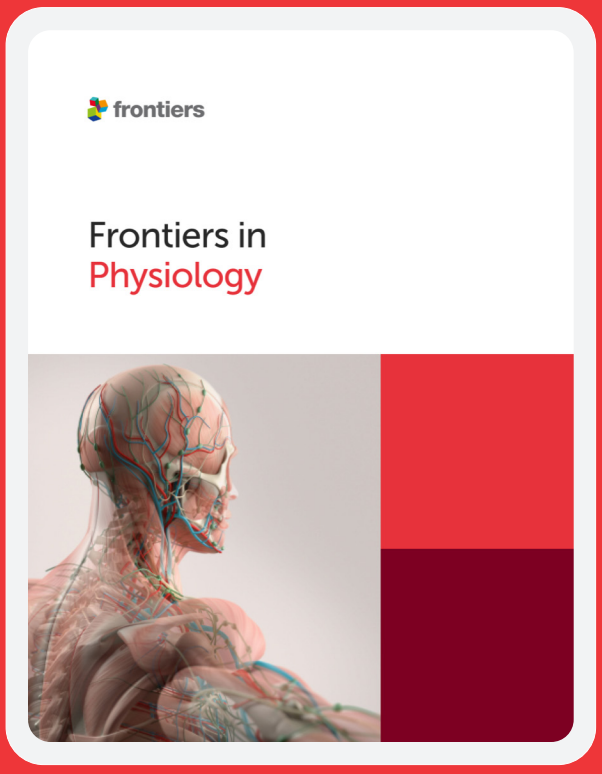


**Frontiers**

Avenue du Tribunal-Fédéral 34
1005 Lausanne, Switzerland
frontiersin.org

**Contact us**

+41 (0)21 510 17 00
frontiersin.org/about/contact